WRC



Central Utah Regional Seismotectonic Study

U. S. DEPARTMENT OF THE INTERIOR
BUREAU OF RECLAMATION
ENGINEERING AND RESEARCH CENTER
SEISMOTECTONIC SECTION
DENVER, COLORADO

CENTRAL UTAH REGIONAL SEISMOTECTONIC STUDY FOR USBR DAMS IN THE WASATCH MOUNTAINS

Geology by:

J. Timothy Sullivan

Alan R. Nelson

Seismology by:

Roland C. LaForge

Christopher K. Wood

Roger A. Hansen

SEISMOTECTONIC REPORT 88-5

Seismotectonic Section
Division of Geology
Engineering and Research Center
U. S. Bureau of Reclamation
Denver, Colorado

March, 1988

Prepared by:

Tim Sullivan 3/24/88
Date

J. T. Sullivan
Geologist
Denver, Colorado

Roland C. LaForge 3/24/88
Date

R. C. LaForge
Seismologist
Denver, Colorado

Chris Wood 3/24/88
Date

C. K. Wood
Seismologist
Denver, Colorado

Technical Approval by:

Dean Ostenaa 3/24/88
Date

D. A. Ostenaa
Head, Seismotectonic Section
Denver, Colorado

Reviewed by:

R B MacDonald 3/25/88
Date

R. B. MacDonald
Chief, Geologic Services Branch
Denver, Colorado

Approved by:

Harold D. Markwell 3/25/88
Date

S. D. Markwell
Chief, Division of Geology
Denver, Colorado

IN SECTION 7, SEISMOTECTONIC CONCLUSIONS ARE PROVIDED FOR THE FOLLOWING USBR DAMS

Newton Dam, Newton Project

Hyrum Dam, Hyrum Project

Causey Dam, Weber Basin Project

Lost Creek Dam, Weber Basin Project

Pineview Dam, Weber Basin Project

Arthur V. Watkins Dam, Weber Basin Project

East Canyon Dam, Weber Basin Project

Echo Dam, Weber Basin Project

Wanship Dam, Weber Basin Project

Jordanelle Damsite, Central Utah Project

Deer Creek Dam, Provo River Project

Soldier Creek Dam, Central Utah Project

Monks Hollow Damsite, Central Utah Project

Mona Dam, Central Utah Project

Joes Valley Dam, Emery County Project

Scofield Dam, Emery County Project

SUMMARY

This report presents the results of a Bureau of Reclamation seismotectonic evaluation for dams in the Wasatch Mountains in north-central Utah. The major objectives of this study were to identify potential earthquake sources in the region and to estimate MCEs (maximum credible earthquakes) for these sources. The conclusions presented in this report are based on geologic mapping, trenching, study of aerial photography, mapping and correlation of Quaternary deposits, soil profile descriptions and sampling, and analysis of historic seismicity. The Regional Study area includes an area on the eastern margin of the Basin and Range province that extends east from the Wasatch Front to the Uinta Mountains and from the Idaho-Wyoming border south to the Wasatch Plateau.

The Regional Study area lies within the ISB (Intermountain seismic belt), a 100-km-wide zone of contemporary seismicity on the eastern margin of the Basin and Range Province that is considered to have the highest level of earthquake risk in the United States outside of California and Nevada. Plots of historical seismicity in this portion of the ISB show that the earthquake activity is concentrated in two diffuse north-trending bands, one west of the Wasatch fault, and the other 20 to 50 km east of the Wasatch fault within the Wasatch Mountains.

In the ISB, large-magnitude historic earthquakes and recent, well-studied, moderate-magnitude earthquakes have been shown to result from dip-slip displacement on generally north-trending normal faults. The large-magnitude earthquakes at Hebgen Lake (M 7.5), Borah Peak (M 7.3), and Hansel Valley (M 6.6) have occurred at focal depths of 10 to 15 km on mapped faults with an identifiable history of late Quaternary surface displacements. These historical examples indicate that potential sources of large-magnitude earthquakes in the region are normal faults with evidence of a history of late Quaternary surface displacements. We consider faults that have been identified from previous geologic investigations and those identified in investigations undertaken as a part of this study as potential sources of large-magnitude earthquakes.

Geologic investigations for this study focused on the back valleys of the Wasatch Mountains, Cenozoic structural basins bounded by normal faults, smaller but similar to the late Cenozoic basins in the Basin and Range Province to the west. Typically the principal faults are known or inferred on the margins of the basins at the base of bedrock escarpments. Our review of aerial photography and low sun-angle overflights of all of the back valleys disclosed only one, previously unrecognized fault scarp in unconsolidated Quaternary deposits in the Regional study area.

A 3-km-long, east-trending fault scarp displaces outwash deposits along the 7-km-long James Peak fault adjacent to the East Cache fault at the south end of Cache Valley. Colluvial stratigraphy in a trench across the 4-m-high fault scarp indicates that two surface displacement events, each with about 2 m of vertical displacement, have occurred in the last 140 ka on the James Peak fault. This suggests an average return period for surface displacements of 70 ka and an average slip rate of about 0.03 mm/yr for the James Peak fault. Surface displacements of 2 m are typically associated with rupture lengths of > 20 km suggesting that adjacent portions of the East Cache fault

rupture simultaneously with the James Peak fault. Although Holocene displacements have occurred on the East Cache fault near Logan, Utah, published mapping indicates that lacustrine deposits of Lake Bonneville overlie the southern portion of the East Cache fault adjacent to the James Peak fault suggesting that the most recent event on the James Peak fault occurred prior to about 14 ka.

Morgan Valley is a Cenozoic basin bounded by north-trending normal faults in the northern Wasatch Mountains. The basin is filled with east-tilted Eocene and younger basin fill. The principal fault in the valley, the Morgan fault, is located on the eastern margin of the valley. Along the northern portion of the Morgan fault, erosion surfaces, probably of early or mid-Quaternary age, are tilted into the fault. Triangular facets are preserved in Paleozoic rocks along the central portion of the fault. The Morgan fault was exposed in trenches across the base of the facets. Colluvial stratigraphy in the trenches show that surface displacements of 0.5 - 1.0 m have occurred on the Morgan fault. Based on correlation of the faulted deposits with alluvial fan deposits dated by aminostratigraphy, an average Quaternary slip rate of 0.01 - 0.02 mm/yr and an average return period for surface displacements of 25 - 100 ka were estimated.

Previous mapping, review of aerial photography, and our mapping indicate that Cenozoic normal faults are also present in Ogden Valley and along the East Canyon fault in the northern Wasatch Mountains. Based on a comparison of stratigraphic and morphological evidence from these faults with the Morgan fault, we concluded that late Quaternary surface displacements have also occurred on segments of back valley normal faults in Ogden Valley and in the East Canyon area. All of these faults are considered potential sources of large-magnitude earthquakes.

In the southern Wasatch Mountains late Quaternary surface displacements have also occurred on back valley normal faults. Trenching of fault scarps in late Quaternary alluvial fans along the Strawberry fault indicates that the most recent event occurred during the Holocene, and that surface displacements have an average return period of 5 to 15 ka. Based on the similarity of the morphology of escarpments associated with the Stinking Springs fault, the Little Diamond Creek fault, and faults in Round Valley to the morphology of the escarpments associated with the Morgan and Strawberry faults, we concluded that late Quaternary surface displacements have also occurred on these faults. They are considered potential sources of large-magnitude earthquakes.

In the central Wasatch Mountains Cenozoic normal faults were mapped in Keetley and Kamas Valleys, and were inferred in Heber Valley and Deer Valley. The principal fault in Kamas Valley is the East Kamas fault on the east side of the valley, where borehole logs and gravity data indicate a minimum Cenozoic displacement of 500 m. Mapping shows that alluvial fans with an estimated age of > 140 ka overlie the East Kamas fault in two locations. The principal fault in Keetley Valley is the the Bald Mountain fault. It was exposed in trenches on the southwest margin of Keetley Valley. There, trenches also show that basin fill deposits with an estimated age of > 140 ka overlie the fault. Trenching of a scarp in alluvial deposits along the south margin of Heber Valley showed that it had an erosional origin. Mapping also showed that other scarps along the margins of Heber Valley were terrace

remnants. Thus, although bore holes suggest that Cenozoic faults are present in Heber Valley, the locations of these faults is unknown and there is no evidence that late Quaternary surface displacements have occurred in the valley. In Deer Valley, no scarps are present in alluvial fan deposits with an estimated age of > 140 ka. In Mountain Meadows, an east-trending synclinal valley developed in Mesozoic rocks and overlying early Tertiary volcanics, air photos revealed a linear, 3-km-long, east-trending scarp associated with a mapped fault on the south margin. A trench across this scarp showed that it was a fault-line scarp. As there is no evidence that late Quaternary surface displacements have occurred on any of these faults, we concluded that there are no potential sources of large-magnitude earthquakes in the back valleys of the central Wasatch Mountains.

The principal source of large-magnitude earthquakes in the region is the Wasatch fault, a 370-km-long, north-trending normal fault that forms the western boundary of the Regional study area. While no investigations of the Wasatch fault were undertaken for this study, previous geologic studies have shown that the fault consists of 6 to 10 segments and that repeated surface displacement events averaging about 2 m have occurred on the central segments of the fault during the Holocene (Schwartz and Coppersmith, 1984). An MCE of magnitude 7 1/2 has been assigned to each of the segments of the Wasatch fault. MCEs with magnitudes ranging from 6 3/4 to 7 1/2 are assigned to late Quaternary faults in the northern and southern portions of the back valleys of the Wasatch Mountains and to the late Quaternary faults on the Wasatch Plateau.

Seismological studies of mainshocks and monitoring of aftershocks of moderate-magnitude earthquakes in the ISB have shown that they occurred on "blind faults" (faults that have not been mapped at the surface) at depths of 8-15 km. Therefore, we also consider a moderate-magnitude earthquake source, unrelated to mapped faults and without accompanying surface rupture, for all sites in the Regional study area. As the threshold for surface faulting in the ISB is within the magnitude range of 6 to 6 3/4, we have estimated an MCE of magnitude 6 1/2 for this potential source. Based on an analysis of the recurrence of moderate-magnitude earthquakes in the region, this MCE is considered a local event at any site in the back valleys. In the final chapter of the report, MCEs and appropriate epicentral distances are tabulated for fourteen existing and two proposed USBR dams in the study area, and the hazard posed by potential foundation displacements is discussed for each of the dams.

A statistical analysis of historical seismicity in the back valleys of the Wasatch Mountains, included as an appendix to this report, concludes that there is no evidence that RIS (reservoir induced seismicity) has occurred at any of the USBR reservoirs in the region.

ACKNOWLEDGEMENTS

We thank the Upper Colorado Region, in particular the Land Acquisitions Branch in Salt Lake City headed by Gib Davies, and the Bonneville Construction Office in Provo for their assistance in the investigations reported here. The Geology Division headed by Dennis R. Williams and the Materials Branch headed by Jerry Eller, provided the logistic support essential to the excavation, shoring, and restoration of backhoe trenches and soil test pits, often in challenging terrain. Bruce Bryant of the U.S. Geological Survey (Denver) provided us a draft copy of the SLC 1° x 2° sheet as well as helpful discussions of the geology of the area. Discussions with Walter Arabasz (University of Utah), Ron Bruhn (University of Utah), Don Currey (University of Utah), Tony Crone (USGS - Denver), and Bruce Kaliser (Utah Geological and Mineral Survey were also helpful. Lael Hardy (Soil Conservation Service, Coalville, Utah) provided a great deal of unpublished data. Rolf Kihl and Vance Holiday (INSTARR, University of Colorado) and the Soil Testing Laboratory, Colorado State University, provided detailed grain size, carbonate, and organic matter analyses of soil samples. Gifford Miller (INSTARR) provided amino acid analyses with the help of Dan Goter. We also thank all the landowners who allowed us access to their property, particularly Karl Jenson, Tremonton, Utah and Leland Kippen, Morgan, Utah for permission to excavate trenches on their land.

Ed Baltzer and Carol Krinsky were integral parts of the investigations reported in this study. Ed assisted in the geologic mapping, trench siting, and trench logging. In addition to providing assistance with the trench logging, Carol mapped Quaternary deposits along the Weber River and described soil profiles on the deposits. Both Ed and Carol helped formulate the interpretations of the trenches. Capable assistance in mapping and logging of trenches was also provided by Rebecca Stoneman and Karen Janowitz. Discussions with Dean Ostenaa and Lucy Foley were helpful throughout the study, particularly in interpreting the trenches in Morgan Valley and Keetley Valley.

CONTENTS

Section		Page
	SUMMARY	i
	ACKNOWLEDGEMENTS	iv
1.0	INTRODUCTION AND REGIONAL SETTING	1
1.1	Introduction	1
1.2	Late Mesozoic and early Cenozoic stratigraphy and structure	4
1.3	Late Cenozoic faulting	6
1.3.1	Basin and Range	6
1.3.2	Basin and Range transition zone	8
1.3.3	The back valleys of the Wasatch Mountains	9
2.0	SEISMOLOGY	10
2.1	Introduction	10
2.2	Seismicity of north-central Utah	13
2.2.1	The historical era: 1850-1962	13
2.2.2	The regional network era: 1962-1974	16
2.2.3	The local network era: 1974-present	18
2.3	The relationship between seismicity and subsurface structure	22
2.3.1	Focal depth distribution and the thermal-mechanical mode of deformation	22
2.3.2	The influence of structure on background seismicity	23
2.3.3	Focal depths of design earthquakes	24
2.4	The state of crustal stress	25
2.4.1	*In situ* stress measurements	25
2.4.2	Seismic estimates of crustal stress	27
2.4.3	Discussion of stress variations	30
2.5	An earthquake occurrence model for the ISB	32
2.5.1	Large-magnitude ISB earthquakes: Hebgen Lake and Borah Peak	32
2.5.2	Moderate-magnitude earthquakes in the ISB	34
2.5.3	Summary	35
2.6	Recurrence rates for moderate-magnitude earthquakes	37
2.6.1	Recurrence rates based on historic seismicity and geologic information	37
2.6.2	Probabilistic estimates of epicentral distance	40
2.7	Summary	42
3.0	QUATERNARY STRATIGRAPHY AND CHRONOLOGY	44
3.1	Introduction	44
3.2	Previous studies	45
3.2.1	The back valleys of the eastern Wasatch Mountains	45
3.2.1.1	The back valleys of the eastern Wasatch Mountains	45
3.2.1.2	Glaciation	47
3.2.2	Lake Bonneville	47
3.2.2.1	Morgan and Ogden Valleys	48
3.2.2.2	Cache Valley	48
3.2.3	Western Uinta Mountains	48
3.2.4	Bear River Range	49
3.3	Stratigraphic terminology	50

CONTENTS (cont.)

3.4 Relative and numerical dating 52
3.4.1 Soil profile relative-dating methods 52
3.4.1.1 Relative-dating methods 52
3.4.1.2 Indices of soil development 52
3.4.1.3 Relative age groups based on soil development in the eastern Wasatch Mountains 53
3.4.1.4 Rates of secondary carbonate and clay accumulation 55
3.4.2 Age estimates using amino acid-ratios 58
3.4.3 Relative dating using magnetic polarity of sediment . 61
3.4.3.1 Quaternary polarity stratigraphy 61
3.4.3.2 Polarity evaluation and age estimates 61
3.4.4 Other dating methods 61
3.4.4.1 Tephrochronology 61
3.4.4.2 Radiocarbon analysis 62
3.4.4.3 Fault and terrace scarp morphology 62
3.5 Quaternary history of Weber and Provo Rivers 65
3.5.1 Weber River drainage 65
3.5.1.1 Upper Weber River Valley 65
3.5.1.2 Central Weber River Valley 71
3.5.1.3 Lower Weber River Valley 74
3.5.2 Provo River drainage 74
3.5.2.1 Upper Provo River Valley 75
3.5.2.2 Heber Valley 81
3.5.2.3 Lower Provo River Valley 83
3.6 Summary of late Cenozoic geomorphic development of the eastern Wasatch Mountains 86
3.6.1 Late Tertiary and early Quaternary 86
3.6.1.1 Paleo-Weber drainage 87
3.6.1.2 Paleo-Provo drainage 87
3.6.2 Middle and late Quaternary 88
3.6.2.1 Weber River drainage 88
3.6.2.2 Provo River drainage 90
3.6.3 Neotectonic conclusions 92
3.6.3.1 Areas with the highest Quaternary Rates of relative uplift 92
3.6.3.2 Apparent sequence of basin development 93
3.6.3.3 Rates of incision along the Webewr River 93
3.6.3.4 Rates of incision along the Provo River 94
3.6.3.5 Relative rates of uplift on major faults 95

4.0 CENOZOIC FAULTING IN THE NORTHERN WASATCH MOUNTAINS 97
4.1 Setting 97
4.2 Morgan Valley 98
4.2.1 Setting 98
4.2.2 The Morgan fault 98
4.2.2.1 The northern section 102
4.2.2.2 The central section 103
4.2.2.3 The southern section 103
4.2.3 Age of Quaternary deposits adjacent to the central section of the Morgan fault 105

CONTENTS (cont.)

4.2.4 Trench investigations of Quaternary faulting on the central section of the Morgan fault 108
4.2.4.1 Stratigraphy in Trench M4 110
4.2.4.2 Stratigraphy in Trench M2U 112
4.2.4.3 Stratigraphy in Trench M1 113
4.2.4.4 Stratigraphy in Trench M2L 114
4.2.4.5 Stratigraphy in Trench M3 114
4.2.4.6 Ages of faulted deposits at the Robeson Springs trench site 115
4.2.4.7 Events in Trench M4 116
4.2.4.8 Stratigraphy in Trench M6 at the Mahogany Canyon trench site 116
4.2.5 Slip rates on the Morgan fault 119
4.2.5.1 Quaternary slip rates 119
4.2.5.2 Cenozoic slip rate 119
4.2.6 Conclusions 121
4.3 Southern Cache Valley region 122
4.3.1 Late Quaternary displacement on the East Cache fault . 122
4.3.2 The James Peak fault 124
4.3.2.1 Quaternary deposits in southern Cache Valley . . 125
4.3.2.2 Scarp and mountain front morphology 125
4.3.2.3 Age of faulted deposits 126
4.3.2.4 Fault displacement history 130
4.3.2.5 Slip rates and recurrence 134
4.3.2.6 Relationship with the East Cache fault 134
4.3.2.7 Conclusions 136
4.3.3 Faults in western Cache Valley 136
4.3.4 Faults in the Mantua area 137
4.3.5 Faults east and southeast of Cache Valley 138
4.3.5.1 Bear Lake faults 138
4.3.5.2 Bear River fault zone 139
4.3.5.3 Crawford Mountain fault 139
4.3.5.4 Faults in the Bear River Range 139
4.4 Ogden Valley 141
4.4.1 Faulting in Ogden Valley 141
4.4.1.1 Northeastern margin of Ogden Valley 143
4.4.1.2 Southwestern margin of Ogden Valley 145
4.4.2 Conclusions 148
4.5 East Canyon Area 149
4.5.1 Geologic setting 149
4.5.2 Quaternary deposits in the East Canyon area 149
4.5.3 The East Canyon fault 153
4.5.3.1 Southern segment of the East Canyon fault . . . 153
4.5.3.2 Northern segment of the East Canyon fault . . . 154
4.5.4 Central Weber River Valley 155
4.5.5 Conclusions 155

5.0 CENOZOIC FAULTING IN THE CENTRAL WASATCH MOUNTAINS 157
5.1 Tectonic setting 157
5.2 Tertiary igneous chronology of the central Wasatch Mountains 158
5.3 Back valleys of the central Wasatch Mountains 160

CONTENTS (cont.)

5.4 Parleys Park and Richardsons Flat 161
5.4.1 Geologic setting 161
5.4.2 Quaternary deposits 161
5.4.3 Age of faulting 165
5.5 Deer Valley 166
5.6 Keetley Valley 168
5.6.1 Geologic setting 168
5.6.1.1 Hawkeye-McHenry fault zone 168
5.6.1.2 Mayflower-Pearl fault zone 169
5.6.1.3 Cottonwood fault 169
5.6.2 Tertiary clastic deposits 170
5.6.3 Quaternary deposits 171
5.6.4 Faulting Keetley Valley 172
5.6.4.1 Bald Mountain fault 172
5.6.4.2 Other north-trending faults 173
5.6.5 Conclusions 173
5.7 Browns Canyon - Mountain Meadows 175
5.7.1 Mountain Meadows scarps 175
5.7.2 Trenching of the Mountain Meadows scarps 175
5.7.3 Conclusions 178
5.8 Kamas Valley 179
5.8.1 Geologic setting 179
5.8.2 Structure of Kamas Valley 179
5.8.2.1 East Kamas fault 181
5.8.2.2 West margin of Kamas Valley 182
5.8.3 South Flank fault 184
5.8.4 North Flank fault 184
5.8.5 Conclusions 185
5.9 Heber Valley 186
5.9.1 Geologic setting 186
5.9.2 Tectonic geomorphology 186
5.9.2.1 Northwestern margin 188
5.9.2.2 Northeastern margin 188
5.9.2.3 Southern margin 189
5.9.3 Trenching of the scarp at Big Hollow 189
5.9.4 Origin of Heber Valley 194
5.9.5 Conclusions 195

6.0 CENOZOIC FAULTING IN THE SOUTHERN WASATCH MOUNTAINS 196
6.1 Tectonic setting 196
6.2 Back Valleys of the southern Wasatch Mountains 197
6.3 Round Valley and Wallsburg Ridge 198
6.3.1 Geologic setting 198
6.3.2 Faulting in Round Valley 200
6.3.3 Trenching in Round Valley 201
6.3.4 Conclusions 201
6.4 Strawberry Valley 204
6.4.1 Geologic setting 204
6.4.2 Seismotectonic investigations 204
6.4.3 Conclusions 205
6.5 Diamond Fork area 206
6.5.1 Geologic setting 206

CONTENTS (cont.)

6.5.2 Little Diamond Creek fault 206
6.5.3 Sam's Canyon fault 207
6.5.4 Conclusions 207
6.6 Wasatch Plateau 209

7.0 CONCLUSIONS 210
7.1 Late Quaternary faulting in the back valleys of the Wasatch Mountains 210
7.2 Fault displacement models for the back valleys of the Wasatch Mountains 211
7.3 Earthquake sources in the ISB 212
7.4 Seismic sources and maximum credible earthquakes 213
7.4.1 Late Quaternary faults 213
7.4.1.1 Wasatch fault 213
7.4.1.2 The James Peak and East Cache faults 214
7.4.1.3 The Morgan fault 215
7.4.1.4 The Strawberry fault 216
7.4.1.5 Back valley faults in the northern and southern Wasatch Mountains 216
7.4.1.6 Back valley faults in the central Wasatch Mountains 216
7.4.2 Random earthquake 216
7.5 Maximum credible earthquakes and USBR dams 219
7.5.1 Newton Dam 219
7.5.2 Hyrum Dam 221
7.5.3 Causey Dam 224
7.5.4 Lost Creek Dam 226
7.5.5 Pineview Dam 227
7.5.6 Arthur V. Watkins Dam 229
7.5.7 East Canyon Dam 229
7.5.8 Echo Dam 231
7.5.9 Wanship Dam (Rockport Lake) 233
7.5.10 Jordanelle Damsite 234
7.5.11 Deer Creek Dam 235
7.5.12 Soldier Creek Dam 237
7.5.13 Monks Hollow damsite 238
7.5.14 Mona Dam 239
7.5.15 Joes Valley Dam 240
7.5.16 Scofield Dam 241
7.6 Reservoir-induced seismicity (summary) 243

8.0 REFERENCES 244

APPENDIX A: Probabilistic determination of epicentral distances

APPENDIX B: An analysis of reservoir-induced seismicity in the back valleys of the Wasatch Mountains

FIGURES

Figure		Page
1.1	Physiographic subdivisions of Utah	1
1.2	Late Cenozoic faults and physiographic provinces of the western United States	7
2.1	Index map of the Intermountain seismic belt	11
2.2	Epicenter map of north-central Utah, 1850 to June 1962	14
2.3	Epicenter map of north-central Utah, July 1962 through September 1974	17
2.4	Comparison of least principal stress direction determined by several methods	26
2.5	Schematic summary of fault-plane solutions (lower hemisphere projections) for the Wasatch front area	28
3.1	Soils indices graph for all soil profiles in the Regional study area with some independent age control	54
3.2	Total secondary clay content and estimated ages for soils with some independent age control in the Regional study area	57
3.3	Weber River terrace profiles	64
3.4	Rubification and non-arid profile indices for soils in the Weber River Valley, East Canyon area, and Parleys Park area	70
3.5	Provo River terrace profiles	76
3.6	Rubification and non-arid total profile indices for soils in the Provo River Valley, Kamas Valley, Heber Valley, and Round Valley	79
4.1	Geology of the northern Wasatch Mountains	99
4.2	Cenozoic geology map of Morgan Valley	100
4.3	Generalized topographic profiles and geologic sections parallel to the strike of the Morgan fault	101
4.4	Geologic map of the central section of the Morgan fault	104
4.5	Geologic map of the Mahogany Creek trench site	117
4.6	Log of the Mahogany Canyon trench (M6)	118
4.7	Geologic map of southern Cache Valley	123
4.8	Soil development indices for soils near the James Peak trench site and in Ogden Valley	128
4.9	Log of a trench across the James Peak fault	131
4.10	Geologic map of Ogden Valley	142
4.11	Geologic map and cross section of the East Canyon fault, including the East Canyon dam area	150
5.1	Geologic map of the central Wasatch Mountains	162
5.2	Geologic map of Parleys Park	163
5.3	Geologic map of Keetley Valley	167
5.4	Geologic map of Mountain Meadows	176
5.5	Log of a trench across the Mountain Meadows scarp	177
5.6	Geologic map of Kamas Valley	180
5.7	Geologic map of Heber Valley	187
5.8	Geologic map of the Big Hollow trench site	190
5.9	Log of a trench on the Big Hollow scarp	191
6.1	Geologic map of Round Valley	199
6.2	Log of the Round Valley trench	202
7.1	Geologic map of Newton Dam and Reservoir area	220
7.2	Geologic map of Hyrum Dam and Reservoir area	223
7.3	Geologic maps of Causey Dam and Lost Creek Dam areas	225

FIGURES (CONT.)

7.4 Geologic map of Ogden Valley including Pineview Dam and Reservoir 228
7.5 Geologic map and cross section of the East Canyon fault, including East Canyon Dam area 230
7.6 Geologic maps of Echo Dam (A) and Wanship Dam (B) areas . . . 232
7.7 Geologic map of the Deer Creek Dam area 237

TABLES

table		page
2.1	Completeness periods for north-central Utah	38
2.2	Return periods for larger earthquakes in north-central Utah	38
2.3	Return periods for moderate earthquakes in north-central Utah	39
2.4	Rate of occurrence per unit area for magnitude 6-plus earthquakes in the Wasatch front and Wasatch fault areas . . .	40
2.5	Probabilistic epicentral distances for magnitude 6-plus earthquakes in the study area	41
3.1	D-alloisoleucine/L-isoleucine ratios in the total (free + peptide-bound) amino-acid fraction and calculated ages for fossil gastropods from alluvial and colluvial sediments along the Weber and Provo River Valleys, Utah	59
3.2	Selected properties of soils on fan and terrace remnants along the Weber River, north-central Utah	67
3.3	Selected properties of soils on fan and terrace remnants along the Provo River, north-central Utah	77
4.1	Selected properties of soils on alluvial, colluvial, and lacustrine sediments along the Morgan fault, Morgan Valley, north-central Utah	106
4.2	D-alloisoleucine/L-isoleucine ratios in the total (free + peptide bound) amino-acid fraction and calculated ages for *Oreohelix cf. strigosa* from alluvial and colluvial sediments along the Morgan fault, Morgan Valley, Utah	109
4.3	Selected properties of soils on the north flank of James Peak, north-central Utah	129
4.4	Selected properties of soils on alluvial fan sediments in Ogden Valley, north-central Utah	144
4.5	Selected properties of soils on alluvial fans along East Canyon Creek, north-central Utah	152
5.1	Selected properties of soils on terraces and moraines in the Park City - Richardson Flat area, north-central Utah	164
5.2	K-Ar dates for intrusives near Jordanelle	170
5.3	Selected properties of soils on alluvial fans in Kamas and Round Valleys, north-central Utah	183
5.4	Heber Valley soils	193
7.1	Average late Quaternary displacement parameters for individual segments of the Wasatch fault	214
7.2	Average displacement paramters and maximum credible earthquakes for late Quaternary faults in the back valleys of the Wasatch Mountains	217

TABLES (cont.)

7.3 Maximum credible earthquakes for Newton Dam 221
7.4 Maximum credible earthquakes for Hyrum Dam 222
7.5 Maximum credible earthquakes for Causey Dam 224
7.6 Maximum credible earthquakes for Lost Creek Dam 226
7.7 Maximum credible earthquakes for Pineview Dam 229
7.8 Maximum credible earthquakes for Arthur V. Watkins Dam 227
7.9 Maximum credible earthquakes for East Canyon Dam 231
7.10 Maximum credible earthquakes for Echo Dam 233
7.11 Maximum credible earthquakes for Wanship Dam (Rockport Lake) . 234
7.12 Maximum credible earthquakes for Jordanelle Damsite 235
7.13 Maximum credible earthquakes for Deer Creek Dam 236
7.14 Maximum credible earthquakes for Soldier Creek Dam 238
7.15 Maximum credible earthquakes for Monks Hollow Damsite 239
7.16 Maximum credible earthquakes for Mona Dam 240
7.17 Maximum credible earthquakes for Joes Valley Dam 241
7.18 Maximum credible earthquakes for Scofield Dam 242

PLATES
(in back cover pocket)

Plate

1A Seismicity, October, 1974 - March, 1986, and Cenozoic Faults in the northern Wasatch Front
1B Seismicity, October, 1974 - March, 1986, and Cenozoic Faults in the central Wasatch Front
1C Seismicity, October, 1974 - March, 1986, and Cenozoic Faults in the southern Wasatch Front
2 Trench Logs and Site Map for the Robeson Springs Trench Site, Morgan Valley, Utah

1. INTRODUCTION AND REGIONAL SETTING

1.1 Introduction

This report presents the results of a seismotectonic study for a portion of central Utah prepared by the Seismotectonic Section, Engineering and Research Center, USBR (U.S. Bureau of Reclamation). The Regional Study area includes the back valleys of the Wasatch Mountains between the Idaho-Wyoming thrustbelt to the north, the focus of a USBR Seismotectonic Study for Palisades Dam (Piety and others, 1986) and the Wasatch Plateau to the south, the focus of a USBR Seismotectonic Study for Joes Valley and Scofield Dams (Foley and others, 1986) (fig. 1.1). The report reviews current geological and seismological data, evaluates current models of earthquake occurrence, and applies these models to a regional and site-specific characterization of earthquake hazards by identifying earthquake sources and associated Maximum Credible Earthquakes (MCEs). The report supersedes the previous Draft Report (Sullivan and others, 1983). Within this part of the USBR Upper Colorado region there are 11 existing USBR dams, and 2 proposed dam sites (pls. 1a and 1b).

Within the area of this Regional Study the Strawberry (Nelson and Van Arsdale, 1986), East Cache (Cluff and others, 1974; Swan and others, 1983) and the Bear Lake faults (Williams, 1962) are the only faults east of the Wasatch fault with recognized late Quaternary (< 125 ka) displacements on the Quaternary fault compilations of Nakata and others (1982) and Anderson and Miller (1979). Present day seismicity in this portion of the Intermountain Seismic Belt (ISB) is concentrated in a diffuse band extending from north to south through the area, but shows little correlation with specific geologic structures. However, within this portion of the Basin and Range transition zone both single event and composite fault plane solutions, and drillhole hydrofracture measurements suggest contemporary stress release is occurring on north-trending normal faults. The physiography of the back valleys of the Wasatch Mountains suggests to us, as it did to Gilbert (1928), that development of the valleys through normal faulting has continued during the Quaternary (Sullivan and Nelson, 1983), and in some valleys during the late Quaternary.

Our emphasis in this investigation is on the evidence for recurrent late Quaternary surface displacements on specific faults in the study area. Most of these faults are found or are inferred on the margins of the back valleys of the Wasatch Mountains which are the youngest structural elements in the region and are expressed topographically as linear bedrock escarpments. These faults share many characteristics with normal faults in the Basin and Range province to the west; most are range-bounding faults that have localized the deposition of unconsolidated deposits in basins in the hanging walls of the faults. The aggregate thickness and age of these deposits are interpreted to be related to the displacement history of the faults. In general, the thickness of the unconsolidated deposits in the back valleys is significantly less than that in the larger basins west of the Wasatch fault suggesting lower slip rates on back valley faults. However, Wallace (1984) has discussed significant variation in late Quaternary slip rates on late Cenozoic faults in the Basin and Range Province and has suggested that fault activity has been episodic throughout the late Cenozoic. Thus, obtaining specific data on slip rates on late Cenozoic faults in the Regional study

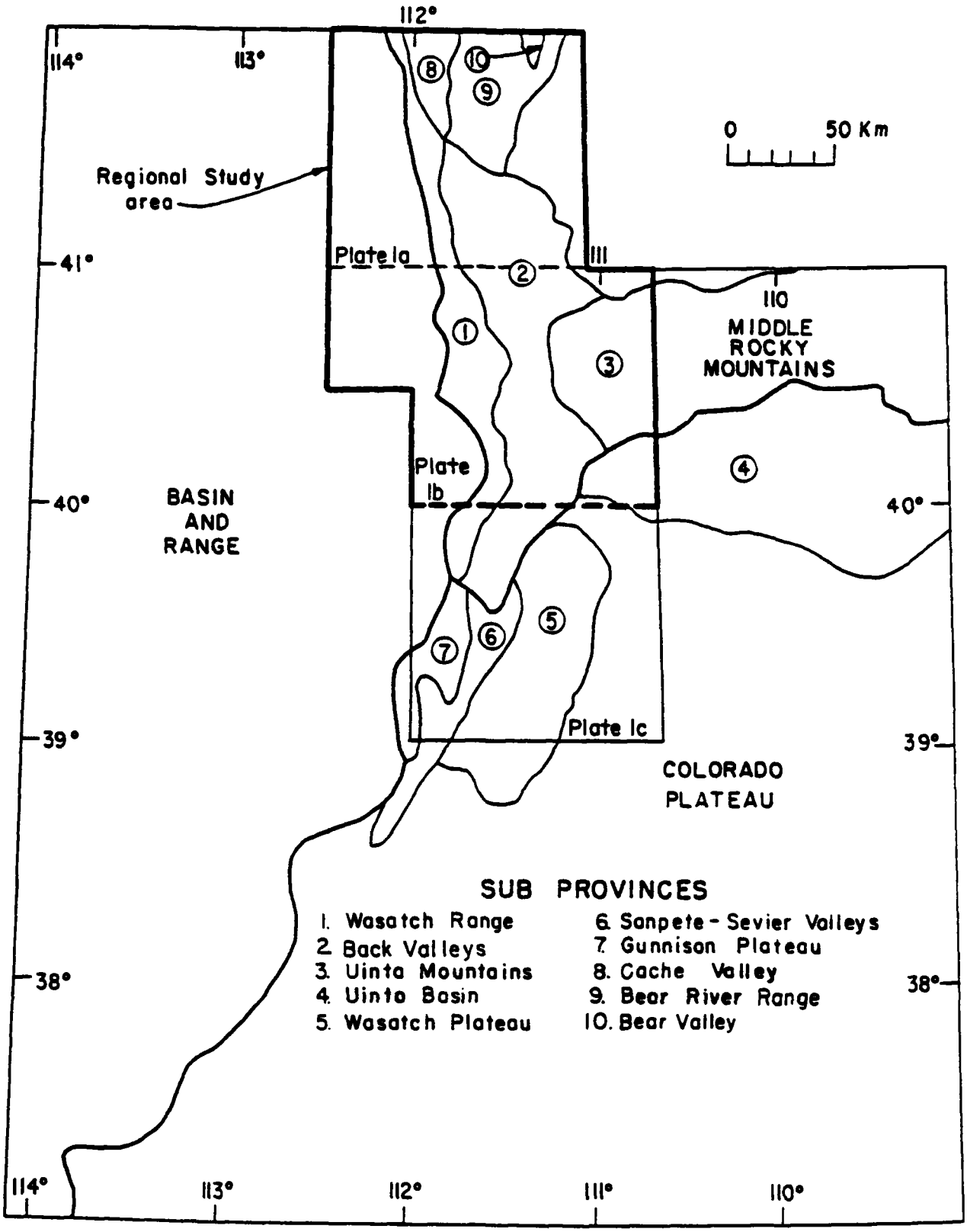


Figure 1.1 Physiographic subdivisions of Utah.

area was our goal.

A close causal relationship has been established between the occurrence of historical earthquakes with associated surface displacements and faults with a history of recurrent late Quaternary surface displacements. The principal method used to recognize such faults is by identifying fault scarps in late Quaternary deposits. However, within area of this study determining the age of most recent displacement for many of the faults has proven to be difficult. While no scarps in unconsolidated deposits are associated with most of the faults, the deposits overlying or in the vicinity of the faults are mostly too young (<15 ka) to provide useful data for faults with recurrence intervals for surface displacements of 10-50 ka, the range we infer in this region. Late Cenozoic uplift of the Wasatch Mountains, primarily related to displacement on the Wasatch fault, has resulted in deep erosion and the removal of late Quaternary deposits from the vicinity of many of the faults. We have identified faults in the region with displaced late Quaternary datums and have relied in part on a qualitative comparison of geomorphic features to draw conclusions for other faults in the region. These geomorphic parameters include the linearity of late Cenozoic fault traces and the height and steepness of triangular facets on the footwalls of late Cenozoic range-bounding faults.

Our reconnaisance study of the neotectonics of the eastern Wasatch Mountains focused on mapped and inferred Quaternary faults bounding the back valleys east of the Wasatch fault (fig. 1.1). Although some faults were mapped previously, most are inferred from our geomorphic interpretation of 1:58,000 scale color IR photography of the whole area and 1:15,000 to 1:40,000 scale BW photography of selected areas. Various investigators have discussed the value of low-sunangle air photos in the identification of late Quaternary faults scarps (for example, Cluff and others, 1970; 1974). As low-sunangle airphotos are only available for the Wasatch fault, we undertook a series of three morning and afternoon low-sun angle overflights of each valley in a fixed-wing aircraft. We reviewed 35 mm photographs of each valley margin taken during the low-sunangle overflights. These overflights and photos revealed possible Quaternary fault-related features in several area all of which were investigated in more detail on the ground.

Mapping and relative dating of Quaternary deposits within most of the back valleys along with our complilations of water well logs (Utah State Engineers Office) and unpublished soils data (Soil Conservation Service) support our concept of continuing Basin and Range style deformation within the region, but with low Quaternary fault slip rates. This work is also the basis of our summary of the geomorphic history of the Provo River and Weber River drainage basins (sec. 3.6), which also argues for relatively low rates of deformation. Finally, mapping and exploratory trenching of scarps at several sites provides our only detailed data on individual fault slip rates, and surface displacement event size and recurrence. We use our conclusions from these selected trenching sites to estimate these parameters for other faults in the study area.

1.2 Late Mesozoic and early Cenozoic stratigraphy and structure

On the western margin of the North American craton in central Utah, marine carbonate and clastic deposition continued without major interruption from the Precambrian into the Jurassic. Two sedimentary sequences developed: a platform sequence in eastern Utah where Paleozoic carbonate and clastic rocks are 1500 m (5000 ft) to 3000 m (10000 ft) thick, and a thicker miogeoclinal sequence in western Utah where correlative rocks are 7500 m (25000 ft) to 10000 m (35000 ft) thick (Burchfiel and Davis, 1972). Lower Mesozoic rocks thicken westward in a similar fashion. The hingeline or transition between these two sequences has been obscured by subsequent deformation, but it nearly corresponds with the eastern margin of late Cenozoic extensional deformation. Isopachs of Cretaceous rocks indicate a marked change in sedimentary patterns following deposition of the Jurassic Morrison Formation. A wedge of clastic strata that thickens from 1800 m (6000 ft) in eastern Utah to 5000 m (16000 ft) in central Utah and abruptly thins out in west-central Utah indicates a western orogenic source (Burchfiel and Hickcox, 1972).

During the late Jurassic to Eocene Sevier Orogeny, the miogeoclinal sequence was thrust many tens of kilometers eastward onto the platform on stacks of imbricate thrust faults (Armstrong and Oriel, 1965). The main features of this thin-skinned deformation, as originally described from the Canadian fold and thrust belt, are the accommadation of displacement on near horizontal, bedding plane faults in incompetent rocks above a basal decollement near the top of crystalline basement, and ramps or higher angle faults that step upsection to the east in competent strata (Dahlstrom, 1970; Royse and others, 1975; Boyer and Elliot, 1982). North of the Uinta Mountains in the Idaho-Wyoming Thrustbelt four major thrust plates have been identified: the Darby, Absoraka, Meade, and Willard-Paris from east to west and youngest to oldest (Armstrong and Oriel, 1965; Royse and others, 1975; Blackstone, 1977; Woodward, 1981; Wiltschko and Dorr, 1982; Dixon, 1982). Although studied in less detail south of the Uinta Mountains, the Charleston, Nebo, and Strawberry thrusts are mapped as the easternmost major thrusts (Eardley, 1944; Bissel 1952; Baker, 1976). Six younger thrusts above the Charleston-Nebo decollement to the west are described by Morris (1983).

Late Cretaceous to Eocene age Laramide deformation contrasts in setting, timing, and style with Sevier deformation. The Laramide mountain blocks of the Rocky Mountains occur east of the leading edge of the Cordilleran Thrustbelt in Wyoming, Utah, and Colorado and overlap only in a few localities. Although orogeny was continuous in the Rocky Mountains through the Cretaceous and Paleogene, Armstrong and Oriel (1965) conclude that major Sevier age deformation occurred in the Cretaceous while major Laramide deformation occurred in the Paleogene. The structure of Laramide mountain blocks is characterized by basement involved, steeply- or shallow-dipping, reverse and thrust faults such as the 30°- 35° dipping Wind River Thrust which can be traced on reflection profiles to a depth of at least 24 km and has an estimated minimum shortening of 21 km (Brewer and others, 1980). Within the study area the east-west trending Uinta anticline had previously been considered a Laramide structure, and is bounded both on the north and south by mountainward dipping reverse faults that developed during the late Cretaceous to Eocene (Campbell, 1975; Ritzma, 1969; Hansen, 1983).

Non-marine clastic deposition of alluvial fan and fluvial facies eroded from

the eastward migrating thrust sheets began in the Cretaceous in central Utah and continued into the Eocene (Nelson, 1971; Mann, 1974). Within the northern Wasatch Mountains parts of the Frontier Formation are related to the Paris-Willard thrust, the late Cretaceous Echo Canyon Formation is related to the Crawford-Meade thrusts, and the early Tertiary Evanston Formation is related to the Absoraka thrust (Armstrong and Oriel, 1965; Wiltschko and Dorr, 1982). The generally flat-lying Eocene Wasatch Formation is the most extensive early Cenozoic deposit in the northern Wasatch Mountains. It appears to have been deposited as a continuous blanket of alluvial fan and fluvial sediment that overlies the synorgenic conglomerates and Paleozoic and Mesozoic rocks with marked angular unconformity in most areas, and it has subsequently been deformed in Cenozoic structural basins. In the central Wasatch Mountains the Wasatch formation had been removed during the early Tertiary and the Keetley volcanics overlie Mesozoic and Paleozoic sedimentary rocks.

In the southern Wasatch Mountains, Mann (1974) suggests that the late Cretaceous Price River Formation and the late Cretaceous and early Tertiary Currant Creek and North Horn Formations are related to the emplacement of the Charleston and Nebo Thrust plates. These are overlain by the Wasatch, Green River and Uinta Formations that thicken eastward into the Uinta basin.

1.3 Late Cenozoic faulting

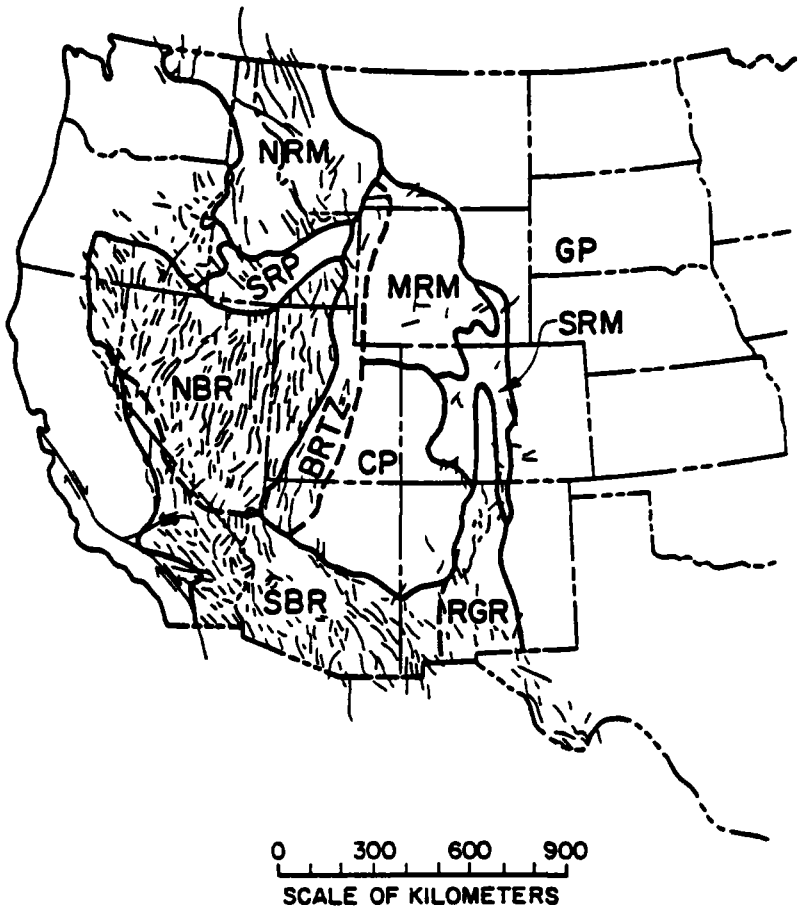
Here we review late Cenozoic deformation in the Basin and Range and the transition zone with the Colorado Plateau and the Middle Rocky Mountains on its eastern margin (fig. 1.2). Historic surface faulting and the surface expression of late Quaternary (last 125 ka) normal faulting in the transition zone suggest deformation related to crustal extension as in the Basin and Range. However, recent interpretations of normal fault geometries and their relationship to the structural fabric inherited from Mesozoic and Early Cenozoic deformation suggest some differences in the styles of Late Cenozoic deformation in the two regions.

1.3.1 Basin and Range

The mid and late Cenozoic evolution of the western Cordillera, east of the Sierra Nevada Mountains has been dominated by extensional deformation as evidenced by physiography, late Cenozoic fault patterns, and surface faulting associated with historic earthquakes. The Basin and Range physiographic province, including the surrounding transition areas with similar geological and geophysical characteristics, occupies an area of more than one million square kilometers (Eaton, 1982) (fig. 1.2). The Basin and Range province consists of a series of generally north-trending linear mountain blocks, typically 15 to 20 kilometers in width, separated by structural basins of similar width. The ranges consist of tilted and faulted Tertiary volcanic rocks and older igneous and sedimentary rocks which are separated by normal faults, on one or both margins, from valleys filled with late Tertiary sediment. The resulting structural relief of individual range-basin pairs is estimated to vary from 2000 to 5000 m (Stewart, 1978). The relative scarcity of sedimentary basin fill deposits older than 17 to 18 Ma and the occurrence of numerous sheetlike ash flow tuffs of early Neogene age (25 to 20 Ma) deposited across areas of little relief (Christiansen and McKee, 1978) indicate that this more recent phase of Basin and Range faulting dates from about 17 m.y. ago.

The Basin and Range exhibits characteristics that are similar to those of continental rift zones in which crustal extension is the fundamental mechanism of deformation. Recent papers by Stewart (1978), Eaton (1982), Zoback and others (1981), and Zoback (1983) discuss a basin-range topography of linear, fault-bounded ranges separated by graben valleys controlled by late Cenozoic normal faults as only one characteristic which distinguishes this region from surrounding areas. Others include: high heat flow, thin lithosphere, the occurrence of low seismic velocities in the underlying upper mantle, a history of long-lived episodic magmatism, and a pronounced crustal low velocity layer (Eaton 1982).

Two general models of Basin and Range faulting have been proposed: 1) a listric fault model, in which normal faults flatten with depth and sole into a near horizontal detachment at depths of 5 to 17 km (e.g. Anderson, 1971; Proffet, 1971; Effimoff and Pinezich, 1981), and 2) a horst and graben model, in which planar, high-angle normal faults are terminated by a low-angle normal fault (e.g. Wernicke, 1981; Anderson and others, 1983) or root in a mid-crustal zone of intrusion or plastic flow (Eaton, 1982; Stewart, 1971; 1978). Interpretation of seismic reflection profiles in the Sevier desert in south-central Utah (MacDonald, 1976; Allmendinger and others, 1983; Anderson



Late Cenozoic extensional faults from Stewart (1978)

Physiographic province boundaries from Stewart (1978)

Sub-province boundaries

Figure I.2 Late Cenozoic faults and physiographic provinces of the western United States. Provinces and sub-provinces are: NRM, Northern Rocky Mountains; MRM, Middle Rocky Mountains; SRM, Southern Rocky Mountains; SRP, Snake River Plain; CP, Colorado Plateau; NBR, Northern Basin and Range: SBR, Southern Basin and Range; BRTZ, Basin and Range Transition Zone; RGR, Rio Grande Rift.

and others, 1983) has suggested the presence of a low-angle detachment in that portion of the Basin and Range that terminates planar, high-angle normal faults. One such high-angle fault truncated by this detachment is on the east side of the Cricket Mountains. This fault has a minimum of 187 m of late Cenozoic displacement and a 2-m-high scarp, thought to be of Holocene age (Crone and Harding, 1984). These authors conclude that Holocene surface displacements probably have occurred in response to movement on the low-angle detachment and suggest that if low angle normal faults can store and release strain energy the most intense ground shaking associated with a large-magnitude earthquake may be located many kilometers from the surface displacements.

1.3.2 Basin and Range Transition Zone

The Basin and Range transition zone refers to a transition in geologic structure and crustal thickness, delineated by contemporary seismicity of the ISB, that occurs over a distance of up to 100 km east of the eastern margin of the Basin and Range (fig. 1.2). The Regional Study Area includes part of the transition zone in central Utah between the Wasatch fault and the relatively stable Colorado Plateau and Middle Rocky Mountains Provinces on the east. As a result of profound, generally east-west oriented extension in western North America, crustal thickness varies from 15-20 km in the Basin and Range to 40 km further east (Keller and others, 1975) with related higher heat flow in the Basin and Range (Bodell and Chapman, 1982). Both contemporary stress indicators and earthquake focal mechanisms indicate a change from east-west extension in the Basin and Range to compression in the Colorado Plateau (Zoback and Zoback, 1980). Recent studies have better defined the location of this change in the direction and magnitude of least principal stresses both in the Uinta basin (Martin and others, 1985) and on the Wasatch Plateau (McKee and Arabasz, 1983; Arabasz and Julander, 1986). Recent hydrofracture studies at two locations within the transition zone have also shown that the region is characterized by east-west and northeast-southwest least principal stresses (Haimson, 1984).

This transition zone is also manifested in regional topography. Average elevations of closed basins in the eastern Basin and Range vary from 4000-5000 ft and the basins are separated by tilted range blocks about 30 km apart. These basins typically have 1000 to 1500 m of late Cenozoic basin fill and are bounded by normal faults on one or both sides with estimated displacements of 2 to 5 km (Stewart, 1978). In contrast to the closed basins in the Great Basin, the transition zone in central and southern Utah is an upland surface disrupted by north and northwest trending structural basins with floors at elevations of 6000-8000 ft that are incised by west-flowing drainages. In northern Utah, Wyoming, and Idaho the transition zone is not as well defined topographically; as displacement diminishes to the north on the Wasatch fault, a clear physiographic boundary between the Basin and Range and the Middle Rocky Mountains is not present.

The ISB and the Basin and Range transition zone are coincident with the foreland of the Sevier Thrust Belt where geophysical data generated for oil and gas exploration, locally detailed surface mapping, and seismologic investigations indicate a complex interaction between late Cretaceous and early Tertiary thrust faults and younger normal faults. In the Idaho-Wyoming Thrustbelt portion of the Basin and Range transition zone, seismic reflection

record sections delineate a well-defined reflector in lower Paleozoic rocks near the top of crystalline basement. On the records this reflector appears undeformed, although normal faults localizing the deposition of as much as 3 km of late Cenozoic basin fill are evident above this reflector on the sections. Fault scarps as much as 10 m high in latest Quaternary deposits are mapped along one of these normal faults, the Star Valley fault (Piety and others, 1986), and late Quaternary displacements are inferred on others (Witkind, 1975a; 1975b). On the basis of the reflection data, late Cenozoic normal faults in the Thrustbelt have been interpreted as listric faults that shallow in dip with depth to join a near horizontal thrust faults in the subsurface (Royse, 1975; 1983; Dixon, 1982). Late Cenozoic displacements of more than 3 km on individual normal faults are interpreted to have been accommodated by a reversal of the original sense of displacement on these formerly east-directed thrust faults that root in the basement tens of km to the west.

1.3.3 The Back Valleys of the Wasatch Mountains

The back valleys of the Wasatch Mountains, as originally described by Gilbert (1928), refer to structural and topographic basins in the Wasatch Mountains including Ogden Valley, Morgan Valley, Kamas Valley (Rhodes Valley), and Heber Valley (Plates 1a and 1b). The structural basins of Cache Valley and the Bear Lake to the north and Strawberry Valley and Little Diamond Creek Valley to the south are also located within the transition zone and are discussed in this report.

The back valleys of the Wasatch Mountains have developed in a diverse geologic terrain bearing the imprint of late Mesozoic and early Cenozoic compressional deformation, Oligocene intrusion and volcanism, and subsequent Basin and Range style extensional deformation. The back valleys of the Wasatch Mountains are similar to basins in the Basin and Range in that they are structural and topographic basins, localizing the deposition of Tertiary and Quaternary sediment. However there are some differences: (1) in some back valleys unconsolidated deposits are thinner, based on modeling of residual Bouguer gravity anomalies (Stewart, 1958; Quitzau, 1961; Peterson, 1970) and water well drilling (discussed in secs. 4.0, 5.0 and 6.0), (2) bounding normal faults have shorter strike lengths in the back valleys; and (3) as a result of late Cenozoic uplift of the Wasatch Mountains, the back valleys are drained by west-flowing streams in contrast to the closed basins that have formed in the Basin and Range.

2.0 SEISMOLOGY

2.1 Introduction

The CUP study area occupies the central, north-south-trending portion of the Intermountain seismic belt, or ISB. The ISB is a 100-km-wide, 1300-km-long zone of active seismicity that extends from northwestern Arizona north through Utah, western Wyoming, and eastern Idaho, and terminates in northwestern Montana (fig. 2.1). It is sometimes defined to include an easterly trending zone of seismicity north of the Snake River Plain which extends into central Idaho.

The ISB marks the eastern margin of a broad zone of late Cenozoic extensional deformation in the western United States (sec. 3.1). In the study area it is roughly coincident with the boundary between the Basin and Range to the west, and the Colorado Plateau and Middle Rocky Mountains provinces to the east. Normal faulting due to general east-west extension predominates in the region, although strike-slip and thrust faulting have been observed in localized areas. Earthquakes occur in the ISB at relatively low rates when compared to plate margins. Low strain rates (10^{-8} to 10^{-9} per year) are indicated from moment release calculations using contemporary seismicity, and from examination of late Quaternary faulting (e.g., Doser, 1980; Greensfelder and others, 1980; Doser and Smith, 1982).

Commonly observed features of earthquake occurrence within the ISB have been described by Smith and Sbar (1974), Smith (1978), and Arabasz and Smith (1981), and will be briefly reviewed. Among these features are: 1) diffuse seismicity which shows only general correlation with locations exhibiting late Quaternary surface faulting; 2) an apparent lack of correlation between small to moderate earthquakes and surficial faults or other geologic structures; 3) shallow focal depths (less than 15 to 20 km); 4) sporadic occurrence of earthquakes both spatially and temporally; and 5) a persistent pattern of normal faulting indicating predominantly east-west extension.

Historic seismicity and the late Quaternary geologic record both indicate that moderate to large magnitude earthquakes occur infrequently; since the 1880's there have been only two events with magnitude greater than 7 and roughly twenty events with magnitude greater than 6 within the entire ISB (Coffman and others, 1982; NOAA, 1985). Return periods of large magnitude earthquakes (7 or greater) for active faults, as determined from the late Quaternary geologic record, are typically on the order of one to ten thousand years or greater (Arabasz and Smith, 1981; Wallace, 1981; Doser and Smith, 1983). Magnitude 6+ events are more frequent, and have occurred since the 1880's at an average rate of roughly once every five years for the entire ISB (Coffman and others, 1982; NOAA, 1985).

The dominant geologic structure within the study area, the Wasatch fault, trends north-south for 370 km and is expressed topographically as the impressive Wasatch Front. While the Wasatch Front marks the physiographic boundary of the Basin and Range, the presence of north-south trending valleys to the east (termed the back valleys) indicates that east-west extension has also occurred east of the Wasatch fault (see sec. 3.2). Although the fault is included in the western portion of the ISB within the study area, very little, if any, seismic activity has been directly associated with it. The

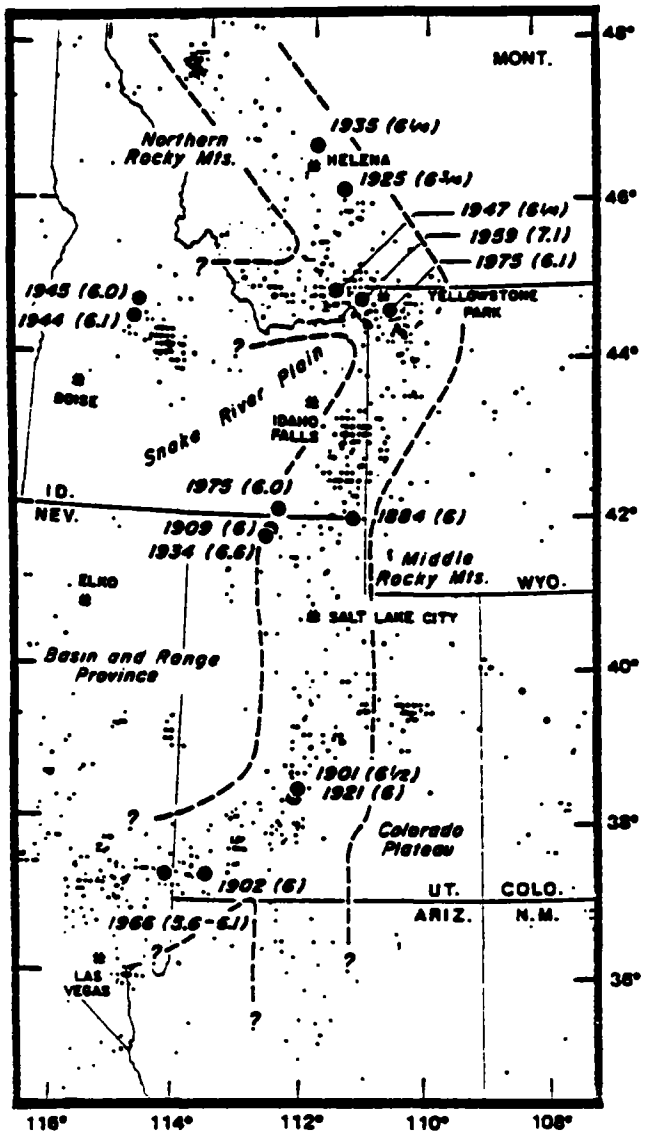


Figure 2.1 Index map of the Intermountain seismic belt. Epicenters of historical mainshocks ($M \geq 6$) shown as large circles, NOAA epicenters through 1974 as smaller circles. From Arabasz and Smith (1981).

largest earthquake in the historical record of the study area, the M_L 6.6 Hansel Valley event of 1934, occurred about 50 km west of the Wasatch fault, and is the only one for which surface displacement has been documented.

Detailed observations of earthquakes occurring within the ISB suggest a complicated relationship between contemporary tectonic processes and regional seismicity patterns. The precise mechanisms are poorly understood, though several tectonic models have been presented. Contemporary seismicity has been related to a complex interaction among subplates of the North American plate (Atwater, 1970; Suppe and others, 1975; Smith, 1977; 1978). The resulting stress field is superposed on Laramide thrust faults, which further modifies an already complicated deformation process.

In this section the seismological characteristics of the CUP study area will be discussed in light of the potential earthquake hazards of the region. Section 2.2 presents and describes the historical seismicity of the study area, and section 2.3 describes current thought on relationships between the seismicity and subsurface structures. Section 2.4 discusses the state of crustal stress from seismological and *in situ* techniques, and section 2.5 describes what we consider to be an appropriate earthquake occurrence model for the Intermountain seismic belt and the CUP study area. Section 2.6 presents the results of studies of earthquake recurrence and seismic moment rates within the area of interest, and finally, the major findings are summarized in section 2.7.

2.2 Seismicity of North-Central Utah

In this section, the historic record of seismicity occurring within the study area will be presented, described, and discussed. The data sources for the epicentral plots are the University of Utah earthquake catalog and previously published figures of University of Utah origin. Descriptions of the larger, more significant earthquakes will be presented, along with those for which special field studies were conducted. Finally, the entire historic seismicity record and how it relates to the regional evaluation of seismic hazards will be discussed.

Because of several distinct changes in detection and recording capabilities that have occurred in this region through time, the historic record has been divided into three periods. The Historical Era covers the period 1850-1962, when earthquakes were located largely on the basis of felt reports and sometimes with the aid of a small number of widely spaced, low magnification seismographs scattered throughout the western United States. The Regional Network Era, 1962-1974, covers a period when several independently recorded, higher magnification seismograph stations were established in the state of Utah. The Local Network Era covers the period 1974-1986, corresponding to the time when dense networks of high magnification, radio telemetered instruments were established throughout the region. The following discussions will be grouped according to these three time periods. Estimates of location accuracies and detection thresholds will also be made.

2.2.1 The Historical Era: 1850-1962

The written record of earthquake occurrence in Utah begins with the entrance of Mormon settlers into the region in 1847. In a fortunate historical coincidence (from the standpoint of documenting historical seismicity), the geographical development of human settlement has followed the trend of the ISB. Although a seismograph was established in Salt Lake City in 1907, this instrument operated at a very low magnification, and many of the seismograms have been lost or misplaced (Arabasz, 1979). The station was therefore of little use in locating earthquakes occurring in the regional study area. The earthquake record from 1850 through 1949 relies almost exclusively on felt reports compiled and documented by Williams and Tapper (1953). By 1950 the U.S. Coast and Geodetic Survey had established a sufficient number of seismograph stations in the western United States to allow the routine location of earthquakes of magnitude 3 or greater in the Rocky Mountain region. Although this network represented a vast improvement over previous recording conditions, the location of earthquakes from felt reports continued to be an important aspect of catalog compilation until about 1962 (Arabasz, 1979). It is estimated that the historic record within the study area is complete for events of magnitude 6.3 and above since 1850, magnitude 5.7 and above since 1880, magnitude 5.0 and above since 1940, and magnitude 4.3 and above since 1950 (Arabasz and others, 1980). Location accuracies vary greatly within the entire time period, and are difficult to judge. Early events based on felt reports are usually placed at the town reporting the effects, and may be in error in maximum intensity as well as location. Accuracies of instrumentally located earthquakes would be difficult to estimate without examining the individual solutions, but are probably on the order of 5 to 20 km.

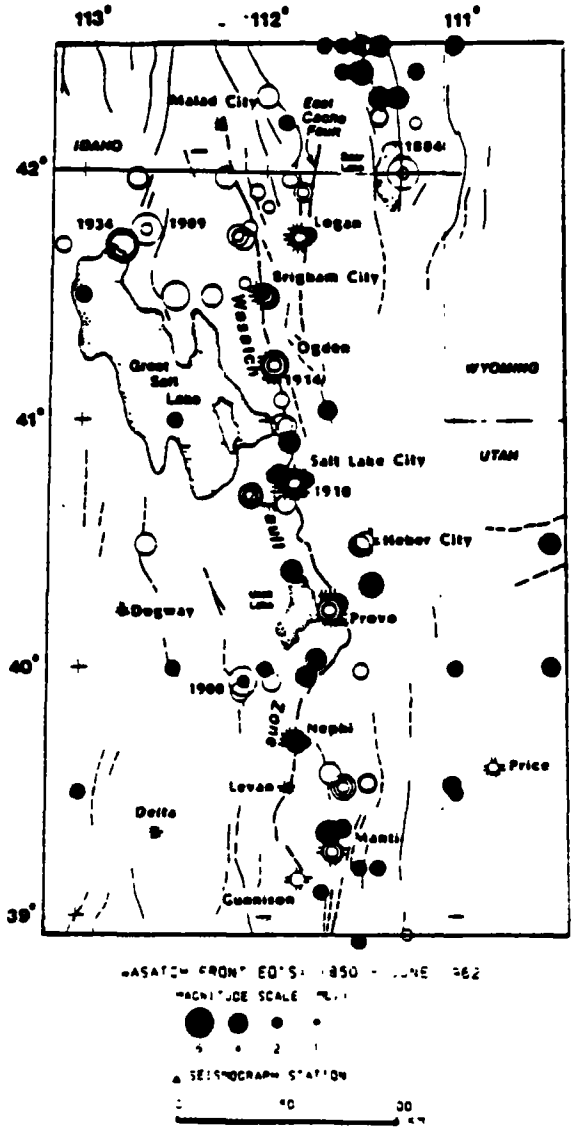


Figure 2.2 Epicenter map of north-central Utah, 1850 to June 1962. Locations of 1850 to 1949 earthquakes shown as open circles, those for 1950 to 1962 as solid circles. Young faults shown for reference. Significant events labelled by year. From Arabasz and others (1980).

Epicenters from the 1850-1962 period are shown in figure 2.2. This figure has been reproduced from Arabasz and others (1980), and relies chiefly on seismicity documented by Williams and Tapper (1953) and Cook and Smith (1967). The open circles are from the period 1850-1949, and represent locations based primarily on felt reports. The solid circles represent primarily instrumental locations from the period 1950 through June, 1962.

Earthquakes of intensity VII or greater are labelled in figure 2.2, and are described briefly below. Most of the magnitudes of events in the 1850-1949 period were determined from intensity data by Williams and Tapper (1953); magnitudes for earthquakes in the 1950-1962 period are generally instrumentally determined and were taken from U.S. Coast and Geodetic Survey publications. All intensities are in Modified Mercalli (MM) units.

1884, November 10, M 6. This event occurred at Bear Lake Valley, near the Idaho-Utah border. Originally associated with the Crawford Mountain fault (Williams and Tapper, 1953), Arabasz and others (1980) infer a location within Bear Lake Valley. Intensity VIII effects were reported in the epicentral area; intensity V was reported in Salt Lake City.

1900, August 1, M 5 1/2. Called the Eureka earthquake (seen about 50 km southwest of Provo in fig. 2.2), this event caused intensity VII effects in the epicentral area.

1909, October 5, M 6. The first large Hansel Valley earthquake, seen at the north end of the Great Salt Lake. Intensity IX effects were noted in the epicentral area, and the earthquake was felt over an area of 30,000 square miles (78,000 km^2) (Williams and Tapper, 1953).

1910, May 22, M 5 1/2. Near Salt Lake City; VII-VIII effects were reported in that city.

1914, May 13, M 5 1/2. Near Ogden; felt over an area of 8,000 square miles (21,000 km^2). Intensity VI effects were noted in Ogden; V-VI in Salt Lake City.

1934, March 12, M_S 6.6 and 6.0. The second large Hansel Valley event (also called the Kosmo earthquake) was felt over an area of 170,000 square miles (440,000 km^2). Intensity VII effects were reported in the epicentral area; intensity VI at Salt Lake City (Neumann, 1936; Coffman and Von Hake, 1982). The two shocks occurred about 3 hours apart. Large quantities of water were emitted from the ground, and a scarp 0.5 m high was formed (Shenon, 1936).

In summary, figure 2.2 shows a trend of activity that coincides well with that of the ISB as defined by more recent seismicity. While many of the earthquakes, and in particular the 1910 and 1914 events, appear to be closely associated with the Wasatch fault, location accuracies of this period are not adequate for drawing such a correlation. It must be kept in mind that many population centers are located at the very base of the Wasatch Front, and that epicenters of this period are understandably biased to those locations. The epicentral locations of the 1884 and 1900 events, and the 1909 and 1934 Hansel Valley events show that moderate (as large as M_S 6.6) earthquakes have

occurred away from the Wasatch Fault. The plot also indicates that the ISB has been a stable feature in this region for at least the past 139 years.

2.2.2 The Regional Network Era: 1962-1974

The implementation of the Worldwide Standardized Seismograph Network (WWSSN) in 1962 greatly benefited the status of seismological instrumentation in the state of Utah. During that year three-component short and long period seismometers were established at Dugway Proving Grounds (about 100 km southwest of Salt Lake City), Price, and Salt Lake City. In the 1960's and early 70's a station at Logan (originally installed in 1940) was upgraded, an array of 10 seismometers was emplaced in the Uinta basin, and a new station was opened at Cedar City (Arabasz, 1979).

Epicenters cataloged for the period July 1962 to September 1974, taken from Arabasz and others (1980), are shown in figure 2.3. These earthquakes were located with information from stations within and outside Utah, with distances between stations being on the order of 75-150 km. Comprehensive efforts were made to revise the epicentral locations from this period using all possible data and more advanced computational techniques (Kastrinsky, 1977; Arabasz, 1979). It is estimated that during this period the earthquake record for north-central Utah is complete for events of about magnitude 2.5 and above (Arabasz and others, 1980). Figure 2.3 shows a north-south trending zone of activity similar to that seen in figure 2.2, about 100 km wide and roughly centered about the Wasatch fault. With the increased resolution, however, some patterns become evident. One of the most remarkable is that in only in a few isolated areas, namely near Brigham City, Salt Lake City, and south of Nephi, does it appear that seismicity is geographically associated with the Wasatch fault. The gaps in activity that are evident along the Wasatch fault in this figure and in the pattern of more recent seismicity have important implications for the occurrence of larger earthquakes, and are discussed in more detail in sec. 2.4. To the east of the Wasatch, seismicity occurs in a north-south trending band coincident with the back valleys, and scattered activity is seen to the west.

In addition to routine data collection and earthquake location procedures carried out by the University of Utah, a number of special microearthquake studies were conducted in this portion of the ISB during this time period. In 1969 a portable 6-station network was deployed in 2 areas of the Utah ISB within the area of figure 2.3 by scientists from Columbia University. The Cache Valley area near Logan and the central part of the Wasatch fault zone were each monitored by six stations for roughly two weeks. The results, summarized by Sbar and others (1972), showed a moderate level of activity at shallow (< 5 km) depths in the Cache Valley area, with a composite fault plane solution indicative of east-northeast extension. A remarkably small number of earthquakes were recorded along the central portion of the Wasatch fault zone, adding credence to the quiescence seen along the fault south of Salt Lake City in figure 2.3.

During the 12 year period shown in figure 2.3, a number of earthquakes in the magnitude 4 to 6 range occurred in the study area, the largest reaching magnitude 5.7. The six largest events that occurred in this period are labeled in figure 2.3. Special studies conducted for the aftershock sequences of four of these earthquakes are described below.

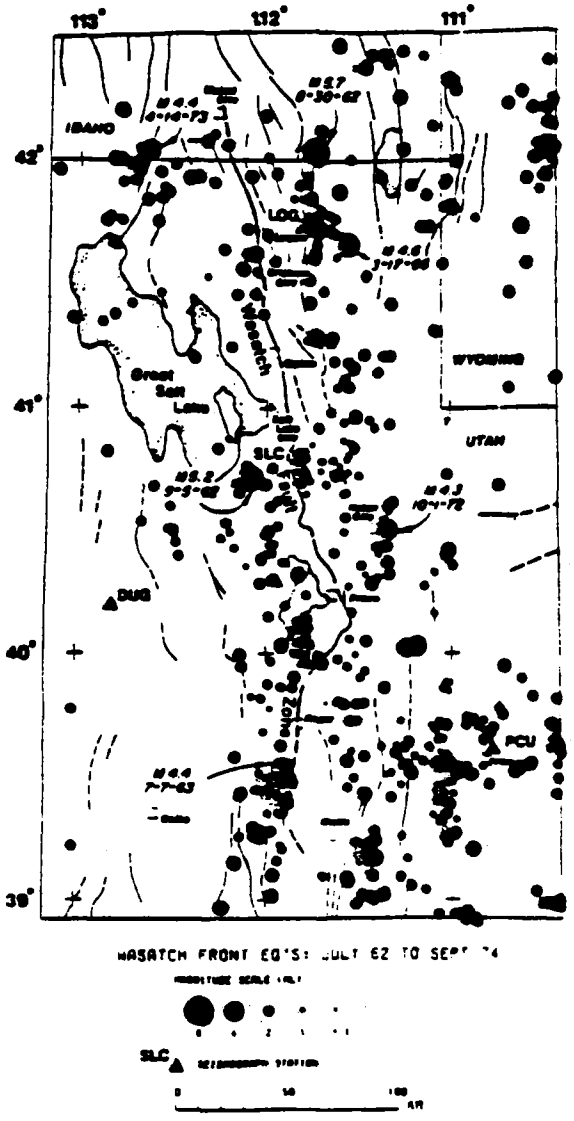


Figure 2.3 Epicenter map of north-central Utah, July 1962 through September 1974. Young faults shown for reference. Significant events are labelled by magnitude and year. From Arabasz and others (1980).

1962, August 30, M_L 5.7. The Cache Valley earthquake (near Logan in fig. 2.3), the largest Utah earthquake since the 1934 Kosmo event, caused about $1 million in damage. Intensity VII was assigned for the epicentral area; intensity V effects were reported in Salt Lake City (Lander and Cloud, 1964). A fault plane solution for the mainshock showed normal faulting on a north-south trending plane (coincident with the trend of the East Cache fault) that dips either east or west (Smith and Sbar, 1974). An aftershock survey by Westphal and Lange (1966) showed an east-dipping aftershock zone (contrary to the west-dipping East Cache fault) at depths of 6 to 16 kilometers. Additional effects of the earthquake are discussed by Cook (1972).

1962, September 5, M_L 5.2. The Magna earthquake (directly west of Salt Lake City in fig. 2.3) occurred a few days after the Cache Valley event, and resources were not available to study it in detail (Arabasz, 1979). Intensity VI effects were reported in the epicentral area and in Salt Lake City (Lander and Cloud, 1964).

1963, July 7, M_L 4.4. The Juab Valley earthquake can be seen at the southern end of the Wasatch fault zone in figure 2.3. Intensity VI effects were noted in the epicentral region and at Nephi (Von Hake and Cloud, 1965). An aftershock study by Westphal and Lange (1963) indicated an association with a fault bounding the west side of the Juab Valley graben.

1972, October 1, m_b 4.7. Aftershocks of the Heber City earthquake (about 30 km northeast of Provo on fig. 2.3) were studied by Langer and others (1979). A 5 km long northwest-trending zone was identified, with hypocenters forming a steeply dipping zone from 5 to 14 km in depth. The distribution of aftershocks and a composite fault plane solution indicated down to the northeast normal faulting on a northwest trending plane. No correlation with surface faults was evident. The maximum intensity in the epicentral area was reported to be VI (Coffman and Von Hake, 1982).

2.2.3 The Local Network Era: 1974-present

Prior to October, 1974, only nine widely scattered seismograph stations existed in the state of Utah (Richins, 1979). After that date, with the support of various agencies, the University of Utah began the emplacement of a network of short period seismometers located primarily in the north-central portion of the state. The signals are telemetered by radio or telephone link to Salt Lake City. Signals were at first recorded continuously on photographic film and earthquakes identified by visual inspection, but in the early 1980's this system gave way to the digitization of the incoming signals and the identification of seismic events by computer algorithm. Arrival times are picked interactively, and locations computed using a standard inversion technique which minimizes differences between observed and computed travel times. As of 1983 three different velocity models were used, corresponding to varying crustal properties in different areas covered by the network. Magnitudes are derived from the signal duration in a manner designed to equate the computed values to Richter local magnitude (M_L). These and other technical details of the network operation and earthquake location procedures are given in Richins and others (1984). As of 1983 about

40 stations were operating within the area of figure 2.3. It is estimated that within the study area the catalog is complete for earthquakes of magnitude 2.0 and greater for this time period (Arabasz and others, 1980; Richins and others, 1984). Kastrinsky (1977) estimates that epicentral errors in north-central Utah for this period are on the order of 2 km, with depth errors of about 4 km when the closest station is nearer to the epicenter than the value of the focal depth. For epicenters recorded with no near stations focal depths are poorly constrained.

Epicenters for the regional study area are shown in plates 1a, 1b, and 1c. The data source, the Utah Region Catalog, was received from the University of Utah in July, 1986. Although the area covered is smaller than that shown in figures 2.2 and 2.3, all regions important in assessing earthquake hazards to the Central Utah Project have been included. The data presented cover the time period October, 1974 through March, 1986. The regional pattern and its significance is discussed below, along with descriptions of special studies associated with specific earthquakes or seismicity in localized areas. The discussion largely follows descriptions by Arabasz and others (1979; 1980) and Kastrinsky (1977).

Seismicity occurring in the northern part of the study area is shown in plate 1a. The Wasatch fault trends north-northwest in this area, and the East Cache fault trends roughly north-south about 20 km to the east of it. The pattern shows a cluster of events in the northwest portion of the plot, a north-south trending band of activity coincident with the Bear River Range and bordered by the East Cache fault on the west, and with the exception of a small cluster of earthquakes north of Brigham City, an almost complete lack of activity in the vicinity of the Wasatch fault.

The north-south trending band of activity persists to the south down to about latitude 40.0, and is an important feature of the seismicity of north-central Utah. The northern portion of this band has been quite active historically, as shown in figure 2.3 and by the occurrence of the M_L 5.7 Cache Valley event of 1962. That earthquake, however, showed no correlation with the East Cache fault despite its occurrence directly beneath it (Westphal and Lange, 1966). Zandt and others (1986), in a special study of the seismicity, geodetic data, and geologic structures of this area, concluded that very few, if any, earthquakes were occurring directly on the East Cache fault.

Although the zone of activity in the northwest portion of the plot has been active historically (fig. 2.3), many of the earthquakes seen there on plate 1a are aftershocks of the M_L 6.0 Pocatello Valley earthquake that occurred about 20 km north of the map boundary on March 28, 1975. An aftershock study and tectonic analysis of this event are described by Arabasz and others (1981). Normal faulting was found to have occurred on a northeast trending, northwest-dipping fault that had not been previously mapped. A complex aftershock zone developed that involved normal, strike slip, and oblique faulting. No surface faulting was discovered.

Plate 1b shows seismicity in the next segment of north-central Utah to the south, which includes the Salt Lake City area. The band of activity trending north-south about 20 km east of the Wasatch fault persists in this region, although the level of activity appears to decrease significantly at about the latitude of Salt Lake City. This is also the latitude at which the Uinta

Mountains trend intersects the Wasatch fault. Although this relationship has been noted by researchers (e.g. Arabasz and others, 1980), to our knowledge no hypothesis for the relationship between the seismicity pattern and the geometry of these structural trends has been presented. Scattered activity is seen about 30 km to the west of the Wasatch fault. Although the fault dips to the west, these events are too shallow to be associated with it (Arabasz and others, 1979). About 20 km to the east of Salt Lake City, in the epicentral area of the M_L 5.2 Magna event of 1962, a series of small earthquakes (maximum magnitude M_L 3.2) occurred in February and March of 1978. This sequence and its effects are described by Cook (1979). With the exception of a cluster of earthquakes adjacent to Salt Lake City, the Wasatch fault is completely devoid of seismic activity. The resolution of the seismic network in the Salt Lake City area is high, however, and a close examination of these events shows a negative correlation with the fault (Walter Arabasz, oral communication, 1986). At the south end of Utah Lake, an east-west trending cluster of activity may be related to strike-slip faulting (Kastrinsky, 1977). The epicentral zone of the 1972 m_b 4.7 Heber City earthquake (about 40 km northeast of Provo) also continued to be active during this period.

Plate 1c shows the next segment of central Utah seismicity to the south of plate 1b. The plot shows substantial activity, despite station coverage being less favorable in this region than to the north (Arabasz and others, 1980). The south end of the Juab Valley, site of the M_L 4.4 1963 event, continued to be active. Some of this activity appears to be be coincident with the southern end of the Wasatch fault. To the east of the Wasatch fault there is scattered activity, but with the well-defined north-south trend seen to the north no longer evident. The dense cluster of epicenters in the northeast part of plate 1c has been related to coal mining (e.g., Smith and others, 1974).

Three special studies have been performed on earthquakes occurring south of latitude 40.0. In a study of events in this area using group location techniques, Wechsler and Smith (1979) found a north-south trend coincident with the northern end of Joes Valley, and that epicenters in the remainder of the Wasatch Plateau remained diffuse. McKee and Arabasz (1982) report the results of a ten-week, twelve station microearthquake survey conducted in the area of plate 1c in 1979. The authors found unusually shallow focal depths and a poor correlation of seismicity with mapped faults and physiographic features. None of the activity could be correlated with the Wasatch fault. Aftershocks of an M_L 4.4 event that occurred in Goshen Valley (near the northern end of Juab Valley) in May, 1980 were also investigated by Mckee and Arabasz (1980). Normal faulting at depths of 8-12 km due to east-west extension was ascertained from single and composite fault plane solutions, but the resolution of a fault plane based on the aftershock distribution was not possible.

In the summer of 1984 a 40-station temporary network was operated in the vicinity of the mining-related activity in the southeastern part of plate 1c by the University of Utah, the Bureau of Reclamation, and Woodward-Clyde Consultants. This 5-week multi-objective study focussed largely on the mining-induced activity, but also involved the eastern Wasatch Plateau. Only two earthquakes were located in this region during the study period, and were found to have occurred at shallow (< 5 km) depths beneath Joes Valley graben.

This result supports the observation of low levels of activity seen in this area in plate 1c. The hypocentral resolution was not sufficient to be able to correlate these events with surface faults associated with the graben (Arabasz and Williams, 1985).

In summary, the seismicity distribution in north-central Utah during this time period shows a distinct lack of correlation with the major faults (Wasatch, East Cache, and others) of the region. To date, in no location has seismicity been proven to have occurred directly on the Wasatch fault. In all localities other than the cluster near Brigham City, network resolution has been sufficient to disprove a possible correlation. The question of whether any of the seismicity north of Brigham City is occurring on the fault has yet to be resolved (Walter Arabasz, oral communication, 1986). The general pattern in north-central Utah shows a well-defined band of north-south trending activity, centered about 20 km east of the Wasatch fault, extending from the northern boundary of the study area south to about latitude 40. Below that, activity exists along this trend but becomes more diffuse. Pockets of seismicity occur to the west of the Wasatch fault, but this zone of activity appears to have less continuity along the north-south trend than the band to the east. The overall pattern of seismicity from the 1962-1974 period (fig. 2.3) is very similar, implying a continuity in the style of earthquake occurrence for at least the past 24 years. The lack of correlation between seismicity and major faults is remarkable, and the occurrence of the 1975 M_L 6.0 Pocatello Valley earthquake demonstrates that events of at least this size can occur without being related to features mapped on the surface. The development of physical models explaining the seismicity in terms of the properties and mechanical nature of the crust is currently an area of intensive research (e.g., Arabasz and Julander, 1986) and is reviewed in the remainder of this section.

2.3 The Relationship Between Seismicity and Subsurface Structure

In this section we examine the distribution of seismicity in the subsurface, and explore possible interactions with local structure and with rheological properties of the upper crust. It was shown previously that while earthquake epicenters in the study area occurred in the vicinity of gross geologic features such as the Wasatch Front, the two-dimensional distribution (e.g., fig. 2.3) of contemporary seismicity was scattered and showed no obvious association with local surficial geology. Although uncertainty in earthquake locations likely played some part in masking the relation between seismicity and structure, the complex epicentral distribution observed remains unaccounted for.

Two modes of deformation in the upper crust are suggested in the recent literature: 1) Deformation largely controlled by the thermal and rheologic properties of the upper crust (e.g., Sibson, 1982; Meissner and Strehlau, 1982; Smith and Bruhn, 1984), and, 2) Deformation controlled primarily by the mechanical and structural properties of the upper crust (e.g., Arabasz and Julander, 1985). Understanding the interaction between release of seismic energy and local geologic structure requires a precise three dimensional knowledge of hypocentral distribution and earthquake source properties, in conjunction with a detailed description of the subsurface geology.

2.3.1 Focal Depth Distribution and the Thermal-Mechanical Model of Deformation

A fundamental characteristic of ISB earthquakes is that nearly all focal depths are less than 15 km, thus limiting brittle deformation to the upper crust (Smith, 1978). Earthquakes recorded in the period 1974 to 1978 by the University of Utah regional seismograph network which were located along, and west of, the Wasatch Front showed a sharp decrease in numbers of events at about the 10 to 13 km depth, with a peak at about 7 to 9 km (Arabasz and others, 1980). A bimodal focal depth distribution, with peaks at about 1 to 3 km and 7 to 9 km was suggested for those earthquakes located along the Wasatch front. Detailed aftershock studies of the 1975 Pocatello Valley and 1976 Hansel Valley earthquakes indicated peaks in the focal depth distribution at about 4 to 7 km, with a rapid decrease in numbers of events at about 7 to 8 km.

Focal depth distributions of low-level seismicity have been used to indicate the vertical extent of brittle deformation in the crust, and to predict probable depths for the nucleation of large earthquakes (e.g., Sibson, 1982, 1984; Meissner and Strehlau, 1982; Smith and Bruhn, 1984). The upper crust is modelled by two zones: 1) a shallow zone where deformation occurs largely through frictional stick-slip faulting described by Byerlee's law (Byerlee, 1968), and, 2) a zone where deformation occurs by quasi-plastic creep. The boundary between the two zones is controlled by the temperature profile of the upper crust. Within these two zones, shear resistance as a function of depth can be calculated for a given strain rate and temperature profile. Shear resistance increases linearly with depth in the frictional zone, peaks at the frictional/quasi-plastic boundary, and decays exponentially with depth in the quasi-plastic zone. If shear resistance is taken as a measure of the maximum value of shear stress with depth, then the occurrence of earthquakes with depth should generally follow the shear resistance distribution.

Regions of high shear resistance can also be shown to represent concentrations of elastic strain energy (Sibson, 1974), and have been interpreted to indicate potential zones for large earthquakes to nucleate (Sibson, 1982; 1984). Smith and others (1985) suggest that large magnitude earthquakes nucleate slightly deeper where shear resistance is changing at its maximum rate.

The application of the shear resistance model to the focal depth distributions found for the Wasatch Front indicates that the frictional/quasi-plastic transition zone is at about the 7 to 8 km depth (Smith and Bruhn, 1984). Large earthquakes are suggested to nucleate at depth (Das and Scholz, 1983), and the shear resistance model indicates that earthquakes larger than about magnitude 5.5 are likely to nucleate at depths equivalent to the maximum depths of aftershocks and low-magnitude seismicity (Smith and Bruhn, 1984). The depth cut-off for seismicity, and the maximum depth of frictional slip is therefore largely controlled by the thermal and rheological properties of the upper crust.

The rapid decrease in numbers of earthquakes at the 10 to 14 km depth, with maximum depths of 15 to 16 km suggests that large magnitude earthquakes should nucleate at 10 to 16 km depths, which are similar to depths of nucleation observed for the Hebgen Lake and Borah Peak earthquakes. Cenozoic normal faults which are steeply dipping, at least in the seismogenic zone at a depth of 8 to 15 km, appear to be likely candidates for faulting given the contemporary state of stress.

2.3.2 The Influence of Structure on Background Seismicity

While the maximum depth of seismicity is relatively constant in the regional study area, detailed microearthquake studies indicate that background (magnitude 3 or less) seismicity is strongly influenced by preexisting geological structure. McKee and Arabasz (1982) present results from a microseismic survey across the Basin and Range - Colorado Plateau (BR - CP) transition in central Utah showing that half of all well-resolved focal depths were less than 4 km. Most hypocenters were located in sedimentary rocks above the approximately 10 km-deep Precambrian basement interface. While the subsurface structure obtained from seismic reflection data indicated predominantly low-angle faulting, fault plane solutions suggested slip on moderate to high-angle faults. They concluded that seismic slip occurred on moderate to high-angle fracture planes that possibly were the upper portions of listric faults, related antithetic faults, or secondary faults within major fault blocks.

For the BR - CP transition in central Utah Arabasz and Julander (1986) suggest that most background seismicity occurs shallower than about 6 to 7 km, and lies above low-angle detachments. They also state that while background earthquakes apparently occur at greater depths (below low-angle detachments) such events are much less frequent. Arabasz and Julander also present aftershocks from a magnitude 4.7 shock in the Thrustbelt in southeastern Idaho, where seismicity is clearly localized above subhorizontal detachments. They conclude that low-angle detachments exert a fundamental influence on background seismicity, and that the frequency distribution of focal depths in the upper crust may locally be controlled by structure rather than rheological and thermal properties. They further suggest that maximum

focal depths, rather than depth of maximum numbers of earthquakes, are indicative of the transition from frictional to quasi-plastic behavior.

2.3.3 Focal Depths of Design Earthquakes

Based on the above discussion we conclude that large ($M \geq 7$) earthquakes will nucleate at depths of 10 to 15 km in the CUP study area. Rupture of the fault surface from such an event would continue upwards into zones of lower shear stress resistance. For earthquakes in the magnitude range of 5.5 to 6.5-7, a similar depth of nucleation should be expected. Smaller magnitude earthquakes, however, may occur as shallowly as 4 km, and will be strongly influenced by preexisting geological structure. While the apparent paradox of normal faulting on listric versus planar faults is not resolved (sec. 2.5), the down dip lengths of listric faults should still be limited by the maximum depth of frictional sliding (Smith and Bruhn, 1984).

2.4 The State of Crustal Stress

For the purposes of evaluating earthquake hazards in the study region, it is desirable to determine, as best as possible, the nature of crustal deformation including principal stress orientations, geometry of seismically active structures, and, in particular, generation and type of episodic large surface-faulting earthquakes. Earthquake studies within the study region have provided timely information relevant to the geometry of seismically active structures and to patterns of contemporary crustal deformation in this region of predominantly intraplate extension.

In the remainder of this section we will discuss experiments that have been designed to lead to an evaluation of the stress state in an area that encompasses the study region. These experiments range from in situ estimation of the three principal stress directions obtained from hydrofracture techniques to microseismicity experiments that involve temporary seismic arrays that serve to determine the sense of crustal deformation that results in earthquake activity. From such earthquake data the fault plane, sense of ground motion, and principal stress directions can be estimated.

2.4.1 In Situ Stress Measurements

The importance of making in situ stress measurements has long been recognized by earth scientists and engineers. The prediction and type of crustal earthquakes, and the proper interpretation of a variety of geologic phenomena require knowledge of the principal directions and magnitudes of the stress field. One way of estimating in situ stress is known as the "hydrofrac" method (e.g. Zoback and others, 1977). The procedure involves measuring stress parameters after hydraulically fracturing unfractured bedrock at depth in a drill hole. From the measured parameters, the maximum, minimum, and intermediate principal stress directions can be calculated assuming that one of them is vertical.

Three hydrofracture experiments have been supported by the Bureau of Reclamation in two different locations within the study region. Two experiments were conducted at the Fifth Water Underground Powerplant site (labeled on pl. 1b) in drill holes DH-103 and DH-101 which are separated by about five hundred feet (Zoback, 1981, and Haimson, 1981). The third experiment was carried out at the Jordanelle damsite (Haimson, 1985)(see pl. 1b for location).

Following Zoback (1981), the results of the study of the state of stress in drill hole DH-103 in the North Horn Formation can be summarized as follows: The greatest principal stress is vertical and results from the weight of the overburden. The magnitude of the least horizontal stress is quite low and is the same as that expected in areas of active normal faulting. The maximum horizontal stress is of intermediate value between the least horizontal stress and the vertical stress, however much closer to the value of the minimum horizontal stress. The direction of extension, or least compression, is S73W $\pm$ 15°, which is quite similar to other stress field indicators for the region. Figure 2.4 (from Zoback, 1981) illustrates the similarity of least principal stress directions determined by four different methods.

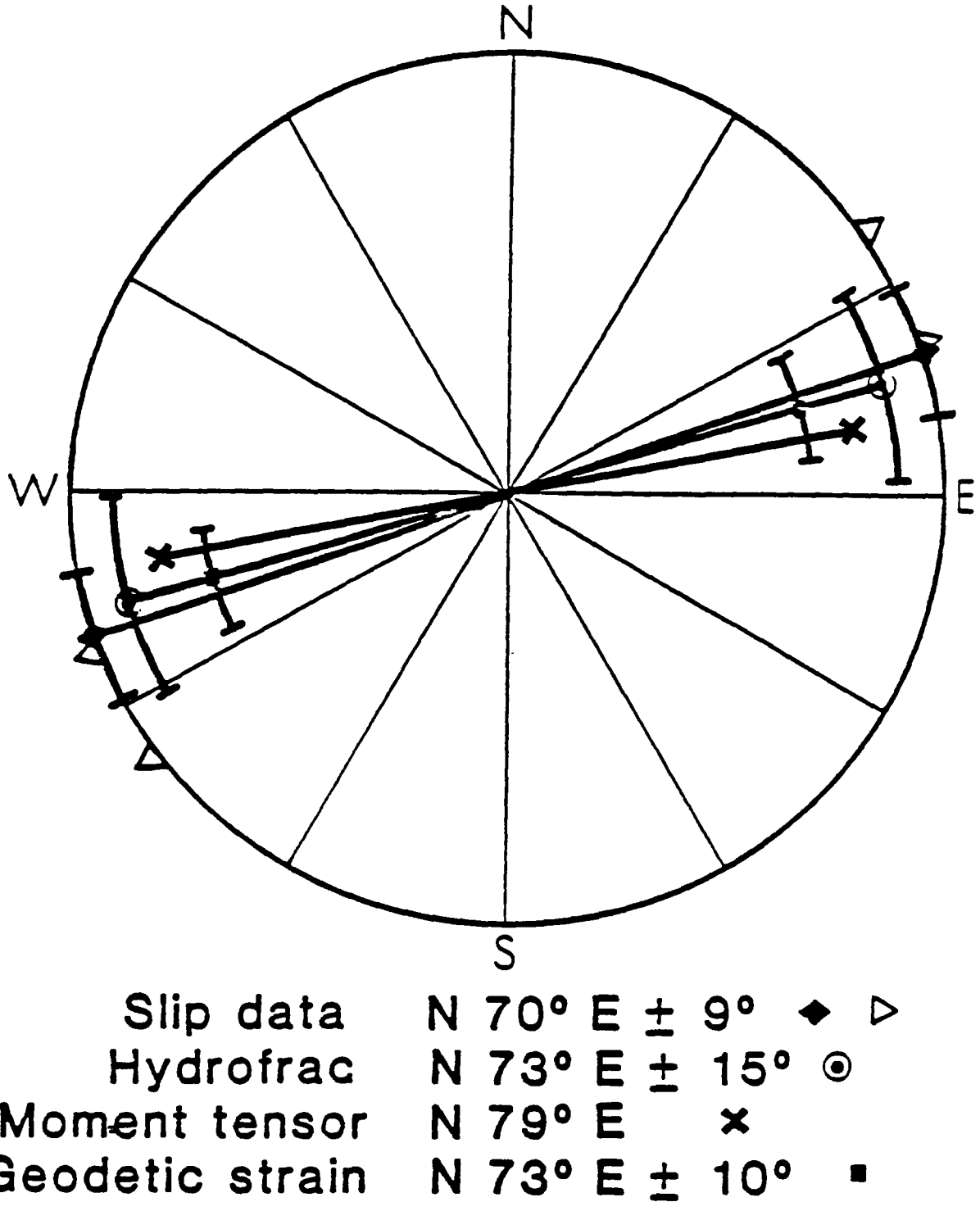


Figure 2.4 Comparison of Least Principal Stress Direction Determined by Several Methods (from Zoback, 1981).

Likewise, Haimson (1981) concludes that the stress estimates in hole DH-101 are in general agreement with those in hole DH-103, indicating extension in a N15E $\pm$ 10° direction. Furthermore, Haimson (1985) again estimates a general NE-SW extensional environment at the Jordanelle drill site also with stress magnitudes which suggest a stress regime close to the limit of stability based on a simple model of frictional sliding on properly oriented preexisting fractures. This conclusion was also reached by Zoback (1981) at the Fifth Water site.

The results of these studies confirm that extensional stresses oriented east-west to east-northeast - west-southwest are dominant in the central Wasatch Mountains. The magnitude of the stresses measured and their orientation indicate that favorably oriented (north-south to northwest-southeast) normal faults in the area will likely be subject to future earthquake activity.

2.4.2 Seismic Estimates of Crustal Stress

Principal stress directions and type of faulting throughout the study region can be estimated from the analyses of seismic data from earthquakes. Pressure and tension axes derived from the earthquake focal mechanisms is one of the most commonly used indicators of tectonic stress. However, principal stress orientations obtained from fault plane solutions are inherently the least reliable indicators of stress orientations. McKenzie (1969) demonstrated that for the general case of triaxial stress the only restriction on the greatest principal stress imposed by the fault plane solution is that this stress direction must lie in the same quadrant as the P axis but could in fact be nearly normal to the P direction. This analysis is based on the evidence that most shallow crustal earthquakes occur on preexisting faults whose fault plane solution incorrectly estimates the principal stress directions. However, Zoback and Zoback (1980) present arguments that lead to the conclusion that principal stress directions estimated from fault plane solutions are likely not to be in error by more than about 20 degrees.

Several studies have been cited in section 2.2.3 that have produced conclusions on the stress regime throughout the study region (e.g., Arabasz and others, 1980; Arabasz and Julander, 1986; Zandt and others, 1986). Focal mechanisms have been determined for widely spaced earthquakes throughout the Intermountain seismic belt. Figure 2.5 (from Arabasz and others, 1980) schematically summarizes all available data for the Wasatch front area (which includes CUP) at that time. Most of the solutions shown on figure 2.5 are composite solutions which comprise first motions from several closely spaced events.

Solution (a) for events along the East Cache Fault indicates dip-slip extensional faulting and is similar to solution (f) determined by Smith and Sbar (1974) and discussed by them for the M_L 5.7 Cache Valley (Logan) earthquake of 1962. Solutions (b) and (e) are similar to the majority of focal mechanisms in the study region which indicate a clear predominance of solutions that are interpreted to represent normal faulting, with slightly varying trends of extension. Solutions (c) and (d), on the other hand, which reflect components of thrust or high-angle reverse faulting, point out that there are local complications.

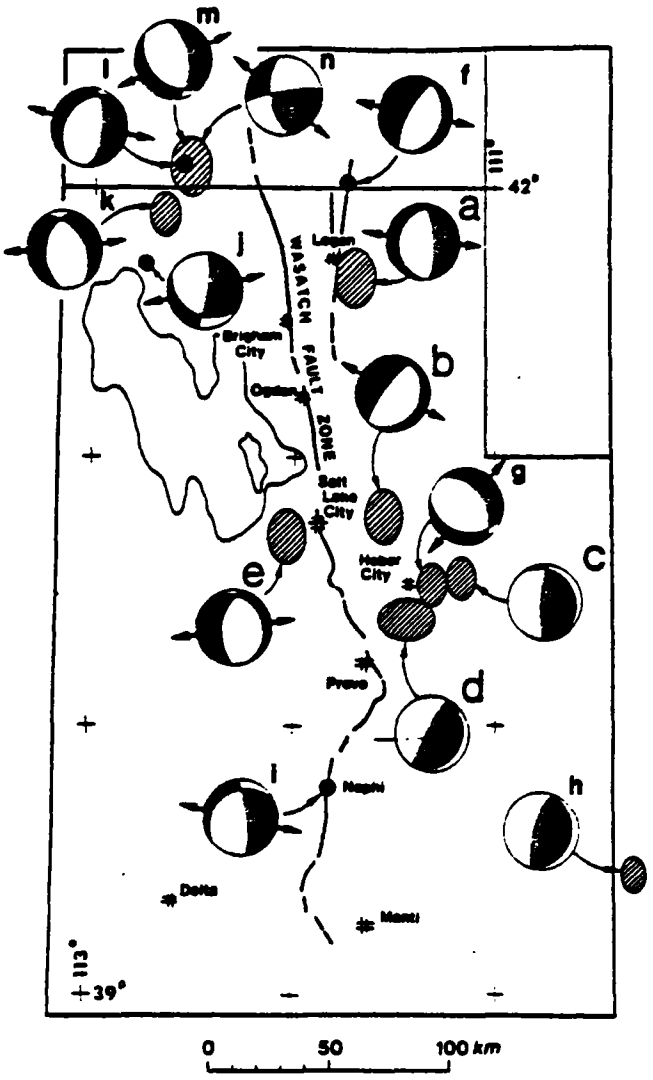


Figure 2.5 Schematic summary of fault-plane solutions (lower hemisphere projections) for the Wasatch front area. Compressional quadrants are shaded. Trends of T axes are shown by heavy arrows. Large dots show location of single-event solutions, and hachured zones show sample areas for composite solutions. Sources: (a to e), this study (keyed to Figure 9); (f and i), Smith and Sbar (1974); (h), Smith et al. (1974); (j), Dewey et al. (1973); (l), Bache et al. (1980); (g, k, m, n), from aftershock studies included in Arabasz et al. (1979). (From Arabasz, et al., 1980).

Although aftershocks of the m_b 4.7 Heber City earthquake of 1972 reflect normal faulting [solution (g)], solutions (c) and (d) for nearby clusters of earthquakes indicate significant horizontal components of compressional stress. Earthquakes in this area are near the intersection of the Wasatch front and the major east-west trending Uinta fold axis. Solution (h) determined by Smith and others (1974) for shallow earthquakes suggests thrust faulting and is similar to solutions (c) and (d) suggesting that stress orientations in the southeastern part of the CUP region may have some influence from the tectonics of the northwestern part of the Colorado Plateau. The contrast in stress orientation across the boundary of the Basin and Range Province in this area differs from that to the north of Salt Lake City, where fault plane solutions imply that general east-west extensional strain extends well east of the Wasatch fault zone and encompasses all of the northern CUP region.

Zandt and others (1986) recognized local complications to the general east-west extensional stress regime in a region north and east of Brigham City. North of Brigham City, a series of earthquakes occurred in 1976-1980 with depths ranging from 2 to 7 km (pl. 1a). A composite mechanism using six events shows normal faulting representative of the general east-west extension. However, about 25 km north, near the town of Fielding, a two day sequence of earthquakes in July, 1978 was also located near the Wasatch fault. A single event mechanism was determined for the largest event in the two day sequence of earthquakes (July 29, 1978 14:04, M_L 3.1, Depth = 4.2 km). This mechanism shows reverse dip-slip motion on a NW-striking plane indicating a nearly horizontal P-axis with azimuth S65W. About 15 km to the east, another reverse mechanism was determined for an earthquake on the edge of a "horst"-like structure within the Cache valley. These reverse mechanisms are unusual in this generally extensional tectonic regime but must lead to the observation that there exists a complex pattern of predominant extension with locally significant areas of apparent compression. Zandt and others (1986) used this information and some published geodetic data (Prescott and others, 1979) to hypothesize westward block motion of a portion of the adjacent Wasatch Mountains along a low-angle detachment with the mountain block. Modelling of the strain field defined by the geodetic observations led to a conclusion that relates to the complexity of strain release patterns in the northern Wasatch Front area and the likely importance of low-angle decollement faults in accommodating extensional strain. In particular they suggested two tectonic models: aseismic slip on a buried portion of a major normal fault that will produce a zone of compression at the surface above the fault plane, or alternatively, aseismic slip on a "listric" normal fault within the footwall block of a major normal fault that will also produce a zone of compression. These (non-unique) descriptions may relate to the formation of back valleys and listric back-valley faults. In any case, a compressional stress regime can occur in isolated regions within the CUP region. However, the stress regime and sense of major faulting of concern to engineering applications will only reflect the major east-west extensional environment.

Another area where the focal mechanisms indicate a local complication is the Idaho-Utah border area north of the Great Salt Lake (Arabasz and others 1980). Focal mechanisms in the Hansel Valley area [solutions (j) and (k) of fig. 2.5] reflect a predominance of normal faulting with general east-west extension, as does the main shock of the 1975 M_L 6.0 Pocatello Valley

earthquake. However, aftershocks of this earthquake (again smaller magnitude events) displayed mixed mechanisms involving normal, oblique, and strike-slip faulting. Solutions (m) and (n) are two of eight aftershock mechanisms that illustrate some of the complexity of the aftershock sequence.

2.4.3 Discussion of Stress Variations

Several lines of evidence have been presented from which to assess the overall picture of stress variations within the CUP region. Although we are handicapped by a lack of information on large-scale seismic slip related to motion on major faults, and we face uncertainties of dealing with limited *in situ* stress field determinations and measurements based on seismic deformation, we believe there are important clues for understanding crustal deformation and the generation of episodic large surface-faulting earthquakes in this complex region. We note that the Basin and Range extensional environment undergoes a transition to the compressional environment of the Colorado Plateau near the southeastern part of the study region. However, the *in situ* stress estimations made near the seismically determined compressional anomalies (and in particular at the Jordanelle damsite) indicated the more general extensional environment common to the study region as a whole.

The overwhelming majority of evidence leads to the conclusion that although there exist small anomalies to a uniform isotropic stress field, the predominant stress regime that will control major faulting of concern to engineering applications is that of east-west extension conducive to normal faulting.

One last observation that may relate to strain variations along the Wasatch front is the observation of apparent seismicity gaps. Several studies have recognized that anomalously low seismicity along segments of the Wasatch Fault deserves special discussion (see Sbar and others, 1972; Smith, 1974, 1978; Smith and Sbar, 1974; and Arabasz and others, 1980). For example, quiescence of seismic activity could be due to low strain following a large prehistoric earthquake, or could be precursory, occurring at a high level of strain (e.g., Wyss and others, 1978). Two sites that are particularly noted by Arabasz and others (1980) where gaps in seismicity appear to exist can be seen on plate 1. There appear to be two segments located to the north and to the south, respectively, of Salt Lake City that have been seismically quiet since at least 1962. They mark areas of unusually low earthquake activity within a broadly active earthquake zone and along a major active fault. Unfortunately, existing data are inadequate either to characterize seismicity during a complete cycle for a large rupture event on the Wasatch Fault, or to determine which segments, if any, are in a late pre-earthquake stage. Uncertainties discussed by Swan and others (1980) regarding the timing of the last surface-faulting events within the seismic gaps and the variation of interevent times of such events are such that one cannot confidently determine whether the corresponding segments of the Wasatch Fault are in the initial or the later stages of a seismic cycle. Thus, if a large earthquake is indeed due somewhere along the fault, the segments characterized by the persistent seismicity gaps are not necessarily the segments most likely to rupture next. Finally, it is interesting to note that the compressional strain field from geodetic measurements by Prescott and others (1979) lie within the seismicity gap north of Salt Lake City. However, once again

conclusive data as to whether this is precursory evidence for an impending large earthquake are not available.

2.5 An Earthquake Occurrence Model for the ISB

The relationship between contemporary seismicity and geologic structure in the ISB is not well understood. Targeting potential sources of moderate to large magnitude earthquakes using seismologic versus geologic data often leads to conflicting interpretations, since data from these two avenues of study are frequently not complimentary. As an example, locations of recurrent sources of large-magnitude (greater than 7.0) earthquakes are typically indicated from geologic field studies since evidence of displacement will generally be preserved in the Quaternary record. However, studies of contemporary seismicity have not demonstrated that epicenters of small- and moderate- magnitude earthquakes, which generally do not produce surface rupture, are concentrated near late Quaternary faults. Furthermore, the occurrence of events such as the 1975 Pocatello Valley earthquake in southeastern Idaho (magnitude 6.0), where seismologic evidence indicates that faulting cuts across preexisting late Quaternary faults, suggests that locations of moderate-magnitude earthquakes (up to 6.5) may not be indicated in the surficial geology (Arabasz and Smith, 1981; Arabasz and others, 1981).

Because many of the characteristics of moderate- and large- magnitude earthquakes are dissimilar, it is useful to treat separately the two categories of earthquakes, and formulate a model of earthquake occurrence which recognizes the distinction. We subsequently review observations of large and moderate magnitude earthquakes for the ISB historic catalog.

2.5.1 Large-magnitude ISB earthquakes: Hebgen Lake and Borah Peak

Two earthquakes of magnitude exceeding 7.0 have been recorded within the entire ISB. On August 18, 1959, a sequence of earthquakes shook the area around Hebgen Lake, Montana, causing in excess of 11 million dollars in damage and the loss of 28 lives. On October 28, 1983, a large earthquake occurred in central Idaho, near Challis, which resulted in 2 deaths and a property loss of over 12 million dollars. These are the largest documented earthquakes in the historic catalog for the ISB, and provide direct evidence for characterizing ground motion and surface faulting for a "maximum credible event". Geologic data from surface cutting faults in the ISB and Basin and Range supplement these observations and suggest a model for the recurrence of major earthquakes.

The Hebgen Lake earthquake was originally assigned a magnitude (approximately M_L, Tocher, 1962) of 7.1, but recent analyses of the data suggest more likely magnitude values of M_L 7.7 (Bolt, 1984); also M_L 7.6, m_b 7.0, and M_S 7.2 (Doser, 1984); and finally M_S 7.5 (Doser, 1985). The Borah Peak earthquake has been assigned magnitudes of M_L 7.2 (Bolt, 1984), and M_S 7.3 (National Earthquake Information Service, 1983). The seismic moment of the Hebgen Lake earthquake was estimated at 9.2×10^{26} dyne-cm by Doser (1984). The moment for the Borah Peak earthquake was estimated at about 2.1×10^{26} dyne-cm by Doser and Smith (1985), which is in good agreement with the value of 3.12×10^{26} dyne-cm found by Ekstrom and Dziewonski (1985). These values are very close to the geodetically determined moment of 3.3×10^{26} dyne-cm determined by Stein and Barrientos (1985). Stress drops for the Hebgen Lake and Borah Peak events were estimated at 97 and 17 bars, respectively (Doser, 1984; Doser and Smith, 1985).

Geodetic and seismological evidence strongly suggests that the Hebgen Lake and Borah Peak events occurred on normal faults dipping 45 to 60°. Rupture propagated unilaterally from one end of the fault, and nucleation of rupture occurred at about the 15 km depth for both events. Doser (1984) determined a fault dip of 45 to 60° for the Hebgen Lake earthquake from a detailed re analysis of the original seismic records. Waveform modeling indicated a focal depth of 15 km, near the base of the seismogenic zone, with rupture propagating upwards to the surface and along the length of the fault zone. Many varied observations of the Borah Peak earthquake indicate that slip occurred on a 45 to 60° dipping planar normal fault (e.g., Barrientos and others, 1985; Doser and Smith, 1985; Stein and Barrientos, 1985; Ekstrom and Dziewonski, 1985). The main shock hypocenter had a depth of 14 to 16 km, and rupture propagated unilaterally along the fault. Barrientos and others (1984) modeled observed vertical deformation associated with the earthquake and suggested that moment release was concentrated in the depth range of 8 to 12 km.

Near-field acceleration data are not available for either the Hebgen Lake or Borah Peak earthquakes, however the Borah Peak event was recorded by strong motion instruments located at INEL (Idaho National Engineering Laboratory) some 100 km southeast of the main shock. These data were presented by Jackson (1985) and Jackson and Boatwright (1985). Peak horizontal accelerations recorded at two free-field sites were 0.04 and 0.08 g. Duration of the record segment where peak horizontal accelerations exceeded 0.02 g was 10 to 15 s, and the acceleration amplitude spectra peaked in the frequency band of 5 to 15 Hz. Extrapolation of aftershock data recorded both at INEL and in the epicentral area suggested an upper limit of 0.8 g for near field ground acceleration of the main shock.

The Hebgen Lake and Borah Peak earthquakes produced extensive surface rupture, with maximum recorded displacements of 6.7 and 2.7 m, respectively (Myers and Hamilton, 1964; Crone and Machette, 1984). The Hebgen - Red Canyon fault system showed an average surface displacement of about 2 m over a length of about 30 km (Myers and Hamilton, 1964). Crone and Machette (1984) measured an average surface displacement of 0.8 m along the 34 km scarp at Borah Peak. Both events occurred on faults exhibiting multiple late Quaternary displacements (Myers and Hamilton, 1964; Malde, 1971; Hait and Scott, 1978; Pierce, 1985).

Observed displacements from the Hebgen Lake and Borah Peak events were similar to paleoseismic single-event displacements measured on late Quaternary normal faults elsewhere in the ISB and Basin and Range. For example, Schwartz and Coppersmith (1984) measured single-event displacements exposed in trenches across several segments of the Wasatch fault zone. They found that displacements ranged between 1.6 to 2.6 m, with an average displacement per event of 2 m. This suggests that the Hebgen Lake and Borah Peak earthquakes are representative of large-magnitude events elsewhere in the ISB.

Further examination of the paleoseismic record of the Wasatch fault suggests a model for earthquake occurrence on recurrently active faults. Although Schwartz and Coppersmith (1984) were not able to rule out single-event displacements of less than 0.5 m, they felt that displacements of between 0.5 and 1.6 m, had they been present, would have been observed. These

observations led them to suggest that a "characteristic earthquake" model, where individual faults and fault segments tend to generate only earthquakes having magnitudes and displacements in a narrow range about the maximum, was applicable to the Wasatch and other faults.

The characteristic event model of faulting is in marked contrast to the log linear relationship between earthquake frequency versus magnitude (Gutenberg and Richter, 1954) widely observed for seismically active regions. The characteristic earthquake model was initially suggested by Allen (1968) from observations of seismicity along the San Andreas fault, and may also describe faulting in other tectonic environments. In a detailed study of both seismicity data and late Quaternary displacement on strike slip and reverse faults in Japan, Wesnousky and others (1983) concluded that the characteristic earthquake model better describes the behavior of individual faults than does the Gutenberg-Richter relationship.

The characteristic sizes of the Hebgen Lake and Borah Peak earthquakes are assumed to provide estimates of earthquake parameters which can be applied to other normal faults in the ISB. While sufficient data do not yet exist to conclusively demonstrate the universal applicability of the characteristic earthquake model to late Quaternary faults in the ISB, it is presently the most favored model. Thus, it is assumed that earthquakes that occur on late Quaternary normal faults in the ISB will be of a size which is in a narrow range about the maximum for the particular fault. For a suite of faults, or for the region around a fault, a Gutenburg-Richter type relation is still assumed to be valid.

2.5.2 Moderate-magnitude earthquakes in the ISB

Since 1870 there have been fifteen earthquakes reported in the ISB with magnitudes in the range of approximately 6.0 to 7.0 (Coffman and others, 1982; NOAA, 1985). This figure does not include foreshocks or aftershocks. Earthquakes in this magnitude range, which we have called moderate-magnitude events, typically produce no surface displacement, and do not appear to be related to active late Quaternary faults. The occurrence of these earthquakes is suggested to follow a process quite distinct from that of the large-magnitude earthquakes discussed in the previous section.

Precise magnitude determination for earthquakes occurring before 1930 is difficult, since these magnitudes were often based on the maximum intensity of ground shaking reported in the epicentral region, or on the size of the felt area. Comparison with recent earthquakes in the ISB for which instrumental magnitudes are available suggests that an earthquake of magnitude 6 or greater produces a maximum Modified Mercalli Intensity of VII or more, and is felt over an area on the order of 10 000 km^2. Uncertainty in the magnitude determination for events not recorded instrumentally makes it possible that three or more of the assumed fifteen magnitude 6.0 to 7.0 earthquakes were actually in the magnitude 5.5 to 6.0 range. Regardless of the ambiguity in some of the magnitude determinations, detection of moderate magnitude earthquakes has probably been uniform since at least 1870 because of the large felt areas such events produce.

Surface rupture resulting from moderate-magnitude earthquakes has rarely been observed. Of the fifteen magnitude 6.0 to 7.0 earthquakes documented in the

ISB, only the magnitude 6.6 1934 Hansel Valley, Utah, earthquake has been associated with surface rupture (Shenon, 1936). This event produced 0.5 m maximum surface displacement along a discontinuous 10-km-long zone of en echelon scarps in predominantly unconsolidated sediments. Pardee (1926) reported that the 1925 magnitude 6.7 Clarkston, Montana, earthquake produced only isolated surface cracks of up to 0.6 m related to local subsidence, but no observable scarp with surface displacement was found.

Within the ISB there is evidence for the existence of a threshold magnitude for the occurrence of surface rupture. This magnitude apparently lies in the magnitude 6 to 6-3/4 range, and likely varies somewhat with location. Doser (1985) has noted that surface rupture has not been observed for magnitude 6.0 to 6.5 earthquakes in the ISB, and suggests that magnitude 6-1/2 is the threshold for surface rupture. This was based on the observation that no surface rupture was recorded for the 1975 M_L 6.1 Yellowstone, Wyoming, 1975 M_L 6.0 Pocatello Valley, Idaho, and the 1947 M 6.3 Virginia City, Montana earthquakes. Though the magnitude determinations for the Hansel Valley and Clarkston earthquakes are somewhat uncertain, they appear to have been near the threshold magnitude.

Locations of moderate-magnitude earthquakes suggest that these earthquakes occur without correlation to late Quaternary faults. Evidence from the Pocatello Valley earthquake indicates that the earthquake ruptured on a fault which cuts across a major late Quaternary fault in the area (Bache and others, 1980; Arabasz and others, 1981). None of the magnitude 6 to 6-3/4 ISB earthquakes have been shown to have occurred on recurrently active range bounding faults. Earthquakes of this magnitude within the ISB may therefore occur on hidden subsurface faults, without apparent correlation to the surficial geology.

2.5.3 Summary

The Hebgen Lake and Borah Peak earthquakes are assumed to be representative of maximum magnitude earthquakes which occur on late Quaternary normal faults in the ISB. Earthquake occurrence on recurrently active normal faults appears to be limited to characteristic surface rupturing events that produce displacements greater than 0.5 m. Quoting Doser (1985), we suggest a model for large earthquakes (magnitude 7 - 7.5) in the ISB which "would predict a fault rupture length of 20 to 30 km, an average surface displacement of 1 to 4 m, a paucity of foreshocks, displacement along major fault systems showing repeated movements in Quaternary-Holocene times, and unilateral rupture nucleating at a depth that is at or near the base of the seismogenic zone." Ground motion parameters for such earthquakes are expected to be similar to those observed for the Hebgen Lake and Borah Peak events.

Because moderate-magnitude earthquakes in the ISB have not produced observed surface rupture or other evidence of nucleating on late Quaternary faults, it is unlikely that potential sites of moderate-magnitude earthquakes may be predicted from Quaternary geology. Detailed geologic field studies of each of the fifteen magnitude 6.0 to 7.0 earthquakes observed in the ISB have not been conducted, but the available literature suggests that the specific locations of these events could not have been targeted from the surface geology (Arabasz and Smith, 1981). Potential sites of future earthquakes in the magnitude 6 to 7 range might therefore remain unidentified if based on

geologic data alone. Without further advances in earthquake prediction, enabling use of contemporary seismicity data, it may only be possible to assume that these events will occur on "blind" structures having no surface expression.

2.6 Recurrence Rates for Moderate-Magnitude Earthquakes

The ISB is defined by a concentration of low-level earthquake activity, most of which occurs on unmapped or "blind" structures having no apparent correlation to late Quaternary surface faults. The frequency distribution of this activity, and the predictability of likely locations for future events, is quite distinct from that of large-magnitude earthquakes which apparently occur only on recurrently active surface faults.

Seismically active regions or suites of active faults have widely been observed to obey a log-linear relation between earthquake frequency and magnitude (Gutenburg and Richter, 1954). The log-linear relation, however, has been shown to inadequately describe seismicity on individual faults exhibiting recurrent surface rupture. Analysis of trenches dug across active late Quaternary faults indicates that the amount of slip produced by single events does not vary greatly for a particular fault (e.g., Coppersmith and Schwartz, 1984). This observation has suggested that large-magnitude earthquakes within the ISB may be described by the "characteristic earthquake" model, which postulates that for any recurrently active late Quaternary fault only large earthquakes with magnitudes in a narrow range are likely to occur. The geologic record therefore provides information on the occurrence of large-magnitude earthquakes, their rate, and their likely locations.

In contrast to large-magnitude earthquakes, events within the ISB of magnitude less than about 6-1/2 have not been observed to occur on faults which displace the surface. Aside from minor local subsidence, these events have not formed scarps. Because earthquakes of this size may cause significant ground motion, it is necessary to characterize their probable locations and average rates of occurrence. Such information cannot be obtained solely from the geologic record. The remainder of this section reviews seismicity rates based on the historic earthquake catalog, and also on the geologic record, and estimates the frequency of occurrence of moderate-magnitude earthquakes for the CUP region.

2.6.1 Recurrence Rates Based of Historic Seismicity and Geologic Information

Earthquake recurrence studies for the north-central Utah area have been presented by Arabasz and others (1980) and Kastrinsky (1977), based on the entire record of seismicity, from 1850 through 1978. Arabasz and others (1980) analyzed earthquake recurrence in north-central Utah as a whole (the area shown in figs. 2.2 and 2.3) using three major documentation periods (1850-1962, 1962-1974, and 1974-1978). In doing so the completeness periods for various magnitude detection thresholds were determined, and accounted for in the computations, utilizing the methodology of Stepp (1972). Because these completeness periods are important in interpreting historical seismicity at local sites, they are reproduced in Table 2.1.

Table 2.1 Completeness Periods for North-Central Utah

Period	Intensity ≥	$M_L \geq$ *
1974-1986		2.0
1962-1986		2.3
1950-1986	V	4.3
1940-1986	VI	5.0
1880-1986	VII	5.7
1850-1986	VIII	6.3

* converted from intensity by $M_L=(2/3)I + 1$

Earthquake recurrence times were computed from the standard log-linear recurrence formula $\log(N) = a - b(M)$ (Gutenberg and Richter, 1954), where N is the number of events of magnitude M or greater, and the a- and b- values are constant. N was computed both as a cumulative number (the number of events greater than or equal to M) and as an incremental number (the number of events with a given maximum intensity or within a certain magnitude range).

In comparing recurrence intervals for the recent data set (1962-1978) to those calculated for the entire historic record, Arabasz and others (1980) found that the rate of occurrence of $M_L \geq 4$ events was significantly lower in the recent period than would be expected from the extrapolation of the entire record. Specifically, 21 earthquakes of this size or greater would be expected in the 1962-1978 period based on the entire record, whereas only 12 actually occurred. They suggested that the current level of activity is anomalously low, and may be related to the prescence of seismicity gaps along much of the Wasatch fault.

Arabasz and others (1980) suggest that recurrence estimates based on the entire 129-year record are more appropriate for earthquakes of M_L 6.0 and greater. The computed values, derived from the methodologies described above, are listed in table 2.2. The narrow range of recurrence times shows that the results are consistent despite the usage of varying mathematical techniques.

Table 2.2 Return Periods for larger earthquakes in north-central Utah *

$M_L \geq$	Years
6.0	22-25
7.0	111-115
7.5	232-262

* based on the 129 yr. (1850-1978) record

Kastrinsky (1977) also computed recurrence intervals for earthquakes within the same study area, but with data only from the 1962-1974 period. While his

computed values for earthquakes of M_L 6 and greater are very different from those calculated by Arabasz and others(1980) based on the entire historic record, this can be attributed to the extreme sensitivity of the extrapolated values to the b- value in the recurrence relation $\log(N) = a - b(M)$. However, for magnitudes of 5.0 and less, Kastrinsky (1977)'s values are probably more realistic, and are listed in table 2.3.

Table 2.3 Return Periods for moderate earthquakes in north-central Utah *

$M_L \geq$	Years
5.0	35
4.0	3.9
3.0	0.43

* based on a 12 yr. (1962-1974) record

Note that according to tables 2.2 and 2.3 M_L 6.0 events are predicted to occur more frequently than M_L 5.0 events. This points out again that the modern seismicity rate appears to be lower than the historic rate.

Estimates of long-term seismicity based on slip rates for Quaternary faults in Utah were made by Doser and Smith (1982). They implicitly assumed that seismicity in the region surrounding (and including) the Wasatch fault, could be described by a log-linear cumulative frequency versus magnitude recurrence relation. They further assumed that most of the net moment release in the region was accounted for by slip on Quaternary faults. By measuring parameters which relate magnitude to moment, and using b-values from contemporary seismicity, they were able to estimate the recurrence rate of earthquakes in the region. In essence, they estimated an a-value from geologic data and magnitude-moment relations, and combined that with the b-value from historic seismicity. While they inappropriately combined relations obtained by Anderson (1979), who assumed a truncated form of the recurrence density distribution, with Molnar (1979), who assumed a truncated form of the cumulative recurrence relation, the errors introduced are probably within the precision of the estimates of the measured parameters.

Doser and Smith (1982) found good agreement between their estimates of seismicity based on geologic data with estimates obtained solely from historic seismicity, with the exception of the Wasatch Fault area. They attributed that discrepancy (about a factor of 2 greater for the geologic estimate of occurrence rates) to the short (20-year) period of historic seismicity data along the Wasatch fault. For the Wasatch front area (the Wasatch fault and subsidiary fault systems) Doser and Smith (1982) found good agreement between the geologic and historic data. In table 2.4 below we have extracted their estimates of seismicity rates for magnitude 6 -plus earthquakes for both the Wasatch fault and Wasatch front areas, normalized to a unit area of 1 km^2. Maximum and minimum estimates are shown because of the different estimates provided by the geologic and historic data.

Table 2.4 Rate of occurrence per unit area for magnitude 6-plus earthquakes in the Wasatch front and Wasatch fault areas. Data are from Doser and Smith (1982) and are based on geologic data as well as historic seismicity.

Rate of magnitude 6-plus earthquakes (10^{-7}/year/km^2)

	Wasatch front (74 000 km^2)	Wasatch fault (27 000 km^2)
Maximum rate	5.38	5.35
Minimum rate	4.57	2.41

2.6.2 Probabilistic Estimates of Epicentral Distance

We have used a probabilistic approach to assess the likelihood of a moderate magnitude earthquake occurring in the vicinity of an arbitrary site in the CUP region. It is assumed that earthquakes occur over time as a Poisson process and that the regional earthquake activity occurs uniformly over all sub-areas. Specifying an annual probability of occurrence then fixes the size of an area required to produce at least one event in any particular magnitude range. The appropriate equations on which these computations are based are detailed in Appendix A. The occurrence rate for earthquakes of this range is taken from table 2.4.

Probabilistic epicentral distances of moderate-magnitude earthquakes were estimated for a wide range of annual probabilities of occurrence. Selecting an annual probability of occurrence fixed the radius of an area in which no event will occur, and this radius was interpreted as an epicentral distance. Because of the direct trade-off between annual probability of occurrence and epicentral distance, the distance is essentially fixed by selection of the probability rather than by the recurrence relation. It should be emphasized that the concept of a "recurrence time" when applied to these probabilistic earthquakes is distinct from that of a localized source such as a fault. This results because, for the probabilistic case, we are defining the recurrence time by specifying an annual probability of occurrence. A distance is then calculated. Equivalently a distance could be specified, and then an annual probability or recurrence time could be calculated. For the case of a localized source, the annual probability of occurrence, and recurrence interval, are independent of epicentral distance. We have listed in table 2.5 epicentral distances at an arbitrary site in the study area for a magnitude 6-plus earthquake for various annual probabilities of occurrence.

Table 2.5 Probabilistic epicentral distances for magnitude 6-plus earthquakes in the study area. Recurrence rates on which these estimates are based are given table 2.4.

Recurrence rate used	Epicentral distance (Annual probability**) 1/100,000	1/50,000	1/10,000	1/1000
Wasatch Front max	2.4	3.4	7.7	24
Wasatch Front min	2.6	3.7	8.3	26
Wasatch Fault max	2.4	3.4	7.7	24
Wasatch Fault min	3.6	5.1	11	36

* All focal depths are assumed to be 7 km
** Probability of occurrence of the event with magnitude 6 or greater within the epicentral distance

Given the degree of uncertainty in recurrence of magnitude 6-plus earthquakes, the values listed in table 2.5 provide only a general indication of the potential for the local occurrence of events originating on "blind" structures. It seems clear, however, that for commonly used probabilities of occurrence, the epicentral distance for magnitude 6-plus events is likely to be less than 10 km. Applied to an arbitrary sub-area within the region, such as the area around a damsite, these calculations imply that for a wide range of annual probabilities (about 1 in 10 000 to 1 in 100 000), a near-field earthquake of magnitude 6-plus can be expected. As noted previously, ISB earthquakes in this magnitude range are not expected to produce surface rupture and are likely to occur on "blind" faults.

2.7 Summary

The study area lies within the seismically active Wasatch front area of the ISB. Earthquakes in the magnitude 3 to 5 range, which are felt over areas of up to 10 000 km^2, have commonly occurred in the study region. Smaller magnitude events, which usually are not felt, are widely distributed throughout a well-defined band of seismic activity which extends from northern Montana to northern Arizona, and passes through the study area. The presence of seismicity is interpreted as an indication of ongoing extensional tectonic deformation. Contemporary seismicity has been analyzed to help evaluate the potential for the occurrence of damaging earthquakes throughout the study area, and to characterize their likely effects.

Potential sites for large-magnitude earthquakes (magnitude greater than 6.5) are generally identifiable from geologic data, since these events tend to produce surface rupture which is preserved in the late Quaternary geologic record. The likely sites of smaller magnitude events are much more difficult to identify from either seismologic or geologic evidence. Moderate-magnitude earthquakes (magnitude less than 6.5) have not produced surface rupture, and poor correlation of contemporary seismicity to mapped geologic structures has been observed.

Although there have been only two large-magnitude earthquakes recorded within the ISB, there are important characteristics common to both events. Large magnitude earthquakes appear to nucleate at depths of about 15 km and rupture to the surface. Rupture is initiated at one end of the fault and propagates unilaterally. Fault planes are steeply dipping, with 45 to 60° dips. There is no indication that the fault planes become subhorizontal at depth, and the geodetic data are well explained by simple planar faults. A relationship of the fault plane with older thrust faults is suggested, but the fault planes extend into the basement rocks.

Earthquakes with magnitude less than about 6.5 may occur without apparent correlation to late Quaternary faults in the ISB. These events apparently occur on subsurface or "blind" structures which are not revealed in the surface geology. Other than in a general sense, the location of contemporary seismicity does not necessarily indicate the probable sites of future events of this size. The depth of nucleation of these moderate events is most likely to be in the 8-15 km range.

The estimation of average rates of occurrence and locations of earthquakes with magnitude less than about 6.75 has been treated with a probabilistic approach. Based on the historic earthquake record for the CUP study area, an earthquake of magnitude 6.0 or greater will occur closer than 1 km at an annual probability of 1 in 100,000 for any site.

Fault plane solutions obtained from individual events and groups of earthquakes indicated east-west extension on normal faults, but with local variations. The strikes of possible fault planes were similar in orientation to preexisting Laramide thrust faults. It therefore seems likely that the present state of stress provides conditions favorable to slip on these planes.

Although the Wasatch fault shows abundant geomorphic evidence of Holocene

movement, seismicity documented since 1962 shows no direct association with the fault. The presence of seismic gaps along much of the fault's length is intriguing, but offers no clues as to the timing of future large earthquakes.

3. QUATERNARY STRATIGRAPHY AND CHRONOLOGY

3.1 Introduction

Accurate mapping and dating of Quaternary deposits are critical to seismic hazard assessment because displacement of Quaternary deposits where they overlie faults is usually the chief evidence for fault activity in the recent geologic past. Understanding of the geomorphological development of an area on local as well as regional scales also requires maps of well-dated Quaternary deposits whose genesis is correctly interpreted. A geomorphological history of an area, in turn, is the means for assessing the degree to which landform development has been controlled by tectonism (including large-scale deformation as well as local faulting) and for estimating rates of deformation. Both indiviual fault assessment and regional tectonic geomorphology approaches are necessary for a full understanding of regional neotectonics and the resulting seismic hazard posed by tectonic structures in the region.

Below we outline the regional geomorphology and previous Quaternary geology studies in the Regional study area (fig. 1.1). Much of this section is devoted to a discussion of our age estimates for Quaternary deposits using several independent methods. Following this, we summarize our interpretation of the geomorphic history of the area based on our mapping and age estimates, but focusing on the fluvial terrace remnants along the Provo and Weber Rivers (pls. 1a and 1b). The detailed mapping of Quaternary deposits in the back valleys and assessment of specific faults is left to sections 4 through 6 where we discuss the neotectonics of specific areas within the Regional study area.

3.2 Previous Studies

Previous work on the Quaternary geology of the area has focused on the most extensive and easily correlated landforms and deposits. These include the erosion surfaces of the back valleys of the Wasatch Mountains; the shorelines and deposits of Lake Bonneville in Cache, Ogden, and Morgan Valleys; and the glacial deposits of the Wasatch, Bear River, and Uinta Mountains and the Wasatch Plateau. The colluvial and alluvial valley margin and fill deposits which overlie most of the mapped and inferred faults in the area have not been the subject of any detailed studies. However, the complilations of Stokes and Madsen (1961) and Hintze (1980) show some Quaternary deposits not mapped by others.

An earlier seismotectonic study for Soldier Creek Dam (Nelson and Martin, 1982) and studies for Joes Valley and Scofield Dams on the Wasatch Plateau (Foley and others, 1986) and for Monks Hollow Dam (Diamond Fork drainage)(Sullivan and others, 1987) are within the Central Utah Project Regional Seismotectonic Study area. Because these studies will review the Quaternary geology in these areas we will not discuss it here.

3.2.1 The back valleys of the eastern Wasatch Mountains

Although earlier authors (such as Davis, 1903) discussed the evolution of the Wasatch Front, Gilbert (1928) provided the first detailed discussion of the physiographic development of the Wasatch Range as a whole and the back valleys between it and the western terminus of the Uinta Mountains (pl. 1). Each of the back valleys was briefly described and Mantua, Ogden, and Morgan Valleys were suggested to be grabens with Parleys Park, Rhodes Valley, and Heber Valley inferred to be at least partially fault bounded. Gilbert (1928) concluded that the back valleys developed during uplift of the Wasatch Range as a horst, and that the cross drainage of the range is due to antecedence. More recently, Hunt (1982) attributes the transverse canyons of the Wasatch Range to a combination of superposition and antecedence termed anteposition. Threet (1959) and Hunt (1982) commented briefly on the physiographic development of most of the back valleys, but aside from soil surveys (Carley and others, 1980; Erickson and Mortensen, 1974) and generalized USGS quadrangle mapping no detailed studies of pre-Bonneville Quaternary deposits have been made. Except for comments on the diversion of the Provo River (Anderson, 1915; Gilbert, 1928; Baker, 1970, p. 7) and an abstract on pre-Bonneville terraces in the Weber Canyon by Eardley (1970), the river terraces of the area are also unstudied (Marsell, 1963). Of particular interest would be work by N.C. Williams in the headwaters of the Provo and Weber Rivers, referred to by Threet (1959), which has not been published.

3.2.1.1 Weber Valley erosion surface

The most detailed work on the Quaternary history of the area is that of Lofgren (1955) and especially Eardley (1933; 1944; 1955) and his students (Egbert, 1954; Schick, 1955; Coody, 1957). Eardley (1944; 1952; 1955) argued that the main relief features of the region, including the main lines of drainage, developed by north-south oriented folding and faulting beginning in the late Eocene. Faulting and folding continued in the early Oligocene with deposition of the Norwood Tuff and Keetley volcanics. A long period of erosion followed, lasting until early Pliocene time in Cache Valley and

possibly to late Pliocene time in Morgan Valley. Due to antecedence (Eardley, 1944), possibly basin capture in the early Cenozoic (Threet, 1959), or more likely a combination of antecedence and superposition termed anteposition by Hunt (1956; 1983) the Provo, Weber, and Ogden Rivers must have crossed the Wasatch Range near their present valleys by the end of the Pliocene. The Herd Mountain erosion surface, which Eardley felt was correlative with the Gilbert Peak surface of Bradley (1936) in the Uinta Mountins, was cut during this period of stability. Renewed faulting and uplift along many old faults in the late Pliocene elevated and greatly dissected the Herd Mountain erosion surface and extensive fanglomerates were deposited on the valley margins (for example, Lofgren, 1955).

The Weber Valley erosion surface of Eardley (1944) then gradually formed as fanglomerate deposition gave way to pediment development during another long period of relative stability in the Pliocene and early Pleistocene. Eardley (1944) pictured the Weber Valley erosion surface as consisting of almost all gently sloping pediments, ridge crests, and older alluvial and colluvial surfaces between the crest of the Wasatch Mountains to within a few hundred feet of present back valley floors. "Submature" topography was thought to have developed by the end of this period, but total relief approached that of today. Renewed movement on the Wasatch fault in Pleistocene time with eastward tilting of the Wasatch Mountain block (Eardley, 1933; Hunt, 1982) led to dissection of the Weber Valley erosion surface and deepening of the back valleys.

Two erosion surfaces of possible Quaternary age, the Rendezvous Peak surface and the McKensie Flat surface, have been described from southern Cache Valley by Williams (1958) and Mullens and Izett (1964). Blau (1975, p. 22) reports that Williams considers the basin on the north flank of James Peak (see discussion in sec. 4.3) to be a remnant of the McKensie Flat surface. Because both surfaces are lower than Eardley's (1944) Herd Mountain erosion surface, they may have formed during development of the Weber Valley erosion surface. Both authors (Williams, 1958; Eardley, 1955) feel the Herd Mountain surface once extended over the Cache Valley area. Other studies of Quaternary features in Cache Valley are limited to Lake Bonneville deposits which cover most of the valley.

In a thoughtful review of the geomorphology of the area, Threet (1959) accepted this overall scheme, but the Herd Mountain surface was abandoned and the Weber Valley surface restricted to "local pediment remnants of questionable cyclic significance." Threet (1959) lists nine types of topographic surfaces present in the eastern Wasatch Mountains and argues that very few of these features can be shown to have been produced by cyclic periods of erosion and pediment formation. For instance, he interprets the Herd Mountain surface as a stripped structural surface with no necessary cyclic significance because it coincides with flat-lying resistant beds and does not have a cover of datable deposits. Campbell (1978) also notes that the Weber Valley erosion surface was not entirely developed prior to block faulting in the back valleys as suggested by Eardley (1944). Thus, many of the features grouped by Eardley (1944) into the Weber Valley erosion surface developed during the late Tertiary and Quaternary, but they may well span this entire period.

3.2.1.2 Glaciation

Atwood (1909) did the first detailed survey of glaciation in the Wasatch Mountains. At least two periods of glaciation, the latter less extensive than the former, were recognized based on differences in downvalley moraine position and in the degree of dissection and soil development of moraines and weathering of valley walls. Most glacial deposits occur on the western slope of the mountains, but only a few of these areas have been investigated in more detail than in the studies by Atwood (1909). In particular, early work by Atwood (1909), Hunt and others (1953), Richmond (1964), and Morrison (1965) in Little Cottonwood and Bells Canyons (where moraines and deposits of Lake Bonneville interfinger) led to the recent chronology of Madsen and Currey (1979) and their students. These latter investigators found evidence for: "an early canyon-mouth glaciation, probably during isotope stage 6; on a till, a paleosol dated at about 26 ka; overriding that soil, a later canyon-mouth glaciaton probably beginning prior to about 19 ka; a midcanyon deglacial pause prior to 12.3 ka; an upper-canyon deglacial pause prior to 7.5 ka; and late Holocene periglaciation." Except for the study by Anderson and Anderson (1981) on Mount Timpanogos and the regional mapping of Bryant (written communication, 1983), recent work on glacial deposits in the rest of the range consists only of generalized mapping of undifferentiated moraines (Stokes and Madsen, 1961; Baker and Crittenden, 1961; Crittenden and others, 1966; Bromfield and others, 1970; Hintze, 1980) and scattered abstracts (for example, Nielson, 1979).

3.2.2 Lake Bonneville

The rise of Lake Bonneville and outwash deposition during the glacial periods of the Pleistocene filled the valleys with alluvium and in the case of Cache, Ogden, and Morgan Valleys with lake sediment (for example, Legette and Taylor, 1937). The most recent fall of Lake Bonneville allowed the alluvial trenching of Bonneville deposits in Morgan and Ogden Valleys (Eardley, 1944; Lofgren, 1955) and the lower Provo River Canyon (Hunt, 1982).

The extensive work on the chronology of the deposits of Lake Bonneville begun by Gilbert (1890) and continued by Hunt and others (1953), Eardley and others (1957), Bissell (1963), Broecker and Kaufman (1965), and Morrison (1965) among many others has been revised and summarized by Scott and others (1983). The following summary of the lake chronology is taken from the abstract of that latter paper: "A substantially modified history of the last two cycles of Lake Bonneville is proposed. The Bonneville lake cycle began prior to 26 ka; the lake reached the Bonneville shoreline about 16 ka. Poor dating control limits our knowledge of the timing of subsequent events. Lake level was maintained at the Bonneville shoreline until about 15 ka, or somewhat later, when catastrophic downcutting of the outlet caused a rapid drop of 100 m. The Provo shoreline was formed as rates of isostatic uplift due to this unloading slowed. By 13 ka, the lake had fallen below the Provo level and reached one close to that of Great Salt Lake by 11 ka. Deposits of the Little Valley lake cycle are identified by their position below a marked unconformity and by amino acid ratios of their fossil gastropods. The maximum level of the Little Valley lake was well below the Bonneville shoreline. Based on the degree of soil development and other evidence, the Little Valley lake cycle may be equivalent in age to marine oxygen-isotope stage 6."

3.2.2.1 Morgan and Ogden Valleys

Studies of late Quaternary faulting along the Wasatch Front (for example, Swan and others, 1980) have been greatly facilitated by dated Bonneville deposits associated with the Wasatch fault. Bonneville deposits cover much of the floors of Morgan and Ogden Valleys, but no shoreline deposits continuously cover the margins of the valleys where valley-bounding faults have been mapped or inferred.

Lake Bonneville silts and sands in Morgan Valley were described by Gilbert (1890, p. 163-164) and mapped by Mullens and Laraway (1973). A considerable amount of deltaic material was deposited in the valley during the high stand of Lake Bonneville and the valley was filled with sediment after the fall to the Provo level below the north end of the valley (Eardley, 1944). Legette and Taylor (1937), Lofgren (1955), Doyuran (1971), and Sorensen and Crittenden (1979) provide somewhat more detail on the Quaternary sediments of Ogden Valley. Sands and silts deposited over the floor of the valley up to an elevation of 1570 m (5150 ft) are typically 12 m thick. The floor of the valley is graded to the Provo Lake level at the mouth of Ogden Canyon. Under the last-cycle Bonneville sediments lie about 30 m of dark, micaceous silt which is underlain by stream-laid gravels and sands more than 120 m thick in the center of the valley.

It should be emphasized that although many of the deposits of Lake Bonneville can be identified by their lithology and elevation, none have been dated directly in either Morgan or Ogden Valleys.

3.2.2.2 Cache Valley

William's (1962) mapping of Bonneville and Provo lake stage shorelines and deposits in southern Cache Valley (pl. 1) remains the only detailed work on the Quaternary geology of a large part of the valley since Gilbert's (1890) work in the area. Mullens and Izett (1963; 1964) followed William's (1962) mapping in their study of the Paradise area. Maw's (1968) chronology of Lake Bonneville events in the Cutler Dam area agrees with Scott and others (1983), except for a reversal of flow through the Bear River narrows with a rise and fall of the lake between the Bonneville and Provo high stands (possibly due to the isostatic effects outlined by Curry (1980)). Unlike workers in Utah Valley, Williams (1962), Mullens and Izett (1964), and Maw (1968) found little or no direct evidence for an "Alpine" stage of the lake predating the Bonneville stage which agrees with the more recent interpretations of Scott and others (1983).

3.2.3 Western Uinta Mountains

The Central Utah Project Regional Study area includes only the westernmost portion of the Uinta Mountains. The Quaternary chronology of the Uintas is reviewed in the recent seismotectonic study for Upper Stillwater and Taskeech damsites (Martin and others, 1985), and by Nelson and Osborn (in press). For this reason, we mention here only the few studies that deal with the western end of the Uintas. Other regional chronologies are discussed in the section on regional correlation (sec. 3.6.2).

Atwood's (1909) survey of glaciation was the first detailed study of Quaternary features in the Uinta Mountains and is still the basic reference for the western Uintas. Atwood (1909) recognized the deposits of two episodes of glaciation and found limited evidence for a third, earlier glacial event. Moraines of each event and adjacent outwash deposits were mapped in all the major drainages.

Other studies in the western Uintas are limited to largely unpublished theses. Eskelsen (1953, p. 31) traced the high-level Tertiary Gilbert Peak erosion surface of Bradley (1936) as far west as the North Fork of the Duchesne River and commented briefly on drainage development in the Soapstone Basin area. As part of a glacial and periglacial geomorphic study of a part of the Uinta Mountains, Barnhardt (1973) identified a late "Pinedale" advance of very limited extent in the western Uinta Mountains for which he obtained a minimum radiocarbon age of 8.2 ka. Younger deposits at Bald Mountain consist only of talus cones, avalanche boulder tongues, and protalus ramparts, with some dating control provided by a second radiocarbon age and lichenometry. The thesis work of Grogger (1974) is for the most part concerned with Holocene and Neoglacial deposits in the upper parts of drainages on the north flank of the Uintas and provides only generalized descriptions of the moraines deposited during earlier periods of major glaciation. Grogger (1974) offers no detailed relative-age data or mapping to substantiate his application of a more detailed subdivision of Bradley's (1936) glacial chronology (which was based on correlations to Blackwelder's (1915) studies in the Wind River Mountains) to the moraines in the Uintas (Grogger, 1974, p. 43) or his correlation of this sequence to others in the western United States (Grogger, 1974, p. 202).

3.2.4 Bear River Range

Young (1939) and Williams (1964) recognized glacial deposits of two ages in the Bear River Range (pl. 1). Williams (1964) correlated these deposits with "Pinedale" and "Bull Lake" deposits elsewhere in the Rocky Mountains. In a more recent, detailed study of the entire range, DeGraff (1976a) mapped a number of geomorphic features including cirques (1979), moraines, landslides, alluvial fans (1975), and relict patterned ground (1976b). At least three periods of glaciation (Bull Lake, early Pinedale, late Pinedale) were identified and seven ages of alluvial fans mapped using soil profile descriptions and the relationship of the younger fans to Lake Bonneville deposits. A more recent manuscript on the alluvial fans by DeGraf, Oaks, and Southard (written communication, 1983) used relative position, degree of dissection, and the degree of soil profile development to identify four episodes of alluvial fan deposition which they tentatively correlated with interglacial-interlacustrine intervals during the late Pleistocene. The most recent episode of alluvial fan deposition is younger than the Provo shoreline and probably coincides with semi-arid conditions during the mid-Holocene. The youngest of these fans are the only relative-age dated features that cross potentially active faults on the eastern margin of Cache Valley.

3.3 Stratigraphic Terminology

Most Quaternary chronology studies in the Rocky Mountain region have subdivided deposits of the most recent major glaciations into those deposited during Bull Lake glaciation and Pinedale glaciation and designated older deposits as pre-Bull Lake (Richmond, 1965; Madole, 1976; Pierce, 1979). These groupings are usually based on relative-age (RD) data (Birkeland and others, 1979) such as relative position in the landform sequence, landform morphology (such as the degree of humockyness of moraines or of dissection of terraces), the degree of soil development, and surface weathering data (for example, number of boulders on the surface, thickness of weathering rinds on clasts, boulder weathering pit size and depth; see Burke and Birkeland, 1979). Because the criteria used to subdivide these deposits into these relative-age groups are relative within the local sequence, deposits from different sequences in the region assigned to the same relative-age group may be of widely differing ages (Pierce, 1979; Colman and Pierce, 1981; Porter and others, 1983). Confusion has resulted from the use the terms "Pinedale", "Bull Lake", and "pre-Bull Lake" by some as names for glacial events with specific ages and by others (for example, Nelson and others, 1979) as informal regional diachronous allostratigraphic units (North American Committee for Stratigraphic Nomenclature, 1983) with time-transgressive boundaries based on major, mappable weathering and morphologic breaks in the local late Quaternary sequence. Following Pierce (1979) and Porter and others (1983) we use these terms to name the more recent major Quaternary glaciations in the Rocky Mountains and assume ages (discussed below) for the deposits of each glaciation in our area based on correlations using RD data to numerically-dated glacial deposits.

The marine oxygen-isotope record (Shackelton and Opdyke, 1973) indicates several periods of extensive worldwide glaciation younger than 600 ka, but older than dated Bull Lake deposits (discussed below). Eardley and others (1973) and McCoy (1981) have found evidence for events possibly correlative with some of these glaciations in the Bonneville Basin. Uranium-series dates on speleothems suggest two cold intervals during the younger part of this period in the northern Rocky Mountains (Harmon and others, 1977) and Madole and Shroba (1979) have estimated the age of a pre-Bull Lake till in the Colorado Front Range at 400-500 ka. But no easily correlatable pre-Bull Lake deposits have been numerically dated in the central Rocky Mountains.

Oxygen-isotope ratios from the marine record suggest the more recent major periods of world-wide glaciation date from roughly 210-290 ka (stage 8), 130-190 ka (stage 6), and 15-75 ka (stages 2,3,4) (Shackelton and Opdyke, 1973), but correlation of even these more recent major climatic events between marine and continental records is difficult at best because of the complexity of responses to climate change and the problems of dating deposits beyond the range of radiocarbon dating. However, numerical ages have been obtained for Bull Lake deposits in several areas (Pierce and others, 1976; Szabo, 1980; Colman and Pierce, 1981; Shroba and others, 1983) and a number of ^{14}C analyses set upper limits on the ages of the various phases of Pinedale glaciation (Porter and others, 1983; Carrara and others, 1984). Many Bull Lake deposits are probably about the same age as those at West Yellowstone dated at about 140 ka (Pierce and others, 1976; Shroba and others, 1983); some others may correlate with the glacial event identified by Colman and Pierce (1981) dated at about 60 to 70 ka. Although some may be as old as

this latter event, most deposits assigned to a major Pinedale glaciation are probably in the range of 15 to 30 ka (Pierce, 1979; Porter and others, 1983). Most latest Pinedale deposits are older than 11.5 ka (Madole, 1980; Porter and others, 1983; Carrara and others, 1984), and those deposited during Pinedale deglaciation probably date from 15-18 ka.

Throughout the Central Utah study area, where we lack numerical-age estimates based on independent data (discussed below) we use relative-age (RD) data (chiefly, measures of the degree of soil development) first to group our deposits into different relative-age groups (RAGs) and then secondly, to correlate the RAGs with numerically-dated Pinedale and Bull Lake deposits in the Rocky Mountain region. On this basis we assume that the undated deposits of each RAG are about the same age as dated deposits with similar soil development characteristics in the Rocky Mountain region.

3.4 Relative and Numerical Dating

In our mapping of Quaternary deposits in the Central Utah Project area we have attempted to date deposits wherever practical using several RD and numerical-age techniques (as defined by Colman and Pierce, 1981). Only radiocarbon analysis and tephrochronology provide reliable numerical ages. Ages calculated using other methods are based on a number of presently unverifiable assumptions. However, where several of these methods can be used independently in the same landform sequence and compared with regional correlations based on RD data, we can be reasonably confident of our age estimates.

3.4.1 Soil Profile Relative Dating

3.4.1.1 Relative-dating methods

Relative dating (RD) using the characteristics of soil profiles described on landforms was by far the most common dating method we used. Other surface and subsurface weathering techniques are much less suitable because of the large differences in lithologies (even locally) from one area to another. Methods utilizing differences in landform morphology such as qualitative or quantitative measures of fluvial dissection (for example, Bull and McFadden, 1977) or scarp morphology (for example, Hanks and others, 1984) were not particularly useful either because no single type of Quaternary depositional landforms are well-preserved or widely distributed in the Central Utah Project area.

Despite the many problems in using relative soil development data for chronocorrelation (Pierce, 1979; Birkeland, 1984a), careful comparison of quantitative relative-age data from deposits of unknown age with data from similar deposits in areas where numerical ages are available allows first approximation age limits to be set for some of the deposits of unknown age.

3.4.1.2 Indices of soil development

To compare the degree of development of soils within the CUP Regional study area with each other and with soils in other areas where numerical ages are available, measures of soil development are needed. A number of indices which express how soil properties vary with time have been calculated using profile data from chronosequences in the Rocky Mountain region (for example, Birkeland, 1984a; Meierding, 1977; Machette, 1978; Shroba and Madole, 1979; Pierce, 1979; Colman and Pierce, 1986; Hall and Heiny, 1983; Shroba and Birkeland, 1983) and elsewhere (for example, Harden and Marchand, 1977; Burke and Birkeland, 1979; Torrent and others, 1980; Meixner and Singer, 1981; Gile and others, 1981; Muhs, 1982; Harden and Taylor, 1983; Birkeland, 1984b; Rockwell and others, 1984). A chronosequence is an array of related soils in the same area that differ primarily in the length of time over which they formed (Jenny, 1941, 1980). Other soil-forming factors such as climate, organisms, topography, and parent material texture and lithology are assumed to be relatively constant for all soils in the sequence. Chronosequences and the many problems in the solution of chronofunctions have been reviewed by Stevens and Walker (1970), Vereeken (1975), Yaalon (1971,1975), Bockheim (1980), Harden and Taylor (1983), and Birkeland (1984a).

The soil properties that vary the most systematically with time in the Rocky Mountain region include those related to horizon thickness, color, texture, and carbonate accumulation. Indices which express changes in these properties include simple, widely-used indices (for example, depth to base of Cox horizon and maximum clay increase), profile summations (for example, Machette, 1978), and the indices of Harden (1982) and Harden and Taylor (1983). Harden's indices are a refinement of those proposed by Bilzi and Ciolkosz (1977) and incorporate in a quantitative way most of the concepts represented by development indices used previously in the western U.S. The profile development index (Harden, 1982) is particularly useful because the degree of development of all selected properties can be objectively summarized in a single value. However, it should be emphasized that many of these indices are derived from ordinal scale data and cannot be quantitatively compared using parametric methods. To avoid these problems we follow Harden and Taylor (1983) in using x-y plots to compare indices for different soils (methods of Nelson and Taylor, 1985).

3.4.1.3 Relative age groups based on soil development in the eastern Wasatch Mountains

To determine broad, relative-age groupings of soils on Quaternary deposits in the eastern Wasatch Mountains we selected 16 soil profiles from the area which had some independent age control. The age control for each of these profiles is discussed in the section on the area where they occur. Age control consisted of direct association of deposits with moraines inferred to be of Pinedale (15-18 ka) or Bull Lake (130-150 ka) age, amino acid ratios on snails from deposits beneath soils, and, in one case, a radiocarbon date beneath a soil. All of the soil development indices of Harden (1982) and Harden and Taylor (1983) and g/cm^2 and g/cm^3 clay and carbonate values for these 16 soils were compared using two-variable plots. The plots demonstrated the general age dependency of changes in color, textural, and structural properties and clay and carbonate accumulation, but no plot produced distinct, widely-separated groups of soils. A plot of the rubification index versus the non-arid total profile index provided groupings most consistent with our previously determined ages (fig. 3.1). Using standardized profile depths, weighted means of profile properties, or other commonly used soil development indices did not produce more distinct or consistent groupings.

Only four broad groups of soils of differing relative age (RAGs) can be distinguished on figure 3.1. However, almost all previous studies attempting to demonstrate the utility of soil development indices for estimating ages have used chronosequences where most of the soil forming factors could be assumed to be relatively constant. The variablility in source rock lithologies, parent material texture, site surface stability, local variation in rainfall, and distance from major dust sources for our soils is greater than for the soils studied in most other chronosequences. In this regard, it is probably typical of many areas where mapped Quaternary deposits are undated but need to be (for example, Hall and Heiny, 1983). Considering the variablility of the soil forming factors, the distribution of soils in figure 3.1 is, perhaps, more consistent than might be expected.

Using our independent age estimates for the soils in each relative-age group (RAG) and considering regional correlation of major soil properties and

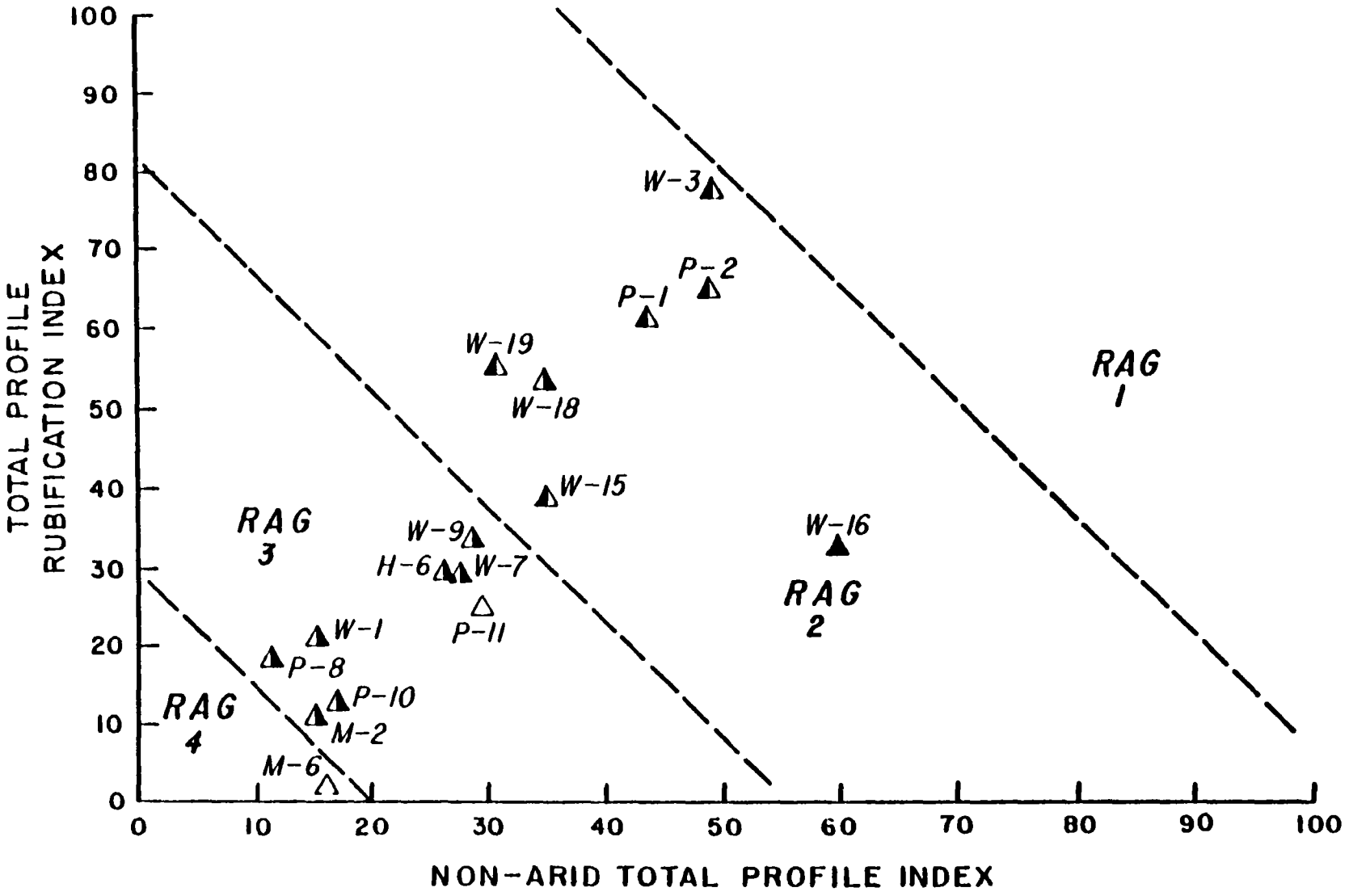


Figure 3.1 Soils indices graph for all soil profiles in the Regional study area with some independent age control.

glacial events, rough ages are assigned to each RAG. The sediments in which soil W-16 in relative-age group 1 (RAG 1) is developed are >730 ka (sec. 3.5.1), but this soil has been eroded and is not necessarily representative of this great age. On the basis of our estimated age for RAG 2, RAG 1 deposits are probably >200 ka. In most regional comparisons (Richmond, 1965; Madole, 1976) others have used the same reasoning to place correlative deposits in a "pre-Bull Lake" age category. Age estimates for the soils in RAG 2, except for WR-18 (discussed in sec. 3.5.1), suggest deposition of the sediments on which these soils are developed during the Bull Lake glaciation near the end of oxygen-isotope stage 6 (130-150 ka). The thick, reddish argillic horizons of these soils are similar to those in soils on Bull Lake age deposits elsewhere in the Rocky Mountain region (Shroba and Birkeland, 1983; Hall and Heiny, 1983, table 11) which have been dated in this age range in a few areas (discussed above). Except for soil P-11, the soils in RAG 3 are developed on deposits associated with Pinedale deglaciation (15-18 ka) or with the fall of Lake Bonneville from its high stand (14-15 ka). These soils are variable, some with cambic B horizons and others with thin argillic horizons, but these characteristics are typical of soils in this age range in the region (Shroba, 1980; Shroba, 1984; Machette, 1985b; Southard and Southard, 1985). Soil P-11, on coarse, cobbly modern floodplain deposits, may be no more than a few hundred years old. Extensive infiltration of silt and minor amounts of clay into these coarse gravels (probably during flood subsidence) and bright orange groundwater staining of the gravels give this profile soil indices much higher than are typical of Holocene soils. A radiocarbon date on peat beneath the C horizon of soil M-6 (sec. 4.2) shows the soil is <8 ka. The fine-grained character of the slopewash deposits in which this soil is developed may account for its high carbonate content (7 g/cm^2) and high non-arid index (fig. 3.1) relative to our other Holocene soils in the area. Thus, RAG 1 soils are thought to be <10-14 ka.

3.4.1.4 Rates of secondary carbonate and clay accumulation

Rates of total secondary carbonate accumulation in soils and to a lesser extent secondary clay accumulation have proven useful in estimating the age of soils in a number of areas in the arid and semi-arid western U.S. (Machette, 1985a; 1985b; Pierce, 1979; Shroba, 1984; Colman and others, 1986; Reheis, 1984). Except in areas of very calcareous parent material or deposition of carbonate by ground water, most carbonate in soils on stable sites is derived from aerosolic sources such as dust and from Ca++-enriched rainfall (Machette, 1985a; Gile and others, 1981). Similarly, much of the secondary clay in argillic horizons originated as dust or precipitation nucleii falling on the soil surface and this clay has been translocated into the B horizon (Colman, 1982; Shroba and Birkeland, 1983; Shroba, 1984). Increased rates of precipitation and accompanying vegetation changes due to higher soil elevations or climate change can leach soils of carbonate (Machette, 1985a; Birkeland, 1984a). It is also clear that dust influx rates must have varied greatly in most regions with the climate changes of the Quaternary (Bachman and Machette, 1977; Mayer, 1984; MacFadden and Wells, 1984). Thus, age estimates based on total carbonate or clay accumulation values cannot be relied on for soils significantly younger than the last interglacial (125 ka) (unless many regional calibration (independently dated) soils are available) because of the probable major changes in accumulation rates over this period. However, over longer time spans (50-100 kyr), multiple cycles of climate change tend to attenuate accumulation rate changes

and this results in relatively more accurate age estimates for older soils (Machette, 1985a; 1985b; Shroba and Birkeland, 1983; Colman and others, 1986).

Based on the above studies, we attempted to use total secondary clay and carbonate values as an independent method of assessing the age of soils in the eastern Wasatch Mountains (methods of Machette, 1978; 1985a; 1985b; Nelson and Taylor, 1985).

Total secondary carbonate values provide only minimum age estimates for our soils because most soils have little or no carbonate and those few (6) independently-dated soils that do yield carbonate accumulation rates significantly higher than those for most other areas in the region. Based on 3 soils (M-2, M-6, table 4.1; H-6, table 5.3) in Morgan and Heber Valleys, latest Pleistocene-Holocene rates could be as high as 1 $g/cm^2/kyr$; however, groundwater may have added carbonate to soil M-2 and primary carbonate values are difficult to estimate for soils M-6 and H-6. Our longer-term (0-150 ka) rate (again based on 3 soils, W-3, W-15, W-19, tables 3.2 and 3.3) is roughly half (0.5 $g/cm^2/kyr$) of our Holocene-latest Pleistocene rate. Based on their locations east of the crest of the Wasatch Mountains, it is unlikely that latest Pleistocene-Holocene carbonate accumulation rates for our soils are higher than those calculated by Shroba (0.5 $g/cm^2/kyr$) (in Scott and others, 1982) for soils near Salt Lake City. Based on rates of about 0.15 $g/cm^2/kyr$ for Fisher Valley (Colman and others, 1986), 0.14 $g/cm^2/kyr$ for the Beaver area (Machette, 1985a; 1985b), and maximum rates of 0.14-0.26 $g/cm^2/kyr$ for Spanish Valley (Harden and others, 1985) elsewhere in Utah, Quaternary rates in the eastern Wasatch Mountains may well have been <0.2 $g/cm^2/kyr$. We use 0.5 $g/cm^2/kyr$ as a maximum rate to estimate minimum ages. Even so, this rate combined with amino acid age estimates for deposits on which some of our most carbonate-rich soils are developed suggests some of our secondary carbonate estimates are too high.

Many more of our soils for which we have independent age estimates have significant secondary clay accumulations than those with secondary carbonate, but less is known about clay rates and their spacial and temporal variablilty in the region than is known about carbonate rates. Shroba (1984), working with soils on till in the Rocky Mountains, derived rates of 0.02-0.04 $g/cm^2/kyr$ for the Holocene, 0.01-0.06 $g/cm^2/kyr$ for the latest Pleistocene (Pinedale), and 0.03-0.04 $g/cm^2/kyr$ for the late and middle Pleistocene. Middle Pleistocene rates from Fisher Valley are much higher (0.11 $g/cm^2/kyr$)(Colman and others, 1986) similar to late Quaternary rates of 0.14 $g/cm^2/kyr$ from McCall, Idaho, which are partially due to clay formation by in-situ weathering of basaltic parent material (Colman and Pierce, 1986). Our rate for the eastern Wasatch Mountains is about 0.08 $g/cm^2/kyr$, but the amount of scatter in our data, especially for latest Pleistocene soils, should be noted (fig. 3.2). Because clay accumulation is so variable in soils that are <50 ka, this average rate is less useful for estimating the age of younger soils. We are uncertain whether or not our rate applies to soils >200 ka in the eastern Wasatch Mountains because we have no dated profiles >150 ka. However, rates from Fisher Valley suggest assumming an average rate of 0.08 $g/cm^2/kyr$ for the middle Quaternary in the eastern Wasatch Mountains is reasonable.

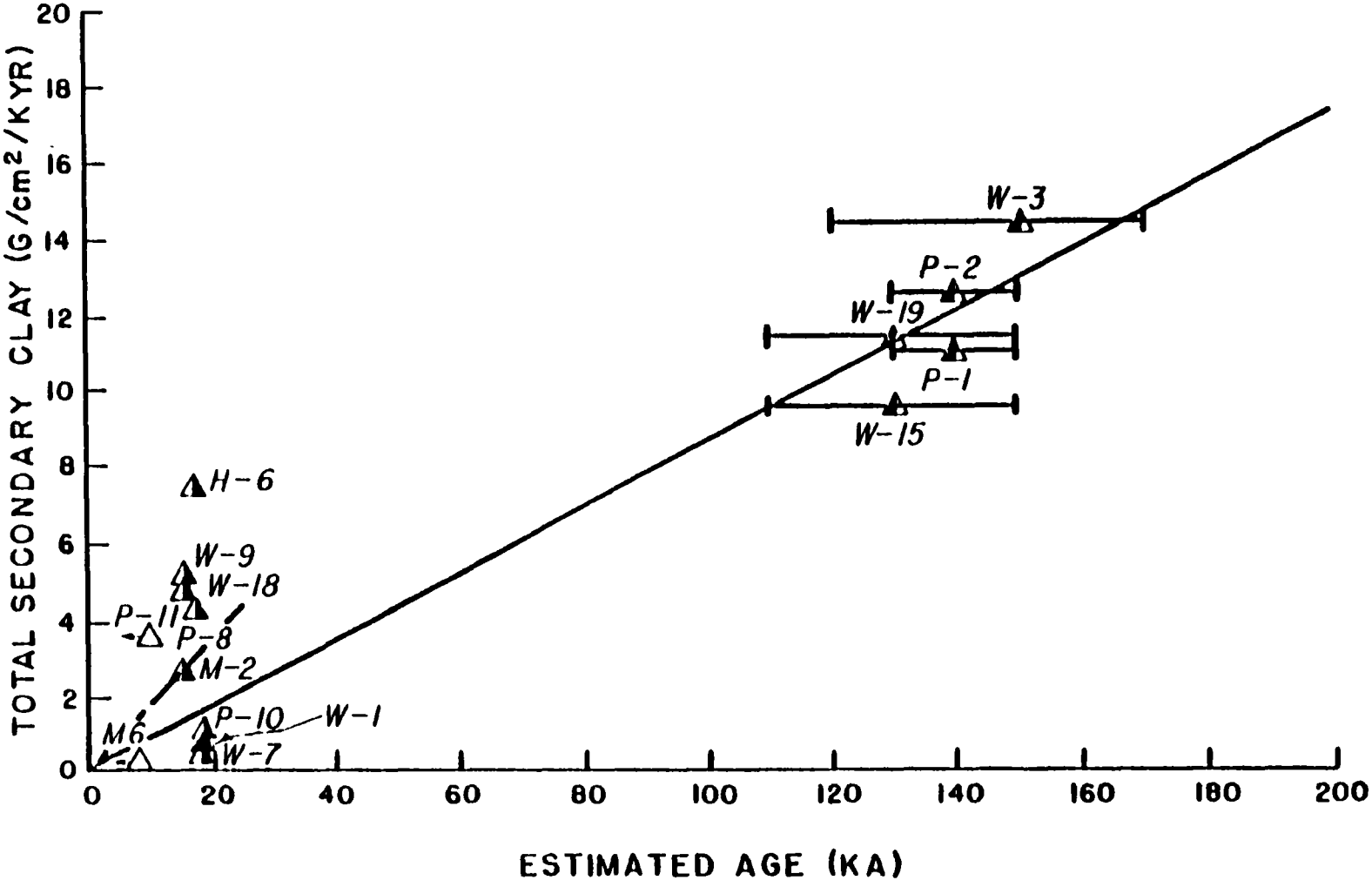


Figure 3.2 Total secondary clay content and estimated ages for soils with some independent age control in the Regional study area.

3.4.2 Age Estimates Using Amino Acid Ratios

Amino acid ratios derived from the analysis of the organic matrix within carbonate fossils have proven useful in the relative dating and correlation of a variety of Quaternary stratigraphic units worldwide (Schroeder and Bada, 1976; Wehmiller, 1982). This methodology, termed aminostratigraphy by Miller and Hare (1980), is valid within a region as long as all samples have had very similar temperature histories and the if the amino acids in the species analyzed racemize at about the same rate (Williams and Smith, 1977). Thus, D/L isoleucine ratios on fossil gastropods from Morgan Valley (table 4.2) and along the Weber River Valley (table 3.1) can be used to determine the age of the gastropods relative to each other with no further assumptions.

Numerical age estimates are much more difficult to obtain from amino acid ratios. These estimates require accurate kinetic models of amino acid racemization (AAR) along with estimates of the temperature histories for the fossil samples. A $\pm$ 1°C uncertainty in the effective diagenetic temperature (EDT)(integrated chemical effect of the sample's temperature history) results in a 20% uncertainty in the age estimate. Still, D/L stereomeric ratios on carbonate shells have provided useful age estimates (often minimum ages) in many areas (Wehmiller, 1982). If sufficient independently-dated calibration samples are available from the same region as the samples to be dated, fairly accurate age estimates for the undated samples can be made (for example, Bada and Protsch, 1973).

Three types of parameters must be estimated in order to use the kinetic models proposed for amino acid racemization (the dependency of aIle/Ile ratios on time and temperature) in mollusks (Wehmiller and Belknap, 1978; Lajoie and others, 1980; Miller and others, 1983) to estimate ages from snail aIle/Ile ratios: 1) genus-dependent parameters in the kinetic equations must be estimated for the snail genera analyzed, 2) the non-linearity of racemization (epimerization) kinetics in carbonate fossils must be quantified, and 3) the temperature history of the sample must be estimated including the effects of near surface heating due to shallow (<2 m) burial.

The rate of the isoleucine epimerization reaction has been shown to vary by as much as a factor of two from one mollusk genus to another (Miller and Hare, 1980). Only recently have attempts been made to use amino acid ratios measured on terrestrial and freshwater gastropods in dating Quaternary deposits (Miller and others, 1979; 1982; McCoy, 1981; Scott and others, 1983; Harmon and others, 1983; Nelson and others, 1984). Detailed kinetic data are available for only one of the gastropod genera we have analyzed, Vallonia (Nelson and others, 1984), but aIle/Ile ratios on the other genera used from the same sites (Miller and Hare, 1980; Nelson, unpublished data) suggest that isoleucine racemizes at about the same rate in all genera used in the eastern Wasatch Mountains.

For this reason, in all our calculations for all genera we used kinetic data for Vallonia. In any case, paleotemperature uncertainties and the non-linearity of racemization kinetics have a much more profound effect on the age estimates than do inter-generic differences in racemization rates. Pyrolysis of modern shells (Miller and others, 1982; Miller and others, 1983) and analysis of independently dated fossil shells (Wehmiller and Belknap, 1978; 1982) show that the isoleucine racemization reaction in fossil shells

Table 3.1 D-alloisoleucine/L-isoleucine ratios in the total (free + peptide-bound) amino acid fraction and calculated ages for fossil gastropods from alluvial and colluvial sediments along the Weber and Provo River valleys, Utah.

INSTAAR Lab No. (Univ. of Colo.)	Species	Depth below surface (m)	Mean sample weight (mg)	Average no. of shells used	No. of sample preps	Mean Total alle/Ile ratio*	Minimum age estimates Holocene EDT~	Quaterna EDT**
Deer Creek Reservoir (EDT = 6.8-7.2 deg C); A on pl. 1B								
DAN-177	Oreohelix cf. strigosa	2	25.6	<1	5	0.32+0.06	97-103	398-427
East shore of Rockport Reservoir (EDT = 7.2-7.7oC); B on pl. 1B								
DAN-218A	Oreohelix cf. strigosa	2.8	11.0	<1	1	0.19	49-54	202-221
DAN-218B	Oreohelix cf. strigosa	2.8	8.7	<1	4	0.30+0.05	82-90	337-369
DAN-218C	Pupilla blandi	2.3	2.5	2	1	0.13	36-39	146-160
DAN-218D	Vallonia gracilicosta	2.3	1.9	3	1	0.13	36-39	146-160
DAN-174A	cf. Catinella	2.3	3.0	1	1	0.20	57-62	232-254
DAN-174B	Pupilla sp.	2.8	3.7	1	1	0.18	51-55	208-227
DAN-173	cf. Catinella	5.4	3.7	1	2	0.14+0.01	39-42	159-174
West shore of Rockport Reservoir (EDT = 7.1-7.6oC); C on pl. 1B								
DAN-175	Oreohelix cf. strigosa	1.7	11.4	<1	3	0.29+0.02	81-88	331-362
Wanship gravel pit (EDT = 7.2-7.7oC); D on pl. 1B								
DAN-215A	Vallonia sp.	5	0.5	1	1	0.15	42-46	171-187
DAN-215B	cf. Catinella	5	2.7	1	1	0.18	51-55	208-227
DAN-213	Oreohelix cf. strigosa	20	3.2	<1	1	0.39	110-120	451-494
Pecks Canyon gravel pit (EDT = 7.3-7.8oC); E on pl. 1B								
DAN-211A	cf. Catinella	4.2	5.6	1	3	0.14+0.01	38-42	117-171
DAN-211B	Pupoides albilabus	4.0	2.4	1	2	0.13+0.02	35-38	109-118
Gravel pit west of Coalville (EDT = 7.3-7.8oC); F on pl. 1B								
DAN-214A	Oreohelix cf. strigosa	8	6.4	<1	1	0.14	34-37	138-151
DAN-214B	Oreohelix cf. strigosa	8	9.2	<1	1	0.20+0.03	51-56	210-230
DAN-214C	Vallonia cf. cyclophorella	8	0.9	1	2	0.11+0.02	29-32	92-100
DAN-214D	Pupilla blandi	8	3.0	3	4	0.11+0.01	29-32	92-100
DAN-217	cf. Catinella	10	4.2	<1	1	0.17	47-51	192-210
Fan southwest of Henefer (EDT = 7.3-7.8oC); G on pl. 1A								
DAN-176,192	Oreohelix cf. strigosa	2.1	16.3	<1	4	0.15+0.02	37-40	150-164
DAN-191	Oreohelix cf. strigosa	2.7	19.3	<1	3	0.39+0.01	108-118	443-485
Terrace north of Henefer (EDT = 7.4-7.9oC); H on pl. 1A								
DAN-210	Oreohelix cf. strigosa	3.0	18.1	<1	3	0.05+0.003	7.1-7.8	
DAN-210D	Vallonia cf. cyclophorella	2.8	4.0	2	1	0.05	11.4-12.4	

* Alle/Ile ratio (peak area) measured using methods of Miller and Hare (1980). Mean ratios include one standard deviation. Extraneous values rejected using methods of Dixon (1965).

Age calculated using a linear kinetic model of isoleucine racemization (eqn. 18 in Williams and Smith (1977), with $k' = 0.77$, a modern ratio of 0.025 for Oreohelix and 0.014 for other species (Nelson, unpub. data), Arrhenius parameters determined for Vallonia by Nelson and others (1984), and values of constants in in Arrhenius eqn. 9 in Williams and Smith (1977).

~ Age calculated using an EDT (Wehmiller, 1977) for the Holocene estimated using instrumental mean annual temperatures in the region (NOAA, 1981), limited soil temperature data (Conrad, 1965, and unpub. data of Lael Harvey, Soil Conservation Service, Coalville, UT), and data of Miller and others (1982).

** Age calculated using an EDT for the late Quaternary in this region of 8 deg C less than present mean annual temperature (Nelson and others, 1984)(for example, Wehmiller and Belknap, 1982). Age range calculated using +/-0.25oC range in estimated EDT.

follows linear kinetics at least to aIle/Ile ratios of 0.25-0.4 (Wehmiller, 1982). For older samples with higher ratios, the apparent reaction rate decreases by 0.3 to 0.1 of the initial rate over a transition zone of variable width between ratios of 0.25-0.6 (Kriausakal and Mitterer, 1980; Wehmiller, 1982). The point at which the reaction rate decreases (break point) and the amount of decrease are dependent both on the shell genus and probably on the absolute temperature history of the shell as well (Wehmiller, 1982). AIle/Ile ratios from snails in the Weber River Valley (table 3.1) are all <0.4 and most are <0.2, and therefore, we do not need to consider non-linear models for minimum age estimates on these samples. The older samples from Morgan Valley (table 4.2) have ratios as high as 0.61. For these samples, with ratios >0.4, we assume reaction rate parameters typical of those available for other mollusks (Wehmiller, 1982): a rate decrease of 0.2 of the initial rate and a break point of 0.4.

Attempting to estimate the temperature histories (EDTs) of the snail samples adds even more uncertainty to our age estimates. Because of the lower temperatures during the Pinedale glaciation, the average EDT experienced by our pre-Holocene samples was considerably lower than the Holocene effective temperature. Recent paleotemperature estimates for the last glacial-interglaical cycle (the last 125 kyr) in the Rocky Mountain region (for example, Mears, 1981; McCoy, 1981; McCoy and Williams, 1983: Barry, 1983) suggest the period 25 to 125 ka experienced an average temperature of about 10°C less than present MAT in the eastern Bonneville Basin and that the full glacial-interglacial change in temperature was between 9°C and 16°C, similar to values suggested by Pierce (in Porter and others, 1983) using different methods. McCoy (1981) used aIle/Ile ratios and radiocarbon ages to estimate temperatures 8.5°C below MAT for the same area from 11 to 15 ka. Using pollen data from Clear Lake cores in the northern California coast ranges, Adam and West (1983) estimate only 7°C to 8°C temperature change during the last glacial cycle, but with a period of fluctuating climate averaging 4°C to 5°C below present about 75 to 125 ka. Most recently, Nelson and others (1984) have estimated an average EDT for the period 0-600 ka in the Rocky Mountain region of 8°C less than present mean annual temperature.

To calculate minimum age estimates for our snail samples we used the average Quaternary EDT estimated by Nelson and others (1984) because it is the simplist and most reasonable paleotemperature model available with the present limited database. The model consists only of an EDT of 8°C less than the present MAT for the middle and late Quaternary. This value was estimated using some of the same snail species analyzed here and it applies to the same region. Furthermore, almost all of our samples appear to have experienced at least one full glacial-interglacial cycle making an average Quaternary EDT for the region a reasonable approximation of the integrated thermal history of each sample. Almost all of our samples have been buried deeply enough that an increases in ratios due to near-surface heating effects (Wehmiller, 1977; Miller and others, 1982) do not need to be considered. Considering the large uncertainties in the temperature estimates used, more complex models (for example, Wehmiller, 1982; Nelson and VanArsdale, 1986) are not justified. Although there is considerable uncertainty in these calculations, for several reasons (discussed in the literature cited above), these age estimates are much more likely to be minimum rather than maximum ages.

3.4.3 Relative dating using magnetic polarity of sediment

3.4.3.1 Quaternary polarity stratigraphy

Paleomagnetism has been used extensively for determining the age of Cenozoic rocks and sediments. The earth's magnetic field polarity has reversed in the past and the record of these reversals is preserved in lavas and sediments. The geomagnetic polarity time scale is a record of normal and reversed polarities compiled from dated paleomagnetic sequences (Cox, 1969). This time scale can be used for correlation of stratigraphic sequences whose general age is known, but for which radiometric dates are not available. The most recent major polarity change occurred about 730 ka (Mankinen and Dalrymple, 1979); most Quaternary deposits containing only one component of magnetization in a normal direction are probably younger than 730 ka. Quaternary deposits formed prior to the begining of the present normal polarity epoch will retain a reversed component of magnetization unless this component is so strongly overprinted with more recent normal polarity components that the original reversed component cannot be recognized. Because earlier normal polarity epochs preceded the last major reversed epoch prior to 900 ka, it is difficult to determine the age of Quaternary sediments with a normal polarity.

3.4.3.2 Polarity evaluation and age estimates

A paleomagnetic study of Quaternary sediments in Keetley Valley and others sites in the eastern Wasatch Mountains (pl. 1) was conducted to determine whether sampled sediments retained a well-defined reversed polarity component and were therefore likely to be >730 ka (App. A).

Samples from 12 of the 30 sites sampled contain a strong indication of a reversed component. On this basis samples from sites JT-2, JT-7A, JT-7B, JT-11, J-13, J-16, HV-2, DC-1, and WV-16 are considered to be >730 ka. Some samples from the following drill cores from Keetley Valley also contain an unambiguous reversed component and thus must also be at least this old: DH-R-101, DH-R-110, DH-R-111, DH-R-114, DH-R-115.

Several samples contain scattered remanence directions which are relatively stable upon demagnetization or directions which deviate away from the present normal field direction upon demagnetization. Although these samples contain a suggestion of reversed magnetization (App. A), the data are not compelling enough for us to conclude that these sediments are reversed. We group these sediments with those that are dominated by normal components and conclude nothing about their age on the basis of the paleomagnetic analysis. These include samples from sites JT-8, JT-9, J-4,J-17,HV-1, JT-10, J-6A, J-6B, J-15, RV-1, WD-1.

3.4.4 Other Dating Methods

3.4.4.1 Tephrochronology

Volcanic eruptions during the Quaternary produced tephra which was deposited over much of the western U.S. Layers of tephra found in sediments downwind from the volcanic source (often slightly reworked by colluvial and alluvial processes), when correlated using morphologic, optical, and chemical

properties with tephra of known age, are used to date the deposits in which the layers occur. Tephra from two major volcanic centers, Long Valley in eastern California and Yellowstone in northwestern Wyoming, have been identified in central Utah (Izett, 1982; Nash and Pope, 1977; Izett and Wilcox, 1982). Two of these tephras, the Lava Creek B Ash and the Bishop Ash, dated elsewhere at 620 ka (Izett and Wilcox, 1981) and 730 ka (Izett and others, 1970) respectively, have distinct mineralogical and chemical characteristics which allow them to be readily identified. Both of these tephras were found in Keetley Valley, but nowhere else in the eastern Wasatch Mountains. A one-meter-thick bed of ash discovered in soil pit JS-15 (fig. 3.3) was identified as Lava Creek B ash by Ray Wilcox (U.S. Geological Survey, Denver, written comunication, 1983) on the basis of petrographic criteria. The Bishop Ash was found in a nearby roadcut and identified in the same manner (discussed in sec. 5.6).

3.4.4.2 Radiocarbon analysis

Radiocarbon analysis is the most accurate and commonly used method for dating late Quaternary deposits, but its use is severely limited in the eastern Wasatch Mountains because of the lack of suitable material for analysis associated with deposits near faults. The two ^{14}C ages from a single peat deposit in Morgan Valley (sec. 4.2) are the only radiocarbon dates obtained from our studies in the eastern Wasatch Mountains. Except for some minimum ages from fault scarp deposits along the Strawberry fault (Nelson and VanArsdale, 1986), we are aware of only two published ^{14}C ages from the area east of the Wasatch Front. However, special organic concentration proceedures for soil samples (Scharpenseel, 1971; Mathews, 1980; Kihl, 1975) and ^{14}C atom counting by accelerator techniques (Stuiver, 1978; Tucker, 1981) are being used in other seismotectonic studies (Nelson and VanArsdale, 1986; West, 1984; Foley and others, 1986) in the central Rocky Mountains.

3.4.4.3 Fault and terrace scarp morphology

Analysis of topographic profiles across fault scarps developed in alluvium is the most widely used method of estimating the recency of fault movement in the Basin and Range (for example, Wallace, 1977; Bucknam and Anderson, 1979; Nash, 1980; Machette, 1982; Colman and Watson, 1983; Hanks and others, 1984; Mayer, 1984). Most often the relation between fault scarp height or offset and maximum fault-scarp-slope angle have been used as a relative-age measure, but other parameters such as the degree of scarp crest rounding (Wallace, 1977; Sterr, 1981; Peterson, 1983) also appear to be age dependent. However, these methods require a reasonably large sample of profiles across scarps of significantly differing heights for realtive-age comparisons to be made. Additional problems in comparing profile data from one area to another include differences in climate, lthology, aspect, and fault displacement histories (single vs. multiple events of different sizes) all of which affect the rate of scarp degradation and thus, the measures of scarp morphology. For example, a slope-height plot for the Strawberry Valley fault scarps on the southeast edge of the eastern Wasatch Mountains was not particularly useful in estimating their age (Nelson and Martin, 1982; Nelson and VanArsdale, 1986).

No fault or stream scarps of sufficient extent and of differing height in similar lithologies of unconsolidated materials were found in the eastern

Wasatch Mountains. Thus, the other methods discussed above were judged to be most-likely to yield accurate age estimates.

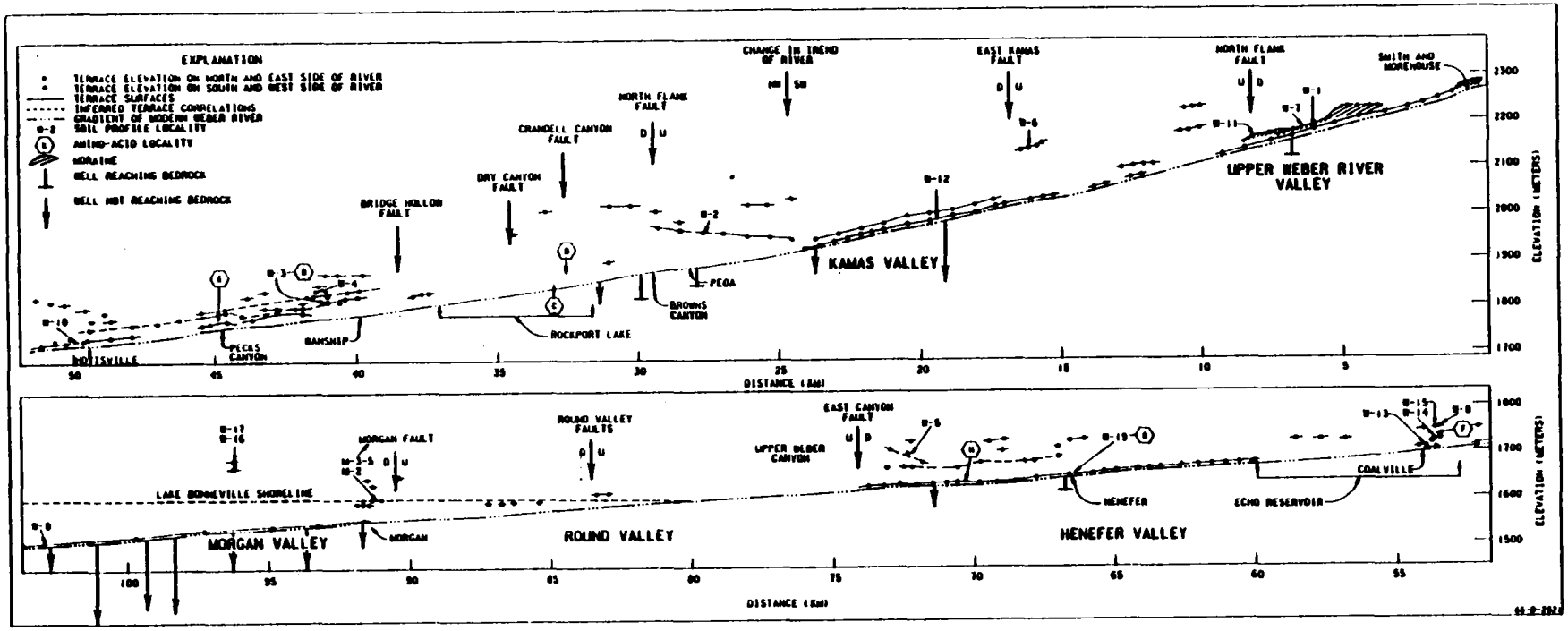


Figure 3.3 Weber River terrace profiles.

3.5 Quaternary history of Weber and Provo Rivers

The drainage basins of the Provo and Weber Rivers encompass most of the CUP Regional study area (pl. 1). Although they are nowhere continuous for any significant distance, the fluvial terrace and fan remnants preserved along the center of these two river valleys are the most widely distributed Quaternary landforms in the area. Terraces have the additional advantages of providing stable sites where erosion is usually not significant. Thus, soils should reflect the age of the terrace surface at these sites to a greater degree than soils developed on less stable landforms such as moraine crests. For the same reason, fault scarps, if present, should be preserved on the terraces longer than on other landforms in unconsolidated deposits in the area. Thus, we chose to collect most of our soils data for relative-age dating from terrace and fan remnants along the Provo and Weber Rivers. The soils data combined with other RD data allow us to outline the history of the development of these drainage basins and to estimate the contribution to this development made by neotectonic movement on faults in the area. The pre-Quaternary history of the area is reviewed in section 3.6.

3.5.1 Weber River drainage

The Weber River drainage basin is much larger than the basins of other streams in the Wasatch Mountains, encompasing an area of about 6200 km^2 in the central Wasatch and western Uinta Mountains. The river heads in the cirques of the Uintas, flows westward and northward through several back valleys, and then cuts directly west through the core of the Wasatch Range into Salt Lake Valley (pl. 1). Remnants of fluvial terraces and alluvial fans graded to them along several portions of the river valley provide a partial record of Quaternary events in the basin. Most remnants are highly dissected, and only the lowest terraces are continuous for more than short distances (fig. 3.3). Terrace and fan remants can be grouped into 1) those in the headwaters area including northern Kamas Valley, 2) those along the central portion of the valley from Peoa to the East Canyon fault, and 3) those along the lower portion of the river in Morgan Valley. No remnants are preserved in the narrow upper and lower canyons of the river below the central portion of the valley (fig. 3.3).

3.5.1.1 Upper Weber River Valley

Remnants of at least five fluvial surfaces of at least three different relative ages are preserved in the upper Weber River Valley and Kamas Valley above Rockport Reservoir (fig. 3.3).

The lowest major terrace, 10-12 m above the modern Weber River, appears to be continuous from above the mouth of Smith and Moorehouse Canyon to the northwestern corner of Kamas Valley, except for a short reach in the narrow canyon where the river enters the valley. This terrace grades into a set of arcuate moraines deposited by a glacier issuing from Smith and Moorehouse Canyon (Atwood, 1909). About 2 km above the mouth of the canyon, moraines and glacier trimlines are found near the valley floor indicating that the Weber River Valley glacier reached this position in the valley. Athough they are small and partially buried by outwash, the moraines in this area are hummocky with sharp crests. This morphology and the distance of these moraines from the cirques in the mountains suggests these moraines were

deposited during the later part of the last major glaciation (Atwood, 1909), the Pinedale glaciation. Exposures of coarse, bouldery gravel capped by 20-40 cm of loess in the 12 m terrace confirm it is an outwash terrace deposited during deglaciation. Soil development indices (figs. 3.1 and 3.2) for the soil on this terrace near the moraines (soil W-1, table 3.2) suggest it is of latest Pleistocene age (<20 ka); the outwash terrace probably dates from 15-18 ka (Porter and others, 1983).

A second terrace at 25 m above the river is preserved between two dissected moraines on the south side of the river about 6 km below Smith and Moorehouse Canyon (fig. 3.3). A soil pit in the terrace exposed gray, sandy till, like that in the moraines, indicating that at least this part of the terrace is ground moraine rather than outwash. Development indices for soils on the till are low (figs. 3.1 and 3.4) indicating a Pinedale age for the moraines. However, a 5-m-deep exposure in the eastern moraine shows coarse outwash with a 60-cm-thick, reddish argillic horizon developed on it underlying gray till. Alluvial fan terraces from a small drainage on the south side of the river about 5 km down river from the 25 m terrace appear graded to a former floodplain at about this relative elevation. Thus, although Pinedale glaciers advanced down the valley as far as the moraines as recently as 15-18 ka, a valley train of outwash was apparently deposited at this relative elevation (about 25 m) in the valley long before the deposition of the Pinedale moraines and the 12 m outwash terrace.

Two small, dissected remnants of surfaces at 76 m and 122 m above the river are preserved about 2 km west of the moraines adjacent to the 25-m terrace. The slight down-valley gradient of these remnants suggests they are remnants of fluvial terraces, but small alluvial fans and colluvium obscure their surfaces.

A terrace about 10 m above the north side of the Weber River extends from the mouth of the upper Weber canyon to near the western edge of Kamas Valley where it gradually merges with present floodplain deposits. On the basis of relative elevation above the river this terrace correlates with the 12 m terrace up valley (fig. 3.3), but soils on this lower terrace in northern Kamas Valley suggest it is much older. Development indices (fig. 3.4) and total secondary clay for a soil on this terrace (soil W-12, table 3.2) suggest it is somewhat younger than most soils in RAG 2. However, other soils on this terrace (unpub. profile descriptions, Lael Harvey, Soil Conservation Service (SCS), Coalville, UT, 1982) have thick (60-100 cm), clay-rich B horizons with 5YR color hues indicating a RAG 2 age. Regional correlations suggest this terrace is probably related to Bull Lake glaciation (130-150 ka)(discussed in sec. 3.4).

A 25-m terrace of coarse, bouldery gravel also extends across most of the northern end of Kamas Valley. Eroded soils near the edge of this terrace have >30-cm-thick argillic horizons overlying carbonate with stage II to III morphology. However, coalesing alluvial fans along the hills which form the northern edge of Kamas Valley appear to overlie or grade into the 25-m terrace and soils on the fans are more strongly developed than those on the 10-m terrace. Most fan soils have >100-cm-thick very clay-rich B horizons (unpub. SCS profile descriptions, soil WR-2, table 3.2), some with stage III to IV carbonate. Although development indices place soil W-2 on the distal edge of a fan in RAG 2 (fig. 3.4), this soil has been eroded, and its stage

Table 3.2 Selected properties of soils on fan and terrace remnants along the Weber River, north central Utah (continues next 2 pages).

Profile	Horizon*	Average depth (cm)		Parent material	Munsell dry color	ESTIMATED PERCENT BY VOLUME Pebbles (0.2-8cm)	Cobbles (8-25cm)	Boulders (>25cm)	PERCENT BY WEIGHT~ Sand (2-0.5mm)	Silt (50-2um)	Clay (<2um)	Percent** organic matter	Percent§ carbonate
W-1	A1	0	12	loess	10YR 5/3	10	5	0	44	35	21	3.8	0.0
	A2	12	28	loess	10YR 6/4	10	5	0	49	31	19	1.1	0.0
	2Bt	28	53	outwash	10YR 5/4	20	30	30	60	25	15	0.4	0.0
	2CB	53	80	outwash	7.5YR 5/4	20	30	30	81	10	10	0.5	0.0
	3Cox	80	180+	outwash	7.5YR 5/4	20	30	30	55	28	18	1.8	0.0
W-2	Ap	0	4	loess	7.5YR 5/3	2	5	0	40	34	26	5.8	2.5
	Akj	4	18	loess	10YR 5/3	2	5	0	40	31	29	3.4	3.7
	AB	18	43	loess	10YR 7/2	5	5	2	45	21	34	1.6	46.4
	2Btk1	43	75	alluvium	5YR 5/4	10	15	5	48	14	38	1.0	62.8
	2Btk2	75	142+	alluvium	5YR 5/7	10	10	2	52	23	25	0.3	14.7
W-3	Ap	0	27	loess-colluvium	7.5YR 7/3	2	0	0	23	50	27	1.3	0.6
	Bt	27	69	loess-colluvium	7.5YR 6/4	2	0	0	21	40	39	0.6	0.6
	2Bt	69	80	alluvium	7.5YR 6/6	20	10	0	31	37	32	0.9	1.4
	2Btkm	80	110	alluvium	7.5YR 7/4	5	2	1	56	23	21	1.2	65.5
	2Bkm	110	150	alluvium	7.5YR 8/0	10	10	2	72	20	8	0.4	45.1
	2Btk	150	200	alluvium	5YR 7/6	40	10	2	63	26	10	0.4	22.0
	2Bk	200	255	alluvium	5YR 6/6	60	10	1	76	17	7	0.1	10.0
	2C	255	355+	alluvium	5YR 6/6	60	10	1	76	17	7	0.1	7.9
W-4	Ap	0	8	colluvium	7.5YR 5/2	5	5	0	33	34	34	2.9	15.9
	Ak	8	24	colluvium	7.5YR 6/2	5	5	0	30	32	38	1.8	21.9
	AB	24	44	colluvium	7.5YR 7/3	2	3	0	32	33	35	1.4	40.4
	Btk	44	59	colluvium	7.5YR 5/4	2	3	0	41	30	29	0.6	25.1
	2Bkm	59	122	alluvium	7.5YR 8/0	10	10	0	43	25	32	0.6	75.3
	2Bk1	122	177	alluvium	7.5YR 5/4	30	10	3	49	31	20	0.4	52.5
	2Bk2	177	240+	alluvium	7.5YR 6/4	20	30	3	51	36	13	0.2	11.0
W-5	Ap	0	10	loess-colluvium	7.5YR 5/3	5	2	0	12	56	32	1.3	0.0
	A	10	23	loess-colluvium	7.5YR 5/3	5	2	0	13	58	29	1.3	0.0
	Bt	23	54	loess-colluvium	5YR 4/4	5	2	0	10	34	56	0.6	0.0
	Bkj	54	73	loess-colluvium	5YR 4/4	2	2	0	16	69	16	0.6	8.0
	Bk1	73	95	loess-colluvium	5YR 8/0	2	2	0	14	64	22	0.6	40.0
	Bk2	95	154+	loess-colluvium	5YR 4/6	2	2	0	16	64	20	0.1	25.0
W-6	A	0	18	loess-colluvium	7.5YR 3/4	5	5	5	56	29	15	1.7	0.0
	AB	18	27	loess-colluvium	7.5YR 4/4	5	5	5	50	29	21	0.8	0.0
	2Bt	27	83	alluvium	5YR 4/5	10	20	15	65	15	21	0.6	0.0
	2Bk1	83	126	alluvium	7.5YR 8/0	10	10	10	74	24	2	0.1	14.4
	2Bk2	126	184+	alluvium	5YR 8/0	10	20	10	71	18	11	0.6	44.8

* Horizon nomenclature of Guthrie and Witty (1982) and Birkeland (1984) except that master K horizon is not used.
~ Particle size distribution of <2 mm fraction using sieve-pipette methods (for example, Carver, 1971) and a Sedigraph for some silt-clay fractions with prior removal of carbonates and organic matter using methods of Jackson (1956).
**: Percent organic matter by method of Walkley and Black (1934).
§ Percent carbonate by method of Dreimanis (1962).

Table 3.2 Selected properties of soils on fan and terrace remnants along the Weber River, north central Utah (continues next page).

Profile	Horizon*	Average depth (cm)		Parent material	Munsell dry color	ESTIMATED PERCENT BY VOLUME Pebbles (0.2-8cm)	Cobbles (8-25cm)	Boulders (>25cm)	PERCENT BY WEIGHT~ Sand (2-0.5mm)	Silt (50-2um)	Clay (<2um)	Percent** organic matter	Percent‡ carbonate
WR-7	A1	0	13	loess	10YR 2/3	5	5	0	25.2	57.4	17.4	3.1	0.0
	A3	13	42	loess-till	10YR 4/3	10	20	0	29.8	52.4	17.8	1.6	0.0
	2Bw	42	115	till	7.5YR 7/4	20	15	10	57.9	33.6	8.5	0.3	0.0
	2Cox	115	157+	till	7.5YR 7/4	20	15	10	70.9	22.1	7.0	0.1	0.0
WR-8	Ap	0	7	loess	7.5YR 6/3	0	0	0	29.3	49.8	20.9	2.4	3.7
	Bwj	7	21	loess	7.5YR 6/4	0	0	0	28.3	50.9	20.8	2.3	3.6
	2Bkm	21	62	loess-colluvium	7.5YR 6/4	0	0	0	30.8	50.2	19.0	0.8	25.4
	2Bk	62	141+	loess-colluvium	10YR 7/4	0	0	0	38.8	49.1	12.1	0.7	23.8
WR-9	Ap	0	12	loess	7.5YR 4/2	5	3	0	21.9	40.1	38.0	2.0	0.0
	BA	12	22	loess	7.5YR 5/4	5	3	0	22.2	31.6	46.2	0.7	0.0
	Bt	22	47	loess	7.5YR 6/4	3	0	0	29.2	41.3	29.5	0.6	0.0
	2Bt	47	69	alluvium	7.5YR 6/6	15	3	0	53.8	33.5	12.7	0.4	0.0
	2Cox1	69	120	alluvium	10YR 6/5	20	20	0	85.3	7.9	6.8	0.3	0.0
	2Cox2	120	171+	alluvium	7.5YR 6/5	20	20	0	88.1	5.9	6.0	0.3	1.1
WR-10	Ap	0	22	loess	7.5YR 5/3	1	0	0	45.2	35.3	19.5	2.3	0.7
	2Bw	22	52	loess-colluvium	7.5YR 5/3	1	0	0	50.7	34.3	15.0	1.3	11.6
	2C	52	71	loess-colluvium	7.5YR 5/3	1	0	0	54.2	30.3	15.5	0.8	14.5
	3Btb	71	99	alluvium	7.5YR 6/4	1	0	0	42.8	36.5	20.7	0.6	10.0
	3Cb	99	115	alluvium	7.5YR 6/3	50	0	0	81.6	10.6	7.8	0.5	12.1
	4Btb	115	144	alluvium	7.5YR 5/6	30	10	0	73.7	16.7	9.6	0.4	17.0
	4Coxb	144	165+	alluvium	7.5YR 4/6	30	10	0	79.2	13.4	7.4	0.3	16.8
WR-11	A	0	18	loess-till	7.5YR 3/3	10	5	0	59.4	28.1	12.5	5.1	0.1
	2Bw	18	22	loess-till	7.5YR 5/4	10	5	0	55.2	34.4	10.4	0.6	0.1
	2C1	22	45	till	5YR 7/3	15	15	30	77.2	17.5	5.3	0.5	0.1
	2C2	45	100+	till	5YR 7/4	15	15	30	70.2	21.4	8.4	0.5	0.1
WR-12	Ap	0	16	loess	7.5YR 4/3	5	0	0	36.7	39.6	23.7	4.3	0.6
	AB	16	45	loess	7.5YR 3/3	5	0	0	29.1	40.3	30.6	2.0	0.4
	Bt	45	70	loess	7.5YR 4/4	3	0	0	32.9	38.3	28.8	1.4	0.3
	2Bt	70	110	outwash	7.5YR 4/4	5	30	5	62.4	21.8	15.8	1.1	0.1
	2Btkj	110	160	outwash	7.5YR 4/4	15	20	10	77.1	13.1	9.8	1.3	3.0
	2Bk	110	185+	outwash	7.5YR 6/4	15	20	10	79.7	11.9	8.4	0.7	5.5
M-13	A	0	3	loess	10YR 3/3	0	0	0	31	47	22	6.9	0.1
	Bt1	3	27	loess	7.5YR 5/4	5	0	0	29	47	24	1.3	0.2
	Bt2	27	42	alluvium	7.5YR 6/4	10	5	0	30	45	26	1.2	0.1
	2Bk1	42	49	alluvium	7.5YR 7/4	10	5	0	63	21	16	2.0	35.2
	2Bk2	49	75	alluvium	5YR 5/6	20	5	0	87	8	5	0.8	26.0
	3Cox	75	90	alluvium	7.5YR 6/4	5	0	0	93	4	3	0.2	4.6
	4Ck	90	145	alluvium	7.5YR 7/3	40	25	5	86	9	5	1.2	30.0
	4Ckj	145	180+	alluvium	7.5YR 6/4	40	25	5	92	5	3	0.2	10.3

* Horizon nomenclature of Guthrie and Witty (1982) and Birkeland (1984) except that master K horizon is not used.
~ Particle size distribution of <2 mm fraction using sieve-pipette methods (for example, Carver, 1971) and a Sedigraph for some silt-clay fractions with prior removal of carbonates and organic matter using methods of Jackson (1956).
** Percent organic matter by method of Walkley and Black (1934).
‡ Percent carbonate by method of Dreimanis (1962).

Table 3.2 Selected properties of soils on fan and terrace remnants along the Heber River, north central Utah.

Profile	Horizon#	Average depth (cm)		Parent material	Munsell dry color	ESTIMATED PERCENT BY VOLUME Pebbles (0.2-8cm)	Cobbles (8-25cm)	Boulders (>25cm)	PERCENT BY WEIGHT~ Sand (2-0.5mm)	Silt (50-2um)	Clay (<2um)	Percent## organic matter	Percent$ carbonate
H-14	A	0	6	loess	10YR 5/3	5	0	0	25	64	12	4.5	4.7
	2Bt	6	21	alluvium	10YR 5/4	10	5	0	24	55	21	1.7	3.9
	2Btk	21	29	alluvium	10YR 7/4	15	5	0	23	55	22	0.9	36.0
	3Btkb	29	48	alluvium	7.5YR 8/4	30	5	0	67	26	7	0.7	49.6
	3Ckb	48	59	alluvium	10YR 8/3	70	10	0	71	24	5	0.7	51.2
	3Ckjb	59	70+	alluvium	10YR 8/3	65	10	0	74	23	3	0.3	10.8
H-15	Ap	0	17	loess	10YR 5/3	20	0	0	49	29	23	2.3	0.2
	A	17	35	alluvium	10YR 4/4	20	20	0	47	27	26	2.1	1.1
	2Bt	35	52	alluvium	7.5YR 5/6	5	5	0	52	26	22	1.0	4.4
	2Btk	52	63	alluvium	7.5YR 7/3	5	5	0	51	28	21	1.0	33.2
	3Bk1	63	103	alluvium	7.5YR 5/8	10	20	20	59	26	15	0.7	44.0
	3Bk2	103	130+	alluvium	7.5YR 7/6	40	5	5	67	25	8	0.1	21.8
H-16	A	0	25	colluvium	10YR 4/3	10	25	5	46	28	27	2.1	0.4
	BA	25	36	colluvium	5YR 5/4	10	25	5	40	22	38	1.3	0.2
	Bt1	36	81	loess-colluvium	5YR 6/4	5	5	0	33	35	32	0.5	0.1
	Bt2	81	122	loess-colluvium	5YR 6/5	5	5	0	34	35	31	0.3	0.1
	Btkj	122	137+	loess-colluvium	5YR 6/4	5	5	5	39	34	27	0.1	9.8
H-17	Ap	0	13	colluvium	10YR 3/3	5	10	10	49	31	20	2.8	0.4
	A	13	30	colluvium	10YR 3/3	5	10	10	45	27	28	2.5	0.2
	Bt1	30	48	alluvium	7.5YR 4/4	10	20	20	48	13	39	1.0	0.6
	Bt2	48	91	alluvium	5YR 4/6	10	20	20	55	14	31	0.4	0.4
	Bt3	91	127+	alluvium	5YR 4/6	10	20	20	56	15	29	0.3	0.5
H-18	Ap	0	9	loess	7.5YR 5/4	0	0	0	42	45	13	2.5	0.0
	A	9	24	loess	7.5YR 6/4	0	0	0	42	43	15	2.1	3.2
	AB	24	42	loess	7.5YR 6/4	0	0	0	40	44	16	1.9	1.3
	Bt1	42	58	loess	5YR 6/6	0	0	0	33	48	19	0.7	0.0
	Bt2	58	114	loess	5YR 6/6	0	0	0	32	49	19	0.4	0.0
	BC	114	130	loess	7.5YR 6/6	0	0	0	42	44	14	0.4	0.0
	Cox	130	154	loess	7.5YR 6/8	2	0	0	75	19	7	0.2	0.0
	2Cox	154	187+	alluvium	7.5YR 7/6	35	2	0	94	3	3	0.1	0.0
H-19	Ap	0	10	loess-colluvium	7.5YR 5/4	10	2	0	39	43	19	3.0	13.8
	A	10	19	loess-colluvium	7.5YR 5/4	10	2	0	36	44	20	2.0	11.8
	Bt	19	34	loess-colluvium	7.5YR 7/4	10	2	0	32	49	19	1.6	14.6
	2Bk1	34	120	loess	7.5YR 8/3	5	0	0	51	44	5	0.7	58.0
	2Bk2	120	169	loess	7.5YR 8/5	8	1	0	34	61	6	0.4	21.4
	2Bkj	169	225	loess	7.5YR 7/6	8	1	0	39	54	7	0.3	16.8
	3Btkb	225	265+	loess	5YR 6/6	8	1	0	52	36	12	0.3	31.2

Horizon nomenclature of Guthrie and Witty (1982) and Birkeland (1984) except that master K horizon is not used.
~ Particle size distribution of <2 mm fraction using sieve-pipette methods (for example, Carver, 1971) and a Sedigraph for some silt-clay fractions with prior removal of carbonates and organic matter using methods of Jackson (1956).
Percent organic matter by method of Walkley and Black (1934).
$ Percent carbonate by method of Allison and Moodie (1965, p. 1387).

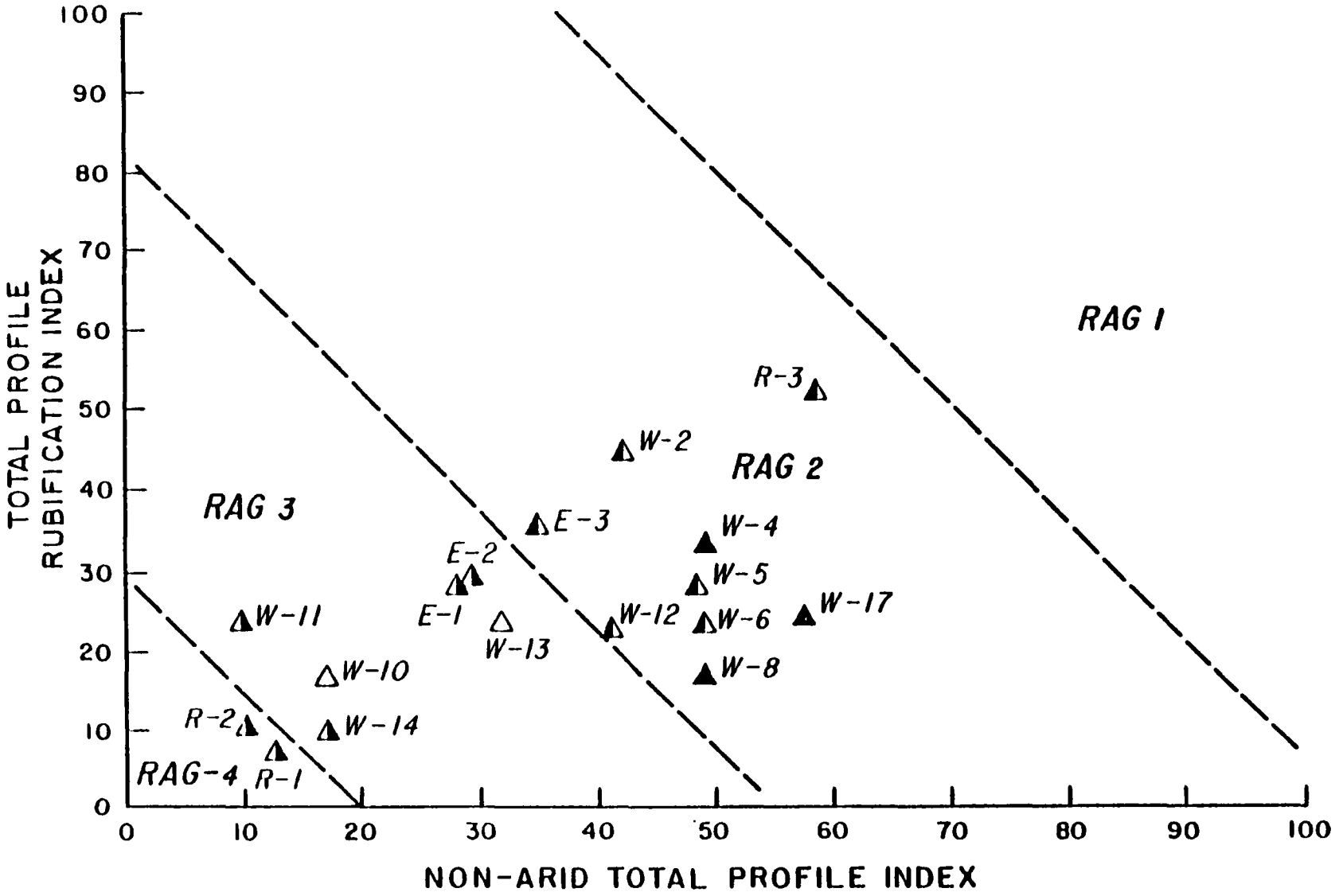


Figure 3.4 Rubification and non-arid profile indices for soils in the Weber River Valley, East Canyon area, and Parleys Park area.

IV carbonate morphology and 32 g/cm$_2$ of secondary clay suggest it is much older. On this basis the 25-m terrace and the associated alluvial fans are probably in RAG 1 (pre-Bull Lake) and are >200 ka and possibly 300-400 ka (sec. 3.4).

A soil pit (soil WR-6, table 3.2) on the terrace remnant 120 m above the river at the northeast corner of Kamas Valley exposed coarse, bouldery gravels with at least stage IV carbonate (dense carbonate prevented a bulldozer from deepening the pit to the base of the carbonate). Secondary clay in the argillic horizon overlying the carbonate (15 g/cm^2) suggests an age of roughly 190 ka (fig. 3.2). Solely on the basis of relative elevation, this surface may correlate with the small isolated remnant farther up the Weber valley or with remnants of small strath terraces cut on the Keetley volcanics near the northwest corner of Kamas Valley (fig. 3.3). However, because this surface 1) may have been displaced by faulting (discussed in sec. 5.6), 2) is of such limited extent, and 3) is probably quite old (>mid-Quaternary), correlations are speculative.

3.5.1.2 Central Weber River Valley

In the central part of the Weber River Valley between Browns Canyon and the escarpment of the East Canyon fault (fig. 3.3), remnants of alluvial fans are preserved at the mouths of tributary drainages; all other remnants of fluvial surfaces are small and discontinuous. There are at least five major levels of fluvial features (fig. 3.3), but reconstruction of former floodplains is difficult because only the lowest terrace extends contiuously along the valley for more than 2 km. More importantly, fan remnants that were once graded to the same level of the river now occur at widely varying elevations because 1) the cone shape of the fans makes their axial portions higher than their flanks, 2) the fans vary in size depending on the size of their drainage basins, and 3) many fans slope steeply into the valley so that the greater the extent of valley-side erosion by the river the higher the elevation of the fan remnant that is preserved. However, the larger fan sequences such as those near Wanship, near Henefer, and at the mouth of Pecks Canyon have at least two distinct fans inset below the highest fan remnants suggesting at least three different levels of former floodplains. On figure 3.3, the dashed lines between remnants along the central part of the Weber Valley show the most likely correlation of fan remnants and surfaces; the lines rise and fall because of the varying sizes, distances from the river, and degree of preservation of the remnants.

The lowest major terrace along the river is marked (fig. 3.3) primarily by alluvial fans extending into the center of the valley above Echo Reservoir and by a continuous terrace, 5-8 m high, from the reservoir to the East Canyon fault. Both the fans and the terrace have smooth surfaces and are undissected. Where the river has eroded the fans their edges are 5-15 m high, but elsewhere they appear to grade into terraces that are <2 m above the present river.

Exposures in the low terrace and the fans show they are composed primarily of massive to interbedded clayey silts and sandy silts with a few dispersed, subangular clasts and occasional gravel lenses. Towards their heads the fans have more interbedded sand and gravel beds, but none contain cobbles or boulders. Thus, the fans appear to be the product of fluvial events of small

to moderate discharge alternating with deposition of loess and colluvium. The terrace deposits probably also consist mostly of loess and colluvium near the sides of the valley. Near the valley center, they must have mostly a slack-water fluvial origin (except for the low, cobbly terrace below Coalville).

Several lines of evidence indicate the low fans and terrace are early Holocene to latest Pleistocene in age. Soils on these deposits generally have cambic or weak argillic horizons and often, stage I carbonate morphology. Shroba (1980) has described similar soils of early Holocene to Bonneville (15 ka) age near Salt Lake City. Soils on modern floodplain deposits in the Weber Valley generally lack B horizons (unpub. soils descriptions, SCS, Coalville). Near the edge of the valley fine-grained colluvial deposits that appear to overlie or grade into the fans tend to have thick, moderately developed argillic horizons, often with stage I and even stage II carbonate. However, it is difficult to tell whether these deposits are the same age as the more distal parts of the fans or whether they are older. Soil indices (fig. 3.4) suggest a fan south of Hoytsville (profile W-10, table 3.2) and the low terrace just below Coalville (profile W-13, table 3.2) are in RAG 3, which is correlated with Pinedale-age deposits. The boulders and cobbles in the low terrace below Coalville (fig. 3.3) indicate it was probably deposited during Pinedale deglaciation, but the fine-grained character and position in the center of the valley of most of the other low fans and terrace suggest they are younger and post-date periods of high discharge associated with deglaciation. This is confirmed for the low terrace at Henefer (site H, table 3.1) where aIle/Ile ratios on snails in the terrace suggest an age of 7-12 ka.

The next major level of fluvial deposits are almost all parts of alluvial fans. They occur mostly as small, discontinuous remnants of fans plastered against the valley walls near tributaries at 25-40 m, but below the highest fan remnants. Gravel pit exposures in these remnants show sequences of interbedded fine (clayey silts, fine sandy silts, fine sands) and coarse (cobbly gravels and coarse pebbly sands) units. The buff to pink, fine-grained units are 0.2-1 m thick and are usually massive or faintly stratified. Buried cambic and weak argillic horizons are sometimes developed in these units. Sands are 0.5-2 m thick, horizontally stratified, and occasionally planar cross-stratified. Gravels are usually thicker (0.5-3 m) and are mostly planar cross-bedded units of sand-matrix-supported gravel or clast-supported gravel with a finer matrix. Muddy matrix-supported gravel is not as common. Cobbles and most clasts are Uinta Mountain Group quartzites, but these may have been reworked from the Cretaceous Wasatch Formation; they have not necessarily been transported by outwash streams from the Uinta Mountains. Bed contacts are parallel and continuous with limited channel fills. These units have features characteristic of the more distal portions of alluvial fans where they merge with braidplain deposits, possibly in a climate more humid than the present with more evenly distributed rainfall (Rust and Koster, 1984). Most of the fine-grained units are loess and slopewash deposits, but some are probably fluvial slackwater deposits. No good evidence remains of the characteristics of the floodplains to which these alluvial fans were graded. A relatively wetter climate seems to characterize Pinedale deglaciation (Porter and others, 1983; Pierce and Scott, 1984; Funk, 1977) and this may be the case for the wanning phases of earlier glaciations. These alluvial fan deposits appear coarser than those

now being deposited in the valley in similar settings. For these reasons, these fan remnants may have been deposited during an early deglaciation.

Amino acid and soils evidence from these fan deposits suggest they are broadly correlative with oxygen isotope stage 6. Alle/Ile ratios on snails from these deposits at four sites along the valley suggest ages of 90-250 ka (table 3.1, fig. 3.3). Shells yielding much higher ratios are reworked. Deposits of several ages may well be present at the same or different sites, but the normal variation in ratios on snails in alluvial deposits and the likelihood of reworking in sediments of this type also mean that all these remnants could also be about the same age. If so, deposition during the end of Bull Lake glaciation (130-150 ka) seems likely. However, with a few exceptions, soils on these deposits are almost as strongly developed as many of the soils on much higher fan remnants (figs. 3.1 and 3.4). Thick, clay-rich argillic horizons with 5YR color hues overlie horizons with stage III and even weak stage IV carbonate development. Ages for these soils based on secondary carbonate and clay accumulation rates are generally >130 ka, but the total secondary clay in soil W-3 near Wanship (table 3.2) gives an age of about 250 ka. In contrast, a soil on the gravelly fan sediment at this level at the mouth of Cherry Canyon at Wanship has only a weak argillic horizon suggesting a relatively young age (this soil is probably eroded). However, snails in colluvium under a soil (W-19, table 3.2) that yields ages of >160 ka (carbonate) and 141 ka (clay) have ratios similar to those for snails in these alluvial fan deposits. Considering their poor preservation we are unlikely to obtain more accurate ages on these deposits. For this reason, we assume an average age of about 140 ka for most of these deposits and suggest that they were deposited near the end of Bull Lake glaciation.

Fan remnants occur at the mouths of the largest tributary drainages, such as near Wanship, Pecks Canyon, Hoytsville, and Henefer, roughly 20-30 m above the remnants disscussed above (fig. 3.3). Isolated erosional remnants occur at similar elevations between Hoytsville and Wanship, at Coalville, and near Henefer. Soils on these surfaces are generally no better developed than those discussed above, probably at least partly due to erosion at most sites, but secondary clay (32 g/cm^2) in soil W-4 (table 3.2) near Wanship suggests an age of 400 ka. Based on their height above the river, degree of dissection, and overall degree of soil development we suggest that these deposits pre-date isotope stage 6 (>200 ka) despite the fact that the soils are not distinctly different than those on deposits we interpret to be about 140 ka. A further problem is that some profiles (W-5 and W-8, table 3.2) are developed in fine-grained loess and colluvium which may overlie older, coarser fluvial deposits. Soils develop more rapidly in fine-grained deposits and this adds further uncertainty as to the age of these surfaces. These higher remnants in the central Weber Valley are about same height above inferred stage 6 deposits as are similar fan deposits in northern Kamas Valley (discussed above).

Finally, the highest recognizable erosion surface remnants occur near Rockport Reservoir, Hoytsville, and below Henefer at 80-150 m above the river (fig. 3.3). Clay pits near Henefer expose partially lithified, debris flow deposits of quartzite clasts supported in a red, clayey matrix; this is probably the Pliocene? Huntsville fanglomerate of Eardley (1952). Remnants of erosional surfaces cut on this deposit were labeled the Weber Valley erosion surface by Eardley (1944). Other remnants near Rockport Reservoir

are cut on the Keetley volcanics. There is no way for us to correlate any of these highest isolated remnants. Based solely on elevation they must be >500 ka, but we have no other age information.

3.5.1.3 Lower Weber River Valley

No terraces or alluvial fans of any significant extent are preserved in the narrow twisting upper canyon of the Weber River between Henefer and Round Valleys. The few very small, steep alluvial fans and talus cones are probably of Holocene age.

During its last high stand about 15 ka (Scott and others, 1983), Lake Bonneville extended through the lower canyon of the Weber into Morgan and Round Valleys (fig. 3.3). Except for very small, young fans and talus cones, no fluvial features of any extent are preserved in the canyon. A number of small alluvial fans and large fluvial terraces at the mouths of Cottonwood, Peterson, Deep, and East Canyon Creeks are graded to levels at or just below the high stand of the lake in Morgan Valley (fig. 4.2). On this basis we assume that these features and wave-eroded scarps at this level elsewhere in Morgan Valley are about 15 ka. A lower fluvial terrace extends along much of Morgan Valley at about 7 m above the river. Because the lake dropped to below the level of the floor of Morgan Valley during its fall to the Provo shoreline about 14 ka (Scott and others, 1983), the 7-m terrace probably dates from 14-15 ka.

A few remnants of older alluvial fans and extensive fans along the Morgan fault occur 10-50 m above the Bonneville shoreline in Round and Morgan Valleys (fig. 3.3). On the basis of relative elevation, degree of fan dissection, and soil development on the Morgan fault fans (discussed in sec. 4.2) these fans are >100 ka, probably roughly correlative with remnants correlated with the isotope stage 6 upvalley. Patches of rounded quartzite cobbles 45 m above the river on the hillside north of the town of Morgan (fig. 4.2) may be the remnants of a terrace of this age.

Higher, older remnants of fans and erosion surfaces occur 70-400 m above the river, especially in the northern half of Morgan Valley (figs. 3.3 and 4.2). These surfaces were included by Eardley (1944) in his Weber Valley erosion surface. A soil on one of the lowest of these surfaces (W-16, table 3.2) is strongly developed (RAG 2, fig. 3.1), but its degree of development does not accurately reflect its age because this soil site has been eroded and the rate of most soil development processes greatly slows in soils this old (Birkeland, 1984). Paleomagnetic analysis shows that sediments in the B horizon of this soil are reversely magnetized and therefore >730 ka (sec. 3.4.). Surfaces above this soil must be considerably older than 730 ka and the highest surfaces, which have been rotated into the Morgan fault (sec. 4.2), may well be pre-Quaternary.

3.5.2 Provo River drainage

The Provo River drainage basin is about 1/4 the size of the Weber River Basin and prior to the last interglacial it was considerably smaller (discussed below). Like the Weber, the river heads in the cirques of the Uintas (pl. 1), flows westward and southward through several back valleys, and then cuts directly west through the core of the Wasatch Range into Utah Lake

Valley. Fluvial terraces in the upper Provo River Valley and terrace remnants and alluvial fans graded to them along several portions of the lower valley provide a partial record of Quaternary events in the basin (fig. 3.5). Reconstructing the history of the river through Heber Valley is difficult because the valley is so wide (5-13 km) making remnants far apart. Terrace and fan remants can be grouped into 1) those in the headwaters area including southern Kamas Valley, 2) those in Heber Valley, and 3) those in the lower canyon of the river below Heber Valley. Few remnants are preserved in the narrow upper and lower canyons of the river (fig. 3.5).

3.5.2.1 Upper Provo River Valley

Four main terraces are preserved in the upper Provo River Valley and the southern part of Kamas Valley. The lowest terrace, composed of bouldery gravel about 4-6 m above the river, is found at the junction of the South Fork of the Provo River with the main Provo River and along the North Fork just upstream (pl. 1). Farther up the North Fork the terrace cannot be distinguished from floodplain deposits. A soil on this terrace at the junction lacks a B horizon (soil P-4, table 3.3); soil development indices suggest a late RAG 3 (Pinedale) age (fig. 3.6) and the bouldery sediment of the terrace suggest it was deposited during the final retreat of the cirque glaciers about 20 km up the valley.

A second terrace composed of bouldery gravel just below the confluence with the South Fork is about 12 m above the river. Based on its relative elevation this terrace is part of the valley train which rises sharply to join the moraines at the mouth of the North Fork of the Provo River valley. At this confluence with the North Fork, sharp-crested, narrowly-breached moraines from both the North Fork and the main Provo valley coalese. However, arcuate moraines and an outwash terrace partially dammed up against the moraines show that the last advance of the North Fork glacier was slightly more extensive than that of the main Provo valley glacier. The morphology of these moraines and their distance from the cirques suggest they were deposited during the last major glaciation (Atwood, 1909), probably about 15-18 ka (sec. 3.4). Development indices (figs. 3.1 and 3.6) for soils on the moraines (soil P-10, table 3.3) and on outwash (soil P-8, table 3.3) confirm a RAG 3 (Pinedale) age. Development indices show the soil on the 12 m terrace at the confluence with the South Fork (soil P-3, table 3.3) is also in RAG 3 (fig. 3.6) and therefore about the same age.

There are no exposures in the deposits of the next highest terrace, which occurs along much of the upper valley about 20-30 m above the river. A soil on this terrace near Woodland (unpub. description, SCS, Coalville) has a thick (86 cm), clay-rich (30-40% clay) argillic horizon with 5YR color hues like the soils on the extensive terrace about 10 m above it which is correlated with the Bull Lake glaciation (discussed below and in sec. 3.4). However, this is the highest terrace preserved upstream along the North Fork (pl. 1) and it extends almost as far upvalley as the morphologically subdued terminal moraines descending the valley sides. These moraines have wider crests and gentler slopes than the moraines 2 km to the north at the confluence of the North Fork. This moraine morphology and development indices (RAG 2, fig. 3.6) for a soil on these moraines (soil P-9, table 3.3) suggest they are significantly older than the Pinedale moraines just north of them. A thick (60 cm) but very patchy argillic horizon consisting of

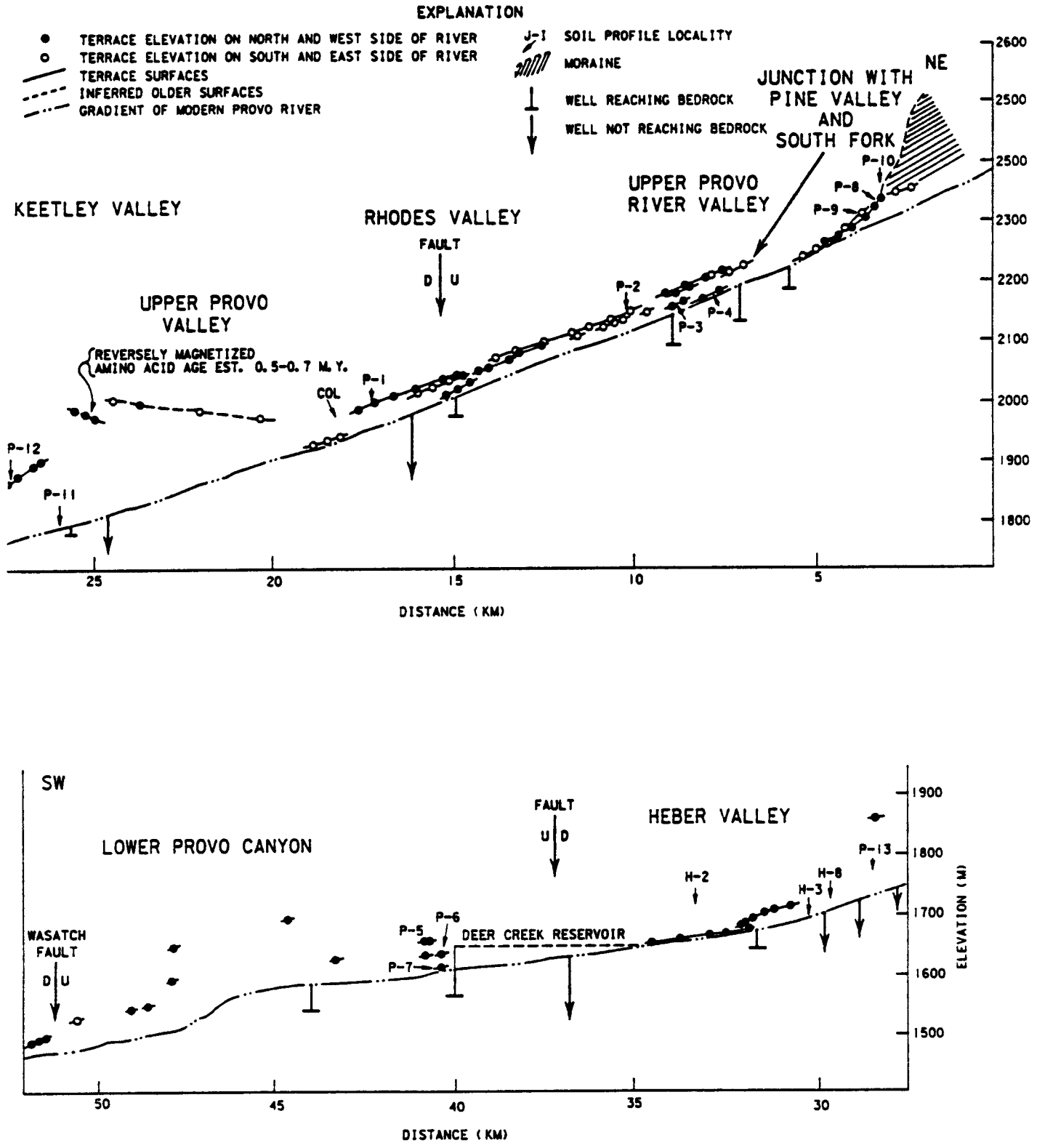


Figure 3.5 Provo River terrace profiles.

Table 3.3 Selected properties of soils on fan and terraces remnants along the Provo River, north central Utah (continues next page).

Profile	Horizon*	Average depth (cm)	Parent material	Munsell dry color	ESTIMATED PERCENT BY VOLUME Pebbles (0.2-8cm)	Cobbles (8-25cm)	Boulders (>25cm)	PERCENT BY WEIGHT~ Sand (2-0.5mm)	Silt (50-2um)	Clay (<2um)	Percent§ carbonate	Percent** organic matter
P-1	Ap	0-10	loess	7.5YR 4/3	2	0	0	55	24	22	0.0	1.0
	A	10-24	loess	7.5YR 5/3	2	0	0	51	25	24	0.0	1.7
	AB	24-41	loess	7.5YR 4/3	2	0	0	54	25	21	0.0	1.3
	Bt	41-80	loess	7.5YR 6/4	5	0	0	38	33	28	0.0	0.8
	2Bt	80-113	outwash	7.5YR 5/6	20	10	2	62	20	18	0.0	0.4
	2CB	113-156	outwash	7.5YR 5/6	20	10	2	83	8	10	0.0	0.4
	2Cox	156-200+	outwash	7.5YR 6/7	30	20	2	88	5	7	0.0	0.2
P-2	Ap	0-14	loess	7.5YR 5/3	5	1	0	27	54	19	0.5	6.6
	A	14-48	loess	7.5YR 5/4	5	1	0	26	55	19	0.0	4.1
	2AB	48-61	outwash	7.5YR 7/4	30	20	0	39	41	20	0.0	1.1
	2Bt/CB	61-131	outwash	5YR 5/7	30	20	1	60	17	24	0.0	0.5
	2CB	131-170+	outwash	5YR 7/6	30	20	1	73	11	16	0.0	0.3
P-3	Ap	0-10	loess	7.5YR 6/3	5	3	0	34	43	23	0.0	4.6
	A	10-22	loess	7.5YR 5/3	5	3	0	35	43	22	0.0	3.2
	Bt	22-51	loess	7.5YR 6/5	5	7	5	34	46	20	0.0	0.7
	2BC	51-68	outwash	7.5YR 5/6	20	1	5	36	45	20	0.0	0.5
	2Cox	68-100+	outwash	7.5YR 5/6	30	20	35	85	7	8	0.0	0.4
P-4	Ap	0-7	loess	7.5YR 5/3	5	10	5	52	29	19	0.0	7.7
	A	7-30	loess	7.5YR 4/3	5	10	5	60	24	16	0.0	2.9
	2Cox	30-142+	outwash	7.5YR 6/4	20	20	20	94	4	3	0.0	0.4
P-5	Ap	0-18	loess	10YR 5/3	15	0	0	27	51	22	0.0	1.1
	A	18-34	loess	10YR 4/3	40	0	0	31	44	25	0.0	1.4
	2Bt1	34-67	alluvium	5YR 5/4	50	10	0	31	29	40	0.1	0.7
	2Bt2	67-167	alluvium	5YR 4/6	20	40	30	46	26	28	0.2	0.4
	2BC1	167-207	alluvium	5YR 4/6	10	10	70	49	25	26	0.2	0.3
	2BC2	207-247+	alluvium	7.5YR 4/6	20	20	30	49	29	22	0.2	0.3
P-7	A	0-16	alluvium	10YR 5/3	50	10	0	57	28	15	0.0	1.1
	Bt	16-36	alluvium	10YR 5/6	50	20	0	54	25	21	0.0	0.6
	Bk	36-67	alluvium	10YR 7/4	45	35	5	89	4	7	0.0	0.3
	2Ckj	67-150+	alluvium	10YR 6/4	10	0	0	56	30	14	0.0	0.2

* Horizon nomenclature of Guthrie and Witty (1982) and Birkeland (1984) except that master K horizon is not used.
~ Particle size distribution of <2 mm fraction using sieve-pipette methods (for example, Carver, 1971) and a Sedigraph for some silt-clay fractions with prior removal of carbonates and organic matter using methods of Jackson (1956).
§ Percent carbonate by method of Dreimanis (1962).
** Percent organic matter by method of Walkley and Black (1934).

Table 3.3 Selected properties of soils on fan and terrace remnants along the Provo River, north central Utah.

Profile	Horizon*	Average depth (cm.)	Parent material	Munsell dry color	ESTIMATED PERCENT BY VOLUME Pebbles (0.2-8cm)	Cobbles (8-25cm)	Boulders (>25cm)	PERCENT BY WEIGHT~ Sand (2-0.5mm)	Silt (50-2um)	Clay (<2um)	Percent§ carbonate	Percent§§ organic matter
P-8	A1	0 14	loess-outwash	10YR 4/4	15	5	0	47	39	15	0.0	4.7
	A2	14 23	loess-outwash	7.5YR 4/4	15	5	0	47	39	15	0.0	3.1
	BA	23 34	loess-outwash	7.5YR 7/4	15	5	0	60	31	9	0.0	0.6
	2Bt	34 43	outwash	7.5YR 7/4	30	10	5	75	19	6	0.0	0.3
	2Bt/C	43 73	outwash	10YR 7/4	40	20	10	84	14	2	0.0	0.2
	2Cox	73 85+	outwash	10YR 7/4	40	20	10	87	12	2	0.0	0.2
P-9	A1	0 12	till	10YR 5/2	30	25	5	50	37	13	0.1	5.1
	A2	12 25	till	10YR 5/3	30	25	5	54	35	11	0.0	2.5
	EB	25 48	till	7.5YR 7/4	30	25	5	76	18	6	0.1	0.1
	Bt/C	48 110	till	10YR 7/4	30	20	5	66	17	17	0.1	0.2
	Cox	110 160+	till	10YR 7/4	30	20	5	64	21	15	0.0	0.2
P-10	A1	0 18	till	10YR 2/2	20	25	5	51	36	13	0.1	6.7
	A2	18 36	till	7.5YR 3/3	20	25	5	63	25	12	0.1	4.7
	AB	36 57	till	7.5YR 5/3	20	25	5	57	31	12	0.1	2.4
	Bt	57 93	till	10YR 7/3	20	25	5	62	31	7	0.0	0.5
	C	93 135+	till	10YR 7/3	20	25	5	72	23	5	0.0	0.2
P-11	A1	0 22	loess	10YR 3/2	0	0	0	37	40	24	0.1	5.7
	A2	22 84	loess	10YR 4/2	0	0	0	39	36	25	0.1	3.2
	AB	84 96	alluvium	10YR 4/2	25	5	0	58	26	16	0.1	1.3
	2Bt	96 120	alluvium	7.5YR 4/8	40	20	0	76	14	10	0.2	0.7
	2C/B	120 170	alluvium	10YR 5/2	40	20	0	80	12	8	0.2	0.5
	2C	170 210+	alluvium	10YR 5/2	40	20	0	83	12	5	0.2	0.2
P-12	A	0 22	loess	7.5YR 4/2	5	1	0	42	39	20	0.1	3.8
	Bt	22 38	loess	7.5YR 4/5	5	1	0	18	23	59	0.1	1.3
	2Bt1	38 78	alluvium	7.5YR 4/3	30	10	10	45	25	30	0.1	0.7
	2Bt2	78 114	alluvium	7.5YR 6/5	30	10	10	55	22	23	0.1	0.2
	3Btk	114 138+	alluvium	7.5YR 5/4	30	10	10	43	28	29	4.1	0.1
P-13	Ap	0 19	loess	10YR 5/3	3	0	0	29	48	23	0.0	3.0
	AB	19 45	loess	10YR 5/3	3	0	0	55	30	15	0.0	2.4
	Bt	45 75	loess	10YR 6/4	3	0	0	64	24	12	0.0	1.0
	BC	75 87	loess-colluvium	10YR 6/4	30	5	0	71	20	9	0.0	0.4
	2C	87 178+	alluvium	10YR 7/3	60	10	0	92	6	3	0.0	0.2

* Horizon nomenclature of Guthrie and Witty (1982) and Birkeland (1984) except that master K horizon is not used.
~ Particle size distribution of <2 mm fraction using sieve-pipette methods (for example, Carver, 1971) and a Sedigraph for some silt-clay fractions with prior removal of carbonates and organic matter using methods of Jackson (1956).
§ Percent carbonate by method of Allison and Moodie (1965, p. 1387).
§§ Percent organic matter by method Walkley and Black (1934).

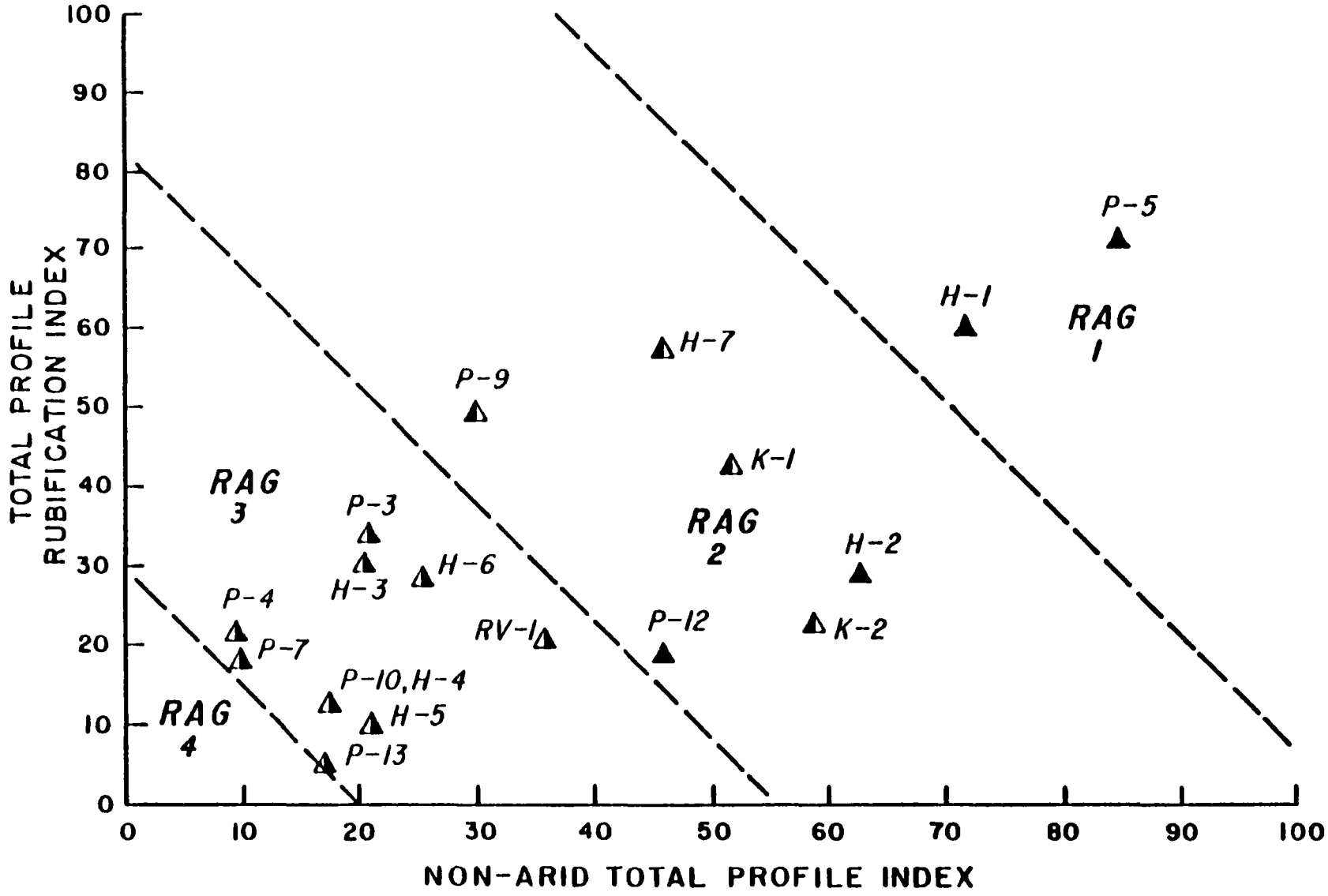


Figure 3.6 Rubification and non-arid total profile indices for soils in the Provo River Valley, Kamas Valley, and Round Valley.

coallesing clay bands (for example, Gile, 1979) characterizes this soil. Secondary clay values (4 g/cm2) suggest an age of roughly 54 ka. Thus, it is possible that these moraines are correlative with an earliest Pinedale glacial event dated by Colman and Pierce (1981) at about 60-70 ka near McCall, Idaho (sec. 3.4). However, because the 20-30 m terrace extends almost to the subdued moraines and does not extend beyond them, we conclude it is probably about the same age as the moraines, and that both the terrace and the moraines probably date from the Bull Lake glaciation (130-150 ka).

The most extensive fluvial terrace in the Wasatch Mountains extends along most of both sides of the Provo River from its confluence with the South Fork of the Provo to the former col at the southwestern corner of Kamas Valley (fig. 5.6). The terrace is fairly constant in height at about 35-40 m above the river. The slopes of the scarps of this terrace above the 20-30 m terrace are gentle (8°-9°), but the terrace is little dissected. Exposures in the terrace deposits show it consists of horizontally-bedded, coarse bouldery to cobbly outwash. Sand-matrix-supported units are less common than clast-supported units, but 10 m vertical exposures in a gravel pit show reddish (5YR hues) clay infiltrated into the matrix of much of the sequence, especially in the upper 2 m. The terrace cannot be traced to any moraines upvalley, but the Provo Valley glacier was probably at about the position of the subdued moraines (discussed above) when the terrace was deposited. The thick, reddish, clay-rich B horizons of the soils on this terrace (soils P-1 and P-2, table 3.3, and unpub. soil descriptions, SCS, Coalville) led us to correlate these deposits with the Bull Lake glaciaton (sec. 3.4) and to infer an age of about 130-150 ka for them (sec. 3.4).

The age of the 35 m terrace is important in the development of the Weber and Provo River drainage basins because this age provides a maximum age for the diversion of the Provo River above Kamas Valley into the present Provo drainage. Formerly, the upper Provo flowed north though Kamas Valley where it joined the Weber River (Anderson, 1915; Gilbert, 1928). A combination of headward erosion of the Provo River up the present upper Provo Canyon (Woodfill, 1972) and the filling of southern Kamas Valley with an extensive sheet of outwash (Peterson, 1970) during the Bull Lake glaciation allowed a low col at the southwestern corner of Kamas Valley to be breached (Anderson, 1915). Rapid down-cutting, probably by high-discharge meltwater streams, lowered the col, incised the outwash to form the extensive 35 m terrace, and confined further outwash deposition to the narrow valley below the terrace (Nelson and Krinsky, 1982). The extent of the 20-30 m terrace along the valley suggests a period of floodplain stablility or aggradation 10 m below the high terrace, also during Bull Lake time. Thus, the diversion of the upper Provo took place about 130-150 ka and the cutting of the present upper canyon of the river began at that time and has continued to the present.

Few remnants of terraces or fans are preserved in the straight, narrow canyon of the upper Provo River. Tributary drainages into the canyon are small and most of the few small fans appear graded to the present floodplain. Exposures in these small fans show colluvium with angular clasts and weakly developed soils, some with stage I carbonate, suggesting a Holocene age. At the head of the canyon the river has eroded a fan on its south side to form a terrace about 7 m high (fig. 3.5). Based on its height this terrace may correlate with the lowest terrace upriver; if so, it probably formed during the last phases of Pinedale deglaciation.

The most significant fluvial feature along the upper canyon is the well-developed paleovalley cut on the Keetley volcanics on either side of the rim of the canyon. The paleovalley slopes about 2.4 m/km to the east and its tributary drainages trend eastward and join it at acute angles showing that the predominant drainage pattern in the canyon area was into southern Kamas Valley before the cutting of the present canyon. Woodfill (1972, p. 25) noted a terrace deposit of fluvial cobbles of Uinta Mountain Group quartzite, on the north rim of the canyon, which he felt was a remnant of a terrace deposited by the upper Provo River when it flowed north through Kamas Valley to join the Weber.

3.5.2.2 Heber Valley

Reconstruction of the history of the Provo River in Heber Valley is difficult because the valley is too wide (5-15 km) for most of the fan and terrace remnants preserved on the valley margins to be directly related to a former floodplain along the present river. In addition, fluvial events in the several large tributaries which join the Provo in the valley also influenced the distribution of most remnants in the valley. Alluvial deposits in the valley can be grouped into 1) high, older fan sediments and pediments near the north end of the valley, 2) mid- to late Quaternary alluvial and colluvial fans with a complex history on the valley margins, and 3) the younger large, gently sloping fans and alluvium that floor the valley. Moraines extend to near the valley floor in several drainages (fig. 5.7).

At the north end of Heber Valley, about 2-15 m of dissected alluvial fan sediments are exposed overlying a bedrock (Oligocene Keetley volvanics) pediment. The fan surfaces slope 5-7° towards the river from 40 to 100 m above the river on the east side and from 30 to 120 m on the west side of the river (Qafo on fig. 5.7). Cuts in these deposits on the east side of the river show a complex sequence of clast-supported channel fills and matrix-supported debris flow units interbedded with fine-grained loess and colluvial units. Shallow, west-dipping bed contacts characterize the upper few meters of the sequence, but many dips in the lower third of the exposures are 5-15° to the east and southeast. Because westward dips would be expected in fans that slope to the west, eastward dips could be interpreted as evidence for tectonic rotation of the lower part of the sequence. However, the geometries of indiviual beds are not well-exposed and the eastward dips are more likely to be depositional, especially if a large alluvial fan once occupied the northern end of Heber Valley.

In any case, all the alluvial fan sediments pre-date the late Quaternary and the lower part of the sequence is pre-mid-Quaternary. The relative elevation and degree of dissection of the fans and pediment suggest it is much younger than the paleovalley above the upper Provo Canyon (fig. 3.5), but older than lower alluvial and colluvial fans on the margins of the valley to the south (Qaf on fig. 5.7). Paleomagnetic samples from the lower part of the fan sequence east of the river retain a reversed component of magnetization indicating they are >730 ka (sec. 3.4.). The lithology, relative elevation above the river, and reversed magnetization of the sediments in the lower part of the sequence suggest they are correlative with similar dissected basin fill sediments 5 km to the north in Keetley Valley (at 25 km on fig. 3.5)(sec. 4.5) which have also been shown to be at least this old.

Development indices for a soil on the fan surface (fig. 3.6, soil P-12, table 3.3) place the soil in RAG 2, but the highly weathered clasts in the soil suggest it may be much older.

On all three margins of Heber Valley alluvial and colluvial fans slope from the valley floor to as high as 150 m (Qaf on fig. 5.7). The fans are generally little dissected, but scarps have been cut into the distal portions of many by streams paralleling the valley margins. Limited shallow cuts in the fans expose a variety of lithologies reflecting both a number of different source lithologies for the fan sediments and complex depositional histories extending over much of the mid- and late Quaternary.

The middle and upper portions of many fans are probably several hundred thousand years old. Their position below the pediment at the north end of the valley and the col between Deer Creek Reservoir and Round Valley (discussed below) (fig. 3.5) indicate at least the surface sediments on these fans are of late and mid-Quaternary age. Development indices (fig. 3.6) show that a soil (soil H-1, table 5.3) on a gravelly alluvial fan in Big Hollow (fig. 5.8) predates RAG 2 (correlated with the Bull Lake glaciation) and total secondary clay (39 g/cm^2) suggests a age of almost 500 ka. Clay contents are high in argillic horizons and stage III carbonate is common in fine-grained colluvial deposits (stage IV carbonate is found in some exposures) overlying gravelly alluvial fan deposits here (soil H-2, table 5.3 and fig. 5.9) and near the mouths of other drainages on all three margins of Heber Valley.

Some of the smaller fans and the more distal portions of the larger fans and the channels within them on the margins of the valley appear to be younger, of latest Quaternary age. Shallow exposures in near-surface deposits show cambic and weak argillic horizons developed on fine gravelly alluvium, slopewash, and loess indicating that these portions of the fans have been active during the last 10-15 ka. For example, development indices for a soil developed in loess and alluvium on the distal portion of a fan northeast of Midway (soil P-13, figs. 3.5 and 5.7, table 3.3) place it on the border between RAG 3 and RAG 4. In the Midway area (fig. 5.7), outwash and alluvial fan sediment from Snake and Pine Creeks is interbedded with and overlain by tuffa deposits from thermal springs (Baker, 1968). Soil indices (fig. 3.6) show that soils on the morphologically distinct terminal moraines near the mouths of Pine Creek (soil H-4, table 5.3) and Snake Creek (soil H-6, table 5.3) are in RAG 3, correlated with the Pinedale glaciation. If older glacial deposits are preserved in these drainages they have not been identified. Thus, the outwash which probably makes up much of the fan sediment near Midway is probably about 15-18 ka. The surface tuffa deposits which are >22 m thick in places (Baker, 1968) are probably mostly Holocene in age. The present Provo River has cut a 8 to 10-m-high scarp in these deposits along much of this side of the valley (figs. 3.5 and 5.7).

The floor of Heber Valley consists mostly of gravelly alluvium deposited in large, gently sloping (0.5-1°) fans from the Provo River entering the valley on the north, Lake and Center Creeks flowing from the east, and Daniels Creek draining the highlands southeast of the valley (fig. 5.7). Distributary channels can be identified on all three fans and those on the Provo River fan appear especially well-preserved suggesting many of these channels have been active during the Holocene. A soil (P-11, table 3.3) on the Provo fan

adjacent to the present channel (figs. 3.5 and 5.7) is probably less than a few hundred years old, but development indices place it in RAG 3 (fig. 3.1). Rapid infiltration of slack-water fines into the cobbly gravel parent material of this soil accompanied by groundwater staining due to a high water table produced higher than expected indices for this soil. Cuts in fluvial deposits along Daniels Creek near the mouth of Daniels Canyon, about 6 m below the level of the fan deposited by Daniels Creek expose similar cobbly Holocene soils with infiltrated silt and groundwater staining.

On the main surfaces of the Daniels Creek and Lake Creek-Center Creek fans a number of exposures show soils with cambic and weak argillic horizons. Development indices (fig. 3.6) place a soil on the Daniels Creek fan (soil H-3, table 5.3) near Big Hollow and a soil on the Lake Creek-Center Creek fan southeast of Heber City (soil H-5, table 5.3) in RAG 3 suggesting a latest Pleistocene age (10-15 ka) for much of the surfaces of the fans. The morphology and degree of soil development on the terminal moraines in Lake Creek valley east of the valley (fig. 5.7) indicate a similar age. Outwash spread out into the valley during Pinedale deglaciation is of this age. However, a well-developed soil on the distal edge of the Daniels Creek fan (soil H-7, table 5.3) has indices which clearly place it in RAG 2 (fig. 3.6), suggesting it considerably predates much of the surrounding alluvium and the Pinedale glaciation. Total secondary clay (11 g/cm^2) in this soil suggests it may correlate with soils on Bull Lake outwash deposits with similar clay values in the upper Provo Valley.

Soils of RAG 4 (Holocene), RAG 3 (Pinedale), and RAG 2 (Bull Lake) on alluvial deposits of about the same elevation in the central part of Heber Valley indicate that alluvium has been deposited at about this relative elevation, at least in the central part of the valley, for the last 130-150 kyr. Much of the Provo River fan may be younger than the Daniels Creek and Lake Creek-Center Creek fans; the present river has cut about a 5-m-high scarp into the distal edge of the Daniels fan north of Deer Creek Reservoir (fig. 5.7). Older scarps with gentle slopes on the edge of fans north of Heber City show that the Provo River flowed along this part of the valley since these fans were active. Apparently, more recent deposition on the fans from Lake Creek and Daniels Canyon has kept the river from occupying the east side of the valley.

The complex sequence of deposits of differing ages in the fans bordering Heber Valley and isolated deposits of RAG 2 in the center of the valley suggest that fans graded to a floodplain at close to the present relative elevation have persisted for hundreds of thousands of years. Scarps in the fans may be due entirely to lateral cutting by streams; downcutting (as suggested by Eardley, 1933) is not required.

3.5.2.3 Lower Provo River Valley

Alluvial and colluvial fans on the sides of the valley along Deer Creek Reservoir are similar in their degree of dissection and position in the valley to the late and mid-Quaternary fans in Heber Valley, although the lower portions of the fans are now covered by the reservoir. Around the shores of the reservoir and in cuts along the adjacent highway, exposures show the fans lining the valley are composed mostly of fine gravelly stream and debris flow deposits, with overlying and occasionaly interbedded

slopewash and loess. No very strongly developed, reddish argillic horizons were observed on these deposits. Surface soils and some buried fine-grained units in some cuts have cambic to weakly developed argillic horizons, such as those in the sequence of 3 alluvial cut and fill units along the west shore of the reservoir. Carbonate contents are highly variable, but stage III carbonate morphology is common on fan units in the lower half of exposures along the west shore of the reservoir and stage IV was observed on colluvial sediments in the road cut in the col between the Provo River Valley and Round Valley. Amino acid ratios in snails from the sediments along the west shore suggest the lower fan sediments in the exposure (the lower portions of these fans are now beneath the reservoir) are at least several hundred thousand years old (table 3.1) and paleomagnetic analysis of samples from the road cut in the col suggest these deposits are >730 ka (sec. 3.4 and App. A). Thus, as in Heber Valley, the surfaces of many fans have been active in the latest Pleistocene and perhaps the Holocene, but mid- to early Quaternary sediments underlie these thin younger sediments in many areas, especially on the upper portions of the fans. This suggests that these older Quaternary sediments are slowly being eroded as the river valley is deepened.

Pre-reservoir topographic maps (10 ft. contour interval) of the Provo River valley now covered by Deer Creek Reservoir do not show any major terraces along the river. The alluvial fans on the sides of the valley slope smoothly to the valley floor, but there appears to be a sharp decrease in gradient where the fans merge with present floodplain deposits. There is also a sharp break in slope where the floodplain sediments meet the steep sides of the valley and on the sides of bedrock inliers in the valley. The gradient of the valley floor is considerably reduced near Deer Creek Dam and the river begins to meander considerably 6 to 8 km above the dam. These features indicate relatively recent aggradation of the river above the site of Deer Creek Dam; the erosion of the river valley at the dam has not kept pace with the deepening of the valley upstream.

The roadcut in the col between the Provo Valley and Round Valley (fig. 3.5) exposes fluvial sands and rounded cobbles of Keetley volcanics under the sediments with a magnetically reversed component. The lithology of the cobbles with a source in Heber Valley (14 km to the east) shows that the Provo River once flowed through the col (Baker, 1976), more than 730 ka.

Quaternary deposits in the lower Provo Canyon below Deer Creek Reservoir (fig. 3.5) provide only limited evidence of the Quaternary history of the river (Crone and others, 1983). Deposits along the canyon consist chiefly of Holocene alluvium in the floodplain, alluvial and colluvial fans (including debris flow, mudflow, talus, and avalanche deposits) deposited from tributary drainages, landslides (usually related to outcrops of the Manning Canyon shale), and coarse deltaic and shoreline sediments below 1651 m (5360 ft) near the mouth of the canyon deposited during the most recent high stand of Lake Bonneville (sec. 3.)(Baker, 1964a; 1964b; Baker, 1972; Baer and Rigby, 1980). At five sites, small isolated surfaces 50 to 100 m above the river may be remnants of older late Quaternary mainstream alluvium (fig. 3.5), but these are too discontinuous to correlate and are unlikely to be datable. The few exposures in the lower remnants of fluvial terraces and fans show very weakly developed soil profiles on gravelly alluvium in the lower canyon and somewhat better developed soils on similar deposits at about the same relative elevation above the river upstream. This suggests a greater degree

of relative uplift and dissection in the lower canyon as would be expected nearer the Wasatch fault. Soil development on landslide deposits in the lower canyon is minimal (no argillic horizons in soils on clayey parent material, maximum carbonate stage is I) suggesting many slides have been active in Holocene time.

The marked steepening in the river gradient for 1.5 km below Vivian Park (fig. 3.5) is probably the result of some combination of 1) the upstream migration of a knickpoint produced by relatively rapid uplift on the Wasatch fault, 2) the river's inability to remove the alluvial fill deposited in the canyon when Lake Bonneville reached this elevation, and possibly 3) the damming effect from the large alluvial fans on the north wall of the canyon.

The best preserved older fluvial deposits in the lower Provo Canyon are found immediately below Deer Creek Dam (fig. 3.5). Weeks Bench, a remnant of a large, coarse, probably deltaic fan 60 m above the river, was deposited into the canyon from Provo Deer Creek, probably during glaciation in the headwaters of the creek. The position of a large landslide in the Manning Canyon shale south of the bench does suggest this fan was built by damming of the river to this level (1675 m; 5480 ft) by the landslide (Baer and Rigby, 1980). Development indices (fig. 3.6) for very well-developed soil with 5YR hues and up to 50% highly weathered clasts (soil P-5, table 3.3) developed on the gravelly alluvium of Weeks Bench indicate it probably predates the Bull Lake glaciation (sec. 3.4). The hummocky topography of the landslides north and west of the bench along with evidence of recent movement (Baer and Rigby, 1980) show the slides have been active, probably many times, since the deposition of the bench. Landslides may also have influenced the development of an intermediate terrace, 28 m above the river below Weeks Bench, and several lower terraces at 5 to 10 m. The intermediate terrace surface was disturbed during construction of Deer Creek Dam making a soil developed on it (soil P-6, fig. 3.5) of little use in estimating its age, but indices for a weakly developed soil (soil P-7, table 3.3) on the 10 m terrace indicate a latest Pleistocene age (10-15 ka).

3.6 Summary of Late Cenozoic Geomorphic Development of the Eastern Wasatch Mountains

We present below our interpretation of the geomorphic development of the Weber and Provo River drainage basins, including the back valleys, based on our reconnaissance study of the eastern Wasatch Mountains (pl. 1). This summary provides a framework within which to evaluate the late Tertiary and Quaternary neotectonics (and hence, seismic hazards) of the area. Each of the back valleys is unique in some ways and although the best approach for future detailed work would be consider the origin of each valley separately (Threet, 1959), existing data indicate that the back valleys developed in response to the same tectonic, climatic, and geomorphic processes during the late Cenozoic. Particularly because of the cross-drainage of the major rivers through the Wasatch Mountains, events in some of the back valleys profoundly influenced the development of other back valleys.

3.6.1 Late Tertiary and Early Quaternary

We have no argument with Eardley's (1944, 1955) and Hunt's (1982) discussions of the early physigraphic development of the area (sec. 3.2), although the Herd Mountain erosion surface attributed to this period may not have regional significance (Threet, 1959). Before the middle Tertiary, drainage in the vicinity of the Wasatch Range was generally from west to east, but the present drainage pattern shows that streams also flowed to the north and south around the Uinta Mountains. In the late Eocene and Oligocene the back valleys began to develop by north-south oriented folding and faulting, but the northward course of the present Weber River and erosion surfaces near Smith and Moorehouse Valley in the Weber River headwaters shows that the regional slope in the area of the back valleys north of Heber Valley was in this direction, towards Cache Valley and the Bear River Range. During a long period of erosion in the Oligocene and Miocene, the eastern part of the area was uplifted higher than the western part and the consequent drainage that had been directed to the east and north, north of Heber Valley, and to the southeast south of Heber Valley was reversed (Gilbert, 1928). Hunt (1956, 1982) explains the transverse canyons of the Wasatch Range, including the Weber and Provo Canyons, by a combination of consequent and antecedent drainage termed anteposition. Displacement on the Wasatch fault and the relative uplift of the range, begun in the Miocene, continued in the Pliocene with renewed activity on back valley faults. During this period the larger consequent drainages gradually became incised into the Wasatch block by antecedence, forming the narrow canyons that join some of the back valleys and cut through the Wasatch Range. Moderately high rates of uplift on the Wasatch fault have continued into the late Quaternary (Machette, 1984) with lower rates on some back valley faults, but no evidence precludes periods of relative tectonic quiescence on any of these faults during some parts of the Quaternary.

Because no numerical-age dates have been obtained on post-Oligocene units, the following chronology of events is entirely relative. To some extent the development of the Weber and Provo basins can be linked, but the chronological position of events in one basin with those in the other is not always clear.

3.6.1.1 Paleo-Weber Drainage

The size of the Weber drainage basin shows it has been the dominant basin in the area from early Tertiary times. The size of the basin and fortuitous back valley faulting may have allowed this basin to capture drainages on its eastern margin (Hansen, 1969) and south of the Uinta axis, but relative uplift of the Wasatch block must have also helped by increasing the rate of headward erosion of streams due to the lowering of the base level of the river. The northward slope of high erosion surfaces above Daniels Canyon southeast of Heber Valley suggest that even this area may once have been part of the paleo-Weber drainage before the development of Heber Valley. Eardley (1944) points out that the Weber River once flowed through the East Canyon area.

Faulting clearly disrupted the paleo-Weber drainage, probably repeatedly. Paleochannels and numerous erosion surfaces which are lower than and therefore younger than those above Daniels Canyon and on Herd Mountain indicate the Park City-Parleys Park area drained into Kamas Valley, which was still part of the headwaters of the Weber Valley during this period. If the concentration of drainage along the central Weber Valley was due to displacement on faults, the faulting in this area predates significant displacement on the faults that now form the margins of Parleys Park, Richardson Flat, Deer Valley, and Keetley Valley, because these younger faults cut across the paleochannels and erosion surfaces. Faulting along the margins of Heber Valley also must have been later than the cutting of the younger erosion surfaces because lowering of the valley by faulting would have allowed the Provo River to capture the Keetley Valley drainage much earlier than it did. Whether the Weber Valley erosion surface predates or postdates faulting (Eardley, 1955) is not relevant because Eardley's (1944) concept of the surface includes features of probably late Tertiary to at least mid-Quaternary age (sec. 3.2). These repeated temporary drainage disruptions must have rapidly filled the back valley basins and kept the river channels on the higher areas between basins within a few tens of meters of bedrock.

The basin fill deposits in Keetley valley are too coarse-grained and extensive to have been deposited by the present drainages on the western side of the valley. For this reason, the basin-fill deposits (dated by paleomagnetics, amino acid ratios, and tephrochronology at >730 ka) were deposited prior to displacement on the Frog Valley fault and faults with similar morphologies to the north. Thus, the development of Keetley Valley post-dates the paleochannels and surfaces sloping into Kamas Valley and pre-dates displacement on the Frog Valley fault and, by analogy, similar faults to the north. Because the escarpments in the western parts of Parleys Park and the Park City and Deer Valley areas are steeper and the valleys are covered with young sediment, faults bounding these valleys may have had more recent displacements than those in Richardson Flat and in Keetley Valley.

3.6.1.2 Paleo-Provo Drainage

In contrast to the Weber River, the Provo River has had a more difficult time enlarging its drainage basin although it has still managed to maintain its course across the Wasatch Range and to extend its basin eastward (for example, Hansen, 1969) due to gradient steepening by uplift on the Wasatch

block. As in other back valleys, the lowering of Strawberry Valley due to displacement on the Strawberry fault preserved some of the southeastward flowing drainage in this area from capture by streams eroding eastward from the Wasatch Front. However, barbed drainages west of Strawberry Resrvoir suggest that some of the present western part of the Strawberry Valley drainage may have once drained into Hobble Creek or Spanish Fork River. If so, the lowering of Strawberry Valley was early enough or the drainages small enough that their capture was prevented. Lowering of Heber Valley (the shape and size of the present valley suggest little of this was due to erosion by the Provo River) rejuvenated the drainage basin of the Provo, possibly capturing the drainage in an area that originally flowed northward. This allowed drainage from the Daniels Canyon area to cut its narrow canyon and allowed the stream at the north end of Heber Valley to capture Keetley Valley. However, the entire Strawberry Valley area did not necessarily ever drain into Heber Valley. A drainage divide near the present location of Daniels Pass may have shifted back and forth depending on where the greatest amount of headward erosion was taking place. Thus, the lowering of Heber Valley and Strawberry Valley must be roughly contemporaneous and both are younger than the high erosion surfaces north of Heber Valley and the canyon cutting by headward erosion of Wasatch Front streams.

Heber and Keetley valleys may have initially developed during the same period, but some displacement on Heber Valley faults which is more recent than that in Keetley Valley (probably correlative with displacements in Deer Valley and Parleys Park) seems required to explain the 1) depth of Heber Valley, 2) the depth of Daniels Canyon, and 3) the capture of the Keetley drainage by the Provo River in Heber Valley.

The cols on Wallsburg Ridge (fig. 6.1) were probably cut by streams roughly paralleling the Provo River. Thus, displacements on the faults bounding Round Valley cannot be older than the major period of lowering of Heber Valley, but they could be younger.

3.6.2 Middle and Late Quaternary

Our evidence of mid- and late Quaternary events in the eastern Wasatch Mountains consists mainly of the position and relative age of alluvial fan and terrace remnants along the major river valleys. The major valleys provide the local base level for fluvial events in smaller tributary drainages. Because the effect of base level changes decreases exponentially upstream (Hamblin and others, 1981), evidence of depositional responses to events in the tributary basins is less distinct and less well-exposed than evidence in the major valleys; exceptions are glaciated basins or those with large landslides. Using our evidence from the major valleys (discussed above) we infer the following sequences of events:

3.6.2.1 Weber River Drainage

1) It is clear that there is a distinct group of fan and terrace remnants in Kamas Valley and the central Weber River Valley that are significantly older than the remnants correlated with the Bull Lake glaciation (130-150 ka), but younger than the erosion surfaces discussed above (sec. 3.6.1). This does not necesarily imply that these remnants are all the same age; they may differ in age by as much as 100-300 kyr. However, indices for

soils on the remnants, the degree of dissection of the remnants, their position above better-dated, better-preserved remnants, and their probable association with one or more of the pre-Bull Lake glaciations recorded by the marine isotope record suggest these remnants are >200 ka and <500 ka, possibly correlative with isotope stages 8 (230-300 ka), 10 (350-370 ka), and/or 12 (440-470 ka).

These remnants are 20-30 m above the Bull Lake remnants and vary from 45 m to 70 m above the present river. By projecting the slope of some of the better preserved of these pre-Bull Lake remnants into the center of the valley, we estimate that floodplains during this period were about 30-50 m above the present valley floor in the central Weber Valley and about 25 m above the present floor of northern Kamas Valley. Scarps, 10-15 m high, at the toe of alluvial fans on the east side of Kamas Valley may have been cut when the channel of the Weber River was pulled towards the east side of the valley, perhaps by displacements on the East Kamas fault during this period before the Bull Lake glaciation. However, the scarps may also have been cut by the building of an outwash fan at the northeast corner of the valley which might have periodically deflected the channel of the river to the south during pre-Bull Lake and later glaciations. The fluvial deposit 30 m above the southwestern corner of Kamas Valley deposited by the former south fork of the Weber River (Woodfill, 1972)(discussed below), may be correlative with remnants in this age group. The net average degradation along the river above the East Canyon fault since these remnants were deposited appears to be <50 m.

2) Fluvial remnants about 25-40 m above the central Weber River (projected to about 20-30 m above the present river), 0-10 m above the river in Kamas Valley, and about 25 m above the upper Weber River Valley are correlated with the Bull Lake glaciation (130-150 ka). Based only on their elevation on the valley side, gravel remnants near the town of Morgan may also be correlative. These are outwash deposits in Kamas Valley and the upper Weber, although it is possible some of these deposits in the upper Weber pre-date the Bull Lake glaciation. Terraces cut in alluvial fans during this period in northern Kamas Valley show that the Weber flowed both west and probably south during this period. The correlation of fan and terrace remnants along the central valley with a deglacial episode during this period is less certain, but this is the most reasonable correlation. These remnants cannot be significantly younger than the Bull Lake glaciation. Thus, roughly 10-20 m of degradation in both Kamas and the central valley appears to have taken place between the end of the Bull Lake glaciation and previous major depositional (probably glacial) periods.

3) During the Bull Lake glaciation the former south fork of the upper Weber River was captured by the present Provo River, significantly reducing the size of the Weber drainage basin and removing over half of the area of its glaciated headwaters from its basin. Formerly, the upper Provo flowed north though Kamas Valley where it joined the Weber River (Anderson, 1915; Gilbert, 1928). A combination of headward erosion of the Provo River up the present upper Provo Canyon through a zone of weakness in the Keetley volcanics (produced by hydrothermally-altered intrusives (Woodfill, 1972)) and the filling of southern Kamas Valley with an extensive sheet of outwash (Peterson, 1970; Hansen, 1969) allowed a low col at the

southwestern corner of Kamas Valley to be breached (Anderson, 1915). Rapid down-cutting, probably by high-discharge meltwater streams, lowered the col, incised the outwash in the southern part of Kamas Valley to form the extensive 35 m terrace, and confined further outwash deposition to the narrow valley below the terrace (Nelson and Krinsky, 1982). The extent of a lower 20-30 m terrace along the Provo River suggests a period of floodplain stablility or aggradation about 10 m below the high terrace, also during Bull Lake time. Thus, the diversion of the upper Provo took place about 130-150 ka.

4) Deposition during Pinedale deglaciation (15-18 ka) produced distinct terminal moraines in the upper Weber River Valley and an outwash terrace at 10-12 m which grades into the present floodplain deposits near the northeastern corner of Kamas Valley. A coarse, bouldery terrace deposit, 8 m above the river near Coalville, may have been produced at this time, but other exposures in the central valley show mostly finer-grained sediments. Thus, Pinedale glacial deposits are apparently near the level of or below the modern floodplain between the upper Weber Valley and Morgan Valley. No net degradation seems to have occurred since the end of the Pinedale glaciation. This must be at least partially due to the reduced discharge into the Weber River following the diversion of the present upper Provo River.

5) In Morgan Valley, the high stand of Lake Bonneville about 15-16 ka produced wave-cut scarps, deltas where major tributaries to the Weber River enter the valley, and nearshore deposits at and below 1580 m (5180 ft). During the lower stand of the lake at the Provo shoreline, below the lower canyon of the Weber River (13-14 ka), a fluvial terrace was deposited over most of the valley at about 7 m above the present river. Because the river flows on or near bedrock in the upper canyon of the Weber above Morgan Valley, the filling of Morgan Valley by the lake probably had a negligible effect on the river gradient upstream.

6) In the central Weber Valley, a continuous fluvial terrace below Echo Reservoir at 5-8 m above the river and correlative alluvial and colluvial fans that grade to near the present floodplain probably date from the mid- to early Holocene. Some of these deposits may be as old as the end of Pinedale glaciation (15 ka), but the fine-grained character of most of these sediments indicates they post-date deglaciation. Possibly, most of these deposits date from the mid-Holocene altithermal, a period of low effective precipitation when a reduced vegetative cover may have resulted in much higher-than-present sediment yields during major storms. Thus, no more than 7-8 m of degradaion has taken place along the river valley since the mid- to early Holocene.

3.6.2.2 Provo River Drainage

1) Evidence of mid-Quaternary fluvial events in the Provo drainage basin is found only in Heber Valley and the upper part of the lower Provo River Canyon. Probable remnants of moraines predating the Bull Lake glaciation are found above the 35 m outwash terrace on the north side of the river near the junction with the South Fork of the Provo (Bryant, in press)(pl. 1). Thus, earlier glaciations were more extensive than the Bull Lake glaciation in the Provo headwaters, but no outwash deposits above the 35 m

terrace are preserved. The size and bouldery lithology of the large fan making up Weeks Bench just below Deer Creek Dam (fig. 5.7) suggest it was deposited during a pre-Bull Lake glaciation, but we have no direct evidence linking it with a glacial episode. It may be a response to the damming of the canyon by a landslide. Exposures of soils on some of the alluvial fans on the margins of Heber Valley and the Provo Valley along Deer Creek Reservoir show some parts of the fans considerably predate the Bull Lake glaciation. Because the fans are being eroded and younger sediments have been deposited in channels and on the distal portions of the fans, the local base level for the tributary drainages (the main river) must be being lowered. However, because portions of the fans are hundreds of thousands of years old and the fans are near the present floor of the valley, the relative depth of the Provo Valley in the past cannot have been greatly deeper than it is now. If it had been, extensive old fans like these would not be preserved on the valley sides. This also argues for either relatively little displacement on valley-bounding faults or concurrent rapid aggradation which has kept the floor of the valley near its present elevation during most of the mid-and late Quaternary.

2) During the Bull Lake glaciation glaciers advanced down the North and South Forks of the Provo River building moraines in the valley of the North Fork and depositing an extensive valley train which filled the southern half of Kamas Valley with outwash. This aggradation raised the level of the river to the col at the southwest corner of Kamas Valley, diverting the river into the upper canyon of the Provo River and into Heber Valley. The river then incised the outwash plain and the canyon at least 10 m and probably enlarged the upper canyon considerably. A large amount of outwash must have been deposited in northern Heber Valley where the river spread out over the wide floor of the valley. We have no information on timing, but quite possibly, the main river channel was deflected to the east side of its alluvial fan at the head of Heber Valley during this period and may have cut the subdued scarps in the distal parts of the fans on this side of the valley at this time. The dissection of older basin fill deposits in Keetley Valley, begun by headward erosion of the Provo River before the diversion, must have accelerated during this period. A single soil on the edge of the Daniels Creek alluvial fan shows that a large fan was also deposited from this drainage at this time. Probably, parts of the alluvial fans along the margins of Heber Valley and near Deer Creek Reservoir were periodically active during this period.

3) Pinedale glaciation in the headwaters of the Provo River was marked by the deposition of prominent moraines in the valleys of the North and South Forks. The outwash terraces deposited at this time are much less extensive down-valley from the moraines than those deposited during the Bull Lake glaciation, probably because the river was confined to the narrow valley in the upper canyon and to below the 25 m terrace in southern Kamas Valley. High meltwater discharges, probably during deglaciation (15-18 ka), must have deeply (up to 25 m) incised the older outwash, deepened the upper canyon, and spread large quantities of outwash over the northern end of Heber Valley. During the same period much less outwash was being spread into the valley from glaciers in Snake and Pine Creek valleys on the northwest margin of Heber Valley and from Lake Creek valley in the southeast corner of Weber Valley. Alluvium was also deposited from Daniels Canyon, although no large glaciers occupied this

drainage. Based on the position of the Provo River on the west side of the valley during at least the later part of this period, deposition from Lake Creek and Daniels Canyon must have been more extensive than from the northwest margin, forcing the river to the west side of the valley. Another possibility is that earlier fans from these drainages were larger than those from the northwest margin and thus, that the lowest part of the valley was along the northwest margin. We have not identified any Bull Lake glacial deposits in any of these drainages suggesting Bull Lake glaciers in these valleys were no more extensive than Pinedale glaciers. Lake Bonneville extended into the lower canyon about 15 ka and left shoreline deposits in the canyon and an extensive delta at its mouth.

4) The latest Pleistocene (<15 ka) and Holocene history of the river is marked by a low terrace along parts of the upper river valley, Holocene channel scars over much of the northern third of Heber Valley, by scarps in deposits of this age near Midway and on the distal edge of the Daniels Canyon fan above Deer Creek Reservoir, and by a few isolated terrace remnants in the lower canyon of the river, such as the 10 m terrace below Weeks Bench. Up to 7 m of incision were apparently produced above the lower canyon of the river during this period, but there is considerably more incision nearer the Wasatch fault due to rapid relative uplift of the Wasatch Mountain block. Parts of the distal portions of the alluvial fans along the margins of Heber Valley and near Deer Creek Reservoir were active during this period.

Thus, the wide floor of Heber Valley seems to have been near its present relative level for the last several hundred thousand years even though the lower and probably the upper Provo Canyons have been deepened considerably over the same period.

3.6.3 Neotectonic Conclusions

A key premise in our interpretation of the contribution of tectonic deformation to the development of the Weber and Provo basins is that the larger streams in the area have been able to downcut at rates that equal or exceed the highest Quaternary uplift rates in the eastern Wasatch Mountains (for example, Hamblin and others, 1981). Following these authors, at any given point along a river the apparent uplift of the river profile due to fault displacement is the sum of the true uplift plus the amount of channel degradation (or minus channel aggradation) that would have occurred without displacement.

3.6.3.1 Areas with the Highest Quaternary Rates of Relative Uplift

Total relief and the degree of fluvial dissection are the variables we used to distinguish areas with the highest relative rates of Quaternary uplift. Statistical analysis of quantitative measures of drainage basin, stream profile, and valley morphology (methods of Bull and McFadden, 1977; Soule, 1978; Mayer and Maclean, 1986) would document and show more subtle differences in relative uplift from one area to another than the qualitative approach used here; however, major conclusions should be the same whether or not quantitative methods are used.

The greatest relief and steepest valleys in the eastern Wasatch Mountains

occur near the crest of the range about 15 km east of the Wasatch Front. Relief is high west of the crest, but gradually decreases to a rolling, moderately dissected topography about 40-50 km east of the Wasatch fault. The Uinta Mountains are a major positive relief element on the east edge of the area. In the central portion of the area, total relief drops more sharply about 25 km east of the fault along the western edge of the more easterly back valleys (Richardson Flat, Heber, Kamas, Strawberry) and the central Weber River Valley. The widespread preservation of pre-Quaternary erosion surfaces in this area shows that late Cenozoic uplift was much less here than in the main part of the range to the west. Thus, except where the increasing height of the range is broken by back valleys (Morgan, Ogden, East Canyon), evidence of relative late Cenozoic uplift seems to increase from east to west to the Wasatch fault. However, the development of the eastern back valleys has lowered much of the landscape in the eastern part of the area reducing total relative relief and the degree of fluvial dissection. In a relative sense, this could be interpreted as evidence for the western Wasatch Range rising more as a horst (Gilbert, 1928) rather than as a slab displaced along the Wasatch fault being tilted eastward. However, downward displacement of Salt Lake Valley along the Wasatch fault (Eardley, 1970) with much lower rates of slip on the western back-valley-bounding faults would produce the same topography.

3.6.3.2 Apparent Sequence of Basin Development

Only broad generalizations can be made about the timing of displacements on faults that formed the margins of the back valleys. Kamas Valley was one of the earliest basins to develop in the central eastern Wasatch Mountains, but the presence of the Norwood Tuff shows Ogden Valley, Morgan Valley, and the East Canyon area may have had an earlier history of normal faulting. The present physiography of the other back valleys south of East Canyon is a more recent development, but the present valleys are certainly pre-Quaternary. Some faults on the margins of these valleys may not have moved since this time, but many clearly have had more recent displacements that are contemporaneous with those in Deer Valley and Parleys Park. Portions of the faults bounding some of the valleys have continued to move during the late Quaternary. Thus, all the basins have had a long and complex history, but those south of the central Weber Valley (except for Kamas Valley) may have had a shorter history than those farther north. In any case, patterns of drainage development and valley margin morphologies show that rates of development and thus of faulting varied both spacially and temporally.

3.6.3.3 Rates of Incision along the Weber River

Rates of incision along the Weber River vary with the age of the datums used to estimate the rates. Rates are highest, 0.5-0.8 mm/yr, where latest Pleistocene and Holocene deposits are used as datums (upper Weber Valley, Henefer area, and Morgan Valley), and less than half these (0.18-0.3 mm/yr) where Bull Lake deposits are used. Rates derived from projected pre-Bull Lake datums (RAG 1) in the central Weber Valley are 0.1-0.25 mm/yr with the true rates probably closer to 0.1 than to 0.25. Rates in Kamas Vallley are lower (0 mm/yr for Pinedale, 0-0.07 mm/yr for Bull Lake, and 0.05-0.12 mm/yr for pre-Bull Lake) because the relative elevation of remnants is lower. However, it is unclear whether the lower elevation of the remnants is due entirely to aggradation in the valley during Bull Lake and Pinedale

glaciations or to agradational filling as a result of actual downward displacement of the valley floor on valley-bounding faults. The difference in relative elevation between the remnants in Kamas Valley and those in the central valley (fig. 3.5) is too small (<20 m) and the remnants too discontinuous to argue for significant displacement on normal faults along this part of the river. We have no other evidence that faults crossing this part of Kamas Valley or the central valley have been active during the Quaternary (sec. 5.8 and 4.5). No correlatable pre-Bull Lake remnants are preserved above Kamas Valley.

It is clear that the river valley above the East Canyon fault has not been greatly deepened during the last 200-500 kyr. Bedrock is at shallow depths on either side of the East Canyon fault in East Canyon Creek valley (sec. 4.5) and the Weber River Valley, suggesting that apparent uplift rates on the fault have not exceeded river incision rates on the downthrown block of the fault. This and other well data showing shallow depths to bedrock in the central valley suggest downcutting between episodes of aggradation in the Weber Valley may have been limited to roughly the depth of fill by bedrock at shallow depths beneath the river.

The lack of dated remnants <730 kyr old along the river below the East Canyon fault makes it difficult to draw conclusions about rates of valley erosion. However, this lack of remnants might well be due to their removal as a result of high rates of erosion due to the high rates of relative uplift near the Wasatch fault in and near Morgan Valley. The maximum rate in Morgan Valley derived from the paleomagnetically-dated erosion surface is <0.18 mm/yr. Incision rates must have been much higher near the Wasatch fault than upstream of Morgan Valley because of the high uplift rate on the fault; although discontinuous, pre-Bull Lake remnants are higher above the river closer to the Wasatch fault suggesting present and reconstructed pre-Bull Lake river profiles diverge downstream. Also, the modern river profile steepens in the lower canyon of the river indicating this portion of the river has not fully adjusted to recent uplift on the Wasatch fault. Thus, incision rates upstream were probably considerably less than this maximum rate over the same period of time. About 0.1 mm/yr is a reasonable maximum rate from the mid-Quaternary to present for uplift-related incision by the river above the East Canyon fault; rates below the fault were higher, but probably <0.15 mm/yr except adjacent to the Wasatch fault.

3.6.3.4 Rates of Incision along the Provo River

There are less datums along the Provo River than along the Weber from which to calculate incision rates. As along the Weber, latest Pleistocene and Holocene rates derived from terraces in the upper Provo Valley and in Heber Valley (0.5-0.7 mm/yr) are clearly much higher than long-term rates. Rates determined from Bull Lake deposits in the upper valley are 0.18-0.25 mm/yr, but it appears that there has been little net degradation in Heber Valley over the last several hundred thousand years. The maximum rate derived from Weeks Bench, just below Deer Creek Dam, is similar (<0.2 mm/yr). Longer-term maximum rates derived from the paleomagnetically-dated cols at the north end of Heber Valley and near Deer Creek Reservoir are <0.13 mm/yr. Incision rates must be much higher than this in the lower canyon of the river near the Wasatch fault, but there are no dated deposits in this area, except for the Bonneville deposits at the mouth of the canyon (which yield a rate of 3 mm/yr

since 15 ka).

The present profile of the Provo River is smooth except near Deer Creek Dam and at Vivian Park. A decreasing gradient above the dam and a steepening below the dam suggest the river has not been able to maintain its grade along this reach, probably due to landsliding or fault displacement. The marked steepening in the river gradient for 1.5 km below Vivian Park is probably the result of some combination of 1) the upstream migration of a knickpoint produced by relatively rapid uplift on the Wasatch fault, 2) the river's inability to remove the alluvial fill deposited in the canyon when Lake Bonneville reached this elevation, and possibly 3) the damming effect from the large alluvial fans on the north wall of the canyon.

Thus, our conclusions on incision rates for the Weber River seem to also apply to the Provo River: maximum mid-Quaternary rates above Deer Creek Dam are probably <0.1 mm/yr, while rates are higher than this closer to the Wasatch fault.

3.6.3.5 Relative Rates of Uplift on Major Faults

Our outline of the geomorphic development of the two major drainage basins of the region and estimated incision rates provide only limited constraints on slip rates on faults in the region. Because we have no numerical-age estimates for latest Tertiary-early Quaternary units in the area, pre-mid-Quaternary rates cannot be calculated. Except perhaps immediately adjacent to the Wasatch fault, river incision has kept pace with uplift (Hamblin and others, 1981). For this reason, the rate of river incision into the upthrown block of a fault may be a good maximum estimate of the slip rate on the fault if there is no aggradation above or below the fault. However, terrace and fan remnnats are much less likely to be preserved on an uplifted block (more rapid erosion) unless slip rates are very low. Incision rates for parts of river valleys on downthrown blocks (such as Kamas and Heber Valleys) measure only net incision and because aggradation usually is extensive in this type of setting, a slip rate component cannot be separated from the incision rate.

Along the Weber River incision rates and the relationship of terrace and fan remnants to the modern river profile suggest that mid- and late Quaternary slip rates on faults that cross the river above Morgan Valley are <0.1 mm/yr. Higher incision rates derived from Bull Lake and younger deposits are not the result of tectonic displacement on faults, but deposits of these ages cannot be used to preclude displacements on faults except at a few localities. Incision rates provide little direct information on the slip rate of the Morgan fault because no old remnants are preserved on the upthrown side of the fault and because the valley is filled with >200 m of lake and alluvial sediment on the downthrown side. Below Morgan Valley our assumptions about incision rates and slip rates may not apply.

We infer similar conclusions about faults crossing the Provo River above Deer Creek Dam, but because the principal faults bound valleys (Kamas and Heber) with thick aggradational fills, incision rates provide little direct data on slip rates. However, the complex sequence of deposits which are up to several hundred thousand years old in the fans bordering Heber Valley and isolated deposits of Bull Lake age in the center of the valley suggest that fans graded to a floodplain at close to the present relative elevation have

persisted for this length of time. This suggests inferred maximum slip rates of 0.1 mm/yr on these faults are reasonable.

The many northwest-trending thrust faults which trend across the canyon of the lower Provo River were active during the late Cretaceous (Baker, 1964a). One of the largest normal faults in the canyon, the East Aspen Grove fault displaces some thrust faults and the earliest Tertiary volcanics in the area, but does not displace the youngest Teriary volcanics. The East Aspen Grove fault and the related West Aspen Grove fault are therefore no older than Eocene (Baker, 1964a). Structural relationships at several other sites in the area indicate Tertiary extension along preexisting thrust planes (R. L. Bruhn, oral communication, 1982).

Because the lower Provo Canyon area is undergoing rapid dissection due to uplift on the Wasatch fault, scarps produced by relatively small displacements (cumulative displacement <50 m) on faults in the area would be rapidly eroded. However, the major Tertiary faults in the area appear to have had little effect on the present topography, and are thus, thought to be much older than the Wasatch fault (Baker, 1964a) and the inferred faults bounding the back valleys.

The higher elevation of bedrock beneath Deer Creek Dam than the base of wells drilled entirely in alluvium upstream in Heber Valley indicates displacement on valley-bounding faults beneath Deer Creek Reservoir (Baker, 1964a), probably with aggradation along this part of the river due to intermittent ponding of drainage during episodes of uplift (Baker, 1976; Hunt, 1982). However, Weeks Bench (pre-Bull Lake fan) is not much higher than the present elevation of Deer Creek Reservoir and even if minimal relative uplift of the bench is assummed, damming due to either landslides or uplift here cannot account for most of the alluvial filling of Heber Valley. Still, the change in gradient of the present river profile at Deer Creek Dam and aggradational landforms just upstream suggest Quaternary events of some sort perturbed the river's profile. Bonneville shoreline sediments at the mouth of the lower Provo Canyon reach almost twice the height above the present river that Weeks Bench is above bedrock beneath the river. This argues for relatively little uplift of Weeks Bench relative to uplift on the Wasatch fault at the mouth of the canyon. There is no prominent mountain front escarpment near the dam and regional evidence discussed above shows displacement rates must be much lower than those on the Wasatch fault. Thus, faults beneath Deer Creek Reservoir may have had Quaternary displacements, but long-term slip rates on faults in this area are low.

4. CENOZOIC FAULTING IN THE NORTHERN WASATCH MOUNTAINS

4.1 Tectonic Setting

Although obscured by early and middle Tertiary sedimentation and the development of the back valleys, north-south trending late Cretaceous and early Tertiary, east-directed thrust faults extend south from the Idaho-Wyoming thrustbelt through the northern Wasatch Mountains to the westward projection of the Uinta Axis where they then turn east on the northern margin of the Uinta reentrant (Armstrong, 1968; Beutner, 1977). Except for the older Precambrian and some Paleozoic rocks between Ogden and Salt Lake City in the lower plate of the Willard thrust, all of the northern Wasatch Mountains are a large allocthonous block (Armstrong, 1968). The Willard thrust, exposed in Ogden Canyon, emplaces younger Precambrian rocks over older Precambrian and Paleozoic rocks (Eardley, 1969). Further east a series of younger, structurally higher thrusts including the Crawford, Absoraka and Darby thrusts are interpreted to flatten with depth to join a detachment surface (Armstrong, 1968; Royse and others, 1975; Lamerson, 1982).

Although reflection records from the back valleys in the northern Wasatch Mountains are few and of poor quality, published interpretations of subsurface structure in this Utah portion of the Thrustbelt suggest that some back valley faults are similar to late Cenozoic normal faults in the Idaho-Wyoming thrustbelt such as the Grand Valley and Star Valley faults (Dixon, 1982; Piety and others, 1986). The East Cache, Morgan, East Canyon, Bear Lake and Ogden Valley faults have been interpreted as listric normal faults that sole in a sub-horizontal detachment at depth (Lamerson, 1982; Royse and others, 1975; Royse, 1983).

Gilbert (1928) described the back valleys of Cache Valley, Ogden Valley and Morgan Valley as grabens. He referred to the Wasatch Mountains to the west as a horst with the Wasatch fault bounding the west side of the horst and back valley normal faults bounding its east side. Eardley (1933) acknowledges the possible contribution of normal faulting to the development of Ogden and Morgan Valleys, but attributes the topographic expression of the basins primarily to erosion, and interprets a 3-4° eastward tilting of the Wasatch Mountains as a response to displacement on the Wasatch fault, ascribing the evolution of Heber Valley to preexisting erosional relief and migration of a knickpoint in the Provo River. Eardley (1944) related the Herd Mountain and Weber Valley erosion surfaces of Miocene and Pliocene age, respectively, to displacement on the Wasatch fault, their dissection to regional uplift, and concluded that the back valleys are early Cenozoic synclines, deepened by erosion. Eardley (1952) reviewed early Cenozoic folding in the north central Wasatch Mountains and describes the East Canyon fault. Eardley (1959) discusses Cenozoic volcanic stratigraphy and suggests that the Morgan and East Canyon faults are late Cenozoic normal faults. In unpublished theses his students conclude that late Cenozoic displacement has occurred on normal faults in the back valleys of the Wasatch Mountains (Brimhall, 1951; Egbert, 1954; Schick, 1955; Nelson, 1971). Threet (1959) reviewed the evidence for contrasting interpretations of the back valleys as eroded early Cenozoic synclines and Cenozoic grabens and concludes that the origin of each valley should be considered separately, as we have done below.

4.2 Morgan Valley

Morgan Valley is located in the northern Wasatch Mountains, 35 km northeast of Salt Lake city and about 20 km east of the Wasatch fault (pl. 1a and fig. 4.1). Interstate 84 and the Union Pacific Railroad follow a 20-km-long, 2 to 3 km wide northwest-trending floodplain of the Weber River across this 10- to 15-km wide, north-trending basin. East Canyon Creek enters Morgan Valley from the south and joins the Weber near the town of Morgan and Cottonwood Creek enters the valley from the east 10 km downstream of Morgan.

4.2.1 Setting

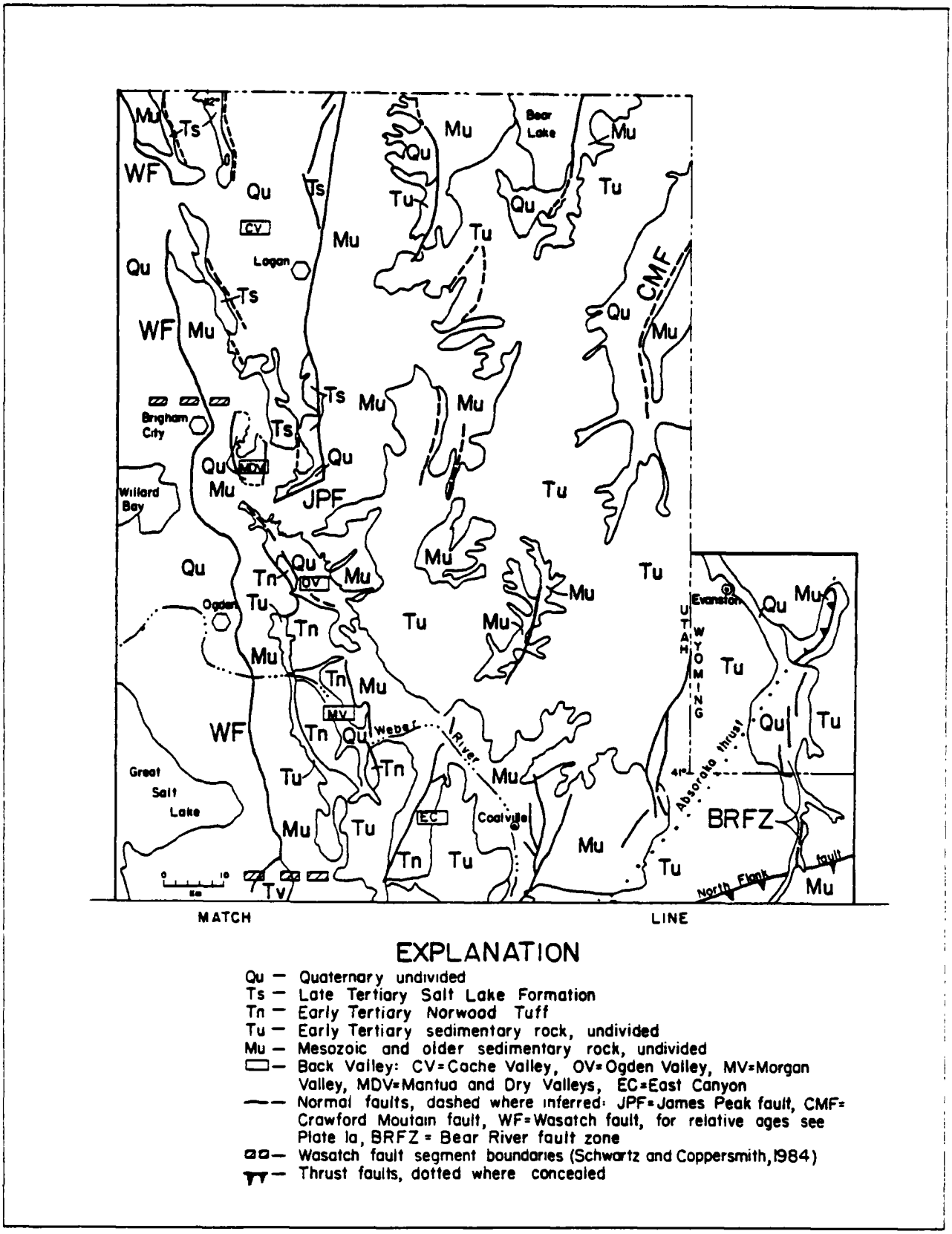
Cenozoic deposits of three ages, separated by angular unconformities, are present in Morgan Valley and suggest a deformational history dating from the Eocene. The conglomerates of the Eocene Wasatch Formation, dipping 40 to 65° to the east and northeast, are exposed on the west margin of the valley unconformably overlying Mesozoic and Paleozoic sedimentary rocks (Mullens and Laraway, 1973; Bryant, 1984). The overlying tuffaceous sandstones and conglomerates of the Norwood Tuff, described and dated as late Eocene to early Oligocene by Eardley (1944), are exposed throughout the valley dipping 10° to 40° to the northeast. Schick (1955) and Coody (1957) mapped a fanglomerate unconformably overlying the Norwood Tuff on the east side of the valley (Thv on fig. 4.2) that they informally correlated with the Huntsville fanglomerate, which is mapped in Ogden Valley and near the East Canyon fault (fig 4.1).

Northeast dips that increase with age in the Tertiary rocks in the basin suggest that the dip of the fault shallows with depth, and it is inferred to join the regional detachment below the north-central Wasatch Mountains (Hopkins and Bruhn, 1983). The estimated 6800 m of Cenozoic displacement on the fault (Hopkins, 1982) is consistent with estimates of a minimum of 3300 m of structural relief between the crest of the Wasatch Mountains and Morgan Valley (Naeser and others, 1983). A gravity study of the back valleys of the Wasatch Mountains (Quitzau, 1961) defines a 20 mgal residual Bouguer anomaly in the valley which also supports an interpretation of a significant thickness of low density Cenozoic deposits in Morgan Valley.

4.2.2 The Morgan fault

The Morgan fault is mapped on the east side of Morgan Valley at the base of an escarpment formed in Paleozoic rocks (Mullens and Laraway, 1973). The escarpment consists of three linear, 4- to 8-km-long sections that correspond with en-echelon steps in the trace of the fault and with differences in escarpment height and the elevation of hanging wall deposits (figs. 4.2 and 4.3). There are no fault scarps in unconsolidated deposits along the three sections of the fault; however, triangular facets along the base of the escarpment that are 100 to 250 m high and slope 20° to 25° suggest that Quaternary displacements have occurred on the fault.

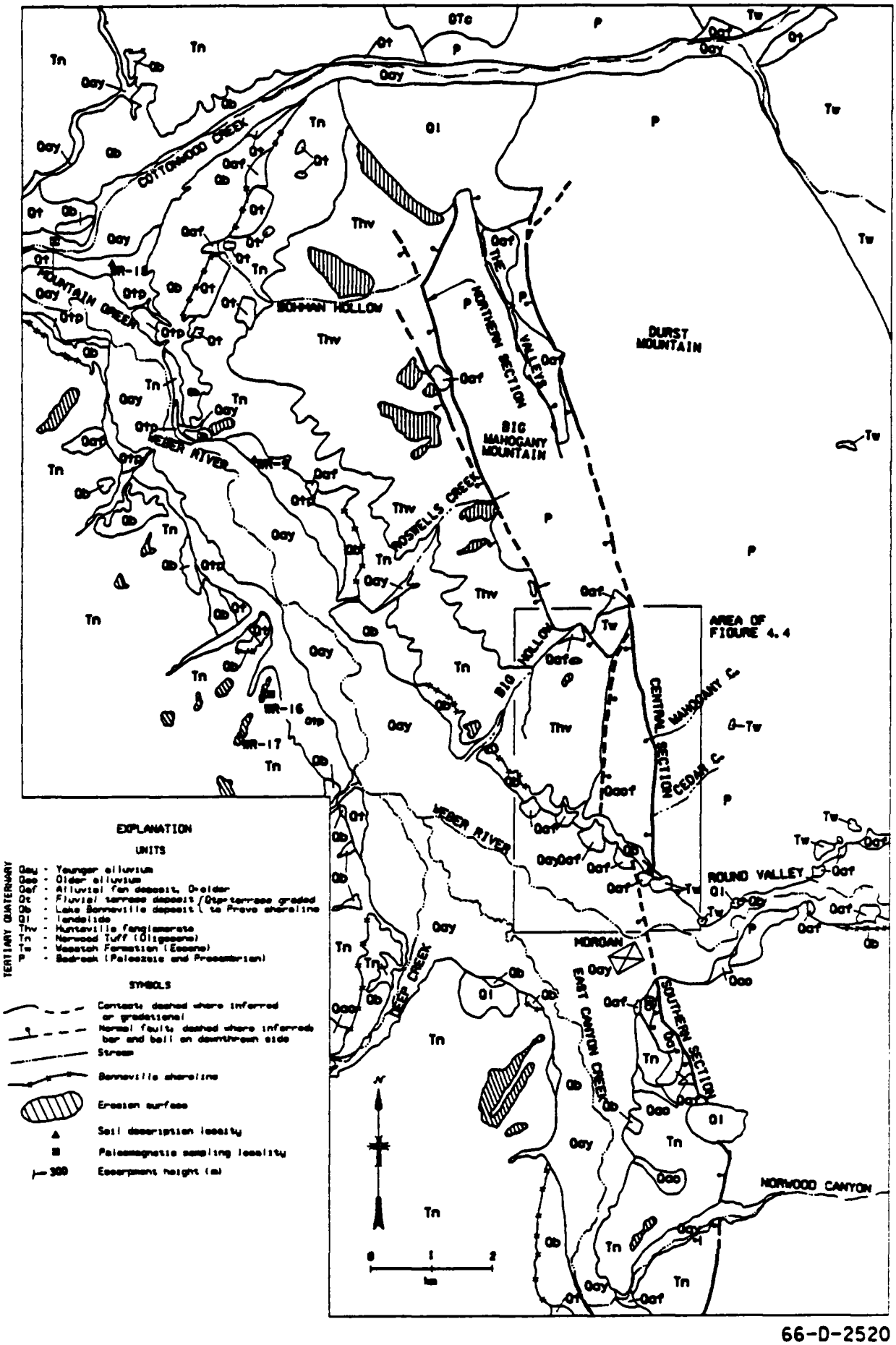
In the following discussion, we have divided the Morgan Valley into three sections with some contrasting characteristics; however, available evidence suggests but does not establish differing late Quaternary slip rates, recurrence, or age of most recent displacement as has recently been proposed for segments of the Wasatch fault by Schwartz and Coppersmith (1984).



EXPLANATION

Qu — Quaternary undivided
Ts — Late Tertiary Salt Lake Formation
Tn — Early Tertiary Norwood Tuff
Tu — Early Tertiary sedimentary rock, undivided
Mu — Mesozoic and older sedimentary rock, undivided
▭ — Back Valley: CV=Cache Valley, OV=Ogden Valley, MV=Morgan Valley, MDV=Mantua and Dry Valleys, EC=East Canyon
—— Normal faults, dashed where inferred: JPF=James Peak fault, CMF=Crawford Moutain fault, WF=Wasatch fault, for relative ages see Plate 1a, BRFZ = Bear River fault zone
▫▫ — Wasatch fault segment boundaries (Schwartz and Coppersmith,1984)
▼▼ — Thrust faults, dotted where concealed

Figure 4.1 Geology of the northern Wasatch Mountains.



66-D-2520

Figure 4.2 Cenozoic geology of Morgan Valley.

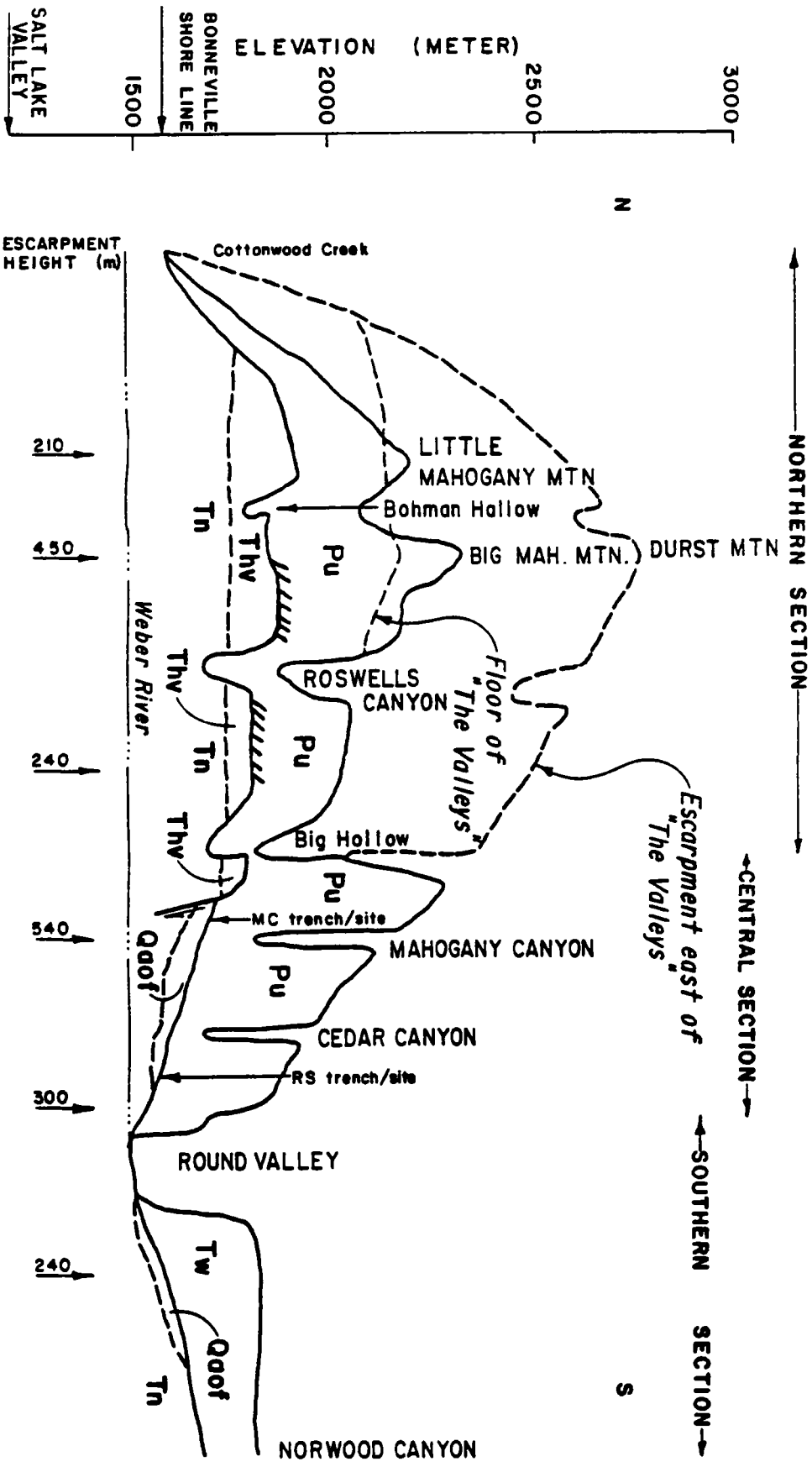


Figure 4.3 Generalized topographic profiles and geologic sections parallel to the strike of the Morgan fault.

4.2.2.1 The northern section

The preservation of triangular facets and the tectonic rotation of early Quaternary erosion surfaces suggest that late Quaternary displacements have occurred on the northern section of the Morgan fault. This 10-km-long section of the fault is mapped from from Big Hollow north almost to Cottonwood Creek (fig. 4.2) as a series of parallel and en-echelon fault traces at or near the eroded facets at the base of the bedrock escarpment. We have shown the late Quaternary Morgan fault dying out between Bohman Hollow and Cottonwood Creek where the escarpment associated with the fault has diminished in height to less that 50 m.

Adjacent to the northern section of the Morgan fault, near Roswell Canyon, the Huntsville fanglomerate (QTc of Mullens and Laraway, 1973) overlies the Norwood Tuff on a planar, east-dipping contact. Hopkins (1982, fig. 5) shows the Huntsville fanglomerate dipping 13° to the east with an estimated thickness of 1000 m adjacent to this section of the fault. As this fanglomerate is locally derived from the footwall of the Morgan fault its original dip is assumed to have been to the west, thus the present east dips are interpreted to be the result of rotation by displacement on the Morgan fault. Locally well-preserved, gently (0.5 - 1.7°) east-dipping erosion surfaces, cut on the Huntsville fanglomerate, are preserved adjacent to the northern section of the fault at an elevation of about 6100 ft (fig. 4.2). The position of these surfaces, adjacent to the Morgan fault scarp at Durst Mountain, suggests they were once graded to the Weber River and sloped to the southwest. We infer that subsequent displacement on the Morgan fault has tilted these surfaces into the fault plane.

No scarps were observed in unconsolidated deposits along this section of the fault, but there are no deposits older than mid-Holocene that directly overlie this section of the fault (fig. 4.2). A few eroded, discontinuous, mid-to late Quaternary of fluvial terrace remnants at about 100 m (330 ft) and 175 m (585 ft) above Cottonwood Creek are found south of the creek (sections 20 and 29) near the westernmost trace of the northern fault section (fig. 4.2), and the morphology and drainage patterns of small tributaries on much of this side of Cottonwood Creek valley (near the end of the northern fault segment) suggest large-scale landsliding during the mid- and possibly late Quaternary. Bonneville-age shorelines near the most-likely projection of the fault section are undeformed but do not cross the fault and a less continuous pre-Bonnevillle (>15 ka) terrace about 40 m above the Bonneville shoreline angle does not appear to be significantly displaced, but also does not extend far enough up the creek to preclude post-Bonneville displacements on the fault.

About 1 km to the east of the northern section of the Morgan fault a narrow north-trending valley in Paleozoic rocks ("the Valleys") south of Cottonwood creek is interpreted to be a narrow late Cenozoic graben on the basis of its striking linear trend on topographic maps and air photos and its crosscutting relationship with the regional drainage pattern. An eroded escarpment extends south from "the Valleys" on trend with the projection of the strike of the central section of the fault suggesting that the features are related. Except for thin alluvial fan deposits and colluvium which lack scarps in "the

Valleys", no Quaternary or Cenozoic rocks are preserved in the center of the graben. Structural relief in the graben appears to be less than 500 m, significantly less than the 6800 m estimated for the northern section (Hopkins, 1982). We interpret these as subsidiary faults that join the main trace of the northern section at depth.

4.2.2.2 The central section of the Morgan fault

Our investigation of the Morgan fault focused on the central section of the fault, for along this section Quaternary alluvial fans (Qaof) appear to have been displaced by the Morgan fault (figs. 4.2, 4.3, and 4.4). We infer the topographic low on the hanging wall of the fault to be a 0.5- to 1-km-wide graben filled with alluvial fan deposits that is bounded on the east by the main trace of the central section of the Morgan fault and on the west by an inferred east-facing antithetic fault (figs. 4.2 and 4.4). Dissected alluvial fan deposits (Qaof) slope 6-9° to the southwest within this inferred graben. The lower 50 m of some of the facets slope 1-3° more steeply than their upper portions. Thus, we infer the surface trace of the fault to be at the 50 to 100 m wide break in slope between the facets and the fans. Although a few small, discontinuous, Holocene fans along the break in slope in the larger drainages are undissected, channels (some up to 20 m deep) are incised into the surfaces of all the larger alluvial fans along the central section (fig. 4.4). Longitudinal profiles down these channels show they are graded to the Bonneville shoreline along all but their lowest reaches. Knickpoints in the profiles due to the fall of the lake (dated at 15 ka by Scott and others, 1983) do not appear to have migrated more than 100 m up the fan channels. Holocene alluvial fans have been deposited where the channels reach the floodplain of the Weber River. Thus, we conclude that most of the sediment derived from the footwall of the fault is being carried beyond the hanging wall fan surfaces. Distinguishing tectonic from climatic or changing baselevel responses in alluvial fan systems is difficult at best (for example, Funk, 1977; Bull, 1977), but the dissection of older fans along the central section suggests fault slip rates are lower than stream downcutting rates.

4.2.2.3 The southern section of the Morgan fault

The southern section of the Morgan fault is mapped at the base of an escarpment in the west-dipping Wasatch Formation over a distance of 4.5 km from the Weber River south to beyond Norwood Canyon. Triangular facets with slopes of 18°-20° and heights of 90-120 m are preserved on a one km long portion of this section of the fault south of the Weber River. We have mapped the south end of the southern section of the fault in the vicinity of Norwood Canyon where its associated bedrock escarpment is obscured by very subdued landslide topography (fig. 4.2). An east-facing escarpment in the Norwood Tuff is ineterpreted as an antithetic fault forming a narrow (150 m wide) graben filled with alluvial fan deposits south of the Weber River.

We did not map the southern section in detail, but note that the alluvial fans flooring the graben have slopes and incised channels very similar to those along the central section. Small facets along the southern section have 20-25° slopes and also steepen near their bases like those on the central section. Thus, late Quaternary displacement seems likely on the southern section. However, total Cenozoic displacement on the southern

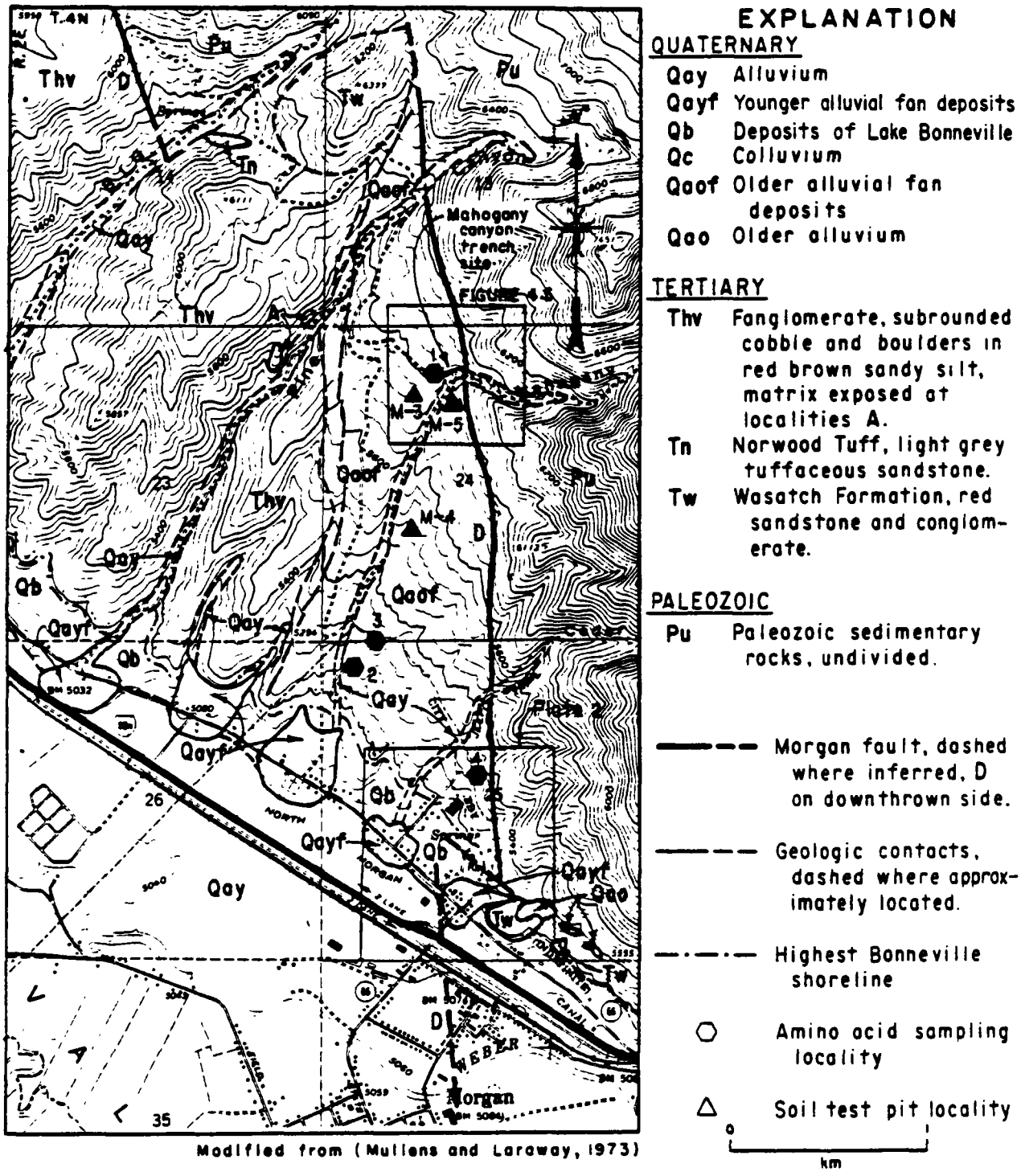


FIGURE 4.4 Geologic map of the central segment of the Morgan fault.

section appears to be less than on the sections to the north as discussed by Hopkins (1982, p.35). She suggests that a syncline, defined by the west dips in the Norwood Tuff in the hanging wall of the fault, formed when the Morgan fault became locked as extension continued.

4.2.3 Age of Quaternary deposits adjacent to the central section of the Morgan fault

The Quaternary deposits along the central section of the Morgan fault consist of Holocene alluvium in the major drainages, deposits of Lake Bonneville, and older colluvial and alluvial deposits at elevations above the Bonneville shoreline (fig. 4.4). Soils developed in the alluvium in the larger drainages (Qay on figs. 4.4 and pl. 2) and in the fans (Qayf) deposited where the drainages reach the floor of Morgan Valley are weakly developed without argillic B horizons. Comparison of these soils with the Holocene soils described by Shroba (1982) indicates that the alluvium is of Holocene age. Soils began forming on the buff-colored sands and silts between the present floodplain and the highest stand of Lake Bonneville in the valley following the fall of the lake about 14 to 15 ka. A soil developed on these deposits near Robeson Springs (M-2, table 4.1 and pl. 2) lacks an argillic horizon, but contains substantial amounts of pedogenic carbonate. A sequence of older fan deposits (Qaof on figs. 4.3, 4.4, and pl. 2) derived from the mountains to the east are exposed above the Bonneville shoreline. These deposits are overlain by thin (1- to 3-m-thick) hillslope colluvium (not shown on fig. 4.4 except south of Cedar Creek) that thickens to 7 m adjacent to the Morgan fault near Mahogany Canyon. Exposures and test pits (all sampling localities on fig. 4.4) show thick calcium carbonate soil horizons (stages II and III of Gile and others, 1966) on both the colluvial and alluvial deposits; a 1-m-thick petrocalcic horizon (stage IV) in fan deposits was exposed beneath about 3 m of colluvium near Mahogany Canyon (locality 1, fig. 4.4). Thus, based on comparisons with similar soils developed in similar deposits elsewhere in the region (Machette, 1985a), many of these alluvial and colluvial sediments are probably of middle Quaternary age (125 to 730 ka). However, the differing degree of carbonate development in units of similar lithology, unconformities between most alluvial and overlying colluvial units, and uncertainty in correlating individual alluvial units between isolated exposures suggests units deposited during a number of episodes during the Pleistocene may be present.

We used three relative dating methods to attempt to more accurately estimate the ages of the older colluvial and alluvial sediments along the central section of the Morgan fault -- two measures of the degree of soil development and amino-acid ratios measured on fossil gastropod shells in the deposits.

Soil development indices (Harden and Taylor, 1983) provide an objective way of comparing the degree of soil development on deposits of unknown age with the degree of soil development on deposits of similar lithology in areas where numerical ages are available (Birkeland, 1984a). Several calibrated (independently dated) soil profiles are available from Morgan Valley (discussed in sec. 3.4): 1) soil M-6 which overlies a peat dated at 8.3 ka and 9.1 ka in a trench near Robeson Springs (table 4.1 and pl. 2), 2) soils (M-2, table 4.1; W-9, W-18, fig. 4.2) on both fine and coarse materials younger than the Bonneville shoreline (14-15 ka), and profile W-16 with a reversely-magnetized B horizon that shows it to be >730 ka (fig. 4.2).

ble 4.1 Selected properties of soils on alluvial, colluvial, and lacustrine sediments along the Morgan fault, Morgan Valley, north-central Utah.

file	Horizon*	Average depth (cm)		Parent material	Munsell dry color	PERCENT BY VOLUME(EST) Pebbles 0.2-8cm	Cobbles 8-25cm	Bldrs (>25cm	PERCENT BY WEIGHT~ Sand 2-0.5mm	Silt 50-2um	Clay <2um	Percent# organic matter	Percent** carbonate
-1	A	0	10	slopewash colluvium	10 YR 6/2	5	0	0	27	56	18	1.7	16.5
	Bwk	10	23	slopewash colluvium	10 YR 5/3	5	0	0	28	52	21	1.2	24.9
	Bkm	23	50	slopewash colluvium	10 YR 8/0	5	0	0	28	58	15	0.5	43.7
	BK1	50	84	slopewash colluvium	7.5 YR 8/2	5	0	0	18	75	7	0.4	48.9
	Bk2	84	161	slopewash colluvium	7.5 YR 7/3	2	0	0	14	79	7	0.3	35.6
	C	161	228+	slopewash colluvium	7.5 YR 7/3	2	0	0	28	62	11		3.3
-2	Ap	0	9	loess and lake seds	7.5 YR 5/3	0	0	0	21	73	6	1.5	
	A	9	20	loess and lake seds	7.5 YR 5/3	0	0	0	22	70	9	1.1	
	Bw	20	42	lake sediments	7.5 YR 6/4	0	0	0	44	43	13	0.3	
	Cox1	42	50	lake sediments	7.5 YR 7/4	0	0	0	50	40	11	0.1	5.5
	Bk1	50	61	lake sediments	7.5 YR 7/4	0	0	0	44	45	11	0.2	13.9
	Bk2	61	71	lake sediments	7.5 YR 8/3	0	0	0	39	47	15	0.4	35.5
	Bk3	71	107	lake sediments	7.5 YR 8/3	0	0	0	6	81	14	0.1	21.7
	Cox2	107	155+	lake sediments	7.5 YR 7/3	0	0	0	6	82	12	0.1	13.0
-3	Ap	0	10	loess and alluvium	7.5 YR 5/3	10	10	2	28	57	15	6.5	
	Bt	10	32	loess and alluvium	7.5 YR 5/3	10	10	2	20	52	28	3.4	14.3
	2Bkm	32	35	alluvium	7.5 YR 8/0	20	5	2	17	66	17	1.2	50.4
	2Bk	35	73	alluvium	7.5 YR 8/3	20	5	2	20	66	14	0.4	56.0
	2Bt	73	128	alluvium	7.5 YR 6/3	5	0	0	19	73	7	0.2	21.6
	3Ckm	128	135+	alluvium	7.5 YR 8/1	20	10	2	27	41	32	0.3	51.0
-4	A1	0	13	loess and colluvium	7.5 YR 4/3	10	5	1	22	57	20	4.5	21.6
	A2	13	37	loess and colluvium	7.5 YR 4/3	10	5	1	22	62	16	3.2	28.0
	2BA	37	50	alluvium	7.5 YR 7/3	30	1	0	36	50	15	1.3	53.8
	2Bk	50	71	alluvium	7.5 YR 7/4	30	1	0	31	43	26	0.7	54.6
	3Ck	71	120	alluvium	7.5 YR 8/3	10	5	2	17	73	10	0.4	47.6
	3C	120	140+	alluvium	7.5 YR 7/3	10	5	2	19	53	29	0.2	39.8
-5	Ap	0	9	loess and colluvium	7.5 YR 5/3	15	10	1	24	58	18	4.7	
	A	9	30	loess and colluvium	7.5 YR 5/4	15	10	1	21	53	26	2.7	12.8
	BA	30	44	loess and colluvium	7.5 YR 7/4	15	10	1	29	48	23	1.4	46.1
	2Bkm	44	52	alluvium	7.5 YR 8/2	20	10	0	32	48	20	0.4	47.9
	2Bk	52	88	alluvium	7.5 YR 8/3	20	10	0	38	43	19	0.4	46.6
	3CB	88	138	alluvium	7.5 YR 7/4	40	1	0	31	48	21	0.2	41.6
	4C	138	149+	alluvium	7.5 YR 7/4	5	0	0	34	48	18	0.2	46.0
-6	Ap	0	16	slopewash colluvium	7.5 YR 4/2	5	0	0	31	56	13	9.8	10.7
	A	16	37	colluvium	7.5 YR 4/3	5	0	0	28	55	17	3.4	19.8
	Bt	37	69	colluvium	7.5 YR 5/3	5	0	0	30	55	14	2.2	25.0
	Ck	69	98	colluvium	7.5 YR 7/3	5	0	0	33	57	10	1.4	12.4
	2C1	98	135	colluvium	10 YR 7/3	10	0	0	28	49	23	0.9	36.4
	2C2	135	175+	colluvium	10 YR 7/3	5	2	0	23	50	27	1.0	11.6

*Horizon nomenclature of Guthrie and Witty (1982) and Birkeland (1984) except that master K horizon is not used.

~Particle size distribution of <2 mm fraction using sieve-pipette methods (for example, Carver, 1971) and a sedigraph for some silt-clay fractions with prior removal of carbonates and organic matter using methods of Jackson (1956).

#Percent organic matter by method of Walkley and Black (1934).

**Percent carbonate by method of Allison and Moodie (1965, p. 1387).

Unfortunately, the variable but high carbonate content of the soils described on alluvial and colluvial deposits along the central section of the Morgan fault (table 4.1, fig. 4.4) makes the indices of Harden and Taylor (1983) (table 4.1) less useful in estimating the age of these soils than the ages of many of the soils elsewhere in the Wasatch Range (sec. 3.4).

Rates of total pedogenic carbonate accumulation in soils is another method that has proven useful in estimating the age of soils in a number of areas in the arid and semi-arid western United States (Machette, 1985a). Age estimates based on total carbonate values cannot be relied on for soils significantly younger than the last interglacial (125 ka) (unless many independent age estimates for similar soils in the region are available) because of the probable major changes in carbonate accumulation rates over this period. However, over longer time spans, multiple cycles of climate change tend to attenuate accumulation rate changes and this results in relatively more accurate age estimates for older soils (Machette, 1985b; Colman and others, in press).

Using the methods of Machette (1985a) amounts of carbonate in g/cm^2 in the total profile were calculated for the Morgan soils and compared with values for carbonate-rich soils in the northern Wasatch Range with some independent age control. Latest Pleistocene-Holocene (0 to 15 ka) carbonate accumulation rates as high as 1 $g/cm^2/kyr$ were calculated (sec. 3.0) using two soils (M-2 and M-6, table 4.1) in Morgan Valley and one soil in Heber Valley (about 65 km to the south). However, groundwater may have added carbonate to soil M-2 and primary carbonate values are difficult to estimate for all soils. The longer-term (0-150 ka) rate is 0.5 $g/cm^2/kyr$ (again based on only 3 soils along the Weber River) is roughly half the latest Pleistocene-Holocene rate. Based on their locations east of the crest of the Wasatch Range, it is unlikely that latest Pleistocene-Holocene carbonate accumulation rates for the back valley soils are higher than the 0.5 $g/cm^2/kyr$ calculated by Scott and others (1982) for soils of similar age near Salt Lake City. Based on rates of about 0.15 $g/cm^2/kyr$ for Fisher Valley (Colman and others, in press), 0.14 $g/cm^2/kyr$ for the Beaver area (Machette, 1985b), and maximum rates of 0.14-0.26 $g/cm^2/kyr$ for Spanish Valley (Harden and others, 1985) elsewhere in Utah, middle and late Quaternary rates in the eastern Wasatch Range may well have been <0.2 $g/cm^2/kyr$. We use 0.5 $g/cm^2/kyr$ as a maximum rate to estimate minimum ages of 70 to 100 ka for soils M-3, M-4, and M-5 (table 4.1). These calculations suggest soils on the alluvial fans (unit Qaof on fig. 4.4) are certainly >50 ka and probably of pre-last interglacial age (>125 ka). Because the fans are being eroded even finite soil ages would be minimum ages for the fan sediments.

Amino-acid ratios derived from the analysis of the organic matrix within carbonate fossils have proven useful in the relative dating and correlation of a variety of Quaternary stratigraphic units worldwide (Wehmiller, 1982). This methodology, termed aminostratigraphy by Miller and Hare (1980), is valid within a region as long as all samples have had very similar temperature histories and if the amino acids in the species analyzed racemize at about the same rate (Williams and Smith, 1977). Although most studies have used marine mollusks (Wehmiller, 1982), recent work indicates amino acid ratios from non-marine gastropods are useful for relative dating (Miller and others, 1982; Scott and others, 1983; Nelson and others, 1984; Clark and others, 1986). The Paleozoic carbonates and alluvial fan surfaces with

carbonate-rich soils along the central section of the Morgan fault provide a favorable environment for lime-loving terrestrial gastropods. The large terrestrial gastropod Oreohelix cf. strigosa is abundant in the surface litter along the trace of the fault and fragments and whole shells of this species were found in the older alluvial fan sediments (Qaof) and overlying colluvium (Qc) at four sites (fig. 4.4 and table 4.2). Ratios of D-alloisoleucine to L-isoleucine in these samples in the alluvium are >0.4 while those in the colluvial units range from 0.20 to 0.57, suggesting the shells are of several ages.

Accurate numerical-age estimates are difficult to obtain from amino-acid ratios. These estimates require accurate kinetic models of amino-acid racemization in the mollusk genera of interest along with estimates of the temperature histories of the fossil samples. A $\pm$ 1° uncertainty in the effective diagenetic temperature (EDT) (integrated chemical effect of the sample's temperature history) results in a 20% uncertainty in the age estimate and we have no way of estimating the uncertainty in our EDTs. The diagenetic models we used were developed using different genera (table 4.2), but the models for many genera differ little and at the present time there is no reason to think these models do not apply to Oreohelix shells in Morgan Valley.

We used two kinetic models to calculate ages (minimum ages) for the samples (table 4.2). The linear model assumes a constant rate for the isoleucine racemization reaction in shells, but it probably only applies to our younger samples because the reaction rate has been shown to decrease markedly in older samples (Wehmiller, 1982). One of several possible non-linear models suggests much greater ages for the older samples. A few of the samples which were collected <2 m below the surface may have been affected by seasonal temperature changes (which would increase their apparent age), but because the alluvial fan sediments are being eroded most samples must have been buried more deeply during most of their burial history. If the shallower samples were <2 m deep for their entire burial history, the maximum possible surface heating effect would reduce our calculated ages by about half (for example, Wehmiller, 1977). Because of the large uncertainties in sample temperature histories and appropriate kinetic models only the linear-model age estimates (table 4.2) are used, which provide only minimum age estimates. However, enough is known about EDTs in the region and the reaction rate in gastropods to suggest that the samples from the colluvium with ratios of 0.20 and 0.27 are < 400 ka and <500 ka respectively.

Thus, based on 6 samples (table 4.2), the older alluvial fan deposits are >400 ka. The colluvial deposits overlie these older fan deposits at all the sampling sites. The lowest ratio obtained from colluvium, in the trench near Mahogany Canyon, suggests an age of >200 ka. Higher ratios from other colluvial units indicate that either these units are older or that shells in the slope colluvium are reworked from the older fan deposits. The minimum age estimates from the soil carbonate data are consistent with these age estimates from amino-acid ratios.

4.2.4 Trench investigations of Quaternary faulting on the central section of the Morgan fault

The Morgan fault is exposed at the base of the escarpment in 2-m-high

Table 4.2 D-alloisoleucine/L-isoleucine ratios in the total (free + peptide-bound) amino acid fraction and calculated ages for Oreohelix cf. strigosa from alluvial and colluvial sediments along the Morgan fault, Morgan Valley, Utah

INSTAAR Lab No. (Univ. of Colo.)	Depth below surface (m)	No. of sample preparations	Mean Total aIle/Ile ratio*	Minimum age estimates (ka): Linear kinetic model# Holocene EDT**	Linear kinetic model# Quaternary EDT##	Non-linear model~	Location on fig. 6.2, pl. 2 Site	Unit
Modern surface float (MAT = 7.2-7.7oC)								
DAN-194	0	8	0.025+0.005	-	-	-	1	-
North Morgan Springs (EDT = 7.5-8.0oC)**								
DAN-190	>4	3	0.61+0.05	174-189	709-777	1511-1660	4	Qaof
Gravel pit (EDT = 7.4-7.9oC)**								
DAN-207	2.3	3	0.27+0.06	71-77	317-289		2	Qc
DAN-209	0.7	3	0.35+0.06	95-103	422-386		2	Qc
DAN-189	3	2	0.41+0.06	113-123	456-503		2	Qaof
DAN-208	5.5	3	0.43+0.04	119-129	485-530		3	Qaof
Mahogony Canyon roadcut (EDT = 7.2-7.7oC)**								
DAN-198	>1.6	3	0.30+0.04	82-90	337-369		1	Qc
DAN-193,195,196 197,199	>2	8	0.49+0.06	142-155	582-637	861-942	1	Qaof
Trench M-6, Mahogony Canyon (EDT = 7.2-7.7oC)**								
	Trench unit							
DAN-206	4a	1.7	3	0.20+0.01	52-57	214-234	1	4a
DAN-201	2	5.0	3	0.35+0.05	98-107	400-438	1	2
DAN-200	2	5.1	3	0.57+0.03	169-184	691-757	1350-1478	1 2
DAN-203	2	6.0	3	0.40+0.05	113-123	463-508	1	2
DAN-204	1	4.8	3	0.44+0.03	126-137	515-564	1	1
DAN-205	1	5.8	3	0.46+0.03	132-144	542-593	677-740	1 1

* Alle/Ile ratio (peak area) measured using methods of Miller and Hare (1980). Mean ratios include one standard deviation. Extraneous values rejected using methods of Dixon (1965).

Age calculated using a linear kinetic model of isoleucine racemization (equation 18 in Williams and Smith (1977) wit k` = 0, a modern ratio of 0.025 for Oreohelix (Nelson, unpub. data), Arrhenius parameters determined for Vallonia by Nelson and others (1984), and values of constants in Arrhenius equation (no. 9 in Williams and Smith, 1977).

~ Age calculated using a non-linear model (e.g. Wehmiller, 1982) with the same relationships as for the linear model except that the reaction rate is assumed to decrease to 1/5 the initial rate for samples with alle/Ile ratios >0.4.

** Age calculated using an EDT (mean effective diagenetic temperature)(Wehmiller, 1977) for the Holocene estimated using instrumental mean annual temperatures in the region (NOAA, 1981), limited soil temperature data (Conrad, 1965) and unpub. data of Lael Harvey, Soil Conservation Service, Coalville, UT), and data of Miller and others (1982).

Age calculated using an EDT for the late Quaternary in this region of 8 C less than present mean annual temperature (Nelson and others, 1984; Wehmiller and Belknap, 1982). Age range calculated using +/-0.25oC range in estimated EDT.

exposures at Robeson Springs (pl. 2) as a planar, N7°W striking, 65° west-dipping sheared contact between Paleozoic carbonates and light brown, silty colluvium. Sheared and altered dolomite is exposed for a distance of about 15 m to the east in the footwall of the fault, but no other shears are evident in the colluvial deposits in the exposure that extends about 25 m west of the fault. This exposure and additional exposures at North Morgan Springs (pl. 2) showed that unconsolidated deposits, exposed above the Bonneville shoreline, were displaced by a single trace of the Morgan fault at the base of the triangular facets on the escarpment.

The Robeson Springs trench site is located at the southern end of the central section of the Morgan fault, about 150 m south of Robeson Springs (pl. 2). The linear trace of the footwall escarpment ends at a small, east-trending ephemeral drainage south of the trench site. South of this drainage red sandstone and conglomerate of the Wasatch Formation are exposed dipping 40° to the west and extending across the projection of the central section of the fault. Projection of the southern section of the fault north across the Weber River indicates that the Morgan fault steps westward about 200 m between the southern and central sections (fig. 4.4 and pl. 1).

At the Robeson Springs site four trenches were excavated at or near the break-in-slope at the base of the footwall escarpment of the Morgan fault (pl. 2). The trench logs, a site map, unit descriptions and a discussion of the bases for unit correlations are included on plate 2. Two of these trenches (M2U and M4) exposed the main trace of the Morgan fault. Another normal fault trending northwest between the central and southern sections of the Morgan fault is exposed in trenches M2U, M1, and M3. The Devonian and Cambrian dolomite which forms the escarpment is exposed in all the trenches. To the east it is overlain by Devonian and Mississippian sedimentary rocks that generally dip to the west, but that have been complexly folded and faulted (Mullens and Laraway, 1973). In trenches (M2U and M4) colluvial deposits overlie the dolomite in the hanging wall of the fault, but in the exposures at North Morgan Springs the colluvial deposits overlie older alluvial fan deposits that are correlated with similar deposits exposed at four locations north of the Robeson Springs site (sec. 4.2.3, fig. 4.4, and pl. 2).

4.2.4.1 Stratigraphy in Trench M4

In trench M4 the Morgan fault is clearly expressed as a zone of sheared dolomite and fault gouge from within a meter of the ground surface to the base of the trench (pl. 2). The fault zone juxtaposes colluvial deposits and bedrock along a N7W striking, 50° west-dipping planar contact. The east boundary of the fault zone is an abrupt planar shear separating fractured bedrock (unit 1) from rock flour (unit 1b) which is interpreted to be a fine-grained fault breccia derived from the bedrock. Near the base of the trench a plastic clay gouge (unit 1c) forms part of the fault zone.

On the west margin of the fault zone a 4-m-thick sequence of colluvial deposits have been displaced by the fault (pl. 2, units 3, 6, 7a, and 7b). The colluvial deposits are all of similar lithology--clayey silts with variable but small (<15%) amounts of dispersed, angular pebbles of dolomite. Using slight differences in color, clay content, carbonate content and induration, three main colluvial units (unit 3, unit 6, and unit 7) have been mapped and separate facies within each unit (small letters) have been

identified. Unit 3 is massive, well-indurated, and contains upper and lower zones of pedogenic carbonate (stage II). Unit 6 is siltier, lacks carbonate, and is loose and unconsolidated. The modern soil is developed in unit 7, including a the cambic B-horizon with weak stage II carbonate in some parts (unit 7a).

Discrete, downslope-thinning, colluvial wedges that are derived from erosion of the free face of a fault scarp are typically found adjacent to faults with scarps more than a meter high in unconsolidated deposits. The stratigraphy and thickness of these colluvial wedges have been used to estimate the size of the individual surface displacements on faults (for example, Schwartz and Coppersmith, 1984). Near the floor of trench M4, two 0.1-m-thick, 0.5- to 0.8-m-long fingers of fault breccia (unit 1b) are interbedded with colluvial unit 3c (pl. 2). This interbedding of fault breccia and colluvium appears to have resulted from the erosion of fault breccia from the free face of a scarp that was formed during two separate surface displacements on the fault. The colluvium between these fingers of fault breccia is 0.4 m thick, and 0.5 m of colluvium is preserved between the lower finger and the underlying bedrock. These thicknesses provide minimum estimates of the height of the scarp and the vertical displacement that produced it.

The lack of discrete horizons within unit 3a suggests that it did not accumulate as a succession of scarp-derived colluvial wedges. Unit 3a consists of 2 m of massive pebbly, clayey silt deposited by surface wash aand creep from above the trench site. The uniform thickness of fault breccia preserved adjacent to this unit along a planar 50o west-dipping contact indicates that unit 3a has been faulted into its present position. We interpret this unit to consist of multiple, indistinguishable colluvial units that have been downdropped along the fault during successive small surface displacements and subsequently buried by continuing deposition from the escarpment above the fault. These colluvial units inferred to comprise unit 3 are lithologically identical; unconformities between them or any differences in soil development from one unit to another have apparently been masked by carbonate accumulation. Based on the depth of carbonate in the modern soil (unit 7a) the pedogenic carbonate zones of unit 3 probably developed 1 to 2 m below the ground surface. The lack of interbedding within unit 3 (other than at the floor of the trench where fingers of fault breccia divide portions of unit 3c) indicates that the displacements did not expose the fault breccia in the scarp free face. This indicates that the individual surface displacements were not significantly greater than the present thickness of slope colluvium (unit 7c), about 0.5 m, on the footwall of the fault. Thus, the displacements were probably about the size of the minimum displacements inferred from the thickness of colluvium preserved below the fingers of fault breccia near the floor of the trench.

The total displacement since the deposition of unit 3c has been estimated by projecting the base of the unit 3 to the footwall of the fault using the same slope as the ground surface (pl. 2). The measured vertical displacement between the bedrock surface and the top of unit 3 is about 4.0 m.

In the upper portion of trench M4 the apparent displacement of the base of unit 6a records the most recent displacement event on the fault at this locality. Unit 6b is a slightly pebblier upslope facies of unit 6a, a key stratigraphic unit which is present in all of the trenches at the site and

which overlies a dated peat deposit in trenches M2 and M3 (discussed below). The amount of this displacement has been estimated by projecting the base of unit 6a to the footwall of the fault using the same slope as that of the present ground surface (pl. 2). The measured vertical displacement between the bedrock surface and the base of unit 6a is about 1.0 m. The fault plane on which this displacement occurred is preserved in unit 2, a lighter colored, well-indurated, pocket of colluvium, as a carbonate-impregnated plane dipping 50° to the west.

Estimated displacements of 0.5 to 1 m per event are small compared with those estimated for other Quaternary faults in Utah (for example, Schwartz and Coppersmith, 1984; Nelson and Van Arsdale, 1986; sec. 4.3). These small displacements and empirical relationships (for example, Bonilla and others, 1984) between earthquake magnitude and the amount of surface displacement suggest paleoearthquake magnitudes of 6 1/2 to 7 for the Morgan fault. Similar relationships between earthquake magnitude and fault rupture length also suggest paleoearthquake magnitudes of 6 1/2 to 7 for the 16-km-long Morgan fault.

The preservation of unit 3b directly above the main fault appears to be related to an earlier displacement. A near-vertical carbonate-filled shear extends from the base of unit 3b to the floor of the trench in the bedrock east of the main fault and strikes N8E across the trench. Unit 7a and its more pebbly upslope facies, unit 7b, are interpreted to be parts of a horizon of slope colluvium downdropped to its present position by the most recent displacement event on the main fault zone. Unit 6b thins upslope to its contact with unit 2 in the hanging wall of the fault and it is not clear if it ever extended across the fault. The predominance of silt and the lack of induration in unit 6 suggest that it consists principally of loess (or loess redeposited by surface wash) rather than slope colluvium eroded from the escarpment. It is the only colluvial unit in this and other trenches that thickens downslope suggesting that it was deposited only on the lower parts of the slope and may not have extended across the fault zone.

4.2.4.2 Stratigraphy in Trench M2U

In trench M2U the Morgan fault is manifested as a near vertical step in the bedrock surface striking N7W across the upper part of the trench that is on the projection of the fault exposed in trench M4 (pl. 2). However, no planar fault contact is evident along the irregular contact between the bedrock and colluvium, or within the bedrock at the base of the trench. A gradational contact between relatively hard bedrock and the fault breccia below the vertical step is interpreted as the fault zone in this trench.

Both the bedrock and the colluvial units are correlated with those in M4. The upper slopewash (Units 7a and 7c) is about 1.5 m thick and extends undisplaced across the fault. A middle unit of loose silt (unit 6) pinches out about a meter downslope of the fault. The sequence of older colluviul deposits (unit 3) overlying the bedrock on a 21° west-dipping contact in the hanging wall of the fault has the same lithology and stratigraphic position as correlative deposits in trench M4.

Although there is no clear evidence of shearing in the colluvial deposits in this trench, we infer that the preservation of unit 3 results its

downdropping along the Morgan fault. The base of unit 3 is estimated to have been displaced about 3.5 m (pl. 2). Although the contacts are masked by carbonate the upper, 0.2 m thick portion of unit 3a appears to extend undisplaced across the bedrock step. Unit 7a is displaced in M4, but no displacement of this unit is discernable in this trench although the contact between units 3a and 7a are difficult to distinguish between stations 22 and 24 where evidence of the most recent displacement would be preserved. Two, 0.2 m thick colluvial horizons preserved at the base of unit 3 may record evidence of small, individual surface displacement events.

This trench originally was 31 m long, reaching a maximum depth of 3.5 m, but the central portion of this excavation, between stations 6.5 and 14 was not logged in detail because it was backfilled immediately in an attempt to retard the rapid inflow of groundwater. Prior to backfilling the central portion of M2 we observed that both the upper units 7 and 6 and the bedrock are continuous between the upper (M2U) and lower (M2L) portions of the trench shown on plate 2.

4.2.4.3 Stratigraphy in Trench M1

Trench M1, located about 8 m south of trench M2, exposes a planar, southwest-dipping contact between bedrock and colluvium, interpreted to be a fault, that strikes N65W and appears to terminate the north-trending fault exposed in trench M2U and M4. In the trench, particularly on the north face, the contact has two distinct segments: a lower, planar fault contact dipping 70° to the southwest that is highlighted by a seam of red clayey silt (unit 8) varying from 1 to 200 mm in thickness; and an upper irregular contact that appears to be unfaulted. Along both its upper and lower segments this contact juxtaposes massive, brown silty colluvium and bedrock. The bedrock (unit 1a) is the same in M2 and M4 with local zones of yellow and green alteration and carbonate impregnated, steeply dipping fractures striking N65W across the trench.

The upper segment of this contact juxtaposes massive light brown silty colluvium and bedrock. Based on the color and weak induration of the matrix and pebble lithologies this colluvium is correlated with unit 6 in trench M4. The contact with an apparent dip of about 60° on the south wall of the trench and an apparent dip of 35° on the north wall of the trench. We interpret this difference to reflect local variation in the strike of the contact across the trench and interpret this as indicating that this upper portion is an erosional contact. This interpretation is also supported by the irregularities in the contact and the truncation of a N65°W striking 50 - 70° dipping shear fabric in the bedrock.

Based on its similarity to the fault contact in trench M4, the N65°W-striking 70° southwest-dipping contact between bedrock and colluvium in the lower portion of the trench is interpreted as a fault contact. A thin zone of red clayey silt is smeared along this fault contact on both faces of the trench and on the south face it extends into the upper portion of the contact. While its presence along the fault contact suggests that it may be fault gouge, its lithology indicates it is not derived from either the bedrock or the colluvium. Based on its occurrence in trenches M2L and M3 discussed below we have concluded that this is sediment derived from the underlying Wasatch formation that has been deposited along the fault plane by

groundwater upwelling.

The colluvium adjacent to the fault contact in the lower portion of this trench (unit 4?) includes pebble lithologies distinct from colluvial unit 3a that underlies unit 6a in trenches M2U and M4. The upper contact with unit 6a is clearly defined between stations 13 and 15 on the south face of the trench. Based on matrix color in this area, pebble lithologies, and correlation with units underlying unit 6a in M3 and M2L, the basal colluvium in the trench is interpreted to be unit 4, correlative with units described in M3 and M2L. The upper contact of this unit is inferred to meet the bedrock contact at the segment break about level 7.5.

Overlying both the bedrock and the colluvium is a 0.3 m thick, undisplaced, gravelly, silty slopewash (unit 7c), similar to its correlative in trench M4 with a weakly developed soil profile (MV-1) again suggesting a Holocene age for this unit.

4.2.4.4 Stratigraphy in Trench M2L

In trench M2L a N55°W, 60° southwest-dipping contact between bedrock and colluvium occurs on the projection of the the N65W striking fault contact in trench M1. This contact juxtaposes bedrock (units 1a and 1d) and a distinct orange silty clay (unit 4c), that is underlain by a similar, but brownish-red colluvium (unit 4b). In this trench the contact is not sharp or planar like the fault contacts in M4 and M1, rather it is irregular, and in detail the bedrock and colluvium appear to intertoungue.

Bedrock in this trench consists of a limestone or dolomite with distinctive blobs of yellowish, limey siltstone (unit 1d) which could be interpreted either as part of the Devonian dolomite or as the Cambrian limestone (C1 of Mullens and Laraway, 1973) that underlies unit 1a along a 20° west-dipping contact. A 20° west dipping, 5 cm-thick red clay seam (unit 8) follows this stratigraphic contact, across the fault into the colluvail deposits where it follows the contact between units 4b and 4c. Deposition of unit 8 post dates the most recent displacement and is interpreted to result from the circulation of ground water. A small spring is present northwest of this trench on the projection of this fault (pl. 2). We suggest that the red fines are derived from the reddish matrix of the Wasatch Formation in the hanging wall of the subsidiary fault at depth (and exposed southeast of the trench site), carried up along fracture planes, and redeposited along permeable contacts, including the fault contact in this trench.

At the upper end of M2L a 1-m-thick peat deposit is preserved in a depression in the bedrock (unit 1a) underlying unit 6a. The continuity of the peat and the coeval, relic A-horizons near the base of unit 6a in trench M2L establish that there has been no displacement of this subsidiary fault since the deposition of unit 6.

4.2.4.5 Stratigraphy in Trench M3

Trench M3 was excavated across the slope between M1 and M2 exposing the peat deposits and the northwest-trending fault identified in M1 and M2L (pl. 2). The 1.2 m thick peat deposit (unit 5) exposed in M2L overlies bedrock at the north end of the trench in the footwall of the northwest-trending fault. It

underlies units 6a, 6b, 7a, and 7c which extend across an intertonguing, 60° southwest-dipping fault contact between bedrock and colluvial deposits (units 4a and 4c). This contact is on the projection of the fault contact in M1, it is also interpreted as a fault contact which has been modified by groundwater circulation as in trench M2L.

Colluvial horizons are exposed in the hanging wall of the fault with a distinctive reddish color suggesting that may have been in part derived from the Wasatch Formation. Despite their similar positions below unit 6, the predominance of siltstone and sandstone clasts in unit 4a in this trench and in trenches M1 and M2L distinguish this unit from unit 3 in M2U and M4. At the base of M3 a colluvial unit (2b) is exposed with a relic carbonate horizon (unit 2a) which may be the older alluvial fan deposits exposed at North Morgan Springs and elsewhere along the central section of the fault.

A 20° west dipping (no apparent dip in trench wall), discontinuous lenses of red, clayey silt (unit 8) follow the contact between units 6a and 4a to station 59.5 where they become a continuous seam that extends uninterrupted across the fault into the bedrock. As in trenches M2L and M1 we interpret this unit as being derived from underlying units and deposited by groundwater upwelling along the fault.

4.2.4.6 Ages of faulted deposits at the Robeson springs trench site

Estimates of the ages of displaced colluvial deposits at the Robeson Springs trench site are based on radiocarbon dates on peat interbedded with colluvial deposits in trenches M2L and M3, and on amino-acid ratios from snails in colluvial and alluvial fan deposits exposed in four other locations along the central segment of the Morgan fault. In trenches M2L and M3 a small (3 m by 6 m) bog deposit of peat is exposed that underlies colluvial unit 6 and overlies bedrock in the hanging wall of the Morgan fault. Unit 6 is correlated between trench M4 and the other trenches, 32 m to the south (pl. 2), on the basis of similar lithology and stratigraphic and geomorphic position. Radiocarbon dates of 8.3 ka on peat (Beta-9244) and 9.1 ka on wood (Beta-9244) from this deposit indicate an early Holocene age for the bog and an early or middle Holocene age for the overlying colluvial unit 6.

We infer a middle to late Pleistocene age for the older colluvial deposits (unit 3) in trench M4 by using their similar lithology, degree of carbonate development, stratigraphic position, depth, and position adjacent to the fault to correlate them with the sequence at Mahogony Creek for which we have amino-acid age estimates (table 4.2). At Mahogany Creek about 2.5 km north of the Robeson Springs trench site (fig. 4.4), a similar sequence of colluvial deposits varies in thickness from 7 m in a trench at the mountain front to about 1 m in a roadcut 180 m to the west. In the trench at Mahogany Canyon this colluvium overlies older alluvial fan deposits in which a petrocalcic horizon with stage IV carbonate is developed. This degree of pedogenic carbonate development suggests that the fan deposits are at least 200 to 300 ka and probably >500 ka. Snails from this colluvium at depths of 1 to 5 m, and from other sites at similar depths have estimated ages of 200 to 400 ka or greater (discussed above, table 4.2). However, the upper parts of unit 3 may date from the late Pleistocene (10-125 ka), for individual units can not be correlated from Mahogany Creek to Robeson Springs.

4.2.4.7 Events in Trench M4

On the basis of the stratigraphic relations in trench M4 and our estimates of the age of the colluvial deposits we have interpreted the following sequence of events:

1) During the middle and late Pleistocene units 3 and 3c were deposited as a series of 0.5 to 1.0 m thick horizons of slopewash that were downdropped and preserved by a series of small displacement events comprising a total of 3 m of displacement on the Morgan fault. Prior to or during this period unit 3b was deposited as slopewash across the fault zone, and displaced about 1 m on a near vertical shear which resulted in its preservation from erosion above the main fault zone.

2) Following an interval of non-deposition of unknown duration, a depression in in the hanging wall of the fault exposed in trench M2L (pl. 2) was filled with bog deposits (radiocarbon dates of 8.3 and 9.1 ka).

3) Unit 6 was deposited above unit 3 and the bog deposits principally as loess that may have been derived from exposed Lake Bonneville sediments in the valley.

4) Units 7a and 7b were deposited by surface wash across the fault zone.

5) Units 3b, 7a, and 7b were displaced about 1.0 m along the main fault zone.

6) Modern surface wash continued to deposit colluvium (unit 7c) on the slope across the fault zone.

4.2.4.8 Stratigraphy in Trench M6 at the Mahogany Canyon trench site

Mapping along the central segment of the Morgan fault about 2.5 km north of the Robeson springs site revealed a cut along a private road on the north side of Mahogany Creek (figs. 4.2 and 4.4) exposing 14° southwest dipping, snail bearing, carbonate stage IV to V cemented gravels below 3 m of colluvial deposits. These older alluvial fan deposits (Qaof) have been incised about 20 m in this area by Mahogany Creek, which heads to the east in the Paleozoic carbonates exposed on Durst Mountain. Three trenches were excavated at the base of the facet about 180 m to the east of this exposure on the updip projection of these older fan gravels in an attempt to expose the stratigraphic relationships among dateable, faulted colluvial deposits on the main trace of the Morgan fault.

Trench sites were selected along the bedrock facet north of Mahogany Creek, where headward erosion by a small tributary along the strike of the Morgan fault has incised the surface of the older fan deposits (Qaof) projected from the roadcut a maximum of 10 m (fig. 4.5). Trench M6 on what appeared to be the base of the triangular facet, was 8 m deep and 15 m long. Alluvial and colluvial deposits were exposed in the trench, but not the Morgan fault (fig. 4.6). Carbonate stage V fan gravels (unit 1b), correlative with those exposed in the roadcut on the basis of similar D/L ratios of snails (table 4.2), lithologies, and stratigraphic position, were exposed in the base of the trench. The horizontal upper surface of this petrocalcic horizon in the trench contrasts with its 14° southwest dip in the roadcut and suggests local

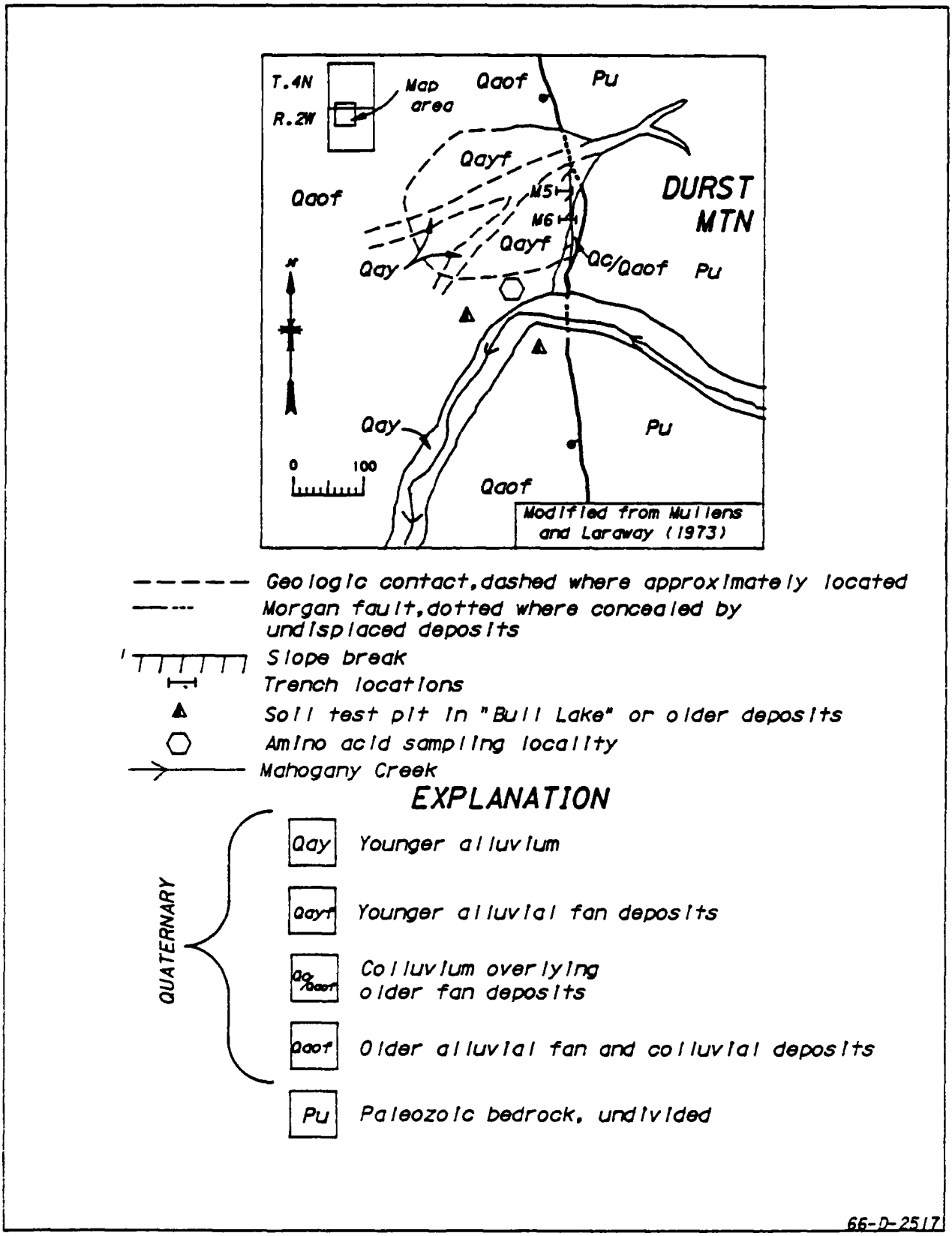
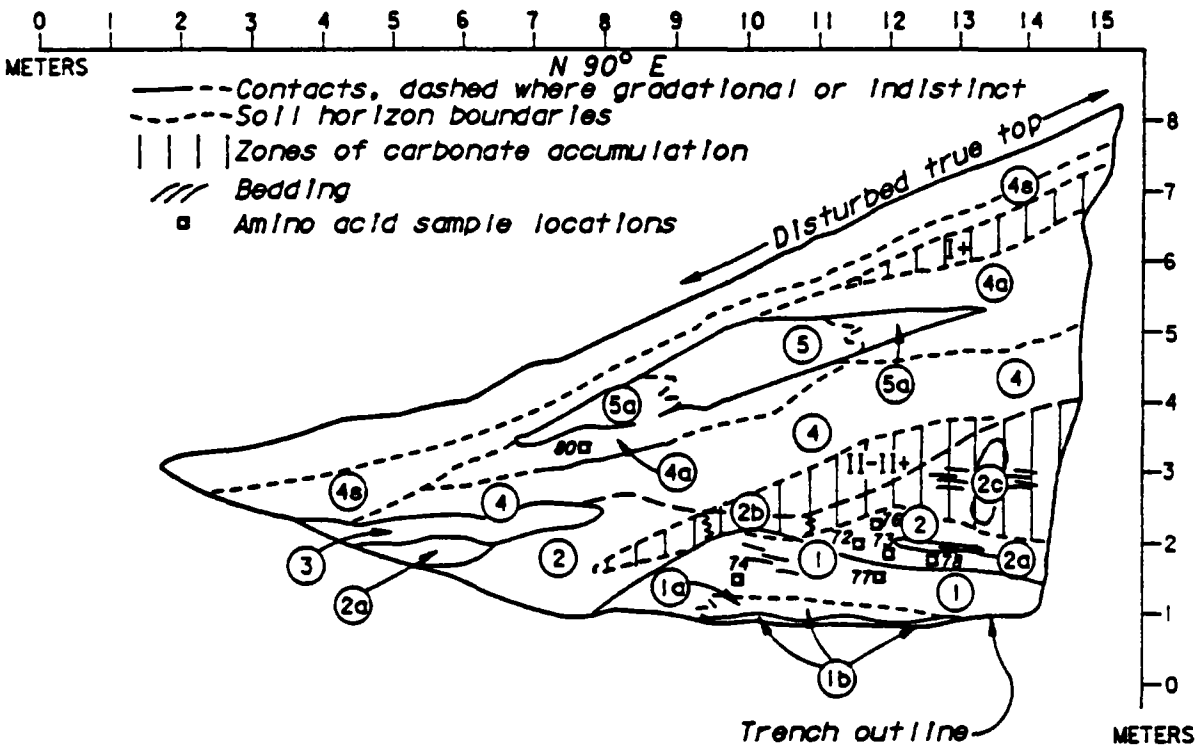


Figure 4.5 Geologic map of the Mahogany Creek trench site.



UNIT DESCRIPTIONS

Alluvial fan deposits (Qaof on figure 4.1.3)

1. Light brown (10YR 7/6) gravelly clayey silt. Unit consists of 30% subangular to subrounded limestone and dolomite pebbles and occasional cobbles in a moderately indurated clayey silt matrix. Contains local zones of bedding dipping 10° east.
1a. Light brown (10YR 7/4)sandy silty gravel. Unit consists of 60% subangular to subrounded limestone and dolomite pebbles and cobbles in a moderately indurated clayey silt matrix.
1b. Tan (10YR 8/2) gravelly silt. Unit consists of 40% subangular and subrounded limestone and dolomite pebbles and cobbles in a very hard, stage U carbonate cemented clayey silt matrix.
2. Yellow (10YR 7/6) to very pale brown (10 YR 7/4) in stage II carbonate zone gravelly clayey silt. Unit consists of variably concentrated (0-30%) subangular limestone and dolomite pebbles and cobbles in a moderately indurated clayey silt. Contains local zones of crude bedding as shown.
2a. Pebble lens, other less distinct lenses not shown.
2b. Same as 2 but no gravels.
2c. Brownish yellow (10YR 6/3) clayey silt. Unit consists of massive, poorly indurated clayey silt. Contact is abrupt but irregular. This incorporated block of sediment interrupts stage II carbonate zone but has not deformed bedding.
3. Yellow (10YR 7/6) gravelly silt. Unit consists of 40% subangular and subrounded limestone and dolomite cobbles and pebbles in a moderately indurated matrix of clayey silt.

Colluvium (Qc on figure 4.1.3)

4. Light brown (10YR 5/4) clayey silt. Unit consists of 1-5% coarse sand and pebbles in an unstratified, moderately indurated clayey silt matrix.
4a. Same as 4 with 20% subangular limestone and dolomite pebbles.
4s. Yellowish brown (10YR 5/4) clayey silt. Weak argellic B-horizon and overlying A-horizon developed on units 4, 4a, and 5.

Alluvial fan deposits

5. Yellow (10YR 8/6) silty gravel. Unit consists of 50% subangular limestone and dolomite pebbles and occasional cobbles in a loose sandy silt matrix. Interpreted to be the eroded remnant of gravels deposited in south flowing channel.
5b. Same as 6 but very pale brown (10YR 8/4)

FIGURE 4.6 LOG OF THE MAHOGANY CANYON TRENCH (M6)

66-D-2518, 33

rotation of the fan surface into the fault.

These basal gravels were overlain by debris flow deposits (units 1 and 2) with local, crude, east-dipping bedding again suggesting local tectonic rotation subsequent to their deposition (fig. 4.6). The upper portion of the trench consists of interbedded, fine-grained colluvial deposits (units 2 and 4) locally derived from upslope, and gravels (unit 5) with geometries and imbrication suggesting deposition in south flowing channels in the strike drainage. Snails collected from colluvial units in the trench (fig. 4.6 and table 4.2) and yielded minimum age estimates of 500 kyrs for units 1 and 2 and 200 - 400 kyrs (sec. 4.2.3) for unit 4a which is interbedded with the channel gravels. These dates on late Quaternary deposits adjacent to the Morgan fault at this site suggest a relatively low the slip rate on the fault, but because the fault is not exposed, we are unable to estimate slip rate, surface displacement size, or recurrence at this locality.

4.2.5 Slip rates on the Morgan fault

4.2.5.1 Quaternary slip rates

Mapping and trench investigations on the central section of the Morgan fault provided evidence that middle to late Pleistocene and Holocene displacements have occurred on this back valley fault. At the Robeson Springs trench site, two faults were identified: 1) the north-trending central section of the main fault that displaces middle to late Pleistocene and Holocene colluvial deposits 4 m, and 2) a northwest-trending trace of a subsidiary fault that displaces similar middle to late Pleistocene colluvial deposits. Radiocarbon dates of 8.3 and 9.1 ka provide a maximum age for the younger colluvium that has been displaced about 1 m by the main fault in trench M4. Assuming the lower part of the underlying sequence of colluvial deposits in trench M4 is 200-400 ka, 4 m of displacement yields a middle to late Pleistocene slip rate of 0.01 to 0.02 mm/yr. Because only 1 event is recorded an Holocene slip rate can not be calculated. These Pleistocene slip rates are an order of magnitude lower than long-term Pleistocene rates on the Wasatch fault (Machette, 1984), but some other faults in the region may have rates nearly this low (Nelson and Van Arsdale, 1986; sec. 4.3).

We interpret the colluvial stratigraphy in trench M4 as suggesting recurrent Quaternary surface displacements of 0.5 to 1.0 m have occurred on the Morgan fault at the Robeson Springs trench sites. If 0.5 m most nearly represents the average size of the surface displacement events that are represented by the 4 m of displacement in at least the last 200 to 400 ka as suggested by the lack of discrete scarp-derived colluvial wedges in the trench, about 8 individual events have occurred. These estimates yield a minimum average middle to late Quaternary event recurrence interval of 25 to 50 kyr. If only four events of 1 m displacement have occurred, the minimum average recurrence interval would be 50 to 100 kyr.

4.2.5.2 Cenozoic slip rate

The effect of the late Cenozoic uplift of the Wasatch Range on the evolution of landforms in Morgan Valley partly depends on the distribution of late Cenozoic faults. Naeser and others (1983) estimate uplift rates of 0.8 mm/yr over the last 5 Ma and 0.4 mm/yr over the last 10 Ma for the north-central

Wasatch Range west of Morgan Valley. As shown in a section across the northern section of Morgan Valley constructed by Hopkins (1982, her fig. 5), the faults bounding the west side of Morgan Valley mapped by Bryant (1984) have limited displacement and the structural relief in the valley is primarily due to Cenozoic displacement on the Morgan fault. If the late Cenozoic slip rate on the Wasatch fault is much greater than that of the Morgan fault, the effect of this relative uplift of the Wasatch Range would be to accelerate late Cenozoic erosion in Morgan Valley. The Weber River has incised the Norwood Tuff more than 300 m in Morgan Valley (fig. 4.3) indicating that this is the case and suggesting that the average late Cenozoic slip rate on the Morgan fault is much lower than that of the Wasatch fault.

The thickness and attitude of the Huntsville fanglomerate adjacent to the northern section of the Morgan fault provide an estimate of the average Cenozoic slip rate on the fault. In the cross section of Hopkins (1982), the Huntsville fanglomerate overlies the late Eocene-early Oligocene Norwood Tuff and dips 13° to the east with an estimated maximum thickness of 1000 m adjacent to the Morgan fault which provides a minimum estimate of displacement since deposition of the fanglomerate. The age of this deposit is poorly constrained; the previous workers have suggested it is of Pliocene age (Eardley, 1944; Coody, 1957). However, similar unconsolidated gravel deposits of Oligocene age have been mapped further south in the Wasatch Range overlying and interbedded with the Oligocene Keetley volcanics (Bromfield and Crittenden, 1971). Using an age range of 5 - 35 Ma for the Huntsville fanglomerate and a minimum displacement estimate of 1000 m yields an estimated average middle and late Cenozoic slip rate of 0.03 to 0.2 mm/yr.

The tilting of late Cenozoic erosion surfaces adjacent to the northern section of the fault also provides a crude estimate of the average late Cenozoic slip rate on the fault. In this area locally well-preserved, gently (0.5° - 1.7°) east-dipping erosion surfaces, cut on the Huntsville fanglomerate, slope up to 1.7° northeast, into the fault (fig. 4.2). Based on our observations in less dissected terrains of the Weber River drainage, these surfaces probably once sloped at least 3° towards the center of the valley; therefore, we interpret the back tilting of these surfaces to have resulted from displacement on the Morgan fault. If the most steeply tilted surface, south of Bohman Hollow and 1.7 km west of the main trace of the fault, has been uniformly rotated from a 3° westerly dip to its present 1.7° easterly dip, then projection of this surface to the fault indicates about 150 m of displacement. If the erosion surface has been down dropped relative to the footwall as well as rotated, total displacement would be greater. These erosion surfaces are probably significantly older than a much lower erosion surface on the west side of the valley paleomagnetically dated at >730 ka (fig. 4.2). Assuming an age of 1 to 5 Ma for this surface yields an average latest Cenozoic slip rate of 0.03 to 0.15 mm/yr for this section of the fault, which is consistent with the rate estimated from the thickness and age of the Huntsville fanglomerate.

These slip rate values are poorly constrained and do not take into account probable significant variations in slip rates during the late Cenozoic. Estimates of 0.01 to 0.02 mm/yr determined at the Robeson Springs trench site for the middle to late Quaternary are at the low end of the ranges of late Cenozoic slip rates. Because we infer only one Holocene event and our

estimates of average minimum recurrence intervals range from 25-100 ka, we have no way of judging whether the Holocene slip rate or recurrence differs from our estimates for the middle to late Quaternary, as has been suggested for the Great Basin by Wallace (1984) and for the Wasatch fault by Machette (1984). Our dating control is too imprecise to determine whether there has been a significant change in slip rates during the late Cenozoic. If there is a difference in rates, middle to late Quaternary rates on the Morgan fault are probably lower than for earlier periods.

4.2.6 Conclusions

Two west dipping normal faults are exposed in trenches at the Robeson Springs trench site at the south end of the central section of the Morgan fault. The main north-trending fault, exposed at the base of triangular facets on the footwall escarpment, displaces colluvial deposits underlain by a peat deposit with ^{14}C dates of 8.3 and 9.1 ka. This fault ends or is terminated by a northwest-trending fault. The termination of the north-trending fault and mapped bedrock relationships suggest that the northwest-trending fault connects or transfers displacement between the central and southern sections of the Morgan fault. Although the expression of this northwest-trending fault has been modified by groundwater circulation at the trench site, the fault does not displace the colluvial deposits underlain by the peat, and it is interpreted to displace older colluvial deposits, suggesting that during at least some of the surface displacement events rupture occurs on both the central and southern section of the Morgan fault.

A post-early Holocene displacement event of 1 m might be expected to have produced scarps along the central section of the fault that would still be visible today. Scarps 1 m high on gently sloping alluvial fans probably would be preserved for tens of thousands of years (Hanks and others, 1984). However, the Morgan fault is mapped at the base of a 20° to 25° sloping escarpment and figure 6 shows that the 1-m-high scarp has been completely covered since the deposition and faulting of unit 6. Erosion and deposition of younger alluvial deposits apparently obliterated the scarp in drainages crossing the escarpment.

Mapping and trenching of the central section of the Morgan fault demonstrates that surface displacements have occurred on the fault during the middle Pleistocene and Holocene. Colluvial deposits, estimated from amino-acid ratios on gastropods found in correlative deposits to be at least 200 - 400 ka, are displaced 4.0 m at the Robeson Springs trench site. These data yield an average middle to late Pleistocene slip rate of 0.01 to 0.02 mm/yr. These rates are near the low end of the range of estimates of the late Cenozoic slip rate on the Morgan fault based on the tilting of late Cenozoic erosion surfaces and estimates of the displacement of a Cenozoic fanglomerate. Radiocarbon dates of 8.3 ka and 9.1 ka on bog deposits beneath Holocene alluvial units show that the most recent surface displacement event (approximately 1 meter) post-dates deposition of the bog deposits. The colluvial stratigraphy in one trench at the site is interpreted as showing that individual surface displacements on the fault have been small (0.5 to 1 m). These small displacements, the limited length of the fault, and empirical displacement-earthquake magnitude relationships suggest that paleoearthquakes in the magnitude range 6 1/2 to 7 have occurred on the Morgan fault.

4.3 Southern Cache Valley Region

The Regional Study Area includes the southern portion of Cache Valley in Utah and the adjacent Wasatch and Bear River Mountains and Bear Lake area to the east (fig. 1.1). Only a brief reconnaisannce has been made of the Bear River Range and the areas to the east and southeast. We mapped in detail only two areas in this region: north of James Peak in southern Cache Valley and west of Little Mountain near Newton Reservoir (fig. 4.7). The East Cache fault, on the east side of Cache Valley, extends 100 km north from James Peak into Idaho. Shorter Quaternary faults are inferred on the west margin of the valley and on the margins of horst blocks within the valley. The James Peak fault appears to be a splay at the southern end of the East Cache fault. Scarps associated with faults on the margins of Cache Valley mapped from low-sun-angle photographs by Cluff and others (1974) and limited investigations of the East Cache fault near Logan are the only seismotectonic investigations reported in Cache Valley (Swan and others, 1983b).

Cache Valley is a late Cenozoic structural and topographic basin, bounded by normal faults, that developed in the Cache Allocthon, the upper plate of the Willard and Woodruff thrusts (Bjorkland and McGreevy, 1971; Crittenden, 1972; Hintze, 1980)(fig. 4.7). The East Cache fault, the principal fault in the valley, is marked by triangular facets cut on the east-dipping Precambrian and Paleozoic rocks at the western base of the Bear River Range. Geophysical data (Stanley, 1972; Petersen, 1974) complied by Zoback (1983) suggest that the late Cenozoic basin fill in the valley is 1.7 to 2.1 km thick. A seismic reflection profile across the East Cache fault shows that Cache Valley is an asymmetric basin, deepest on the east margin adjacent to the East Cache fault (Smith and Bruhn, 1984). Consistent east dips of reflectors in the late Tertiary basin fill are similar to those observed in the basins adjacent to the Grand Valley and Star Valley faults which have been interpreted as listric faults (Royse and others, 1975; Dixon, 1982; Piety and others, 1986).

4.3.1 Late Quaternary Displacement on the East Cache fault

A number of early investigators, including Gilbert (1890), Bailey (1927), and Peterson (1936), noted scarps in unconsolidated deposits along the East Cache fault, bounding the east side of Cache Valley (fig. 4.7), as evidence of relatively recent displacements on the fault. Displaced Bonneville gravels on the East Cache fault were clearly visible at one time at the mouth of Logan Canyon (Peterson, 1927, pl. 10). Cluff and others (1974) mapped probable late Pleistocene and Holocene fault traces along most of the East Cache fault zone in detail, including post-Provo age (<14 ka) scarps near the mouth of Logan Canyon. They suggested that fault displacement here is older than that along the Wasatch fault near Salt Lake City. On the basis of test pits across west-facing scarps just north of Logan Canyon, Rogers (1978) also concluded that displacements on the fault had occurred in recent geologic time. Temporary exposures in several other areas along the East Cache fault have also revealed post Bonneville displacements (B.N. Kaliser, oral communication, 1981), but these investigations are undocumented.

Swan and others (1983b) completed the most detailed investigation of recent displacements on the East Cache fault. Based on a review of all previous work, detailed mapping and topographic profiling, and several 20-m-long test pits they concluded:

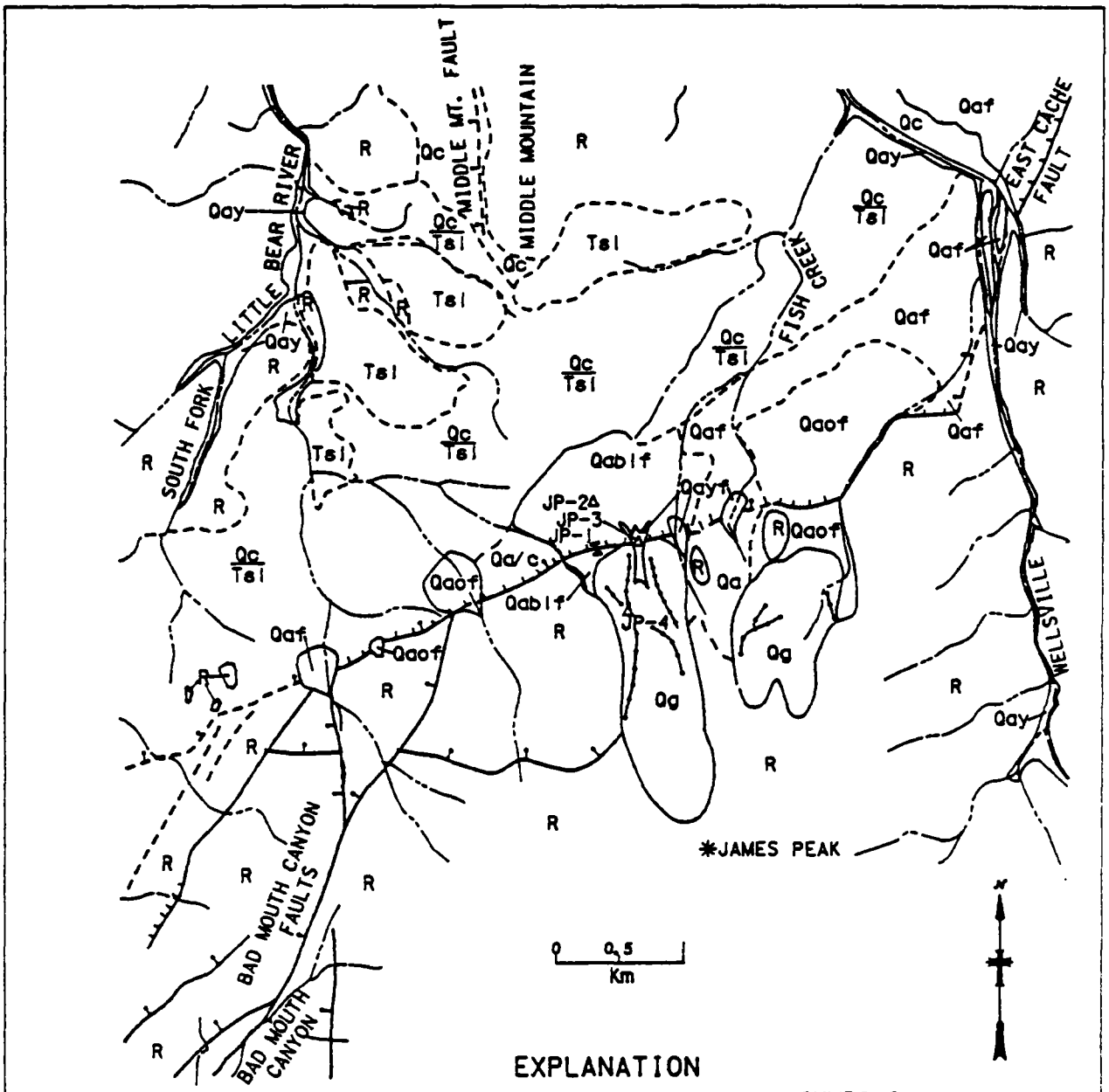


FIGURE 4.7 GEOLOGIC MAP OF SOUTHERN CACHE VALLEY

56-D-2502.33

Two surface faulting events have occurred along the East Cache fault east of Logan, Utah since Lake Bonneville receded from the Bonneville shoreline between 15,000 and 14,000 years ago. The first event occurred prior to 13,500 year B.P. and may have been temporally related to the catastrophic drop in the level of Lake Bonneville from the Bonneville to the Provo shoreline. The most recent event post-dates the recession of the lake below the Provo shoreline (about 13,500 years ago). Extensive burial of the fault scarp by alluvial fans suggest that this event occurred prior to about 6,000 to 8,000 years B.P. The average recurrence based on two events is calculated to be 7,250 $\pm$ 250 years. The actual interval between the two events could have been as short as 2,000 to 3,000 years or as long as 7,000 to 8,000 years. The recurrence of major surface faulting events along the East Cache fault is markedly different than for the Wasatch fault zone between Brigham City and Nephi, where there have been repeated surface faulting events during the late Holocene.

Estimates of the net vertical tectonic displacement for each of the past two surface faulting events at Logan are approximately 1.4 m. Distortion resulting from graben formation and backtilting has increased scarp height approximately twice the net vertical tectonic displacement during each of these events. Empirical relationships between displacement per event and earthquake magnitude suggest that these displacements were associated with earthquakes in the magnitude range of Ms 6.5 to 7.25.

The late Pleistocene-Holocene slip rate along the segment of the East Cache fault at Logan is between 0.1 and 0.2 mm per year, which is significantly slower than the slip rate along the Wasatch fault zone south of Brigham City.

Diminishing estimates of the thickness of basin-fill in southern Cache Valley (Zoback, 1983) and decreasing topographic relief on the bedrock escarpment of the East Cache fault suggest the fault diminishes in total displacement south of Logan. Near the southern end of the fault Swan and others (1983b) found few deposits to work with because the main trace of the fault is at the range front, well above the Bonneville shoreline, and because scarps along the fault are nearly completely masked by recent (post-Provo) alluvial fan deposits. They speculate, however, that the rupture segment studied near Logan may be dying out south of Providence Canyon. However, no abrupt changes in rangefront morphology suggest the location of a fault segment boundary in this area. Mullens and Izett (1964) also reported that Lake Bonneville deposits in the Paradise area (fig. 4.7) are unfaulted.

4.3.2 The James Peak fault

The scarp of the James Peak normal fault is the only previously unreported fault scarp in unconsolidated deposits in the northern Wasatch Mountains. The scarp marks the southern edge of an unnamed structural and topographic basin between James Peak and Middle Mountain at the southern end of Cache Valley and 5 km north of Ogden Valley (pl. 1 and fig. 4.7). The basin, about 3 km wide and 9 km long, contains Tertiary Salt Lake Formation with a cover of Quaternary colluvium and alluvium (Blau, 1975; Hintze, 1980). The basin

is bounded on the north by highly dissected Paleozoic limestones, shales, dolomites, and quartzites and on the south by Paleozoic and Precambrian orthoquartzites, argillites, and volcanics that make up the highlands around James Peak (King, 1965; Blau, 1975; Davis, 1983).

The James Peak normal fault, at the base of the escarpment in Paleozoic and Precambrian rocks on the north side of James Peak, marks the southern boundary of the east-west-trending basin at the southern end of Cache Valley (fig. 4.7). Isolated outcrops of Paleozoic sedimentary rocks suggest that the Salt Lake Formation may be <100 m thick in the basin indicating cumulative subsidence is much less here than in Cache Valley. North of the basin, north-dipping, lower Paleozoic rocks are cut by north-trending normal faults including the Middle Mountain fault. Near Broadmouth Canyon on the west side of James Peak, Blau (1975) maps north-trending normal faults with estimated displacements of about 1500 m that are about on trend with the Middle Mountain fault. Escarpments in bedrock mark these north-trending faults, but north-trending scarps are not developed in the sediments in the basin. No east-west-trending faults are mapped along the northern edge of the basin where fluvial dissection has produced extensive outcrops of the Salt Lake Formation. Thus, the basin appears to be a shallow half-graben connecting the larger and deeper grabens at the southern end of Cache Valley and the northwest end of Ogden Valley (Zoback, 1983; sec. 4.4).

4.3.2.1 Quaternary Deposits in southern Cache Valley

Quaternary deposits in the basin consist of locally-derived, bouldery, colluvial deposits (unit Qc/Tsl on fig. 4.7) in the central and northern portions which thicken and are interbedded with fan alluvium to the south. Alluvial fan deposits (Qaf), including two large, bouldery outwash fans (Qaof and Qablf) derived from the quartzites exposed on James Peak, occur along the southern edge of the basin. These fans become larger and appear to thicken from west to east; if so, this thickening may indicate downfaulting, tilting, or deeper erosion of the eastern part of the basin near Wellsville Creek and the East Cache fault. Sandy till (Qg) makes up the high, steep moraines built by the glaciers that deposited the outwash fans in two of the unnamed drainages on the north flank of James Peak.

4.3.2.2 Scarp and Mountain Front Morphology

Mountain front slopes developed in bedrock along the James Peak fault are steep, especially on James Peak (26°), despite the fact that this side of the peak has been extensively eroded by glaciers. On the lower half of the mountain, eroded spurs (ridge crests) are faceted. Three breaks in slope on the spurs, as well as the north-facing faceted spur (25° slope) just west of Wellsville Creek at the east end of the basin (fig. 4.7), suggest a history of recurrent Quaternary displacements on the fault (for example, Gilbert, 1928; Hamblin, 1976). To the east, the mountain front is lower and more dissected with gentler slopes, although here, as elsewhere, the steepest facets are at the base of the slopes along the fault. However, by comparison, the facets along the fault are smaller, less continuous, and less steep than those along the East Cache and Wasatch faults. The short (<7 km) mountain front along the James Peak fault makes quantitative comparisons with other mountain fronts (for example, Bull and MacFadden, 1977) of little value. Overall, the mountain-front morphology of the north flank of James

Peak suggests much lower Quaternary slip rates than that on major nearby faults such as the East Cache and Wasatch faults.

The James Peak fault scarp is expressed primarily as a scarp in bedrock over much of its length, but along the central part of the fault the scarp cuts alluvial and colluvial deposits and the large alluvial fans (units Qablf and Qaof, fig. 4.7) issuing from the glaciated drainages on the north flank of the mountain. The scarp is generally higher (10-30 m) and steeper (20-35° maximum slope angle) in bedrock (or thin colluvium over bedrock) than in fan sediments (1-4 m; 15-30°). Where the scarp is in alluvium undissected by small drainages, it is uniformly 3-4 m high.

An en echelon offset at the east end of the scarp forms a junction with the prominent scarp at the southern end of the East Cache fault; the scarps join at about a 110o angle. The eastern half of the scarp is subdued (<2 m high, 20° maximum slope angle) where it crosses the apex of the easternmost alluvial fan (Qaof on fig. 4.7), but the scarp is steeper (20-25o) in the Cambrian quartzite on the en echelon segment (500 m west of Wellsville Creek). The lower slopes of the Paleozoic limestone and sandstone bedrock facets, 2.7 km to the north on the East Cache fault, are steeper still (25-30°). Just west of the large alluvial fans, the western half of the scarp is steep (22-30° maximum slope angle) near the base of dissected facets in quartzite, but farther west the scarp is indistinct because the bedrock hills west of James Peak are lower and more rounded than the faceted mountain flanks to the east.

Just south of the western end of the basin, the Broadmouth Canyon normal faults trend about N30°E through low, dissected bedrock hills (Blau, 1975). A major topographic boundary between the west flank of James Peak and the lower hills to the west marks the largest normal fault, with 1500 m of throw, that extends into Broadmouth Canyon. One large (120 m difference in elevation) and several smaller topographic steps (most down-to the-northwest) (fig. 4.7) that parallel the largest fault are interpreted as related subsidiary faults.

4.3.2.3 Age of Faulted Deposits

Our chronology of Quaternary deposits and the scarps bounding or cutting them near James Peak is based on the morphology and relative position of fans, moraines, and scarps, and data from 4 soils developed on deposits in the largest glaciated drainage. Most mapped Quaternary deposits are undifferentiated as to age (fig. 4.7), but even the oldest are probably no more than a few hundred thousand years old.

The height of topographic scarps along the Broadmouth Canyon faults suggests Pliocene to Quaternary, but not necessarily late Quaternary displacement. Most of the faults cannot be traced into the Salt Lake Formation in the basin to the north and thus, they appear to be buried by Tertiary sediments. However, in two areas where the Broadmouth Canyon faults meet the James Peak fault faint lineaments extend into dissected Salt Lake Formation sediments; exposures are not sufficient to resolve the relationships between the lineaments and the faults. Although the Broadmouth Canyon faults may join the James Peak fault, the young scarp on the latter fault indicates the Broadmouth Canyon faults have been displaced by it.

The steep, continuous scarp in the alluvial fans along the central part of the James Peak fault suggests late Quaternary displacement on the fault. However, except for the smallest, youngest fans, which lack scarps where the fault crosses them, fans of significantly different ages (in which to compare scarp heights) were not identified. Topographic profiling across the scarp was difficult because of the thick alder-aspen forest and the soft, loose organic-rich soil on the surface of the scarp. For this reason, profiling to obtain displacement and relative-age estimates (for example, Bucknam and Anderson, 1979) was not attempted.

To estimate ages we followed Harden and Taylor (1983) in using X-Y plots to compare development indices for the soils we described and sampled near the trench site (table 4.3; fig. 4.8) with soils of known age elsewhere in the Wasatch Mountains (sec. 3.4; fig. 3.1). Soils on a lateral moraine (JP-4) and on the outwash fan in front of it (JP-2) were described to determine whether these were Bull Lake or Pinedale deposits (discussed in sec. 3.3). For comparison, a Holocene soil (JP-3) was described on very coarse, bouldery alluvium in a narrow channel where the moraines are narrowly breached. The thick soil developed on the colluvial wedges in the trench (JP-1) was also described to help estimate their age. Soils JP-1 and JP-2 are developed in deposits of more than one age. To help estimate the time interval represented by the degree of soil development in the younger deposits as well as by the whole soil we calculated soil indices for each depositional unit of these two soils (table 4.3; fig. 4.8).

Soil development indices (fig. 4.8) calculated using field and laboratory data shows that the outwash gravels (unit Qablf on fig. 4.7) in the lower parts of soils JP-1 and JP-2 are in RAG 2 (relative-age group 2) and are probably chronocorrelative with outwash from the Bull Lake glaciation. Although it is possible that this outwash significantly post-dates the last interglacial (125 ka), the reddish, clay-rich argillic horizons of these soils suggest they began forming about 140 ka (sec. 3.4).

Soil JP-4 on the steep, high, left lateral moraine (fig. 4.7) is poorly developed with soil indices lower than those for most soils on tills and outwash of the Pinedale glaciation (fig. 4.8). However, the till on which the soil is developed is derived entirely from quartzites, which do not weather easily. In addition, the steep slopes and narrow crests of the moraines indicate this soil may have been partially stripped by erosion on the moraine crest. Thus, both because soil development proceeds so slowly in quartzite-derived tills and because of erosion the moraine is probably much older than the soil indices suggest.

The bouldery surfaces, narrow crests, and steep slopes of the moraines on the north flank suggest they were built during the Pinedale glaciation, but the indices for soils developed on the outwash apron in front of the moraines suggest an older, probably pre-last interglacial age (>125 ka). The most probable interpretation of the age of the moraines is that Pinedale and Bull Lake glaciers extended the same distance downvalley, but that during the Pinedale glaciation, high Bull Lake lateral moraines protected all but the center of the fan surfaces from burial by younger outwash. Thus, the outwash fans that are displaced by the James Peak fault (Qablf and Qaof on fig. 4.7)

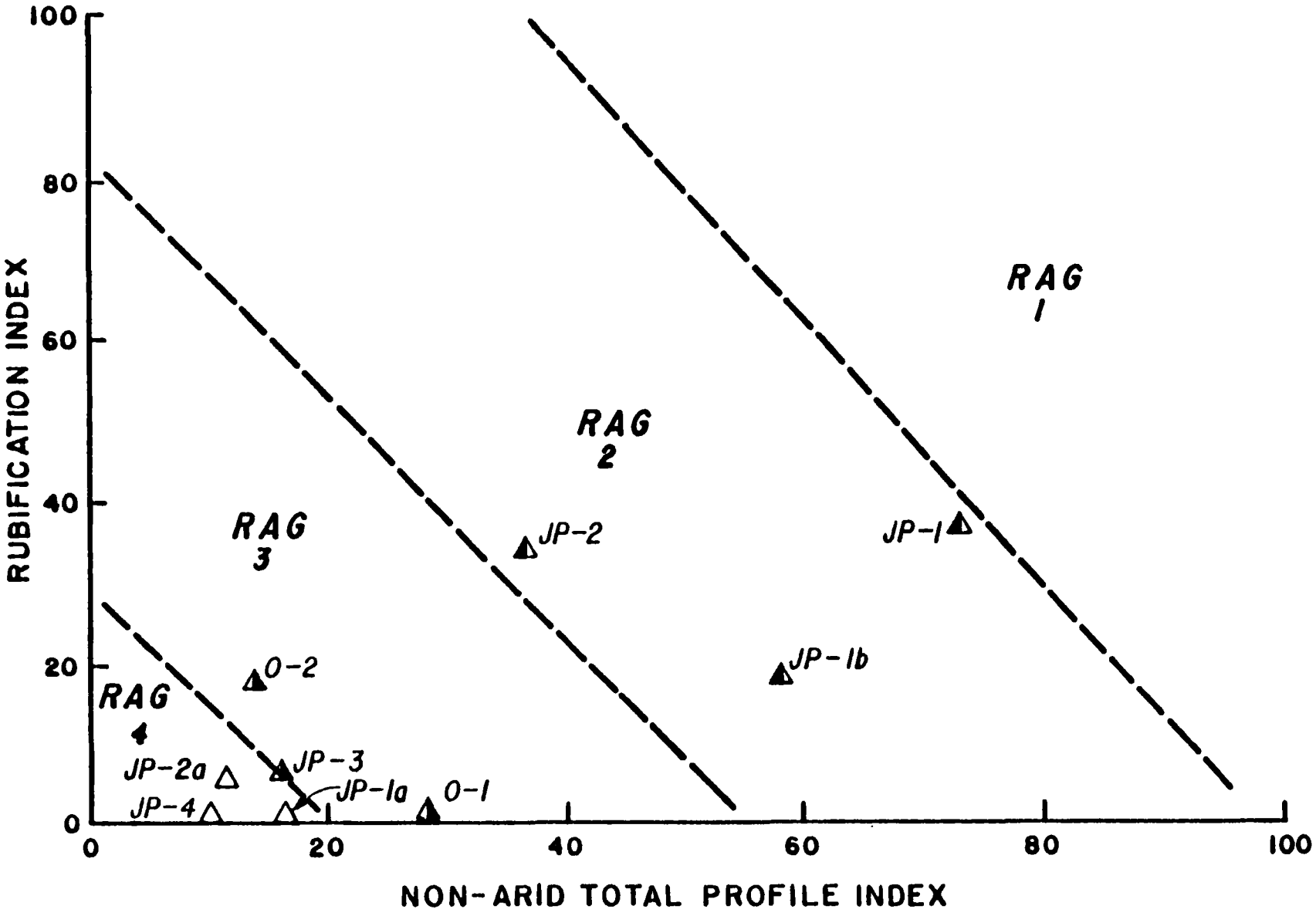

RUBIFICATION INDEX
NON-ARID TOTAL PROFILE INDEX
0
20
40
60
80
100
RAG 1
RAG 2
RAG 3
RAG 4
JP-1
JP-1a
JP-1b
JP-2
JP-2a
JP-3
JP-4
O-1
O-2

Table 4.3 -- Selected properties of soils on the north flank of James Peak, north central Utah.

Profile	Trench log unit	Horizon*	Average depth (cm)	Parent material	Munsell dry color	ESTIMATED PERCENT BY VOLUME Pebbles (0.2-8cm)	Cobbles (8-25cm)	Boulders (>25cm)	PERCENT BY WEIGHT~ Sand (2-0.5mm)	Silt (50-2um)	Clay (<2um)	Percent# organic matter
JP-1	4b	A1	0 10	colluvium-loess	7.5YR 2/2	10	2	0	20	57	23	9.4
	4b	A2	10 46	colluvium-loess	7.5YR 3/2	10	2	0	22	54	24	8.8
	4a	Bw	46 83	colluvium-loess	7.5YR 5/3	10	5	0	28	51	21	3.2
	3b8	2Bt1	83 100	colluvium-loess	7.5YR 5/4	10	5	0	26	53	21	2
	3a8	2Bt2	100 205	colluvium-loess	7.5YR 6/4	25	15	0	28	48	24	0.7
	2	3Cox/3Bt	205 248	scarp colluvium	7.5YR 7/4	20	20	2	33	45	23	0.6
	1B	4Bt	248 278	outwash	5YR 4/6	30	30	10	54	18	28	0.3
	1	4Cox	278 390+	outwash	7.5YR 7/3	30	30	10	90	8	3	0.2
Extra **	2b	3C	260	scarp colluvium	7.5YR 7/6	10	15	25	36	45	19	0.9
samples	2a	3C	355	scarp colluvium	7.5YR 6/4	10	20	20	21	39	40	0.4
JP-2		Ap	0 10	sheetwash-loess	10YR 6/3	20	25	0	29	52	19	5.2
		A	10 20	sheetwash-loess	7.5YR 6/4	20	25	0	28	52	20	3.7
		Bt	20 53	sheetwash-loess	7.5YR 6/4	20	25	0	37	37	26	1.4
		2Bt	53 85	outwash	2.5YR 4/6	50	25	0	72	17	11	0.6
		2BC	85 114	outwash	5YR 7/4	50	25	0	88	7	5	0.2
		2Cox	114 136+	outwash	5YR 7/4	40	35	1	84	11	5	0.3
JP-3		A1	0 16	loess-alluvium	7.5YR 4/3	15	20	25	35	53	12	13.4
		A2	16 41	loess-alluvium	7.5YR 5/3	15	20	25	41	41	19	5.2
		Bt	41 85	loess-alluvium	7.5YR 5/4	15	20	25	63	27	10	1.2
		2C	85 132+	alluvium	7.5YR 7/3	25	20	30	82	13	5	0.4
JP-4		A1	0 13	sheetwash-till	7.5YR 3/3	20	5	10	62	31	8	10.4
		A2	13 48	sheetwash-till	7.5YR 4/3	10	20	10	66	27	6	3.6
		2Bt	48 72	till	7.5YR 8/1	20	10	10	72	20	9	0.4
		2C	72 105+	till	7.5YR 8/0	20	15	10	81	15	4	0.4

* Horizon nomenclature of Guthrie and Witty (1982) and Birkeland (1984) except that master K horizon is not used.

~ Particle size distribution of <2 mm fraction using sieve-pipette methods (for example, Carver, 1971) and a Sedigraph for some silt-clay fractions with prior removal of organic matter using methods of Jackson (1956). No samples contained carbonate.

Percent organic matter by method of Walkley and Black (1934).

** From center of units 2a and 2b at station 21 (fig. 4.9).

are probably primarily of Bull Lake age (130-150 ka).

Soil JP-3 and the upper parts of JP-1 and JP-2 are only weakly developed, falling in RAG 4 (fig. 4.8). Cambic and weak argillic B horizons have developed in the mixed, fine-grained sheetwash and loess deposits in the upper parts of soils JP-1 and JP-2. Soil JP-3 has a weak argillic horizon, but no increase in hue or chroma to bright reddish colors (table 4.3). Soil indices suggest a Holocene or very latest Pleistocene age for this soil, and its position near the main stream channel of the largest drainage basin on the north flank also suggests it is of Holocene (probably late Holocene) age. Argillic horizon development in deposits this young is probably due to a locally high rate of eolian dust influx (fine silt as well as clay) from the large areas of exposed Bonneville lake sediments in southern Cache Valley. Shroba (1980) has also described argillic horizons from deposits of mid- to early Holocene age along the Wasatch fault.

4.3.2.4 Fault Displacement History

To estimate the size, number, and age of the more recent surface displacement events on the James Peak fault a single trench was excavated across the 7-m-high scarp on the outwash fan 200 m west of the left lateral moraine (fig. 4.7). Dense aspen forest and soft soils prevented access to all other promising trench sites. The trench exposed white, coarse sandy, quartzite-derived outwash (unit 1; fig. 4.9) with a reddish, argillic horizon developed on it (unit 1B) overlain by bouldery, silty colluvial wedges (unit 2). The wedges were overlain by silty colluvial units (3 and 4) with thick cambic and argillic B horizons. Despite the slumping and raveling of the very loose, unconsolidated outwash in the lower trench walls we were able to expose the fault zone and former free face of the scarp at the south end of the trench. A topographic profile across the scarp indicates the fan has been displaced about 4.2 +0.6/-0.2 m at this site. The stratigraphic relationships, unit contacts, lithologies of the outwash and the colluvial wedges, and the soils developed on them do not clearly show whether one event of about 4 m displacement or two events of about 2 m displacement have occurred on the same fault in the trench. As discussed below, we favor a two-event interpretation.

Based on regional correlation of map and trench units (fig. 4.8), we infer the following sequence of events:

1) Moraines and an extensive outwash fan were deposited on the north flank of James Peak, probably during the Bull Lake glaciation (about 130-150 ka). Soils developed on stable areas of moraines and outwash, but gradual erosion prevented well-developed soils from forming on moraine crests. The length of time required to develop the reddish argillic B horizons on the outwash is difficult to estimate, partly because the soil north of the trench site (JP-2) appears to have been stripped. The fact that the argillic horizon and the fine-grained units overlying it are thin suggests soil JP-2 has been eroded, perhaps by meltwater in braided, outwash channels (which did not reach the trench site) during the later Pinedale glaciation. These horizons may have developed rapidly because of high dust influx rates due to the silt and clay from lake sediments exposed in Cache Valley to the north. Because the B horizons on these deposits are much more strongly developed than the B horizons on late Pinedale or Holocene deposits, these horizons must have

UNIT DESCRIPTIONS

COLLUVIUM

2 Scarp-derived proximal facies
- 2a Gravelly clay
- 2b Loose, gravelly, sandy-silt

3B Slopewash and loess facies argillic B horizon
- 3a Gravelly clayey silt
- 3b Pebbly silt loam

4 Slopewash and loess facies
- 4a Pebbly silt loam - cambic B horizon
- 4b Pebbly silt loam - A horizon

OUTWASH

1 Clean, loose, coarse sandy gravel
- 1a Zone of some infiltrated silt and clay
- 1B Zone of patchy argillic horizon development and iron-staining

EXPLANATION

- Lithologic and soil horizon contact; dashed where gradational
- Soil horizon contacts not coincident with lithologic unit contacts
- Fault, arrow indicates relative sense of displacement
- Surface of erosional scarp
- Argillic B horizon
- Cobbles and boulders

NOTES

n1 Upper 5-30cm is less sandy, reddish (5YR 4/6) clayey silt.

n2 Shear zone in outwash marked by 3-cm-wide reddish clay seam and imbricated cobbles.

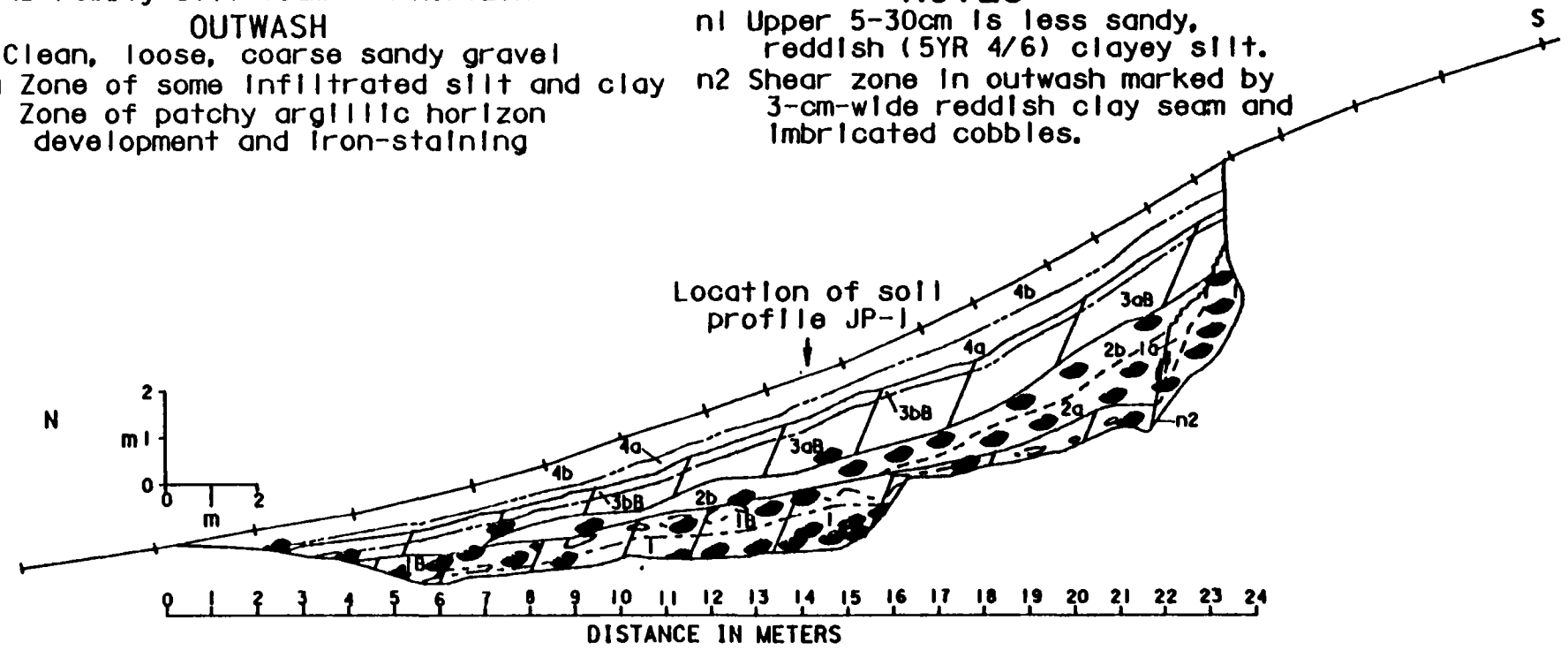


FIGURE 4.9 LOG OF A TRENCH ACROSS THE JAMES PEAK FAULT

taken at least a few tens of thousands of years to develop, perhaps as many as 70 ka.

2) Surface faulting vertically displaced the outwash (unit 1, fig. 4.9) about 1.6-2.2 m, down-to-the-north. A proximal, colluvial debris wedge (unit 2a), formed by spall, slump, and slopewash, rapidly buried the argillic horizon developed on the outwash (unit 1B) and the lower part of the free face of the scarp. The source of the bouldery debris wedge, with a matrix of silty clay (table 4.3), must have been the surface colluvium of similar lithology overlying the outwash on top of the scarp (not exposed in our trench). Although it is mapped as part of the soil developed on unit 1, the thickening of the reddish, clayey silt near the top of outwash unit 1B adjacent to the fault (note n1, fig. 4.9) and the inclusion of reddish clayey peds in the matrix of less-reddish clayey silt near the base of unit 2a suggest that material along the unit 1B-unit 2a contact may be fragments of the argillic horizon eroded from the scarp right after this event. We infer that none of the loose, sandy outwash (unit 1) was exposed in the free face by this event; if it had been the free face would have slumped almost immediately after faulting, contributing much coarse sand to the debris wedge. Equilibrium scarp degradation models at gently sloping sites suggest the maximum fault displacement is about two times the maximum colluvial wedge thickness (for example, Nash, 1981). However, the steep slope above the site and the inferred active surface transport processes (discussed below) suggest the amount of vertical displacement during this event was probably not much greater than the wedge thickness (1.6 m).

3) After the argillic horizons had formed and probably after the first fault event, soil development on the lower part of the outwash fan continued. However, the steep (20°-25°) slope of the fan above the trench site, the lack of well-developed B horizons on the proximal wedges, and the high clay content of surface colluvium above the scarp suggest that creep and solifluction may have been the dominant slope processes during periods of cold, moist climate (onset of Pinedale glaciation, about 75 ka?) during or after the deposition of the first proximal wedge. These processes may have eroded existing soils or prevented well-developed soils from forming at and above the site.

4) A second displacement event on the same fault moved unit 2a down against the outwash. The looser, sandier lithology of the proximal debris wedge (unit 2b) produced following this event indicates that some outwash was exposed in the free face in addition to the bouldery, clayey silt (not exposed in the trench) overlying the outwash. Erosion of the scarp following the first event also probably reduced the proportion of bouldery silt to outwash exposed in the free face during the second event, resulting in a sandier wedge. Slumping of the outwash in the lower part of the free face helped to spread loose debris downslope and buried the debris wedge from the first event. The loose debris produced a thinner wedge (unit 2b) that extended farther downslope than the first wedge (unit 2a); this geometry is typical of debris wedges produced by later events on multiple-event scarps (Ostenaa, 1984). Displacement during the second event is more difficult to estimate from the thickness of the debris wedge; it must be close to the difference between total topographic displacement across the scarp and the displacement of the first event (4.2 m - (1.6-2.2 m)) = 2.0-2.6 m). We could not measure total throw because the top of the outwash unit in the footwall

was not exposed in the trench. The lack of any evidence of soil development on the debris wedge resulting from the first event suggests that the two events may have occurred less than a few tens of thousands of years apart. However, the active surface processes on the steep fan (discussed above) could also have eroded a moderately-developed soil or prevented one from forming. It is also possible that weak soil development near the top of wedge 2a is masked by later development of more strongly developed soils on units 2b and 3aB (fig. 4.9).

An alternate interpretation that must be considered is that both units 2a and 2b are proximal debris wedges produced following a single displacement event of about 4 m. This would explain the absence of 1) an abrupt contact between units 2a and 2b, 2) any evidence of soil development on unit 2a, and 3) deformation of the first debris wedge (2a) during the second event. The apparent overlap of the time estimates for pre-first-event and post-second-event soil forming intervals (discussed below) would also be explained by a single event. Clear evidence of shearing along the contact between units 2a and 1a was not observed, but 3 cobbles were imbricated parallel with the contact near the base of unit 1a and the outwash is so unconsolidated that evidence of shearing may not have been preserved. Possibly, unit 1a is a fissure which filled with outwash that slumped from the free face after a second event. In any case, the stratigraphic relationships near the fault show that most of unit 2a must have been deposited immediately after faulting and its lithology shows this unit was derived from units which contained little sand. Because we find it difficult to explain how a thick, proximal debris wedge could be deposited adjacent to a several-meter-high, almost vertical free face of loose, sandy outwash without the outwash contributing any sediment to the wedge, we favor a two event fault history. In addition, 2-m displacement events are much more typical of faults in the region, even faults that are much longer than the James Peak fault (Schwartz and Coppersmith, 1984).

5) A silty colluvial wedge (unit 3) was deposited over the proximal debris wedges by wash erosion of the scarp crest and by rill and wash transport of fines from above the site. The thickness and high silt content of the wedge (table 4.3) suggests it has a strong eolian component, probably due to exposed lake sediments in Cache Valley. As the deposition rate of the colluvial wedge decreased, B horizon development in the upper part of the wedge became more distinct, culminating in a 122-cm-thick, argillic horizon (table 4.3) on the wedge. Because of its position on the scarp slope, this soil is not directly comparable to soils in more stable landscape positions whose age is better known. We interpret this soil as forming in a climate not greatly different from the present; thus, it must either pre-date the main Pinedale glaciation (18-25 ka) or post-date the fall of Lake Bonneville from its high stand (15 ka, Scott and others, 1983). The total amount of clay in this soil (9 g/cm^2) compared with regional rates of clay accumulation (for example, Colman and others, 1986) and most other soil indices for this part of the soil on unit 3 (fig. 4.9) suggest an age as great as 100-150 ka because these horizons are so thick. However, 1) the limited soil reddening and weak B horizon structure, 2) the probable high dust influx rate during part of the history of the site, and 3) the likelihood of some of unit 3 being derived from clay-rich soils upslope all suggest a much younger age. Thus, we estimate this soil, which post-dates both fault events, developed over 30-70 ka.

6) Finally, an episode of rapid slopewash deposition, probably with some eolian influx, produced a silty colluvial unit (4) which is very similar to unit 3. A weak cambic B horizon (4B) and a thick, silty A horizon (4A) on this unit, indicate a Holocene age (soil JP-1a, fig. 4.9). Deposition during the warmer, and probably drier Altithermal of the mid-Holocene (Baker, 1983) is likely.

4.3.2.5 Slip Rates and Recurrence

The topographic profile across the scarp at the trench site (fig. 4.9) shows the outwash, most likely about 140 ka, is displaced about 4.2 m for an average late Quaternary vertical slip-rate of 0.03 mm/yr on the James Peak fault.

Because the soils developed on the outwash and on the colluvium overlying the faulting-related wedges provide only maximum and minimum age estimates for the wedges, the true recurrence of surface faulting events is difficult to estimate. Displacement data for each of the two fault events is uncertain, but scarp erosion models that consider the position of the scarp at the foot of a steep slope, the thickness of the first colluvial wedge, and the volumes and lithologies of both wedges suggest the second event may have been larger than the first. We estimate average displacements of about 1.8 +0.4/-0.2 m for the first event and 2.4 +0.8/-0.6 m for the second event. The reddish argillic horizon on the outwash beneath the colluvial wedges probably required at least several tens of thousands of years (we assume >30 ka) to develop before burial, perhaps even 70 ka. This well-developed soil adjacent to the fault shows that no significant displacement occurred on the fault for a long period of time after outwash deposition ceased. Thus, the first event could have occurred as early as 110 ka (140-30 ka) or as late as 70 ka (140-70 ka). The thick argillic horizon on unit 3, which post-dates the second displacement event, also suggests a soil forming interval of at least 30 ka and perhaps 70 ka. With these broad constraints, a time interval of 80 ka (from 110 ka to 30 ka) is available in which the two events could have occurred. If we take the mean of possible times at which each event occurred (first event, x = 90 ka, second event, x = 50 ka) the events are separated by 40 ka (90-50 ka). Because the maximum estimates of the length of the soil forming intervals following each event overlap, no minimum estimate of the length of this period can be made. If the two events were separated by 40 ka, the recurrence interval between these events and earlier and future events would be >50 ka (50 + 40 + 50 = 140 ka). Thus, the average recurrence interval for the two events since 140 ka is at least 50 ka, but the lack of a soil between the two debris wedges suggests non-uniform recurrence. However, if there was only one event (discussed above), it probably occurred about 70 ka.

4.3.2.6 Relationship to the East Cache fault

The location of the James Peak fault at the southern end of the East Cache fault suggests their surface rupture histories may be related. Blau's (1975) mapping shows that the East Cache fault is abruptly terminated at its high-angle intersection with the James Peak fault (fig. 4.7) because no north-trending fault extends up Wellsville Creek. The James Peak fault is also oriented at near right angles to the contemporary regional extensional stress

field (Zoback and Zoback, 1980). However, portions of the Wasatch fault which intersect at high angles have ruptured concurrently during the Holocene (Personius, 1985) and similar fault patterns are found along late Quaternary fault zones elsewhere in the Basin and Range (for example, Wallace, 1979). The morphology of the bedrock scarps on the Broadmouth Canyon faults (fig. 4.7) does not suggest recurrent late Quaternary displacement, but also does not preclude some Quaternary slip. These scarps trend southwesterly, nearly parallel to the southern part of the East Cache fault. We speculate that the Broadmouth Canyon faults may be the southernmost part of a Quaternary rupture zone encompassing all three faults.

Some of the larger surface displacement events on the James Peak fault may have ruptured part of the East Cache fault. Empirical relationships between the amount of surface displacement and fault rupture length (Bonilla and others, 1984) suggest that more than 7 km of surface faulting is associated with events that produce the 2 m of displacement that we infer from our trench stratigraphy. On the Wasatch fault surface displacements of 1.6 to 2.6 m are thought to be associated with ruptures on fault segments 30 to 60 km long (Schwartz and Coppersmith, 1984). The 1983 Borah Peak earthquake had a maximum displacement of about 2.5 m and a total rupture length of 36 $\pm$ 3 km (Crone and Machette, 1984). Thus, even if small, unrecognized ruptures occurred on the Broadmouth Canyon faults during the events recorded at James Peak, at least 15 to 20 km of the southern part of the East Cache fault may also have ruptured. Near the southern end of the East Cache fault, Swan and others (1983b) could not determine the age of most recent displacement because the main trace of the fault is well above the Bonneville shoreline at the range front, and because scarps along the fault are almost completely masked by younger (post-Provo) alluvial fans. Thus, average recurrence on the section of the East Cache fault marked by the post-Provo scarps near Logan since the high stand of Lake Bonneville appears to be about 7 ka, but the actual interval between events could be as short as 2 to 3 ka (Swan and others, 1983b).

Site-specific fault slip data indicate differing histories for the East Cache and James Peak faults, but little reliable information on the southern half of the East Cache fault is available to distinguish among several possible relationships. One possibility is that displacements on the James Peak fault occur near the end of surface ruptures produced by very large, but infrequent (average recurrence of >50 ka) earthquakes which break a large part of the East Cache fault (>50 km). The length of these ruptures and the fact that the amount of displacement is likely to be greater near the center than near the end of the rupture segment indicate these earthquakes would be as large as or larger than those inferred on the central segments of the Wasatch fault (Bonilla and others, 1984; Schwartz and Coppersmith, 1984), which seems very unlikely. Alternatively, the East Cache fault may consist of unrecognized segments, with the southern part of the fault (and the James Peak fault) having an order of magnitude longer recurrence than the East Cache fault near Logan. The southern part of the East Cache fault could also have a slip rate and recurrence similar to that for the central part of the fault; if displacements were occurring near the base of the facets along the range front, on faults buried by the post-Provo alluvial fans along the range front, or on faults basinward of the alluvial fans, scarps on these unrecognized faults would be either buried or quickly eroded.

Although the apparent slip rates on the East Cache and James Peak faults differ by a factor of 3 to 6, it should be emphasized that the age of the datums used to estimate the rates differ by almost an order of magnitude. A similar situation is reported by Machette (1984) whose mapping suggests that the high slip rates and short recurrence intervals on the central segments of the Wasatch fault zone may only apply to the latest Pleistocene and Holocene; longer-term late Quaternary rates appear to be much lower, closer to those estimated for other faults in the region (for example, Nelson and VanArsdale, 1986; sec. 4.2). The rapid changes in subsurface pore pressures and isostatic loading and unloading accompanying the rise and fall of Lake Bonneville about 15 ka may have triggered many earthquakes on the Wasatch and East Cache faults resulting in a latest Pleistocene and Holocene recurrence rate several times that for the late Quaternary (Swan and others, 1983b; Machette, 1984). Thus, we speculate that late Quaternary slip rates on the East Cache fault and the James Peak fault, and perhaps recurrence as well, do not differ nearly as much as suggested by the apparent slip rates above.

4.3.2.7 Conclusions

Two surface displacement events of about 2 m each have occurred on the James Peak fault in the last 140 ka indicating a late Quaternary slip rate of about 0.03 mm/yr. Surface faulting recurrence intervals are difficult to estimate because of poor age control, but the average recurrence between events is at least 50 ka. The fault may be a westerly splay of the East Cache fault rather than a separate valley-bounding fault like those to the south. The lack of detailed slip and recurrence data from the southern half of the East Cache fault precludes determining whether the central part of the East Cache fault behaves independently from the southernmost part of the fault and from the James Peak fault or whether all parts of both faults have had a similar late Quaternary history.

4.3.3 Faults in western Cache Valley

The Wellsville and Clarkson faults, termed the West Cache fault by Oviatt (1985), are down-to-the-east normal faults that displace the Tertiary Salt Lake Formation on the west side of southern Cache Valley (fig. 4.7). East dips in the Salt Lake Formation beneath Cache Valley shown by reflection data (Smith and Bruhn, 1984) indicate that these faults have significantly less displacment than the East Cache fault, suggesting these faults are antithetic to the East Cache fault. However, the amount of relief of the range front and the steepness of some facets on this side of the valley suggest late Quaternary displacement on some faults here. Cluff and others (1974) mapped a number of scarps of possible tectonic origin in latest Quaternary deposits along these faults. More recent mapping by Oviatt (1985) and Personius (1985) shows that some of the scarps are Quaternary faults and that a few displace Bonneville-age sediments (Oviatt, written comm., 1986). However, recurrence intervals are longer and displacement event sizes are probably smaller on the West Cache faults than for late Quaternary events on the East Cache and Wasatch faults. For this reason and because all USBR structures are not significantly closer to the West Cache faults than they are to the Wasatch and East Cache faults, we do not consider the West Cache faults further.

4.3.4 Faults in the Mantua area

Near Mantua in the Wasatch Mountains east of the East Cache fault and northwest of Ogden Valley (fig. 4.1) are a number of partially closed, roughly equidimensional basins, from a few hundred meters to a few kilometers in diameter. The basins are smaller, but physiographically very similar to the larger back-valley basins in the Wasatch Mountains to the south, such as Ogden and Morgan valleys. Many of the east and west margins of the Mantua basins are linear, with steep, faceted ridges with coalesing alluvial fans at their bases; other margins of the basins are eroded with gentle slopes. The floors of the basins vary greatly in elevation, and some basin floors are dissected by streams while others are flat, filled with Quaternary alluvial sediments. The youngest basin fills are Holocene, but a road cut in basin fill sediments along the highway south of Dry Lake shows that at least some of the sediments filling these basins date from the early Quaternary. The ash exposed in the road cut is the Lava Creek B Ash (Oviatt, written comm., 1986) deposited about 720 ka (Izett and others, 1978). Major drainages flowing from the Wasatch Mountains into Cache Valley are clearly disrupted by the steeper margins of the small basins. The best examples of headwaters areas that are beheaded by escarpments in this part of Utah are found on the east edge of Mantua and Dry valleys.

Three possible orgins for the basins in the Mantua area have been suggested: 1) they are primarily karst features, 2) the basins were formed by normal faulting in the middle and late Tertiary, were filled with sediment, and are presently being exhumed by uplift and fluvial erosion, and 3) the basins are primarily the result of Quaternary normal faulting on pre-existing Tertiary faults bounding the basins, but most if not all displacment pre-dates the late Quaternary. Like Crittenden and Sorensen (1985) we favor the third explanation for the development of these basins for the following reasons, although origin 2 above may be of secondary importance. Karst features are present locally in some of these basins, but they are small (much smaller than the larger basins) and the features are not widely distributed throughout the area underlain by Paleozoic carbonates. The basins are much too large to have been produced entirely by karst processes. If karst was a dominent process in the area features of all sizes would be expected to be developed throughout the areas of carbonate bedrock.

Like the back valleys to the south the Mantua basins probably initially developed by normal faulting during the Tertiary. However, if the postulated faults and steep escarpments bounding these basins are entirely exhumed (representing a former Tertiary landscape) then the prominent beheaded drainages which now drain into Cache Valley are also exhumed. Because the Wasatch Range has been uplifted relatively rapidly during the late Cenozoic (Naeser and others, 1983) and because streams in the region are generally able to downcut at rates equal to uplift rates, even over resistent lithologies (Hamblin and others, 1981), we think it unlikely that the present drainage pattern in this part of the Wasatch Range is largely inherited from the middle and late Tertiary. Some of the Mantua basins with dissected floors are no longer topographically closed, but others are still being filled with Holocene sediment. In addition, the straightest, longest, highest, and steepest escarpments all trend nearly north-south -- parallel with the Wasatch fault in this area (Personius, 1985) and perpendicular to the regional extensional stress regime (Zoback, 1983). The disruption of

major drainages combined with the steep, faceted escarpments found in some north-trending basins strongly suggests to us that most of the basins have had at least tens of meters of displacement during the Quaternary. This does not preclude cumulative Tertiary displacement on the basin-bounding faults exceeding Quaternary displacement.

Thus, although we have no direct evidence, such as scarps in Quaternary deposits, we conclude that the Mantua area basins are bounded by normal faults and that significant Quaternary displacements have occurred on many of these postulated faults on the east and west basin margins (fig. 4.1). The escarpments along the central portions of many of our inferred Quaternary faults are higher and steeper than other parts of the escarpments. This suggests that these portions of the faults may have ruptured more often or more recently than the northern and southern ends of the faults. Inferred fault lengths are in the 10-20 km range, but the steeper central parts of the fault escarpments are only about 3 to 6 km long. We have marked the central part of some inferred faults as suggestive of late Quaternary displacement (plate 1a) on the basis of their morphologic similarity with escarpments in back valleys farther south which have had late Quaternary displacements. However, we have no direct evidence that displacments have occurred on these parts of the faults.

As with the West Cache faults, the inferred faults in the Mantua area pose much less hazard to USBR structures than do the Wasatch, James Peak, and East Cache faults. Thus, the Mantua basins were not studied further.

4.3.5 Faults east and southeast of Cache Valley

In this section we provide a summary of published information on the Bear Lake and Crawford Mountain faults supplemented by a brief review of aerial photography of the southern portion of Bear Lake and the eastern Bear River Range and a half day field reconnaisance along the southeastern shore of Bear Lake.

The Bear Lake fault and the Crawford Mountain normal fault occur in the Idaho-Wyoming Thrustbelt in the northern Wasatch Mountains east of Cache Valley at or near the eastern margin of the Basin and Range transition zone (fig 4.1). Both of these late Cenozoic normal faults have developed in the upper plate of the Crawford Mountian thrust, an imbricate splay of the Absoraka Thrust.

4.3.5.1 Bear Lake faults

Bear Lake occupies the southern portion of an arcuate structural depression drained by the Bear River that extends over a distance of about 100 km from Laketown, Utah north to Soda Springs, Idaho. Seismic reflection data across the southern portion of Bear Lake show east-dipping reflecters within the graben bounded on the east by the west-dipping East Bear Lake normal fault (Lamerson, 1982; Valenti, 1982; Royse, personal comm).

Fault scarps with heights of 3 - 10 m mapped in alluvial fan deposits at the mouth of North Edan Creek, and scarps in lake bottom sediments reported by Williams and others (1962) indicate that late Quaternary surface displacements have occurred on the East Bear Lake fault. Williams and others (1962) discuss the recent history of Bear Lake and describe three abondoned

late Pleistocene shorelines preserved on the margins of the lake. They map fault scarps in unconsolidated deposits, probably of Holocene age, along the east Bear Lake fault from Laketown, Utah to Bennington, Idaho, a distance of about 60 km. Kaliser (1972) discusses exposures of the east Bear Lake fault in alluvial fan deposits, describes the prominent triangular facets developed in bedrock in the footwall of the east Bear Lake fault. He also discusses three earthquakes that occurred in the vicinity of Bear Lake from 1873-1876.

Based on air photo interpretation and reconnaissance mapping of the scarps on the east side of Bear Lake (A. J. Crone, oral communication) we conclude that late Quaternary surface displacements have occurred on the East Bear Lake fault. Therefore, we consider this fault to be a source for large magnitude earthquakes in the northern Wasatch Mountains.

4.3.5.2 Bear River fault zone

Mapping of fault scarps in alluvial deposits has defined the 20-km-long Bear River fault zone south of Evanston, Wyoming (Gibbons and Dickey, 1983; West, 1984), east of the Regional study are (fig. 4.1). Trenching has established that Holocene surface displacements of 2 to 3 m have occurred with a recurrence interval of 1 to 3 kas (West, 1984). These fault scarps, as well as drainage anomalies and a linear bebrock escarpment further to the east are interpreted as resulting from the reactivation of the Darby thrust (West, 1986). These faults should also be considered as potential sources for large-magnitude earthquakes.

4.3.5.3 Crawford Mountain fault

The Crawford Mountains are located southeast of Bear Lake, east of Randolph, Utah and east of the Regional Study area. A normal fault that extends for a distance of at least 30 km has been mapped on the west margin of the Crawford Mountains where it is concealed by the floodplain deposits of the Bear River (Hintze, 1980). Seismic reflection data indicate that this fault has localized deposition of about 2 km of east-dipping Tertiary sediment in the upper plate of the Crawford thrust which is exposed on the east side of the mountains (Royse, 1975; Lamerson, 1982). This fault is also interpreted as a listric normal fault related to the reactivation of an older thrust fault (Royse, 1985, personal communication).

We have done no reconnaissance mapping or air photo study of the Crawford Mountains fault for this study and have identified no faults scarps in late Quaternary deposits associated with the fault, although detailed study of the alluvial deposits on the west side of the Crawford Mountains may reveal fault-related features similar to the Bear River fault zone (West, 1984). Based on similarities with the East Cache and the East Bear Lake fault, we infer that late Quaternary displacements have occurred on this fault (fig. 4.1).

4.3.5.4 Faults in the Bear River Range

In the Bear River Range south of Bear Lake and east of Cache Valley, prominent west-facing linear bedrock escarpments with poorly preserved facets are inferred to mark the positions of down-to-the-west normal faults (fig. 4.1; pl. 1a), some of which appear on published maps (Stokes and Madsen, 1964; Hintze, 1980). Cluff and others (1974) suggest that late Quaternary

faults may be present immediately southwest of Bear Lake (fig. 4.1). Our study of air photo also reveals lineaments at the base of these escarpments and has identified additional escarpments and associated lineaments that suggest late Cenozoic and possibly late Quaternary displacements have occurred on faults in the Bear River Range (fig. 4.1). The faults typically have lengths of 10 - 15 km with early Tertiary and Quaternary deposits in the hanging wall and Paleozoic rocks in the footwalls.

On the basis of this reconnaissance air photo mapping we infer that late Quaternary displacements have occurred on these faults (fig. 4.1; pl. 1a).

4.4 Ogden Valley

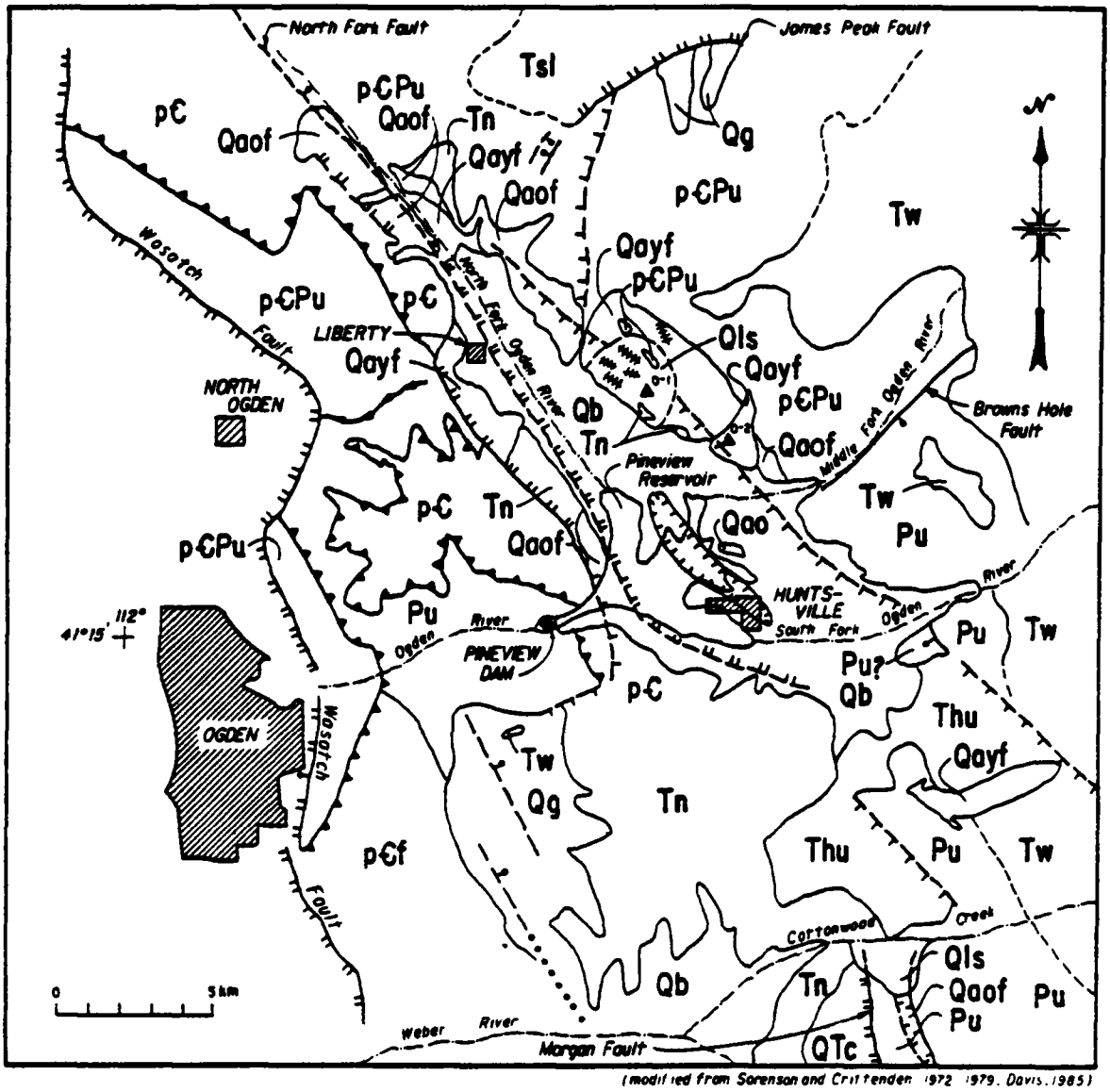
Ogden Valley is a 35-km-long, up to 5-km-wide, northwest-trending structural and physiographic basin in the Wasatch Mountains north of Morgan Valley and east of Ogden, Utah. Three major tributaries of the Ogden River flow into Ogden Valley and the river exits through Ogden Canyon in the Wasatch Mountains (fig. 4.10). Pineview Dam on the Ogden River impounds Pineview Reservoir which occupies the southwestern portion of the Valley.

The preservation of the Oligocene Norwood Tuff and the Pliocene(?) Huntsville fanglomerate within Ogden Valley and a steep faceted bedrock escarpment on the southwest margin of the valley suggest that the subsidence of Ogden Valley began in the early Cenozoic and has continued into the late Quaternary, as in Morgan Valley to the south. Eardley (1955) discusses a displacement history for back valley faults in the northern Wasatch Mountains that includes an early Cenozoic episode of folding and faulting. Based on a late Pliocene(?) fanglomerate in Morgan, Ogden, and Cache Valleys, he infers a late Pliocene episode of major block faulting that defined the present outline of Ogden Valley. We concur that late Cenozoic extension in the back valleys of the Wasatch Mountains has reactivated prexisting normal faults in Ogden Valley; however, we have inferred early and/or mid-Quaternary displacement on several marginal faults and late Quaternary displacement on faults on the southwest margin of the valley.

4.4.1 Faulting in Ogden Valley

Ogden Valley is interpreted as a late Cenozoic graben based on published cross sections of Royse and others (1975) and Sorensen and Crittenden (1979) depicting steeply-dipping normal faults on the margins of Ogden Valley which are associated with a residual gravity low of about 25 mgal centered near Huntsville (fig. 4.10) that is interpreted to represent about 1500 m of low-density Norwood tuff and overlying late Cenozoic basin fill (Stewart, 1958; Zoback, 1983). Northwest-striking normal faults with lengths of 10 - 18 km and late Cenozoic displacements of >500 m are also interpreted from this data by Stewart (1958). Two late Cenozoic normal faults are shown on the southwest margin of the valley (fig. 4.10): the southwesternmost is exposed as a fault contact at the base of the bedrock escarpment bordering the valley with a length of about 10 km from west of Liberty to Ogden Canyon; and the other, referred to as the North Fork fault, is inferred on the basis of gravity data and drilling to extend from the North Fork of the Ogden River to south of Pineview Reservoir. A single fault is inferred on the northeast margin also about 1.5 km basinward of the valley margin (Sorensen and Crittenden, 1979). Logs of waterwells, drilled to develop an aquifer confined below an impermeable horizon in pre-Bonneville deposits within Ogden Valley, demonstrate that pre-Bonneville age, unconsolidated, alluvial and lacustrine deposits in the valley are at least 100 m lower in elevation than Paleozoic bedrock at Pineview Dam at the outlet to the Valley (USBR, 1932; Doyuran, 1972).

Our initial efforts to locate and assess evidence for late Quaternary faulting in the back valleys of the Wasatch Mountains focused on Ogden Valley. Sorenson and Crittenden (1979) show faults displacing Holocene colluvium near the northeast margin of the valley, and Lofgren (1955, p.83) described a fault scarp demonstrating "recent displacement" along the range



(modified from Sorenson and Crittenden 1972 1979. Davis, 1985)

EXPLANATION

- Contact, dashed where approximately located.
- Late Quaternary normal faults, dashed where inferred or approximately located.
- Late Cenozoic normal faults, dashed where inferred or approximately located.
- Cenozoic normal faults, dashed where inferred or approximately located.
- Willard Thrust fault
- Ogden Thrust fault
- Eden water gap
- Maximum residual gravity anomaly from Stewart (1958)
- Lineaments (Sorenson and Crittenden, 1979)
- Streams
- Soil test pit

QUATERNARY

- Qayf — Younger alluvial fan deposits
- Qb — Lake Bonneville sediments and Holocene alluvium, includes post-Bonneville alluvium.
- Qls — Landslide
- Qaof — Older alluvial fan deposits.
- Qao — Pre-Bonneville alluvium.
- Qg — Glacial deposits

TERTIARY

- Thu — *Pliocene? Huntsville fanglomerate*
- Tsl — Neogene Salt Lake formation
- Tn — Late Eocene-Oligocene Norwood Tuff.
- Tw — Eocene Wasatch formation.

PRE-TERTIARY

- Pu — Paleozoic undivided.
- p€Pu — Paleozoic and Precambrian undivided.
- p€f — Precambrian Farmington Canyon Complex.
- p€ — Precambrian in upperplate Willard Thrust, mostly Brigham Group.

Figure 4.10 Geologic map of Ogden Valley.

front east of Liberty, Utah. Our low sun angle overflights and review of aerial photography revealed no fault scarps in unconsolidated deposits either at the margins or within Ogden Valley; however, inferred fault contacts with Cenozoic deposits and our compilation of waterwell data suggest late Cenozoic displacement has occurred on most faults in the valley and the steepness and linearity of the bedrock fault scarp on the southwest margin of Ogden Valley suggested late Quaternary displacement.

4.4.1.1 Northeastern margin of Ogden Valley

A normal fault is mapped on the northeastern margin of the valley, but geologic and geomorphic evidence suggests that it is not a late Quaternary fault. Cambrian and Precambrian rocks, overlain east of the valley by the Wasatch Formation, form the range front opposite Pineview reservoir along the northeastern margin of the valley from Wolf Creek to the South Fork of the Ogden River (fig. 4.10). This portion of the valley margin is linear, but less steep than the escarpment along the Morgan fault, with larger tributary valley embayments eroded into it. The break in slope between the range front and the thin, bouldery alluvium, colluvium, and landslide deposits that mantle bedrock on this side of the valley is gentle, and interpretations differ as to the location of a range-front fault. Previous smaller-scale maps and generalized cross sections (Lofgren, 1955; Doyuran, 1972) depict a range-front fault at the base of the escarpment on this margin of the valley. But we interpret the gravity data and the more recent mapping of Sorenson and Crittenden (1979) as suggesting that the main fault on this margin of the valley corresponds with the contact between the Norwood Tuff and the Cambrian rocks, located 1-2 km basinward of the margin of the valley. Quadrangle-scale-mapping by Sorenson and Crittenden (1979) shows outcrops of Cambrian quartzite beneath the bouldery surface deposits at distances of 1 to 2 km from the range front showing that there is little or no stratigraphic offset between these outcrops and the escarpment. Therefore, we conclude that there is not a significant fault along the break in slope at the base of the escarpment, in contrast to the Morgan fault.

Along this margin of the valley Sorensen and Crittenden (1979) map a subparallel series of < 2 km long, northwest-striking faults in "Holocene colluvium and slopewash" that are nearly coincident with the contact between the Norwood Tuff and Cambrian rocks, that we interpret to be the main fault on this margin of the valley (fig. 4.10). These mapped faults correspond with 1-7 m high, predominantly southwest-facing scarps, evident both on airphotos and on the ground. Several exposures just northwest of the scarps show very well-developed, but eroded soils with thick, 2.5YR-5YR, clay films completely coating peds. The old argillic horizons of these soils, developed on highly-weathered alluvial fan gravels, are >1.5 m thick and stained with manganese oxides. Based on comparisons with soils along the Weber River (sec. 3.5), these soils are at least 200 ka. Overlying the old argillic horizons are 1-2 m of silty loess and slopewash deposits. Boulder streams, patterned ground, and other solufluction features (like those described by Williams and Southard (1962) and Degraff (1976)) on these piedmont deposits along the range front) show the near surface sediments on much of the piedmont have been active during much colder periods in the late Quaternary, but have not been removed or buried by Holocene processes. Indices for a soil (soil O-1, table 4.4, figs. 4.10 and 4.8) with a moderately developed argillic horizon developed in these deposits suggest the soil is pre-

Table 4.4 Selected properties of soils on alluvial fan sediments in Ogden Valley, north central Utah.

Profile	Horizon*	Average depth (cm)	Parent material	Munsell dry color	ESTIMATED PERCENT BY VOLUME Pebbles (0.2-8cm)	Cobbles (8-25cm)	Boulders (>25cm)	PERCENT BY WEIGHT~ Sand (2-0.5mm)	Silt (50-2um)	Clay (<2um)	Percent# organic matter	Percent** carbonate
O-1	A	0 15	loess-colluvium	7.5YR 5/2	5	10	10	18	72	10	2.8	0.2
	2BA	15 51	loess-colluvium	7.5YR 6/2	5	10	10	15	41	44	0.8	0.4
	2Bt	51 76	loess-colluvium	7.5YR 6/3	5	0	0	11	42	46	0.6	0.4
	2BC	76 122+	loess-colluvium	7.5YR 7/3	5	0	0	14	41	45	0.5	0.3
O-2	Ap	0 12	loess-colluvium	10YR 5/3	5	5	20	35	50	15	2.8	0.0
	A	12 28	loess-colluvium	10YR 5/3	5	5	20	34	48	18	1.2	0.0
	Bt	28 59	loess-colluvium	7.5YR 6/4	5	5	20	47	34	18	0.7	0.0
	2Bt	59 83	alluvium	7.5YR 5/5	10	15	20	83	7	9	0.2	0.0
	2Cox	83 121+	alluvium	7.5YR 5/5	10	15	30	87	6	7	0.2	0.0

* Horizon nomenclature of Guthrie and Witty (1982) and Birkeland (1984) except that master K horizon is not used.

~ Particle size distribution of <2 mm fraction using sieve-pipette methods (for example, Carver, 1971) and a Sedigraph for some silt-clay fractions with prior removal of carbonates and organic matter using methods of Jackson (1956).

Percent organic matter by method of Walkley and Black (1934).

** Percent carbonate by method of Allison and Moodie (1965, p. 1387).

Holocene. The total profile index for a soil (soil O-2, fig. 4.10) on a large Holocene alluvial fan to the southeast is about half that for soil O-1 (fig. 4.10), but the high content of fines in this Holocene soil shows that a large amount of silt and clay is being blown onto the east side of the valley, probably from exposed lake sediments. Thus, most of the unconsolidated deposits on the piedmont are probably old alluvial fans, weathered Norwood Tuff, and landslide deposits over bedrock with a thin cover of late Pleistocene and Holocene loess and colluvium. Landslides in the Norwood Tuff are ubiquitous in the back valleys of the Wasatch Mountains. The scarps mapped by Sorenson and Crittenden (1979) are in an area where only a thin veneer of loess and slopewash overlies the Norwood Tuff and old fan deposits, the scarp lengths are very limited, and the distribution of the scarps along the valley margin is very limited. For these reasons, we interpret these scarps as the result of shallow landslides (as discussed by Lofgren (1955, p. 83) and Doyuran (1972 pg. 28) or bedrock knobs protruding through most of the piedmont sediment, rather than to late Quaternary displacement on faults.

South of the South Fork of the Ogden River, southeast of Huntsville, and above the Bonneville shoreline an unconsolidated boulder conglomerate (Thv), inferred to be of Pliocene(?) age, is preserved overlying the Norwood Tuff that is described by Lofgren (1955) and informally referred to as the Huntsville fanglomerate. From aerial photos we have mapped inferred faults along the linear, southeast trending contacts between this Huntsville fanglomerate and older rocks (fig. 4.10). These 2- to 5-km-long inferred faults are presumed to be of late Cenozoic age, but lack the prominent expression of late Quaternary faults such as the Morgan fault. The faults do reflect the preferred northwest trend of late Cenozoic faults in Ogden Valley which are inferred to be related to prexisting structure. Southwest of Huntsville the Norwood Tuff extends up onto the west flank of the Wasatch Mountains where its inferred, northwest-trending fault contact with older rocks mapped by Bryant (in press) is concealed by late Pleistocene moraines. As no faults are mapped north of Cottonwood Creek on the northward projection of the Morgan fault, we conclude that the Morgan fault dies out in the vicinity of the creek and that late Cenozoic extension further north is accommodated on the northwest-trending faults of Ogden Valley.

The Broadmouth Canyon faults (sec. 4.3) extend south from the southern end of Cache Valley to Ogden Valley (fig. 4.10). Although they have been mdified by erosion, the height of the bedrock escarpments on these faults suggests Quaternary displacement, but the scarps decrease in height to the south and cannot be traced into the valley.

4.4.1.2 Southwestern margin of Ogden Valley

Mapping by Sorensen and Crittenden (1979) based on gravity modelling by Stewart (1958) shows two southeast-striking normal faults along the southwestern margin of the valley. Precambrian and Cambrian sedimentary rocks form the prominent escarpment southwest of Liberty. This linear, 10-km-long escarpment continues south of Ogden Canyon as a fault contact between Precambrian rocks and the Norwood Tuff (fig. 4.10). Late Quaternary alluvial fan and colluvial deposits are mapped as displaced in the hanging wall of this fault (Sorensen and Crittenden ,1979) below the Edan Water Gap (el m, 6184 ft) west of Liberty, and " recent displacement" is inferred along

this section of the fault by Lofgren (1955) based on the presence of springs and the steep bedrock fault scarp (28-33°) preserved here. This portion of the fault ends abruptly at Chicken Creek, west of Liberty. Scarps in the distal portions of the alluvial fans along this section are all stream cut and we found no scarps in any sediments along the base of the escarpment. However, these fans are less dissected and grade into late Quaternary fluvial terraces and Bonneville deposits towards the center of the valley suggesting they are probably younger than the fans along the southern section of the fault or those on the northeast margin of the valley. Gilbert (1928, p. 58,59) believed the Eden Water Gap was cut by a stream crossing the Wasatch Range that was captured in Ogden Valley by the Ogden River after a significant amount of uplift on the Wasatch fault, but before much of the more recent Quaternary uplift (Eardley, 1944).

This fault is interpreted to continue with southeasterly strike about 2 km south of Ogden Canyon along the steeply-dipping contact between the Norwood Tuff and Precambrian rocks where the contact with the Norwood Tuff turns abruptly to the southwest (fig. 4.10). At this point, southwesterly-striking facets in Precambrian rocks suggest a fault contact with the Norwood Tuff along a 5-km-long southwest-striking fault section. Further to the southwest, southeast-striking normal faults mapped by Bryant (1979) are concealed by late Quaternary (<125 ka) moraines. The short southwest-striking section is on the projection of the Browns Hole normal fault mapped by Crittenden (1972b) in Precambrian and Cambrian rocks on the opposite side of the valley (fig. 4.10). Along the Middle Fork of the Ogden River the fault does not displace the Wasatch Formation, but the facets south of Ogden Canyon suggest late Cenozoic reactivation of a portion of the Browns Hole fault. As there is no deflection of the gravity contours along this southeast trend within the valley only the southwestern most portion of the fault is interpreted to have been reactivated.

Based on the steepness and linearity of the escarpment on the northwest-striking section of the fault, the height of the Eden water gap, and the late Quaternary age of the fans here in contrast to other margins of the valley, we conclude that late Quaternary displacements have probably occurred on at least this section of this 10-km-long fault.

The second normal fault on this margin of the valley is mapped at the base on the eroded escarpment in the Norwood Tuff north and south of Pineview reservoir, on the basis of an interpretation of gravity data by Stewart (1958). This fault appears to be the southward continuation of the North Fork fault discussed below. Drill hole logs described by Doyuran (1972) confirm the presence of this fault and suggest that it has greater cumulative displacement than the fault at the base of the escarpment in Precambrian rocks further to the southwest. Based on the closure of the residual gravity anomaly and water well data, the reactivated late Cenozoic portion of the North Fork fault is inferred to have a length of about 18 km. Thomas (1945) interpreted logs of water wells drilled through the clayey silt horizon that caps the artesian reservoir in the valley as demonstrating about 8 m of late Quaternary, pre-Bonneville displacement on this fault.

North of Liberty the course of the North Fork of the Ogden River appears to be in part controlled by the northwest-striking North Fork fault (fig. 4.10) mapped by Sorensen and Crittenden (1976; 1985). In cross section this fault

is depicted as high-angle, down-to-the-northeast, normal fault with at least 1000 m of displacement of Paleozoic and Precambrian rocks which they interpret to be pre-Tertiary in age. We concur that there appears to have been at least no late Cenozoic displacement on this fault, for although this fault truncates northeast trending faults mapped in Precambrian and Paleozoic rocks to the northeast, it lacks an associated bedrock fault scarp, and it has not localized deposition of Norwood Tuff or younger deposits.

An escarpment, probably produced by Quaternary faulting, bounds alluvial fans and fluvial terraces along the North Fork of the Ogden River north of the Liberty between the trace of the Willard thrust and the inferred trace of the North Fork fault (fig. 4.10). Facets along the escarpment are eroded, but recognizable and slope about 22°. Fluvial terraces between the escarpment and the channel of the North Fork and the alluvial fans that grade into them are probably of at least three different ages. The two lower terraces, at about 8 m and 15-20 m, and some debris flow deposits on the higher alluvial fans have poorly developed soils on them with Bw horizons or weak argillic horizons with patchy areas of reddish sandy clay. These characteristics suggest they may correlate with Pinedale glacial deposits (sec.s 3.3 and 3.4). Moderately-developed soils with 50-100-cm-thick argillic horizons with 5YR hues that are overlain by 40-75 cm of loess are developed in the gravel terraces about 40-50 m above the river. Based on correlations discussed in sections 3.4 and 3.5, a Bull Lake age (about 140 ka) seems reasonable for these terraces. A few poor exposures of the soils on terrace and fan deposits above the 40-50 m terraces, about 90 m above the river, show argillic horizons with more reddish clay than lower terraces, but less than in the soils developed on the fan sediments along the northeast margin of the valley. These deposits are probably >200 ka. The fan sediments closest to the escarpment have old soils on them like the fans along the other margins of the valley, except for the Liberty section, suggesting significant displacements on the escarpment fault are pre-late Quaternary. The height of the terraces above the North Fork compared to similar-aged terraces elsewhere in the region (sec. 3.5) and the fact that terraces with Bull Lake-type soils are much higher than terraces with Pinedale-type soils is probably partly due to more rapid fluvial dissection of valley deposits as a result of displacement on the Wasatch fault, only 6 km to the east.

The North Fork fault appears to be a 30 or more km long fault, parallel to the Willard Thrust, that has been reactivated as a late Cenozoic fault along only a portion of its length. Northeast of Liberty the escarpment on the west edge of the alluvial terraces appears to be a Quaternary fault on the basis of its linearity and steep slope. Southwest of Liberty, the projection of the the North Fork fault coincides with the basinward, late Cenozoic normal fault defined by the gravity data (fig. 4.10). Based on the shape and the closure of the residual gravity anomaly in the center of the valley, the late Quaternary North Fork fault is inferred to continue south of Huntsville, yielding a late Quaternary fault length of 18 km. Alternatively, the 4 km section west of the North Fork may indicate that Quaternary displacemnt on the North Fork fault has been transferred in an en echelon manner to the southwest-bounding fault. However, there is good evidence for late Quaternary displacement only on the Liberty section of the southwest-bounding fault.

4.4.2 Conclusions

Based on published geologic mapping and our interpretation of air photos, subsurface data and reconnaissance mapping, we conclude that northwest-trending late Cenozoic normal faults are present in Ogden Valley and that late Quaternary displacement has occurred on some of these faults. In Morgan and Cache Valleys we have concluded that late Quaternary faults are present at the base of some of the escarpments on the margins of these valleys. However, on the northeastern margin of Ogden Valley we conclude that no significant fault is present at the base of the escarpment, rather the main fault is inferred from gravity data and geologic mapping to be 1 to 2 km basinward of the base of the escarpment. A smooth bedrock pediment dipping 6-7° southwest extends smoothly across this fault contact and it is overlain by fan sediments with very old soils on them and a thin veneer of bouldery loess and slopewash. In addition, old gravels near the center of the valley just north of Huntsville, which were probably deposited by the Ogden River, have a thick, clay-rich argillic horizon with 5YR hues developed on them, suggesting they are >130 ka. This indicates that deposits at least this old and possibly much older have not been displaced below the present floor of the valley. Therefore, we conclude that no late Quaternary displacement has occurred along this margin of the valley. The faults on the southwest margin of the valley have downdropped pre-Bonneville alluvial deposits in the valley relative to its outlet and are inferred to have displaced late Quaternary alluvial fans along at least one section of the valley margin. We have estimated the late Quaternary fault lengths to be 18 km for the North Fork fault and 10 km for the southwesternmost fault on this margin of the valley (fig. 4.10).

Making an accurate assessment of the potential for surface faulting in Ogden Valley is difficult. We have no trench or site-specific data with which to constrain the late Quaternary slip rate, single event size, or age of most recent displacement. Therefore, based on similarities in late Quaternary fault length and the escarpment morphology of one section, and the estimated young age of alluvial deposits adjacent to the fault, we assume that slip rate and displacement parameters are similar to those calculated for the Morgan fault -- a Quaternary slip rate of 0.01 - 0.02 mm/yr and an average recurrence of surface displacements of 25 - 100 ka.

4.5 East Canyon area

South and east of Morgan Valley, the prominent east-facing escarpment of the East Canyon fault, with maximum relief of about 350 m, trends N25°E over a distance of 28 km from Big Mountain to Croyden, Utah. The Weber River breaches the escarpment near Croyden and enters the Upper Weber Canyon about 12 km east of Morgan, Utah and East Canyon Creek breaches the escarpment at East Canyon Dam, and then flows north joining the Weber River in Morgan Valley (fig. 4.11).

4.5.1 Geologic setting

The East Canyon fault has developed in the Stevensville syncline (Eardley, 1944; Lamerson, 1982) adjacent to the east limb of the large ramp anticline in the lower plate of the Willard thrust that forms the north-central Wasatch Mountains. Nearly vertical Paleozoic and Mesozoic rocks are exposed in the Upper Weber Canyon, downstream of the fault, where they are unconformably overlain by late Cretaceous and early Tertiary conglomerates of the Echo Canyon, Evanston, and Wasatch Formations that are also exposed in the footwall of the fault (Mullens and Laraway, 1964). Rocks exposed in the hanging wall of the fault include the east-dipping Jurassic Preuss Formation, the Wasatch Formation, and the northwest-dipping Norwood Tuff. A Pliocene? fanglomerate has been mapped adjacent to the southern portion of the fault by Egbert (1954) that is probably equivalent to the Huntsville fanglomerate in Morgan and Ogden Valleys.

The escarpment was recognized as a fault scarp by earlier workers (Eardley, 1952; Egbert, 1954) who discuss a complex displacement history for the fault, culminating in late Cenozoic normal displacement. Recognizing that most major late Cenozoic listric normal faults in the Foreland Thrust Belt are west-facing, Royse (1983) interprets the East Canyon fault as an east-facing exception, suggesting that the fault soles in Jurassic salt along a thrust plane, and that its east dip is localized by the east-dipping, thrust rotated Jurassic Press Formation. Lamerson (1982) discusses three drill holes in the Stevensville syncline including No. 1 Gulf-Amoco East Canyon that spudded about 2.7 km east of the East Canyon fault (fig. 4.11a). Based on the omission of the lower Preuss Formation in the well, he interprets a normal fault at the top of salt in the Preuss Formation at a depth of 2.6 km (8,656 ft). Assuming this fault intersection is the East Canyon fault with a 45° southeast dip, our mapping and that of Bryant (written comm., 1983) suggests that the 20° northwest-dipping Norwood Tuff has been displaced a minimum of 2.2 km (fig. 4.11a).

4.5.2 Quaternary deposits in the East Canyon area

At least four relative ages of fluvial deposits can be distinguished in the East Canyon Creek drainage basin in the hanging wall of the East Canyon fault (fluvial deposits of the Weber River Valley are discussed in sec. 3.5.1). A few remnants of erosion surfaces cut on the Norwood Tuff and the Pliocene fanglomerate, 150-180 m above East Canyon Creek, are found in the Taylor Hollow area east and west of East Canyon Reservoir. Roadcuts show quartzite-cobble gravels with a reddish, sandy clay matrix, like that of the Huntsville fanglomerate in its type area, overlying the Norwood Tuff in this area. The largest remnants south of Taylor Hollow slope 3-5° towards the reservoir.

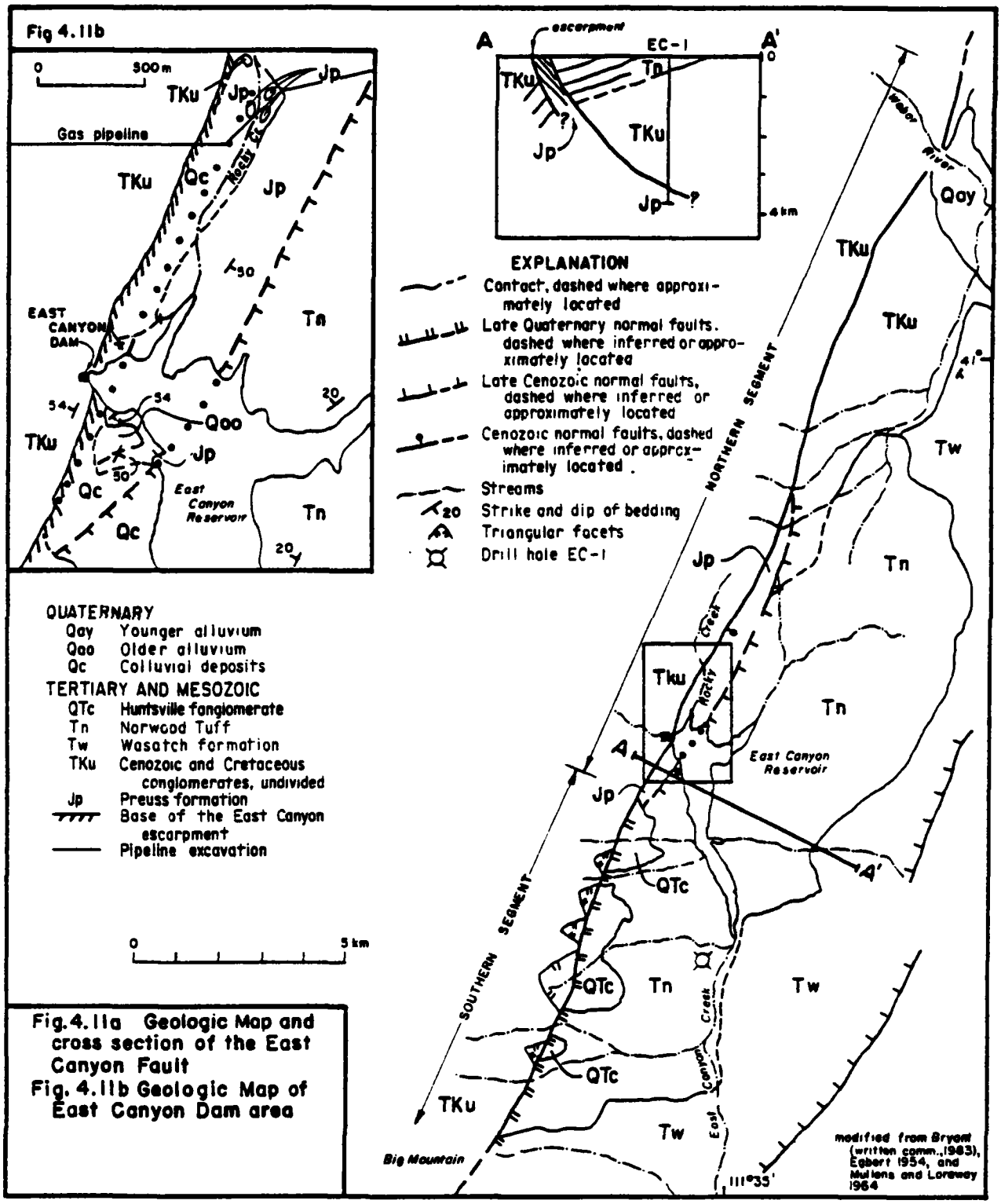


Fig. 4.11a Geologic Map and cross section of the East Canyon Fault

Fig. 4.11b Geologic Map of East Canyon Dam area

Their slope and elevation relative to the creek suggest they are roughly correlative with similar surfaces west of the Weber River in Morgan Valley which are >730 ka (sec. 4.2).

The next lower group of fluvial terraces, 50-70 m above the creek, are best preserved as alluvial fan remnants where tributary drainages meet East Canyon Creek, although in some valleys, such as Taylor Hollow and Big Dutch Hollow, they extend up valley. Most often, only a single remnant at this level is preserved, but at the mouth of Big Dutch Hollow, two levels 12 m apart are found in the largest alluvial fan complex in the drainage. The size of this fan complex relative to those at the mouths of other tributaries is probably due to increased discharge during deglaciation of the small plateau glaciers southwest of Lewis Peak in the headwaters of Big Dutch Hollow. Below the middle level fan remnants, discontinuous terraces are preserved 7-17 m above East Canyon Creek along most of its length.

In an effort to compare the sequence of fluvial terraces in the East Canyon drainage with similar terrace remnants elsewhere in the Weber River drainage (sec. 3.5.1), soils on the fan remnants at the mouth of Big Dutch Hollow were described and analyzed (table 4.5; pl. 1b). Comparison of soil development indices and secondary clay values from these profiles with those from soils in the area with some age control (sec. 3.4)(figs. 3.1 and 3.2) suggest the highest Quaternary fan remnant (65 m) is probably in RAG 2; regional correlations suggest an age of about 140 ka for this remnant. Both the next lower fan remnant (52 m above the creek) and the more extensive terrace at 16 m have much lower soil indices suggesting both soils are in RAG 3 and may be related to Pinedale deglaciation (see discussion in sec. 3.5.1). The terraces at 7-17 m along the creek are not continuous enough to trace below East Canyon Reservoir, but their relative position above the creek and the degree of soil development on them suggest they are correlative with either or both 1) the gravel terrace graded to the Lake Bonneville shoreline at the southern tip of Morgan Valley and 2) the fluvial terrace about 12 m below it. In either case, the terraces are about 14-15 ka (sec. 1.2).

The terrace sequence in the East Canyon Creek drainage suggests a long period of dissection following the cutting of the highest erosion surfaces. The middle level fans and terraces at 50-70 m are probably related to the climate changes accompanying isotope stage 6 glaciation (sec. 3.5.1), but the character of this depositional response is not known. The relatively young age but high relative elevation of the 42 m fan remnant at the mouth of Big Dutch Hollow suggests most of the dissection below the 50 m level along the creek has taken place since the maximum extent of glaciers during Pinedale glaciation (about 18 - 25 ka). The extent of this dissection throughout the basin suggests it is neither a response to local faulting nor to the fall of the high stand of Lake Bonneville in Morgan Valley. Major regional changes in effective precipitation and vegetative cover are probably primarily responsible for this amount of dissection. The lower terraces are probably an aggradational response to events during Pinedale deglaciation (12-18 ka). However, the extent of these terraces also suggests a regional climatic event rather than a base level change.

Thus, because the existing terrace remnants are not continuously preserved along the valleys and because the remnants are best explained as a response to regional climate change, the fluvial deposits in the East Canyon Creek

Table 4.5 Selected properties of soils on alluvial fans along East Canyon Creek, north central Utah.

Profile	Horizon*	Average depth (cm)	Parent material	Munsell dry color	ESTIMATED PERCENT BY VOLUME Pebbles (0.2-8cm)	Cobbles (8-25cm)	Boulders (>25cm)	PERCENT BY WEIGHT~ Sand (2-0.5mm)	Silt (50-2um)	Clay (<2um)	Percent# organic matter	Percent** carbonate
E-1	Ap	0 20	loess	10 YR 4/2	5	0	0	36	43	21	6.9	0.4
	A	20 50	loess	10 YR 3/2	5	0	0	36	41	23	3.2	0.4
	2BA	50 78	fluvial gravels	7.5 YR 6/6	30	10	0	45	40	15	0.5	0.1
	2Bt	78 110	fluvial gravels	7.5 YR 6/5	40	30	5	78	13	9	0.7	0.1
	2Cox	110 163+	fluvial gravels	7.5 YR 5/6	40	30	5	78	10	12	0.2	0.2
E-2	Ap	0 10	loess	10 YR 4/4	5	0	0	36	46	19	4.7	0.3
	A	10 25	loess	10 YR 4/4	5	0	0	32	47	21	1.8	0.2
	B	25 52	loess	7.5 YR 5/5	3	0	0	32	44	23	0.5	0.1
	Bt1	52 77	loess	7.5 YR 5/5	3	0	0	33	44	22	0.5	0.1
	2Bt2	77 112	fluvial gravels	7.5 YR 5/5	20	20	0	57	24	18	0.5	0.1
	2Cox	112 145+	fluvial gravels	7.5 YR 6/6	20	10	20	78	10	12	0.2	0.2
E-3	A	0 30	loess	10 YR 4/4	3	0	0	34	45	21	4.0	0.1
	BA	30 52	loess	7.5 YR 6/4	3	5	0	30	45	24	0.9	0.0
	2Bt1	52 80	fluvial gravels	5 YR 6/8	20	20	5	46	17	37	0.8	0.1
	2Bt2	80 110	fluvial gravels	5 YR 6/6	20	20	5	55	16	29	0.0	0.1
	2BC	110 135+	fluvial gravels	5 YR 6/7	20	20	5	71	14	15	0.2	0.1

* Horizon nomenclature of Guthrie and Witty (1982) and Birkeland (1984) except that master K horizon is not used.

~ Particle size distribution of <2 mm fraction using sieve-pipette methods (for example, Carver, 1971) and a Sedigraph for some silt-clay fractions with prior removal of carbonates and organic matter using methods of Jackson (1956).

Percent organic matter by method of Walkley and Black (1934).

** Percent carbonate by method of Allison and Moodie (1965, p. 1387).

drainage offer little positive or negative evidence of late Quaternary movement on the East Canyon fault.

4.5.3 The East Canyon fault

No fault scarps have been identified in unconsolidated deposits along the East Canyon fault; however, the steepness of the bedrock escarpment and the triangular facets south of East Canyon Dam suggest that late Quaternary displacements may have occurred on this portion of the fault. Therefore, we have divided the East Canyon fault into two segments: a southern, 10-km-long segment exhibiting evidence interpreted to indicate late Quaternary displacement; and a northern, 18 km-long segment consisting of two parallel traces that lack such evidence (fig. 4.11a).

4.5.3.1 Southern segment of the East Canyon fault

On figure 4.11a, south of East Canyon Dam, the East Canyon fault is mapped along a well defined air photo vegetation lineament at the base of the escarpment at the contact between the east-dipping Wasatch Formation in the footwall and the Norwood Tuff and overlying Huntsville fanglomerate in the hanging wall (Egbert, 1954; Bryant, written comm., 1983). This southern segment of the East Canyon fault is distinguished from the northern segment by the prominent of the vegetation linear associated with the fault, triangular facets developed on spurs in the footwall of the fault, and the preservation of a Pliocene(?) fanglomerate in the hanging wall of the fault. The facets reach a maximum height of about 300 m at the head of Monument Creek. South of this creek the facets diminish rapidly in height towards Big Mountain. In this area, the strike of the East Canyon fault turns to the west and its continuation is mapped as the Little Mountain reverse fault (Egbert, 1954; Bryant, written comm., 1983).

In the hanging wall of the southern segment of the fault the Norwood Tuff has an estimated thickness of 2000 m and has been rotated 20 -25° into the fault. It is overlain by a younger fanglomerate, less than 40 m thick, that is described by Egbert (1954, pp. 19-20) as loosely consolidated sub-rounded boulders, cobbles and pebbles in a matrix of reddish-orange sand. The lithology and position of this unit above the Norwood Tuff suggests correlation with the Pliocene? Huntsville fanglomerate in Morgan and Ogden Valleys, although lateral continuity can not be established. As can be seen on figure 4.11a this unit is preserved only adjacent to the East Canyon fault south of East Canyon Dam. We interpret this deposit to have been locally derived from the footwall of the fault in response to late Cenozoic displacement on the southern portion of the East Canyon fault as suggested by Egbert (1954).

Triangular facets on the footwall and the preservation of Norwood Tuff and Huntsville fanglomerate in the hanging wall distinguish this southern segment of the East Canyon fault from the northern segment discussed below. Although we have no direct evidence of the age of the youngest displacement on this segment of the fault, based on similarities with the Morgan fault in the age of hanging wall deposits and morphology of the escarpment, we infer that late Quaternary surface displacements have occurred on the East Canyon fault south of East Canyon Dam.

4.5.3.2 Northern segment of the East Canyon fault

The escarpment of the northern segment of the East Canyon fault north of the Dam lacks the facets developed on the southern segment, presenting an embayed appearance suggesting considerable erosion. The Echo Canyon Formation, a well-indurated conglomerate similar to the Wasatch Formation, forms the escarpment of this segment of the fault. On figure 4.11b two parallel traces of the East Canyon fault are mapped in the vicinity of East Canyon Dam. A western trace of the East Canyon fault is mapped striking parallel to East Canyon Dam, about 60 m (200 ft) upstream of the axis (fig. 4.11b). Exposures along State Highway 66 on the north side of the reservoir reveal steeply west-dipping conglomerates of the Echo Canyon Formation in the footwall faulted against lower-lying steeply southeast-dipping red-brown sandstones and siltstones of the Jurassic Preuss Formation. A chaotic zone of sheared siltstone and sandstone extends for 300 m (1000 ft) east of the contact with northeasterly striking reverse faults exposed in the roadcuts. When the reservoir level is low, outcrops of the sandstone and siltstone can also be traced along the south shore of the reservoir and up the first tributary to the south where they are overlain by mainstream gravels of East Canyon Creek (Qao on Fig. 4.11b).

North of the dam, the Preuss Formation can be traced about up Rocky Creek about 2 km to the point where the canyon turns northwest and breaches the escarpment in the Echo Canyon Formation (figs. 4.11a and 4.11b). Exposures in the canyon show that the fault contact between the Preuss Formation and the Echo Canyon Formation, overlain by 2-7 m of colluvium, is at least 100 m (300 ft) east of the base of the escarpment (fig. 4.11b), demonstrating that a period of escarpment retreat and colluvial deposition postdates displacement on the western trace of the East Canyon fault. In addition, about 500 m (1500 ft) south of that portion of Rocky Creek, a cutslope for a gas pipeline excavation crosses the western trace of the East Canyon fault (fig. 4.11b). Exposure is generally poor on this ravelled cut, but where near vertical cuts are preserved, a stage III-IV carbonate horizon is developed in the colluvium that overlies the fault. Age estimates and regional correlation of deposits with similar carbonate morphology (sec. 3.5.1) suggest that this soil formed over a period of at least 100 ka and probably 200 ka. Based on this evidence we conclude that the escarpment immediately north of the dam is primarily a fault-line scarp and that late Quaternary displacements have not occurred on the western trace of the East Canyon fault.

East of the outcrops of the Preuss Formation near the dam the Norwood Tuff is exposed dipping to the west at reservoir level and in roadcuts indicating the presence of an additional eastern trace of the East Canyon fault displacing the Norwood Tuff (fig. 4.11b), as inferred by Bryant (written comm., 1983). This eastern trace has no associated topographic escarpment. Pediment gravels are mapped by (Bryant, written comm., 1983) overlying the fault. On the basis of their relative elevation above East Canyon Creek, between erosional remnants thought to be >730 ka and alluvial fan remnants with an estimated age of about 140 ka (discussed below), these pediment gravels are probably at least several hundred thousand years old.

North of the dam, the escarpment lacks faceted spurs like those on the southern segment of the fault and the Norwood Tuff does not extend west to

the escarpment. Instead, resistant conglomerates mapped as Wasatch Formation by Bryant (written comm., 1983) and Mullens and Laraway (1964) are exposed east of the escarpment as east-dipping hogbacks (fig. 4.11a). If these beds are actually part of the Evanston or Echo Canyon Formations they may define the east limb of the ramp fold inferred by Royse (1983). As these beds apparently have not been rotated into the fault and the Norwood Tuff is thin or removed, we interpret the northern portion of the East Canyon fault as primarily a fault-line scarp exhumed by the removal of the conglomerates that overlie the less resistant beds of Preuss Formation (Mullens and Laraway, 1964) east of the escarpment.

4.5.4 Central Weber River Valley

We found no evidence of Quaternary displacement on faults in the central portion of the Weber River Valley east of the East Canyoin area (fig. 3.1). The Absoraka and related thrusts have been mapped at near right angles to the valley near Rockport Reservoir (Crittenden, 1974; Baclawski and others, 1984). A series of north-trending normal faults and thrust faults have been mapped near the Coalville anticline (Trexler, 1966; Baclawski and others, 1984) east of Coalville (fig. 4.1). The normal faults displace all Tertiary units but appear to be be related to the dissolution of salt in the underlying Preuss Formation (Baclawski and others, 1984). Bryant (written communication, 1983) has inferred a down-to-the-west normal fault trending up the valley from Wanship to Echo Reservoir. Terrace and fan remnants are too discontinuous in this part of the valley to provide datums with which to demonstrate no movement on these faults during the mid- or late Quaternary (sec. 3.5.1 and fig. 3.5). However, late Cenozoic fluvial dissection in this area has produced a topographically subdued landscape compared to many other areas in the eastern Wasatch Mountains; there are no steep, faceted escarpments, tilted erosion surfaces, or other evidence of Quaternary deformation between the East Canyon fault and Kamas Valley. Thus, both relative and absolute rates of uplift along this portion of the valley must be considerably less in most other areas of the eastern Wasatch Mountains (sec. 3.6).

4.5.5 Conclusions

Stratigraphic and geomorphic evidence support the conclusion that no late Quaternary displacement has occurred on the northern segment of the East Canyon fault. The northern segment consists of two parallel traces north of East Canyon Dam. The eastern trace is interpreted to be the youngest trace because it displaces the Norwood Tuff. We conclude that no late Quaternary surface displacements have occurred on this trace of the northern segment for no topographic escarpment is preserved, and pediment gravels with an estimated minimum age of 200 ka appear undisplaced across this fault. The western trace is near the base of the escarpment which lacks facets associated with late Quaternary faults in other back valleys. The Huntsville fanglomerate and the Norwood Tuff are not preserved in the hanging wall of this trace also suggesting that considerable erosion has occurred since the most recent displacement on this trace of the fault. In addition, colluvial deposits with an estimated age of at least 100 - 200 ka overlie this western trace of the northern segment of the fault near Rocky Creek. Therefore, we conclude that no late Quaternary surface displacements have occurred on either this western trace or the eastern trace of the 16 km long northern

segment of the East Canyon fault. We also conclude that there is no evidence for late Quaternary displacements on faults in the central portion of the Weber River Valley.

Based on presence of triangular facets, the preservation of the Huntsville fanglomerate, and by analogy with similar features associated with the Morgan fault (sec. 4.2), we infer that late Quaternary surface displacements may have occurred on the 10-km-long southern segment of the East Canyon fault south of East Canyon Dam. The late Quaternary fault length of the southern segment of East Canyon fault is 10 km, somewhat less than that of the Morgan fault.

Making an accurate assessment of the potential for surface faulting on the southern segment of the East Canyon fault is difficult. We have no trench or site-specific data with which to constrain the late Quaternary slip rate, single event size, or age of most recent displacement. Therefore, based on similarities in late Quaternary fault length and the escarpment morphology of this segment, we assume that slip rate and displacement parameters are similar to those calculated for the Morgan fault which are a Quaternary slip rate of 0.01 - 0.02 mm/yr and an average recurrence of surface displacements of 25 - 100 ka (sec. 4.2).

5. CENOZOIC FAULTING IN THE CENTRAL WASATCH MOUNTAINS

In this section we discuss faulting in back valleys of the central Wasatch Mountains east of Salt Lake City and west of the Uinta Mountains, bounded on the north and south by the leading edges of late Cretaceous and early Tertiary thrust faults.

5.1 Tectonic Setting

At the intersection of the north-trending Wasatch Range and the east-trending Uinta Arch in the central Wasatch Mountains, Mesozoic and Paleozoic sedimentary rocks are exposed between the surface traces of the Mount Raymond-Absoraka thrust on the north (sec. 4.1) and the Charleston thrust on the south (sec. 6.1). The east-west strikes of these thrusts define a reetrant in the thrust belt in the central Wasatch Mountains referred to by Beutner (1977) as the Uinta reentrant. He concludes that rocks exposed in the Uinta reentrant are paraautocthonous (displaced <10 km) in contrast to autochonous rocks exposed in the upper plates of the major thrust sheets to the north and south (displaced >50 km). He argues that the development of the Uinta reentrant, like the Southwestern Montana reentrant to the north, is a consequence of the interaction between the thrustbelt allocthon and geometric and stratigraphic irregularities of the craton margin. The Uinta reentrant coincides with the westward projection of the early Cenozoic Uinta Arch, an east-west trending, doubly plunging, north verging anticline (Hansen, 1983) exposing Precambrian sedimentary rocks in the core. Subseqently, this Uinta trend influenced sedimentation during the Paleozoic and localized mid-Tertiary igneous activity (Stewart and others, 1977). Based on the trends of the traces of folds in the allocthon that parallel the curving traces of the thrusts, and patterns of synorogenic and post-orogenic sedimentation, Beutner (1977) concludes that the Uinta reentrant is principally a structural reentrant rather than an erosional incursion into the leading edge of the Thrustbelt.

Various interpretations of the relationships between the thrusts north and south of the Uinta reentrant have been presented. Crittenden (1972a) suggests there is linkage between the Charleston and the Willard thrusts that is concealed west of the Uinta reentrant. However, Blackstone (1977) points out inconsistancies in this interpretation and suggests linkage between the Charleston and the Mount Raymond and Dry Canyon - Crandell Thrusts. These thrusts are inferred to be the westward continuation of the Absoraka thrust, although limited stratigraphic separation suggests that the Mt. Raymond thrust is a relatively minor fault (Crittendon, 1974; Lamerson, 1982). In the northern Wasatch Mountains, the Taylor and Ogden thrusts are exposed below the Willard thrust and involve crystalline basement. Crittenden (1972a) interpreted these as local faults, subsidiary to the Willard Thrust, but Blackstone (1977) Bruhn and Beck (1981) suggested they may be a part of the Absoraka system. Bruhn and others (1983) interpret a large anticline in rocks below the Willard thrust as evidence that basement rocks of the north central Wasatch Mountains are underlain by a detachment, as indicated in a cross section of Royse and others (1975). Bruhn and others (1983) also interpret the Uinta Mountains as an anticline developed above a sidewall ramp in the regional detachment and present a structural synthesis requiring that the Wasatch Mountains including the Uinta reentrant are underlain by a regional detachment at a depth of 10 to 20 km.

5.2 Tertiary igneous chronology of the central Wasatch Mountains

The late Eocene - early Oligocene Keetley volcanics are exposed in the eastern portion of the central Wasatch Mountains, masking the westward projection of the Uinta Arch and its intersection with the Wasatch Mountains. Bromfield and others (1970) and Bromfield and Crittenden (1971) have mapped andesite and rhyodacite flows, tuffs, volcanic breccias, and rhyodacite porphyries in the eastern portion of the Park City mining district. Woodfill (1972) in his petrographic and field study of the volcanic field further east describes volcanic breccias, flows, tuffs, lahars and intrusive rocks which range in composition from quartz latite to trachyandesite further east that are interpreted as forming by fractional crystalization of an andesitic parental magma.

A series of mid-Tertiary age calc-alkaline porphyry stocks intrude the Keetley volcanics and older rocks in the Park City Mining District and are aligned along the western projection of the Uinta axis (Stewart and others, 1977). Porphyritic and hypabyssal textures, strongly deformed host rocks, concordant intrusive contacts, and the lack of contact metamorphism indicate shallow emplacement levels (<5 km) for the eastern stocks in the Park City Mining District; discordant intrusive contacts, extensive diking, wider metamorphic aureoles, and equigranular textures indicate indicate deeper emplacement levels (>5km) for the western stocks, west of the Park City District (Woodfill, 1972; Lawton, 1980).

The Little Cottonwood stock is the largest and western-most of these stocks. A radiometric age of 24 - 31 ma for the Little Cottonwood stock based on fission track and K-Ar dates is supported by local geologic relations (Crittenden and others, 1973). Intrusive contacts with Precambrian quartzites and argillites of the Big Cottonwood formation are exposed along the north and east sides of the stock while the post-emplacement Wasatch fault and Deer Creek normal fault bound the western and southern margins respectively. About 8600 m of the Oquirrh formation in the upper plate of the Charleston thrust are exposed in fault contact on the southern margin of the stock along the younger Deer Creek normal fault. This thickness of allocthonous rocks overlying the stock after emplacement is consistent with mineralogical evidence for emplacement depths for the stock of 8-10 km (Lawton, 1980). The Alta and Clayton Peak stocks are exposed further to the east and are not in contact with the Little Cottonwood stock. Geologic relations indicate that the Alta stock intrudes the Clayton Peak stock which is consistent with the radiometric ages of emplacement of 37 - 41 ma for the Clayton Peak stock and 32 - 33 ma for the Alta stock (Crittenden and others, 1973). The Alta magma was intruded in two pulses into pre-Triassic rocks at a depth of about 6.3 km (Wilson,1961).

East of the Clayton Peak stock in the Park City Mining District Boutwell (1912) mapped a large composite porphyry pluton later shown to consist of at least 6 separate intrusions, the Ontario, Mayflower, Glencoe, Valeo, Flagstaff, and Pine Creek stocks (Bromfield and others, 1970). East of the Park City Mining District the sequence of volcaniclastic rocks and subordinate andesitic flows of the Keetley volcanics unconformably overly Paleozoic and Mesozoic sedimentary rocks and are intruded by the Park Premier stock and the Indian Hollow plug that probably mark source vents for at least some of the volcanics (Bromfield and others, 1977; Bromfield and Crittenden,

1971; Bromfield and others, 1970; Woodfill, 1972). Radiometric ages indicate a short history of overlapping igneous events spanning 5 Ma based on K-Ar biotite dates, or at most 10 Ma based on K-Ar horneblende dates, during the late Eocene and Oligocene (Crittenden and others, 1973; Bromfield and others, 1977).

5.3 Back Valleys of the central Wasatch Mountains

The upland surface of the central Wasatch Mountains is broken by a series of intermontane basins, generally smaller than the valleys in the northern and southern Wasatch Mountains. These valleys include Heber Valley, Kamas Valley, and Parleys Park that were originally described by Gilbert (1928), and Keetley Valley which also shares similar characteristics with other back valleys. These back valleys are similar to other back valleys in the northern and southern Wasatch Mountains in that some are bounded by normal faults that displace Oligocene rocks, although the margins of some of the valleys have been modified by fluvial erosion. This is shown by the mapping, drilling, trenching and geophysical studies, discussed below for each valley. However, in contrast to the northern and southern Wasatch Mountains, no late Quaternary faults have been identified in the central Wasatch Mountains.

5.4 Parleys Park and Richardsons Flat

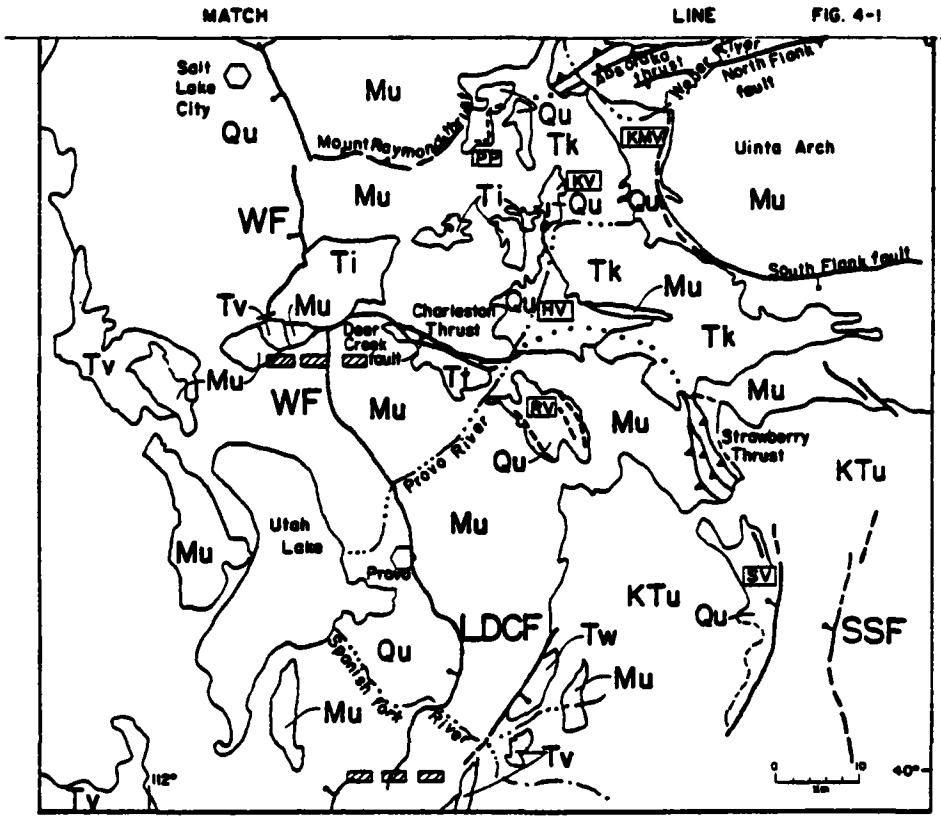
Parleys Park and Richardsons Flat are irregularly-shaped intermontane valleys at the west edge of the Keetley volcanic field north of Park City, Utah (fig. 5.2). Linear portions of some of the margins of these back valleys and gravel sequences more than 100 m thick within the valleys suggested that late Cenozoic and possibly late Quaternary faults were present within the valleys (Sullivan and Nelson, 1983).

5.4.1 Geologic setting

No Cenozoic normal faults are mapped in or near Parleys Park or Richardson Flat. The only fault mapped in the vicinity is the Mount Raymond thrust involving Mesozoic sedimentary rocks west of Parleys Park; to the east the Silver Creek member of the Keetley volcanics unconformably overlies Mesozoic sedimentary rocks (Bromfield and Crittenden, 1971; Crittenden and others, 1966). Unconsolidated gravel deposits (Ttg on fig. 5.2), described as consisting of boulders and cobbles equivalent to or derived from the Wasatch formation, are locally exposed above the Mesozoic rocks and below the Keetley volcanics on the margins of Parleys Park (Bromfield and Crittenden, 1971). The logs of two waterwells collared in the gravels shows that they are at least 90 m thick (fig. 5.2). Additional well logs in Parleys Park and the Silver Creek Basin show that unconsolidated gravel sequences vary in thickness from < 50 to > 200 m. Wells that penetrate the unconsolidated deposits all show that they overlie Mesozoic sedimentary rocks indicating that much of the sequence in Parleys Park is probably the Tertiary gravels mapped by Bromfield and Crittenden (1971) and Crittenden and others (1966). West of Parleys Park the northeast-trending Dutch Draw syncline and the Willow Draw anticline fold the trace of the Mount Raymond thrust (fig. 5.2). The well data on fig. 5.2 is limited but does suggest that the gravels in Parleys Park thicken on the northeastward projection of thie syncline. This suggests that most of the gravel sequence is the same age or older than the folding. Therefore, we conclude that most of the gravel sequence preserved in Parleys Park is of Tertiary age, rather than late Cenozoic alluvial fans deposited in fault-bounded basins as we had earlier suggested (Sullivan and Nelson, 1983).

5.4.2 Quaternary deposits

Alluvial deposits on the flat north of Park City and covering much of Parleys Park are nearly undissected by tributary drainages, suggesting a late Pleistocene (Pinedale) or younger age for the surficial deposits in the valley. Development indices for a soil on the terminal moraine of Ontario Ridge in the southern part of Park City (soil R-2, fig. 5.2, table 5.1) place the soil in RAG 4, but because this soil is on a narrow moraine crest it is probably eroded and therefore provides only a minimum age for the moraine. A similar weakly-developed soil on a moraine remnant surrounded by a large outwash fan in the southwestern corner of Parleys Park also falls in RAG 4 (soil R-1, fig. 5.2, table 5.1). The morphology and elevation of these moraines makes it clear that they and the large outwash fans into which they grade date from the Pinedale glaciation, probably the deglacial phases about 15-18 ka (sec. 3.4). The slope, morphology, and degree of dissection of the other fans on the west margins of these valleys is similar to that of the outwash fans (except in the northwest corner of Parleys Park) suggesting they



EXPLANATION

Qu — Quaternary undivided
Tw — Middle or late Tertiary Wanrhodes volcanics
Tt — Middle Tertiary Tibble Formation
Tk — Middle Tertiary Keetley volcanics
Ti — Middle Tertiary intrusives
Tv — Tertiary igneous rocks, undivided
KTu — Cretaceous and Early Tertiary sedimentary rocks, undivided
Mu — Jurrasic and older sedimentary rocks, undivided
▭ — Back valleys: PP = Parleys Park, KMV= Kamas Valley, KV=Keetley Valley, HV= Heber Valley, RV=Round Valley, SV=Strawberry Valley
— — Cenozoic normal faults, dashed where inferred: SSF=Stinking Springs fault, LDCF = Little Diamond Creek fault, WF = Wasatch fault, for relative ages see Plate 1b
▨ — Wasatch fault segment boundaries (Schwartz and Coppersmith, 1984)
▾▾ — Thrust faults, dotted where concealed

Figure 5.1 Geologic map of the central Wasatch Mountains.

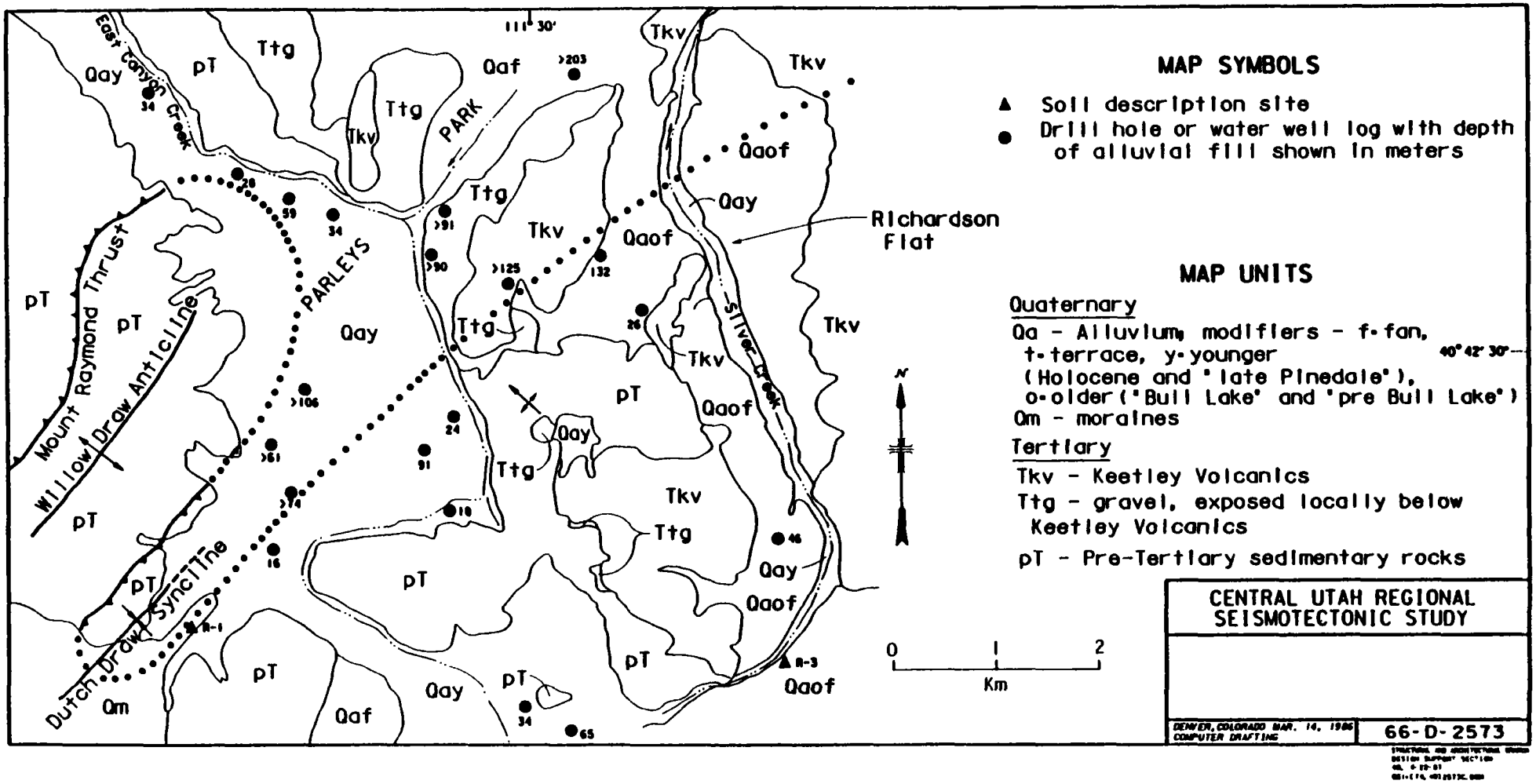


Figure 5.2 Geologic map of Parleys Park.

TABLE 5.1 Selected properties of soils on terraces and moraines in the Park City - Richardson Flat area, north central Utah.

Profile	Horizon*	Average depth (cm)	Parent material	Munsell dry color	ESTIMATED PERCENT BY VOLUME Pebbles (0.2-8cm)	Cobbles (8-25cm)	Boulders (>25cm)	PERCENT BY WEIGHT~ Sand (2-0.5mm)	Silt (50-2um)	Clay (<2um)	Percent** organic matter	Percent# carbonate
R-1	A1	0 40	loess	7.5 YR 4/3	3	0	0	34	46	20	6.7	0.3
	A2	40 55	till	7.5 YR 4/3	3	10	0	34	46	20	5.7	0.3
	Bw	55 87	till	5 YR 5/4	3	3	0	54	31	15	0.5	0.0
	C	87 115+	till	5 YR 4/6	3	3	0	58	27	14	0.6	0.2
R-2	A	0 13	till	10 YR 3/2	20	5	0	35	45	20	6.2	0.0
	BE	13 30	till	10 YR 7/4	30	15	0	40	43	17	4.0	0.0
	C/Bw	30 60	till	10 YR 7/4	30	15	0	41	35	24	2.4	0.0
	C	60 90+	till	10 YR 7/3	30	20	0	59	28	13	1.0	0.0
R-3	A1	0 7	loess	7.5 YR 4/3	10	0	0	29	48	23	3.0	0.0
	A2	7 20	loess	7.5 YR 4/3	10	0	0	31	48	21	2.2	0.0
	BA	20 38	loess	7.5 YR 6/4	10	0	0	31	47	22	1.3	0.0
	Bt	38 52	loess	7.5 YR 6/4	10	0	0	28	41	31	0.8	0.0
	2Bt	52 98	fluvial gravels	5 YR 6/6	60	2	0	57	23	21	0.6	0.0
	2BC	98 175	fluvial gravels	7.5 YR 6/6	50	10	0	67	20	14	0.3	0.0
	2Cox	175 280+	fluvial gravels	7.5 YR 6/6	40	20	0	69	18	14	0.2	0.0

* Horizon nomenclature of Guthrie and Witty (1982) and Birkeland (1984) except that master K horizon is not used.

~ Particle size distribution of <2 mm fraction using sieve-pipette methods (for example, Carver, 1971) and a Sedigraph for some silt-clay fractions with prior removal of carbonates and organic matter using methods of Jackson (1956).

Percent organic matter by method of Walkley and Black (1934).

** Percent carbonate by method of Allison and Moodie (1965, p. 1387).

do not greatly predate the outwash fans. Other shallow cuts in the flat north of Park City and in Parleys Park south of Interstate 80 expose alluvium and loess with similar late Pinedale (RAG 3) and Holocene soils with cambic and very weak argillic horizons.

The valley floor deposits in Richardson Flat and the northeastern part of Parleys Park are more deeply dissected than those in valleys to the south and west and a single soil also suggests that they are older. Soil R-3 (table 5.1) has development indices which place it in RAG 2 (fig. 3.6), but total secondary clay (6 g/cm2) suggests an age of roughly 73 ka. The soil is developed in a gravelly alluvial terrace 8 m above the main channel of Silver Creek which drains the outwash-floored flat north of Park City. The dissected alluvial fan deposits which floor much of Richardson's Flat are about 4 m higher than the terrace. The soil on the terrace is clearly older than the main advance of Pinedale glaciers (18-25 ka). If the terrace is part of a pre-25-ka outwash valley train, like that produced by Pinedale deglaciation, it is most likely correlative with the Bull Lake glaciation (130-150 ka, sec. 3.4). However, total clay values suggest it might correlate with an earliest Pinedale glacial event identified by Colman and Pierce (1981) at about 60-70 ka. If the terrace is unrelated to glaciation it could date from 50-150 ka. The significance of this soil is that it shows that the fan deposits above it are at least this old. Based on the degree of dissection of these fans here and in most of Parleys Park, the surfaces of these fans in most areas may be >200 ka.

5.4.3 Age of faulting

Although parts of the valley floors are covered by late Quaternary deposits, the bulk of the gravel sequence filling Parleys Park and Richardsons Flat is probably of Tertiary age, suggesting that any concealed faults on the margins of these valleys are probably also of Tertiary age. However, at some time before the middle Quaternary the drainage pattern apparently was disrupted by displacement on short normal faults. The present drainage pattern and the slope of paleovalleys and remnants of erosion surfaces show that this area was once a moderately-eroded (described as "subdued" by Eardley, 1944) fluvial terrain that sloped gently to the northeast toward the Weber River (sec. 3.6). We can not be certain whether the margins of these flats are fault-controlled or whether they are partly or entirely stream cut. All of the margins of Richardson Flat and the northern and western margins of Parleys Park have embayments eroded into them and mountain-front facets are either lacking or very eroded. This also suggests that faults, if present, are Tertiary in age. However, the 2-3 km-long, linear eastern and southern margins of Parleys Park north of Park City form steep dipslopes in the Jurrasic Nugget sandstone that meet at right angles (Crittenden and others, 1966). This morphology suggests Quaternary faults may be present here, for these features are difficult to attribute to fluvial erosion.

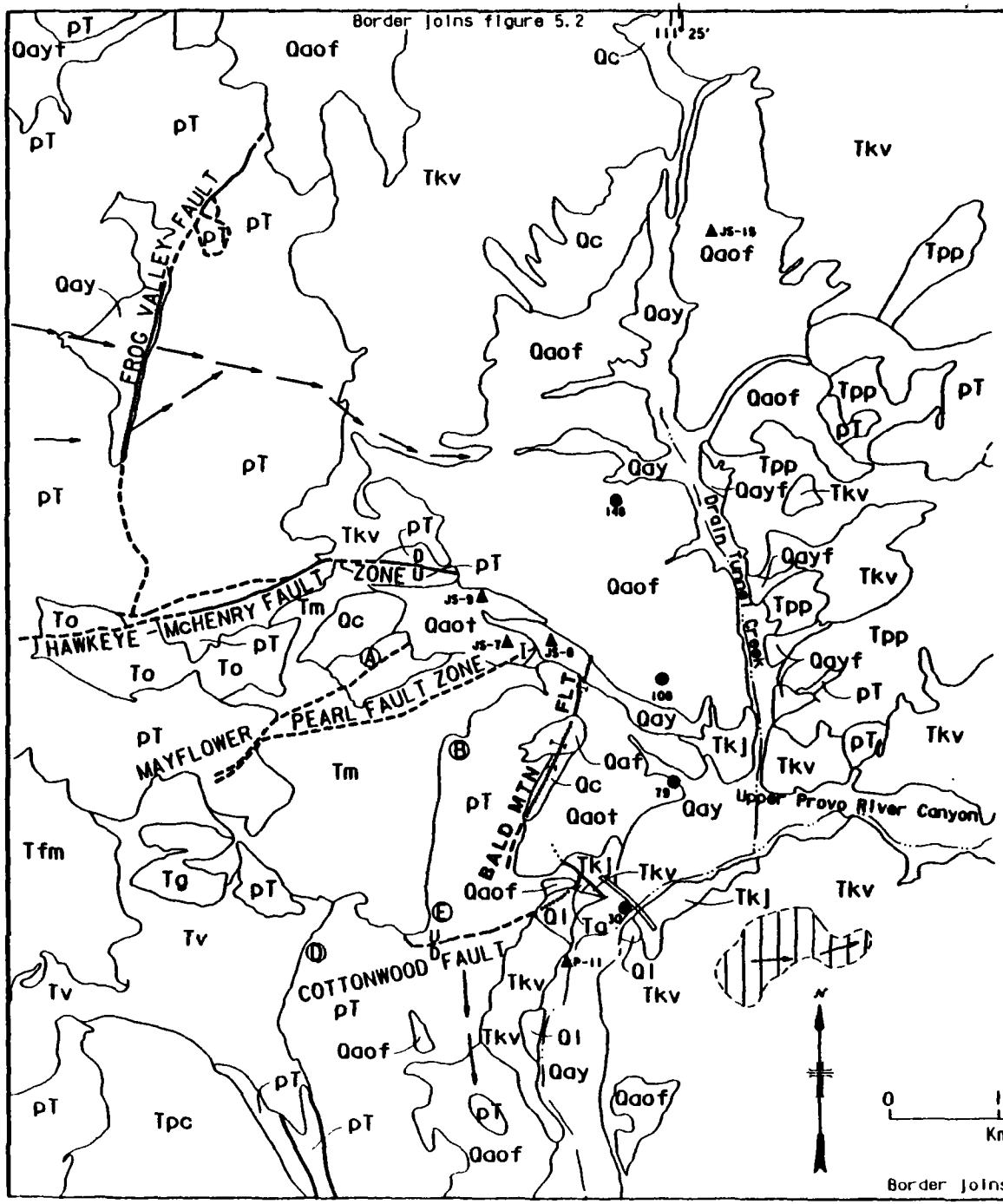
Although no fault scarps in unconsolidated deposits were found in the area, we conclude that some margins of Parleys Park may be bounded by short normal faults with Quaternary displacement. However, we find no evidence for late Quaternary displacement on these faults.

5.5 Deer Valley

Deer Valley is a small closed basin about 1.5 km long and 0.5 km wide in the southwestern portion of the Park City East Quadrangle immediately east of Park City, Utah (fig. 5.3). The north-northeast-trending basin is bounded on the east by a linear, steep, 120 m-high escarpment in the Park City Formation. The Frog Valley thrust fault, known from mine mapping south of Deer Valley caps a hill immediately northeast of the valley, and is mapped at the base of the escarpment (Bromfield and Crittenden, 1971; fig. 5.3). Four v-shaped stream valleys appear to be truncated by the west-facing escarpment suggesting the possibility that Quaternary displacement has disrupted these drainages (Sullivan and Nelson, 1983). These valleys formerly drained the east side of the Park City Mining district and transported most of the basin fill deposits into Keetley Valley (fig. 5.3).

Holocene marsh sediments are found in much of the center of Deer Valley, but exposures in fine-grained colluvium at the base of the escarpment show cumulic soils with 1-1.5-m-thick argillic horizons over stage II carbonate. The valleys to the west and north received much outwash during Pinedale glaciation, but the Deer Valley drainage basin is unglaciated. Thus, comparison of the soils in the alluvium and colluvium around the margins of the valley with other soils in the regional study area (sec. 3.4) suggests sediments on the valley margins are certainly >50 ka and probably >100 ka. No fault scarps were found in these deposits in Deer Valley, although if scarps were formed at the base of the escarpment they could have been eroded in a few thousand years.

The presence of mid-Tertiary age gravels in Parleys Park to the north and Keetley valley to the east suggests that Deer Valley may formerly have been filled with mid-Tertiary age gravels. The lower portions of the basin fill in Keetley valley downstream from the escarpment are inferred to be of mid-Tertiary age (Sec. 5.6). Therefore, east-flowing drainages supplying this sediment must also initially be of mid-Tertiary age. This drainage system may have been initially disrupted by Tertiary displacement on the Frog Valley fault. However, the morphology of the escarpment and the mid-Quaternary age of the upper portion of the unconsolidated deposits in Keetley Valley suggest Quaternary displacements have occurred on this 1.5 km long escarpment although there is no evidence of late Quaternary displacements.



MAP SYMBOLS

- Paleo channel flow direction
- Landform boundaries and drainage divides
- Exploratory trench
- o Outcrop or sampling site
- ▲ Soil description site
- ● Drill hole or water well log with depth of alluvial fill shown in meters
- ■ Paleomagnetic sampling site
- U/D Faults, dashed where inferred, dotted where concealed
- Erosion surface
- Jordanelle damsite

MAP UNITS

Quaternary

Qa - Alluvium, modifiers - f-fan, t-terrace, y-younger (Holocene and late Pinedale), o-older (pre-Bull Lake)
Qc - Colluvium
Ql - Landslides

Tertiary

Tm - Mayflower stock
Tpc - Pine Creek stock
To - Ontario stock
Tpp - Park Premier stock
Tkj - Jordanelle stock
Tv - Valeo stock
Tfm - Flag stock
Tg - Glencoe stock
Ta - Alluvial and colluvial deposits
Tkv - Tertiary Keetley Volcanics

pT - Pre-Tertiary sedimentary rocks

Figure 5.3 Geologic map of Keetley Valley.

DENVER, COLORADO MAR. 4, 1986 COMPUTER DRAFTING

66-D-2581

5.6 Keetley Valley

Keetley Valley is a north- and northeast- trending topographic basin about 7 km long and 2-3 km wide in the eastern portion of the Park City Mining District (fig. 5.3). The proposed Jordanelle Dam on the Provo River will be located at the south end of the valley. For detailed maps and a more detailed report of investigations in Keetley Valley refer to USBR (1986) and Sullivan and others (1986).

The most recent phase of major drainage adjustments in the central Wasatch Mountains was the capture of the upper Provo River in Kamas Valley by headward erosion up the upper Provo River canyon < 150 ka (sec 3.5.2). The subsequent dramatic increase in discharge must have resulted in accelerated erosion of the mainstream channel and its tributaries. Tributaries to the Provo River that drain the margins of Keetley Valley, including McHenry Creek and Drain Tunnel Creek, have incised about 100 m into the unconsolidated deposits in the valley giving the valley a dissected basin morphology unlike that of other adjacent valleys (Parleys, Richardsons, Heber, Kamas) that lack Provo River tributaries.

5.6.1 Geologic Setting

Keetley Valley is located at the intersection of the eastward projection of the Uinta Arch and the north-trending Wasatch Mountains. West of Keetley valley both published quadrangle maps and proprietary Mine maps (Jordanelle Task Force, 1982) provided by the Park City Mining District document a pervasive pattern of east- and northeast-trending faults in Mesozoic and older sedimentary rocks and, to a lesser extent, in Oligocene intrusive and volcaniclastic rocks. The stocks near the west margin of the valley are the previously mapped Mayflower and Ontario stocks (Bromfield and others, 1970; Bromfield and Crittenden, 1971), and the Jordanelle stock defined by drilling and geophysical studies for Jordanelle damsite (Tkj of Bromfield and others, 1970). The principal mapped faults are the east and northeast trending Hawkeye-McHenry, Mayflower-Pearl, and Cottonwood faults (fig. 5.3).

5.6.1.1 Hawkeye-McHenry fault zone

On the Park City East (Bromfield and Crittenden, 1971) and Heber (Bromfield and others, 1970) Quadrangles the east-trending Hawkeye-McHenry fault zone (fig. 5.3) extends from the east limb of the Park City anticline east to the margin of Keetley Valley where its continuation is concealed by alluvial fill. Triassic sedimentary rocks and the overlying Keetly volcanics on the north are faulted against the Pennsylvanian Weber quartzite on the south. At its west end the fault is inferred to displace the Ontario stock, although mapping indicates only limited displacement of the margin of the stock, suggesting the faulting largely predates the stock. Large ore-bodies are localized along the fault zone (Bromfield, 1968). Mine maps show that the fault zone is complex, consisting of footwall and hanging wall strands that are hundreds of meters apart with an average dip of 45° to the north and stratigraphic displacement of at least 300 m (1000 ft) (Bromfield, 1968). Mine geologists and a USBR consultants map of the proposed reservoir (Bridges,1984) infer that the fault continues with a southeast trend across the valley.

Alternatively, the Hawkeye-McHenry fault has been modelled in resistivity traverses in Keetley Valley and has been interpeted to turn and strike south along the southwest margin of the valley (Meiiji, 1980). Neither of these interpretations of the trend of an eastward extension of the Hawkeye-Mchenry fault zone have been confirmed due, in large part, to the thick alluvial fill masking the projection of the fault. Based on reservoir drilling and aeromagnetic data (Fox, 1984) the Jordanelle stock is interpreted to underlie the southern portion of Keetley Valley and may extend as far north as the projection of the Hawkeye-McHenry fault zone. If so, and if the stock is contemporaneous with or youger than the Ontario stock then the fault may not continue beneath the alluvial fill in Keetley Valley.

5.6.1.2 Mayflower-Pearl fault zone

On the Heber quadrangle (Bromfield and others, 1970) south of the Hawkeye-McHenry fault (fig. 5.3) a north-east-trending zone of inferred faults has been mapped near Glencoe Canyon west of Keetley Valley. Mine tunnel map along the northeast-trending Pearl Vein and Mayflower Zone depict pervasive fracturing within the Mayflower stock and the host rocks (Jordanelle Task Force, 1982). Apparent left-lateral offset of about 1000 m of the Weber Quartzite-Round Valley Limestone contact suggests that substantial displacement has occurred on the fault zone. As the west margin of the Mayflower stock is not offset (Bromfield and others, 1970) most of the displacement must predate or be related to the intrusion of the stock (fig. 5.3). Mine maps of the Cunningham Tunnel (Jordanelle Task Force, 1982, pl. A) indicate northeast-striking shears in unconsolidated deposits near the tunnel portal that are inferred to be related to this fault zone. Detailed mapping and trenching on the surface projection of these features (fig. 5.3) show there has been no displacement in overlying late Quaternary (>125 ka) alluvial deposits (Sullivan and others, 1986).

5.6.1.3 Cottonwood fault

On the Heber quadrangle (Bromfield and others, 1970) this east- and north-east trending fault is shown as extending from the south margin of the Mayflower stock east and then northeast above the proposed Jordanelle damsite where its continuation is concealed by older alluvium. Apparent lateral offset of the Weber Quartzite-Park City Formation contact of about 1000 m (3000 ft) again suggests substantial displacement. The fault juxtaposes overturned Triassic Woodside and Thaynes formations in the footwall on the south and Weber Quartzite and Park City Formation in the hanging wall to the north. The overturning of footwall beds, the relative eastward displacement of beds in the hanging wall and the presence of the Mayflower stock in the hanging wall suggest that the fault formed during emplacement of the Mayflower stock (Bromfield, 1968; Bromfield and others, 1977). Stokes and Madsen (1961) depict the fault as extending to the east side of Keetley Valley, although Hintze (1980) shows the fault only on the southwest side of the valley.

USBR mapping combined with drilling data and an analysis of aeromagnetic data have led to the interpretation that the andesite porphyry exposed at Jordanelle is a hypabyssal intrusive (USBR, 1986) as suggested by Woodfill (1972). These findings update previous interpretations of an extrusive origin for this rhyodacite porphyry (Tkj, of Bromfield and others, 1970).

USBR investigations at the proposed Jordanelle damsite have confirmed that the Cottonwood fault is a reverse fault and drilling has shown that it places the locally overturned Triassic Woodside Shale and slivers of Thaynes formation over the Keetley volcanics on the slope south of the Jordanelle stock. In exposures near Jordanelle damsite, north and north-trending normal and reverse faults displace Tertiary unconsolidated deposits. These faults are truncated by, or merge with, the sheared margin of the Jordanelle stock. These north-trending faults, the Cottonwood fault, and other shear zones on the margins and within the Jordanelle stock are interpreted to have formed nearly contemporaneously with the emplacement of the Mayflower and Jordanelle stocks (USBR, 1986).

Radiometric dating indicate a mid-Tertiary age for emplacement of the Jordanelle and Mayflower stocks. Four radiomteric dates ranging from 36 to 40 Ma were obtained from three unweathered drill core samples from depths ranging from 60 to 132 m within the Jordanelle stock (table 5.2). These dates and a published radiometric date on the Mayflower stock indicate nearly contemporaneous emplacement of the stocks (table 5.2).

Table 5.2 K-Ar dates for intrusives near Jordanelle

Intrusive	Mineral (sample #)	Age (Ma)
Mayflower	Hornblende	41.2 +/- 1.6 *
Jordanelle	Biotite (A-7482)	36.5 +/- 1.8
	Biotite (A-7481)	36.3 +/- 1.8
	Biotite (B-7480)	40.0 +/- 1.6
	Hornblende (A-7480)	38.5 +/- 1.9

* Bromfield and others (1977)

5.6.2 Tertiary clastic deposits

Unconsolidated early Tertiary-age deposits of silt, clay, and gravel about 100 m thick underlie breccia of the Silver Creek member of the Keetley volcanics in Parleys Park and on the margins of Mountain Meadows a few kilometers north and east of Keetley Valley (Ttg of Bromfield and Crittenden, 1971). These deposits are locally exposed and unconformably overlie deformed Mesozoic and Paleozoic sedimentary rocks. Crittenden and others (1966) suggest that these gravels are derived from the Eocene Wasatch Formation and that they are in part younger, in part older and in part contemporaneous with the Keetley volcanics, indicating that they are of early Tertiary age.

At the south end of the valley trench exposures near the right abutment of the proposed dam show that unconsolidated deposits are intruded by andesite porphyry of the Jordanelle stock (USBR, 1986, Appendix B). Radiometric ages of 36 - 40 Ma (table 5.2) provide a minimum age for these unconsolidated deposits. They are overlain by Quaternary older alluvial deposits (Qao of Bromfield and others, 1970; Qaof on fig. 5.3). Clasts of quartzite within the andesite porphyry at the base of the unconsolidated deposits at a depth of 79 m in a drill hole further north in Keetley valley (fig. 5.3) suggest

that the Jordanelle stock has intruded unconsolidated deposits in the valley (USBR, 1986). These relationships suggest that at least the lower portion of the basin fill in Keetley Valley is of mid-Tertiary age.

5.6.3 Quaternary deposits

The Quaternary deposits in Keetley Valley mapped on fig. 5.3 include: (1) alluvium consisting of interbedded gravelly clay, sandy gravel, and sandy clay which comprise the upper portion of the more than 150 m of unconsolidated deposits in the valley (Qaof); (2) coarse alluvial gravel which overlies the basin-fill deposits near McHenry Canyon (Qaot); (3) alluvial and colluvial gravels and silty clays derived from these older deposits and from bedrock which mantle the basin fill deposits around the margins of the Valley (Qaf and Qayf); and, (4) overbank alluvium deposited by Ross Creek and the Provo River (Qay).

The oldest unconsolidated deposits in Keetley Valley are the basin-fill alluvium (Qaof), consisting of interbedded gravels, sands, and gravelly clays that are found in drill holes, trenches, soil pits, and natural and man-made exposures throughout the proposed reservoir area. Several independent lines of evidence, including paleomagnetism, tephrostratigraphy, aminostratigraphy, and soil relative age dating, indicate that the upper portion (about 3 m) of the older basin fill, exposed in the shallow excavations on the surface is of pre-middle Pleistocene age (>500 ka) (Sullivan and others, 1986). The lower portion of the older basin fill in the reservoir, accessible only through drill cores, is similar in appearance to the exposed deposits. Paleomagnetic evidence suggests that these sediments are older than 730 ka and there is evidence in one drill core for interbedding of the basin fill deposits with Oligocene volcanic rocks indicating that the lowest part of the basin fill deposits is mid-Tertiary in age.

At the northeast margin of Keetley Valley are coarse alluvial gravels up to about 3 m thick (Pa) that were deposited in fans across the surface of the basin fill deposits (Pao). These deposits consist of partially grussified subrounded gravels derived from Keetley volcanics exposed in the highlands to the east. The age of these alluvial fan gravels can be estimated from their stratigraphic position above the basin fill deposits containing the Lava Creek B ash (620 ka) in soil pit JS-15 and the relative degree of soil profile development on their surface. The soil is similar to soils in other back valleys designated as relative age group 2 inferred to date to about 140 ka (Sullivan and others, 1986). Similar gravels with strongly developed soil profiles are found overlying basin fill deposits at the mouth of McHenry Canyon (soil pits JS-7,9) about 35 m above the present base level.

Over much of the proposed reservoir area the only younger units which are geomorphically distinct from the basin fill deposits are late Pleistocene alluvial deposits that are inset into the basin fill where drainages have incised it about 20 to 40 m (Qay). These deposits exhibit a similar degree of weathering and soil development (soil pit JS-8) to latest Pleistocene soils of RAG 3 in other back valleys and are therefore inferred to date to about 15-18 ka (Sullivan and others, 1986).

5.6.4 Faulting Keetley Valley

Late Cenozoic and Late Quaternary normal faults have been identified in back valleys of the Wasatch Mountains both to the north and south of Keetley Valley. These faults have been exposed or inferred at or near the valley margins. The morphology of Keetley Valley suggested that north to northeast-trending normal faults may also present in this back valley. In the first part of this section we summarize the results of trench investigations and drilling that have confirmed that a previously unrecognized fault is present along the southwestern margin of the valley. In the second part of this section we report the conclusions from a program of seismic refraction profiling undertaken to determine whether other normal faults of similar trend were present within the southern portion of the valley (Sullivan and others, 1986). This program served to map the bedrock surface below the unconsolidated deposits in the valley which provides constraints on the existence and location of faults displacing this surface.

5.6.4.1 Bald Mountain fault

On the southwest margin of the valley northeast-striking, east-dipping Paleozoic rocks form a 3-km-long escarpment near the east margin of the Mayflower stock (fig. 5.3). Although more eroded, this escarpment is similar to those in other back valleys, suggesting that a normal fault was present at the base of the escarpment. Two trenches, described in Sullivan and others (1986), expose a northeast-trending fault between the Paleozoic rocks and Oligocene igneous rocks at the base of the escarpment (fig. 5.3). Alluvial fan deposits 10 to 15 ft thick overlie the igneous rocks exposed in both of the trenches. A fault contact between Paleozoic rocks and igneous rocks is exposed in each of the trenches at the base of the escarpment. In each of the trenches the fault strikes N20°E and an angle drill hole through the fault plane established that this is a steeply east-dipping normal fault juxtaposing Weber Quartzite in the footwall and Oligocene igneous rocks in the hanging wall (Sullivan and others, 1986).

In each trench a wedge of colluvial deposits about 3 m thick overlies the fault. An erosional contact between the colluvial deposits and the Weber quartzite above the fault contact indicates that the colluvial deposits have not been displaced. These deposits have an estimated age of a few tens of thousands of years based on the preservation of a cambic B-horizon in one of the trenches, allowing us to preclude surface displacement during this period. However, the results of trenching in Morgan Valley and in southern Cache Valley suggest that this is about the recurrence interval of surface displacements on some late Quaternary normal faults in the back valleys.

In an embayment in the escarpment between these trench sites, alluvial fan deposits (Qaf) overlie the projection of the fault. Drilling within the alluvial fan further constrained the position of this fault to within a distance of about 30 m, and a trench across the projection of the fault exposed undisplaced alluvial fan deposits (Sullivan and others, 1986). A relic B-horizon with an estimated age of at least 125 ka is exposed over most of the trench showing that there has been no displacement on this fault in at least that period of time.

5.6.4.2 Other north-trending faults

To further investigate the structure of Keetley Valley a staged seismic refraction program was conducted in the southern portion of the valley to map the top of bedrock below the basin fill (Sullivan and others, 1986). The partial cross sections of Keetly Valley provided by the refraction lines confirm the general basin shape of the valley. On some of the lines relatively steep gradients of the bedrock-basin fill refractor are apparent. Based on association with these steep gradients, we have confirmed the projection of Bald Mountain fault exposed at the base of the escarpment on the southwest margin of the valley. and inferred the location of an additional fault that appears to displace the lower portion of the basin fill deposits. No scarp is present on the surface projection of this fault in the older fan deposits suggesting that there also has been no surface displacement on this fault in at least the last 100 ka.

A 100 m deep northeast-trending trough of basin fill extends south below the Provo River floodplain toward Jordanelle. The trough is well-defined on an east-west oriented refraction line where its location and depth below the floodplain have been confirmed by drilling (Sullivan and others, 1986). Additional lines confirm its northeast trend. We had inferred possible fault control on this trough to explain its presence (Sullivan and Nelson, 1983). Although no scarps are present within the valley above any projection of this fault, a series of trenches were excavated in the upper portion of the basin fill deposits (>730 ka) above the projection of the margins of the trough (Sullivan and others, 1986). These trenches establish that there has been no late Quaternary displacement on faults that may bound steep west side of this trough.

Trench exposures demonstrating that the Jordanelle stock intrudes unconsolidated deposits suggest that this trough may not be fault controlled, but that it may represent the upper surface of the Jordanelle stock.

5.6.5 Conclusions

East and northeast-trending faults mapped on the margins of Keetley valley are interpreted as having formed nearly contemporaneously with the emplacement of mid-Tertiary stocks. These faults share few of the morphologic characteristics of late Cenozoic faults in other back valleys of the Wasatch Mountains and they do not displace late Quaternary deposits.

The deposition of >150 m of mid-Quaternary to mid-Tertiary age basin fill sediments suggests a history of Cenozoic subsidence on concealed northtrending normal faults as in the other back valleys of the Wasatch Mountains. One such fault, the Bald Mountain fault, was identified on the southwest margin of the valley. Trenching and mapping have shown that it does not displace alluvial fan deposits with an estimated age of >125 ka. Other concealed faults, inferred from seismic profiles and drilling, may be related to Cenozoic subsidence of the valley. Detailed mapping has reveled no scarps in older alluvial fan deposits (> 125 ka) on the surface projection of these faults.

Although Quaternary displacements on these and other faults in Keetley Valley can not be precluded, direct evidence from trenching, together with the lack

of scarps and the subdued morphology of the valley margins indicates that no late Quaternary displacements have occurred in Keetley Valley.

5.7 Browns Canyon-Mountain Meadows

The nearly flat-lying flows and breccias of the Keetly Volcanics are exposed in the West Hills between Kamas Valley and Keetley Valley. Erosion along Lost Creek and Browns Canyon has exposed the contact between the Breccia of Spring Creek and the underlying Tuffs North and East of Mountain Meadows, and locally exposed Mesozoic sedimentary rocks and Tertiary-age gravels that underlie the volcanics (Bromfield and Crittenden, 1971). No Tertiary gravels intervene between the volcanics and the Mesozoic sedimentary rocks on the south side of Mountain Meadows. Only a thin veneer of Quaternary colluvial deposits overlies the Keetley volcanics within Mountain Meadows.

5.7.1 Mountain Meadows scarps

A 4 km-long series of linear, northeast-trending scarps parallel State Highway 196 along the southeastern margin of Mountain Meadow (fig. 5.4). These scarps vary in height from 2 to 8 m with slope angles of 10 - 20°, but they are as steep as 25° where small slumps on the face of the scarp have increased the slopes. The scarps in part follow the fault contact between the Tuff of Spring Creek and the Tuffs of Mountain Meadows on on the southeast margin of Mountain Meadows (Bromfield and Crittenden 1971). Gully exposures at various locations above and below the scarps show volcanics at shallow depths, overlain by only a thin veneer of regolith and colluvium. Two main tributaries of Lost Creek that head above the scarps have incised 10 - 20 m into the bedrock. The tributaries been filled with fine-grained alluvium composed principlly of dark brown organic matter with an exposed thickness of up to 3 m. The scarps end at the margins of these drainages and do not continue into the alluvial fill.

5.7.2 Trenching of the Mountain Meadows scarps

In order to assess the origin of the Mountain Meadows scarps a backhoe trench was excavated across a scarp about 20 m west of a drainage that breaches the scarp (fig. 5.4). At the trenchsite the scarp is 4.5 m high with a scarp angle of 20°.

The trench exposes a fault between the Mountain Meadows Member and the older Silver Creek Member of the Keetley volcanics with a sense of displacement opposite to that of the scarp (Bromfield and Crittenden, 1971). From station 34 to station 30 the trench exposes extremely hard, barely rippable, grey volcanic breccia of the Silver Creek member (unit 7) below a thin veneer of loess and colluvium. At station 30 a vertical fault juxtaposes this unit 7 and the deeply weathered and decomposed buff-colored tuffs and breccias of the Mountain Meadows Member (units 2-6) that dip about 30° to the northeast. At about station 24 a near vertical, 0.15-m-wide seam of clay is interpreted to be part of a 1.0 m wide fault zone displacing the southeast-dipping sequence of volcanic tuffs. This fault is overlain by unit 1a consisting of 0.15 to 1.0 m of organic material and occassional cobbles in a matrix of loess, and by unit 1b, a locally preserved zone of clay accumulation. The clay unit has a maximum thickness of 0.6 m and is interpreted to be a B horizon > 100 ka. Numerous near-vertical,iron-stained joints occur in the volcanic rocks; in some cases they are filled with clay but they are overlain by the loess and colluvium.

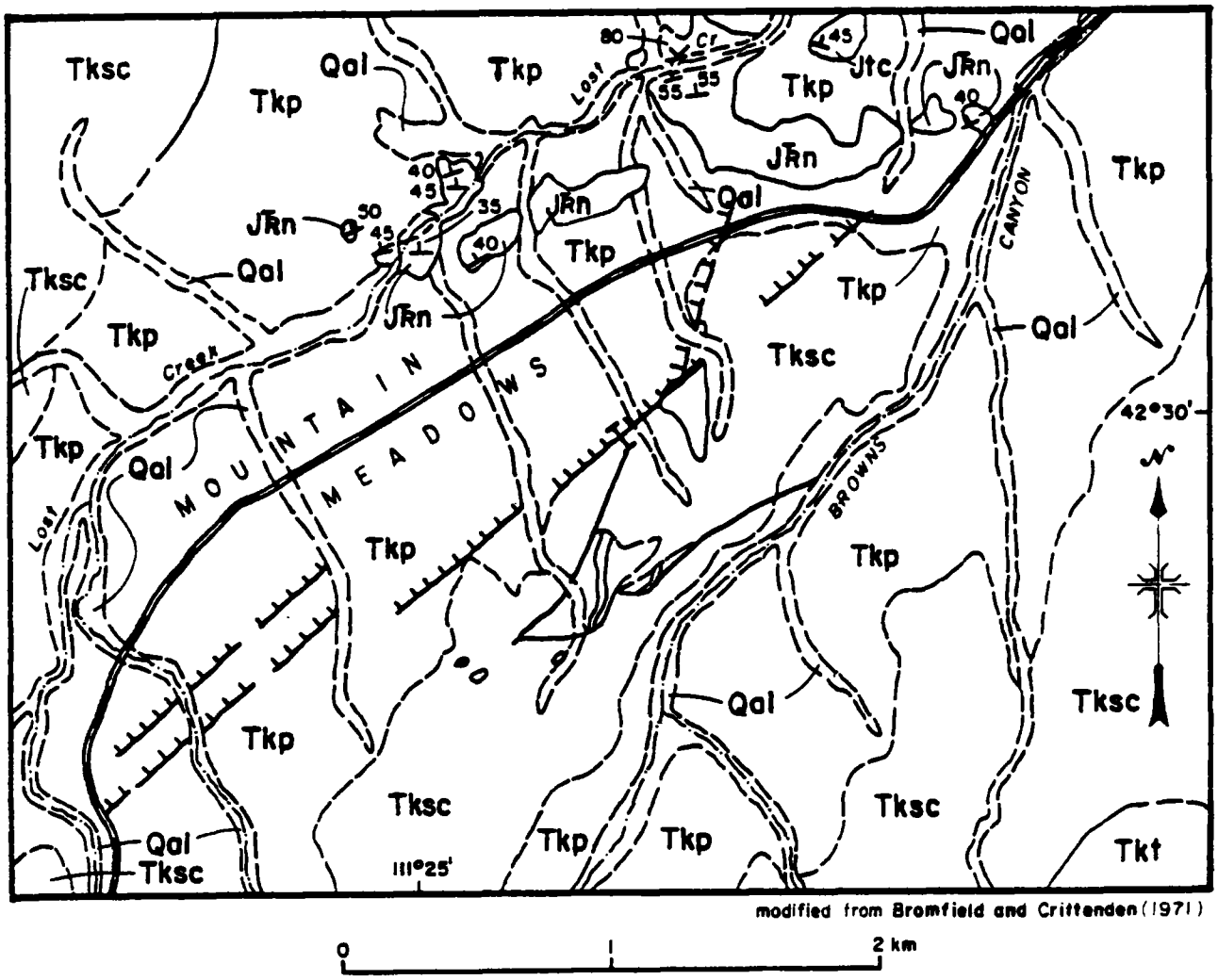
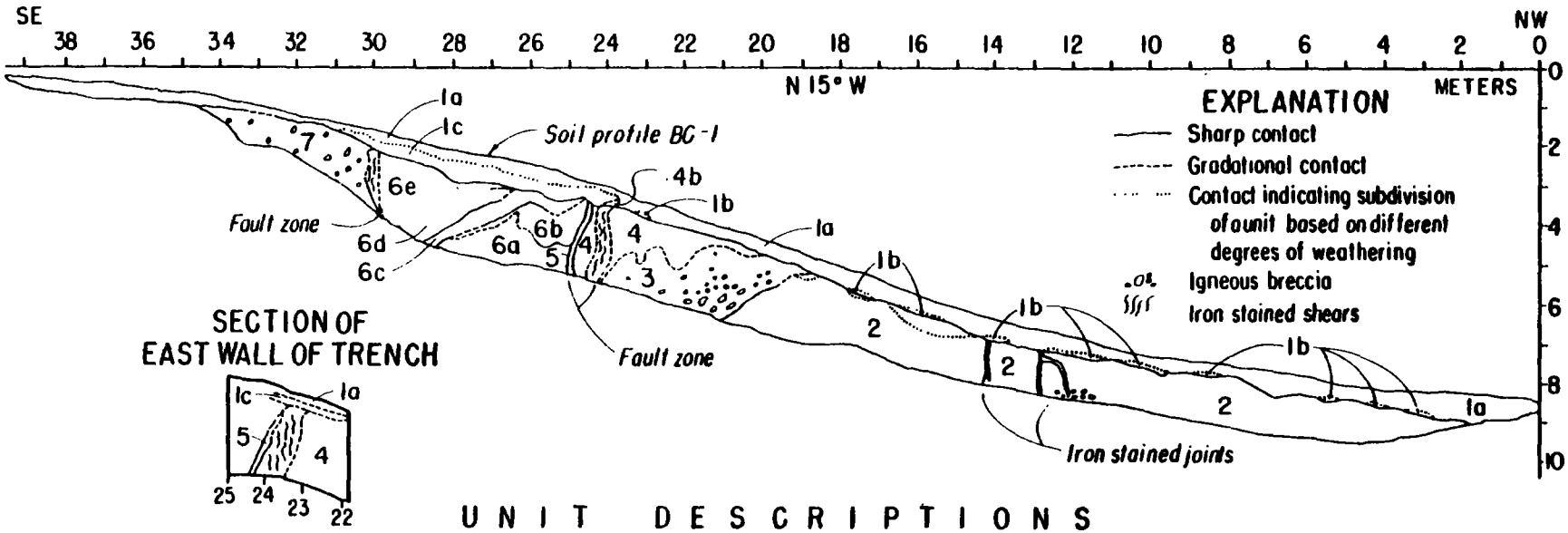


Figure 5.4 Geologic map of Mountain Meadows.



UNIT DESCRIPTIONS

Quaternary loess and colluvium

1a. Dark brown to brownish black (7.5YR 3/2.5) clay loam. Unit consists of loess mixed with a minor amount of colluvium including <5% volcanic pebbles.

1b. Brown (10YR 4/6) clay. Unit is discontinuous, occurring in pockets and lenses. Iron staining is common (7.5YR 5/7).

1c. Brown (7.5YR 4/3.5) clay. Unit consists of argillic soil B horizon developed in loess (unit 1a).

Tertiary Mountain Meadows member (Tkp) of Keetley Volcanics

2. Yellowish brown (2.5YR 5/6) lapilli tuff. Unit consists of 20-30% decomposed subangular to subrounded igneous clasts in a friable crystalline matrix of feldspar and minor quartz (5%) with numerous iron-stained high angle joints. Pedogenic clay in joints at upper surface within dotted areas.

3. Light yellow (2.5YR 7/3) volcanic breccia. Unit consists of 10-40% subrounded igneous clasts, diameter to 50cm in a fining upward sequence dipping 55°55'E. Matrix same as unit 2.

4. Light yellow (2.5YR 7/4) tuff. Matrix same as unit 2.

5. Dark brown (5YR 2/1 - 3/3) clay. Part of fault zone.

6a. Bright yellowish brown (2.5Y 6/6) tuff. Unit consists of highly weathered crystals of feldspar quartz (10%) and biotite (5-8%).

6b. Dull brown (7.5YR 5/4) tuff. Composition same as unit 6a.

6c. Light yellow (2.5Y 7/4) tuff. Composition same as unit 6a.

6d. Light grey (2.5Y 7/3 - 4/6) tuff. Unit consists of weathered crystals of feldspar, quartz (20%) and biotite (5%).

6e. Bright yellowish brown (2.5Y 6/6) tuff. Same as unit 6a with occasional clasts to 10cm.

Tertiary Silver Creek member (Tksc) of Keetley Volcanics

7. Light grey (2.5Y 8/1) volcanic breccia. Unit consists of 40% subrounded igneous clasts in a hard matrix of feldspar and minor quartz and biotite in fault contact with Tkp.

Figure 5.5 Log of a trench across the Mountain Meadows scarp.

The midpoint of the scarp is at about station 18 and if the scarp resulted from a recent displacement on a normal fault, the fault and its associated step in the bedrock surface should be discernable at or downslope from this point. In this lower portion of the trench no fault is present in the volcanics and there is no abrupt thickening of the overlying colluvium and loess. Therefore we conclude this scarp has not formed as a result of recent displacement. The location of the high-angle bedrock fault zone at the upper portion of the scarp suggests that the scarp is a fault-line scarp. The juxtaposition of the weathered friable units and well-indurated units by a fault zone at the top of the scarp suggests that the scarp results from differential erosion. The less resistant units downslope from station 27 have eroded more than the breccias exposed upslope and have been removed, resulting in the present relief on the scarp. In addition the mapping of Bromfield and Crittenden (1971) shows that the breccia above the scarp (unit 7) is the younger Silver Creek Breccia and the tuff and breccia in the footwall of the fault zone (units 2-6) is the older Tuff of Mountain Meadows. As shown on their map, the predominant displacement on the fault must have had the opposite sense of the present relief on the scarp, again suggesting that the scarp results from differential erosion.

5.7.3 Conclusions

Trenching and mapping along scarps on the southeast margin of Mountain Meadows shows that the scarps are fault-line scarps resulting from differential erosion across a fault that juxtaposes volcanic rocks with contrasting erodibility.

5.8 Kamas Valley

Kamas Valley, previously referred to as Rhodes Valley (Sullivan and others, draft report, 1983; Petersen, 1970; Gilbert, 1928), is a north-south trending, nearly rectangular valley about 14 km long and 3 to 7 km wide (fig. 5.6). The Weber and Provo Rivers flow from east to west across the north and south ends of the valley, respectively. Beaver Creek, which drains most of the valley, joins the Weber River in the northwest corner of the valley.

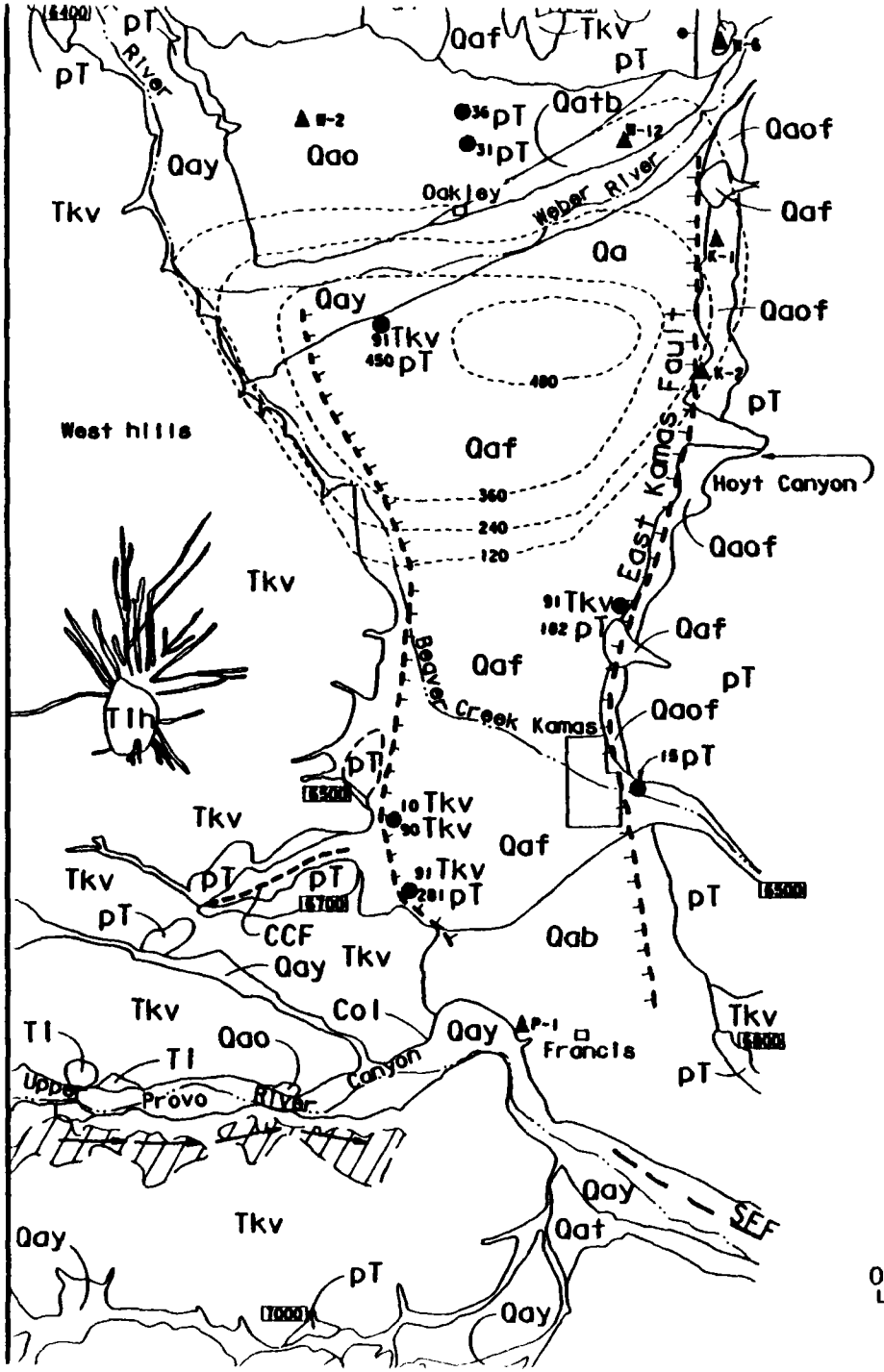
5.8.1 Geologic Setting

Kamas Valley has developed at the eastern edge of the Keetley volcanic field across the west-trending Uinta arch. Dips in the Pennsylvanian and Permian Weber Quartzite and the Permian Morgan Formation (Round Valley Limestone) in the escarpment on the east side of the valley outline the Uinta arch. In the West Hills, west of the broad alluvial plain that floors the valley, the Keetley volcanics unconformably overlie locally exposed, Mesozoic and Paleozoic rocks. Unpublished mapping by Woodfill (1972) of the Kamas and Francis quadrangles are the only detailed geologic maps of Kamas Valley.

The valley floor is a gently west-sloping alluvial plain comprised of alluvial fans deposited by intermittent drainages heading in the Uinta Mountains to the east that overlie fluvial gravels deposited by the Weber and Provo Rivers (fig. 5.6). Following the diversion of the Prove River from its former northerly course to its present westerly course across the south end of the Valley about 125 ka (sec. 3.5.2), both rivers have cut channels through the valley fill exposing mainstream gravels in various terrace remnants. Thus, surficial deposits consist of older (RAGs 1 and 2) outwash terraces and alluvial fan remnants along the northern and eastern edges of the valley (Qao on fig. 5.6), RAG 2 outwash in the southern part of the valley (Qab on fig. 5.6), and younger (RAGs 3 and 4) alluvium deposited as gently sloping fans from the Weber River, Beaver Creek, and other drainages on the east side of the valley (Woodfill, 1972; sec. 3.5). Cuts on the east and west sides of the valley in small alluvial and colluvial fans and aprons expose cambic and weak argillic horizons and stage I to II carbonate indicating the lower portions of these fans are of late Pleistocene to Holocene age.

5.8.2 Structure of Kamas Valley

Although Threet (1959) followed Anderson's (1915) and Eardley's (1944) concept of the origin of the back valleys in suggesting a primarily erosional origin for the valley, geophysical data and drilling establish that Kamas valley is a north-trending graben as earlier suggested by Gilbert (1928). Peterson (1970) inferred north-trending normal faults on the margins of the valley on the basis of a gravity study that defined an 8 mgal residual anomaly in the northern portion of the valley that he interpreted to represent at least 490 m of low-density Tertiary and Quaternary deposits. Logs of three oil test wells in Kamas Valley (fig. 5.6) confirm this interpretation (Montgomery, written comm., 1980). An oil-test well south of Oakley near the center of the anomaly shows about 450 m of low-density materials consisting of 100 m of unconsolidated deposits and about 350 m of Keetley volcanics. The base of the Keetley volcanics is at an elevation of about 1490 m (4900 ft) in this hole suggesting structural relief in the



⊥ ⊥ ⊥ Inferred late Cenozoic faults

Pre-late Cenozoic faults, dashed where approx. located, SFF-South Flank fault, CCF - City Creek fault

Geologic contacts

▲ Soil description site

● Drill hole or water well log with depth in meters and stratigraphic unit encountered

--- 360 --- Estimated thickness in meters of low-density deposits from (Peterson, 1970)

Elevations (feet) of the base of the Keetley Volcanics erosion surface

Erosion surface

40°40'

MAP UNITS

Quaternary

Qa - Alluvium, modifiers - f-fan, t-terrace, y-younger (Holocene and "Pinedale"), b-Bull Lake, o-older (pre-"Bull Lake")

Qc - Colluvium

Ql - Landslides

Tertiary

Tkv - Tertiary Keetley Volcanics,

Tl - Tertiary intrusions

Tlh - Indian Hollow stock with radiating dikes

pT - Pre-Tertiary sedimentary rocks

N

0 1 2

Km

MODIFIED FROM WOODFILL (1972)

Figure 5.6 Geologic map of Kamas Valley.

valley of 300 - 600 m when compared with the elevations of exposures of the base of the Keetley volcanics at 2070-2130 m (6800-7000 ft) on the margins of the Valley (fig. 5.6).

The log of a 600 m (2000 ft) deep oil test well located north of Kamas near the base of the escarpment on the east side of the valley suggests a concealed normal fault, referred to as the East Kamas fault, is present on this margin of the valley. The well log shows the contact between the Keetley volcanics and the Weber Quartzite at a depth of about 182 m. This thickness of volcanics combined with the escarpment height of about 300 m indicates structural relief of as much as 482 m on this fault. A north-striking, down-to-the-west normal fault in Mesozoic rocks, is exposed in the extreme northern portion of the valley on the projection of the concealed East Kamas fault (Woodfill, 1972).

The log of a third hole oiltest well near the west side of the valley, northwest of Francis, shows about 90 m (300 ft) of unconsolidated deposits overlying about 200 m (625 ft) of Keetley volcanics then Weber quartzite. In this hole the base of the Keetley volcanics is at an elevation of about 1670 m (5500 ft). A few hundred meters to the west on the south side of City Creek, southwest dipping outcrops of Weber quartzite are overlain by the Keeley volcanic at an elevation of about 2040 m (6700 ft) suggesting a normal fault with structural relief of as much as 360 m on the west margin of the valley.

5.8.2.1 East Kamas fault

The morphology of the escarpment of the East Kamas fault contrasts with that of the Morgan fault, suggesting that the East Kamas fault is not a late Quaternary fault. The escarpment on this side of the valley is sinuous, due to the erosion of small embayments into the escarpment by streams depositing alluvial fans along this valley margin. The morphology of this escarpment is much more subdued than that of the escarpment along the Morgan fault or the southern portion of the East Canyon fault; remnants of facets cut on spurs are indistinct and rounded with slope angles of 10-18°. In places, the facets are coincident with dipslopes or accentuated by fluvial erosion at the base. Two en echelon fault segments, which trend north and slightly east of north, may be present; one from the Weber River to south of Hoyt Canyon, and the other from west of this point to the town of Kamas. Alternatively, a single, more sinuous segment may be present as shown on fig. 5.6, but in this case, the northern part of the footwall escarpment was probably modified by lateral cutting by the Weber River prior to establishing its present westerly course. The southern part of this side of the valley was similarly modified by the present upper Provo River before its diversion into the Provo drainage (sec. 3.5.2).

A sequence of large alluvial fans of several ages have been deposited across the East Kamas fault where the east flowing drainages north and south of Hoyt Canyon reach the valley floor (Qa on fig. 5.6). Lateral cutting by outwash streams from the Upper Weber River Valley produced a 20 to 30-m-high scarp in these fans along the northern 3 km of the escarpment, probably during both the Pinedale and Bull Lake glaciations. Woodfill (1972) noted that the fans were segmented, and concluded that segmentation might be the result of late Pleistocene displacement on the East Kamas fault, implying that the segments

nearest the mountain front were the youngest (for example, Bull, 1977). In fact, the highest segments of the fans are the oldest. These segments are only shallowly incised relative to other old fans in the region, slope about 5-7° to the west, and head in several-hundred-meter-wide embayments in the escarpment in their tributary valleys. Development indices (fig. 3.6) for soils on the lower parts of these segments (soils K-1 and K-2, table 5.3) place them in RAG 2, correlated with oxygen-isotope stage 6 (sec. 3.4). The soils display carbonate stage II to III morphology and secondary clay values (12 g/cm^2 and 13 g/cm^2) suggest ages of 150-165 ka (fig. 3.6). Because carbonate tends to inhibit clay accumulation, these soils could be considerably older. However, if these fans were deposited during stage 6, they were most likely deposited during a probable period of higher-than-present effective precipitation during Bull Lake deglaciation about 130-140 ka (sec. 3.5.1).

In the two small drainages just north of Hoyt Canyon, two small remnants of alluvial fans that are older than the RAG 2 fans are preserved. The west faces of these remnants are scarps with slopes of < 10°, the highest of which is 20 m. The alignment of the scarps with the inferred trace of the East Kamas fault in this area suggests these may be remnants of fault scarps. However, the presence of a scarp with a parallel trend cut by the Weber River about 1 km to the west and the embayed morphology of the montain front suggest that all the scarps may have an erosional origin. In Hoyt Canyon, landslide deposits have covered or incorporated correlative older remnants.

Two lower segments of the alluvial fans have been identified. The middle portions of the fans are undissected and slope about 2°. Soils on these parts of the fans (unpub. soil descriptions, SCS, Coaville, UT) generally have weak argillic horizons, but the degree of rubification is less than for most Pinedale age soils in the area. Still, because these deposits consist of coarse, cobbly alluvium they were probably deposited during Pinedale deglaciation (15-18 ka) when effective precipitation was greater than now (sec. 3.5). Soils on the lowest segments of the fans, which slope about 0.5-1° and extend several km out into the valley, generally have cambic B horizons or lack B horizons entirely (unpub. soil descriptions, SCS, Coalville, UT). This degree of soil development suggests they are of latest Pleistocene and Holocene age (<15 ka).

There are no scarps in the RAG 2 fan deposits which cross the inferred trace of the East Kamas fault showing that there has been no surface displacement on the fault in at least the last 130-140 ka. Younger alluvial fan deposits with estimated ages of <15 ka are present valleyward of these older fan deposits and their development is related to glaciation and not late Quaternary displacement on the East Kamas fault as suggested by Woodfill (1972).

5.8.2.2 West margin of Kamas Valley

The morphology of the west margin of Kamas Valley is not suggestive of Quaternary faulting. The southern half of the valley margin is deeply embayed, the escarpment is only 120 m high, and no well-developed facets are found. Slopes are steep and the valley margin is fairly straight along the northern half of the west margin, but the position of Beaver Creek on this side of the valley makes it clear that the morphology of much of the west

TABLE 5.3 Selected properties of soils on alluvial fans in Kamas Valley and Round Valley, north central Utah.

Profile	Horizon*	Average depth (cm)	Parent material	Munsell dry color	ESTIMATED PERCENT BY VOLUME Pebbles (0.2-8cm)	Cobbles (8-25cm)	Boulders (>25cm)	PERCENT BY WEIGHT~ Sand (2-0.5mm)	Silt (50-2um)	Clay (<2um)	Percent** organic matter	Percent# carbonate
K-1	Ap	0 15	loess-colluvium	10YR 5/2	15	5	0	30	53	17	4.0	0.0
	AB	15 30	loess-colluvium	7.5YR 4/2	15	5	0	31	45	24	2.4	0.0
	Bt1	30 51	loess-colluvium	7.5YR 4/5	15	5	0	30	37	33	0.9	0.0
	2Bt2	51 81	alluvium	7.5YR 6/6	40	15	0	55	19	26	1.0	0.0
	2Btk	81 114	alluvium	7.5YR 7/6	40	15	0	69	12	19	0.4	16.0
	2CBk	114 173+	alluvium	7.5YR 7/6	40	15	0	74	11	15	0.2	13.0
K-2	Ap	0 12	alluvium	7.5YR 4/3	10	7	0	31	47	22	4.0	0.0
	AB	12 32	alluvium	7.5YR 4/2	10	7	0	30	44	26	2.1	0.0
	Bt	32 64	alluvium	5YR 6/4	10	7	0	32	33	36	0.9	0.0
	2Btk	64 89	alluvium	5YR 8/3	15	7	0	42	35	22	0.8	36.3
	2Bk	89 130	alluvium	5YR 6/4	10	0	0	18	73	9	0.4	17.5
	2CBk	130 168+	alluvium	7.5YR 6/3	10	0	0	30	65	5	0.2	9.6
RV-1	Ap	0 20	loess-colluvium	10YR 5/3	15	10	10	29	54	17	1.7	0.0
	A	20 33	loess-colluvium	10YR 5/4	25	15	10	28	50	22	1.2	0.0
	Bt	33 48	loess-colluvium	7.5YR 5/4	20	25	0	25	49	27	0.8	0.0
	2Btb	48 120	loess-colluvium	7.5YR 5/4	10	0	0	17	37	46	0.5	0.0
	3Btkb	120 140	alluvium	7.5YR 5/4	10	5	0	26	42	32	0.2	0.0
	3Bkb	140 222+	alluvium	7.5YR 4/4	20	50	20	35	38	27	0.2	6.9

* Horizon nomenclature of Guthrie and Witty (1982) and Birkeland (1984) except that master K horizon is not used.

~ Particle size distribution of <2 mm fraction using sieve-pipette methods (for example, Carver, 1971) and a Sedigraph for some silt-clay fractions with prior removal of carbonates and organic matter using methods of Jackson (1956).

Percent organic matter by method of Walkley and Black (1934).

** Percent carbonate by method of Dreimanis (1962).

margin is due to lateral cutting by the creek which has been forced against the west edge of the valley by deposition on the alluvial fans to the east. Based on the log of a drill hole near the west margin of the valley indicating that the base of the Keetley volcanics have been displaced about 300 m, there is no evidence for late Quaternary displacement and little suggestion of late Cenozoic displacement.

In the southwestern part of the valley, Woodfill (1972) mapped an east-northeast-striking fault, the City Creek fault, juxtaposing Triassic and Pennsylvanian rocks across a 60-m-wide breccia zone and concludes that the fault does not displace the overlying Keetley volcanics (fig. 5.6).

5.8.3 South Flank fault

East of the valley the Uinta arch is bounded on the south by the South Flank fault. This east-trending normal fault extends along the south edge of the Uinta Mountains for a distance of about 100 km and is inferred to continue below the course of the Provo River at the south end of the Valley (Stokes and Madsen, 1961). Geomorphic and geologic studies of the fault about 50 km to the east in the Uinta Basin have shown that it does not displace the Oligocene-age Duchesne River formation or younger erosion surfaces (Martin and others, 1985).

Montgomery (written comm, 1980) has suggested that faults on the east and west margins of Kamas valley are north-trending splays of the South Flank fault. However, the base of the Keetley volcanics is at similar elevations on both sides of the concealed trace of the South Flank fault at the southeast corner of the Valley. Thus there appears to be no displacement of the Keetley volcanics along the east-trending trace of the South Flank fault compareable to the 300 m of Cenozoic structural relief in Kamas Valley. If the marginal faults in Kamas valley are related to the South Flank fault, it appears that reactivation has only occurred on favorably-oriented north-trending splays. This is consistent with the generally north-striking, normal fault focal mechanisms characteristic of the ISB (sec. 4.0). However, microearthquake activity appears to be concentrated along the east-trending portion of the South Flank fault and a composite focal mechanism from the south end of Kamas Valley indicates north-south compression along an east-trending nodal plane (sec. 2.0).

5.8.4 North Flank fault

East of the valley the Uinta arch is bounded on the north by the North Flank. The North Flank fault is a south-dipping, east-striking reverse fault that displaces Mesozoic rocks near the northern end of the valley, north and east of the map area (Stokes and Madsen, 1961). Faults along the north flank of the Uinta Mountains have been locally reactivated as normal faults during the late Cenozoic (Hansen, 1983) and the late Quaternary (West, 1984; 1986). However, the North Flank fault does not displace the Keetley volcanics in the vicinity of Kamas Valley (Woodfill, 1972) indicating that it has not been reactivated in this area. A west-trending, down-to-the-south normal fault has been inferred near the north end of the valley (Woodfill, 1972), but no scarps which might be associated with faulting were found in deeply dissected alluvial fans which slope down from the hills at the north end of the valley with soils on them that suggest the fans are >200 ka (sec. 3.5.1). We

conclude that there is no evidence for late Cenozoic displacement on the North Flank fault or other east-trending faults.

5.8.5 Conclusions

Logs of drillholes in the center and at the margins of Kamas Valley confirm that Kamas valley is a graben. The lack of distinct facets and the sinuous embayed escarpment on the margins of the valley contrasts with the escarpments associated with late Quaternary faults in the back valleys to the north. There are no scarps in late Quaternary deposits at or near the east margin of the valley. Along the west margin of the valley preserved remnants of late Quaternary alluvial fans (>> 150 ka) could be intepreted to have been diplaced at least 20 m by the East Kamas fault, although an erosional origin for the scarps seems more likely. No scarps are visible on 1) the alluvial fans (130-150 ka) that overlie the fault near the center of its trace, 2) the extensive outwash terrace (130-150 ka) that overlies the East Kamas fault at the southern end of the valley (Woodfill, 1972), or 3) the 10 m terrace (10-15 ka) that overlies the fault at the north end of the valley (fig. 3.3, sec. 3.5.1).

We conclude that no surface displacements have occured on the East Kamas fault or other faults in or near Kamas Valley in at least the last 130 ka.

5.9 Heber Valley

Heber Valley is a triangular shaped valley about 13 km on a side on the Provo River downstream of Keetley and Kamas Valleys and above Lower Provo Canyon in the Wasatch Mountains. Daniels Creek, Center Creek, and Lake Creek enter Heber Valley from the south and east to join the Provo River, which enters the basin from the north. Deer Creek Dam is located about 8 km down the lower Provo Canyon from Heber Valley and impounds Deer Creek Reservoir, which extends into Heber Valley (fig. 5.7).

5.9.1 Geologic Setting

Rocks of the upper plate of the Charleston thrust (sec. 5.1) are exposed on the southern margin of Heber Valley and lower plate rocks are exposed on the northwestern and northeastern margins of the valley (fig. 5.7) Therefore, the trace of the Charleston thrust zone is constrained to an inferred position beneath Heber Valley. On the Aspen Grove (Baker, 1964) and Timpanogos Cave (Baker and Crittenden, 1961) quadrangles, west of Heber Valley, the Tibble Formation is exposed in a 4 km-wide band of outcrops that extends to the margin of Heber valley at Deer Creek Reservoir in the upper plate of the Charleston thrust. The Tibble Formation is principally a fluvial deposit of consolidated conglomerates, tuffaceous sands and freshwater limestones thought to be contemporaneous with the Keetley volcanics, although it has not been directly dated (Baker and Crittenden, 1961). Almost 1000 m of the Tibble Formation is preserved consistently dipping 20° - 40° to the northeast. This rotation is interpreted to result from displacement on the Deer Creek fault, a 35° southwest-dipping, east-trending normal fault inferred to sole in the Charleston thrust fault (Riess, 1985). Westward displacement of Jurassic and upper Paleozic rocks in the upper plate of the the Charleston thrust fault from their footwall cutoff position is interpreted as evidence of 5-7 km of Cenozoic extension on the Charleston thrust zone (Royse, 1983; Hopkins and Bruhn, 1983). The Deer Creek normal fault displaces the Little Cottonwood stock (24-31 ma) but is truncated by the Wasatch fault, suggesting most of the displacement occurred during the middle Cenozoic.

A group of thermal springs and associated tufa deposits are found in the northwestern part of Heber Valley near Midway, Utah. Baker (1968) describes the springs and concludes that the spring water is meteoric, originating in the mountains to the northwest and emerginging through fractures at Midway. As nearby intrusive rocks are Oligocene in age, the heat source is unknown but attributed to an unusually high geothermal gradient. Kolesar (1981) reports the results of a recent investigation of this geothermal system which included lithologic logs of four wells that show alternating tufa and alluvium to depths of about 60 m. Their favored model for the origin of the springs envisions " a series of relatively young, small intrusions north of Midway" to drive the geothermal system. Minor faults along the crest of an anticline inferred in Mesozoic and Paleozoic rocks beneath Midway may provide the conduits to the surface.

5.9.2 Tectonic Geomorphology

Eardley (1933; 1944) regards the Wasatch Mountains as an east-tilted fault block and concludes that Heber Valley is an erosional valley excavated by the

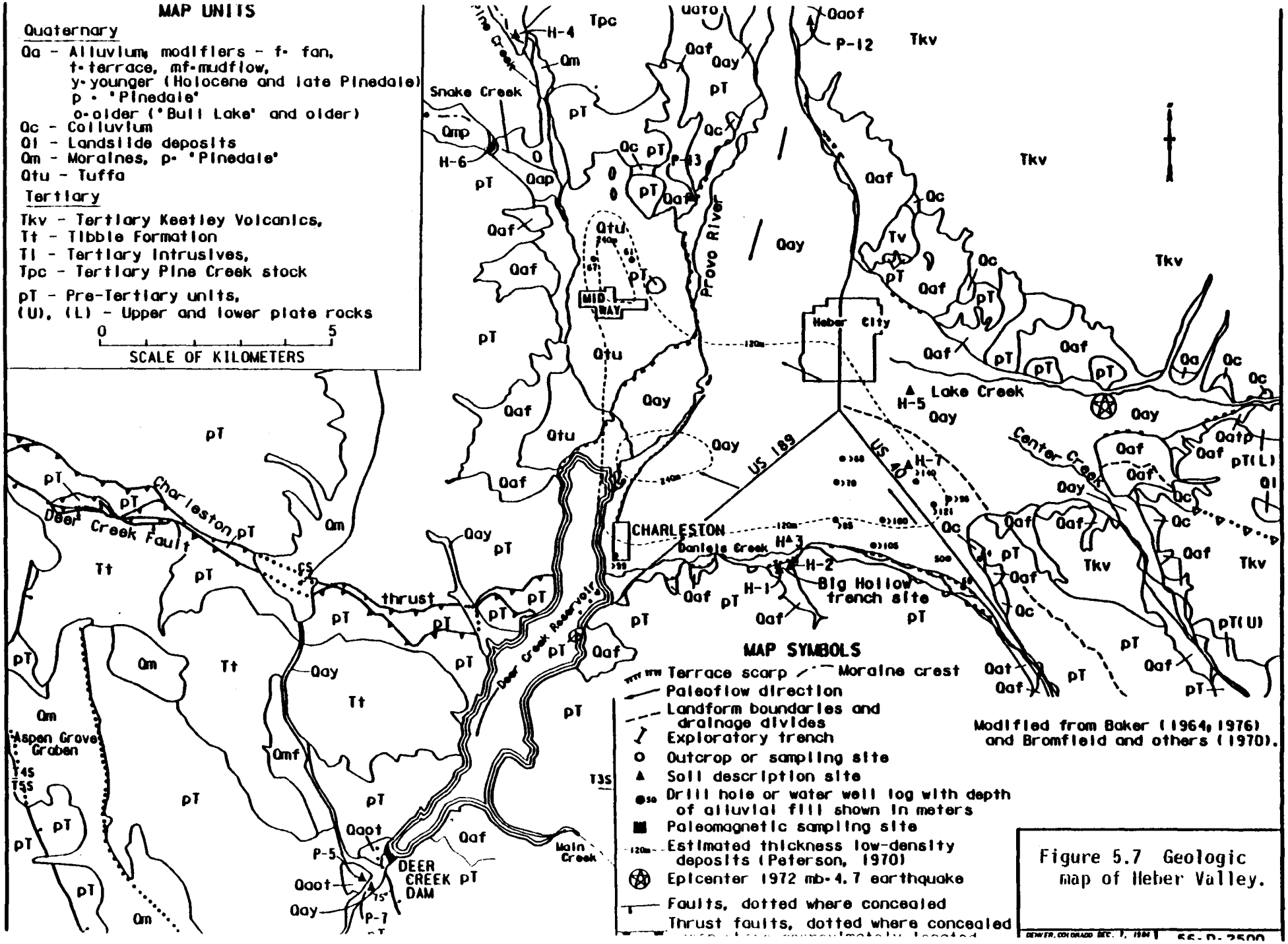


Figure 5.7 Geologic map of Heber Valley.

Provo River and its tributaries at or near the hingepoint of tilting. Although he disputes evidence for a hingepoint of east tilt, Threet (1959) also favors an erosional origin for Heber Valley suggesting that the unconsolidated fill in Heber Valley is <100 m thick overlying a bedrock strath surface. Gilbert (1928) considers the Wasatch Mountains to be a horst and the back valleys to be grabens on the east side of the Wasatch Mountains, and some subsequent investigators (Baker, 1964; 1976; Peterson, 1970; Baer and Rigby, 1980; Hunt, 1982) have inferred that concealed faults have contributed to the development of Heber valley.

To assess the evidence for concealed faults on the margins of Heber Valley we reviewed aerial photography at various scales, conducted two low sun-angle overflights of the valley, and prepared a map of the deposits on the valley margins (fig. 5.7). Most of the discussion of the Quaternary deposits in the valley is included in the section (3.5.2) on the Provo River Valley.

5.9.2.1 Northwestern margin

The sinuous, embayed margin bounding the northwest edge of Heber Valley contrasts with the linear valley margin and little-eroded triangular facets associated with the Morgan fault, the James Peak fault, the southern portion of the East Canyon fault, and faults in Ogden Valley where recurrent late Quaternary surface displacements are inferred (discussed in previous sections). Late Quaternary alluvial fans and outwash deposits on this margin (sec. 3.5.2) extend several km up tributary drainages. These deposits are overlain by tufa along much of the valley margin and waterwells show that tufa and gravel deposits are interbedded to depths of at least 60 m (200 ft). A 7-m-high scarp at the edge of the alluvial fans along much of this side of the valley (fig. 5.7) was cut during the latest Pleistocene or Holocene by the Provo River (sec. 3.5.2); no fault scarps were identified in the area. We conclude that late Cenozoic faults may be present at or near this valley margin that may be related to the thermal springs at Midway, but there is no evidence for recurrent late Quaternary surface displacements on this side of the valley. Available evidence does not allow us to locate the fault; therefore, it is not shown on fig. 5.7.

5.9.2.2 Northeastern margin

The presence of the Charleston thrust fault below Heber Valley and evidence presented in sec 5.1 for Cenozoic reactivation of this fault to accomodate Cenozoic extension, could be interpreted to suggest that down to the west, late Tertiary and possibly late Quaternary displacements may have occurred along this margin of the valley. This margin is somewhat steeper and more linear than the northwestern margin, yet it lacks the triangular facets associated with other late Quaternary faults in the Regional study area. Alluvial fan sediments >730 ka overlie a bedrock pediment at the northern end of the northeast margin (sec. 3.5.2). Although the lowest sediments in the fan sequence appear to dip towards the mountain front, these dips are probably depositional. The alluvial and colluvial fans along this margin, like the fans on the other margins of the valley, are of mid- to late Quaternary age (sec. 3.5.2). No fault scarps were identified along this margin; the discontinuous scarps, 5 to 10 m high, on the distal parts of alluvial fans north and east of Heber City are interpreted to be fluvial scarps cut by the Provo River and Lake Creek before the Provo River moved to

its present position on the west side of the valley. Similar scarps have been cut more recently by Daniels Creek on the south margin of the valley. As on the northwestern margin we conclude that a late Cenozoic normal fault may be present along this margin, but there is no evidence that recurrent late Quaternary surface displacements have occurred on this inferred fault. Available evidence does not allow us to locate the fault; therefore, it is not shown on fig. 5.7.

5.9.2.3 Southern margin

As along the northeastern and northwestern margins of the valley the south margin is embayed by tributary drainages, but it has steep bedrock facets developed between the embayments. The largest, steepest facets are adjacent to Daniels Canyon and appear to have been cut by Daniels Creek during periods of higher discharge. Farther to the west, facets are smaller and Daniels Creek has cut embayments into the late to mid-Quaternary fans in the drainages along this side of the valley. The discontinuous, linear scarps in the alluvial deposits east of Daniels Canyon were cut by Center and Lake Creeks. The scarps in the embayments along the south margin were originally interpreted by Eardley (1933) as erosional remnants of a former higher level of the alluvial floor of the valley that has been abandoned as a result of eastward tilting of the Wasatch Mountains in response to late Cenozoic displacement on the Wasatch fault. However, Threet (1959) concluded that the effects of tilt at distances of more than 20 km from the Wasatch fault would not be recognizable. Although the upper part of the lower Provo Canyon and southwestern part of Heber Valley have probably been eroded a little more deeply than the eastern part of the valley due to uplift on the Wasatch fault, scarps like those on the south and northwest margins of the valley are more likely to have been produced entirely by lateral stream erosion with no uplift relative to other parts of the valley.

5.9.3 Trenching of the scarp at Big Hollow

Although the origin of the scarps on the south side of the valley seems best explained by fluvial erosion, one of the scarps on the south side of the valley is shown as a "suspected" Quaternary fault by Anderson and Miller (1979). This 600 m-long, N75°E trending, linear scarp crosses the mouth of Big Hollow in the NW1/4, sec. 19, T.4S, R.5E on the Charleston Quadrangle. The scarp gradually changes in height from 12 m at the east end to <1 m at the west end, and is nearly on trend with a 60° south dipping, N85°E striking gouge zone in brecciated quartzite of the Oquirrh Formation exposed in the gravel pit less than 100 m east of the scarp (fig. 5.8). As this evidence had been interpreted as suggesting a relationship between the scarp and the shear zone, a backhoe trench was excavated across the scarp.

The 36-m-long, 3 to 7 m deep trench was located near the west end of the scarp, where the scarp height is 6 m and the maximum scarp angle is 26° (fig. 5.8). The trench exposure (fig. 5.9) shows that the scarp is developed in stratified, gently north-dipping, alluvial fan deposits (Qaf) consisting of interbedded, moderately-indurated, sandy, angular and subangular gravels and hard sandy clay. At about station 20 these deposits are truncated by an irregular, about 40° north-dipping contact that continues to the base of the trench at about station 26. Two distinct, unstratified, northward thickening, fine-grained units, reaching a maximum thickness of 3.5 m,

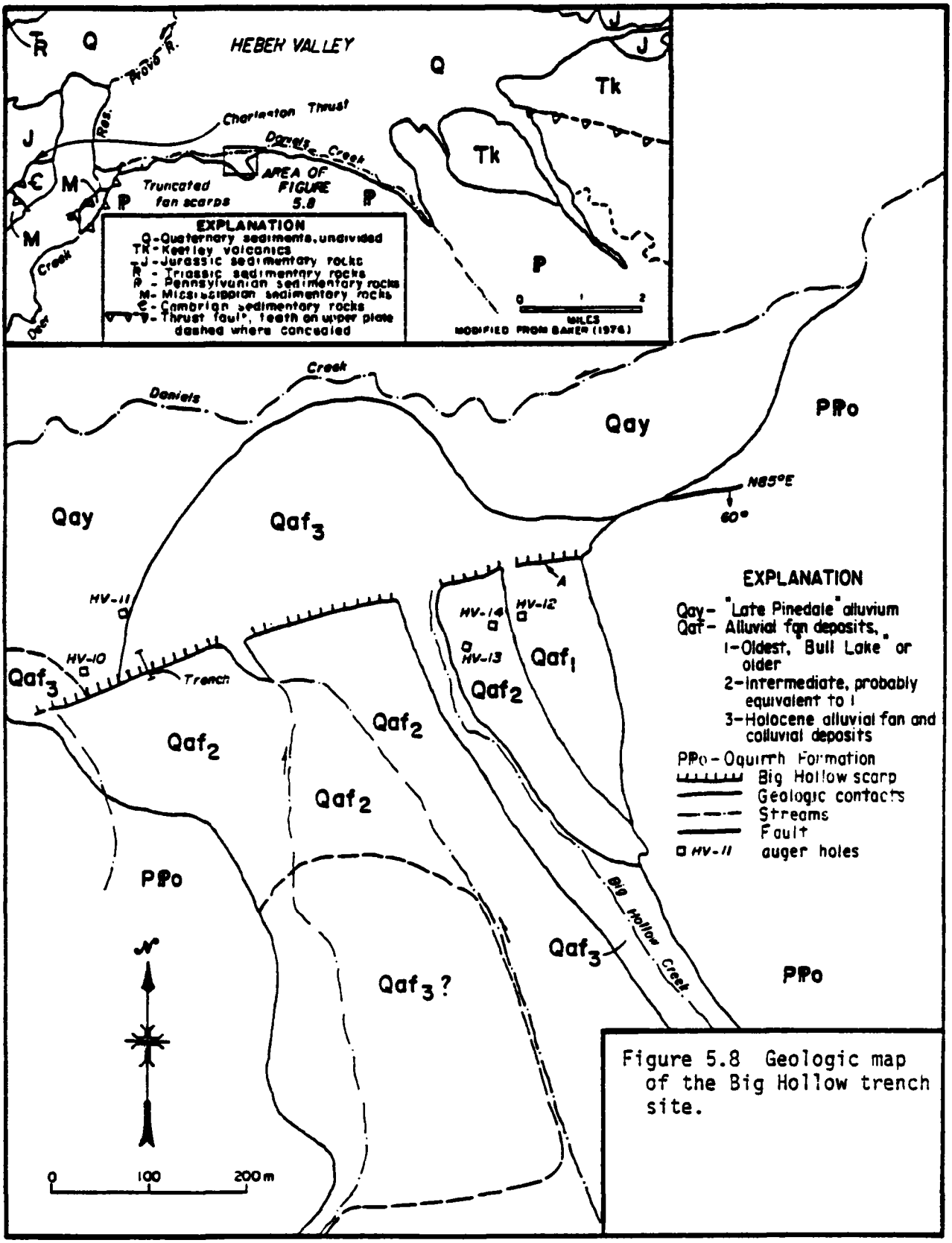
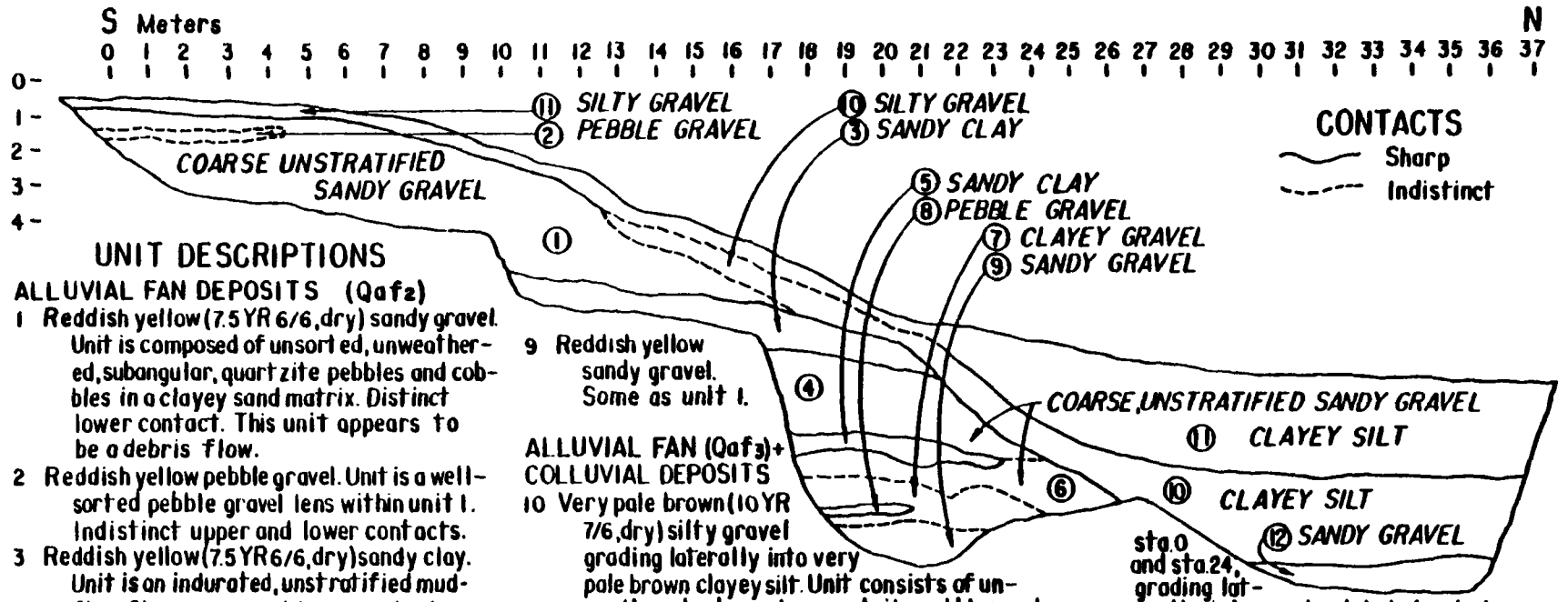


Figure 5.8 Geologic map of the Big Hollow trench site.



UNIT DESCRIPTIONS

ALLUVIAL FAN DEPOSITS (Qafz)

1 Reddish yellow (7.5YR 6/6, dry) sandy gravel. Unit is composed of unsorted, unweathered, subangular, quartzite pebbles and cobbles in a clayey sand matrix. Distinct lower contact. This unit appears to be a debris flow.

2 Reddish yellow pebble gravel. Unit is a well-sorted pebble gravel lens within unit 1. Indistinct upper and lower contacts.

3 Reddish yellow (7.5YR 6/6, dry) sandy clay. Unit is an indurated, unstratified mudflow. Sharp upper and lower contacts.

4 Reddish yellow sandy gravel. Unit is same as unit 1 with faint horizontal imbrication of clasts.

5 Reddish yellow (7.5YR 6/4, dry) sandy clay. Unit is very similar to unit 3.

6 Reddish yellow sandy gravel. Unit has the same description as unit 1.

7 Reddish yellow (7.5YR 6/8, moist) clayey gravel. Unit is composed of unsorted, unweathered, subangular, quartzite pebbles, cobbles, and boulders in a sandy clay matrix. Indistinct upper and lower contacts. This unit appears to be a debris flow.

8 Reddish yellow pebble gravel Unit is a well sorted pebble gravel lens within unit 7. Indistinct upper and lower contacts.

9 Reddish yellow sandy gravel. Some as unit 1.

ALLUVIAL FAN (Qaf3)+ COLLUVIAL DEPOSITS

10 Very pale brown (10YR 7/6, dry) silty gravel grading laterally into very pale brown clayey silt. Unit consists of unweathered subangular quartzite pebbles and cobbles in a moderately indurated clayey silt matrix between sta. 12 and sta. 22 grading laterally into a moderately indurated unstratified clayey silt (10YR 7/6, dry) between sta. 24 and sta. 36. Upper contact is indistinct from sta. 12 to sta. 22 and distinct from sta. 24 to sta. 36. Lower contact is indistinct from sta. 12 to sta. 15 and distinct where exposed from sta. 15 to sta. 36 This unit appears to be a scarp-derived colluvial deposit grading into loess and colluvium.

11 Brown (7.5YR 5/3, dry) silty gravel grading laterally into dark greyish brown (10YR 3/2, dry) clayey silt. Unit consists of unweathered, subangular quartzite pebbles, cobbles, and boulders in a loose silty matrix between sta. 0 and sta. 24, grading laterally into a moderately indurated, unstratified clayey silt between sta. 24 and sta. 36. Lower contact is indistinct between sta. 12 and sta. 21 and distinct between sta. 0 and sta. 12 and sta. 12 and sta. 36. This unit is a surface colluvium grading into loess and colluvium.

FLUVIAL DEPOSITS (Qay)

12 Reddish yellow (7.5YR 7/6, dry) sandy gravel. This unit consists of rounded quartzite pebbles and cobbles in a matrix of fine to coarse sand. This unit is a mainstream gravel deposit representing the period of erosion responsible for the truncation of the fan and the cutting of the scarp.

Figure 5.9 Log of a trench on the Big Hollow scarp.

overlie this contact. The lack of evidence of shearing along this contact, its moderate dip, and its non-planar nature suggest it is an erosional contact.

At the north end of the trench, between stations 29 and 35 at a depth of 3.5 m, fluvial gravels (Qay) are exposed at the base of the trench. These sandy gravels consist of rounded quartzite pebbles and cobbles in a matrix of well-sorted, fine to coarse sand. This suggests the origin of the scarp can be attributed to fluvial erosion. The stratigraphy in auger holes HV-11 and HV-12 (fig. 5.8), below the scarp was similar to that in the northern portion of the trench. Well-rounded gravels were present at depths of 4.2 and 3.0 m respectively, confirming the extent of these gravels and establishing that they form a flat surface beneath the alluvaial fan and colluvial at the base of the scarp.

A series of four pits about 300 m north of Daniels Creek confirm the extent of the fluvial gravels (Qay). These pits exposed 1-2 m of fine-grained loess and colluvium overlying rounded quartzite pebbles and cobbles in a well-sorted sandy matrix (Qay) that are similar to the fluvial gravels (unit 12) in the Big Hollow trench. Survey stations established in the area show that the gravels in these pits, the gravels in the auger holes below the scarp, and the gravels exposed in the trench are at relative elevations within 2 m of each other, and form a flat surface extending south from Daniels Creek to the base of the scarp. Mapping of the fan deposits in the vicinity of the scarp suggests that the greater thickness of overlying fine-grained deposits near the trench site (fig. 5.9) is related to deposition of Holocene fan deposits (Qaf_3) from the active channel of Big Hollow Creek that breaches the scarp 270 m east of the Big Hollow trench (fig. 5.8). Development indices (fig. 3.6) for a soil in one of the pits (soil H-3, table 5.4) north of the scarp, place it in RAG 3, suggesting a latest Pleistocene (10-15 ka) age (sec. 3.5.2). Thus, the erosion of the scarp and the deposition for the fluvial gravels by Daniels Creek probably took place during the period of higher-than-present effective precipitation near the end of Pinedale deglaciation (about 15 ka)(sec. 3.2.2).

Development indices (fig. 3.6) for a soil on the fan surface (Qaf_2) at the south end of the trench (soil H-1, table 5.4) show it is in RAG 1 and is probably several hundred thousand years old (sec. 3.5.2). Borrow pits 150 m south of the trench expose similar soils with even thicker argillic horizons and higher clay contents. Indices place a soil with stage III carbonate development (soil H-2, table 5.4) on colluvial deposits derived from the hillside bordering the eastern edge of the fan in RAG 2. However, total secondary clay values for this soil (32 g/cm^2) suggest it may also be several hundred thousand years old. Similar soil carbonate was encountered in auger hole HV-13, but not in holes HV-12 and HV-14 (fig. 5.8). The fan above the scarp apparently consists mostly of alluvium which is >200 ka, and is covered by and probably interbedded with colluvium from the adjacent hillsides which has been accumulating since deposition of the fan sediments. Carbonate is apparently retained more easily in the fine-grained colluvial soils than in the gravelly fan deposits.

We conclude that the Big Hollow scarp as well as the other scarps on the south margin of Heber Valley have formed as a result of erosion by Daniel Creek during periods of higher flow within the last few hundred thousand

Table 5.4 Selected properties of soils on alluvial fans, moraines, and terraces in Heber Valley, north central Utah.

Profile	Horizon*	Average depth (cm)	Parent material	Munsell dry color	ESTIMATED PERCENT BY VOLU Pebbles (0.2-8cm)	Cobbles (8-25cm)	Bldrs (>25cm	PERCENT BY WEIGHT~ Sand (2-0.5mm)	Silt (50-2um)	Clay (<2um)	Percent§ carbonate	Percen organic m
H-1	Ap	0 12	loess-alluvium	7.5YR 5/3	30	20	0	24	44	32	0.0	6.4
	A	12 24	loess-alluvium	7.5YR 5/3	30	20	0	26	39	35	0.0	3.2
	Bt1	24 52	alluvium	5YR 6/5	30	20	0	54	13	33	0.0	0.6
	2Bt2	52 99	alluvium	5YR 6/5	40	5	0	56	12	31	0.0	0.3
	3Bt3	99 138	alluvium	7.5YR 7/6	35	20	0	37	25	39	0.0	0.3
	3BC	138 230+	alluvium	7.5YR 7/4	35	20	0	60	12	29	0.0	0.2
H-2	Ap	0 28	loess-colluvium	7.5YR 5/3	5	0	0	19	56	25	0.0	1.7
	Bt1	28 42	loess-colluvium	7.5YR 7/4	5	0	0	12	41	48	0.0	0.6
	Bt2	42 90	loess-colluvium	7.5YR 7/4	8	0	0	18	42	40	0.0	0.5
	2CBk	90 121	loess-colluvium	7.5YR 6/5	10	1	0	26	58	16	17.3	0.5
	2Btkm	121 215	loess-colluvium	7.5YR 8/0	8	1	0	37	39	24	50.8	0.2
	3BCk	215 265	loess-colluvium	7.5YR 7/4	15	1	0	41	53	7	28.8	0.1
	4CBt	265 340+	loess-colluvium	7.5YR 7/4	10	1	0	31	65	4	2.7	0.1
H-3	Ap	0 9	loess	10YR 4/3	5	0	0	40	38	22	0.1	2.9
	A	9 42	loess	10YR 4/2	5	0	0	42	35	22	0.1	2.2
	E	42 58	loess	10YR 5/3	5	0	0	52	31	18	0.1	1.0
	2Bt	58 90	alluvium	10YR 4/6	50	20	0	71	16	13	0.1	0.9
	2CB	90 126	alluvium	10YR 6/6	50	20	0	83	9	8	0.1	0.4
	2Cuj	126 160+	alluvium	10YR 7/5	30	5	0	94	3	3	0.3	0.1
H-4	A1	0 22	till	10YR 3/2	5	10	0	63	24	13	0.1	3.2
	A2	22 42	till	10YR 6/3	5	10	0	67	23	10	0.1	0.8
	Bt	42 87	till	10YR 5/4	5	20	0	61	23	16	0.2	0.4
	Cuj	87 124+	till	10YR 5/4	5	5	0	76	16	7	0.3	0.2
H-5	Ap	0 5	loess-alluvium	10YR 4/3	15	0	0	55	30	15	0.1	2.1
	A	5 25	loess-alluvium	10YR 4/3	15	0	0	57	28	15	0.1	1.1
	2Bt1	25 40	alluvium	7.5YR 5/3	25	5	0	54	25	21	0.4	0.6
	2BC	40 85	alluvium	7.5YR 5/3	40	20	0	89	4	7	0.2	0.3
	2Cuj	85 120+	alluvium	7.5YR 7/3	40	20	0	90	5	5	0.1	0.1
H-6	A	0 10	till	7.5YR 4/3	15	20	0	42	43	15	0.0	9.0
	AB	10 27	till	7.5YR 5/3	15	20	0	43	38	19	0.0	3.2
	Bt1	27 46	till	7.5YR 5/5	15	20	0	45	29	26	0.0	1.1
	Bt2	46 79	till	7.5YR 5/6	15	20	0	45	30	25	0.0	0.9
	Cuj	79 160+	till	10YR 7/3	15	20	0	73	19	9	21.4	0.4
H-7	Ap	0 15	loess	7.5YR 4/4	2	0	0	35	40	26	0.0	3.1
	A	5 32	loess	7.5YR 4/4	2	0	0	35	40	25	0.0	2.3
	AE	32 62	loess	7.5YR 5/4	5	0	0	37	40	23	0.0	1.6
	BA	62 73	loess	7.5YR 6/6	5	0	0	36	33	30	0.0	1.1
	2Bt1	73 80	alluvium	5YR 6/7	40	15	0	49	11	40	0.0	0.8
	2Bt2	80 128	alluvium	5YR 5/8	40	15	0	66	10	24	0.0	0.4
	2BC	128 175+	alluvium	7.5YR 6/7	40	15	0	71	11	17	0.0	0.5

* Horizon nomenclature of Guthrie and Witty (1982) and Birkeland (1984) except that master K horizon is not used.
~ Particle size distribution of <2 mm fraction using sieve-pipette methods (for example, Carver, 1971) and a Sedigraph for some silt-clay fractions with prior removal of carbonates and organic matter using methods of Jackson (1956).
§ Percent carbonate by method of Allison and Moodie (1965, p. 1387).
** Percent organic matter by method of Walkley and Black (1934).

years. The origin of the scarps and their positions within the embayments suggests that the bedrock facets between the embayments have also formed as a result of erosion of the brecciated, easily-erodable Oquirrh Formation as a result of channel migration of Daniels Creek on the Daniels Creek fan.

5.9.4 Origin of Heber Valley

Based on a gravity study study Peterson (1970) concluded that a closed, 4 mgal residual Bouguer anomaly low is centered in the southwestern portion of Heber valley. Assuming a density contrast of 0.5 g/cm^3 between bedrock and low-density volcanics and unconsolidated deposits, he estimated a maximum thickness of 240 m (800 ft) of low-density fill in this portion of the valley and concluded from the shape of the amomaly that normal faults bounded the margins of the valley.

To further constrain the thickness of unconsolidated deposits in Heber Valley we have compiled 133 drillers logs of water wells in Heber Valley and compared them with the thickness of low-density fill in the valley estimated from gravity studies (Petersen, 1970). The log of a water well in the valley located near Charleston shows a minimum of 99 m (325 ft) of gravel in an area where the gravity data suggests a thickness of about 120 m of low-density materials. Along the southern margin of the valley where the gravity data suggest a thickness of about 120 m (400 ft) of low-density material, four water wells penetrated 90 to 120 m (300 ft) of unconsolidated deposits (fig. 5.8) without encountering bedrock and in others (not shown) alluvial thicknesses are greater than 60 m. In addition, three holes within Daniels canyon (fig. 5.8) penetrated 30 - 60 m of unconsolidated deposits indicating a minimum thickness of deposits aggraded by Daniels Creek on the upthrown side of any concealed fault on the southern margin of the valley. These wells suggest that Heber valley and its tributary canyons were once excavated more deeply than at present, and support an erosional interpretation of landforms on the southern margin of the valley. In the northwestern portion of the valley three holes have been drilled near Midway to investigate geothermal potential of the Hot Springs (Kolesar, 1981). Two of these holes encountered bedrock (quartzite) at depths of about 60 m within the area where a thickness of 240 m of low-density material had been estimated from the gravity data.

On the basis of the waterwell data we conclude that the alluvium in the valley is typically 60 or more meters thick with a maximum of >120 m. The waterwell data is generally consistent with the estimates of the thickness of the low-density fill from the gravity data except in the northeast portion of the valley where bedrock is significantly shallower than predicted. The maximum thickness of about 240 m (800 ft) and the lithology of the underlying bedrock can not confirmed as no wells were drilled that deep. If the topographic relief of the valley resulted principally from subsidence on concealed faults that post-dates deposition of the volcanics, we would expect to find evidence that the Keetley volcanics are preserved below the alluvial fill as in Kamas valley. The logs of a few wells on the margins of the valley show that the alluvial fill overlies sandstones and shales not volcanic rocks, which may suggest that no significant faults are present on the margins of the valley.

Comparison with the lowest elevation of the Oquirrh Formation exposed across

the channel of the Provo River in the foundation cutoff excavation for Deer Creek Dam (5200 ft) shows that the bedrock surface below the alluvial fill along the southern margin of the valley is lower in elevation than the outlet, as recognized by Baker (1964), which suggests the possibility of recent faulting in the valley. As discussed above, fluvial deposits of the Tibble Formation are exposed in the hanging wall of the Deer Creek normal fault on the western side of Deer Creek Reservoir. If the Deer Creek fault persists beneath the valley, following the trace of the Charleston thrust, then Tibble Formation may also be preserved in Heber Valley. Although the Tibble Formation is described as consolidated we expect that in a saturated condition it would be indistinguishable from younger alluvium on water well logs. If the lower portion of the alluvial fill in the valley is Tibble formation or an equivalent as in Keetley Valley and Parleys Park to the north, then the apparent subsidence of Heber Valley relative to its outlet may be related to reactivation of the Charleston Thrust, which occurred largely during the middle Cenozoic, rather than to late Cenozoic or late Quaternary displacement on concealed faults.

5.9.5 Conclusions

In contrast to the margins of back valley where late Quaternary faults have been identified or inferred, the margins of Heber Valley are sinuous and embayed suggesting that there are no late Quaternary faults at or near the valley margins. Our mapping and trenching in Heber Valley have shown that the scarps at or near the valley margins are the result of erosion by the Provo River and its tributaries. Although we can not preclude the presence of concealed late Cenozoic or Quaternary faults in Heber Valley, we feel a combination of mid-Tertiary extension on the Charleston Thrust and episodes of erosion and aggradation by the Provo River and its tributaries as suggested by Threet (1959) best explain the present physiography. Therefore, we conclude that no late Quaternary surface displacements have occurred in Heber Valley.

6. SOUTHERN WASATCH MOUNTAINS

In this report we refer to the Wasatch Mountains south of Heber Valley and as the southern Wasatch Mountains. In this chapter we discuss late Quaternary faulting south of Heber Valley and north of the Spanish Fork River (fig. 5.1) and summarize the results of other studies to the east (Nelson and Martin, 1982) and south (Foley and others, 1986).

6.1 Tectonic setting

Allocthonous rocks in the upper plate of the Charleston thrust, overlapped on the east by late Cretaceous and Tertiary sedimentary rocks are exposed in the southern Wasatch Mountains (fig. 5.1). The Charleston thrust is the lowermost of a sequence of at least six imbricate stacked thrust faults identified south of the Uinta reentrant (Morris, 1983; Tooker, 1983). The Charleston thrust was first recognized by Baker (1947; Baker and others, 1949) southwest of Heber Valley. The thrust places sedimentary rocks of Precambrian through Permian age over sedimentary rocks of Permian through Jurrasic age along a west-dipping, low-angle thrust fault with an estimated tens of kilometers of late Cretaceous eastward displacement (figs. 5.1 and 5.7). Subsequent mapping has shown that the zone consists of additional related thrusts that cut out most of the lower Paleozoic section leaving >6000 m of brecciated quartzite and limestone of the upper Paleozoic Oquirrh Formation exposed in the upper plate (Baker, 1964). The lower plate paraautocthonous sequence of east-dipping Pennsylvanian Weber Quartzite and overlying Triassic and Jurassic sedimentary rocks are exposed to the north in the Uinta reentrant (Beutner, 1977). The leading edge of the thrust is overlain by conglomerates of the late Cretaceous Price River formation which is overlain by folded and faulted early Tertiary sedimentary rocks of the North Horn, Flagstaff, Green River and Uinta formations and, locally, the Wanrhodes volcanics (Baker, 1976). Southwest of Heber Valley the position of the thrust zone is masked by the overlying Keetley volcanics. The Strawberry thrust has been considered the continuation of the Charleston thrust (Baker, 1976) (fig. 5.1), although recent interpretations suggest that the Strawberry thrust is a structurally higher thrust and that the Charleston thrust is present further to the east in the subsurface (Bruhn and others, 1983).

6.2 Back Valleys of the southern Wasatch Mountains

Generally north-trending Cenozoic normal faults are found in the Basin and Range transition zone east of the Wasatch fault in the southern Wasatch Mountains (Burchfiel and Hickcox, 1972). Late Quaternary displacement has been demonstrated in Strawberry Valley (Nelson and Martin, 1982; Nelson and Van Arsdale, 1986) and has been inferred on other faults in the southern Wasatch Mountains discussed below. South of the Regional Study area, on the Levan segment of the Wasatch fault, both the late Quaternary slip rate and the range front relief associated with the Wasatch fault diminish as the fault dies out at Gunnison, Utah (Schwartz and Coppersmith, 1984). The physiographic boundary between the Basin and Range and the Colorado Plateau becomes a transition zone extending east to Castle valley with late Cenozoic normal faulting evident on the Gunnison Plateau, in Sevier and San Pete Valleys and on the Wasatch Plateau (Burchfiel and Hickcox, 1972; Witkind and others, 1978).

6.3 Round Valley and Wallsburg Ridge

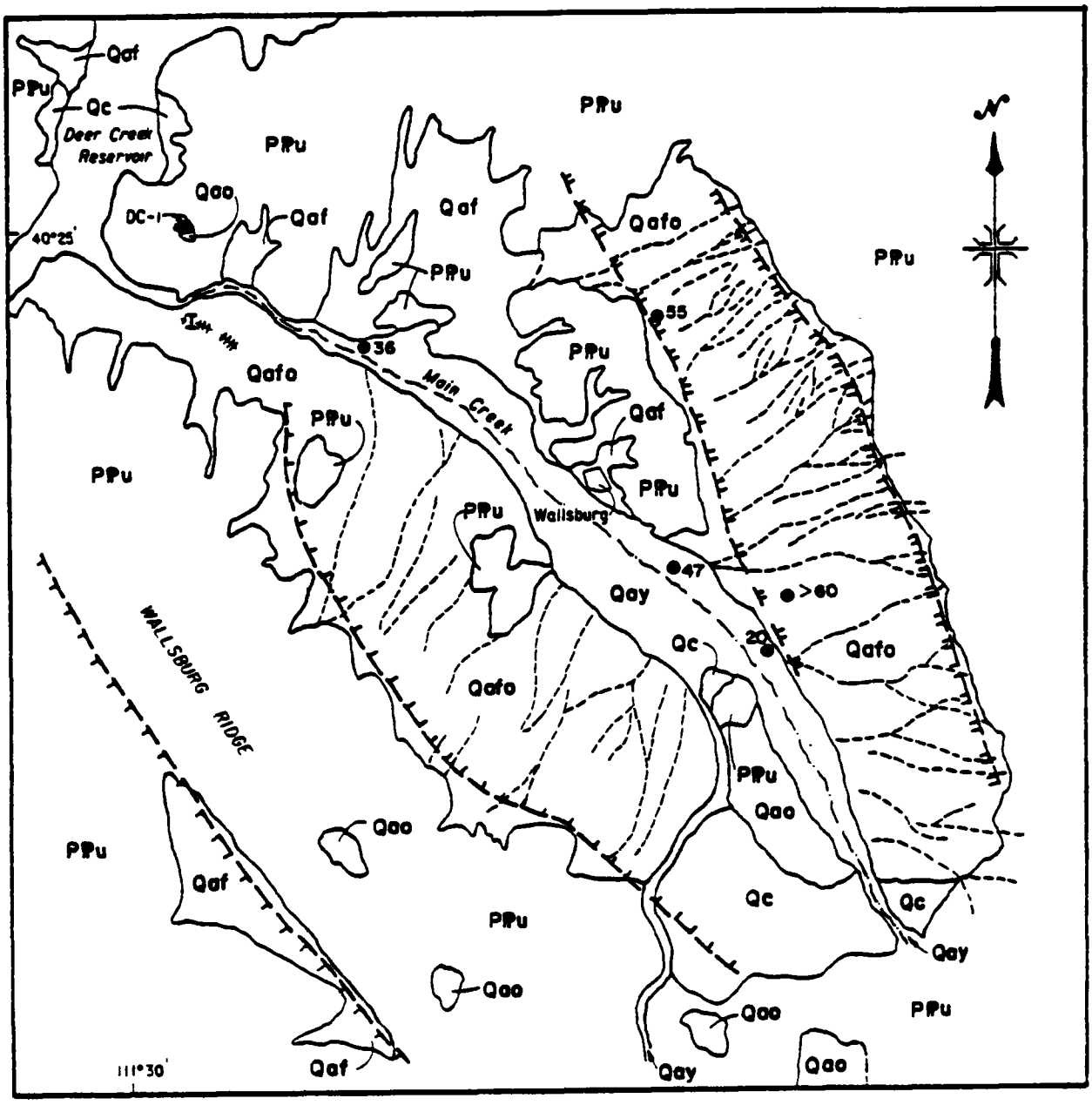
Round Valley is 12-km-long, 6-km-wide basin in the Wasatch Mountains draining into the Provo River about 6 km south of Heber Valley. The outlet of the valley is now occupied by Deer Creek Reservoir (fig. 6.1). Although located adjacent to Heber Valley, we discuss Round Valley with the other valleys of the southern Wasatch Mountains because it contrasts with valleys in the central Wasatch Mountains in several ways including: its structural setting entirely within allocthonous rocks of the upper plate of the Charleston thrust (Baker, 1976), the lack of a significant thickness of mid-Tertiary and younger alluvial fill, and the presence of triangular facets on the margins of the valley.

6.3.1 Geologic Setting

The Permian and Pennsylvanian quartzites and limestones of the Oquirrh Formation in the upper plate of the Charleston thrust are exposed on the margins and the floor of Round Valley (fig. 6.1). In contrast to the other back valleys discussed above, no mid-Cenozoic volcanic rocks or basin fill sediments are exposed in Round Valley. Threet (1959) suggested that the topographic expession of Round Valley was that of a syncline, but Baker (1976) infers an anticline-syncline pair at the south end of the valley and his mapping indicates that the bedrock generally dips away from the valley at the margins. Based on valley morphology and limited waterwell data discussed below we conclude that Round Valley is bounded by normal faults.

Round Valley has a wide (1-2 km), flat, valley floor and Main Creek, which drains the valley, meanders throughout the lower third of the valley. Aggradation of the Provo River above Deer Creek Dam (sec. 3.5.2) may be a partial explanation for a similar fluvial response in Round Valley because the Provo River is the local base level for the valley. However, the gradient of Main Creek steepens just below the narrow canyon at the mouth of the valley suggesting that aggradation in the valley was caused by sediment being supplied to the center of the valley faster than it could be removed through the valley outlet. Shallow exposures in deposits of the valley floor show thin loess over cobbly alluvium. Soil development in these deposits is similar to that in soil H-3 in Heber Valley with cambic and weak argillic horizons developed in the loess and uppermost part of the alluvium. These soils suggest a Holocene and latest Pleistocene (<15 ka) age for these deposits.

Intermediate level erosion surfaces, 210-480 m above the valley floor, and a lower (73 m above valley), long strath terrace remnant capped with gravels in the southeastern end of the valley testify to early periods of lateral fluvial planation, probably during periods of relative tectonic stability (fig. 6.1). Some of these surfaces are probably correlative with older, high surfaces in the Weber drainage (sec. 3.6). The bedrock hill at the northwest end of the long remnant apparently protected it from later erosion. No exposures of the soil developed on this terrace or on higher erosion surfaces were examined. Based on the estimated age of terrace and fan remnants of similar height above the valley floor and similar degree of dissection along the Provo and Weber Rivers (sec. 3.5) the long terrace must be >200 ka and the higher surfaces significantly older. Episodes of fluvial deposition in the valley were controlled by the base level of the Provo River and the



EXPLANATION

- Contact, dashed where approximately located
- Late Quaternary normal faults, dashed where inferred or approximately located
- Late Cenozoic normal faults, dashed where inferred or approximately located
- Trench
- DC-1 Paleomagnetic sampling locality
- Lineament
- Streams
- Drainages
- Water well, with thickness of unconsolidated deposits

Qay Younger alluvium
Qaf Alluvial fan
Qao Older alluvium
Qafo Older alluvial fan
Qc Colluvial deposits
PPu Permian and Pennsylvanian undivided

0 1 2 km

Figure 6.1 Geologic map of Round Valley.

height of bedrock in the creek channel in the narrow canyon at the mouth of the valley. Volcanic clasts with a source in eastern Heber Valley in fluvial sediments exposed in a col between Round Valley and the Provo River Valley (figs. 3.5 and 6.1) show the Provo River once flowed through the col (Baker, 1964) (sec. 3.5.2). The col is now about 67 m above the outlet of Round Valley indicating at least this amount of fluvial downcutting and/or valley floor displacement since the col was occupied by the river. Paleomagnetic analysis of fine colluvial sediments overlying alluvium in a road cut just southeast of the col show that the river occupied the col >730 ka (sec. 3.5.2). Thus, a maximum rate of apparent valley floor lowering is about 0.09 mm/yr.

Extensive coalescing, Quaternary alluvial fans overlie Oquirrh formation within the valley, and hills of Oquirrh formation rise above the fans in several parts of the valley center. The large, coalescing alluvial fans extending out from the mountains bounding Round Valley are interpreted to be both a response to continued displacement on normal faults and climate change. The fans differ from those in most of the other back valleys of the eastern Wasatch Mountains in being more extensive and generally less dissected. Topographic profiles down the fans show the fans on both sides of the valley are convex, but more segments can be recognized in the fan profiles on the northeast side of the valley than in those on the southwest side. On the northeast side, the upper 1/3 of the fans slope about 10-13° and are incised about 5-7 m, the middle half of the fans slope about 5-6° and are incised 3-4 m, while the lower 1/3 to 1/4 of the fans slope about 3-4° and are incised <2 m. Some of the lowest parts of these alluvial fans appear to be graded to a level below the modern floodplain. Segments are not as distinct in profiles of the fans on the southwest side. An upper segment like the upper segment on the northeast side occupies the upper 1/2 to 2/3 of the southwest fan profiles and a segment like the lower segments on the northeast side makes up the lower 1/2 to 1/3 of the profiles. Near the outlet of the valley, 10-m-high scarps have been cut by Main Creek in the distal parts of the alluvial fans as the valley was eroded to keep pace with the Provo River.

6.3.2 Faulting in Round Valley

The triangular facets developed along the moderately steep mountain fronts forming the northeast and southwest margins of the valley are similar to those in Morgan Valley and suggest late Quaternary normal faulting (fig. 6.1). The linearity of the valley margins and the lack of embayed tributary valleys also suggest repeated late Tertiary and probably Quaternary displacement on faults along these 10-km-long valley margins. Two cols with gently sloping sides on Wallsburg Ridge and several high, isolated erosion surfaces at the southeast end of the valley are evidence of an earlier landscape of less relief whose drainage was disrupted by northwest-trending, normal faults (fig. 6.1). The steep escarpment forming the southwest side of Wallsburg Ridge also has the appearance of a late Cenozoic normal fault scarp, but exposures are poor and no faults are mapped in this area (Baker, 1976).

An intra-basin normal fault in Round Valley is defined by isolated, fault-bounded bedrock hills within the valley northeast of Wallsburg (fig. 6.1). These hills are surrounded by older alluvial fan deposits derived from the

northeast margin of the valley. Fan deposits 55 m thick in a waterwell adjacent to the linear, steep-sided, northeast face of these hills suggests they are bounded by a normal fault. Southeast of Wallsburg unconsolidated deposits increase in thickness across the projection of this fault.

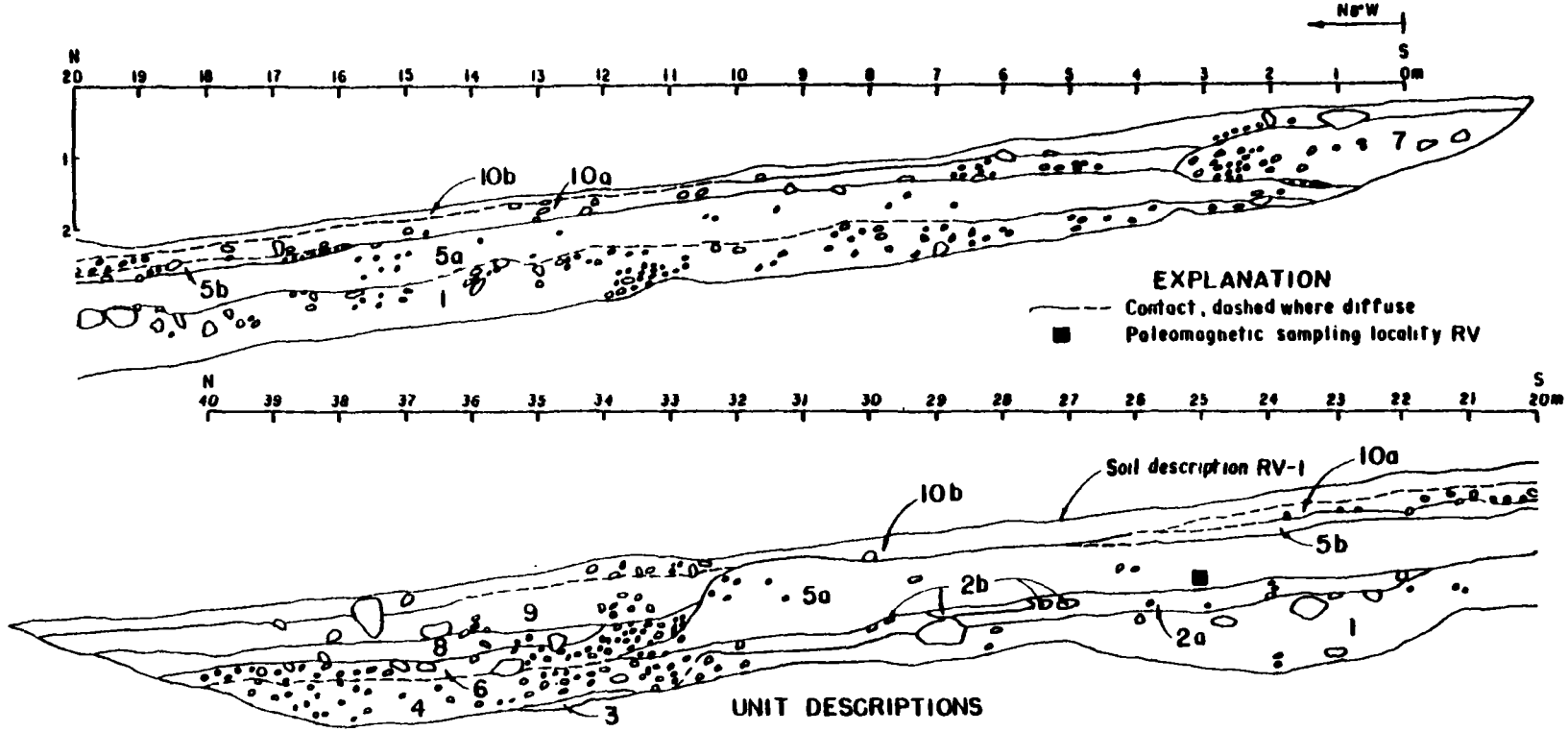
6.3.3 Trenching in Round Valley

Review of aerial photography revealed no fault scarps in unconsolidated deposits along either margin of the valley. However, three, 0.5-1-km-long, northwest-trending vegetation lineaments were observed on the fans along the southwest margin. The lineaments trend discontinuously across the middle portion of two fans parallel to the mountain front in the northwestern part of the valley. A trench excavated across one of the lineaments south of the Main Creek inlet of Deer Creek Reservoir showed a sequence of interbedded debris flow and loess-slopewash units cut by a fan stream channel (fig 6.2). The thickest unit (3a) in the central portion of the trench corresponds with the position of the vegetation lineament which consists of sagebrush that appear to be taller and healthier than sagebrush above and below the lineament. We suggest that the loess-slopewash unit in the middle portion of the trench retains moisture for a longer period than the coarser units (4 and 6-8) in the upper and lower ends of the trench and that greater available moisture produces healthier sagebrush. Thus, the lineament at this site is due to lithologic differences in the near-surface fan sediments -- not to surface displacements. We assume that the other lineaments, which are not as straight or as long as the lineament at this site, are also due to non-tectonic differences in sediment lithologies.

Soils on the fans were only exposed in a few places on the lower half of the fans; they show moderately-developed argillic horizons and stage I to III carbonate on fine-grained loess and debris flow units. Soils are less well-developed on gravelly units and on the most distal portions of the fans. For example, a soil exposed on the distal edge of the fan which was trenched had a 20-cm-thick Bw horizon in Holocene or latest Pleistocene alluvium overlying a 50-cm-thick Btk horizon in late Pleistocene alluvium. Development indices (fig. 3.6) for the soil at the trench site (table 5.3) place the soil in RAG 3 suggesting a latest Pleistocene age for units 1, 2, and 3. Total secondary clay content (8 g/cm^2) suggests a much greater age on the order of 100 ka (fig. 3.2), but the original clay content of debris flow and colluvial units is difficult to estimate. The younger channel-fill unit (6) in the trench has a more weakly developed soil with a cambic horizon suggesting a latest Pleistocene or early Holocene age. There are no exposures in the upper parts of the fans in Round Valley to show if they span as long a time period as the fans on the margins of some of the other back valleys. Weakly developed soils show that parts of the middle and lower portions of the fans have been active in about the last 10-15 ka. These units and the most distal parts of the alluvial fans, like those in Kamas Valley, may be a response the higher effective preciptation during Pinedale deglaciation (for example, Nelson and VanArsdale, 1986).

6.3.4 Conclusions

The large triangular facets and linear bedrock fault scarps bounding Round Valley suggest that late Quaternary surface displacements have occurred in Round Valley. The age of most recent displacement is not constrained; as on



UNIT DESCRIPTIONS

1 Brown (7.5YR 4/4, dry) very gravelly clay, debris flow which contains poorly sorted subangular and subrounded boulders (20%), cobbles (50%) and pebbles (20%) of quartzite and limestone: stage I+ carbonate; very weak sub-horizontal bedding

2a Brown (7.5 YR 5.5/4, dry) gravelly clay, debris flow which contains poorly sorted angular and subangular boulders (<5%), cobbles (10%) and pebbles (15%) of quartzite; stage II+ carbonate in horizontal veins 0.5 - 1cm thick at top of unit and filling tubular pores throughout unit.

2b. Pinkish gray (7.5 YR 6/2, dry) silty sand, forms a discontinuous moderately well-sorted layer and fills possible krotovinas in the top 8cm of layer 2a

3. Brown (10YR 5/3, dry) very gravelly silt; unit (debris flow) is partially exposed at base of trench between stations 33 and 36 and contains poorly sorted subangular cobbles (20%) and pebbles (30%).

4 Brown (7.5YR 5/4, dry) very gravelly silty, clayey sand, channel-fill alluvium which contains moderately sorted subangular to rounded boulders (15%), cobbles (50%) and pebbles (20%) of quartzite

5a. Brown (7.5 YR 5/4, dry) gravelly clay; slopewash derived from loessial deposits which forms the B horizon of the modern soil profile; moderately sorted, contains subangular pebbles (10%) and boulders (<5% near base) of quartzite

5b Brown (7.5YR 5/4, dry) very gravelly clay; slopewash contains moderately sorted subangular and subrounded cobbles (25%) and pebbles (20%) of quartzite.

6 Similar to 4, but contains slightly more boulders (20%) and cobbles (60%).

7. Brown (10YR 5/3, dry) very gravelly silt; debris flow with poorly sorted subangular cobbles (50%) and pebbles (30%) of quartzite.

8 Brown (7.5YR 5/4) silty clay; debris flow which contains poorly sorted, poorly bedded subrounded boulders (20%), cobbles (20%) and pebbles (10%) of quartzite

9 Grayish brown (10YR 5/2, dry) very gravelly sandy clayey silt; slope colluvium which contains poorly sorted angular and subangular boulders (10%), cobbles (20%) and pebbles (20%) of quartzite.

10a Yellowish brown (10YR 5/4, dry) gravelly silt; slope colluvium which contains poorly sorted subangular and subrounded boulders (10%), cobbles (15%) and pebbles (25%) of quartzite.

10b Brown (10YR 5/3, dry) gravelly silt; slope colluvium which contains poorly sorted subangular and subrounded boulders (10%), cobbles (10%) and pebbles (15%) of quartzite. The A horizon of the modern soil is formed in this unit

the Morgan fault (sec. 4.3), displacements may have occurred during the latest Pleistocene or Holocene without scarps being preserved at the fan-escarpment contact. Available exposures suggest that larger areas of the alluvial fans lining Round Valley may be younger than most of the surfaces of alluvial fans in other back valleys; this could be interpreted as evidence for a higher late Quaternary slip rate on valley-bounding faults here than in other valleys. However, air photograph lineaments on the fans on the southwest side of the valley are not related to faulting and the extent of deposition on the fan surfaces is probably controlled to a greater extent by the local base level (the present floodplain of Round Valley) than by displacement along the fan-escarpment contact. The upper parts of fans are more deeply incised and probably older than the middle and lower portions. This suggests the decreasing gradients down the fans are due to aggradation in the valley rather than to renewed deposition due to displacements near the fan-escarpment contact.

Evidence for the reactivation of the Charleston thrust as an extensional fault during the late Cenozoic in Strawbarry Valley to the east (Van Arsdale, 1979a; 1979b; Royse, 1983) and during the mid-Cenozoic west of Heber Valley (Royse, 1983; Hopkins and Bruhn, 1983; Riess, 1985) suggests that extensional faulting in Round Valley may also be related to the reactivation of the Charleston thrust. However, the lack of mid-Cenozoic age deposits in Round Valley suggests that this structural basin developed after mid-Cenozoic reactivation of the Charleston thrust (Deer Creek normal fault) that is discussed in sec. 6.1. If Round Valley and the southwest side of Wallsburg Ridge are structurally analogous to the much larger Strawberry Valley, developed in the same thrust sheet 25 km to the southeast (Nelson and Van Arsdale, 1986), both southwest-facing escarpments may be the scarps of listric normal faults forming grabens or half-grabens.

Limited waterwell data and mapping indicate that no mid-Tertiary volcanic or alluvial deposits are present in Round Valley which we interpret as suggesting that the concealed marginal faults indicated by the landforms in the valley are principally late Cenozoic features. This contrasts with other back valleys in the central Wasatch Mountains which have thicknesses of up to 400 m of mid-Tertiary volcanics and alluvium. Both mid- and late Tertiary deposits fill the back valleys north of the central Wasatch Mountains and we have inferred a history of both late Cenozoic and late Quaternary faulting in the valleys.

The preservation of triangular facets and the linearity and steepness of the footwall escarpment suggest a late Quaternary displacement history similar to that of the Morgan fault. Lacking independent evidence from Round Valley itself we assume that the Quaternary slip rate on faults in Round Valley is similar to that of the Morgan fault, 0.01 to 0.02 mm/yr, for the escarpment morphology is grossly similar. This is consistent with the maximum rate of valley floor lowering or subsidence of 0.09 mm/yr (sec. 6.3.1). We have no independent evidence for the size of individual surface displacements on the faults in Round Valley but as the fault lengths of 10 km for faults in Round Valley and on Wallsburg Ridge are shorter than the 16 km of the Morgan fault, we assume that they are unlikely to be greater than the 0.5 -1.0 m surface displacement events we inferred on the Morgan fault.

6.4 Strawberry Valley

Strawberry valley lies southeast of Heber Valley in the western part of the Uinta basin near the eastern margin of the Basin and Range transition zone. The Strawberry River heads to the west and flows east across the valley to eventually join the Green River. Soldier Creek Dam, completed in 1974 to increase storage in Strawberry Reservoir, is located on the Strawberry River about 11 km downstream of the older Strawberry Dam. In this section we present a summary of the results of the Seismotectonic study for Soldier Creek Dam (Nelson and Martin, 1982).

6.4.1 Geologic setting

In the northern part of Strawberry Valley, the Strawberry thrust fault displaces Paleozoic and Mesozoic sedimentary rocks and projects south below Strawberry Valley where it is covered by early Tertiary sedimentary rocks (Bissell, 1952; 1959; Astin, 1977; Van Arsdale, 1979). The north-trending Strawberry normal fault bounds the east side of Strawberry valley forming a single, 28-km-long, west-facing bedrock escarpment, 100 to 230 m high in the Eocene Uinta formation. While discrete triangular facets are not evident, the steep slope and oversteepening at the base of the escarpment suggest a history of recurrent late Quaternary surface displacements. The Strawberry River and a tributary, Indian Creek, flow from west to east, breaching the escarpment and incising narrow canyons in the footwall of the fault. The absence of a significant north-trending down-to-the-east fault on the west side of the valley suggests that Strawberry valley is a half-graben. The fault has been inferred to be listric merging with the Strawberry or Charleston thrust faults at depth (Van Arsdale, 1979; Royse, 1983). About 11 km further east the north-trending Stinking Springs fault forms an 11 km long escarpment in the Geen River formation similar to that of the Strawberry fault. Near the north end of the main trace of the Strawberry fault, multiple fault scarps in alluvial fan deposits and bedrock are present on a subsidiary trace of the fault.

6.4.2 Seismotectonic investigations

The following summary is drawn from Nelson and Martin (1982) and Nelson and Van Arsdale (1986): Two trenches excavated across a 7-m-high fault scarp in alluvium, subsidiary to the main trace of the Strawberry fault, expose a record of 2 to 3 fault events, each of 1 to 2 m of stratigraphic displacement, over the last 15 to 30 k yrs, but with smaller net vertical tectonic displacement due to graben formation and backtilting. Age estimates based on soil development suggest that the last surface displacement event occurred during the early to middle Holocene. These displacement and age data suggest that the recurrence intervals for surface displacements are in the range 5 to 15 k yrs. The slip rate calculated from estimated displacement across the 7-m scarp is 0.04 to 0.17 mm/yr. In the floodplain of Indian Creek 15 km south of the scarps, cores were recovered from alluvial deposits at depths to 3 m in the footwall of the fault and at depths to 12 m in the hanging wall of the Strawberry fault. Based on ^{14}C and amino acid dating of sediments from the cores the minimum late Quaternary slip rates on the main fault are 0.03 to 0.06 mm/yr.

6.4.3 Conclusions

Evidence from trenching and coring of alluvial sediments indicate that the late Quaternary slip rate on the Strawberry fault is in the range of 0.03 to 0.17 mm/yr which is similar to the slip rates estimated for the Morgan fault in the northern Wasatch Mountains. However, individual displacement events are larger on the Strawberry fault in the range of 1 to 2 m compared with 1 m or less on the Morgan fault; this difference is probably due to the greater length of the Strawberry fault, 28 km compared 16 km for the Morgan fault. The longer fault length and larger surface displacements suggest that larger earthquakes have occurred on the Strawberry fault than on the Morgan fault or other inferred late Quaternary faults in the northern Wasatch Mountains.

6.5 Diamond fork area

South of Heber and Round valleys, the Diamond Fork river heads on the drainage divide at Two Tom Hill west of Strawberry valley and flows east to join the Spanish Fork River before it crosses the Wasatch Mountains and the Wasatch fault east of Spanish Fork, Utah. The proposed Monks Hollow Damsite is located on the Diamond Fork River at Monks Hollow, about 13 km upstream from the confluence with the Spanish Fork River (fig. 5.1). In this section we present a summary of the results of our seismotectonic investigations in the area (Sullivan and others, 1987).

6.5.1 Geologic Setting

East of the Provo segment of the Wasatch fault the north and northeast-trending Wanrhodes syncline and Diamond fork anticline are mapped in the upper plate of the Charleston thrust in the drainage of the Diamond Fork River. The late Cretaceous Price River Formation overlies the Charleston thrust (Baker, 1976), but the folds involve late Cretaceous and early Tertiary sedimentary rocks (Young, 1978). Tilted volcanic rocks overlie the early Tertiary sedimentary rocks in the Wanrhodes syncline (fig. 5.1). These rocks include tuffs and bedded conglomerates referred to as the Wanrhodes volcanics by Baker (1976). They are inferred to be of Oligocene or Miocene age, although they have not been directly dated. Young (1978) considers most of the volcanic rocks north of the Diamond Fork river to be the equivalent of the Tibble Formation (Baker and Crittenden, 1961) and suggests that the volcanic breccias south of the Diamond Fork river are somewhat younger. He also maps Tertiary terraces and pediment gravels, although the deposits have not been dated.

The volcanics are displaced by the northeast-striking Little Diamond Creek fault (Thistle Canyon fault of Pinnnell, 1972; and Young, 1978; fig. 5.1) with cumulative displacement estimated at about 800 m in Paleozoic rocks on the west limb of the Wanrhodes syncline; on the east margin of the syncline the north-striking Sams Canyon fault displaces early Tertiary rocks as much as 1000 m (Baker, 1976; Young, 1978). These two faults are interpreted as outlining the margins of a back valley similar to those further north. Other north-striking faults with displacements less than 50 m are exposed in Mesozoic rocks near the crest of the Diamond Fork anticline along the Diamond Fork river at Monk's Hollow. Baker (1976) suggests that the folded Tertiary rocks with dips of as much as 60° and the near-vertical faults indicate deformation older than Basin and Range type faulting.

6.5.2 Little Diamond Creek fault

The Little Diamond Creek fault is a northeast-striking fault with a mapped length of about 20 km (Baker, 1976; Young, 1978) that shares similar characteristics with late Quaternary faults mapped elsewhere in the back valleys of the Wasatch Mountains. East-flowing drainages have incised canyons along the trace of the fault exposing Paleozoic sedimentary rocks in the footwall and early Tertiary sediments and mid-Tertiary volcanics in the hanging wall (Baker, 1976; Young, 1978). Triangular facets as much as 400 m high are preserved in Paleozoic sedimentary rocks along a 12 km length of the Little Diamond Creek fault. A prominent air-photo lineament is also present at the base of the triangular facets. The deeply incised mid-Cenozoic

Wanrhodes volcanics in the hanging wall of the fault are tilted about 20° to the northwest and form a syncline in the hanging wall of the fault.

Reconnaissance geologic investigations provided no direct evidence of the age of most recent displacement on the fault. Low-sun angle overflights and review of aerial photos at scales of 1:58,000 and 1:15,400 revealed no scarps in consolidated deposits associated with the fault. Reconnaissance geologic mapping shows that only Holocene deposits are preserved across the trace of the fault. On the interfluves between the canyons, colluvial deposits, probably of late Quaternary age, are draped across the trace of the fault at the base of the escarpment. No scarps are preserved in these deposits, but investigations of the Morgan fault in the northern Wasatch Mountains (sec. 4.2) showed that small scarps (<1 m) at or near the base of a similar bedrock escarpment were removed in less than 10 ka. The deformed mid-Cenozoic rocks together with the triangular facets preserved on the footwall escarpment suggest that late Quaternary displacement has occurred on the fault.

6.5.3 Sams Canyon fault

The Sams Canyon fault zone is a 13-km-long, en-echelon zone of high-angle faults on the west side of the Diamond Fork anticline. Near the point of maximum displacement in Tertiary rocks where the Diamond Fork River crosses the fault, an eroded escarpment less than 30 m high in the Price River formation is inferred to mark the position of the fault (Young, 1978). However, for most of its length no escarpment is associated with the fault and locally, along the trace of the fault, the hanging wall is at higher elevation than the footwall (Sullivan and others, 1987). Negative relief is also associated with other high-angle faults in Mesozoic rocks at Monks Hollow (Sullivan and others, 1987).

To further evalute evidence for late Quaternary displacement on the Sams Canyon fault and the faults at Monks Hollow a terrace profile was constructed along the Diamond Fork River (Sullivan and others, 1987). Minimum ages were estimated for the terrace remnants using soil development indices, amino acid ratios, elevation above stream level, and regional correlation. The continuity of the terrace profiles together with these age estimates indicate that there has been no displacement on the faults in at least the last 125 ka. In addition, in an exposure on the right abutment of the proposed Monk's Hollow dam, gravel and sand units within a terrace remnant with an estimated age of at least 250 ka clearly extends uninterrupted across the trace of one of the high-angle faults (Sullivan and others, 1987).

6.5.4 Conclusions

Previous workers (Baker, 1976; Young, 1978) have suggested that the Little Diamond Creek fault is principally a mid-Cenozoic fault with little or no late Cenozoic displacement. No late Cenozoic or late Quaternary datums are preserved across the fault and no suitable trench sites along the fault were identified. However, its prominent topographic expression and the facets preserved along the fault suggest comparison with Morgan fault in the northern Wasatch Mountains. Making an accurate assessment of the potential for surface faulting on the Little Diamond Creek fault is difficult. We have no trench or site-specific data with which to constrain the late Quaternary slip rate, single event size, or age of most recent displacement. Therefore,

based on similarities in late Quaternary fault length and the escarpment morphology, we assume that slip rate and displacement parameters are similar to those calculated for the Morgan fault which are a Quaternary slip rate of 0.01 - 0.02 mm/yr and an average recurrence of surface displacements of 25 - 100 ka.

6.6 Wasatch Plateau

Displacement on the Wasatch fault diminishes at its south end near Gunnison, Utah, where the boundary between the Basin and Range and the Colorado Plateau becomes a wider zone of late Cenozic faults bounding San Pete Valley and disrupting the Wasatch Plateau. Standlee (1982) discusses the role of Sevier age thrust faulting in accomadating late Cenozoic extension in the region and presents cross sections based on seismic reflection profiles and drill holes depicting normal faults joining or being truncated by reactivated low-angle detachments in the subsurface. Based on the results of his field mapping Witkind (1982) emphasizes the role of salt diapirs in the development of normal faults in the region. Both of these conflicting interpretations suggest that normal faults in the region have limited depth extent, which seems to contradict the results of microseismic monitering which include the presence of hypocenters to depths of 15 km, a diffuse pattern which lacks spatial association with mapped faults, and the predominace of normal focal mechanisms with moderate to steep dips (McKee and Arabasz, 1982; Foley and others, 1986).

The Joes Valley graben is the most extensive fault zone on the Wasatch Plateau and scarps in late Plestocene deposits have been documented by Foley and others (1986). The fault zone is more than 100 km long and has been divided into late Quaternary segments with different ages-of most-recent-displacement. Six backhoe trenches were excavated across fault scarps associated with three faults in the Joes Valley graben. Stratigraphic data from these trenches, in addition to scarp heights measured in late Quaternary deposits, were used to estimate apparent vertiacal surface displacements of <1 to >5 m, and average recurrence intervals for surface displacements of 10 to 20 ka (Foley and others, 1986). Three other major fault zones on the Wasatch Plateau exhibit characteristics associated with late Quaternary surface faulting (Foley and others, 1986). These are the Pleasant Valley Snow Lake and Gooseberry fault zones (pl. 1c). Scarps are also present in late Quaternary deposits in Sevier and San Pete Valleys (Witkind and others, 1978).

7. CONCLUSIONS

In this chapter we summarize the results of our geologic and seismologic studies, discuss models of earthquake occurrence in the ISB, and define potential seismic sources. In the final section MCEs and epicentral distances are tabulated for existing and proposed dams in the Regional Study area.

7.1 Late Quaternary faulting in the back valleys of the Wasatch Mountains

Late Quaternary surface faulting manifested as displacements typically of more than a meter on faults tens of kilometers long with recurrence intervals of thousands to tens of thousands of years is concentrated on the east and west margins of the Great Basin (Wallace, 1984). In this study we have found evidence for late Quaternary faulting in the back valleys of the Wasatch Mountains on the eastern margin of the Great Basin (pls. 1A, 1B, and 1C). Middle and late Quaternary slip rates on these faults range from 0.01 - 0.4 mm/yr. This is about an order of magnitude lower than latest Quaternary slip rates for other studied, latest Quaternary faults on the eastern margin of the Basin and Range including the Wasatch fault (Schwartz and Coppersmith, 1984), Teton fault (Gilbert and others, 1983), and Star Valley fault (Piety and others, 1986). Colluvial stratigraphy in trenches has shown that late Quaternary surface displacements on back valley faults range from a maximum of 2 meters on the James Peak fault to a meter or less on the Morgan fault. The identification of late Quaternary normal faults in the back valleys of the northern and southern Wasatch Mountains on pls. 1A and 1B, and on the Wasatch Plateau on pl. 1C, is based on 1) trenching studies that document that late Quaternary surface displacements have occurred, 2) mapping that demonstrates similarities in the stratigraphy of late Cenozoic deposits exposed in the hanging wall of back valley faults, or 3) comparing the morphology of the footwall bedrock escarpments of back valley faults with the escarpments associated with late Quaternary faults identified from trenching studies.

In the central Wasatch Mountains we have identified north-trending normal faults within some of the back valleys (pl. 1B), but we have concluded that surface displacements have not occurred on these faults during the late Quaternary, although early and middle Quaternary displacements may have occurred. Geomorphic evidence indicates that the margins of these back valleys are more sinuous and eroded than valley margins in the northern and southern Wasatch Mountains. We have presented evidence which precludes displacement in at least the last 125 ka for normal faults in Kamas and Keetley valleys. We infer that no late Quaternary displacement has occurred on other similar faults in the central Wasatch Mountains.

Estimates of the thicknesses of early Tertiary basin fill suggest some significant differences in Cenozoic structural relief among the back valleys of the Wasatch Mountains. Throughout the Wasatch Mountains the major portion of the basin fill sequences in the back valleys is of late Eocene and Oligocene age. In Morgan and East Canyon in the northern Wasatch Mountains and adjacent to the Little Diamond Creek fault in the southern Wasatch Mountains, early Tertiary volcanics have an estimated thicknesses of more than 1000 m. In contrast, drill holes and modelling of residual gravity anomalies indicate that the maximum thickness of unconsolidated Tertiary and

Quaternary basin fill is < 500 m in the back valleys of the central Wasatch Mountains.

The diminished basin fill thickness and the lack of evidence for late Quaternary displacement on back valley faults in the central Wasatch Mountains, compared with similar faults in the northern and southern Wasatch Mountains, may be related to differences in inherited subsurface structure. In the northern and southern Wasatch Mountains the structural fabric inherited from early Cenozoic compressional deformation includes stacked imbricate thrust faults that accommodated 50 or more km of crustal shortening in the late Cretaceous and early Tertiary. At the surface, late Cenozoic extensional faults appear to be localized by the positions of ramps in these thrusts and displacement is inferred to be accommodated at depth by reactivation of the thrust planes (for example, Royse and others, 1975; Dixon, 1982; Riess, 1985). While a basal detachment surface has been inferred to underlie the central Wasatch Mountains (Bruhn and others, 1983), thrusts exposed at the surface have limited stratigraphic displacement in rocks equivalent to the lower plates of the major thrusts to the north and south, and no subsurface ramps have been identified. In addition, mid-Cenozoic intrusive rocks are exposed in the central Wasatch Mountains that must intrude detachment surfaces that may underlie the central Wasatch Mountains. Thus, the difference in cumulative Cenozoic displacement and the lack of late Quaternary faults in the central Wasatch Mountains may be related to differences in upper crustal structure.

7.2 Fault displacement models for the back valleys of the Wasatch Mountains

Zandt and Owens (1980) discuss elastic and viscoelastic models of crustal flexure that predict stress fields that are consistent with the observed pattern of seismicity in the Wasatch Front and suggest a causal relationship between seismicity flanking the Wasatch fault and displacement on the fault. Uplift of the Wasatch Mountains is modelled as footwall uplift resulting from isostatic compensation for displacement on the Wasatch fault that extends through the crust to the base of the seismogenic zone. The results indicate that the observed uplift is clearly due to more than isostatic processes. An additional feature of the viscoelastic model is the development of a zone of subsidence east of the uplift that would correspond to the back valleys and imply that back valley faults are not through going crustal features but rather are supra crustal response to bending stresses in the hanging wall of the Wasatch fault.

A somewhat different model of crustal deformation in the Wasatch Front emphasizes the anisotropic fabric in the upper crust in the Wasatch Mountains resulting from Sevier-age thrusting, but still incorporates the basic role of isostatic forces in the development of the Wasatch Mountains (Zandt and Richins, 1981). Cross sections demonstrate the lack of planar clustering of earthquakes east of the Wasatch fault and the lack of association of earthquakes with back valley faults. The focal mechanisms and geodetic data indicate a complex pattern of extension but with regionally significant areas of apparent compression. As there is no evidence for surface fault creep, a model of subsurface fault creep on low-angle faults in the Wasatch Mountains is evaluated in light of the geodetic data. The model considers a rigid block crustal block bounded on the east by the East Cache fault and on the west by the Wasatch fault and indicates that the 0.2 ustrain per year

compression observed at Ogden could be produced by several mm/yr of slip on a hypothetical back valley fault. To evaluate the nature of slip on this postulated back valley fault the net horizontal displacement due to the combined effects of all $M_L > 1.5$ earthquakes was calculated. The result was an order of magnitude less than the geodetically observed strain and they concluded that the major component of the hypothetical block motion was aseismic. Slip rates of several mm/yr are at least an order of magnitude greater than the average late Quaternary slip rate of 0.02 - 0.15 mm/yr estimated for the Morgan or East Cache faults, perhaps suggesting that the longer term strain rate is significantly lower than that measured for the period 1972-1978. Their favored mechanism for the postulated block motion is gravitational as illustrated in their figure 9. Regional extension causes separation across the Wasatch fault which relieves the buttressing effect on the back valley fault in the Wasatch Mountains. This creates gravitational imbalance which is relieved as rotational displacement on the back valley fault. This aseismic motion may be accompanied by some brittle failure and small earthquakes. The focal mechanisms observed in the northern Wasatch Front are consistent with those predicted by the model. Penetrative faulting on systems of many planar normal faults within the crustal blocks east of the Wasatch fault is suggested, and the presence of several decoupling zones within the upper crust that accommodate the low-angle, predominantly aseismic motion is inferred.

Discrete colluvial wedges exposed in trenches on the James Peak and Strawberry faults suggests that discrete single-event displacements have occurred on these faults during the late Quaternary. The colluvial stratigraphy exposed in trenches across the Morgan fault permits various interpretations. The earliest and the most recent events recorded in the trenches displace discrete colluvial horizons 0.5 - 1.0 m. Additional, intermediate-age displacements are also interpreted as resulting from small single-event displacements; however, the trench stratigraphy would permit an interpretation of some aseismic creep. In the back valleys, as elsewhere in the ISB, we assume that these late Quaternary surface displacements have occurred in association with large-magnitude paleoearthquakes.

7.3 Earthquake sources in the ISB

To account for observations of the characteristics of earthquake occurrence in the ISB that are summarized below, two separate earthquake sources are considered for seismotectonic hazard assessments: 1) large-magnitude earthquakes associated with potential surface rupture on late Quaternary faults, and 2) moderate-magnitude, random earthquakes that occur on blind faults--faults not mapped at the surface.

The association of surface displacements and large-magnitude earthquakes is indicated by the fault scarps that formed during three historic earthquakes in the ISB: the 1934 Hansel Valley earthquake of magnitude 6.6 (Shenon, 1936), the 1959 Hebgen Lake earthquake of magnitude 7.5 (Myers and Hamilton, 1964), and the 1983 Borah Peak earthquake of magnitude 7.3 (Crone and Machette, 1984). Important characteristics common to these events are significant to the future occurrence of other large-magnitude earthquakes in the ISB. Doser (1985) concludes that large-magnitude earthquakes nucleate at or near the base of the seismogenic zone (about 15 km), rupture unilaterally to the surface along planar normal faults dipping 45° to 60°, and form fault

scarps on the updip projection of the causative faults. Our current practice is to consider faults with evidence for late Quaternary surface displacement as potential sources of large-magnitude earthquakes. The identification of the faults which are the sources for these earthquakes, as well as their associated MCEs, estimated maximum surface displacements, and average return periods is based on geologic investigations.

Consideration of a moderate-magnitude, random earthquake source is dictated by network monitoring, aftershock studies, and detailed microearthquake studies in the ISB that indicate that small- and moderate-magnitude earthquakes show little or no spatial correlation with late Quaternary faults. Earthquake epicenters plotted on pl. 1 do not show concentrations of activity on the down dip projections of favorably oriented faults; instead, contemporary seismicity occurs as diffuse bands east and west of the Wasatch fault. Studies of recent moderate-magnitude earthquakes including the 1962 Cache Valley earthquake of magnitude 5.7 (Westphal and Lange, 1966), the 1972 Heber earthquake of magnitude 4.7 (Langer and others, 1979), and the 1975 Pocatello Valley earthquake of magnitude 6.0 (Arabasz and others, 1981) indicate that aftershocks of these events occurred at depths of 8 to 12 km on faults that can not be identified at the surface. Recent detailed microearthquake recording in the Basin and Range transition zone in central Utah shows no correlation of earthquake activity with late Quaternary faults (McKee and Arabasz, 1982; Foley and others, 1986). These observations suggest that seismic slip manifested as background seismicity is occurring on moderate- to high-angle segments of blind faults that have no surface expression (Arabasz and Smith, 1981; Arabasz and Julander, 1986).

7.4 Seismic sources and maximum credible earthquakes

Both seismologic and geologic studies indicate that the principal mode of deformation in the region is normal faulting in response to east-west extension. The MCEs (maximum credible earthquakes) discussed in this section are associated with generally north-trending normal faults and are assumed to be principally dip-slip earthquakes.

7.4.1 Late Quaternary faults

One of the principal goals of this study was to identify potential earthquake sources in the back valleys of the Wasatch Mountains. We have documented the presence of late Quaternary (and very limited Holocene) faulting, which we utilize in targeting sources of large-magnitude earthquakes in the Regional Study area.

7.4.1.1 Wasatch fault

The Wasatch fault is the principal source for large-magnitude earthquakes in the Utah portion of the ISB. It has experienced larger, Holocene, single-event surface ruptures with a shorter estimated average return period than other late Quaternary faults in the region.

Detailed geologic studies of the Wasatch fault, summarized by Schwartz and Coppersmith (1984), indicate that at least six individual segments of the Wasatch fault rupture independently. The slip rates and return periods for these segments are shown in table 7.1. Subsequent investigations summarized

by Machette (1987) suggest that the Provo segment of Schwartz and Coppersmith (1984) may consist of as many as three segments (pl. 1B). More recent trench investigations of the central segments of the Wasatch fault yield slip rate and average return period estimates consistent with those in table 5 (Nelson and others, 1987; Personius and Gill, 1987; Machette and Lund, 1987).

Table 7.1 Slip rates and average return periods for surface displacements on individual segments of the Wasatch fault (from Schwartz and Coppersmith, 1984).*

Wasatch fault segment	Segment length (km)	Late Quaternary slip rate (mm/yr)	Average return period (yrs)
Collinston	>30	no data	no data
Ogden	70	1.1 to 1.8	2000
Salt Lake	35	.56 to 1.4	2400 to 3000
Provo	55	.85 to 1.0	1700 to 2600
Nephi	35	1.17 to 1.46	1700 to 2700
Levan	40	<0.35 +/-.05	>5,000 ?

*Segments located on plate 1.

The largest historical earthquakes in the ISB, the 1959 Hebgen Lake earthquake with a magnitude of 7.5 and the 1983 Borah Peak earthquake with a magnitude of 7.3 are considered to be representative of the maximum-magnitude earthquake expected in the ISB (Doser, 1984). These earthquakes are associated with surface displacements of > 2 m and surface rupture lengths of > 20 km. In previous USBR studies we have estimated MCEs of magnitude 7 1/2 for late Quaternary faults in the ISB with surface rupture lengths of > 20 km and/or evidence of maximum individual surface displacements of > 2 m (Gilbert and others, 1983; Piety and others, 1986; Foley and others, 1986). Late Quaternary fault rupture lengths are 30 to 70 km and average surface displacement per event is > 2 m for the central segments of the fault (table 7.1). These rupture parameters suggest that paleoearthquakes with magnitudes of 6 3/4 to 7 1/2 have occurred on the Wasatch fault during the Holocene (Schwartz and Coppersmith, 1984). Concurring with this interpretation, we estimate an MCE of magnitude 7 1/2 for the Wasatch fault (table 7.2). This MCE should be considered a dipslip earthquake occurring on any of the segments of the Wasatch fault. The strikes of the individual segments vary from about N30°E to N20°W (fig. 7.1); all segments dip 45° to 60° to the west.

7.4.1.2 James Peak and East Cache faults

Late Quaternary displacement on the James Peak normal fault at the south end of Cache Valley is indicated by 7-m-high scarp in late Quaternary deposits. Trenching showed that two surface faulting events, each with about 2 m of vertical displacement have occurred in the last 140 ka (sec. 4.1 and Nelson and Sullivan, 1987). The average return period of surface displacements is at least 50 kyr, but recurrence may be non-uniform and the most recent event may have occurred as recently as 30 ka. The James Peak fault has a length of only about 7 km at the base of James Peak at the southern end of the East Cache fault. Individual surface ruptures of 2 m would most likely be associated with surface ruptures > 20 km in length, suggesting that a greater scarp length ruptured when the James Peak scarps formed.

The north-trending East Cache fault has a length of more than 60 km in Utah. The prominent facets on the footwall escarpment suggest that late Quaternary displacements have occurred on the entire length of the fault. Late Quaternary displacement has been demonstrated on the East Cache fault near Logan, Utah (pl. 1A) where Swan and others (1983) concluded that two, 1- to 2-m, post-Bonneville displacement events have occurred. The fault continues south to James Peak where it joins the James Peak fault, but no scarps are present in Bonneville deposits that post-date the estimated age of the most recent event recorded by the James Peak scarp.

We conclude that surface ruptures on James Peak fault would include rupture on the southern portion of the East Cache fault. At Logan 1- to 2-m displacements are associated with a 10-km-long scarp, but we are unable to constrain the rupture length associated with the 2 m displacements at James Peak. As 2 m displacements are associated with the Wasatch fault which has an MCE of magnitude 7 1/2, we also estimate an MCE of magnitude 7 1/2 for the James Peak and the East Cache faults.

7.4.1.3 The Morgan fault

Trenching studies have shown that Quaternary and Holocene surface displacements have occurred on the Morgan fault indicating that it is a potential source of large-magnitude earthquakes. We have estimated the Quaternary slip rate to be 0.01 to 0.02 mm/yr (sec. 4.2 and Sullivan and Nelson, 1987). In order to provide a conservative estimate of the MCE associated with the Morgan fault we consider the fault length to be 16 km, encompassing the possibility of simultaneous rupture on the entire fault. Data on single event size is available for only one site along the Morgan fault, which we consider to be representative of all sections of the Morgan fault. Based on the geometry of colluvial units displaced by the Morgan fault at the Robeson Springs site, the size of individual surface displacements is 0.5 - 1.0 m (sec. 4.2).

The magnitude and displacement parameters for the Borah Peak and Hebgen Lake earthquakes provide an upper bound for MCEs associated with late Quaternary faults in the region. Shorter fault length and smaller surface displacement events associated with the Morgan fault suggest that paleoearthquakes were of smaller magnitude than those historic earthquakes; therefore, we caonsider an MCE with a smaller magnitude to be appropriate. We estimate an MCE of magnitude 6 3/4 to 7 for the Morgan fault (table 7.2). A representative

example of such an earthquake is the 1934 Hansel Valley earthquake which had an estimated magnitude of 6.6, surface rupture over a distance of about 11 km, and maximum surface displacement of 0.5 m. This MCE for the Morgan fault is also consistent with estimates from Bonilla and others (1984) using fault length of 16 km and maximum surface displacement of 1 m.

7.4.1.4 The Strawberry fault

The Strawberry fault is a 28-km-long, north-striking normal fault (pl. 1B). An estimated late Quaternary slip rate of 0.07 - 0.4 mm/yr based on trenching of fault scarps associated with the fault and radiocarbon dating of stream sediments cored in a drainage that crosses the main escarpment (Nelson and Martin, 1982) indicate that late Quaternary surface displacements have occurred on the fault; therefore, the Strawberry fault is considered a potential source of large-magnitude earthquakes. If simultaneous rupture of the entire fault is assumed, the fault length is similar to the length of individual segments of the Wasatch fault. However, trench data indicates that the most recent scarp-forming events resulted from vertical displacements ranging from 0.1 m to 1.8 m; the trench stratigraphy suggests that individual displacements were probably no greater than about one meter (Nelson and Martin, 1982). This displacement data suggests smaller paleoearthquakes than those inferred for the Wasatch fault. Nelson and Martin (1982) have assigned an MCE of magnitude 7 to the Strawberry fault which is adopted in this report (table 7.2).

7.4.1.5 Back valley faults in the northern and southern Wasatch Mountains

In the northern and southern Wasatch Mountains we have documented late Quaternary surface displacements on the Morgan fault, the James Peak fault, and the Strawberry fault. On the basis of similarities in the basin fill stratigraphy and the morphology of footwall escarpments, we have inferred that late Quaternary normal faults are present in other back valleys. Lacking evidence from detailed investigations in these other valleys, we have assumed that the late Quaternary slip rate, average single event displacement, and average return period of surface displacements are similar to the Morgan fault. Mapping shows that late Quaternary fault length for these faults is 20 km or less. This maximum fault length suggests that MCEs associated with these faults should be no greater than the magnitude 7 estimated for the Morgan and Strawberry faults. We have estimated MCEs of magnitude 6 3/4 to 7 and 6 1/2 to 6 3/4 for these back valley faults (Table 7.2).

7.4.1.6 Back valley faults in the central Wasatch Mountains

Based on trenching and mapping of late Quaternary deposits overlying concealed normal faults, and the eroded appearance of footwall escarpments in the back valleys of the central Wasatch Mountains, we have concluded that no late Quaternary (<125 ka) displacements have occurred on these faults. This evidence may reflect extremely long recurrence intervals for surface displacements on these faults (>125 ka), or the inactivity of the faults. In either case, we do not consider these faults to be potential sources of large-magnitude earthquakes.

Table 7.2 Maximum Credible Earthquakes for late Quaternary faults in the Back Valleys of the Wasatch Mountains

FAULT	Late Quaternary Rupture Length (km)	Average Single Event Displacement (m)	Late Quaternary Slip Rate (mm/yr)	MCE (Ms)	Estimated Average Return Period (ka)
Wasatch a)	30 - 70	1.6 - 2.3	0.56 - 1.46	7 1/2	1.7 - 3.0
East Cache b)	10	1.4	0.1 - 0.2	7 1/4	7.2
James Peak c)	>7	2	0.03	7 1/2 c)	70
Strawberry d)	28	0.1 - <1.8	0.07 - 0.4	7	5 - 15
Morgan	16	0.5 - 1.0	0.01 - 0.02	6 3/4 to 7	25 - 100
Ogden Valley	10 - 18	e)	e)	6 3/4 to 7	e)
East Canyon	12	e)	e)	6 1/2 to 6 3/4	e)
Round Valley	10	e)	e)	6 1/2 to 6 3/4	e)
Little Diamond Creek	20	e)	e)	6 3/4 to 7	e)

a) for individual segments from Schwartz and Coppersmith (1984)
b) Swan and others (1983b)
c) MCE assumes simultaneous rupture on the East Cache fault (sec. 4.3.2.6)
d) Nelson and Martin (1982), Nelson and VanArsdale (1986)
e) Assumed to be similar to values for the Morgan fault

7.4.2 Random earthquake

A moderate-magnitude earthquake is considered a potential seismic source for all sites within the back valleys of the Wasatch Mountains. As the threshold for surface faulting in the ISB appears to be within the magnitude range 6 to 6 3/4 (sec. 2.5.2), we estimate an MCE of magnitude 6 to 6 1/2 for this earthquake source. Based on calculations of probabilistic epicentral distances from geologic and seismologic data (sec. 2.6.2), we have concluded that for annual probabilities of occurrence of 1/50 000 to 1/100 000 an earthquake of magnitude 6 or greater could occur within 5 km of any site. Therefore the magnitude 6 to 6 1/2 random earthquake should be considered a local event that could occur in the immediate vicinity of any site within the back valleys. This MCE could occur on a blind fault or on any of the favorably-oriented faults in the region.

7.5 Maximum Credible earthquakes and USBR dams

Fourteen existing USBR dams and two proposed dams are located on pls. 1A, 1B, and 1C within the Regional Study area. On the basis of our investigations of late Quaternary faulting in the area and our analysis of historical seismicity in this portion of the ISB, we have previously provided seismotectonic conclusions for some of these sites. In the following sections we provide summaries of these conclusions for each dam including an assessment of the potential for surface displacements in the dam foundations, the identification of seismic sources, and an estimate of the MCE associated with each source. A local moderate-magnitude random earthquake source is recommended for each of the damsites in addition to the late Quaternary faults that are the sources of large-magnitude earthquakes. The fault parameters used to estimate the MCEs are presented in table 7.2; epicentral distances from the dams to the closest approach of the faults are measured on plates 1A, 1B, and 1C. In the following sections we provide tables of MCEs for each of the dams which also include estimates of the average return periods for the MCEs that can be used in risk analyses for the dams. For a number of the sites we refer to Seismotectonic Reports or technical memorandums that have previously been issued.

7.5.1 Newton Dam

Newton Dam is located in Cache Valley in the northern Wasatch Mountains east of the Wasatch fault (pl. 1A). The principal late Quaternary fault in Cache Valley, the East Cache fault, bounds the east side of the valley. The upper Tertiary Salt Lake Formation fills the valley and is overlain by Quaternary deposits of Lake Bonneville and younger fluvial deposits. The dam is located near the center of the valley west of Little Mountain, a horst block within the valley that is bounded on the east side by the Dayton fault and on the west side by the Newton fault.

7.5.1.1 Site geology

Site-specific seismotectonic investigations for Newton Dam, completed in 1982 and discussed in our memorandum of August 12, 1982, focused on detailed mapping in the vicinity of the dam. The results of this mapping are shown on fig. 7.1. The principal conclusions from this mapping and the gravity data of Peterson and Oriel (1970) are as follows:

1) Different dip directions in exposures of the Salt Lake Formation near Newton Dam, together with evidence of a closed gravity low west of Little Mountain, indicate that a 20-km-long, N20°-30°W striking, down-to-the-west, concealed normal fault (the Newton fault) displaces the Salt Lake Formation on the west side of Little Mountain; the most likely location for the fault is about 300 m east of the dam foundation.

2) Scarps in the vicinity of the dam represent shorelines of Lake Bonneville; no fault-related scarps or lineaments are present.

3) Shorelines between the Provo (4800 ft) and Bonneville (5180 ft) levels of Lake Bonneville can be traced across the Newton fault (fig. 7.1) showing that there has been no surface displacement on the Newton fault in at least the last 14 to 17 ka.

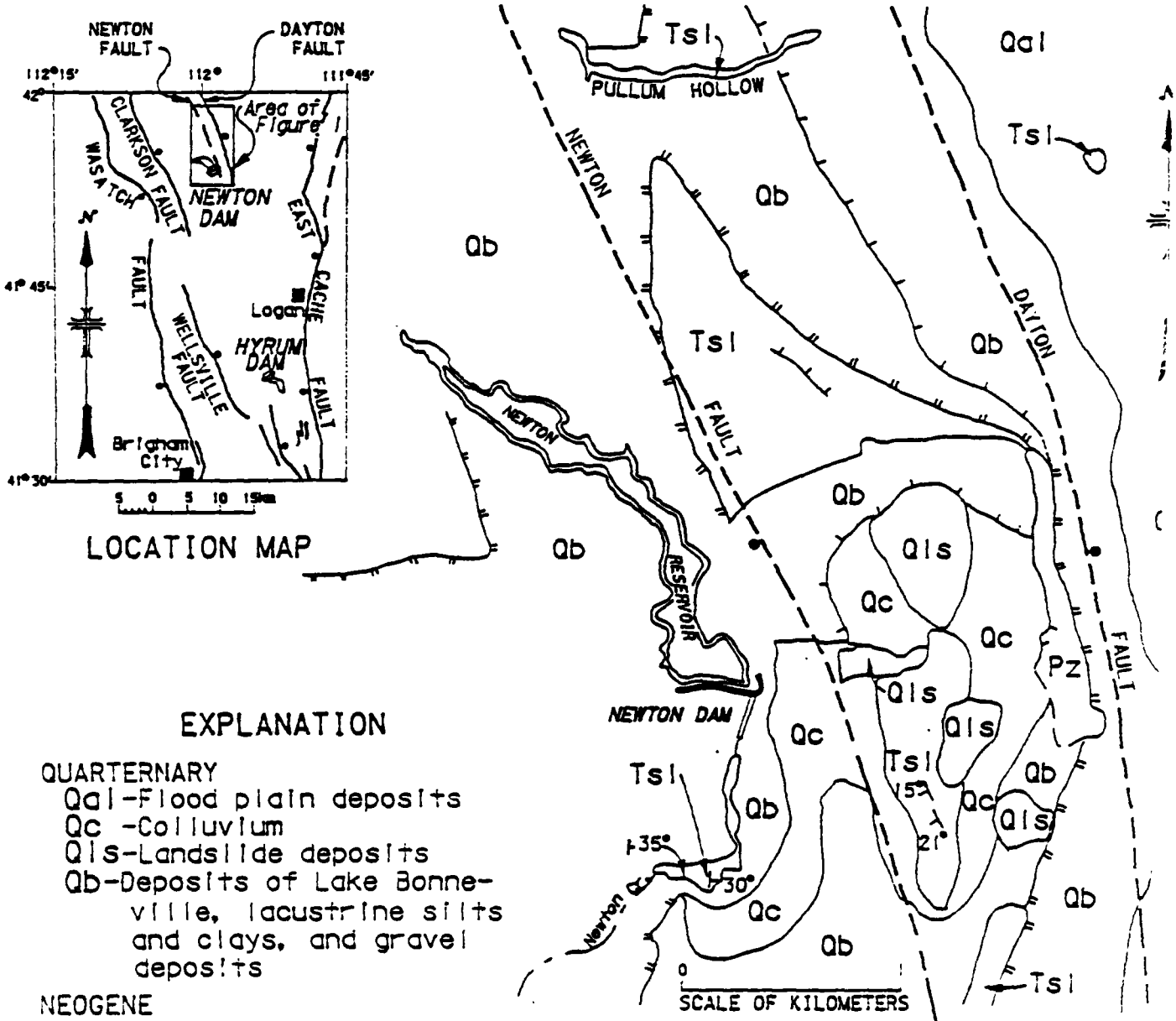


FIGURE 7.1 - GEOLOGIC MAP OF NEWTON DAM AND RESERVOIR AREA

4) No prominent linear escarpment with triangular facets is associated with the Newton fault suggesting that it is not a late Quaternary fault.

7.5.1.2 Seismic sources and MCEs

There is no evidence that latest Quaternary surface displacements have occurred on the Dayton fault or the Newton fault. As these faults also lack the morphologic characteristics of other late Quaternary faults in the back valleys of the Wasatch Mountains, they are not considered potential seismic sources for large-magnitude earthquakes.

The principal seismic sources for Newton Dam include an MCE of magnitude 7 1/2 on the Wasatch fault at a distance of 10 km, and a local random earthquake of magnitude 6 to 6 1/2 (table 7.3). The East Cache fault is also a potential source for a large-magnitude earthquake, but as it is located further from the dam (20 km) than the Wasatch fault, it is not included in table 7.3.

Table 7.3 Maximum credible earthquakes for Newton Dam

Earthquake source	MCE (M_S)	Closest approach to site (km)	Focal depth (km)	Average return period (1000 yrs)
Wasatch fault	7 1/2	7	10-15	no data*
Random earthquake	6 to 6 1/2#	local	8-15	**

* no slip rate or return period data available yet for the Collinston segment
M_L
** for an estimated annual probability of .00001 to .00002

7.5.1.3 Surface faulting

As there is no evidence that late Quaternary surface displacements have occurred on the Newton fault, we have concluded that surface faulting does not pose a hazard to Newton Dam.

7.5.2 Hyrum Dam

Hyrum Dam is located in the southern portion of Cache Valley about 30 km south of Newton Dam (pl. 1A). The the only known late Quaternary faults in the valley are the East Cache fault and its southwestern continuation the James Peak fault. The dam and reservoir are located at the north end of Hyrum Bench, a platform developed on the east-dipping Salt Lake Formation that forms the foundation of the dam.

7.5.2.1 Site geology

Site-specific seismotectonic investigations for Hyrum Dam, completed in 1982 and discussed in our memorandum of September 9, 1982, focused on detailed mapping of known and suspected faults in the vicinity of the dam. The results of the mapping are shown on fig. 7.2. The principal results from this investigation are as follows:

1) The Willow Grove fault, a north-trending normal fault that projects toward Hyrum Dam does not extend into the vicinity of the dam.

2) East-west striking shear zones exposed in a roadcut near the dam most likely have a non-tectonic origin.

3) Review of aerial photography did not reveal fault-related scarps or lineaments in the vicinity of the dam.

4) We have no evidence with which to determine the existence of a previously mapped, inferred fault on the eastern margin of Hyrum bench about 3 km from the dam, but if it is present it would be antithetic to the East Cache fault.

7.5.2.2 Seismic sources and MCEs

The principal seismic sources for Hyrum Dam include an MCE of magnitude 7 1/2 on the Wasatch fault at a distance of 12 km, an MCE of magnitude 7 1/2 on the East Cache fault at a distance of 7 km (encompassing antithetic faults), and a local random earthquake of magnitude 6 to 6 1/2 (table 7.4).

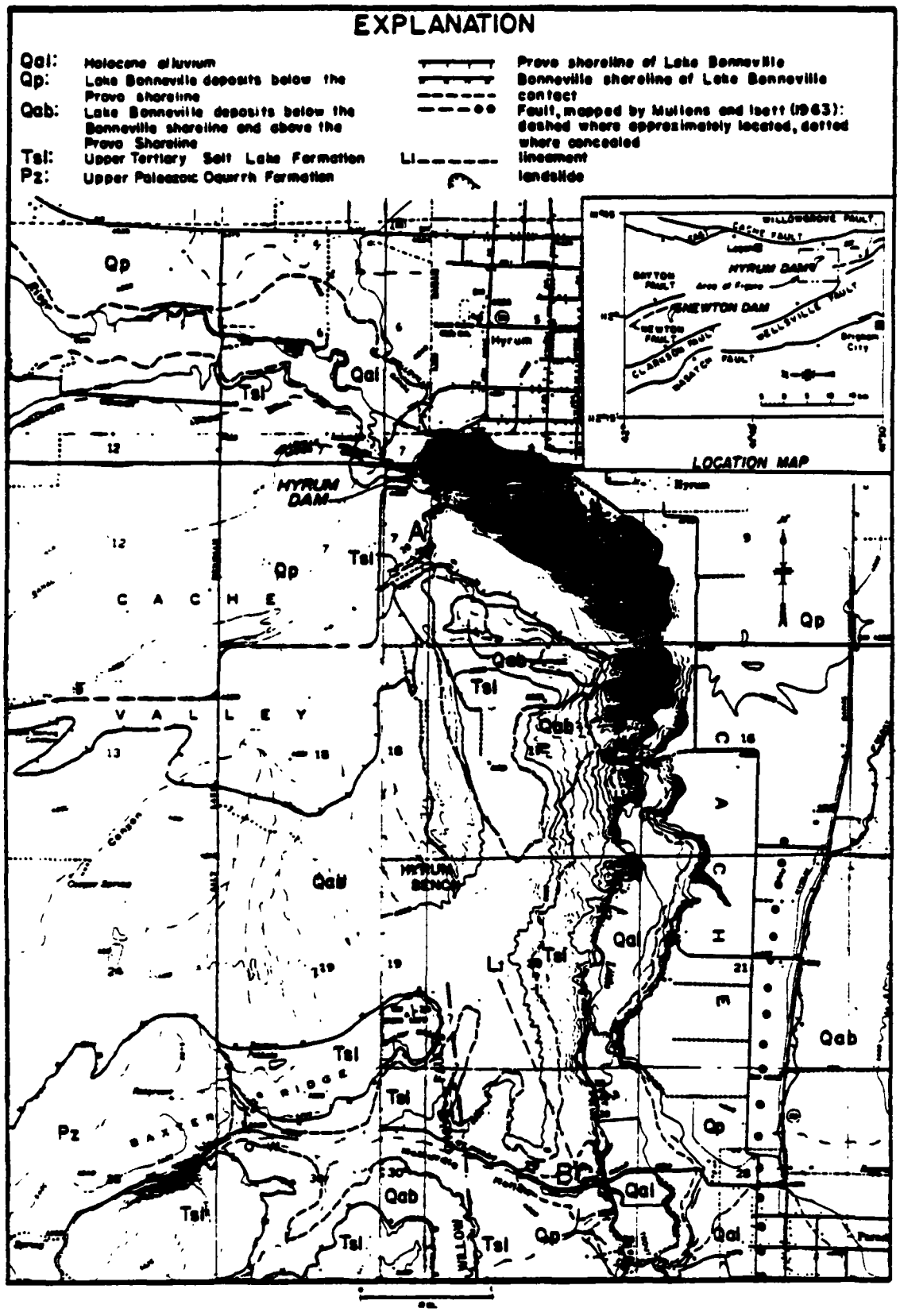
Table 7.4 Maximum credible earthquakes for Hyrum Dam

Earthquake source	MCE (M_S)	Closest approach to site (km)	Focal depth (km)	Average return period (1000 yrs)
Wasatch fault	7 1/2	13	10-15	no data*
East Cache fault	7 1/2	7	10-15	7.2
Random earthquake	6 to 6 1/2#	local	8-15	**

* no slip rate or return period data available yet for the Collinston segment
\# M_L
** for an estimated annual probability of 0.00001 to 0.00002

7.5.2.3 Surface faulting

No late Quaternary faults are known in the vicinity of the dam; therefore, surface faulting is not considered to pose a hazard to Hyrum Dam.



NOTES Fieldwork by T. Sullivan, E. Bartter, L. Foley, June 14, 1982

Modified from T.E. Mullens and G.A. Izett, 1963, Geology of the Paradise Quadrangle, Utah, U.S. Geological Survey, GQ-188

FIGURE 7.2 GEOLOGIC MAP OF HYRUM DAM AND RESERVOIR AREA

7.5.3 Causey Dam

Causey Dam is located east of the northern Wasatch Mountains about 15 km east of Ogden Valley (pl. 1A). In this area folded and faulted Paleozoic sedimentary rocks are unconformably overlain by the gently folded, latest Cretaceous to Eocene Evanston and Wasatch Formations.

7.5.3.1 Site geology

Reconnaissance site-specific seismotectonic investigations for Causey Dam are reported in our technical memorandum of May 21, 1986 (SAR-1632-49). Figure 7.3 is a geologic map of the Causey Dam area modified from Hintze (1980). The principal results from our site-specific investigations are as follows:

1) There are no faults that displace the Tertiary rocks or Quaternary deposits in the vicinity of the dam.

2) A 150-m-wide (500 ft) shear zone in Paleozoic rocks exposed in the spillway excavation for the dam does not appear to displace the Tertiary rocks or Quaternary terrace deposits near the dam.

7.5.3.2 Seismic sources and MCEs

Seismic sources and associated MCEs for Causey Dam are shown in table 7.5.

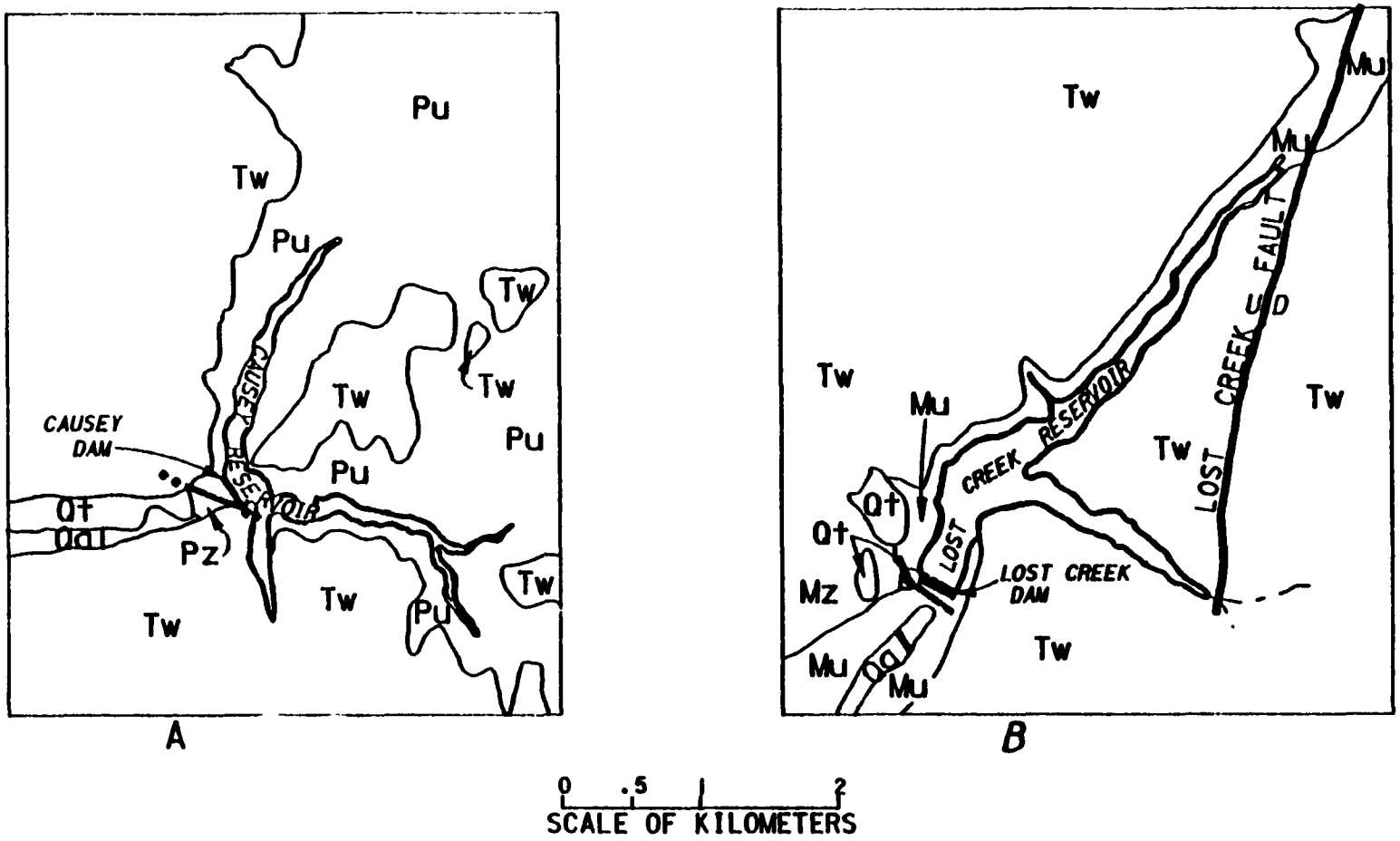
Table 7.5 Maximum credible earthquakes for Causey Dam

Earthquake source	MCE (M_S)	Closest approach to site (km)	Focal depth (km)	Average return period (1000 yrs)
Wasatch fault	7 1/2	28	10-15	2*
James Peak/ East Cache faults	7 1/2	21	10-15	70
Ogden Valley faults	6 3/4 to 7	16	10-15	25-100
Random earthquake	6 to 6 1/2#	local	8-15	**

* Ogden segment of Schwartz and Coppersmith (1984)
M_L
** for an estimated annual probability of 0.00001 to 0.00002

7.5.3.3 Surface faulting

No late Quaternary faults are known in the vicinity of the dam; therefore, surface faulting is not considered to pose a hazard to Causey Dam.



EXPLANATION

Qal	*Quaternary stream alluvium*
Qt	*Quaternary terrace deposits*
Tw	*Lower Tertiary Wasatch and Evanston Formations*
Mu	*Mesozoic sedimentary rocks*
Pu	*Paleozoic sedimentary rocks*
—··	*Fault, dotted where concealed*

FIGURE 7.3 - GEOLOGIC MAPS OF CAUSEY DAM (A) AND LOST CREEK DAM (B) AREAS

7.5.4 Lost Creek Dam

Lost Creek Dam is located in the northern Wasatch Mountains about 25 km southeast of Causey Dam. In exposures along Lost Creek in the vicinity of the dam, nearly flat-lying conglomerates of the early Tertiary Wasatch Formation unconformably overlie Triassic sedimentary rocks.

7.5.4.1 Site geology

Reconnaissance site-specific seismotectonic investigations are reported in our technical memorandum of March 24, 1986 (SAR-1632-114). During construction of the dam, a fault and several shear zones were found in the dam foundation in the Triassic Twin Creek Limestone. They trend about east-west and project beneath undisplaced Tertiary rocks and Quaternary terrace remnants (fig. 7.3). The Lost Creek fault is a north-striking normal fault located about 2 km east of the dam that displaces Mesozoic rocks and the overlying Wasatch Formation (fig. 7.3). No bedrock escarpment or fault scarps in latest Quaternary stream deposits are associated the fault. As these features are characteristic of late Quaternary faults in the back valleys, we concluded that no late Quaternary displacements had occurred on the Lost Creek fault; therefore, it is not considered a potential source of large-magnitude earthquakes.

7.5.4.2 Seismic sources and MCEs

Seismic sources and associated MCEs for Lost Creek Dam are shown in table 7.6.

Table 7.6 Maximum credible earthquakes for Lost Creek Dam

Earthquake source	MCE (M_S)	Closest approach to site (km)	Focal depth (km)	Average return period (1000 yrs)
Wasatch fault	7 1/2	44	10-15	2*
Morgan fault	6 3/4 to 7	25	10-15	25-100
Random earthquake	6 to 6 1/2#	local	8-15	**

* Ogden segment of Schwartz and Coppersmith (1984)
M_L
** for an estimated annual probability of 0.00001 to 0.00002

7.5.4.3 Surface faulting

No late Quaternary faults are known in the vicinity of the dam; therefore, surface faulting is not considered to pose a hazard to Lost Creek Dam.

7.5.5 Pineview Dam

Pineview Dam is located in the northern Wasatch Mountains on the Ogden River upstream of Ogden, Utah (pl. 1A). Pineview Reservoir extends upstream into Ogden Valley, a back valley bounded on the west side by east-dipping late Quaternary faults discussed in sec. 4.4 and shown on fig. 7.4. Our technical memorandum of July 14, 1987 (SAR-1632-107) earlier provided seismotectonic conclusions for the dam.

7.5.5.1 Site Geology

Paleozoic sedimentary rocks in the upper plate of the Absoraka thrust are exposed in Ogden Canyon and form the foundation of the dam. About 2 km upstream of the dam inferred late Quaternary normal faults bound the southwest margin of Ogden Valley, but mapping shows that no late Quaternary faults are present in the dam foundation (fig. 7.4).

7.5.5.2 Seismic sources and MCEs

Seismic sources and associated MCEs for Pineview dam are shown in table 7.7.

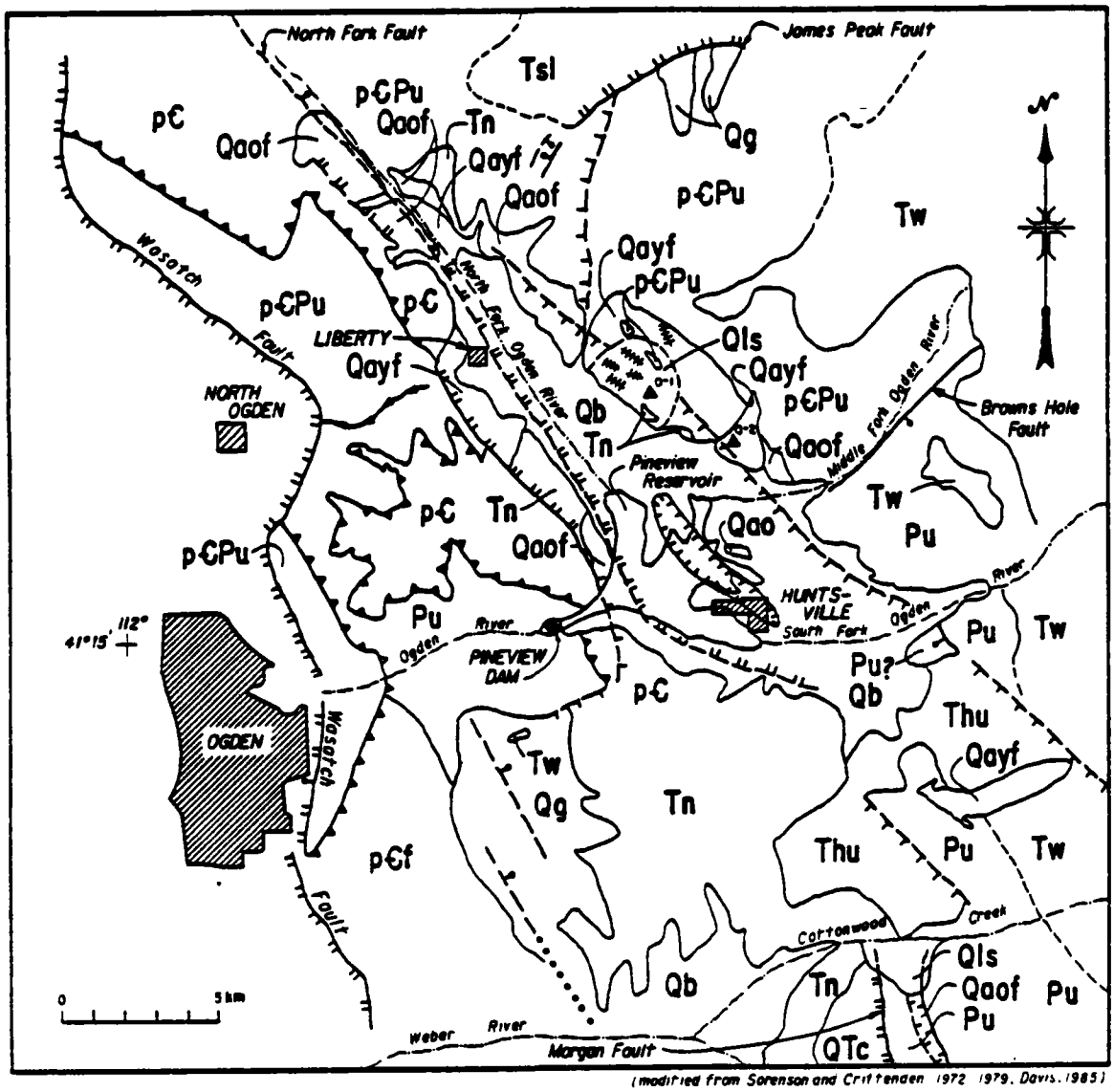
Table 7.7 Maximum credible earthquakes for Pineview Dam

Earthquake source	MCE (M_S)	Closest approach to site (km)	Focal depth (km)	Average return period (1000 yrs)
Wasatch fault	7 1/2	8	10-15	2*
Ogden Valley faults	6 3/4 to 7	2	10-15	25-100
Random earthquake	6 to 6 1/2#	local	8-15	**

* Ogden segment of Schwartz and Coppersmith (1984)
\# M_L
** for an estimated annual probability of 0.00001 to 0.00002

7.5.5.3 Surface faulting

No late Quaternary faults are known in the immediate vicinity of the dam; therefore, surface faulting is not considered to pose a hazard to Pineview Dam.



(modified from Sorenson and Crittenden 1972 1979, Davis, 1985)

EXPLANATION

- Contact, dashed where approximately located.
- Late Quaternary normal faults, dashed where inferred or approximately located.
- Late Cenozoic normal faults, dashed where inferred or approximately located.
- Cenozoic normal faults, dashed where inferred or approximately located.
- Willard Thrust fault
- Ogden Thrust fault
- Eden water gap
- Maximum residual gravity anomaly from Stewart (1958)
- Lineaments (Sorenson and Crittenden, 1979)
- Streams
- Soil test pit

QUATERNARY

- Qayf — Younger alluvial fan deposits.
- Qb — Lake Bonneville sediments and Holocene alluvium, includes post-Bonneville alluvium.
- Qls — Landslide
- Qaof — Older alluvial fan deposits.
- Qao — Pre-Bonneville alluvium.
- Qg — Glacial deposits

TERTIARY

- Thu — Pliocene? Huntsville fanglomerate.
- Tsl — Neogene Salt Lake formation
- Tn — Late Eocene-Oligocene Norwood Tuff.
- Tw — Eocene Wasatch formation.

PRE-TERTIARY

- Pu — Paleozoic undivided.
- pCPu — Paleozoic and Precambrian undivided.
- pCf — Precambrian Farmington Canyon Complex.
- pC — Precambrian in upperplate Willard Thrust, mostly Brigham Group.

Figure 7.4 Geologic map of Ogden Valley including Pineview Dam and Reservoir.

7.5.6 Arthur V. Watkins Dam (formerly Willard Dam)

Arthur V. Watkins Dam is located on the west side of the Great Salt Lake northwest of Ogden, Utah (pl. 1A). Our technical memorandum of July 3, 1985 (SAR-1632-35) earlier provided seismotectonic conclusions for Arthur V. Watkins Dam.

7.5.6.1 Site Geology

This 23-km-long offstream storage structure was constructed on unconsolidated late Quaternary lacustrine and alluvial deposits less than 2 km east of the Wasatch fault. The Wasatch fault is the principal seismic source for the structure.

7.5.6.2 Seismic sources and MCEs

The dam is located 2 km east of the southern end of the Ogden segment of the Wasatch fault. The fault dips west under the dam and reservoir.

Table 7.8 Maximum credible earthquakes for Arthur V. Watkins Dam

Earthquake source	MCE (M_S)	Closest approach to site (km)	Focal depth (km)	Average return period (1000 yrs)
Wasatch fault	7 1/2	2	10-15	2*

* Ogden segment of Schwartz and Coppersmith (1984)

7.5.6.3 Surface faulting

Although the surface rupture of 2 to 3 m anticipated in association with the MCE on the Wasatch fault will most likely occur about 2 km east of the dam and reservoir, secondary displacements of as much as a meter could occur on splay faults below Arthur V. Watkins Dam and Reservoir.

7.5.7 East Canyon Dam

East Canyon Dam is located in the northern Wasatch Mountains east of the southeast margin of Morgan Valley (pl. 1B). The existing dam was constructed about 90 m downstream of the prominent escarpment of the East Canyon fault. Our technical memorandum of August 27, 1987 (SAR-1632-127) earlier provided seismotectonic conclusions for East Canyon Dam.

7.5.7.1 Site Geology

Bedrock in the foundation of the dam is the conglomerates of the late Cretaceous Echo Canyon Formation that dips about 50° northwest and forms the prominent East Canyon escarpment that extends both north and south of the dam (fig. 7.5). The 28-km-long, northeast-trending escarpment forms the footwall of the late Cenozoic East Canyon fault. Based on the presence of triangular

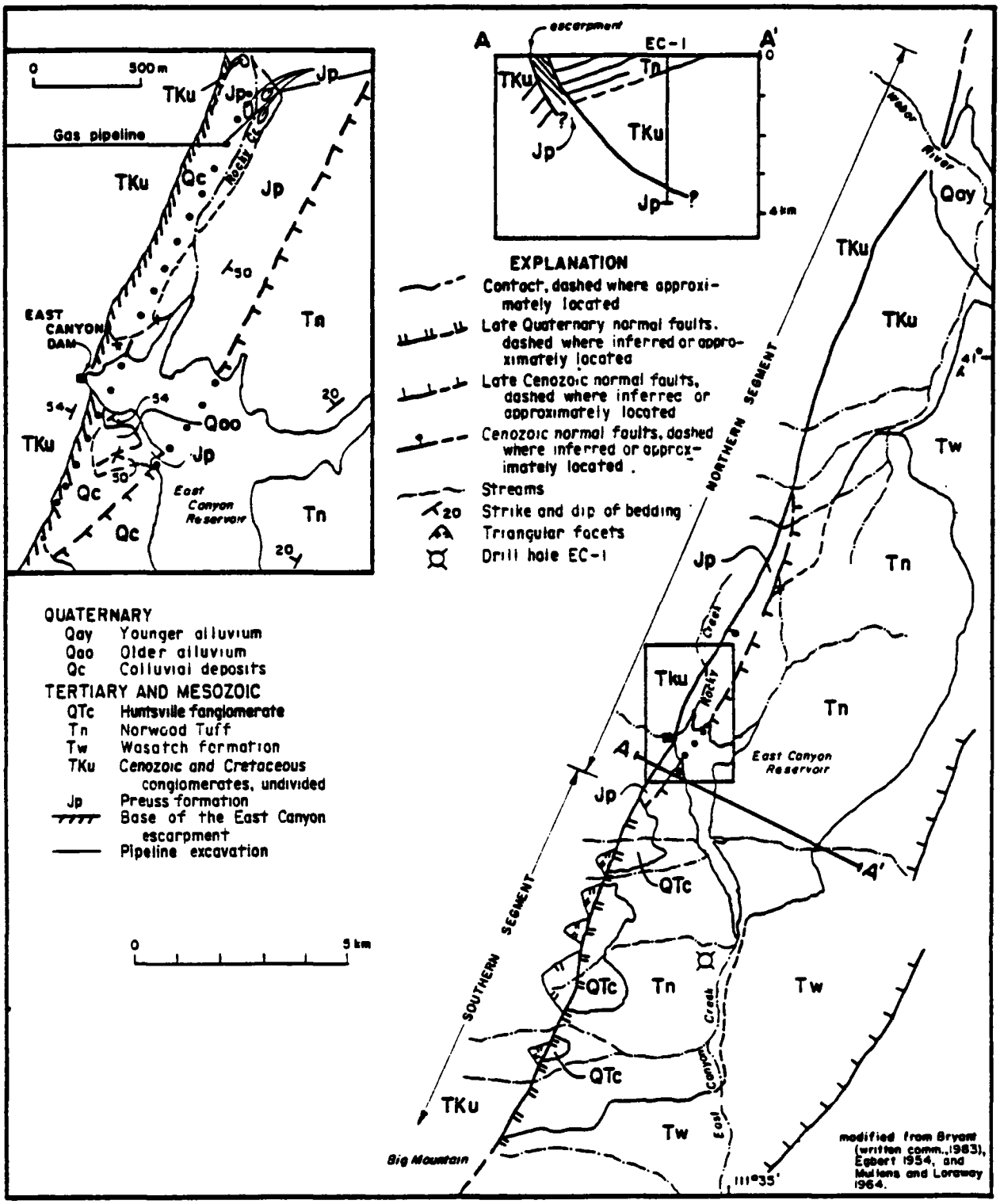


Figure 7.5 Geologic map and cross section of the East Canyon fault including the East Canyon Dam area.

facets, the preservation of the Pliocene? Huntsville fanglomerate, and analogy with similar characteristics associated with the Morgan fault, late Quaternary surface displacements have been inferred on the 12-km-long segment of the fault south of the dam (sec. 4.5).

7.5.7.2 Seismic sources and MCEs

The closest seismic source to the dam is the southern segment of the East Canyon fault. A local MCE of magnitude 6 1/2 to 6 3/4 is estimated for this potential seismic source. Other potential seismic sources are shown in table 7.9.

Table 7.9 Maximum credible earthquakes for East Canyon Dam

Earthquake source	MCE (M_S)	Closest approach to site (km)	Focal depth (km)	Average return period (1000 yrs)
Wasatch fault	7 1/2	22	10-15	2*
Morgan fault	6 3/4 to 7	10	10-15	25-100
E. Canyon fault	6 1/2 to 6 3/4	local	8-15	25-100

* Ogden segment of Schwartz and Coppersmith (1984)

7.5.7.3 Surface faulting

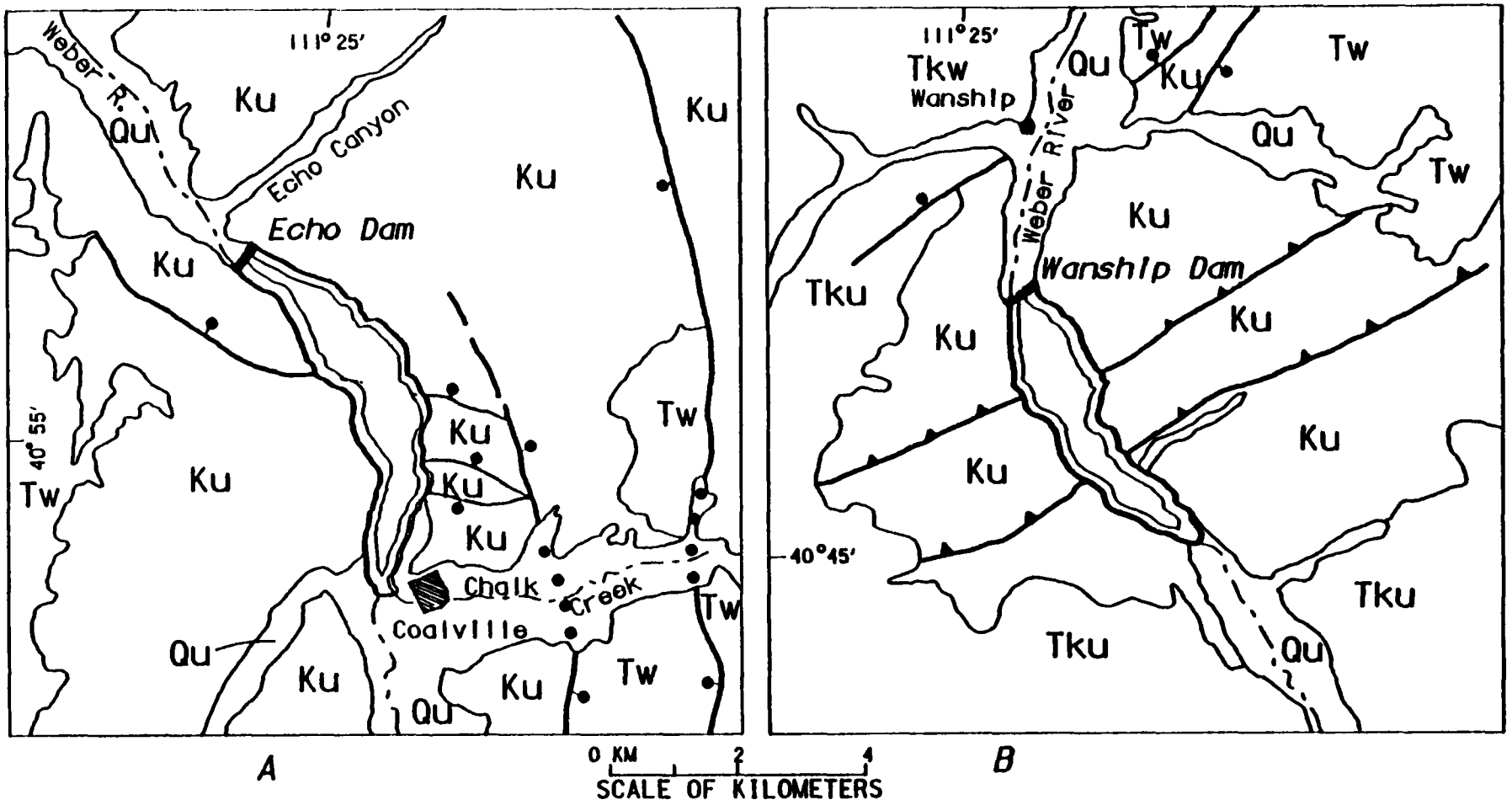
As no faults are known in the dam foundation, surface faulting is not considered to pose a hazard to East Canyon Dam, although some minor adjustments could occur on preexisting joints in the foundation of East Canyon Dam if a large-magnitude earthquake occurred on the East Canyon fault.

7.5.8 Echo Dam

Echo Dam is located on the Weber River in the northern Wasatch Mountains east of the back valley faults (pl. 1B). Northwest-dipping Cretaceous and early Tertiary sedimentary rocks are exposed along the Weber River canyon upstream and downstream of the dam. Our technical memorandum of July 14, 1987 (SAR-1632-112) earlier provided seismotectonic conclusions for Echo Dam.

7.5.8.1 Site Geology

North-striking, high-angle faults and minor east-striking faults in and near the reservoir are shown on fig. 7.6. Late Quaternary deposits overlie some of these faults east of Coalville in fig. 7.6. No bedrock escarpment or scarps in latest Quaternary stream deposits are associated the faults. As these faults lack these morphological characteristics of other late Quaternary faults in the back valleys, we conclude that no late Quaternary displacements have occurred on these faults (sec. 4.5.4).



EXPLANATION

Qu *Quaternary deposits, undivided*
TKu *Late Eocene and Oligocene Keetley volcanics, undivided*
Tw *Eocene Wasatch Formation*
ku *Cretoceous and Jurassic sedimentary rocks, undivided*
Late Cretoceous thrust faults, teethon upper plate
Cenozoic normal faults, dotted where concealed

FIGURE 7.6 - SITE GEOLOGY FOR ECHO DAM (A) AND WANSHIP DAM (B)
MODIFIED FROM STOKES AND MADSEN (1964) AND BRYANT (UNPUBLISHED MAPPING)

7.5.8.2 Seismic sources and MCEs

Seismic sources and associated MCEs for Echo Dam are shown in table 7.10.

Table 7.10 Maximum credible earthquakes for Echo Dam

Earthquake source	MCE (M_S)	Closest approach to site (km)	Focal depth (km)	Average return period (1000 yrs)
Wasatch fault	7 1/2	37	10-15	2*
Morgan fault	6 3/4 to 7	17	10-15	25-100
E. Canyon fault	6 1/2 to 6 3/4	15	8-15	25-100
Random earthquake	6 to 6 1/2#	local	8-15	**

* Ogden segment of Schwartz and Coppersmith (1984)
M_L
** for an estimated annual probability of 0.00001 to 0.00002

7.5.8.3 Surface faulting

No late Quaternary faults are mapped in the vicinity of the dam; therefore, surface faulting is not considered to pose a hazard to Echo Dam.

7.5.9 Wanship Dam (Rockport Lake)

Wanship Dam and Rockport Lake are located on the Weber River in the central Wasatch Mountains about 20 km south of Echo Dam (pl. 1B). North- and northeast-dipping sedimentary rocks of the Frontier Formation are exposed along the Weber River north and south of Wanship Dam. To the east these rocks are unconformably overlain by the Wasatch Formation; to the west they are unconformably overlain by the Keetley Volcanics (fig. 7.6).

7.5.9.1 Site geology

Two southwest-striking thrust faults are mapped crossing Rockport Reservoir in Cretaceous and Jurassic sedimentary rocks. Latest movement on these faults occurred during the late Cretaceous (Crittenden, 1974). A series of generally north-trending normal faults, discussed in sec. 4.5.4, crosses the Weber River about 2 km north of Wanship Dam (fig. 7.6). Late Quaternary deposits overlie some of these faults east of Coalville (fig. 7.6); no footwall escarpment in bedrock is associated with the faults. Therefore, we conclude that no late Quaternary displacements have occurred on these faults; they are not considered potential sources of large-magnitude earthquakes.

7.5.9.2 Seismic sources and MCEs

Seismic sources and associated MCEs for Wanship Dam are shown in table 7.11.

Table 7.11 Maximum credible earthquakes for Wanship Dam (Rockport Lake)

Earthquake source	MCE (M_S)	Closest approach to site (km)	Focal depth (km)	Average return period (1000 yrs)
Wasatch fault	7 1/2	36	10-15	2.4-3*
Morgan fault	6 3/4 to 7	32	10-15	25-100
E. Canyon fault	6 1/2 to 6 3/4	20	8-15	25-100
Random earthquake	6 to 6 1/2#	local	8-15	**

* Salt Lake segment of Schwartz and Coppersmith (1984)
M_L
** for an estimated annual probability of 0.00001 to 0.00002

7.5.9.3 Surface faulting

No late Quaternary faults are known in the vicinity of the dam; therefore, surface faulting is not considered to pose a hazard to Wanship Dam.

7.5.10 Jordanelle Damsite

Jordanelle damsite is located on the Provo River in the central Wasatch Mountains adjacent to the Park City Mining District. In the district early Tertiary calc-alkaline stocks intrude Mesozoic sedimentary rocks and early Tertiary volcanics (Bromfield and others, 1968). Mineralization occurs along early Tertiary, east- and northeast-trending normal and reverse faults in the district. The reservoir will occupy part of Keetley Valley, a north-trending a back valley filled with > 150 m of unconsolidated Tertiary and Quaternary basin fill. The valley is bounded on the west side by the Bald Mountain fault, a north-trending normal fault (pl. 1B). Trench investigations show that late Quaternary deposits with an estimated age of > 130 ka overlie the fault (fig. 5.1). The conclusions from detailed geologic investigations in Keetley Valley and at the damsite have been presented to Boards of Consultants on two occasions (USBR, 1986). The results presented in the final seismotectonic report (Sillivan and others, 1988) are summarized below.

7.5.10.1 Site Geology

Jordanelle Dam will be constructed on a foundation of andesite porphyry and associated volcanic rocks of early Tertiary age. The only major fault mapped in the vicinity of the damsite is the Cottonwood fault, a northeast-trending

reverse fault. Stratigraphy in trenches near the right abutment of the dam shows that faults that are interpreted to be related to the Cottonwood fault are terminated at the margin of the andesite porphyry (USBR, 1986). No other faults are mapped at or near the dam foundation, but boreholes along the foundation alinement indicate that shear zones are present in the dam foundation. Cross sections establish that these zones are intermittent--they lack continuity along strike or down dip. This suggests that the shears are related to the intrusion and subsequent cooling of the andesite porphyry. Available evidence indicates that the foundation is free of faults, although final confirmation awaits mapping of the foundation excavation.

7.5.10.2 Seismic sources and MCEs

Seismic sources and associated MCEs for Jordanelle damsite are shown in table 7.12.

Table 7.12 Maximum credible earthquakes for Jordanelle damsite

Earthquake source	MCE (M_S)	Closest approach to site (km)	Focal depth (km)	Average return period (1000 yrs)
Wasatch fault	7 1/2	30	10-15	1.7-2.6*
Round Valley faults	6 1/2 to 6 3/4	20	10-15	25-100
Random earthquake	6 to 6 1/2#	local	8-15	**

* Provo segment of Schwartz and Coppersmith (1984)
M_L
** for an estimated annual probability of 0.00001 to 0.00002

7.5.10.3 Surface faulting

No late Quaternary faults are known in the vicinity of the dam, so there are no potential sources of large-magnitude earthquakes in the vicinity of the dam. Therefore, coseismic surface rupture associated with a large-magnitude earthquake is not considered to pose a hazard to the dam. However, the occurrence of the random earthquake in the vicinity of the dam could concieveably result in small, secondary displacements on favorably oriented faults in the dam foundation. Although available evidence indicates that such faults are not present in the dam foundation, we have recommended considering the possibility that discrete displacements of as much as 15 cm could occur on north-trending faults, if they are present in the dam foundation (Sullivan and others, 1988).

7.5.11 Deer Creek Dam

Deer Creek Dam is located on the Provo River about 20 km southwest of Jordanelle damsite (pl. 1B). The reservoir extends into Heber Valley, the southernmost back valley in the central Wasatch Mountains (fig. 7.7). Two major faults are mapped on the west side of the reservoir (fig. 7.7)--the Charleston thrust, a late Cretaceous thrust fault, and the Deer Creek normal fault, a Cenozoic normal fault that appears to merge with the Charleston thrust at depth (Riess, 1985). There is no evidence for late Quaternary displacements on either of these faults (sec. 5.9). Concealed Cenozoic normal faults likely are present near the margins of Heber Valley, but there is no evidence for late Quaternary displacements on these inferred faults. Scarps on the valley margins have been shown to be stream cut (sec. 5.9). Late Quaternary faults are inferred in Round Valley east of the dam (pl. 1B) that are potential sources of large-magnitude earthquakes (sec. 6.3).

7.5.11.1 Site Geology

Quartzite and limestone of the upper Paleozoic Oquirrh Formation dipping 30° upstream and striking N30°W in the upper plate of the Charleston thrust were exposed in the dam foundation and abutments (fig. 7.7). A north-striking reverse fault with displacement of as much as 100 m has been mapped in the Oquirrh Formation downstream of the dam. On the right abutment this fault projects below undisplaced alluvial deposits with an estimated age of > 140 ka. No faults were reported in the dam cutoff trench or abutments.

7.5.11.2 Seismic sources and MCEs

Seismic sources and there associated MCEs for Deer Creek Dam are shown in table 7.13.

Table 7.13 Maximum credible earthquakes for Deer Creek Dam

Earthquake source	MCE (M_S)	Closest approach to site (km)	Focal depth (km)	Average return period (1000 yrs)
Wasatch fault	7 1/2	14	10-15	1.7-2.6*
Round Valley faults	6 1/2 to 6 3/4	5	10-15	25-100
Random earthquake	6 to 6 1/2#	local	8-15	**

* Provo segment of Schwartz and Coppersmith (1984)
\# M_L
** for an estimated annual probability of 0.00001 to 0.00002

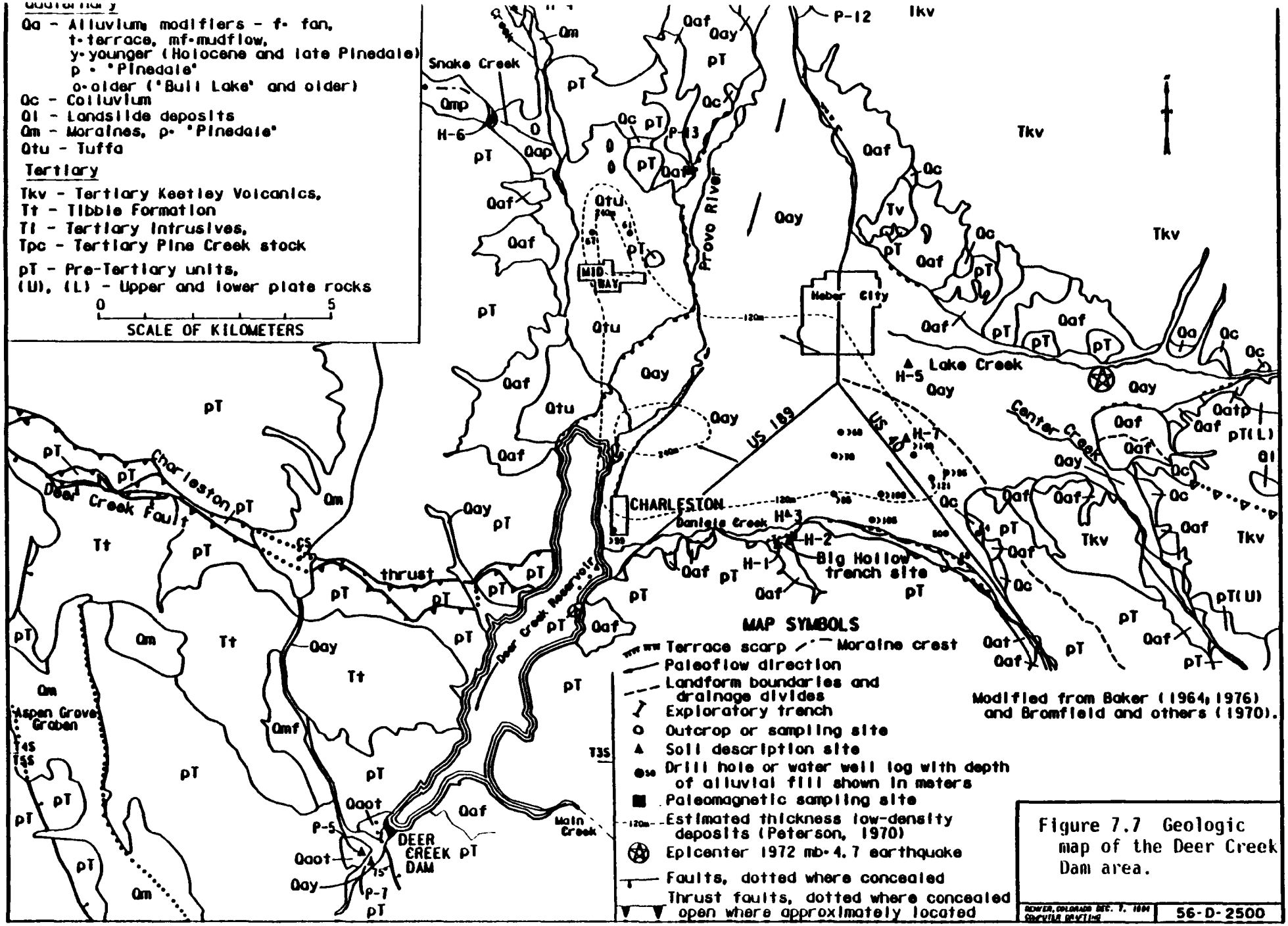


Figure 7.7 Geologic map of the Deer Creek Dam area.

56-D-2500

7.5.11.3 Surface faulting

No late Quaternary faults are known in the vicinity of the dam; therefore, surface faulting is not considered to pose a hazard to Deer Creek Dam.

7.5.12 Soldier Creek Dam

Soldier Creek Dam is located in the southern Wasatch Mountains near the western margin of the Uinta Basin (pl. 1B). The results of investigations and the conclusions from a site-specific seismotectonic study for Soldier Creek Dam (Nelson and Martin, 1982) are summarized below.

7.5.12.1 Site Geology

Soldier Creek Dam was constructed in lower Tertiary sedimentary rocks immediately upstream of the Stinking Springs fault, a north-trending normal fault. The reservoir extends upstream across the Strawberry fault, also a north-trending normal fault. Trenching and coring established that late Quaternary surface displacements have occurred on the Strawberry fault (Nelson and Martin, 1982); therefore, it is considered a potential source for a large-magnitude earthquake. The escarpment associated with Stinking Springs fault is similar to that of the Strawberry fault suggesting that late Quaternary surface displacements have also occurred on the Stinking Springs fault.

7.5.12.2 Seismic sources and MCEs

Seismic sources for Soldier Creek Dam are shown in table 7.14.

Table 7.14 Maximum credible earthquakes for Soldier Creek Dam

Earthquake source	MCE (M_S)	Closest approach to site (km)	Focal depth (km)	Average return period (1000 yrs)
Wasatch fault	7 1/2	45	10-15	1.7-2.6*
Strawberry fault	7	8	10-15	1.5-10**
Stinking Springs fault	6 1/2	local	8-15	no data

* Provo segment of Schwartz and Coppersmith (1984)
** Nelson and Martin (1982)

7.5.12.3 Surface faulting

Surface displacement of as much as one meter could occur on the Stinking Springs fault, 180 m upstream of Soldier Creek Dam, in association with the MCE. Mapping and construction investigations did no reveal any faults trending into or extending under the dam indicating that significant displacements through the dam are extremely unlikely; however, a large-magnitude earthquake on the Stinking Springs fault could produce some shifting of the foundation rock along preexisting joints.

7.5.13 Monks Hollow Damsite

Monks Hollow damsite is located on the Diamond Fork river west of Spanish Fork, Utah in the southern Wasatch Mountains (pl. 1B). Folded and faulted Mesozoic to early Tertiary sedimentary rocks in the upper plate of the Charleston thrust are exposed along the Diamond Fork. The proposed concrete dam will be built on the Jurassic Nugget Sandstone and Twin Creek Formation in the west limb of the north-striking Diamond Fork anticline. The results of investigations and the conclusions from a site-specific seismotectonic study for Monks Hollow Dam (Sullivan and others, 1987) are summarized below.

7.5.13.1 Site Geology

A series of north-trending normal faults that form a north-trending horst have been mapped within about 3 km of the dam, including a fault a few meters upstream of the dam alinement. Longitudinal profiles of late Quaternary terraces on the Diamond Fork River show that no late Quaternary displacements have occurred on any of these faults (Sullivan and others, 1987).

7.5.13.3 Seismic sources and MCEs

Seismic sources and associated MCEs for the damsite are shown in table 7.15.

Table 7.15 Maximum credible earthquakes for Monks Hollow damsite

Earthquake source	MCE (M_S)	Closest approach to site (km)	Focal depth (km)	Average return period (1000 yrs)
Wasatch fault	7 1/2	15	10-15	1.7-2.6*
Little Diamond Cr. fault	6 to 6 3/4	5	10-15	25-100
Random earthquake	6 to 6 1/2#	local	8-15	**

* Provo segment of Schwartz and Coppersmith (1984)
M_L
** for an estimated annual probability of 0.00001 to 0.00002

7.5.13.3 Surface faulting

No late Quaternary faults are known in the vicinity of the dam; therefore, surface faulting is not considered to pose a hazard to the proposed Monks Hollow Dam.

7.5.14 Mona Dam

Mona Dam is located on Long Ridge a north and northeast-trending range block about 6 km west of the Wasatch fault. The reservoir occupies a portion of the adjacent structural and physiographic basin called Juab Valley (pl. 1C). The results of investigations and the conclusions from a site-specific seismotectonic study for Mona Dam (Sullivan and Baltzer, 1986) are summarized below.

7.5.14.1 Site Geology

No faults are mapped in the Eocene volcanic rocks within the foundations of the existing or proposed dams, but late Quaternary faults are inferred on the margins of Long Ridge. The Juab Valley fault on the east side of Long Ridge is a down-to-the-east normal fault antithetic to the Wasatch fault that is inferred beneath Mona Reservoir, a few hundred meters upstream of the dam.

7.5.14.2 Seismic sources and MCEs

Seismic sources and associated MCEs for Mona Dam are shown in table 7.16. As the Juab Valley fault is antithetic to the Wasatch fault any potential MCE associated with this fault is encompassed by the Wasatch fault (Sullivan and Baltzer, 1986).

Table 7.16 Maximum credible earthquakes for Mona Dam

Earthquake source	MCE (M_S)	Closest approach to site (km)	Focal depth (km)	Average return period (1000 yrs)
Wasatch fault	7 1/2	3-6	10-15	1.7-2.7*
Random earthquake	6 to 6 1/2#	local	8-15	**

* Nephi segment of Schwartz and Coppersmith (1984)
\# M_L
** for an estimated annual probability of 0.00001 to 0.00002

7.5.14.3 Surface faulting

No faults or shears have been identified in the foundation of the proposed dam, therefore no significant surface displacements are likely to occur. However, joints are present in the dam foundation and a large-magnitude earthquake on the Wasatch fault could result in displacements on the Juab Valley fault in the reservoir and small adjustments on the joints.

7.5.15 Joes Valley Dam

Joes Valley Dam is located within the ISB on the Wasatch Plateau, an area of nearly flat-lying Mesozoic and lower Tertiary sedimentary rocks south of the back valleys of the Wasatch Mountains (pl. 1C). The Wasatch Plateau is part of the transition zone between the Colorado Plateau on the east and the Basin and Range Province on the west. Cenozoic extension is indicated by north and northeast-trending normal faults on the Plateau. A site-specific seismotectonic study for Joes Valley Dam was conducted by Foley and others (1986).

7.5.15.1 Site Geology

Joes Valley Dam was constructed on a foundation of Tertiary sedimentary rocks adjacent to the north-trending Joes Valley fault zone on the east side of the Joes Valley graben. Scarps preserved in late Quaternary deposits together with the results of trenching establish that late Quaternary surface displacements have occurred on faults in the Joes Valley graben.

7.5.15.1 Seismic sources and MCEs

Seismic sources and associated MCEs for Joes Valley Dam are shown in table 7.17.

Table 7.17 Maximum credible earthquakes for Joes Valley Dam

Earthquake source	MCE (M_S)	Closest approach to site (km)	Focal depth (km)	Average return period (1000 yrs)
Joes Valley graben	7 1/2	local	10-15	10-40
Random earthquake	6 to 6 1/2#	local	8-15	*

M_L
* for an estimated annual probability of 0.00001 to 0.00002

7.5.15.3 Surface faulting

No faults are located in the dam foundation so surface faulting does not pose a hazard to Joes Valley Dam (Foley and others, 1986).

7.5.16 Scofield Dam

Scofield Dam is located on the Wasatch Plateau about 60 km north of Joes Valley Dam (pl. 1C). Cenozoic extension is indicated by north and northeast-trending normal faults on this part of the Plateau. The results of investigations and the conclusions from a site-specific seismotectonic study for Scofield Dam (Foley and others, 1986) are summarized below.

7.5.16.1 Site Geology

Scofield Dam was constructed on a foundation of Tertiary sedimentary rocks adjacent to the north-trending Pleasant Valley fault zone on the east side of the Pleasant Valley graben. Although no scarps are preserved in latest Quaternary deposits in the Pleasant Valley graben, several of the faults exhibit geomorphic characteristics that are similar to the late Quaternary faults in the Joes Valley graben. The faults with inferred late Quaternary displacement closest to the dam are the East and West Pleasant Valley faults both of which underlie the reservoir.

7.5.16.2 Seismic sources and MCEs

Seismic sources and associated MCEs for Scofield Dam are shown in table 7.18.

Table 7.18 Maximum credible earthquakes for Scofield Dam

Earthquake source	MCE (M_S)	Closest approach to site (km)	Focal depth (km)	Average return period (1000 yrs)
Joes Valley fault zone	7 1/2	22	10-15	10-40
Pleasant Valley fault zone	7	local	10-15	no data
Random earthquake	6 to 6 1/2#	local	8-15	*

M_L
* for an estimated annual probability of 0.00001 to 0.00002

7.5.16.3 Surface faulting

No late Quaternary faults have been identified that trend through the dam foundation, so surface faulting is not considered to pose a hazard to Scofield dam (Foley and others, 1986).

7.6 Reservior induced seismicity

RIS (reservoir induced seismicity) refers to the occurrence of small- and moderate-magnitude earthquakes during or after the impoundment of reservoirs. These earthquakes, which have occurred at a number of reservoirs worldwide (Simpson, 1976), are thought to be naturally occurring events that are triggered prematurely by the presence of the reservoir. A statistical analysis of historical seismicity to determine if RIS had occurred at any of the reservoirs in the Regional Study area is reported in Appendix B. The principle conclusions from this study are summarized below:

1) No increase in earthquake activity was noted at any of the subject dams upon initial filling, although all but one of the reservoirs were filled prior to 1967, before installation of the current seismograph network.

2) Based on the statistical analyses reported in Appendix B, there is no evidence for the occurrence of RIS at any but one of the reservoirs in the region. While the analysis pointed to possible RIS at Wanship Dam, further considerations lead to the conclusion that RIS had not occurred.

3) Based on theoretical studies and observed cases of RIS worldwide, the Regional Study area shares a number of attributes that appear to be conducive to RIS. However, the depths and volumes of the reservoirs in the study area are lower than those for which the probability of RIS occurrence has been judged to be significant.

8.0 REFERENCES

Allmendinger, R. W., Sharp, J. W., Tish, D. V., Serpa, L., Kaufman, S., Oliver, J., and Smith, R. B., 1983, Cenozoic and Mesozoic structure of the eastern Basin and Range province, Utah, from COCORP seismic reflection data: Geology, v. 11, no. 9, p. 532-536.

Anderson, G. E., 1915, Stream piracy of the Provo and Weber Rivers, Utah: American Journal of Science, v. 40, p. 314-316.

Anderson, J. G., 1979, Estimating the seismicity from geological structure for seismic-risk studies: Seismological Society of America Bulletin, v. 69, p. 135-158.

Anderson, L. W., and Anderson, D. S., 1981, Weathering rinds on quartz-arenite clasts as a relative-age indicator and the glacial chronology of Mount Timpanogos, Wasatch Range, Utah: Arctic and Alpine Research, v. 13, p. 25-31.

Anderson, L. W., and Miller, D. G., 1979, Quaternary fault map of Utah: Long Beach, California, Fugro, Inc., 39 p., 1:1,000,000.

Anderson, R. E., 1971, Thin-skinned distention in Tertiary rocks of southeastern Nevada: Geological Society of America Bulletin, v. 82, p. 43-58.

Anderson, R. E., Zoback, M. L., and Thompson, G. A., 1983, Implications of selected subsurface data on the structural form and evolution of some basins in the northern Basin and Range province, Nevada and Utah: Geological Society of America Bulletin, v. 94, no. 9, p. 1055-1072.

Arabasz, W. J., 1979, Historical review of earthquake related studies and seismograph recording in Utah, in Arabasz, W. J., Smith, R. B., and Richins, W. D., eds., Earthquake studies in Utah 1850 to 1978: University of Utah Seismograph Stations, Department of Geology and Geophysics, University of Utah, Salt Lake City, Utah, p. 33-56.

Arabasz, W. J., and Julander, D. R., 1986, Geometry of seismically active faults and crustal deformation within the Basin and Range - Colorado Plateau Transition in Utah, in Mayer, L., ed., Extensional tectonics of the Basin and Range Province: A perspective: Geological Society of America Special Paper no. 208.

Arabasz, W. J., and Smith, R. B., 1979, Introduction: What you've always wanted to know about earthquakes in Utah, in Arabasz, W. J., Smith, R. B., and Richins, W. D., eds., Earthquake studies in Utah 1850 to 1978, University of Utah Seismograph Stations: Department of Geology and Geophysics, University of Utah, Salt Lake City, Utah, p. 1-14.

---- 1981, Earthquake prediction in the Intermountain seismic belt -- an intraplate extensional regime, in Simpson, D. W., and Richards, P. G., eds., Earthquake prediction, an international review: American Geophysical Union, Maurice Ewing Series 4, p. 248-258.

Arabasz, W. J., and Williams, D. J., 1985, Analysis and summary of seismographic data recorded in vicinity of Joes Valley dam, Emery County project, eastern Wasatch Plateau, Utah [unpublished report]: Denver, Colorado, U.S. Bureau of Reclamation, 74 p.

Arabasz, W. J., Smith, R. B., and Richins, W. D., 1979, Earthquake studies along the Wasatch Front, Utah: Network monitoring, seismicity, and seismic hazards, in Arabasz, W. J., Smith, R. B., and Richins, W. D., eds., Earthquake studies in Utah 1850 to 1978: University of Utah Seismograph Stations, Department of Geology and Geophysics, University of Utah, Salt Lake City, Utah, p. 253-285.

---- 1980, Earthquake studies along the Wasatch front, Utah: Network monitoring, seismicity, and seismic hazards: Bulletin of the Seismological Society of America, v. 70, no. 5, p. 1479-1499.

Arabasz, W. J., Richins, W. D., and Langer, C. J., 1981, The Pocatello Valley (Idaho-Utah border) earthquake sequence of March to April, 1975: Bulletin of the Seismological Society of America, v. 71, no. 3, p. 803-826.

Armstrong, F. C., and Oriel, S. S., 1965, Tectonic development of the Idaho-Wyoming thrustbelt: American Association of Petroleum Geologists Bulletin, v. 49, no. 11, p. 1847-1868.

Armstrong, R. L., 1968, Sevier orogenic belt in Nevada and Utah: Geological Society of America Bulletin, v. 79, p. 429-459.

Astin, G. K., 1977, Structure and Stratigraphy of the Co-op Creek Quadrangle, Wasatch County, Utah: Brigham Young University Geologic Studies, v. 24, part 1, p. 13-34.

Atwood, W. W., 1909, Glaciation of the Uinta and Wasatch Mountains: U.S. Geological Survey Professional Paper 61, 96 p.

Bache, T. C., Lambert, D. G., and Barker, T. G., 1980, A source model for the March 28, 1975 Pocatello Valley earthquake from time-domain modeling of teleseismic P-waves: Bulletin of the Seismological Society of America, v. 70, p. 405-418.

Baclowski, P., Chidsey, T. C., Bradley, M. D., 1984, Thrust belt and Wasatch-Uinta intersect area: AAPG-SEPM Rocky Mountain Section Meeting Field Trip Guidebook, August 25-26, 1984, 18 p.

Baer, J. L., and Rigby, J. K., 1980, Geologic guide to Provo Canyon and Weber Canyon, central Wasatch Mountains: Brigham Young University Studies for Students no. 10, p. 1-35.

Bailey, R. W., 1927, The Bear River Range fault, Utah: American Journal of Science, 5th series, v. 13, p. 497-502.

Baker, A. A., 1947, Stratigraphy of the Wasatch Mountains in the vicinity of Provo, Utah: U. S. Geological Survey Oil and Gas Preliminary Chart 30.

---- 1964, Geology of the Aspen Grove Quadrangle, Utah: U.S. Geological Survey Geologic Quadrangle Map GQ-239, 1:24,000.

---- 1976, Geologic Map of the west half of the Strawberry Quadrangle, Utah: U.S. Geological Survey Miscellaneous Investigations Series Map I-931, 1:62,500.

Baker, A. A., and Crittenden, M. D., Jr., 1961, Geology of the Timpanogos Cave quadrangle, Utah: U.S. Geological Survey Geologic Quadrangle Map GQ-132, 1:24,000.

Baker, A. A., Calkins, F. C., Crittenden, M. D., Jr., and Bromfield, C. S., 1966, Geologic map of the Brighton quadrangle, Utah: U.S. Geological Survey Map GQ-534, 1:24,000.

Baker, C. H., Jr., 1968, Thermal springs near Midway, Utah: U.S. Geological Survey Professional Paper 600-D, p. D63-D70.

---- 1970, Water resources of the Heber Kamas Park City area, north-central Utah: Utah Department of Natural Resources, Technical Publication no. 27, 79 p.

Barnhardt, M. L., 1973, Late Quaternary geomorphology of the Bald Mountain area, Uinta Mountains, Utah [M.S. thesis]: Salt Lake City, University of Utah, 109 p.

Barrientos, S. E., Ward, S. N., Gonzalez-Ruiz, J. R., and Stein, R. S., 1985, Inversion for moment as a function of depth from geodetic observations and long period body waves of the 1983 Borah Peak, Idaho, Earthquake, in Stein, R. S., and Bucknam, R. C., eds., Proceedings of Workshop XXVIII on the Borah Peak, Idaho, earthquake: U.S. Geololgical Survey Open-File Report 85-290, v. A, p. 485-518.

Beutner, E., 1977, Causes and consequences of curvature in the Sevier orogenic belt in Utah and Montana: Wyoming Geological Association Guidebook, 29th Annual Field Conference, p. 353-366.

Birkeland, P. W., 1974, Pedology, Weathering, and Geomorphological Research, 2nd ed.: New York, Oxford University Press, 285 p.

---- 1984b, Soils and Geomorphology: New York, Oxford University Press, 372 p.

Birkeland, P. W., Colman, S. M., Burke, R. M., Shroba, R. R., and Meierding, T. C., 1979, Nomenclature of alpine glacial deposits -- or what's in a name?: Geology, v. 7, p. 532-536.

Bissell, H. J., 1952, Stratigraphy and structure of northeast Strawberry Valley Quadrangle, Utah: American Association of Petroleum Geologists Bulletin, v. 36, p. 575-634.

---- 1959, North Strawberry Valley sedimentation and tectonics, in Guidebook to the Geology of the Wasatch and Uinta Mountains Transition Area: Intermountain Association Petroleum Geologists, v. 10, p. 159-165.

---- 1963, Bonneville Geology of southern Utah Valley, Utah: U.S. Geological Survey Professional Paper 257-B, p. 101-130.

Blackstone, D. L., 1977, The overthrust belt salient of the Cordilleran fold belt western Wyoming - southeastern Idaho - northeastern Utah: Wyoming Geological Association Guidebook to the 29th Annual Field Conference, p. 367-384.

Blackwelder, Eliot, 1915, Post-Cretaceous history of the mountains of central-western Wyoming: Journal of Geology, v. 23, p. 97-117, 193-217, 307-340.

Blau, J. C., 1975, Geology of the southern part of the James Peak Quadrangle [M.S. thesis]: Logan, Utah, Utah State University, 55 p.

Bodell, J., M., and Chapman, D. S., 1982, Heat flow in the north-central Colorado Plateau: Journal of Geophysical Research, v. 87, p. 2869-2884.

Bolt, B. A., 1984, The magnitudes of the Hebgen Lake 1959 and Idaho 1983 earthquakes [abstr.]: Earthquakes Notes, v. 55, p. 13.

Bonilla, M. G., Mark, R. K., and Lienkaemper, J. J., 1984, Statistical relations among earthquake magnitude, surface rupture length, and surface fault displacement: Bulletin of Seismological Society of America, v. 74, p. 2379-2411.

Boutwell, J. M., 1912, Geology and ore deposits of the Park City district, Utah: U.S. Geological Survay Professional Paper 77, 231 p.

Boyer, S. D., and Elliot, D., 1982, Thrust systems: American Association of Petroleum Geologists Bulletin, v. 66, no. 9, p. 1196-1230.

Bradley, W. H., 1936, Geomorphology of the north flank of the Uinta Mountians: U.S. Geological Survey Professional Paper 185-I, 204 p.

Braile, L. W., Smith, R. B., Keller, G. R., Welch, R. M., and Meyer, R. P., 1974, Crustal structure across the Wasatch Front from detailed seismic refraction studies: Journal of Geophysical Research, v. 79, no. 17, p. 2669-2677.

Brewer, J. A., Smithson, S. B., Oliver, J. E., Kaufman, S. and Brown, L. D., 1980, the Laramide Orogeny: Evidence from COCORP deep crustal seismic profiles in the Wind River Mountains, Wyoming: Tectonophysics, v. 62, p. 165-189.

Brimhall, W. H., 1951, Stratigraphy and structural geology of the northern Deer Creek reservoir area, Provo Canyon, Utah [M.S. Thesis]: Tucson, Arizona, University of Arizona, 75 p.

Broecker, W. S., and Kaufman, A., 1965, Radiocarbon chronology of Lake Lahontan and Lake Bonneville II, Great Basin: Geological Society America Bulletin, v. 76, p. 537-566.

Bromfield, C. S., 1968, General Geology of the Park City region, Utah, in Erickson, A. J., Phillips, W. R., and Garmoe, W. J., eds., Guidebook to the geology of the Park City district: Utah Geological Association Guidebook no. 22, p. 10-29.

Bromfield, C. S., and Crittenden, M. D., Jr., 1971, Geologic Map of the Park City East Quadrangle, Summit and Wasatch Counties, Utah: U. S. Geological Survey Geologic Quadrangle Map GQ-852, 1:24,000.

Bromfield, C. S., Baker, A. A., and Crittenden, M. D., Jr., 1970, Geologic map of the Heber Quadrangle, Wasatch and Summit Counties, Utah: U.S. Geological Survey Geologic Quadrangle Map GQ-864, 1:24,000.

Bromfield, C. S., Erickson, A. J., Jr., Haddadin, M. A., and Mehnent, H. H., 1977, Potassium-argon ages of intrusion, extrusion and associated ore deposits, Park City Mining District, Utah: Economic Geology, v. 72, p. 837-848.

Bruhn, R. L., and Beck, S. L., 1981, Mechanics of thrust faulting in crystalline basement, Sevier orogenic belt, Utah: Geology, v. 9, p. 200-204.

Bruhn, R. L., Picard, M. D., and Beck, S. L., 1983, Mesozoic and early Tertiary structure and sedimentology of the central Wasatch Mountains, Uinta Mountains, and Uinta Basin: Utah Geological and Mineral Survey Special Studies no. 59, p. 63-105.

Brune, J. N., 1968, Seismic moment, seismicity, and rate of slip along major fault zones: Journal of Geophysical Research, v. 73, p. 777-780.

Bryant, B., 1984, Reconnaissance geologic map of the Precambrian Farmington Canyon Complex and surrounding rocks in the Wasatch Mountains between Ogden and Bountiful, Utah: U. S. Geological Survey Miscellaneous Investigations Map I-1447, 1:50,000.

Bucknam, R. C, 1976, Leveling data from the epicentral area of the March 27, 1975, earthquake in Pocatello Valley, Idaho: U.S. Geological Survey Open-file Report 76-52, 6 p.

Bucknam, R. C., and Anderson, R. E., 1979, Estimation of fault-scarp ages from a scarp-height-slope-angle relationship: Geology, v. 7, p. 11-14.

Bucknam, R. C., Algermissen, S. T., and Anderson, R. E., 1980, Patterns of late Quaternary faulting in western Utah and an application in earthquake hazard evaluation, in Proceedings of Conference X, Earthquake Hazards along the Wasatch and Sierra Nevada frontal fault zones: U. S. Geological Survey Open-File Report 80-801, p. 299-314.

Bull, W. B., 1977, The alluvial-fan environment: Progress in Physical Geography, v. 1, p. 222-270.

Bull, W. B., and McFadden, L. D., 1977, Tectonic geomorphology north and south of the Garlock fault, California, in Doehring, D. O., ed., Geomorphology in arid regions: Proceedings, 8th Annual Geomorphology Symposium, State University of New York, Binghamton, N. Y., p. 115-138.

Burchfiel, B. C., and Hickcox, C. W., 1972, Structural development of central Utah: Utah Geological Association Publication no. 2, p. 55-66.

Byerlee, J. D., 1968, Brittle-ductile transition in rocks: Journal of Geophysical Research, v. 73, p. 4741-4750.

Burke, R. M., and Birkeland, P. W., 1979, Reevaluation of multiparameter relative dating techniques and their application to the glacial sequence along the eastern escarpment of the Sierra Nevada, California: Quaternary Research, v. 11, p. 21-51.

Campbell, J. A., 1975, Structural geology and petroleum potential of the south flank of the Uinta Mountain uplift, northeastern Utah: Utah Geology, v. 2, no. 2, p. 129-132.

---- 1978, Cenozoic structural and geomorphic evolution of the Canyon Range, central Utah [Ph.D. thesis]: Salt Lake City, University of Utah, 158 p.

Carley, J. A., Jensen, E. H., Campbell, L. B., Barney, M., Fish, R. H., Chadwick, R. S., and Winkelaar, P., 1980, Soil Survey of Morgan area, Utah: Soil Conservation Service and Forest Service, U.S. Department of Agriculture, 300 p.

Carrara, P. E., Mode, W. M., Rubin, Meyer, and Robinson, S. W., 1984, Deglaciation and postglacial timberline in the San Juan Mountains, Colorado: Quaternary Research, v. 21, no. 1, p. 42-55.

Carver, D., Langer, C. J., Richins, W. D., 1981, Fine details of the aftershock process following the September 30, 1977 Uinta Basin, Utah, earthquakes (abstr.): Earthquake Notes, January - March 1981, v. 52, no. 1, p. 62.

Carver, R. E., 1971, ed., Procedures in Sedimentary Petrology: New York, Wiley-Interscience, 653 p.

Chen, W. P., and Molnar, P., 1977, Seismic moments of major earthquakes and the average rate of slip in central Asia: Journal of Geophysical Research, v. 82, p. 2945-2969.

Christiansen, R. L., and McKee, E. H., 1978, Late Cenozoic volcanic and tectonic evolution of the Great Basin and Columbia intermontane region, in Cenozoic Tectonics and Regional Geophysics of the Western Cordillera: Geological Society of America Memoir 152, p. 283-311.

Cluff, L. S., Glass, C. E., and Brogan, G. E., 1974, Investigation andevaluation of the Wasatch fault north of Brigham City and Cache Valley faults, Utah and Idaho: A guide to land use planning with recommendations for seismic safety [unpublished report, U.S. Geological Survey contract no. 14-08-001-13665]: Oakland, California, Woodward-Lundgren and Associates, 147 p.

Coffman, J. L., Von Hake, C. A., and Stover, C. W., 1982, Earthquake history of the United States: U.S. Department of Commerce.

Colman, S. M., and Pierce, K. L., 1981, Weathering rinds on andesitic and basaltic stones as a Quaternary age indicator, western United States: U.S. Geological Survey Professional Paper 1210, 56 p.

Coody, G. L., 1957, Geology of the Durst Mountain Huntsville area (M.S.thesis): Salt Lake City, University of Utah, 63 p.

Cook, K. L., 1972, Earthquakes along the Wasatch front, Utah -- the record and the outlook, in Hilpert, L. S., ed., Environmental Geology of the Wasatch Front, 1971: Utah Geological Association Publication 1, p. H1-H29.

---- 1979, Effects of earthquakes in the Magna area, Salt Lake county, during February-March, 1978, in Arabasz, W. J., Smith, R. B., and Richins, W. D., eds., Earthquake Studies in Utah, 1859 to 1978, University of Utah, p. 475-487.

Cook, K. L., and Smith, R. B., 1967, Seismicity in Utah, 1850 through June, 1965: Bulletin of the Seismological Society of America, v. 57, p. 689-718.

Crittenden, M. D., Jr., 1972a, Willand thrust and Cache allochthon, Utah: Geological Society of America Bulletin, v. 83, p. 2871-2880.

---- 1972b, Geologic map of the Browns Hole Quadrangle, Utah: U.S. Geological Survey Geologic Quadrangle Map GQ-968, 1:24,000.

---- 1974, Regional extent and age of thrusts near Rockport Reservoir and relation to possible exploration targets in northern Utah: American Association of Petroleum Bulletin, v. 58, p. 2428-2435.

Crittenden, M. D., Jr., and Calkins, F. C., 1966, Geologic map of the Park City West quadrangle, Utah: U.S. Geological Survey Geologic Quadrangle Map GQ-535, 1:24,000.

Crittenden, M. D. Jr., Stuckless, J. S., Kistler, R. N., and Stern, T. W., 1973, Radiometric dating of intrusive rocks in the Cottonwood area, Utah: U.S. Geological Survey Journal of Research, v. 1, p. 173-178.

Crone, A. J., and Harding, S. T., 1984, Relationship of late Quaternary fault scarps to subadjacent faults, eastern Great Basin, Utah: Geology, v. 12, no. 5, p. 292-295.

Crone, A. J., and Machette, M. N., 1984, Surface faulting accompanying the Borah Peak earthquake, central Idaho: Geology, v. 12, p. 664-667.

Currey, D. R., 1980, Events associated with the last cycle of Lake Bonneville - Idaho, Nevada, and Utah: American Quaternary Association, Abstracts of 6th Biennial Meeting, p. 59-60.

Dahlstrom, C. D. A., 1970, Structural geology in the eastern margin of the Canadian Rocky Mountains: Bulletin of Canadian Petroleum Geology, v. 18, p. 322-406.

Davis, W. M., 1903, The Basin ranges of Utah and Nevada: Journal of Geology,v. 11, p. 120-121.

DeGraff, J. V., 1975, Multiple episodes of alluvial fan deposition in the Bear River Range, Utah[abstr.]: Geological Society of America, Abstracts with Programs, v. 7, no. 5, p. 603.

---- 1976a, Quaternary geomorphic features of the Bear River Range, north-central Utah (M.S. thesis): Logan, Utah, Utah State University, 215 p.

---- 1976b, Relict patterned ground, Bear River Range, north-centralUtah: Utah Geology, v. 3, no. 2, p. 111-116.

---- 1979, Numerical analysis of cirques in the Bear River Range, north-central Utah: Modern Geology, v. 7, no. 1, p. 43-51.

Dixon, J. S., 1982, Regional structural synthesis, Wyoming salient of western overthrust belt: American Association of Petroleum Geologists Bulletin, v. 66, no. 10, p. 1560-1580.

Doser, D. I., 1980, Earthquake recurrence rates from seismic moment rates in Utah [M.S. thesis]: Salt Lake City, University of Utah.

---- 1984, Source parameters and faulting processes of the 1959 Hebgen Lake, Montana, earthquake sequence [Ph.D. thesis]: Salt Lake City, University of Utah, 165 p.

---- 1985, The 1983 Borah Peak, Idaho, and 1959 Hebgen Lake, Montana, earthquakes: Models for normal fault earthquakes in the Intermountain seismic belt, in Stein, R. S., and Bucknam, R. C., eds., Proceedings of Workshop XXVIII on the Borah Peak, Idaho, earthquake: U.S. Geological Survey Open-File Report 85-290, v. A, p. 368-384.

Doser, D. I., and Smith, R. B., 1982, Seismic moment rates in the Utah region: Seismological Society of America Bulletin, v. 72, no. 2, p. 525-551.

---- 1983, Seismicity of the Teton - southern Yellowstone region, Wyoming: Bulletin of the Seismological Society of America, v. 73, no. 5, p. 1369-1394.

---- 1985, Source parameters of the 28 October 1983 Borah Peak, Idaho, earthquake from body wave analysis: Bulletin of the Seismological Society of America, v. 75, p. 1041-1051.

Doyuran, V., 1972, Geology and ground-water resources of Ogden Valley, Utah [Ph.D. thesis]: Salt Lake City, University of Utah, 112 p.

Eardley, A. J., 1933, Strong relief before block faulting in the vicinity of the Wasatch Mountains, Utah: Journal of Geology, v. 41, p. 243-269.

---- 1944, Geology of the north-central Wasatch Mountains, Utah: Geological Society of America Bulletin, v. 55, p. 819-894.

---- 1952, Wasatch Hinterland, in Geology of the central Wasatch Mountains, Utah: Utah Geological Society Guide book no. 8, p. 52-60.

---- 1955, Tertiary history of north central Utah in Eardley, A. J., ed., Tertiary and Quaternary geology of the eastern Bonneville Basin: Guidebook to the Geology of Utah, no. 10, p. 37-44.

---- 1959, Review of Geology of northeastern Utah and southwestern Wyoming, in Guidebook to the Geology of the Wasatch and Uinta Mountains Transition area: Intermountain Association of Petroleum Geologists, v. 10, p. 166-171.

---- 1970, Erosion surfaces of the Wasatch Mountains: Utah Academy Sciences Proceedings, v. 47, part 1, p. 272-273.

Eardley, A. J., Gvosdetsky, V., and Marsell, R. E., 1957, Hydrology of Lake Bonneville and sediments and soils of its basin: Geological Society of America Bulletin, v. 68, p. 1141-1202.

Eardley, A. J., Shuey, R. T., Gvosdetsky, V., Nash, W. P., Picard, M. D., Grey, D. C., and Kukla, G. J., 1973, Lake cycles in the Bonneville basin, Utah: Geological Society of America Bulletin, v. 84, p. 211-216.

Eaton, G. P., 1982, The Basin and Range Province: Origin and tectonic significance: Annual Review of Earth and Planetary Sciences, v. 10, p. 409-440.

Effimoff, I. and Pinezich, A. R., 1981, Tertiary structural development of selected valleys based on seismic data: Basin and Range province, northeastern Nevada: Royal Society of London, Philosophical Transactions, Series A, v. 300, p. 435-442.

Egbert, R. L., 1954, Geology of the East Canyon Area [M.S. thesis]: Salt Lake City, University of Utah, 34 p.

Ekstrom, G., and Dziewonski, A. M., 1985, Centroid-moment tensor solutions for 35 earthquakes in western North America (1977-1983): Bulletin of the Seismological Society of America, v. 75, p. 23-40.

Erickson, A. J., Jr., and Mortensen, Vol. L., 1974, Soil Survey of Cache Valley area, Utah: Soil Conservation Service and Forest Service, U. S. Department of Agriculture, 192 p.

Eskelsen, Q. M., 1953, Geology of the Soapstone Basin and vicinity, Wasatch, Summit, and Duchesne Counties, Utah [M.S. thesis]: Salt Lake City, Utah, University of Utah, 46 p.

Fenneman, N. M., 1931, Physiography of the western United States: McGraw-Hill Book Company, New York.

Foley, L. L., Martin, R. A., and Sullivan, J. T., 1986, Seismotectonic study for Joes Valley, Scofield, and Huntington North Dams, Emery County and Scofield Projects, Utah [unpublished report]: Denver, Colorado, U. S. Bureau of Reclamation Seismotectonic Report 86-7, 167 p.

Foley, L. L., 1987, Late Quaternary normal faulting in the Joes Valley graben, Wasatch Plateau, central Utah [abstr.]: Geological Society of America Abstracts with Programs, v. 19, no. 5, p. 275.

Fox, R. C., 1984, Geophysical analysis of Jordanelle damsite [unpublished report]: Provo, Utah, report to the U.S. Bureau of Reclamation.

Gilbert, G. K., 1890, Lake Bonneville: U.S. Geological Survey Monograph no. 1, 438 p.

---- 1928, Studies of Basin and Range structure: U.S. Geological Survey Professional Paper 153, 89 p.

Gilbert, J. D., Ostenaa, D., and Wood, C., 1983, Seismotectonic study for Jackson Lake Dam and Reservoir, Minidoka Project, Idaho-Wyoming [unpublished report]: Boise, Idaho, and Denver, Colorado, U. S. Bureau of Reclamation Seismotectonic Report 83-8, 123 p.

Greensfelder, R. W., Kintzer, F. C., and Somerville, M. R., 1980, Seismotectonic regionalization of the Great Basin and comparison of moment rates computed from Holocene strain and historic seismicity: Geological Society of America Bulletin, Part II, v. 91, no. 9, p. 2039-2111.

Grogger, P. K., 1974, Glaciation of the high Uintas primitive area, Utah,with emphasis on the northern slope [Ph.D. thesis]: Salt Lake City, Utah, University of Utah, 230 p.

Guthrie, R. L., and Witty, J. E., 1982, New designations for soil horizons and layers and the new Soil Survey Manual: Soil Science Society of America Jounal, v. 46, p. 443-444.

Haimson, B. C., 1981, Hydrofracturing studies, Drillhole DH-101, Fifth water underground powerplant site, Diamond Fork Power system - Bonneville unit, Central Utah Project [unpublished report]: Provo, Utah, Report to the U.S. Bureau of Reclamation, 29 p.

Haimson, B. C., and Lee, M. Y., 1985, Stress measurements at the Jordanelle Damsite, Central Utah Project, using wireline hydrofracturing [unpublished report]: Provo, Utah, report to the U.S. Bureau of Reclamation, 34 p.

Hait, M. H., Jr., and Scott, W.E., 1978, Holocene faulting, Lost River Range, Idaho [abstr.]: Geological Society of America Abstracts with Programs, v. 10, no. 5, p. 217.

Hansen, W. R., 1983, Post-Laramide tectonic history of the eastern Uinta Mountains, Utah, Colorado, and Wyoming: The Mountain Geologist, v. 21, no. 1, p. 5-29.

Harmon, R. S., Ford, D. C., and Schwarcz, H. P., 1977, Interglacial chronology of the Rocky and Mackenzie Mountains based upon 230 234 U dating of calcite speleothems: Canadian Journal Earth Sciences, v. 14, p. 2543-2552.

Hill, D. P., 1982, Contemporary block tectonics: California and Nevada: Journal of Geophysical Research, v. 87, no. B7, p. 5433-5450.

Hintze, L. F., 1980, Geologic map of Utah: Utah Geological and Mineral Survey, 1:500,000.

Hopkins, D. L., 1982, A structural study of Durst Mountain and the north-central Wasatch Mountains, Utah [M. S. Thesis]: Salt Lake City, Utah, University of Utah, 50 p.

Hopkins, D. L., and Bruhn, R. L., 1983, Extensional faulting in the Wasatch Mountains, Utah [abstr.]: GeologicalSociety of America, Abstracts with Programs, v. 15, no. 5, p. 402.

Howard, K. A., Aaron, J. M., Brabb, E. E., Brock, M. R., Gower, H. D., Hunt, S. J., Milton, D. J., Muehlberger, W. R., Nakata, J. K., Plafker, G., Powell, D. C., Wallace, R. E., Witkind, I. J., 1978, Preliminary map of young faults in the United States as a guide to possible fault activity: U. S. Geological Survey Miscellaneous Field Studies Map MF-916, 1:5,000,000.

Hunt, C. B., 1956, Cenozoic Geology of the Colorado Plateau: U.S. Geological Survey Professional Paper no. 279, 99 p.

---- 1982, The anomalous transverse canyons of the Wasatch Range, in Nielson, D. L., ed., Overthrust Belt of Utah: Utah Geological Association Publication no. 10, p. 81-90.

Hunt, C. B., Varnes, H. D., and Thomas, H. E., 1953, Lake Bonneville: Geology of northern Utah Valley, Utah: U.S. Geological Survey Professional Paper 257-A, 99 p.

Jackson, M. L., 1956, Soil Chemical Analysis, Advanced Course [unpublished report]: Madison, Wisconsin, University of Wisconsin, Department of Soil Science, 656 p.

Jackson, S. M., 1985, Acceleration data from the 1983 Borah Peak, Idaho, earthquake recorded at the Idaho National Engineering Laboratory, in Stein, R. S., and Bucknam, R. C., eds., Proceedings of Workshop XXVIII on the Borah Peak, Idaho, earthquake: U.S. Geological Survey Open-File Report 85-290, v. A, p. 385-400.

Jackson, S. M., and Boatwright, J., 1985, The Borah Peak earthquake of October 28, 1983 -- strong ground motion: Earthquake Spectra, v. 2, p. 51-69.

Jordanelle Task Force, 1982, Consultant Review Briefing Document for the proposed Jordanelle Damsite and Resevoir, Bonneville Unit, Central Utah Project [unpublished report]: Denver, Colorado, report to U. S. Bureau of Reclamation.

Kaliser, B. N., 1972, Geologic hazards in Morgan County with applications to planning: Utah Geologic and Mineral Survey Bulletin 93, 56 p.

Kaliser, B. N., 1975, Ground cracks resulting from the Pocatello Valley earthquake [abstr.]: Geological Society of America Abstracts with Programs, v. 7, no. 7, p. 1137.

Katrinsky, A. J., 1977, Seismicity of the Wasatch front: Detailed epicentral patterns and anomalous activity [M.S. thesis]: Salt Lake City, Utah, University of Utah, 138 p.

Keller, G. R., Smith, R. B., and Braile, L. W., 1975, Crustal structure alongthe Great Basin-Colorado Plateau transition from seismic refraction studies: Journal of Geophysical Research, v. 80, no. 8, p. 1093-1098.

Knopoff, L., and Kagan, Y., 1977, Analysis of the theory of extemes as applied to earthquake problems: Journal of Geophysical Research, v. 82, p. 5647-5657.

Kolesar, P. T., 1981, Low-temperature geothermal system, Midway, Utah, in Central Wasatch Geology: Utah Geological Association Publication 9, p. 24-30.

Lamerson, P. R., 1982, Fossil Basin area and its relationship to the Absoraka thrust system, in R.B. Powers ed., Geologic Studies of the Cordilleran Thrustbelt: Denver, Colorado, Rocky Mountain Association of Geologists, p. 279-340.

Lander, J. F., and Cloud, W. K., 1964, United States earthquakes, 1962: U.S. Department of Comerce, 1964.

Langer, C. J., Keller, G. R., and Smith, R. B., 1979, A study of aftershocks of the October 1, 1972 m_b = 4.7, Heber City, Utah earthquake, in Arabasz, W. J., Smith, R. B., and Richins, W. D., eds., Earthquake studies in Utah 1850 to 1978: University of Utah Seismograph Stations, Department of Geology and Geophysics, Salt Lake City, Utah, University of Utah, p. 383-394.

Lawton, T. F., 1980, Petrography and structure of the Little Cottonwood stock and metamorphic aureole, central Wasatch Mountains, Utah [Ph. D. Thesis]: California, Stanford University.

Lee, W. H. K. and Lahr, J. C., 1975, HYPO71 (revised), a computer program for determining hypocenter, magnitude, and first motion pattern of local earthquakes: U.S. Geological Survey Open-File Report 75-311, 114 p.

Legette, R. M., and Taylor, G. H., 1937, Geology and ground water resources of Ogden Valley: U.S. Geological Survey Water Supply Paper 796-D, 160 p.

Lofgren, B. E., 1955, Resume of the Tertiary and Quaternary stratigraphy ofOgden Valley, Utah, in Tertiary and Quaternary Geology of east Bonneville Basin: Utah Geological Society Guidebook no. 10, p. 70-84.

MacDonald, R. E., 1976, Tertiary tectonics and sedimentary rocks along the transition -- Basin and Range province to Plateau and Thrustbelt province, Utah, in Hill, J.G., ed., Symposium on the Geology of the Cordilleran Hingeline: Rocky Mountain Association of Geologists, 1976 Symposium, p. 281-317.

Machette, M. N., 1984, Preliminary investigations of late Quaternary slip rates along the southern part of the Wasatch fault zone, central Utah, in Hays, W. W., Gori, P. L., eds., Proceedings of conference XXVI, A workshop on "evaluation of regional and urban earthquake hazards and risk in Utah": U.S. Geological Survey Open-File Report 84-763, p. 391-406.

---- 1985a, Calcic soils of the southwestern United States, in Weide, D. L., ed., Soils and Quaternary geology of the southwestern United States: Geological Society of America Special Paper 203, p. 1-23.

---- 1985b, Late Cenozoic geology of the Beaver Basin, southwestern Utah: Brigham Young University Studies in Geology, v. 32, part 1, p. 19-37.

---- 1987, Recent studies of the late Quaternary history of the Wasatch fault zone, Utah--a review [abstr.]: Geological Society of America, Abstracts with Programs v. 19, no. 5, p.317.

Machette, M. N., Personius, S. F., and Nelson, A. R., 1987, Quaternary geology along the Wasatch fault zone: segmentation, recent investigations, and preliminary conclusions in Hayes, W. W., and Gori, P., eds., Assessment of regional earthquake hazards and risk along the Wasatch Front, Utah: U.S. Geological Survey Open-File Report 87-585, p. A1-A72.

Machette, M. N., and Lund, W. R., 1987, Late Quaternary history of the American Fork segment of the Wasatch fault zone, Utah [abstr.]: Geological Society of America, Abstracts with Programs, v. 19, no. 5, p. 317.

Madole, R. F., 1976, Glacial geology of the Front Range, Colorado, in, Mahoney, W. C., ed., Quaternary Stratigraphy of North America: Stroudsburg, PA, Dowden, Hutchinson, and Ross, p. 297-318.

Madole, R. F., and Shroba, R. R., 1979, Till sequence and soil development in the north St. Vrain drainage basin, east slope, Front Range, Colorado, in Ethridge, F. G., ed., Geological Society of America, Rocky Mountain Section, Guidebook for Fieldtrips, 32nd Annual Meeting: Fort Collins, Department of Earth Resources, Colorado State University, p. 124-178.

Madsen, D. B., and Currey, D. R., 1979, Late Quaternary glacial and vegetation changes, Little Cottonwood Canyon area, Wasatch Mountains, Utah: Quaternary Research, v. 12, no. 2, p. 254-270.

Malde, H. E., 1971, Geologic investigation of faulting near the National Reactor Testing Station, Idaho, with a section on microearthquake studies by Pitt, A. M., and Eaton, J. P.: U.S. Geological Survey Open-File Report 71-338, 167 p.

Mann, D. C., 1974, Clastic Laramide sediments of the Wasatch Hinterland, northeastern Utah [M.S. thesis]: Salt Lake City, Utah, University of Utah, 112 p.

Marsell, R. E., 1963, The Quaternary system in Utah, in Oil and Gas Possibilities of Utah, reevaluated: Utah Geologic and Minerologic Survey Bulletin 54, p. 147-154.

Martin, R. A., Jr., Nelson, A. R., Weisser, R. R., and Sullivan, J. T., 1985, Seismotectonic study for Taskeech Dam and Reservoir Site, Upalco Unit, and Upper Stillwater Dam and Resevoir Site, Bonneville Unit, Central Utah Project, Utah [unpublished report]: Denver, Colorado, U.S. Bureau of Reclamation Seismotectonic Report 85-2, 94 p.

Maw, G. G., 1968, Lake Bonneville history in the Cutler Dam Quadrangle, Cache and Box Elder Counties, Utah [M.S. thesis]: Logan, Utah, Utah State University.

McCalpin, J. R., Robison, R. M., and Garr, J. D., 1987, Neotectonics of the Hansel Valley-Pocatello Valley Corridor, northern Utah and southern Idaho, in Hayes, W. W., and Gori, P., eds., Assessment of regional earthquake hazards and risk along the Wasatch Front, Utah: U.S. Geological Survey Open-File Report 87-585, p. G1-G44.

McCoy, W. D., 1981, Quaternary aminostratigraphy of the Bonneville andLahontan basins, western U.S., with paleoclimatic implications [Ph. D. thesis]: Boulder, University of Colorado, 157 p.

McKee, M. E. and Arabasz, W. J., 1982, Microearthquake studies across the Basin and Range - Colorado Plateau transition in central Utah, in Nielson, D. L., ed., Overthrust Belt of Utah: Utah Geological Association Publication no. 10, p. 137-149.

McKenzie, D. P., 1969, The relationship between fault plane solutions for earthquakes and the directions of the principle stresses: Bulletin of the Seismological Society of America, v. 59, p. 591-601.

Meiiji Resource Consultants, 1980, Results of a geophysical survey of the Jordanelle damsite and reservoir [unpublished report]: Provo, Utah, prepared for U.S. Bureau of Reclamation, 20 p.

Meissner, R., and Strehlau, J., 1982, Limits of stresses in continental crusts and their relation to the depth-frequency distribution of shallow earthquakes: Tectonics, v. 1, p. 73-89.

Molnar, P., 1979, Earthquake recurrence intervals and plate tectonics: Bulletin of the Seismological Society of America, v. 69, p. 115-133.

Montgomery, B., 1980, written communication.

Morris, H. T., 1983, Interrelations of thrust and transcurrent faults in the central Sevier orogenic belt near Leamington, Utah, in Tectonic and Stratigraphic studies of the eastern Great Basin: Geological Society of America Memoir 157, p. 75-82.

Mullens, T. E., and Izett, G. A., 1964, Geology of the Paradise Quadrangle, Cache County, Utah: U. S. Geological Survey Bulletin 1181-5.

Mullens, T. E., and Laraway, W. H., 1964, Geology to the Devils Slide Quadrangle Morgan and Summit Counties, Utah: U.S. Geological Survey Geologic Quadrangle Map MF-290, 1:24,000.

---- 1973, Geologic map of the Morgan Quadrangle, Morgan County, Utah: U.S. Geological Survey Geologic Quadrangle Map MF-318, 1:24,000.

Myers, W. B., and Hamilton, W., 1964, Deformation accompanying the Hebgen Lake earthquake of August 17, 1959, in The Hebgen Lake, Montana, Earthquake of August 17, 1959: U.S. Geological Survey Professional Paper 435, p. 55-98.

Nakata, J. K., Wentworth, C. M., and Machette, M. N., 1982, Quaternary fault map of the Basin and Range and Rio Grande Rift provinces, western United States: U.S. Geological Survey Open-File Report 82-0579, 1:2,500,000.

Nash, D. B., 1981, Fault -- A Fortran program for modelling the degradation of active normal fault scarps: Computers and Geosciences, v. 7, p. 249-266.

National Earthquake Information Service, 1983, Preliminary determination of epicenters, monthly listing: U.S. Geological Survey, October, 1983, 20 p.

National Oceanic and Atmospheric Administration (NOAA), 1985, Earthquake data file: U. S. Department of Commerce.

Nelson, A. R., Millington, A. C., Andrews, J. T., and Nichols, H., 1979, Radiocarbon-dated upper-Pleistocene glacial sequence, Fraser Valley, Colorado Front Range: Geology, v. 7, p. 410-414.

Nelson, A. R., and Martin, R. A., 1982, Seismotectonic report for Soldier Creek Dam, Central Utah Project, Utah [unpublished report]: Denver, Colorado, U. S. Bureau of Reclamation Sesmotectonic Study Report 82-1, 115 p.

Nelson, A. R., and Taylor, E. M., 1985, Lotus 1-2-3 template to calculate soil development indices: Denver, Colorado, Computer Oriented Geological Society, Public Domain Diskettes -- Geological Applications for Your Micro, v. 5, (file SOILIND).

Nelson, A. R., and VanArsdale, R. B., 1986, Recurrent late Quaternary movement on the Strawberry normal fault, Basin and Range -- Colorado Plateau transition zone, Utah: Neotectonics, v. 1, p. 1-30.

Nelson, A. R., and Sullivan, J. T., 1987, Late Quaternary history of the James Peak fault, southernmost Cache Valley, north-central Utah, in Hayes, W. W., and Gori, P., eds., Assessment of regional earthquake hazards and risk along the Wasatch Front, Utah: U.S. Geological Survey Open-File Report 87-585, p. J1-J39.

Nelson, M. E., 1971, Stratigraphy and paleontology of Norwood Tuff and Fowkes Formation, northeastern Utah and southwestern Wyoming [M.S. thesis]: Salt Lake City, Utah, University of Utah, 65 p.

Neumann, F., 1936, United States earthquakes, 1934: U.S. Department of Commerce.

Nielson, R. L., 1979, The glaciation of Slate Canyon, Provo, Utah [abstr.]: Geological Society of America, Abstracts with Programs, v. 11, no. 6, p. 297.

Ostenaa, D. A., 1984, Relationships affecting estimates of surface fault displacements based on scarp-derived colluvial deposits [abstr.]: Geological Society of America, Abstracts with Programs, v. 16, no. 5, p. 327.

Pardee, J. T., 1926, The Montana earthquake of June 27, 1925: U.S. Geological Survey Professional Paper 147-B, 17 p.

Personius, S. F., and Gill, H. E., 1987, Holocene displacement on the Brigham City segment of the Wasatch fault zone near Brigham City, Utah [abstr.]: Geological Society of America, Abstracts with Programs, v. 19, no. 5, p. 326.

Peterson, D. L., 1970, A gravity and aeromagnetic survey of Heber and Rhodes Valleys, in Baker, C. H., Jr., Water resources of the Heber-Kamas-Park City area, north-central Utah: Utah Department of Natural Resources Technical Publication no. 27, p. 54-60.

---- 1974, Bouguer gravity map of part of the northern Bonneville basin, Utah and Idaho: U.S. Geological Survey Miscellaneous Field Studies Map MF-627, 1:250,000.

Peterson, D. L., and Oriel, S. S., 1970, Gravity anomalies in Cache Valley, Cache and Box Elder counties, Utah, and Bannock and Franklin counties, Idaho: U. S. Geological Survey Professional Paper 700-C, p. C114-C118.

Peterson, V. E., 1936, The geology of a part of the Bear River Range and some relationships that it bears with the rest of the range [M.S. thesis]: Logan, Utah, Utah State University, 71 p.

Pierce, K. L., 1979, History and dynamics of glaciation in the northern Yellowstone National Park area: U.S. Geological Survey Professional Paper 729-F, 90 p.

---- 1985, Quaternary history of faulting on the Arco segment of the Lost River fault, central Idaho, in Stein, R. S., and Bucknam, R. C., eds., Proceedings of Workshop XXVIII on the Borah Peak, Idaho, earthquake: U.S. Geological Survey Open-File Report 85-290, v. A, p. 195-206.

Pierce, K. L., Obradovitch, J. D., and Friedman, I., 1976, Obsidian hydration dating and correlation of Bull Lake and Pinedale glaciations near West Yellowstone, Montana: Geological Society of America Bulletin, v. 87, p. 703-710.

Piety, L. A., Wood, C. K., Gilbert, J. D., Sullivan, J. T., and Anders, M. H., 1986, Seismotectonic Study for Palisades Dam and Reservoir, Palisades Project, Idaho [unpublished report]: Denver, Colorado, U. S. Bureau of Reclamation Seismotectonic Report 86-3, 198 p.

Pinnell, M. L., 1972, Geology of the Thistle quadrangle, Utah: Brigham Young University Geology Studies, v. 19, part 1, p. 89-130.

Pitt, A. M., Weaver, C. S., and Spence, W., 1979, The Yellowstone Park earthquake of June 30, 1975: Bulletin of the Seismological Society of America, v. 69, no. 1, p. 187-205.

Platt, L. B., 1975, Recent faulting at Samaria Mountain, southeastern Idaho [abstr.]: Geological Society of America Abstracts with Programs, v. 7 no. 7, p. 1229-1230.

Porter, S. C., Pierce, K. L., and Hamilton, T. D., 1983, Late Wisconsin mountain glaciation in the western United States, in Wright, H. E., Jr., Late Quaternary environments of the western United States, Porter, S. C., ed., The Late Pleistocene, v. 1: Minneapolis, Minnesota, University of Minnesota Press, p. 71-111.

Prescott, W. H., Savage, J. C., and Kinoshita, W. T., 1979, Strain accumulation rates in the western United States between 1970 and 1978: Journal of Geophysical Research, v. 84, p. 5423-5435.

Proffett, J. M., Jr., 1971, Late Cenozoic structure in the Yerington district, Nevada, and the origin of the Great Basin [abstr]: Geological Society of America Abstracts with Programs, v. 3, no. 2, p. 181.

Proffett, J. M., Jr., 1977, Cenozoic geology of the Yerington district, Nevada, and implications for the nature and origin of Basin and Range faulting: Geological Society of America Bulletin, v. 88, p. 247-266.

Quitzau, R. P., 1961, A regional gravity survey of the back valleys of the Wasatch Mountains and adjacent areas in Utah, Idaho and Wyoming [M.S. thesis]: Salt Lake City, Utah, University of Utah, 48 p.

Richins, W. D., 1979, Earthquake data for the Utah region 1850 to 1978, in Arabasz, W. J., Smith, R. B. and Richins, W. D., eds., Earthquake studies in Utah, 1850 to 1978: University of Utah Seismograph Stations, Department of Geology and Geophysics, University of Utah, Salt Lake city, Utah, p. 57-251.

Richins, W. D., Arabasz, W. J., Hathaway, G. M., McPherson, E., Oehmich, P. J., and Sells, L. L., 1984, Earthquake data for the Utah region, January 1, 1981 to December 31, 1983: University of Utah Seismograph Stations, Salt Lake City, Utah, University of Utah, 111 p.

Richmond, G. M., 1964, Glaciation of Little Cottonwood and Bells Canyons, Wasatch Mountains, Utah: U.S. Geological Survey Professional Paper 454-D, 41 p.

---- 1965, Glaciation of the Rocky Mountains, in Wright, H. E., Jr., and Frey, D. G., eds., The Quaternary of the United States: Princeton, Princeton University Press, p. 217-230.

Riess, S. K., 1985, Structural geometry of the Charleston thrust fault, central Wasatch Mountains, Utah [M.S. Thesis]: Salt Lake City, Utah, University of Utah, 73 p.

Ritzma, H. R., 1969, Tectonic resume, Uinta Mountains, in Geologic Guide book of the Uinta Mountains: Intermountain Association of Geologists, 16th Annual Field Conference, p. 57-63.

Rogers, J. L., 1978, Geologic reconnaisance of a portion of the Logan East Bench [unpublished report]: Salt Lake City, Utah, Utah Geological and Mineral Survey, Report of Investigations, 51 p.

Royse, Frank Jr., 1983, Extensional faults and folds in the Foreland Thrust Belt, Utah, Wyoming, and Idaho [abstr.]: Geological Society of America Abstracts, v. 15, no. 5, p.295.

Royse, Frank Jr., Warner, M. A., and Reeves, D. L., 1975, Thrust belt structural geometry and related stratigraphic problems -- Wyoming, Idaho, and northern Utah: Rocky Mountain Association of Geologists Symposium -- Deep Drilling Frontiers of the Rocky Mountains, p. 41-54.

Sbar, M. L., Barazangi, M., Dorman, J., Scholz, C. H., and Smith, R. B., 1972, Tectonics of the Intermountain Seismic Belt, western United States: microearthquake seismicity, and composite fault plane solutions: Geological Society of America Bulletin, v. 83, p. 12-28.

Schackleton, N. V., and Opdyke, 1973, Oxygen isotope and paleomagnetic stratigraphy of equatarial Pacific core V28-238: Oxygen isotope temperatures and ice volumes on a 10^5 and 10^6 scale: Quaternary Research, v. 3, p. 39-55.

Schick, R. B., 1955, Geology of the Morgan-Henefer Area, Morgan and Summit Counties, Utah [M.S. thesis]: Salt Lake City, Utah, University of Utah, 54 p.

Schwartz, D. P., and Coppersmith, K. J., 1984, Fault behavior and characteristic earthquakes -- examples from the Wasatch and San Andreas fault zones: Journal of Geophysical Research, v. 89, n. B7, p. 5681-5698.

Scott, W. E., McCoy, W. D., Shroba, R. R., and Rubin, Meyer, 1983, Reinterpretation of the exposed record of the last two cycles of Lake Bonneville, western United States: Quaternary Research, v. 20, p. 241-265.

Shenon, P.J., 1936, The Utah earthquake of March 12, 1934, (extracts from unpublished report), in Newman, F., United States Earthquakes, 1934: U.S. Coast and Geodetic Survey Serial 4593, p. 43-48.

Shroba, R. R., 1980, Influence of parent material, climate, and time on soils formed in Bonneville-shoreline and younger deposits near Salt Lake City and Ogden, Utah [abstr.]: Geological Society of America, Abstracts with Programs, v. 12, no. 6, p. 304.

Shroba, R. R., and Birkeland, P. W., 1983, Trends in late Quaternary soil development in the Rocky Mountains and Sierra Nevada of the western United States, in Wright, H. E., Jr., Late Quaternary environments of the western United States, Porter, S. C., ed., The Late Pleistocene, v. 1: Minneapolis, Minnesota, University of Minnesota Press, p. 71-111.

Shroba, R. R., Rosholt, J. N., and Madole, R. F., 1983, Uranium-trend dating and soil B horizon properties of till of Bull Lake age, north St. Vrain drainage basin, Front Range, Colorado [abstr.]: Geological Society of America, Abstracts with Programs, v. 15, no. 5, p. 431.

Shuey, R. T., Shellinger, D. K., Johnson, E. G., and Alley, C. B., 1973, Aeromagnetics and the transition between the Colorado Plateau and Basin and Range provinces: Geology, v. 1, p. 107-110.

Sibson, R. H., 1974, Frictional constraints on thrust, wrench, and normal faults: Nature, v. 249, p. 542-545.

---- 1982, Fault zone models, heat flow, and the depth distribution of earthquakes in the continental crust of the United States: Bulletin of the Seismological Society of America, v. 72, p. 151-163.

Sibson, R. H., 1984, Roughness at the base of the seismogenic zone -- contributing factors: Journal of Geophysical Research, v. 89, p. 5791-5800.

Simpson, D. W., 1976, Seismicity changes associated with reservoir loading: Engineering Geology, v. 10, p. 123-151.

Slemmons, D. B., 1977, State-of-the-art for assessing earthquake hazards in the United States, report 6: faults and earthquake magnitude: U.S. Army Corps of Engineers Miscellaneous Paper 5-73-1.

Smith, R. B., 1972, Contemporary seismicity, seismic gaps, and earthquake recurrences of the Wasatch front, in Environmental Geology of the Wasatch Front: Utah Geological Association Publication 1, p. 1-19.

---- 1974, Seismicity and earthquake hazards of the Wasatch front, Utah, July-August, 1974: Earthquake Information Bulletin, v. 6, p. 12-17.

---- 1977, Regional geophysics and intraplate tectonics of the Wyoming-Idaho-Utah thrust belt: Joint Wyoming-Montana-Utah Geological Associations, 29th Annual Field Conference and Symposium, Rocky Mountain Thrust Belt Geology and Resources.

---- 1978, Seismicity, crustal structure, and intraplate tectonics of the interior of the Western Cordillera: Geological Society of America Memoir 152, p. 111-144.

Smith, R. B., and Arabasz, W. J., 1979, Seismicity, tectonics and crustal structure in Utah: Important aspects from new data, in Earthquake studies in Utah 1850 to 1978: Seismograph Stations, Salt Lake City, University of Utah, p. 395-408.

Smith, R. B., and Bruhn, R. L., 1984, Intraplate extensional tectonics of the eastern Basin-Range: Inferences on structural style from seismic reflection data, regional tectonics, and thermal-mechanical models of brittle-ductile deformation: Journal of Geophysical Research, v. 89, p. 5733-5762.

Smith, R. B., and Lindh, A. G., 1978, Fault-plane solutions of the western United States: A compilation, in Smith, R. B., and G. P. Eaton, eds., Cenozoic tectonics and regional geophysics of the Western Cordillera: Geological Society of America, Memoir 152, p. 107-110.

Smith, R. B. and Sbar, M. L., 1974, Contemporary tectonics and seismicity of the western United States with emphasis on the Intermountain seismic belt: Geological Society of America Bulletin, v. 85, p. 1205-1218.

Smith, R. B., Winkler, P. L., Anderson, J. G., and Scholz, C. H., 1974, Source mechanisms of microearthquakes associated with underground mines in eastern Utah: Bulletin of the Seismological Society of America, v. 64, p. 1295-1317.

Sorensen, M. L. and Crittenden, M. D. Jr., 1972, Geologic map of part of the Wasatch Range near North Ogden, Utah: U.S. Geological Survey Geologic Quadrangle Map MF-428, 1:24,000.

---- 1976, Preliminary geologic map of the Mantua Quadrangle and part of the Willard Quadrangle, Box Elder, Weber, and Cache Counties, Utah: U.S. Geological Survey Miscellaneous Field Studies Map MF-720, 1:24,000.

---- 1979, Geologic map of the Huntsville Quadrangle, Weber and Cache Counties, Utah: U.S. Geological Survey Geologic Quadrangle Map GQ-1503, 1:24,000.

Standlee, L. A., 1982, Structure and stratigraphy of Jurassic rocks in central Utah: Their influence on tectonic development of the Cordilleran foreland thrustbelt, in Powers, R. B., ed., Geologic Studies of the Cordilleran Thrustbelt: Rocky Mountain Association of Geologists, p. 357-382.

Stanley, W. D., 1972, Geophysical study of unconsolidated sediments and basin structure in Cache Valley, Utah and Idaho: Geological Society of America Bulletin, v. 83, p. 1817-1830.

Stein, R. S., and Barrientos, S. E., 1985, The 1983 Borah Peak, Idaho, earthquake: Geodetic evidence for deep rupture on a planar fault: U.S. Geological Survey Open-File Report 85-290, p. 459-484.

Stepp, J. C., 1972, Analysis of the completeness of the earthquake sample in the Puget Sound area and its effect on statistical estimates of earthquake hazards, in Proceedings, International Conference on Microzonation for Safer Construction, Research and Application, v. 2: Seattle, Washington, Washington University, p. 897-909.

Stewart, J. H., 1971, Basin and Range structure: a system of horsts and grabens produced by deep-seated extension: Geological Society of America Bulletin, v. 82, p. 1019-1043.

---- 1978, Basin-Range structure in western North America: areview: Geological Society of America Memoir 152, p. 1-32.

Stewart, J. H., Moore, W. J., and Zeitz, I., 1977, East-west patterns of igneous rocks, aeromagnetic anomalies, and mineral deposits, Nevada and Utah: Geological Society of America Bulletin, v. 88, p. 67-77.

Stewart, S. W., 1958, Gravity survey of Ogden Valley in the Wasatch Mountains, north-central Utah: EOS, v. 39, no. 6, p. 1151-1157.

Stokes, W. L., and Madsen, J. H., Jr., 1961, Geologic map of Utah - northeast quarter: Utah Geological and Mineral survey, 1:250,000.

Sullivan, J. T., and Nelson, A. R., 1983, Late Cenozoic faulting in Heber and Keetley Valleys, northeastern Utah, in Crone, A. J., ed., Paleoseismicity along the Wasatch Front and adjacent areas, central Utah, in Geologic excursions in neotectonics and engineering geology in Utah, Geological Society of America, Fieldtrip guidebook for Rocky Mountain and Cordilleran Section Meeting - Part IV: Utah Geologic and Mineral Survey Special Studies 62, p. 55-62.

Sullivan, J. T., Foley, L. L., Martin, R. A., Jr., Foley, L. L., and Ostenaa, D. A., 1986, Draft seismotectonic study for Jordanelle Dam, Central Utah Project, Utah in Volume II of Technical Review Document for consultant review, Sept., 1986 [unpublished report]: Denver, Colorado, U.S. Bureau of Reclamation.

Sullivan, J. T., and Baltzer, E. M., 1986, Seismotectonic study for Mona Dam and Reservoir [unpublished report]: Denver, Colorado, U. S. Bureau of Reclamation Seismotectonic Report 86-4, 17 p.

Sullivan, J. T., Foley, L. F., Krinsky, C. K., and Baltzer, E. M., 1987, Seismic sources, maximum credible earthquakes, and related seismic hazards for Monks Hollow damsite [unpublished report]: Denver, Colorado, U. S. Bureau of Reclamation Seismotectonic Report 87-2, 35 p.

Sullivan, J. T., and Nelson, A. R., 1987, Quaternary displacement on the Morgan fault, a back valley fault in the Wasatch Range of northeastern Utah, in Hayes, W. W., and Gori, P., eds., Assessment of regional earthquake hazards and risk along the Wasatch Front, Utah: U.S. Geological Survey Open-File Report 87-585, p. I1-I53.

Swan, F. H., III, Schwartz, D. P., and Cluff, L. S., 1980, Recurrence of moderate- to large- magnitude earthquakes produced by surface faulting on theWasatch fault zone, Utah: Bulletin Seismological Society of America, v. 70, no. 5, p. 1431-1462.

Swan, F. H., III, Hanson, K. L., Schwartz, D. P., and Knuepfer, P. L., 1981, Study of earthquake recurrence intervals on the Wasatch fault at the Little Cottonwood site, Utah: U.S. Geological Survey Open File Report 81-450, 30 p.

Swan, F. H., III, Hanson, K. L., Schwartz, D. P., and Black, J. H., 1983, Study of earthquake recurrence intervals on the Wasatch fault, Utah: 8th semi-annual technical report: San Francisco, California, Woodward-Clyde Consultants, 36 p.

Szabo, B. J., 1980, Results and assessment of Uranium-series dating of vertebrate fossils from Quaternary alluviums in Colorado: Arctic and Alpine Research, v. 12, no. 1, p. 95-100.

Thomas, H. E., 1945, The Ogden Valley Artesian Reservoir, Weber County: Utah State Engineer Technical Publication no. 2, 37 p.

Threet, R. L., 1959, Geomorphology of the Wasatch-Uinta Mountains junction, in Guide book to the geology of the Wasatch and Uinta Mountains Transition area: Intermountain Association of Petroleum Geologists, v. 10, p. 24-33.

Tocher, D., 1962, The earthquake at Hebgen Lake, Montana, on August 18, 1959 (GCT) -- Introduction: Bulletin of the Seismological Society of America, v. 52, p. 153-162.

Tooker, E. W., 1983, Variations in structural style and correlation of thrust plates in the Sevier foreland thrust belt, Great Salt Lake area, Utah, in Tectonic and Stratigraphic studies of the eastern Great Basin: Geological Society of America Memoir 157, p. 61-74.

Trexler, D., 1966, Stratigraphy and structure of the Coalville area, Utah: Professional contributions of Colorado School of Mines, no. 2, 69 p.

U.S. Bureau of Reclamation, 1932, Report on Huntsville (Pineview) Dam Including Geological Report by William Peterson [unpublished report]: Denver, Colorado, U. S. Bureau of Reclamation.

---- 1986, Draft Geologic Report for Jordanelle Damsite and Reservoir, Bonneville Unit, Central Utah Project, Utah, in Volume I of Technical Review Document for consultant review, Sept. 1986 [unpublished report]: Provo, Utah, U. S. Bureau of Reclamation.

University of Utah, 1982, Earthquake data file [magnetic tape through December 1981]: University of Utah Seismograph Stations, Department of Geology and Geophysics, Salt Lake City, Utah.

Van Arsdale, R. B., 1979a, Geology of Strawberry Valley and regional implications [Ph.D. thesis]: Salt Lake City, Utah, University of Utah, 65 p.

✓---- 1979b, Geometry and most recent movement along Strawberry normal fault, Wasatch County, Utah [abstr.]: Geological Society of America Abstracts with Programs, v. 11, no. 7, p. 531-532.

Von Hake, C., and Cloud, W. K., 1965, United States earthquakes, 1963: U.S. Department of Commerce.

Walkley, A., and Black, I. S., 1934, An examination of the Degtjareff method for determining soil organic matter, and a proposed modification of the chromic acid titration method: Soil Science, v. 34, p. 29-38.

Wallace, R. E., 1977, Profiles and ages of young fault scarps, north-central Nevada: Geological Society of America Bulletin, v. 88, p. 1267-1281.

---- 1979, Map of young fault scarps related to earthquakes in north-central Nevada: U. S. Geological Survey Open-File report 79-1554, 2 pls., 1:125,000.

---- 1981, Active faults, paleoseismology, and earthquake hazards in the western United States, in Simpson, D. W., and Richards, P. G., eds., Earthquake Prediction - An International Review: American Geophysical Union, Washington, D.C., p. 209-216.

---- 1984, Patterns and timing of late Quaternary faulting in the Great Basin province and relation to some regional tectonic features: Journal of Geophysical Research, v. 89, no. B7, p. 5763-5769.

Wechsler, D. J., and Smith, R. B., 1979, An evaluation of hypocenter location techniques with applications to southern Utah: Regional earthquake distributions and seismicity of geothermal areas: U.S. Department of Energy, 131 p.

Wernicke, B., 1981, Low angle normal faults in the Basin and Range province: nappe tectonics in an extending orogen: Nature, v. 291, p. 645-648.

Wesnousky, S. G., Scholz, C. H., Shimazaki, K., and Matsuda, T., 1983, Earthquake frequency distribution and the mechanics of faulting: Journal of Geophysical Research, v. 88, no. B11, p. 9331-9340.

West, M. W., 1984, Recurrent late Quaternary (Holocene?) faulting, Bear River fault zone, Uinta, Wyoming and Summit Counties, Utah [abstr.]: Geological Society of America, Abstracts with Programs, v. 16, no. 4, p. 259.

---- 1986, Quaternary extensional reactivation of the Darby and Absaroka thrusts, southwestern Wyoming and north-central Utah [abstr.]: Geological Society of America, Abstracts with Programs, v. 18, no. 5, p. 422.

Westphal, W. H., and Lange, A. L., 1963, Seismic aftershock investigations -- Project Vela Uniform, Juab Valley, Utah, earthquake of 7 July, 1963: Technical Report no. 4, SRI Project PHU-4322, prepared for Advanced Research Projects Agency by Stanford Research Institute.

---- 1966, Local seismic monitoring: final technical report: Stanford Research Institute Report, 242 p.

Williams, E. J., 1964, Geomorphic features and history of the lower part of Logan Canyon, Utah [M.S. thesis]: Logan, Utah, Utah State University, 64 p.

Williams, J. S., 1958, Geologic Atlas of Utah, Cache County: Utah Geological and Mineralogical Survey Bulletin no. 64, 104 p.

---- 1962, Lake Bonneville: Geology of southern Cache Valley, Utah: U.S. Geological Survey Professional Paper 257, 6 p.

Williams, J. S., and Tapper, M. L., 1953, Earthquake history of Utah, 1850-1949: Bulletin of the Seismological Society of America, v. 43, p. 191-218.

Williams, J. S., Willard, A. D., and Parker, U., 1962, Recent history of Bear Lake Valley, Utah-Idaho: American Journal of Science, v. 260, p. 24-36.

Wilson, J. C., 1961, Geology of the Alta stock, Utah [Ph.D. thesis]: Pasadena, California, California Institute of Technology.

Wiltschko, D. V. and Dorr, J. A., 1983, Timing of deformation in the overthrust belt and foreland of Idaho, Wyoming, and Utah: American Association of Petroleum Geologists Bulletin, v. 67, no. 8, p. 1304-1322.

Witkind, I. J., 1975a, Preliminary map showing known and suspected active faults in Idaho: U.S. Geological Survey Open-File Report 75-278, 1:500,000, 71 p.

---- 1975b, Preliminary map showing known and suspected active faults in Wyoming: U.S. Geological Survey Open-File Report 75-279, 1:500,000, 36 p.

---- 1982, Salt diapirism in central Utah, in Overthrust Belt of Utah, D. L. Nielson (ed): Utah Geological Association Publication no. 10, p. 13-30.

Witkind, I. J., Lidke, D. J., and McBroome, L. A., 1978, Preliminary Geologic Map of the Price 1° x 2° quadrangle: U.S. Geological Survey Open-File Report 78-465, 1:250,000.

Woodfill, R. D., 1972, A geologic and petrographic investigation of a northern part of the Keetley volcanic field, Summit and Wasatch Counties, Utah [Ph.D. thesis]: Purdue University, 168 p.

Woodward, N. B., 1981, Structural geometry of the Snake River Range, Idaho and Wyoming [Ph.D. thesis]: Baltimore, Maryland, Johns Hopkins University, 261 p.

Wyss, M., Habermann, R. E., and Johnston, A. C., 1978, Long term precursory seismicity fluctuations: U.S. Geological Survey Open-File Report 78-943, p. 869-894.

Wyss, M., 1979, Estimating maximum expectable earthquakes from fault dimensions: Geology, v. 7 p. 336-340.

Young, G. H., 1978, Geology of the Billies Mountain Quadrangle, Utah county, Utah: Brigham Young University Geology Studies, v. 24, part 1, p. 205-280.

Young, J. L., 1939, Glaciation in the Logan Quadrangle, Utah [M.S. thesis]: Logan, Utah, Utah State Agricultural College.

Zandt, G., and Owens, T. J., 1980, Crustal flexure associated with normal faulting and implications for seismicity along the Wasatch Front, Utah: Seismological Society of America Bulletin, v. 70, p. 1501-1520.

Zandt, G., and Richins, W. D., 1981, Interaction of high- and low-angle normal faults along the eastern Basin and Range, northern Utah: EOS, v. 52, p. 961.

Zoback, M. D., 1981, Hydraulic fracturing stress measurements and fracture studies in hole DH-103 Fifth Water power site, Central Utah Project, [unpublished report]: Provo, Utah, U.S. Bureau of Reclamation, 42 p.

Zoback, M. D., Healy, J. H., and Roller, J., 1977, Preliminary stress measurements in central California using the hydraulic fracturing technique: Pure Applied Geophysics, v. 115, p. 135-152.

Zoback, M. L., 1981, State of stress inferred from fault-slip data in the northern Basin and Range: EOS, v. 62, no. 17, p. 394.

---- 1983, Structure and Cenozoic tectonism along the Wasatch fault zone, Utah, in Tectonic and Stratigraphic studies of the eastern Great Basin: Geological Society of America Memoir 157, p. 3-27.

Zoback, M. L., and Zoback, M. D., 1980, State of stress in the conterminous United States: Journal of Geophysical Research, v. 85, p. 6113-6156.

Zoback, M. L., Anderson, R. E., and Thompson, G. A., 1981, Cenozoic evolution of the state of stress and style of tectonism of the Basin and Range province of the western United States: Philosophical Transactions of the Royal Society of London, series A, v. 300, p. 407-434.

APPENDIX A

PROBABILISTIC DETERMINATION OF EPICENTRAL DISTANCES

by

Christopher K. Wood
Dean A. Ostenaa

Wood/Ostenaa
Seismotectonic Section
September 1984

PROBABILISTIC DETERMINATION OF EPICENTRAL DISTANCES

When specific sources of earthquake activity are identified, such as faults with evidence of recent recurrent surface displacement, a deterministic assessment of earthquakes for engineering analysis may be made. A conservative method places the assigned event on the fault at the point of closest approach to the site of interest. As long as causative faults or clusters of seismic activity are identified, there is little difficulty in applying this method. Problems arise, however, when seismicity is apparently uncorrelated with specific locations or fault structures.

If the site of interest falls within a zone of seemingly random seismicity, two avenues of interpretation may be followed. A simple deterministic approach would be to assign regional events at the site. This may be overly cautious, however, since the method essentially takes the rate of seismicity for the entire zone and applies it to the site. Scaling the observed seismicity to a smaller zone surrounding the site does not remedy this problem since there is no realistic way of picking an appropriate size for the zone. The alternate procedure is to take into account directly the probabilistic nature of seismicity in the zone.

If the assumption can be made that earthquakes occur as independent events, unrelated both spatially and in time, then a probabilistic procedure may be used to compute epicentral distances. Within the zone, earthquakes are assumed to have a uniform spatial distribution. For this case, the number of earthquakes in any area contained in the zone is independent of the actual location of the area and is dependent only on the area's size and length of exposure time.

A commonly used model of earthquake occurrence over time is the Poisson distribution. This process assumes that events occur at an average rate λ, which does not vary over time, and that events are independent (i.e., there are no trends with time such as aftershock sequences or localized swarms). Although evidence has been presented which suggests that in many instances these assumptions are not accurate, other statistical models have not been shown to have any greater applicability. The Poisson model is thus a simple, well understood parameterization frequently used in seismic hazard analysis.

The general form of the Poisson distribution is given by

$$P(k,\lambda t) = \frac{(\lambda t)^k}{k!} e^{-\lambda \tau} \qquad (1)$$

where P is the probability of k events occurring during time t, with an average rate of occurrence λ. The mean number of events occurring is λt. The probability of no events occurring in time t is

$$P = e^{-\lambda t} \tag{2}$$

In applying the Poisson model to earthquake occurrence over an area of uniform seismicity, λ is defined to be the mean number of events in the area with magnitudes between $m - \Delta m/2$ and $m + \Delta m/2$ per unit time. The magnitude-frequency of occurrence law is

$$\log_{10} N = a - bm \tag{3}$$

where N is the number of events with magnitude m or larger per unit area per unit time, and a and b are constants. Using this relation for an area of radius r then allows λ to be expressed as

$$\begin{aligned} \lambda &= \pi r^2 \left[N(m - \Delta m/2) - N(m + \Delta m/2)\right] \\ &= \pi r^2 \, 10^{a - bm} \left[10^{b\,\Delta m/2} - 10^{-b\,\Delta m/2}\right] \end{aligned} \tag{4}$$

If a probability P of nonoccurrence is specified, then the radius r may be found in terms of known parameters using equations 2 and 4.

$$r = \left[\frac{1}{\pi t} \frac{10^{-a + bm}}{10^{b\Delta m/2} - 10^{-b\Delta m/2}} \ln \frac{1}{P}\right]^{1/2} \tag{5}$$

Equation 5 gives an epicentral distance at the selected probability of nonoccurrence P within an exposure time t. An event of magnitude m within the interval $m \pm \Delta m/2$ has a probability of 1-P of occurring closer than a distance r within a time t. It is illustrative at this point to further examine the Poisson distribution and demonstrate some simple relationships.

Given a probability of nonoccurrence P_n over exposure time t_n, a mean rate of occurrence λ_0 is defined by

$$P_n = \exp\left(-\lambda_0 t_n\right) \tag{6}$$

This rate of occurrence λ_0 is then

$$\lambda_0 = (1/t_n) \ln(1/P_n) \tag{7}$$

From this rate of occurrence one could calculate an epicentral distance r for a given magnitude interval $m \pm \Delta m/2$ by using equation 4. This is the distance given by equation 5.

Given the occurrence rate λ_0 (which is determined by P_n and t_n) the occurrence time t_0 for which the probability of occurrence reaches some value P_0 is determined from

$$P_o = 1 - \exp(-\lambda_o t_o) \tag{8}$$

For the special case $\lambda_o t_o = 1$, the probability of occurrence is

$$P_o = 1 - \exp(-1)$$

$$= 0.63$$

and the occurrence time t_o is

$$t_o = 1/\lambda_o$$

$$= t_n/\ln(1/P_n)$$

$$= t_n/(1-P_n) \text{ for } 1-P_n \ll 1$$

In the time t_n there is a probability of $1-P_n$ of an event occurring. However, in a time $t_n/1-P_n$ there is a probability of 0.63 of an event occurring, provided P_n is close to unity.

For example, let the annual ($t_n = 1$) probability on nonoccurrence P_n of an earthquake in some area be given by $1 - (2 \times 10^{-5}) = 0.99998$. Then there is a probability of 0.63 of having an earthquake occur in time $t_n/1-P_n = 50{,}000$ years.

APPENDIX B

AN ANALYSIS OF RESERVOIR-INDUCED SEISMICITY IN THE BACK VALLEYS OF THE WASATCH MOUNTAINS

by

Roland C. LaForge

An Analysis of Reservoir Induced Seismicity in the Back Valleys of the Wasatch Mountains

by

Roland C. LaForge

B.1.0 Introduction

Reservoir induced seismicity (RIS), the occurrence of earthquakes caused by the artificial storage and regulation of impounded water, is a phenomenon that is generally acknowledged to have occurred in a number of cases. In specific cases, however, RIS has proven very difficult to define, observe, and predict (Meade, 1982). Early reviews of RIS include those by Rothé (1970), Simpson (1976), and Stuart-Alexander and Mark (1976). Packer and others (1977) list 16 "accepted" and 35 "questionable" cases of RIS worldwide. The most destructive induced earthquake appears to be the 1967 magnitude 6.5 Koyna, India event. This quake killed 200 persons and injured 1500 others, and caused significant damage to the dam (Gupta and Rastogi, 1976). Other notable examples include activity at Hoover Dam, Nevada (Carder, 1945), Nurek reservoir in the Soviet Union (Simpson and Negmatullaev, 1981), and Lake Kariba in Rhodesia (Gough and Gough, 1970).

Proposed mechanisms for the physical causes of RIS are presented by Kisslinger (1976) and Simpson (1986). It is generally agreed that two main effects are responsible for the phenomenon: elastic stresses transmitted to the underlying crust due to the weight of the impounded water, and the effect of increased pore pressure on fault planes at depth. In both cases the state of stress on a fault must be very near that required for rupture, so that the impounded water in effect acts as a triggering mechanism. Factors that appear to be important include the volume and depth of the reservoir, the type of rock underlying the reservoir, its permeability, the existence of pre-existing faults, and the magnitude and orientation of the crustal stress field. Packer and others (1980) found that the great majority of RIS events occurred within 5 years of initial impoundment, and all but one occurred within 10 years. It has been suggested (Simpson, 1986; Leith, 1984) that the two main mechanisms described above influence the delay time between initial impoundment and the RIS event. Whereas initial compaction due to the water weight would cause the event to occur within several weeks or months, pore pressure changes due to the downward percolation of water could take several years to manifest as failure of a fault plane. Gupta and others (1972) found that RIS is influenced by the rate of increase of water level, the duration of loading, and the period of time during which high water levels are maintained.

To our knowledge, the only suggested case of RIS in the ISB is at Palisades Reservoir, Idaho (e.g., Smith and Sbar, 1974; Schleicher, 1975). These suggestions, however, are based on the detection of swarms near the reservoir during brief (less than one month) recording periods. Bones (1978), in discussing the results from a 3-week microearthquake survey, disputed Schleicher's (1975) suggestion. Piety and others (1987), during a 3-month microearthquake survey, found swarms lasting several days to be pervasive in the area, and unrelated to fluctuations in reservoir level. Continuous monitoring over several years would be necessary to resolve the question of RIS at Palisades Reservoir.

In this study we analyzed historical seismicity to detect possible RIS occurrence associated with the 13 USBR reservoirs in north-central Utah. The study consists two parts. In the first, a search for an increase in activity following initial reservoir impoundment is made. In the second, the more recent network data are examined statistically to search for consistent seasonal increases in seismic activity that may be related to the normal yearly fluctuations in reservoir level. At the end of this section, the potential for RIS in north-central Utah will be discussed based on the results of this study, published observations of RIS elsewhere, and theoretical studies.

B.2.0 Statistical Analysis of RIS in North-central Utah

This section describes a statistical analysis of earthquake occurrence around USBR dams in north-central Utah. The purpose of the study was to try to determine whether RIS occurred upon initial filling, or has occurred on a seasonal basis in the vicinity of the subject dams. The procedure for the analysis was as follows:

(1) Earthquakes from the entire historic record occurring within 15 km of the 13 subject dams were extracted from the University of Utah catalog. These were plotted in map view in order to examine their spatial distribution, relation to regional seismicity patterns, and relation to mapped faults.

(2) The earthquakes for each dam were plotted in histogram form to show the number of events per year, and detect any significant increases in local earthquake occurrence following initial water impoundment.

(3) A statistical analysis was performed on more recent data (1974-1986) to search for seasonal biases in seismicity levels around the subject reservoirs. A test was made to see if monthly variations in activity in the vicinity of each dam differed significantly from variations in the regional data. Then, the data were grouped into 3-month periods to detect increases in seasonal proportions between the local and regional data sets.

(4) The evidence for RIS around each dam was then discussed in light of the above evidence. and additional factors such as significant changes in network configuration and other sampling problems were considered.

Table B-1 lists the 13 USBR dams that are the subject of this study. Information regarding the location, year of initial filling, and reservoir capacity are listed for each dam. The structural height of the dam is tabulated, and is taken as a reasonable estimate of maximum reservoir depth. The locations of the dams are plotted on Plates 1a, 1b, and 1c.

Earthquakes taken from the University of Utah catalog that occurred within 15 km of the dams are plotted in figure B-1(a-m). This distance is somewhat arbitrary, but was judged to be a reasonable value considering such factors as the size of the reservoirs, the closeness of induced events to reservoirs in documented cases, and the location errors of earthquakes in the catalog. The plotted symbols are scaled to magnitude, and faults are drawn as mapped on Plate 1 on each figure. In contrast to the epicenters plotted on plate 1, those in figure B-1 encompass the entire historical extent of the catalog. In the figure for Joe's Valley dam (B-1f), the cluster of events in the box are the result of mining activity (Smith and others, 1974; Foley and others. 1986; Williams and Arabasz, 1988) and were not used in further analyses.

Histograms that display the epicenters plotted on figure B-1 as number of events per year are shown in figure B-2(a-m). The year of initial reservoir filling is indicated by an arrow. In figures

without arrows, seismicity within 15 km of the dam was not recorded until a number of years after initial filling. Note that scales differ between figures, and that due to the record length at some damsites the histograms may extend for two or three pages. In most of the figures, an increase in activity is evident in the mid-1970's. This is largely due to the installation of a dense, high-magnification network of seismograph stations in central Utah, which allowed for the detection and location of larger numbers of smaller magnitude events. A significant problem with graphs of this type is that changes in detection capabilities sometimes occur within the time span of the displayed data set. In order to compensate for the increase in detection in 1974, earthquakes that occurred between 1962 and 1986 with magnitude greater than or equal to 2.3 are plotted in figure B-2 as solid portions of the histogram. Since Arabasz and others (1980) assert completeness for the Wasatch front area for magnitude 2.3 since 1962, the solid representations give a more accurate picture, from the standpoint of a uniform detection level, of earthquake occurrence around the dams. A discussion of changes in instrumentation and detection capabilities in the study area can be found in section 4.2 in the main body of this report.

Table B-3 summarizes post-impoundment activity in the vicinity of the reservoirs. The largest post-impoundment earthquake within two different radii, 15 and 25 km, is tabulated from a point estimated to be the center of the reservoir. Δt refers to the number of years after initial filling the event occurred, and the length of the observation period is noted in the last column. Simpson (1986) observed that RIS due to pore pressure changes can occur up to 20 km from the reservoir. The 25 km distance was chosen to conform to this distance, and to take into account such variables as irregularities in reservoir outline and epicentral errors.

The purpose of the statistical analysis was to compare monthly seismicity rates between local samples near the reservoirs (figure B-1) and rates recorded in the central Utah region as a whole, in order to detect possible seasonal biases that may be attributable to RIS. The "central Utah region" as defined for this analysis extends from latitude 39.0N - 42.0N, and from longitude 111.0W - 112.5W, and is therefore equivalent to the area shown in Plate 1. Because of uncertainties in catalog completeness before installation of the dense high-gain network, only data recorded since November 1, 1974 are used in the analysis. The catalog was complete through June, 1986 at the time of this study. Although Arabasz and others (1978) state that this catalog can be considered complete only for events of magnitude 1.5 and above, all magnitudes were utilized. While a greater number of events lends greater credence to the statistical conclusions, the danger exists that a change in the station distribution in the vicinity of a specific site can significantly alter the detection capability in that area, and therefore give a biased estimate of the seismicity rate. To account for this possibility, yearly station location maps have been drawn (figure B-3). These, along with knowledge of the operating histories of individual stations, were used to help determine whether significant changes in activity were real or could be attributed to changes in detection capability.

Due to practical considerations, aftershocks and swarms events were not deleted from the catalog before carrying out the statistical analysis. While over a large region these phenomena may occur randomly and frequently enough to not bias the data, for local samples the occurrence of either is bound to signal aberrations in seismicity not necessarily due to RIS. Ideally, it would be preferable for earthquake occurrence to approximate a Poisson process, where events occur independently in time and space. Since it does not for this case, we were forced to identify the effects of aftershocks and swarms on a case by case basis when discussing statistically significant results.

The first statistical test considered was to see whether or not the monthly proportions of events at a given site can be said to differ significantly from those in the region. This "goodness of fit" test has an approximately χ^2 distribution (e.g., Waldpole and Myers, 1985), and was calculated with the statistic

$$\chi^2 = \sum_{i=1}^{12} \frac{(o_i - e_i)^2}{e_i} \tag{1}$$

where o_i = the observed number of events that occurred around the reservoir in month i, and e_i = the expected number of local events in month i, given the proportion of events that occurred in the central Utah region (as defined above) during that month. Tabulations of the number of events occurring in each month of each year, for the region and for the area around each dam, are presented in table B-2. In this and the following test, the events occurring around the reservoir were subtracted from the number of regional events, so that the two samples were independent.

An important limitation to the effectiveness of this statistical test is the small sample size around many of the reservoirs. A number of statistics textbooks (e.g. Waldpole and Meyers, 1985) state that equation (1) should not be used when e_i is less than 5. This means that low confidence should be placed in the analysis of damsites where the earthquake sample size is less than about 50. Table B-2 shows that about half of the dams have sample sizes below this number. However, χ^2 values have been computed for all dams, and problems associated with sampling deficiencies will be discussed later for each case.

The calculated χ^2 values are presented in table B-4. Here we tested the hypothesis that the monthly proportion of activity around a particular reservoir did not differ significantly from that in the region as a whole. Examining the χ^2 table with $n-1 = 11$ degrees of freedom, we find that the χ^2 value is significant at the 95% level if it exceeds 19.675. It can be seen in table B-4 that the χ^2 values for Deer Creek, Echo, Hyrum, Newton, and Wanship Dams exceeded this value. The analysis therefore pointed to these dams as subjects for further examination.

The next step in the process was to isolate the particular month or season that gave anomalous statistical results in individual cases, and see if an annual periodicity in anomalous behavior was evident. For this test the rates for each month were summed into 3-month quarters in order to detect rate changes in a "seasonal" time frame. This grouping is based on the presumption that water level changes responsible for RIS also occur at roughly "seasonal" intervals. Every possible consecutive 3-month combination was utilized, so that if indeed a cause and effect relationship existed, a phase shift of 1 or 2 months would not go undetected. This staggering of quarters was also effective in isolating single months of anomalous activity, as will be seen in the discussion of the results.

In this case we were interested in comparing the quarterly proportions of activity in the area surrounding the dam to that in the region, to see if a significant difference could be detected. For this purpose we used the statistic

$$z = \frac{\frac{x_1}{n_1} - \frac{x_2}{n_2}}{\left[\hat{p}(1-\hat{p})\left(\frac{1}{n_1} + \frac{1}{n_2}\right)\right]^{\frac{1}{2}}}, \qquad (2)$$

$$where\ \hat{p} = \frac{x_1 + x_2}{n_1 + n_2},$$

x_1 is the number of events per quarter around the dam, n_1 is the total number of events around the dam, and x_2 and n_2 are the same values, respectively, for the region. z is a random variable having approximately the standard normal distribution.

In formalizing this problem, our null hypothesis, H_o, was that the local quarterly proportion did not significantly differ from the regional quarterly proportion. Where we set the critical z-value for a given significance level depended on whether the alternative hypothesis, H_1, was that the local proportion was greater than or less than the regional proportion, or whether it was only greater. For the purposes of this study, we chose the second option (with a critical value of 1.645), on the reasoning that for engineering purposes we are only interested in identifying an increased hazard due to possible RIS effects. The first alternative, however, assumes interest in decreased activity as well, and has implications for the physical causes of the fluctuations. This will be discussed further in section B.3.0.

The computed values are shown in table B-5 with values greater than 1.645 marked. The table shows that quarters with abnormally high rates appeared to be distributed equally among the spring, summer, and autumn months. There was no dam around which activity could be characterized as unusually high during the winter months. In no quarter were there more than four dams that exhibited anomalous activity, and thus the evidence does not suggest a regional seasonal preference for abnormally high activity.

B.2.1 Results

In examining the question of whether RIS has occurred at any of the major dams in the CUP region, each dam and reservoir will be discussed in terms of seismicity occurrence upon initial filling, seismicity occurrence in the vicinity of the reservoir and its relation to regional patterns, and results of the statistical analysis. If the analysis showed significantly higher activity during particular periods than that observed in the region, table B-2 was examined to see if the anomaly was due to an isolated swarm or mainshock-aftershock sequence, or if it was caused by consistently higher activity in all or most of the years of record. Because the number of earthquakes varied greatly from sample to sample, there were cases where the occurrence of a small number of events during a given period gave rise to a misleadingly high statistic. These cases were identified where they arise.

Causey Reservoir, filled in 1966, lies on the eastern edge of the north-south trending back valley seismicity trend (plate 1a). Two local (within 15 km of the dam) events were recorded in 1967; then none until 1971 (figure B-2a). The z-test showed one period that slightly exceeded the 95% confidence limit. This anomaly can be traced to a swarm of events that

occurred in September 1978 (table B-2b).

Deer Creek Reservoir, filled in 1941, lies in a zone of sparse activity near Round Valley (plate 1b). No local events were recorded until 1953, 12 years after initial impoundment. The chi-square test (table B-2) shows a significant deviation from the regional norm, which also appears in columns 4,5, and 6 of table B-5. An examination of the monthly event counts (table B-2c) shows June and July to have had a high number of events relative to the rest of the year. Further examination of the table, however, reveals that 17 of 23 monthly readings, or 74%, had zero events, and 9 of the 23 events, or 40%, occurred during only 2 periods. Thus it does not appear that June and July exhibit consistently increased activity.

East Canyon Reservoir, filled in 1966, lies within the back valley seismic trend northeast of Salt Lake City (plate 1b). Local seismicity was negligible in the 8 years following initial impoundment (figure B-2c). While the chi-square test was negative (table B-2), the z-test shows two anomalously high late summer-autumn quarters (table B-5). This observation can be traced to the occurrence of a swarm of small ($M_L < 1.5$) events in September and October of 1976, which is seen in figure B-1c as a cluster about 10 km northeast of the dam. Figure B-3 shows a stable station distribution about this site during the entire recording period. To draw a possible correlation between this swarm and the East Canyon fault is beyond the scope of this study. Aside from the swarm, activity during September and October in all other years appears normal.

Echo Reservoir is located about 20 km east of East Canyon Reservoir. Although the reservoir was filled in 1930, no local earthquakes were documented until 1964 (figure B-2d). The z-values show anomalously high periods in the autumn. This results from the same 1976 swarm that was responsible for high values for East Canyon Reservoir, and aside from that year activity during those months appears normal.

Hyrum Reservoir, filled in 1935, is located about 50 km north of Ogden, several km west of the back valley seismic trend (plate 1a). No anomalous activity was recorded following initial filling of the reservoir (figure B-2e). The statistical tests show anomalously high activity rates in spring and late fall (table B-5). These can be traced to a swarm of 19 small ($M_L < 1.0$) events on June 12, 1982, and a week-long swarm of 25 somewhat larger ($M_L < 2.0$) earthquakes in late December, 1983 (table B-2f). The 1982 swarm can be seen if figure B-1e about 5 km southeast of the dam; the 1983 swarm is part of the cluster on the east side of the East Cache fault. Aside from these two isolated swarms, activity during those months appears normal. Figure B-3 shows that station distribution around the reservoir has been dense and stable since 1978.

Joes Valley Reservoir, filled in 1966, is located on the Wasatch Plateau (plate 1c), in an area of low-level, diffuse seismicity. The dense cluster of activity outlined in figure B-1f has been related to coal mining activity (Smith and others, 1974; Foley and others, 1986; Williams and Arabasz, 1988), and was deleted prior to analysis. No anomalous activity was recorded following initial reservoir filling (figure B-2f). The statistical analysis (table B-5) shows a high quarter during the spring. An examination of actual activity, however, (table B-2g) shows that 12 of the total of 27 events occurred during this period. Given this small total number, and the fact that most of the entries during March, April, and May show zero events, the high z-value computed for this period should be attributed to the small sample size. Sampling problems due to uneven station distribution about the site are also suggested by figure B-3.

Lost Creek Reservoir, also filled in 1966, is located in a region of very low seismicity about 40 km east of Ogden (plate 1a). No unusual activity was recorded following initial reservoir

filling. Although one anomalously high quarter was noted by the statistical analysis (table B-5), arguments presented above regarding the validity of the analysis when small sample sizes are involved apply to this case also.

Newton Reservoir, filled in 1945, is located in a relatively quiet zone about 20 km northeast of Logan (plate 1a). No local activity was recorded until 12 years after initial filling. The statistical analysis shows 3 summer quarters of high activity, which can be traced in table B-2i to a high total number for the month of July. However, since only 3 of the 11 years are responsible for the anomaly, this cannot be considered a consistent seasonal trend.

Pineview Reservoir, located several km east of Ogden (plate 1a), was first filled in 1937, and raised to its current dimensions in 1957. No anomalous activity was noted during the decade following either year (figure B-2i). A high z-value is noted during January, February, and March in table B-5. This is due to 5 swarm events that occurred on February 11, 1976.

Scofield Reservoir, filled in 1946, is located on the Wasatch Plateau in a region of low seismicity (plate 1c). No local activity was noted until 21 years after initial filling. Although seismicity during the months of March, April, and May are noted in table B-5 as being high, the small sample size (30 total events) preclude this from being labeled significant. This site has also suffered from uneven and sporadic station coverage (figureB-3).

Soldier Creek Reservoir is located in a relatively quiescent zone about 30 km east of Provo (plate 1b). Although the dam was constructed in 1973, filling did not begin until 1984. Because filling is not yet complete, the reservoir outline has not been drawn on figure B-1k. Figure B-2k indicates no increase in activity since 1984. Because only 5 local events have been recorded for this site, statistical analyses are probably meaningless. Figure B-3, however, shows that station coverage in this area has always been poor, and an examination of the 5 events shows that none have a magnitude less than 1.2. Therefore it is likely that smaller earthquakes are missing from the sample, and that the low activity rate is somewhat misleading.

Strawberry Reservoir, located a few km west of Soldier Creek Reservoir, was filled in 1913. No local events were recorded until 1971 (figure B-2l). Since the local seismicity sample numbers only 12 events, a statistical analysis, as for Soldier Creek, is probably meaningless. The discussion on station coverage presented in the previous paragraph also applies to this site.

Wanship Dam (Rockport Reservoir), is located on the east side of the back valley seismic trend about 30 km east of Salt Lake City (plate 1b). The reservoir was filled in 1957, and no local activity was recorded until 1970 (figure B-2m). The statistical analysis points to anomalously high activity during the fall months (table B-2,B-5). Table B-2n shows the numbers of events to be fairly well distributed throughout the years, except for a swarm of 4 events that occurred during December 8-10, 1978. The removal of these events would lower the number of anomalous periods. The sample size for this site is relatively small (45 events). Aside from these considerations, two additional observations argue against RIS occurrence at this site. The first is that the anomalous period is during the autumn months, when reservoir levels are generally low and stable. An examination of table B-2n shows that the statistical anomaly is due to heightened activity during the months of October, November, and December. Simpson (1976) and Simpson and Negmatullaev (1981) point out that induced earthquakes seem to occur when the water level is at or near maximum, and also when abrupt decreases in water level or rapid decreases in the rate of filling occur. Considering the normal seasonal water level cycles for reservoirs in the study area, these conditions and level changes are very unlikely to occur during the months of October, November,

and December. The second is that the local seismicity pattern seen in figure B-1m clearly appears to be part of the larger regional pattern seen in plate 1b. We would therefore argue against RIS occurrence at Rockport Reservoir, although the evidence is not conclusive.

B.3.0 Discussion

The results of the statistical analysis show no clear evidence for RIS at any of the 13 USBR dams. However, the limitations of this study require that these results should not be considered conclusive. Earthquake detection capabilities at the dates when many of the reservoirs were initially filled were poor by today's standards, and it is therefore possible that smaller magnitude induced events occurred that were not detected. The University of Utah seismograph network was not designed with the documentation of RIS as a primarily goal, and coverage around a number of the reservoirs has been poor or uneven. Thus it is possible that RIS has occurred in the study area, but that evidence for it is not obtainable from the available data. Also, the statistical analysis looked at only one parameter, number of earthquakes. The examination of other parameters, such as moment release, could yield different results. The possibility that the statistical models used do not adequately approximate the earthquake occurrence process also exists.

Baecher and Keeney (1982) attempted to draw statistical correlations between documented cases of RIS and attributes such as reservoir depth and volume, bedrock type, stress field, and presence of active faulting in the reservoir. They found that of all the characteristics, depth and volume best correlated with RIS occurrence. Specifically, it was found that reservoirs deeper than 92 m or greater than 12 x 10^8 m^3 in volume showed the highest probabilities of exhibiting RIS. A weak correlation between depth and volume, given RIS occurrence, was noted. Reservoirs with parameters less than these values were judged to have probabilities of RIS of close to zero. Other preferred attributes were found to be sedimentary bedrock beneath the reservoir, and active faulting present prior to reservoir impoundment, although the statistical correlation for these characteristics was not as strong as that for depth and volume. Probabilities for RIS were presented given various single and combined attributes. For example, looking only at reservoirs exceeding 92 m in depth gives an RIS frequency of about .14.

A stress field in which extensional or shear faulting predominates appears to be the most conducive for RIS occurrence, based on theoretical studies (Simpson, 1986) and observed cases (Baecher and Keeney, 1982). A sizable body of evidence (section 2.4) indicates that the CUP region is currently experiencing crustal extension. In-situ stress measurements conducted near the Jordanelle damsite (discussed in section 2.4) indicate stress levels that may be close to failure. The measurements also indicated low pore pressures, which would tend to maximize the potential for induced failure on a fault due to water seeping down from a reservoir. Simpson (1986), however, points out that uncertainties in this type of measurement may be large compared to the stress required to initiate failure.

In the description of the statistical analysis, it was mentioned that there was a choice between a one-sided test and a two-sided test when using equation (2) in section B.3.0, depending on whether we were interested in identifying both increases and decreases in activity, or only increases. For the purposes of this study, only increases were noted. In table B-5, there are 27 quarters in which the regional rate was exceeded at the 95% confidence level. It is interesting to note, however, that there were 25 quarters in which the local rate was lower than the regional rate at the same confidence level (i.e., z-value less than -1.645). This implies that if there is one specific mechanism causing the local fluctuations, it has the effect of both raising and lowering the rate of local seismic activity.

Although the great majority of documented RIS cases record an increase in activity due to reservoir related effects, two cases have been described in which a decrease in seismicity has been attributed to effects associated with water impoundment. In the first, a gap in seismicity along the Calaveras fault in central California is postulated by Bufe (1976) to be caused by stable sliding (creep) along the fault due to increased pore pressure, resulting from downward percolation of water from Anderson Reservoir. Bufe (1976) implied that this effect occurs at shallow (less than 5 km) depths, and for small earthquakes on faults already prone to creep. The second case involves Tarbela Dam in Pakistan. Jacob and others (1979) noted a reduction in seismicity during initial reservoir filling, which they attributed to increased loading in a compressional tectonic environment. While the data for this case were not well supported statistically, good theoretical arguments exist for their hypothesis (Simpson, 1976). None of the specialized conditions involved in these two cases appear to exist in north central Utah. Regional stresses are clearly extensional, not compressional, and to our knowledge fault creep has not been shown to play a significant role in tectonic movements. We would therefore expect reservoir related effects to manifest as an increase in activity in the CUP region. The fact that an approximately equal number of periods of decreased as opposed to increased activity were observed argues against RIS as the causative mechanism of the abnormal periods identified in table B-5.

Packer and others (1980), in examining 42 "accepted" RIS cases, tabulated the time between initial filling and the occurrence of the largest suspected RIS event. It was found that 37 of the total, or 88%, occurred within 5 years of initial impoundment, and all but two, or 95%, occurred within 10 years. In examining the case for dams in north-central Utah in table B-3, for only 2 of the 13 dams (excluding Soldier Creek reservoir, which has not been completely filled) did the largest local event occur less than 10 years before initial filling. The two exceptions are a magnitude 3.7 event seen 13 km WSW of Causey dam in figure B-1a, and a magnitude 2.6 event seen at the center of Joes Valley reservoir in figure B-1f. Neither earthquake appears to stand out from the regional seismicity pattern, and neither is unusually large.

The largest earthquake that appears to have been induced by water impoundment is the 1967 Koyna, India event. The actual magnitude of this event, however, varies from source to source in the literature, and the magnitude scale is rarely noted. The magnitude is stated as "magnitude 7.0" in Guha (1977), "magnitude 6.0" in Gupta and Combs (1976), and "M 6.5" in Gupta and Rastogi (1976). Rothé (1973) uses values of "magnitude 6.3" and "magnitude 6.4" in different places in the same article. The only mentions of magnitude scales found by this author were by Gupta and others (1972) ("magnitude 6.0 on Karnik's $L_G H$ scale"), and an M_S 6.3 noted by Gupta and others (1980). The scale preferred by the USBR for magnitudes in this range for use in strong motion analysis is the M_L scale. While it is apparent that no Wood-Anderson seismographs were operating within a favorable distance of the 1967 event, the M_S reading gives some insight into an equivalent M_L value. Based on a comparison between M_S and M_L for 24 western U.S. earthquakes, Nuttli (1979) calculated a regression between the two scales which equates M_S 6.3 to M_L 6.2. This relation should be considered very tenuous, however, because of the fact that there were only three magnitudes greater than 6 in Nuttli's analysis, and also because frequency filtering characterics of the crust in India may be quite different from those in the western U.S. Faced with the necessity of estimating a value for the maximum induced event for central Utah, however, we will assume an M_L 6.5 earthquake to be a reasonable, conservative value for such an event. This value also coincides with the estimated magnitude of the maximum random (i.e., non-surface rupturing) earthquake for the intermountain seismic belt.

Based on observations of RIS worldwide, one may conclude that the CUP region is a favorable environment for RIS occurrence based on the presence of a moderately active, extensional stress field. However, all but one of the USBR dams considered here are smaller and shallower than those considered by Baecher and Keeney (1982) as having a greater than negligible probability of exhibiting RIS. The lone exception, Soldier Creek reservoir, would be classified as shallow (81 m) but has a projected volume of 13.65 x 10^8 m^3. The depth of this reservoir, however, has to date

not exceeded 63 m, and the current volume is 7.821 x 10^8 m^3. This is below the threshold value of 12 x 10^8 m^3 proposed by Baecher and Keeney (1982). In summary, although to the best of our knowledge RIS has not occurred in north-central Utah, reservoirs that have existed to date in the region have not been as large as those for which RIS is considered to have a greater than negligible probability.

B.4.0 Conclusions

(1) Within the resolution of available data, no increase in activity upon initial filling was noted at any of the subject dams. However, all but one of the reservoirs were filled prior to 1967. before the installation of the current seismograph network. Therefore this conclusion must be qualified by the regional detection thresholds discussed in section 2.1 of the main report.

(2) The statistical tests proved useful in isolating seasonal periods of anomalously high seismic activity. In all but one case, however, the anomalous activity was traceable to swarms during specific years and not to consistently higher activity during all of the years. Inadequate sample sizes also provided justifications for questioning the validity of anomalous values. The fact that comparable numbers of anomalously high and low values were identified argues against RIS as the causative mechanism of the fluctuations.

(3) Based on the statistical analysis performed in this report, there is no evidence for the occurrence of RIS at all but one of the 13 USBR reservoirs. While the analysis pointed to possible RIS at Rockport Reservoir (Wanship Dam), further considerations lead us to conclude that RIS was not responsible for the statistical anomaly.

(4) Based on theoretical studies and observed cases of RIS worldwide, the CUP region shares a number of attributes that appear to be conducive to RIS. However, the depths and volumes of the reservoirs analyzed in this report are lower than those for which the probability of RIS occurrence has been judged to have a greater than negligible value. For deeper and larger volume reservoirs, RIS probabilities may be assignable based on the work of Baecher and Keeney (1982).

B.5.0 Acknowledgements

Comments on this appendix furnished by Bill Astle, Mathematics Department, Colorado School of Mines. are greatly appreciated. Dr. Walter Arabasz of the University of Utah made several good suggestions which were incorporated into the final manuscript.

Table B-1 Dam and Reservoir Parameters

Dam	Latitude	Longitude	Year Completed	Capacity ($x10^8$ m^3)	Structural Height (m)
Causey	41.298	111.592	1966	.084	66
Deer Creek	40.400	111.533	1941	1.84	72
East Canyon	40.920	111.600	1966	.593	79
Echo	40.963	111.432	1930	.911	48
Hyrum	41.625	111.875	1935	.189	35
Joe's Valley	39.288	111.270	1966	.678	59
Lost Creek	41.185	111.400	1966	.247	76
Newton	41.900	111.983	1945	.067	31
Pineview	41.250	111.833	1937	.543	32
Pineview			1957	1.359	42
Scofield	39.789	111.125	1946	.812	38
Soldier Creek	40.153	111.015	1973,1983*	13.650	81
Strawberry	40.157	111.114	1913	3.330	22
Wanship	40.790	111.403	1957	.751	53

*filling began in 1983;
reservoir depth is at 63 m, volume is at 7.821 x 10^8 m^3 (March, 1988)

Table B-2a. Monthly event counts for study region.

NORTH-CENTRAL UTAH

YEAR	JAN	FEB	MAR	APR	MAY	JUN	JUL	AUG	SEP	OCT	NOV	DEC
1974											16	29
1975	21	12	12	15	10	16	26	14	21	40	17	30
1976	24	33	44	24	29	24	49	45	31	33	50	55
1977	39	42	19	19	28	21	25	17	20	19	18	16
1978	32	13	21	7	14	22	14	15	31	21	39	23
1979	53	33	15	24	34	14	21	30	9	15	13	34
1980	24	13	21	28	20	10	30	16	33	12	12	22
1981	19	10	10	41	21	6	5	15	15	19	16	15
1982	5	10	21	15	23	51	15	21	32	26	45	28
1983	14	19	16	27	25	37	21	30	22	36	22	48
1984	6	4	12	3	7	40	17	23	29	38	15	30
1985	23	15	13	14	22	15	10	17	14	17	12	9
1986	18	13	37	17	10	18						
TOTALS	278	217	241	234	243	274	233	243	257	276	275	339

TOTAL NUMBER OF EVENTS = 3110

Table B-2b. Monthly event counts for Causey Dam.

CAUSEY DAM

YEAR	JAN	FEB	MAR	APR	MAY	JUN	JUL	AUG	SEP	OCT	NOV	DEC
1974											1	0
1975	0	1	0	0	1	0	1	0	1	0	1	1
1976	1	1	1	0	0	1	4	2	0	0	1	1
1977	1	0	0	0	2	0	1	2	1	0	1	0
1978	0	0	1	0	0	2	0	2	8	5	1	3
1979	10	1	1	0	0	0	0	1	0	0	0	1
1980	0	0	0	1	0	0	0	1	2	1	2	2
1981	0	1	1	1	1	0	0	1	0	0	1	0
1982	0	0	0	1	0	1	0	3	0	1	0	0
1983	0	4	2	2	0	0	0	1	2	2	0	0
1984	0	0	2	0	0	1	0	0	0	0	0	1
1985	1	0	1	0	0	0	2	0	0	0	1	1
1986	3	0	1	0	0	4	0					
TOTALS	16	8	10	5	4	9	8	13	14	9	9	10

TOTAL NUMBER OF EVENTS = 115

Table B-2c. Monthly event counts for Deer Creek Dam.

DEER CREEK DAM

YEAR	JAN	FEB	MAR	APR	MAY	JUN	JUL	AUG	SEP	OCT	NOV	DEC
1974											1	1
1975	0	0	0	0	0	3	1	1	1	1	0	0
1976	1	0	0	0	0	0	0	0	0	0	1	1
1977	0	0	1	0	0	0	4	0	0	0	0	0
1978	0	0	0	1	1	0	0	0	0	0	0	0
1979	1	1	0	2	0	0	0	0	0	0	0	0
1980	0	0	0	0	0	0	0	0	0	0	0	0
1981	1	0	0	0	1	0	0	0	0	0	0	1
1982	0	0	0	0	0	5	0	3	0	1	1	0
1983	0	0	0	0	0	0	0	0	0	0	0	0
1984	0	0	2	1	0	3	3	1	0	0	0	1
1985	0	0	0	0	1	2	2	0	2	0	0	0
1986	1	0	0	1	0	0						
TOTALS	4	1	3	5	3	13	10	5	3	2	3	4

TOTAL NUMBER OF EVENTS = 56

Table B-2d. Monthly event counts for East Canyon Dam.

EAST CANYON DAM

YEAR	JAN	FEB	MAR	APR	MAY	JUN	JUL	AUG	SEP	OCT	NOV	DEC
1974											0	1
1975	3	0	0	0	1	0	1	1	4	2	0	4
1976	1	0	1	0	0	0	4	3	6	10	1	2
1977	2	2	0	3	3	1	1	1	1	3	1	0
1978	0	0	0	0	0	1	0	0	1	0	0	5
1979	0	1	1	1	0	0	0	0	0	0	1	0
1980	0	2	0	0	0	0	0	1	3	0	1	0
1981	2	0	0	0	0	0	0	1	0	0	0	1
1982	0	0	1	0	0	2	0	1	1	0	1	1
1983	1	2	0	0	0	0	0	0	0	0	1	0
1984	0	0	0	0	0	3	1	0	0	0	1	0
1985	0	1	1	0	0	1	0	0	0	0	0	0
1986	1	1	0	0	0	0						
TOTALS	10	9	4	4	4	8	7	8	16	15	7	14

TOTAL NUMBER OF EVENTS = 106

Table B-2e. Monthly event counts for Echo Dam.

ECHO DAM

YEAR	JAN	FEB	MAR	APR	MAY	JUN	JUL	AUG	SEP	OCT	NOV	DEC
1974											0	0
1975	0	0	0	0	0	0	0	0	2	1	0	5
1976	1	0	0	1	0	0	4	4	6	9	3	3
1977	1	0	0	2	0	3	3	2	2	2	2	0
1978	1	0	0	0	0	1	0	0	1	0	1	1
1979	0	1	0	1	0	0	0	0	0	0	0	2
1980	0	0	0	0	0	0	0	0	0	0	1	0
1981	2	0	0	0	0	0	0	1	0	0	0	1
1982	0	0	0	0	0	1	0	0	0	0	0	0
1983	1	0	0	0	0	0	0	1	0	0	0	0
1984	0	0	0	0	0	3	0	0	0	0	1	0
1985	0	1	0	0	0	0	0	0	0	0	0	0
1986	0	0	0	0	0	0						
TOTALS	6	2	0	4	0	8	7	8	11	12	8	12

TOTAL NUMBER OF EVENTS = 78

Table B-2f. Monthly event counts for Hyrum Dam.

HYRUM DAM

YEAR	JAN	FEB	MAR	APR	MAY	JUN	JUL	AUG	SEP	OCT	NOV	DEC
1974											0	0
1975	0	0	3	0	0	0	1	1	0	2	0	1
1976	1	1	1	2	4	1	0	1	0	1	0	1
1977	2	1	0	0	0	0	0	0	0	0	0	0
1978	1	0	1	0	1	1	0	1	1	1	2	1
1979	1	2	0	1	0	0	0	0	0	0	0	0
1980	0	1	3	0	2	0	0	0	2	0	2	0
1981	0	0	1	0	0	0	1	0	1	0	0	1
1982	0	1	1	0	0	21	0	0	0	1	8	5
1983	0	0	0	0	7	7	1	1	3	1	0	26
1984	0	0	0	0	0	2	0	2	1	0	3	2
1985	0	0	0	2	4	0	0	1	0	1	2	0
1986	0	0	1	0	0	0						
TOTALS	5	6	11	5	18	32	3	7	8	7	17	37

TOTAL NUMBER OF EVENTS = 156

Table B-2g. Monthly event counts for Joes Valley Dam.

JOE'S VALLEY DAM (MINING EVENTS DELETED)

YEAR	JAN	FEB	MAR	APR	MAY	JUN	JUL	AUG	SEP	OCT	NOV	DEC
1974											0	0
1975	0	0	0	0	0	0	1	0	0	0	0	0
1976	0	0	1	0	0	0	0	0	0	0	1	0
1977	0	0	2	0	0	0	0	0	0	0	0	0
1978	0	0	0	0	0	0	0	0	2	0	0	0
1979	0	1	0	0	0	0	0	0	0	0	0	1
1980	0	0	0	2	1	0	0	1	0	0	0	1
1981	0	0	0	0	0	0	0	0	0	0	0	0
1982	0	0	0	0	0	0	0	0	0	0	0	0
1983	1	1	0	1	3	0	1	0	0	0	0	2
1984	0	0	0	0	0	0	0	0	0	0	1	0
1985	0	0	0	0	0	0	0	0	0	1	0	0
1986	0	0	0	2	0	0						
TOTALS	1	2	3	5	4	0	2	1	2	1	2	4

TOTAL NUMBER OF EVENTS = 27

Table B-2h. Monthly event counts for Lost Creek Dam.

LOST CREEK DAM

YEAR	JAN	FEB	MAR	APR	MAY	JUN	JUL	AUG	SEP	OCT	NOV	DEC
1974											1	0
1975	0	0	0	0	0	0	0	0	1	0	0	0
1976	0	1	0	0	0	0	2	0	1	1	1	0
1977	0	0	0	0	0	0	0	0	0	2	0	0
1978	1	0	0	0	0	0	0	0	2	0	0	0
1979	1	0	0	1	0	0	0	0	0	0	0	0
1980	0	0	0	0	0	0	0	0	0	0	0	0
1981	0	0	0	0	0	0	0	0	0	0	2	0
1982	0	0	0	1	0	0	0	0	0	0	1	0
1983	1	1	0	0	0	0	0	1	0	0	0	0
1984	0	0	0	0	0	0	0	0	0	0	0	0
1985	0	0	0	0	0	0	0	0	0	0	0	0
1986	1	0	0	0	0	0						
TOTALS	4	2	0	2	0	0	2	1	4	3	5	0

TOTAL NUMBER OF EVENTS = 23

Table B-2i. Monthly event counts for Newton Dam.

NEWTON DAM

YEAR	JAN	FEB	MAR	APR	MAY	JUN	JUL	AUG	SEP	OCT	NOV	DEC
1974											0	1
1975	0	0	0	0	1	0	0	0	0	0	0	0
1976	1	0	0	0	0	1	4	0	0	0	1	1
1977	1	0	0	0	0	0	0	0	0	0	0	0
1978	1	1	1	0	0	0	6	0	0	0	0	0
1979	0	0	0	0	0	0	0	0	0	0	0	0
1980	1	0	0	0	0	0	9	0	0	0	0	0
1981	0	0	0	0	0	0	0	0	0	0	0	1
1982	0	0	0	0	0	0	0	0	0	0	1	1
1983	0	1	2	2	0	1	0	0	0	0	0	0
1984	0	0	0	0	0	2	0	0	1	0	0	0
1985	0	0	0	1	0	0	1	0	0	0	0	0
1986	0	0	0	1	0	0						
TOTALS	4	2	3	4	1	4	20	0	1	0	2	4

TOTAL NUMBER OF EVENTS = 45

Table B-2j. Monthly event counts for Pineview Dam.

PINEVIEW DAM

YEAR	JAN	FEB	MAR	APR	MAY	JUN	JUL	AUG	SEP	OCT	NOV	DEC
1974											1	0
1975	0	0	0	0	0	0	1	0	1	0	1	1
1976	2	5	1	0	0	2	3	2	0	0	3	1
1977	3	0	0	0	2	0	0	0	1	0	0	1
1978	1	0	1	0	0	0	0	0	2	1	0	0
1979	4	1	0	0	0	0	0	0	0	0	0	0
1980	0	0	0	0	0	0	0	1	2	3	3	0
1981	0	0	0	1	1	0	0	0	0	0	0	0
1982	0	0	0	0	0	0	0	2	0	1	0	0
1983	0	1	2	0	0	0	0	0	0	1	0	0
1984	0	0	0	0	0	0	0	0	0	0	0	1
1985	1	0	0	0	0	0	1	0	0	0	1	0
1986	1	0	0	0	1	4						
TOTALS	12	7	4	1	4	6	5	5	6	6	9	4

TOTAL NUMBER OF EVENTS = 69

Table B-2k. Monthly event counts for Scofield Dam.

SCOFIELD DAM

YEAR	JAN	FEB	MAR	APR	MAY	JUN	JUL	AUG	SEP	OCT	NOV	DEC
1974											0	2
1975	1	0	0	0	0	0	0	0	0	2	0	0
1976	1	0	0	0	0	0	0	1	0	0	0	0
1977	0	0	0	0	0	0	0	0	1	0	1	0
1978	0	0	0	0	3	0	1	0	0	0	0	0
1979	0	0	0	2	0	0	0	1	1	1	0	0
1980	0	0	2	1	2	0	0	0	1	1	0	0
1981	0	0	0	0	0	0	0	1	0	1	0	0
1982	0	0	0	0	0	0	0	0	0	0	0	0
1983	0	0	0	0	0	0	0	0	0	0	0	0
1984	0	0	0	0	0	0	0	0	0	0	0	0
1985	0	0	2	0	0	0	0	0	0	0	0	1
1986	0	0	0	0	0	0						
TOTALS	2	0	4	3	5	0	1	3	3	5	1	3

TOTAL NUMBER OF EVENTS = 30

Table B-2l. Monthly event counts for Soldier Creek Dam.

SOLDIER CREEK DAM

YEAR	JAN	FEB	MAR	APR	MAY	JUN	JUL	AUG	SEP	OCT	NOV	DEC
1974											0	0
1975	0	0	0	0	0	0	0	0	0	0	0	0
1976	0	0	0	0	0	0	0	0	0	1	0	0
1977	0	0	0	0	0	0	0	0	0	0	0	1
1978	0	0	0	0	0	0	0	0	0	0	0	0
1979	0	0	0	0	0	0	0	1	0	0	0	1
1980	0	0	0	0	0	0	0	0	0	0	0	0
1981	0	0	0	0	0	0	0	0	0	0	0	0
1982	0	0	0	0	0	0	0	0	0	0	0	0
1983	0	0	0	0	0	0	0	0	0	0	0	0
1984	0	0	0	0	0	0	0	0	0	0	0	0
1985	0	0	0	0	1	0	0	0	0	0	0	0
1986	0	0	0	0	0	0						
TOTALS	0	0	0	0	1	0	0	1	0	1	0	2

TOTAL NUMBER OF EVENTS = 5

Table B-2m. Monthly event counts for Strawberry Dam.

STRAWBERRY DAM

YEAR	JAN	FEB	MAR	APR	MAY	JUN	JUL	AUG	SEP	OCT	NOV	DEC
1974											0	1
1975	0	0	0	0	0	0	0	0	0	0	0	0
1976	0	1	0	0	0	0	0	0	0	1	0	0
1977	0	0	0	0	0	0	0	0	0	0	0	2
1978	0	0	0	0	0	0	0	0	2	0	0	0
1979	0	0	0	0	0	0	0	1	0	0	0	1
1980	0	0	0	0	0	0	0	0	0	0	0	0
1981	0	0	0	0	0	0	0	0	0	0	0	0
1982	0	0	0	0	0	0	0	0	0	0	0	0
1983	0	0	0	0	0	0	0	0	0	0	0	0
1984	0	0	0	0	0	0	0	0	0	0	0	1
1985	0	0	0	0	1	0	0	0	0	0	1	0
1986	0	0	0	0	0	0						
TOTALS	0	1	0	0	1	0	0	1	2	1	1	5

TOTAL NUMBER OF EVENTS = 12

Table B-2n. Monthly event counts for Wanship Dam.

WANSHIP DAM

YEAR	JAN	FEB	MAR	APR	MAY	JUN	JUL	AUG	SEP	OCT	NOV	DEC
1974											1	0
1975	0	0	0	0	0	0	1	1	0	1	0	1
1976	0	2	0	0	0	0	0	0	0	1	0	0
1977	0	0	0	1	0	0	1	0	0	1	2	0
1978	0	0	0	0	0	1	0	0	1	2	1	5
1979	0	1	0	1	0	0	0	0	0	3	1	0
1980	2	0	0	0	0	0	0	0	0	0	0	0
1981	0	0	0	0	1	0	0	1	0	0	1	1
1982	0	0	0	0	2	0	0	0	0	1	0	1
1983	0	0	0	0	0	0	1	0	0	0	2	0
1984	0	0	0	0	0	0	0	0	0	0	0	0
1985	0	2	0	0	0	0	0	1	0	0	0	0
1986	0	0	0	0	0	0						
TOTALS	2	5	0	2	3	1	3	3	1	9	8	8

TOTAL NUMBER OF EVENTS = 45

Table B-3 Largest Post-Impoundment Earthquakes

Dam	Year Filled	M_{max} r=15 km	Δt (yrs)	M_{max} r=25 km	Δt (yrs)	Years Since Initial Filling
Causey	1966	3.7	1	**		20
Deer Creek	1941	5.0	17	**		45
East Canyon	1966	2.7	12	2.8	17	20
Echo	1930	2.8	28	3.7	25	56
Hyrum	1935	4.1	29	4.3	11	51
Joes Valley	1966	2.6	9	3.1	16	20
Lost Creek	1966	2.8	17	3.6	20	20
Newton	1945	3.1	33	3.1	17	41
Pineview	1937	3.7	30	**		49
Pineview	1957	3.7	10	**		29
Scofield	1946	2.7	39	2.9	37	40
Soldier Creek*	1983	2.6	2	**		3
Strawberry	1913	2.8	72	4.0	50	73
Wanship	1957	2.7	21	2.7	25	29

*filling not completed
**M_{max} at r=15 km exceeds M_{max} at r=25 km

Table B-4 Computed χ^2 Values

Dam	χ^2
Causey	13.528
Deer Creek	30.240*
East Canyon	18.864
Echo	25.698*
Hyrum	88.676*
Joe's Valley	11.734
Lost Creek	17.855
Newton	104.268*
Pineview	13.315
Scofield	13.715
Soldier Creek	9.757
Strawberry	16.574
Wanship	23.620*

*exceeds 95% level

Table B-5 Computed z-values

Dam	3-Month Period					
	Jan Feb Mar	Feb Mar Apr	Mar Apr May	Apr May Jun	May Jun Jul	Jun Jul Aug
Causey	1.515	-.513	-1.704	-2.164	-1.490	.510
Deer Creek	-1.688	-1.123	-.618	2.361*	3.945*	4.575*
East Canyon	-.487	-1.566	-2.927	-2.211	-1.511	-.586
Echo	-2.823	-3.132	-3.813	-1.827	-1.017	1.129
Hyrum	-2.885	-2.513	-.395	3.335*	2.962*	.849
Joe's Valley	-.178	1.845*	2.644*	1.123	-.228	-1.384
Lost Creek	.273	-.563	-1.645	-1.736	-1.733	-1.244
Newton	-.584	-.367	-.852	-.651	4.972*	4.621*
Pineview	1.828*	-1.041	-2.056	-1.633	-.527	-.244
Scofield	-.476	.142	2.208*	.327	-.527	-1.385
Soldier Creek	-1.246	-1.197	-.164	-.216	-.214	-.214
Strawberry	-1.253	-1.162	-1.216	-1.281	-1.279	-1.279
Wanship	-1.290	-1.089	-1.921	-1.704	-1.349	-1.349

Table B-5 (Cont'd)

Dam	3-Month Period					
	Jul Aug Sep	Aug Sep Oct	Sep Oct Nov	Oct Nov Dec	Nov Dec Jan	Dec Jan Feb
Causey	1.766*	1.602	.458	-1.034	.676	.676
Deer Creek	1.524	-1.239	-2.015	-2.098	-1.511	-1.833
East Canyon	-1.399	2.864*	2.355*	1.237	.128	1.018
Echo	2.056*	3.056*	2.805*	2.454*	.918	-.239
Hyrum	-3.636	-3.215	-1.600	2.970*	2.587*	1.141
Joe's Valley	-.622	-1.223	-.889	-.312	-.319	-.106
Lost Creek	.778	1.093	2.874*	.656	1.111	-.080
Newton	3.676*	-3.550	-2.977	-2.286	-.966	-.702
Pineview	-.143	-.132	.744	-.010	1.581	1.425
Scofield	-.032	1.489	.503	.167	-1.058	-1.262
Soldier Creek	-.189	.778	.306	1.553	.560	.665
Strawberry	.116	.672	.581	2.281*	1.635	1.815*
Wanship	-1.277	.613	2.159*	4.026*	1.689*	.993

*exceeds 95% confidence level

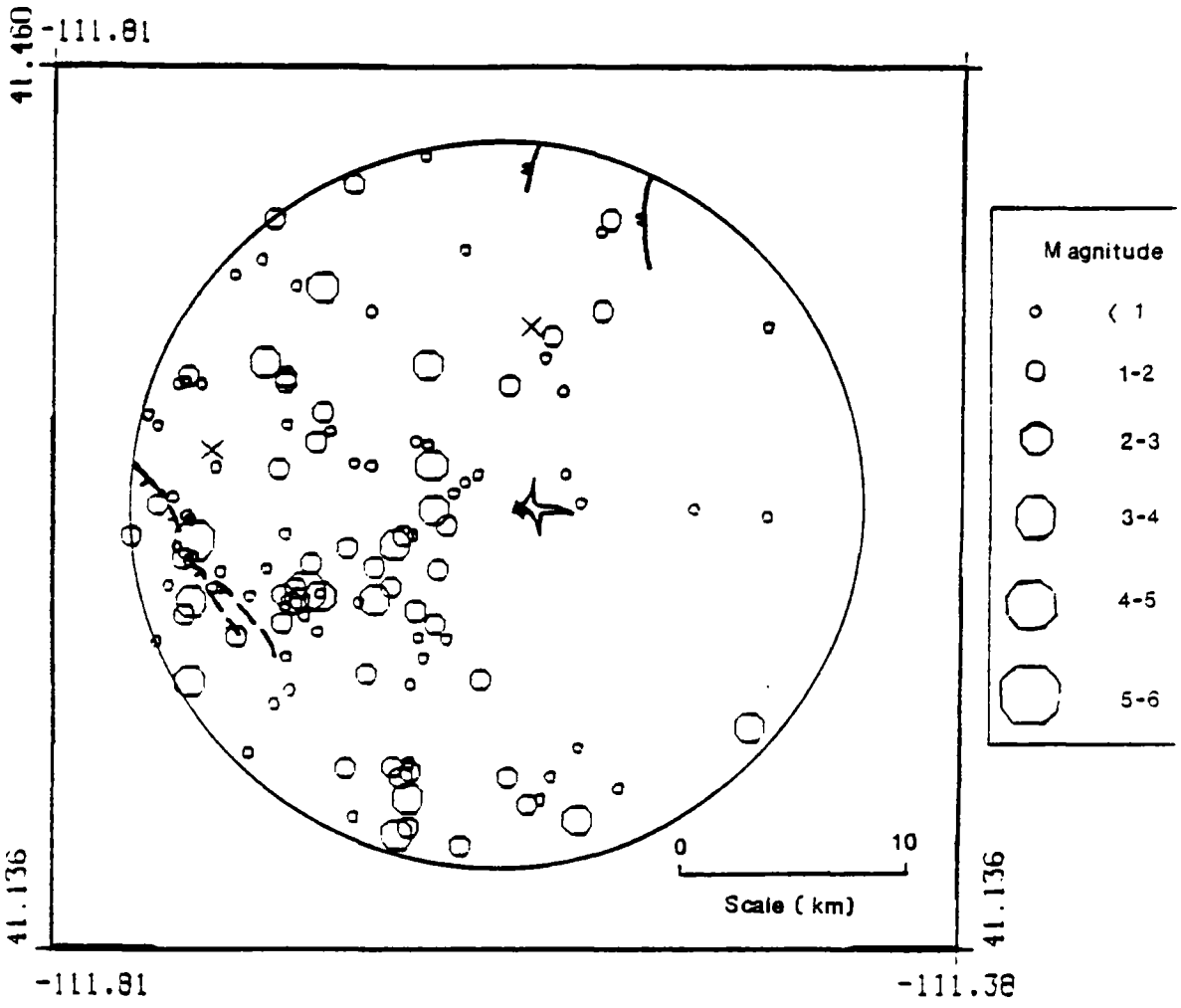


Figure B-1a Seismicity within 15 km of Causey Dam, through 6/86. Symbols scaled for magnitude; x signifies magnitude not computed. Faults plotted as on plate 1. Reservoir area outlined.

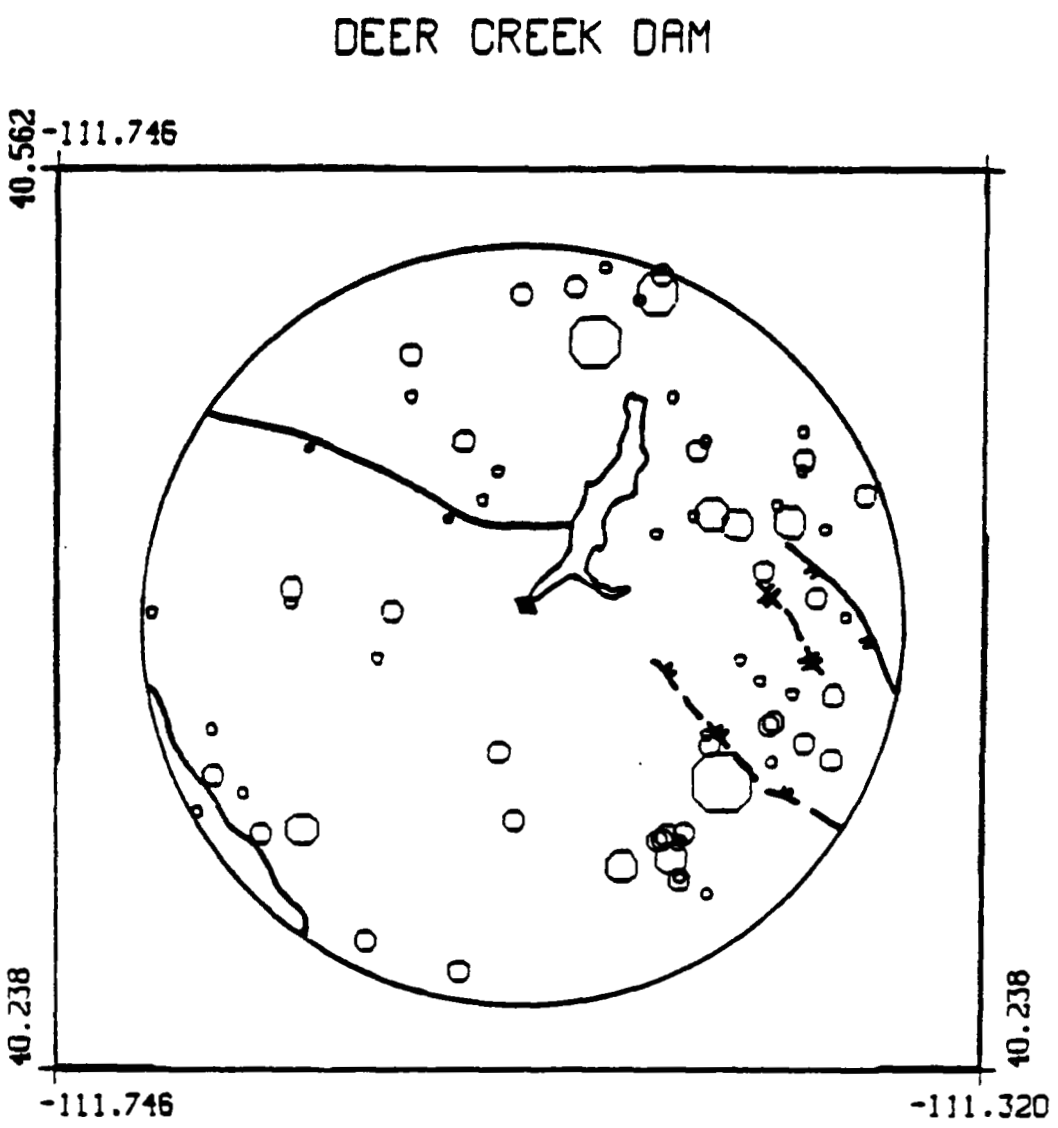


Figure B-1b Seismicity within 15 km of Deer Creek Dam, through 6/86. Symbols scaled for magnitude; x signifies magnitude not computed. Faults plotted as on plate 1. Reservoir area outlined.

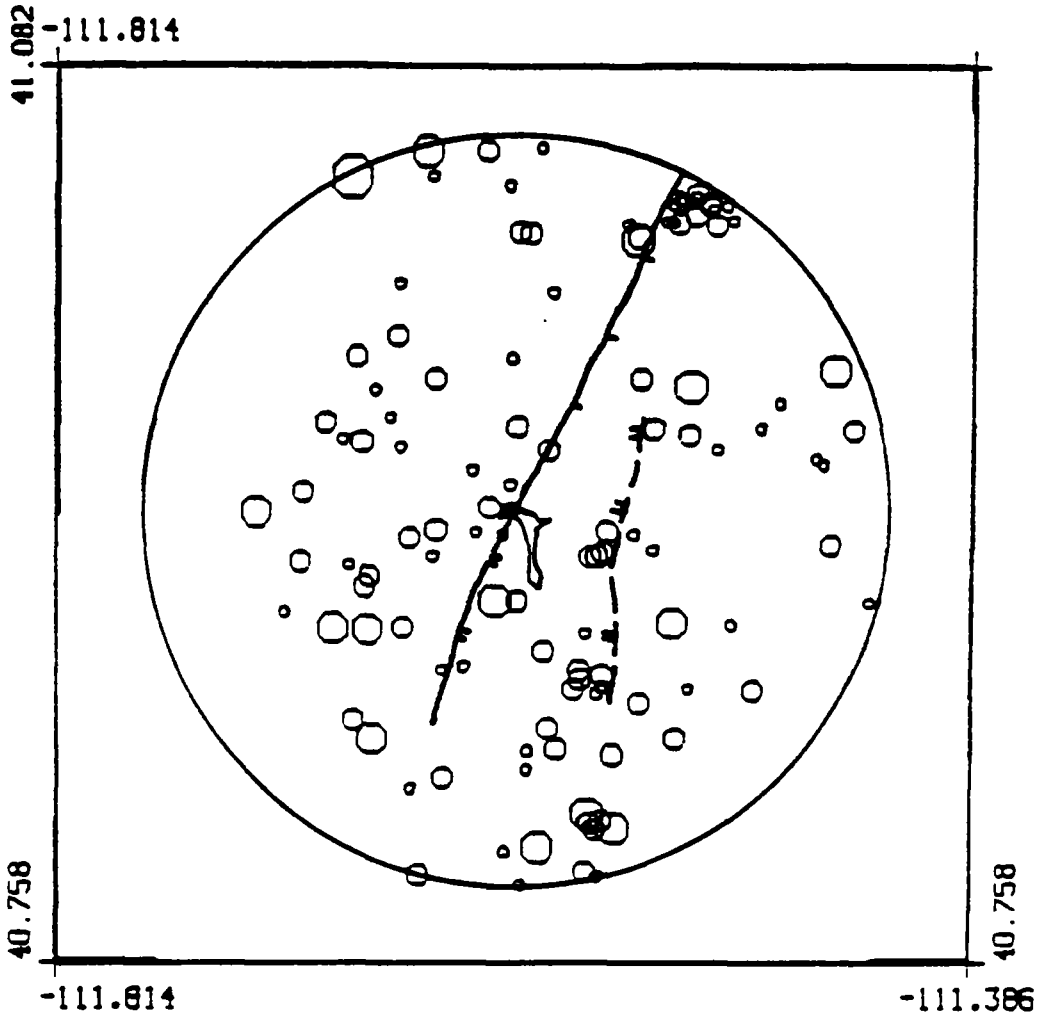


Figure B-1c. Seismicity within 15 km of East Canyon Dam, through 6/86. Symbols scaled for magnitude; x signifies magnitude not computed. Faults plotted as on plate 1. Reservoir area outlined.

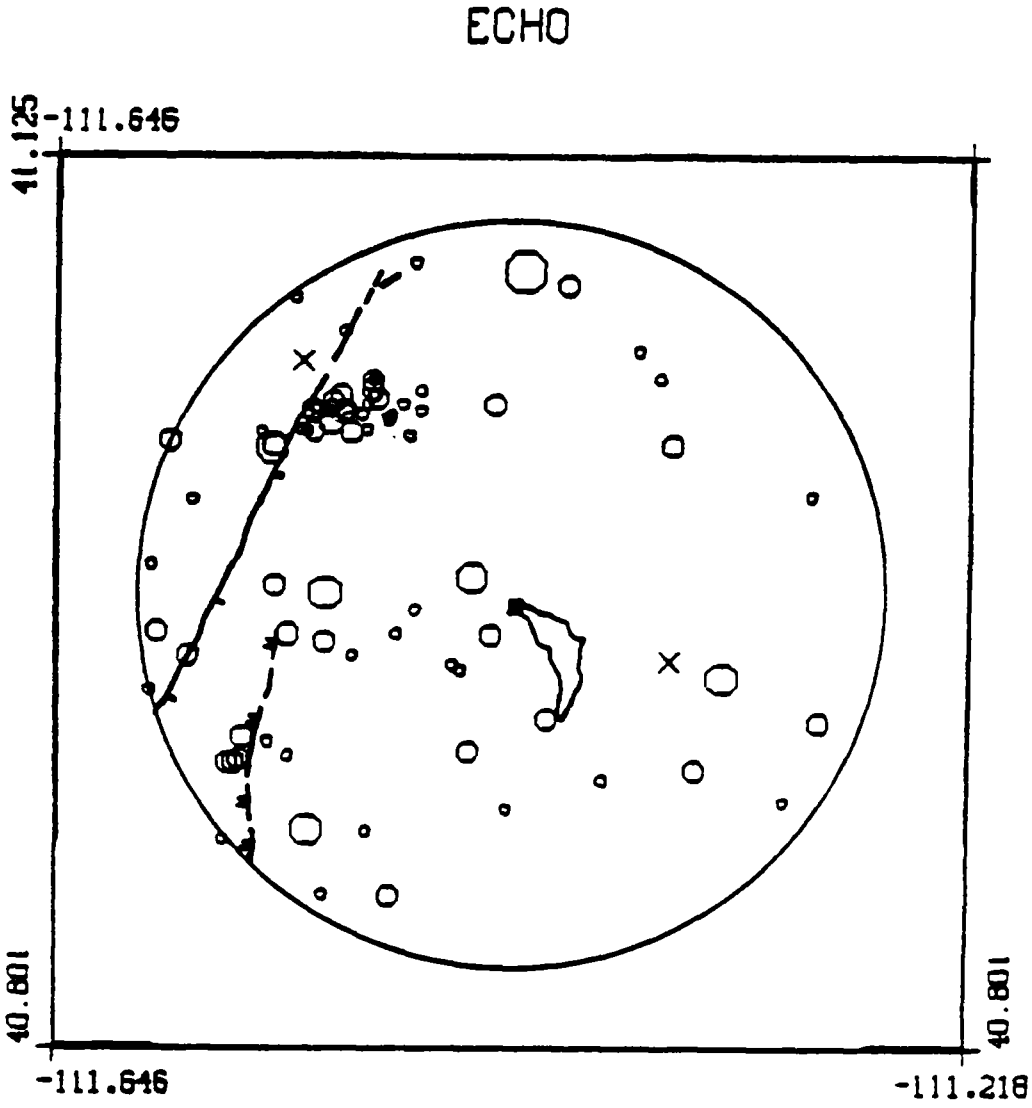


Figure B-1d. Seismicity within 15 km of Echo Dam, through 6/86. Symbols scaled for magnitude; x signifies magnitude not computed. Faults plotted as on plate 1. Reservoir area outlined.

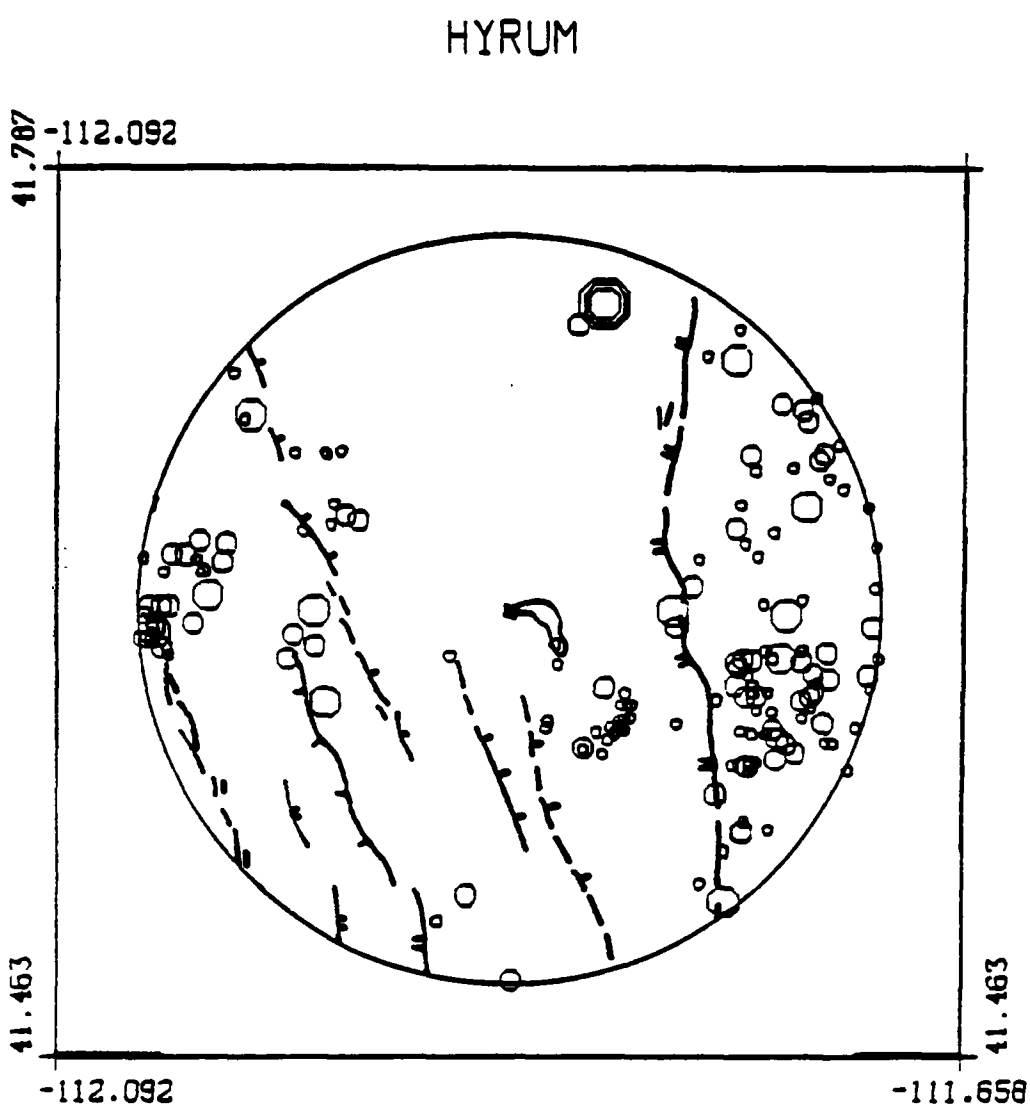


Figure B-1e. Seismicity within 15 km of Hyrum Dam, through 6/86. Symbols scaled for magnitude; x signifies magnitude not computed. Faults plotted as on plate 1. Reservoir area outlined.

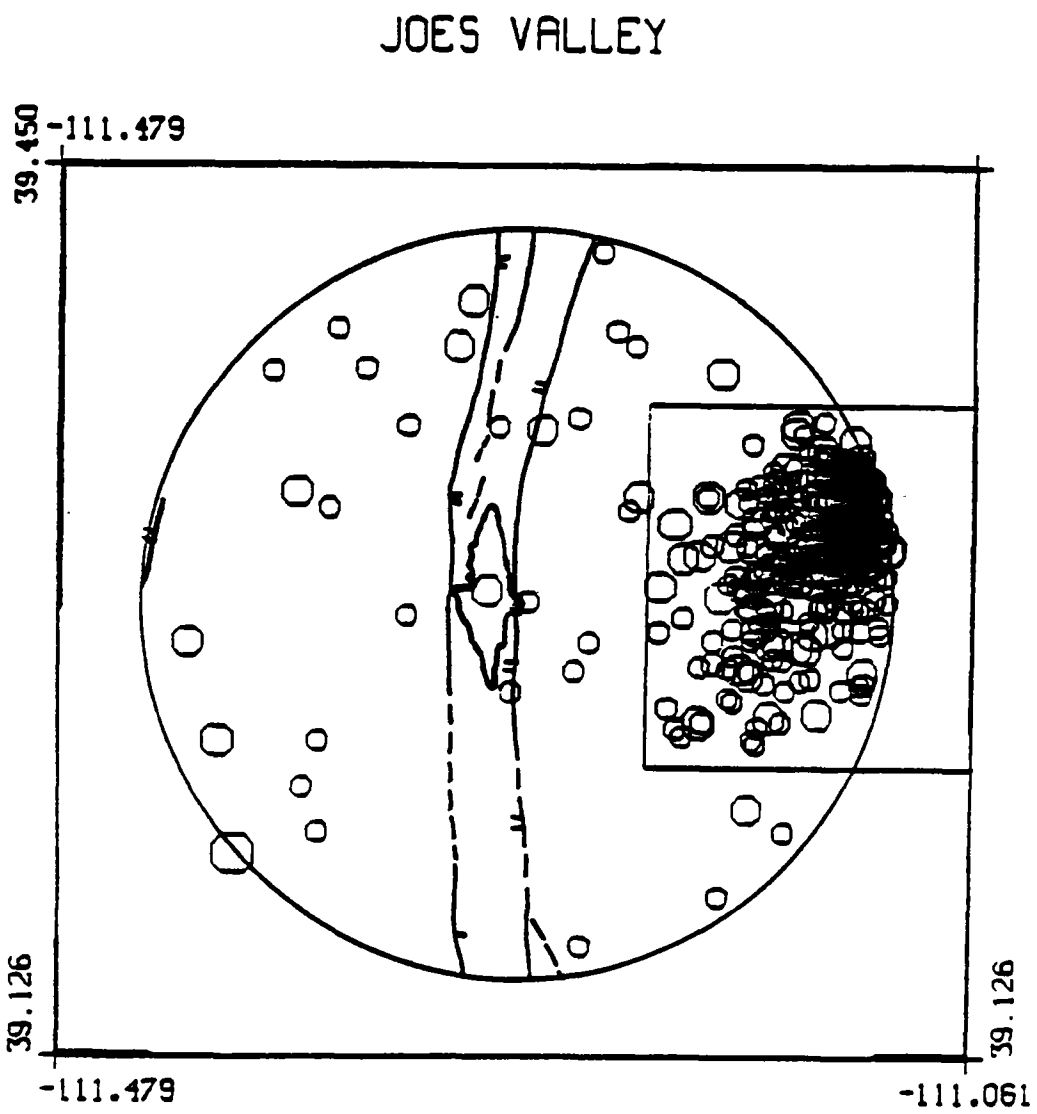


Figure B-1f. Seismicity within 15 km of Joes Valley Dam, through 6/86. Symbols scaled for magnitude; x signifies magnitude not computed. Faults plotted as on plate 1. Reservoir area outlined.

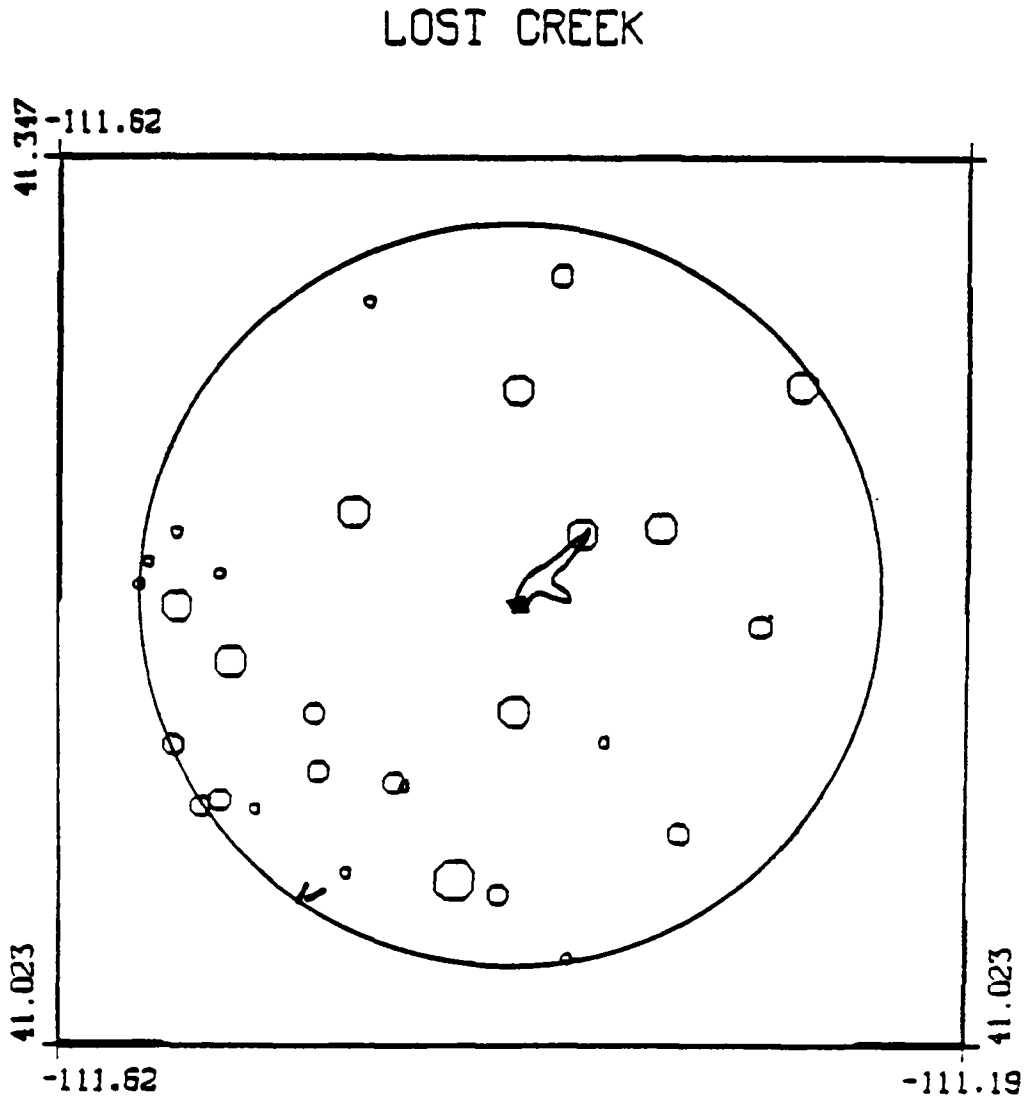


Figure B-1g. Seismicity within 15 km of Lost Creek Dam, through 6/86. Symbols scaled for magnitude; x signifies magnitude not computed. Faults plotted as on plate 1. Reservoir area outlined.

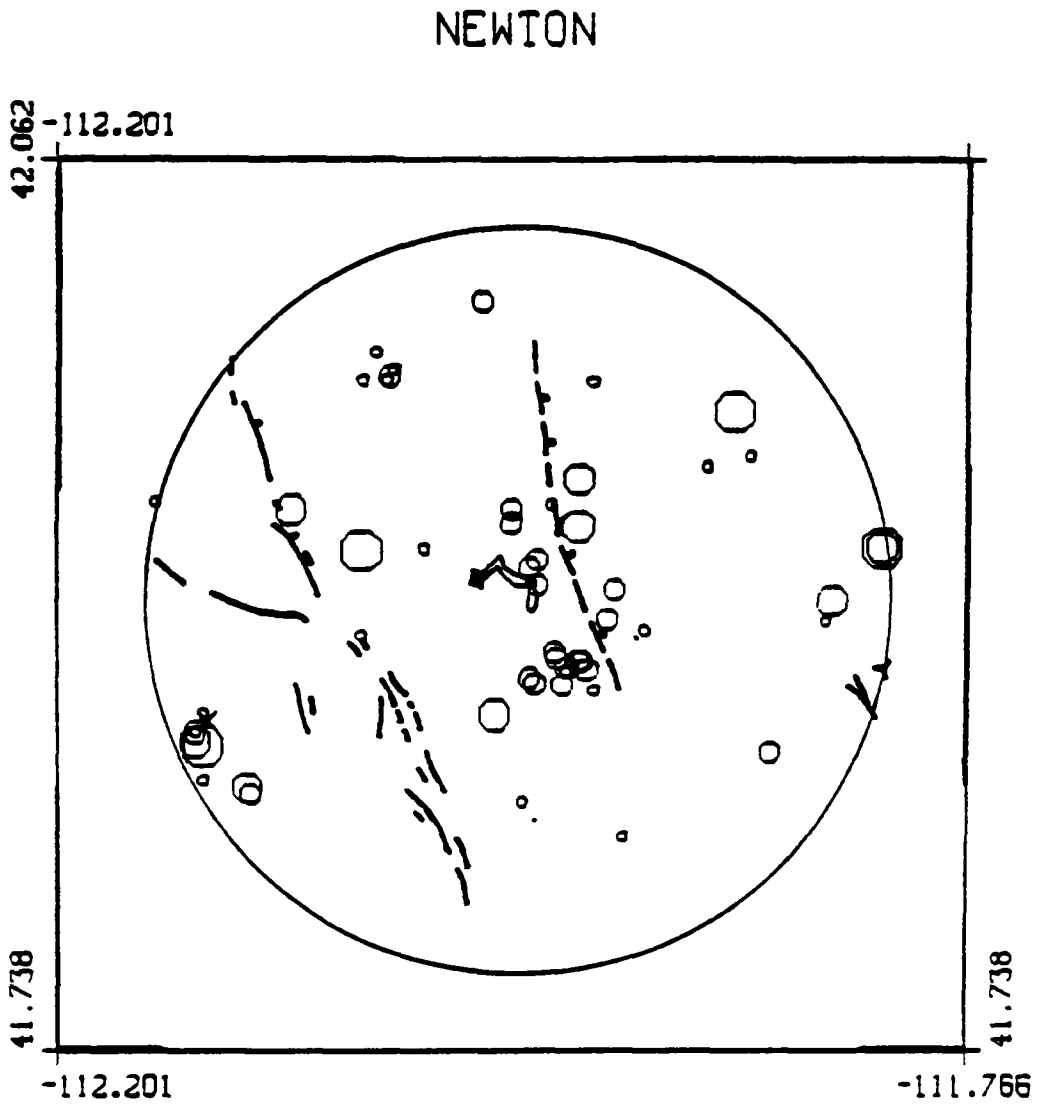


Figure B-1h. Seismicity within 15 km of Newton Dam, through 6/86. Symbols scaled for magnitude; x signifies magnitude not computed. Faults plotted as on plate 1. Reservoir area outlined.

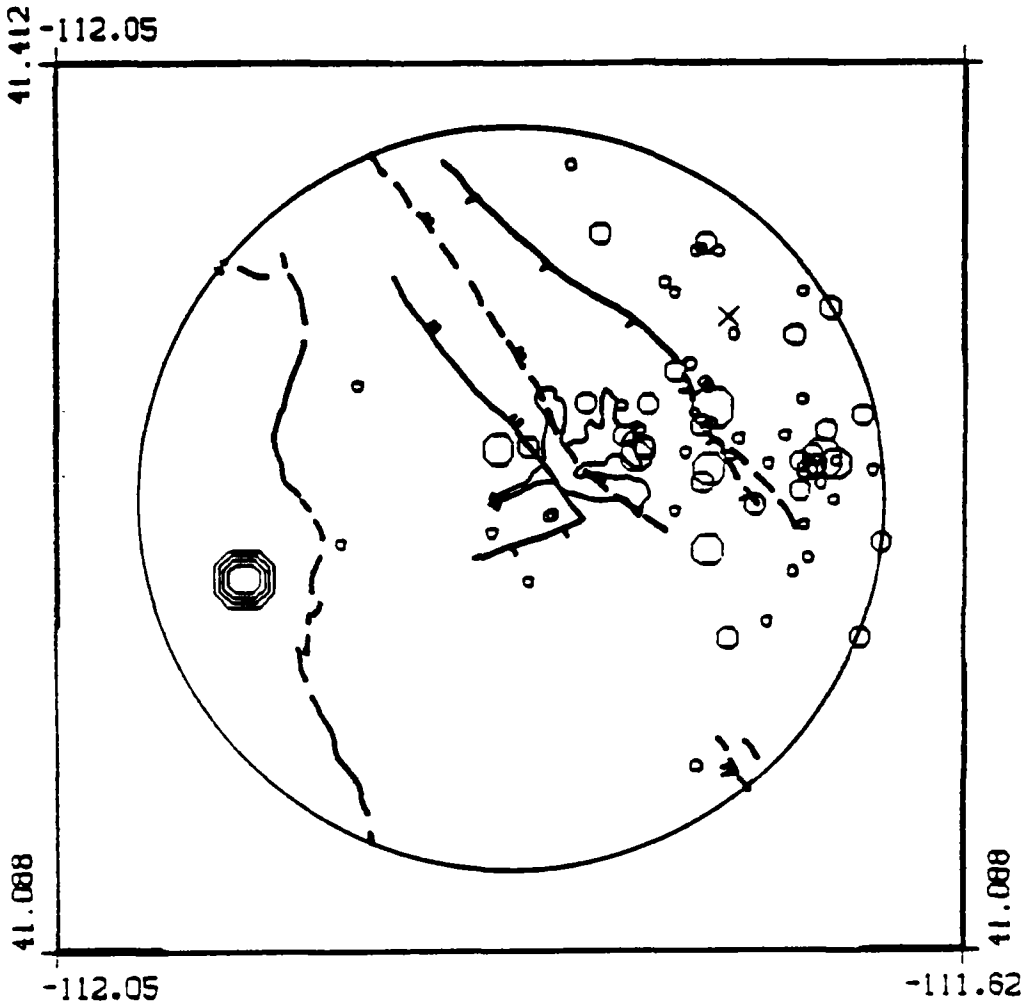


Figure B-1i. Seismicity within 15 km of Pineview Dam, through 6/86. Symbols scaled for magnitude; x signifies magnitude not computed. Faults plotted as on plate 1. Reservoir area outlined.

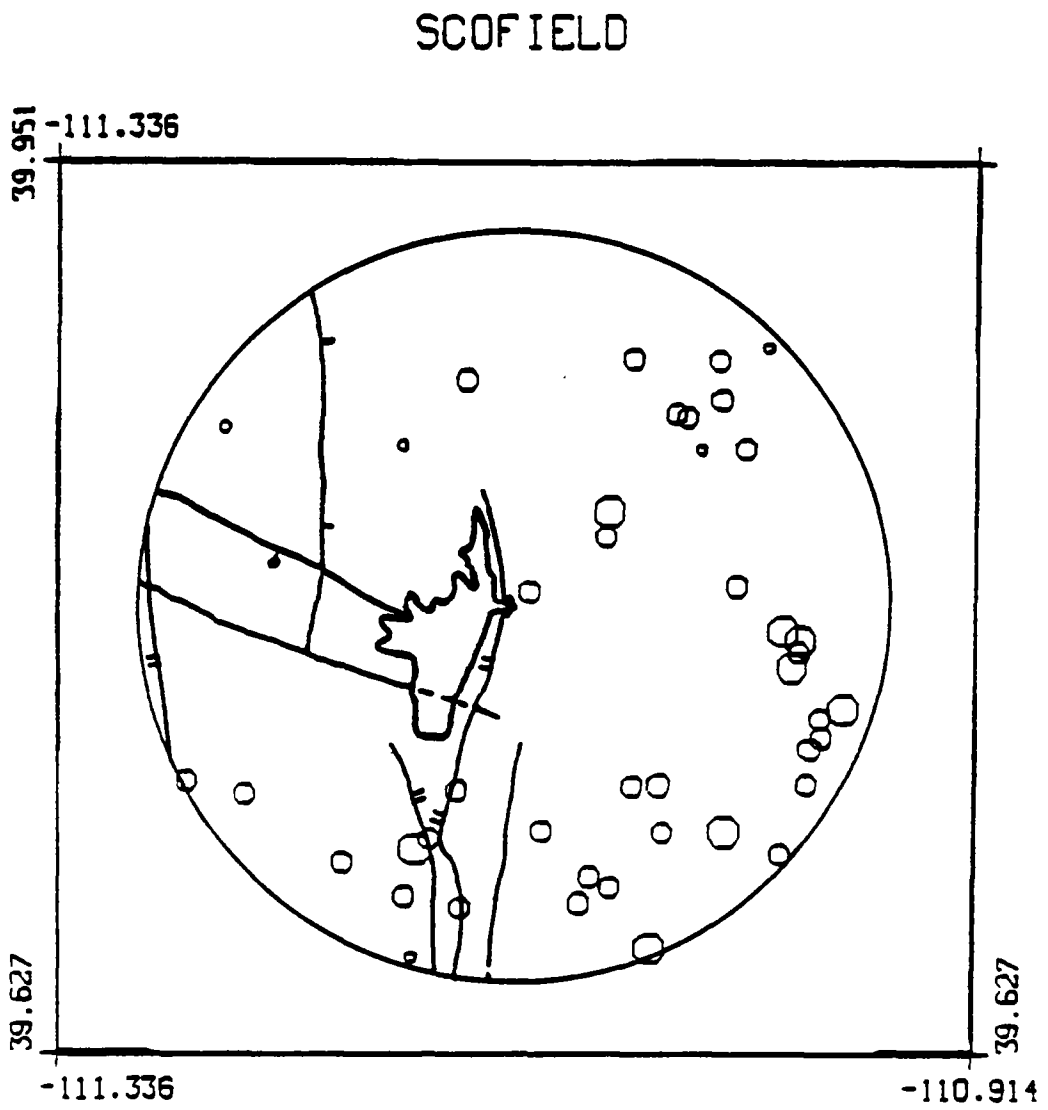


Figure B-1j.. Seismicity within 15 km of Scofield Dam, through 6/86. Symbols scaled for magnitude; x signifies magnitude not computed. Faults plotted as on plate 1. Reservoir area outlined.

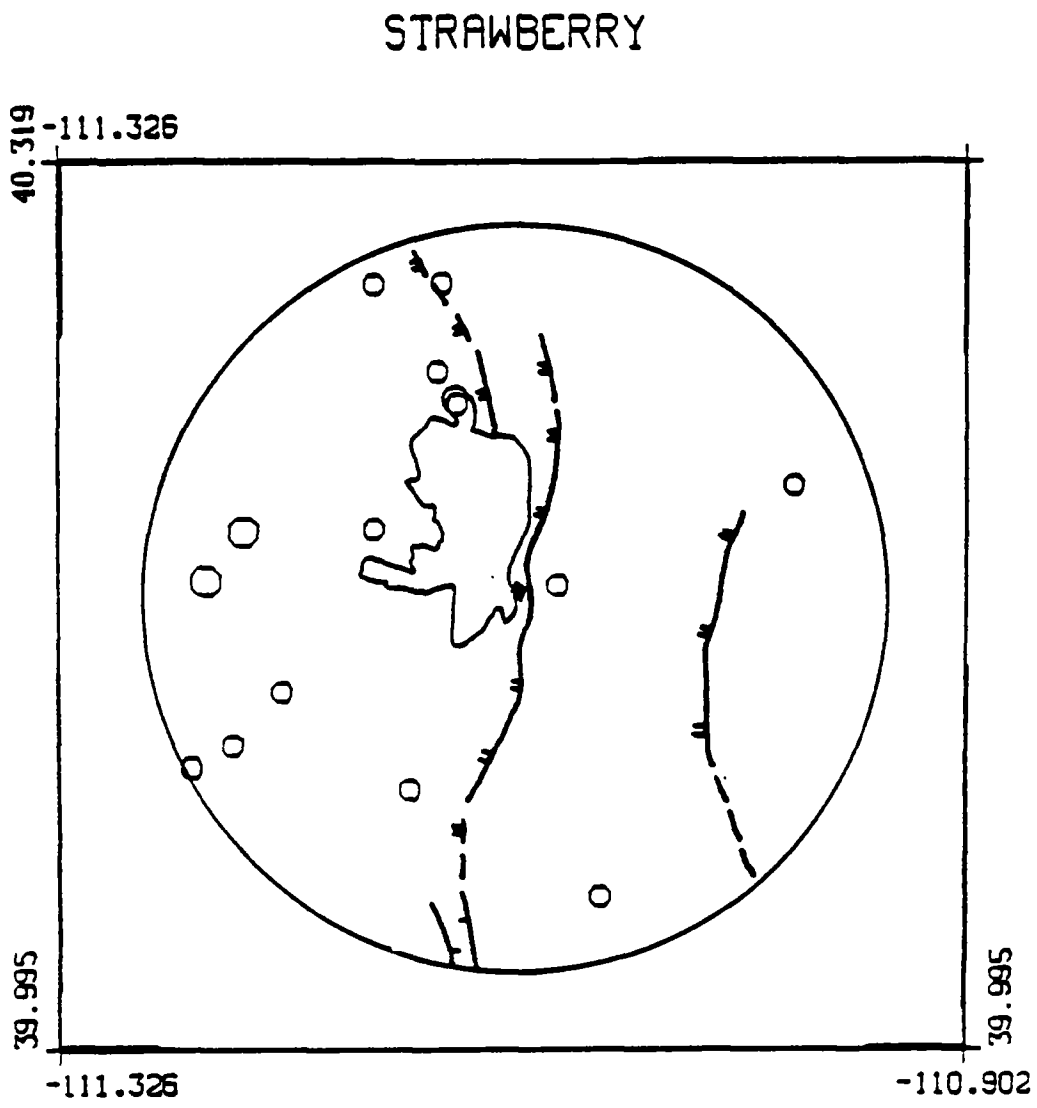


Figure B-1k. Seismicity within 15 km of Strawberry Dam, through 6/86. Symbols scaled for magnitude; x signifies magnitude not computed. Faults plotted as on plate 1. Reservoir area outlined.

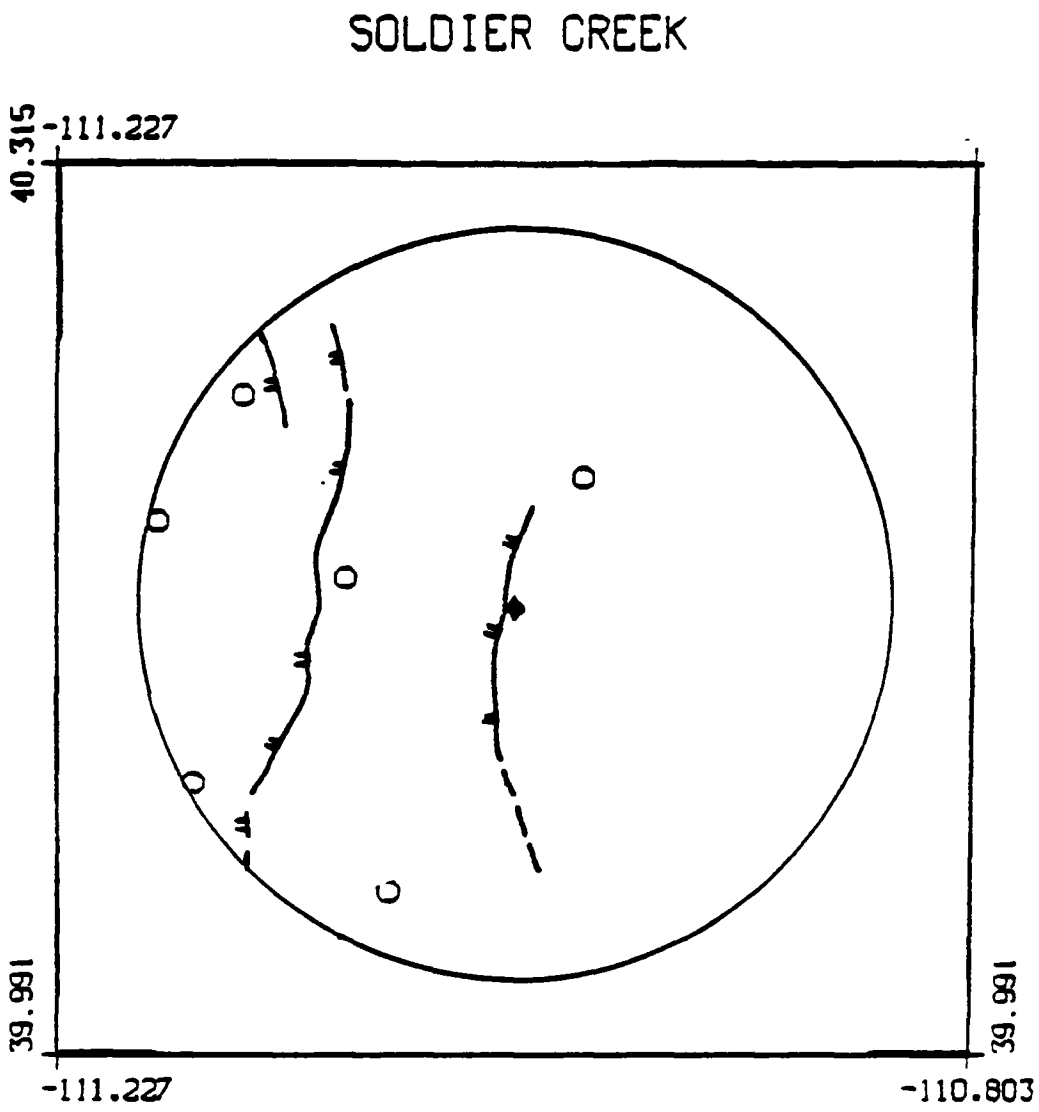


Figure B-11. Seismicity within 15 km of Soldier Creek Dam, through 6/86. Symbols scaled for magnitude; x signifies magnitude not computed. Faults plotted as on plate 1.

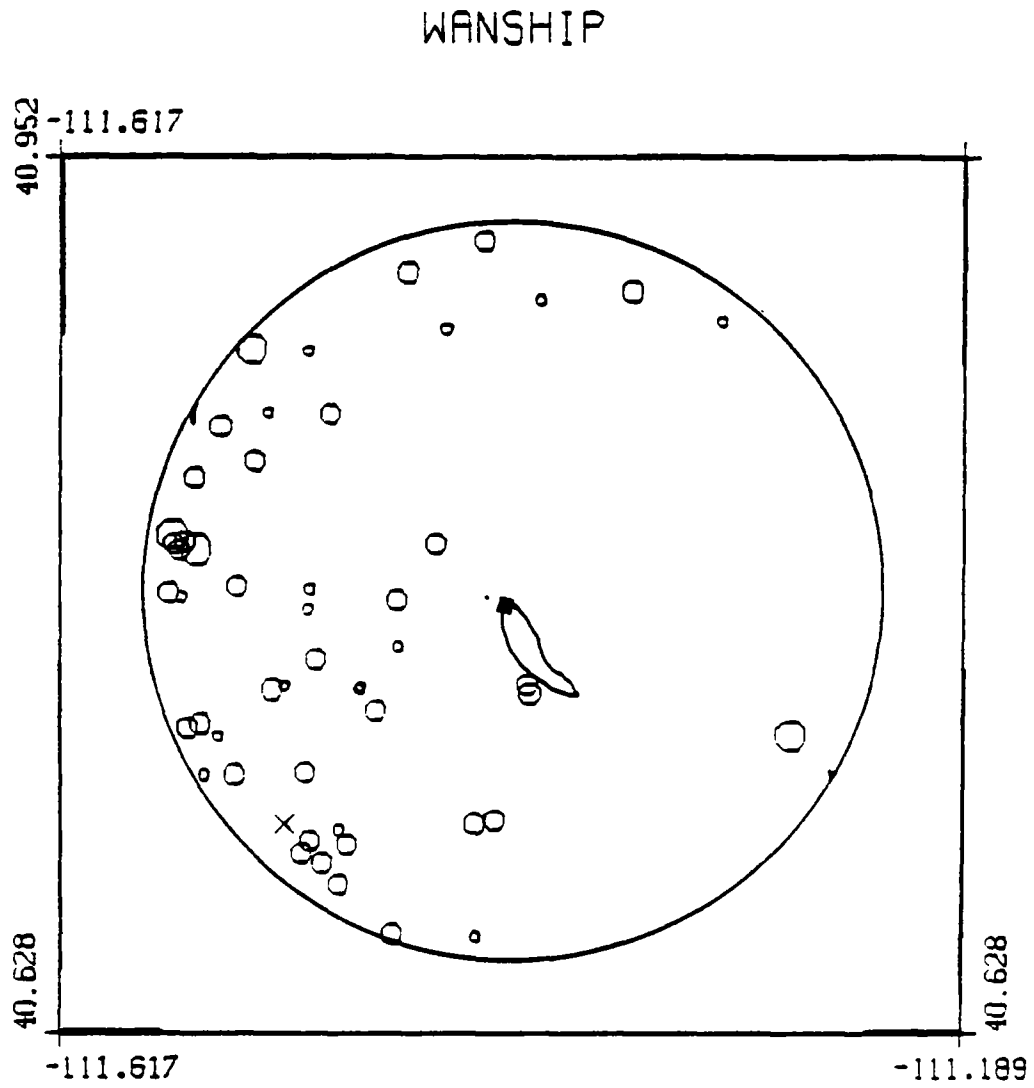


Figure B-1m Seismicity within 15 km of Wanship Dam, through 6/86. Symbols scaled for magnitude; x signifies magnitude not computed. Faults plotted as on plate 1. Reservoir area outlined.

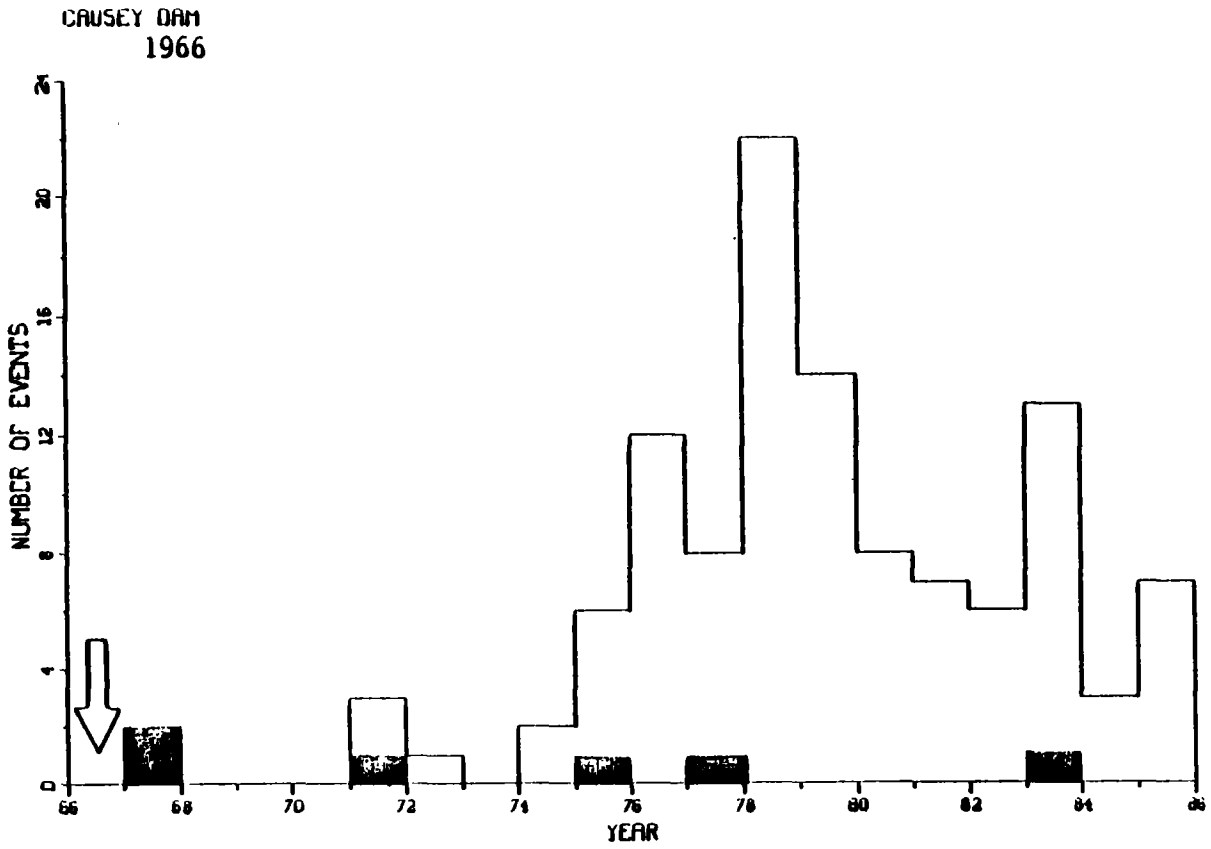


Figure B-2a. Yearly event count for Causey Dam. Arrow signifies year of initial reservoir filling. Solid portions indicate events ≥ magnitude 2.3.

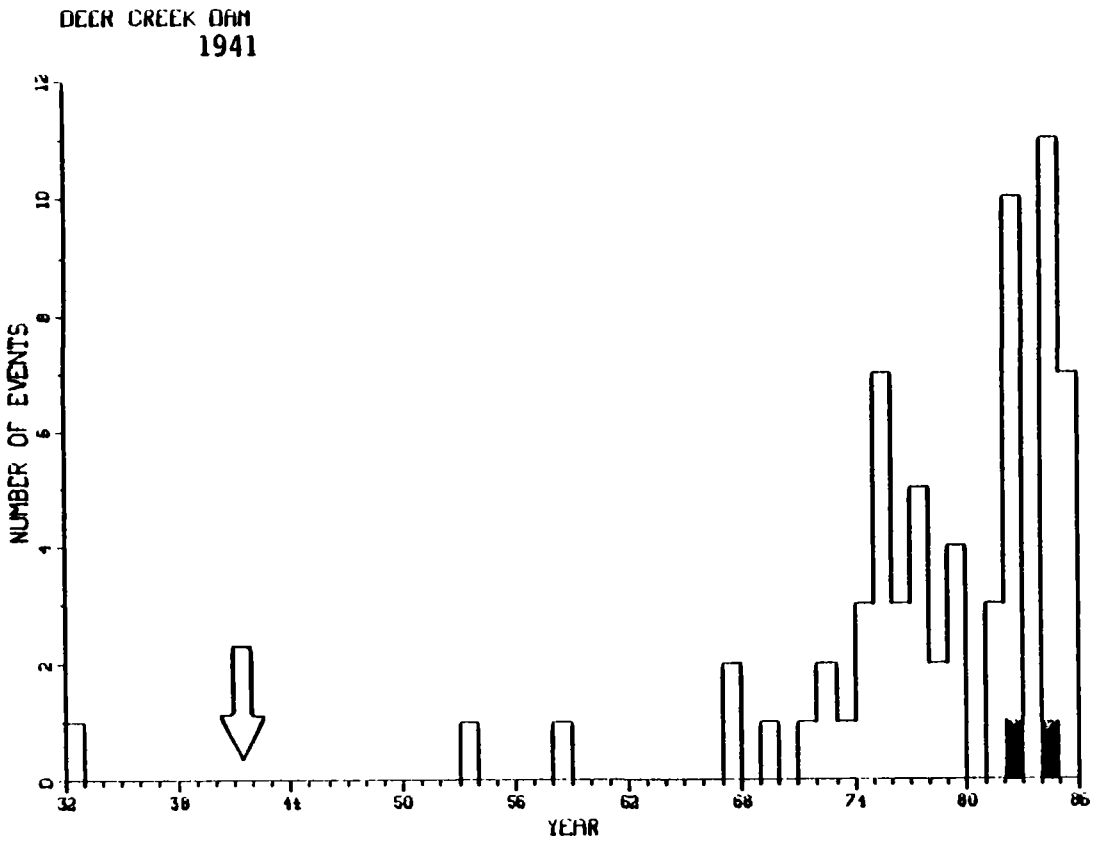


Figure B-2b. Yearly event count for Deer Creek Dam. Arrow signifies year of initial reservoir filling. Solid portions indicate events

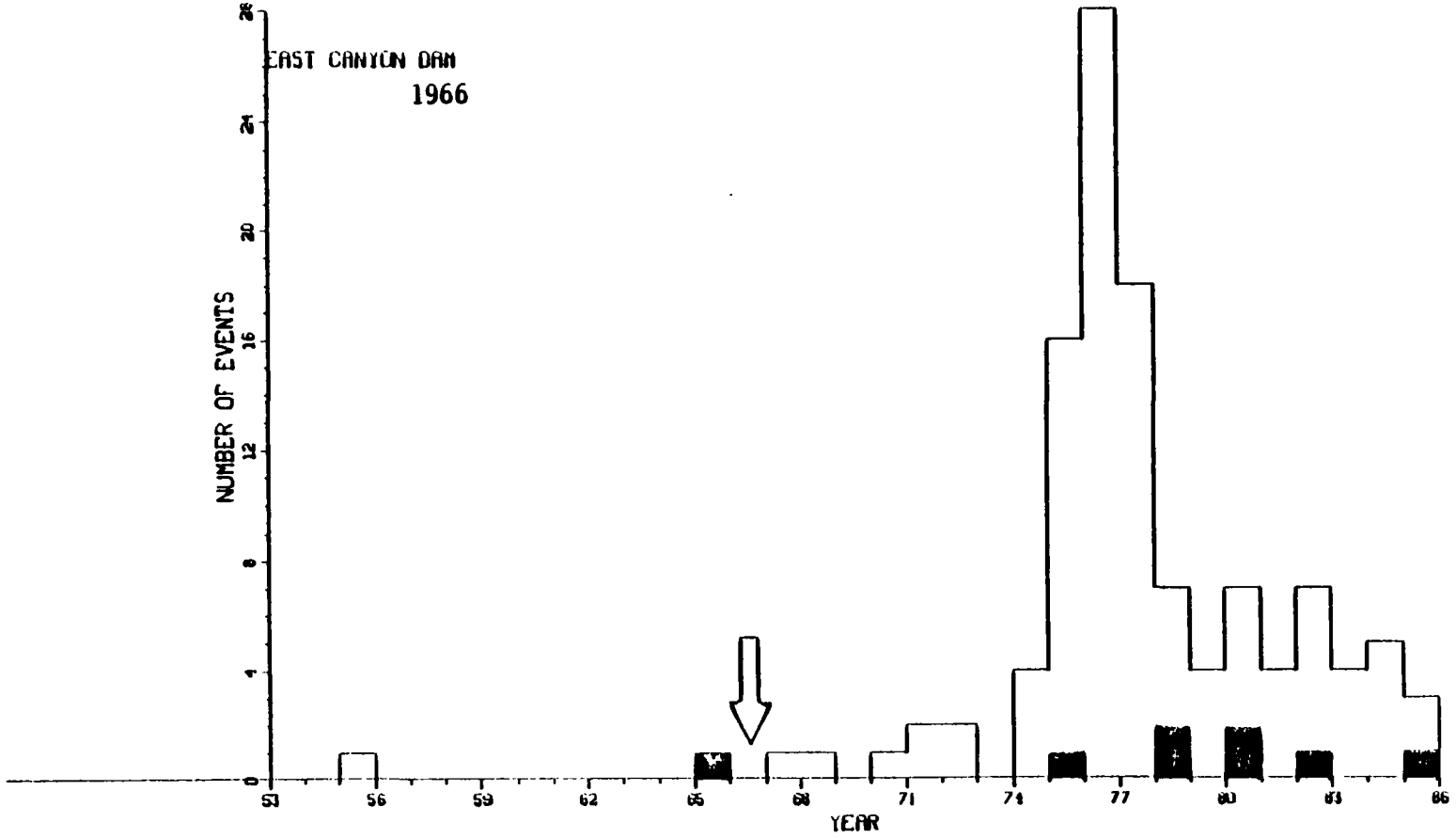


Figure B-2c. Yearly event count for East Canyon Dam. Arrow signifies year of initial reservoir filling. Solid portions indicate events $\geq$ magnitude 2.3

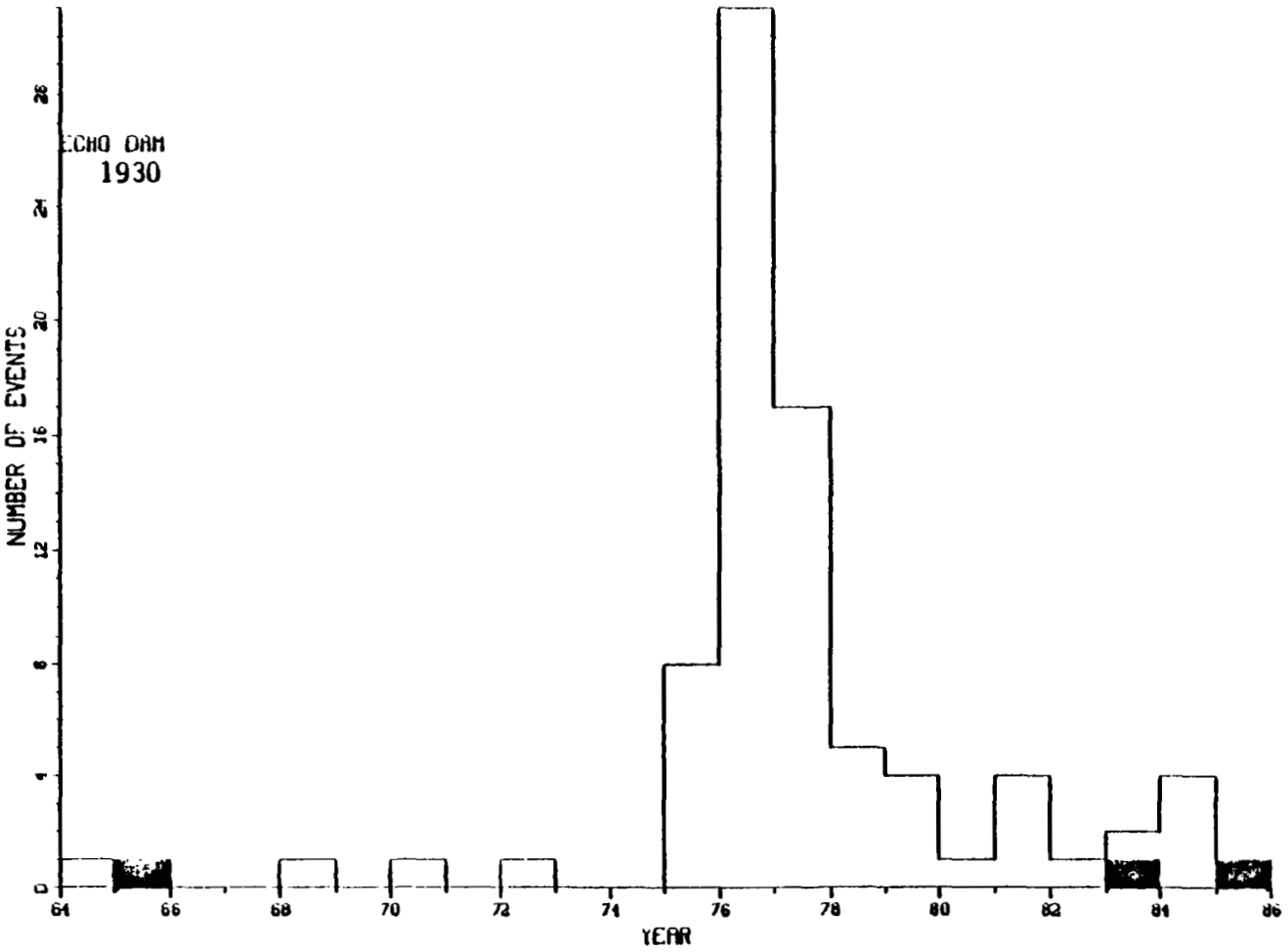


Figure B-2d. Yearly event count for Echo Dam. Arrow signifies year of initial reservoir filling. Solid portions indicate events

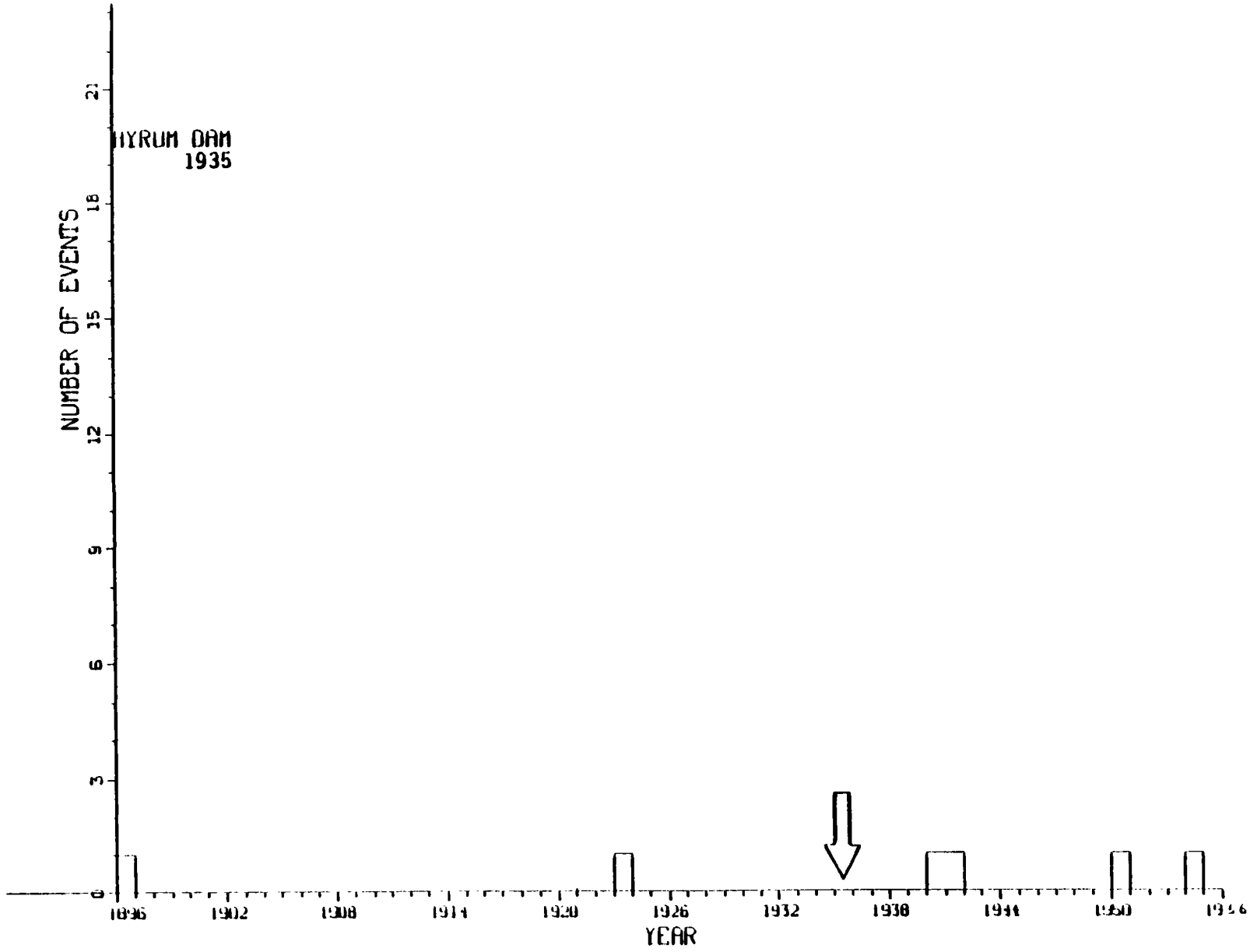


Figure B-2e. Yearly event count for Hyrum Dam. Arrow signifies year of initial reservoir filling.

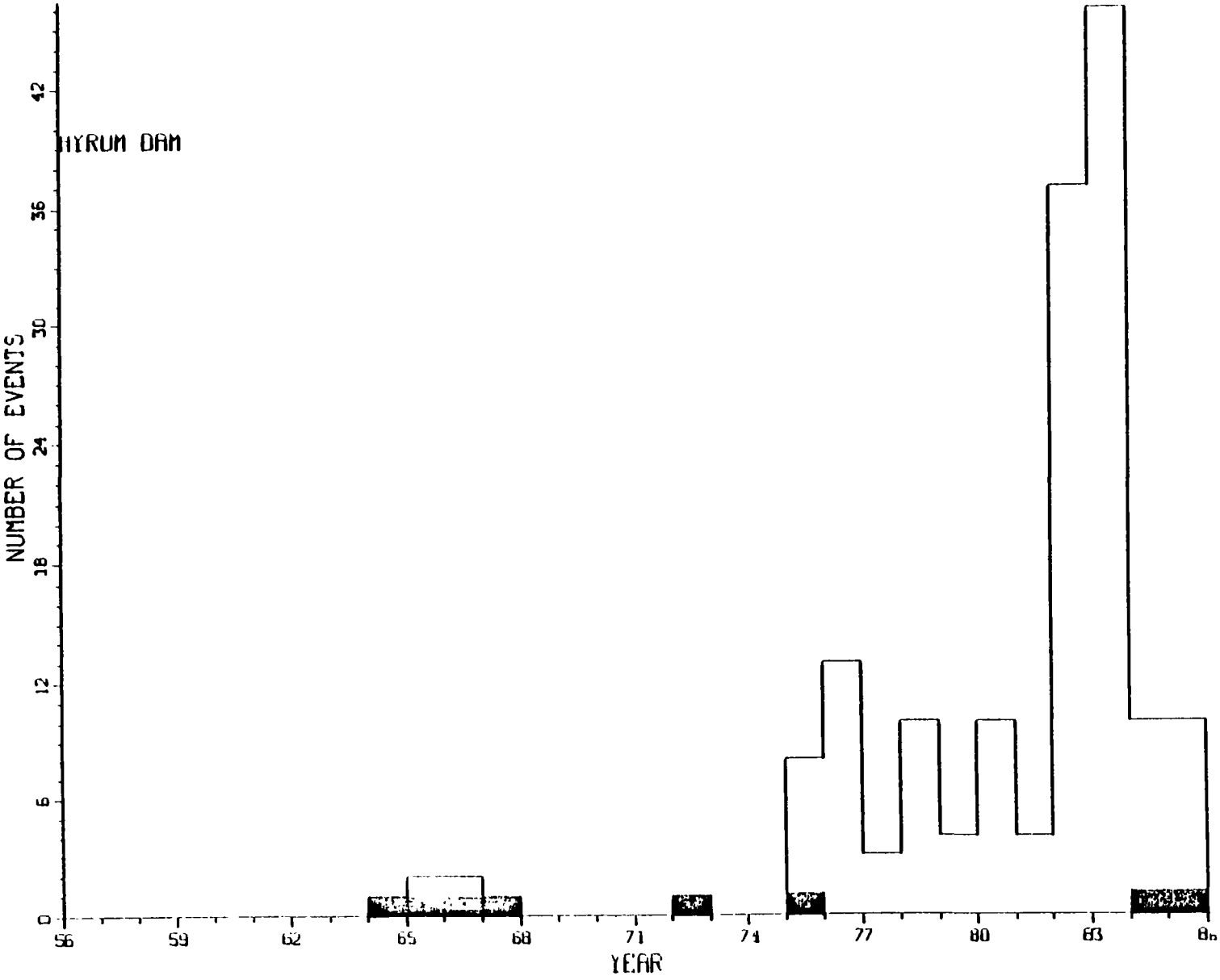


Figure B-2e (Cont'd) Solid portions indicate events ≥ magnitude 2.3.

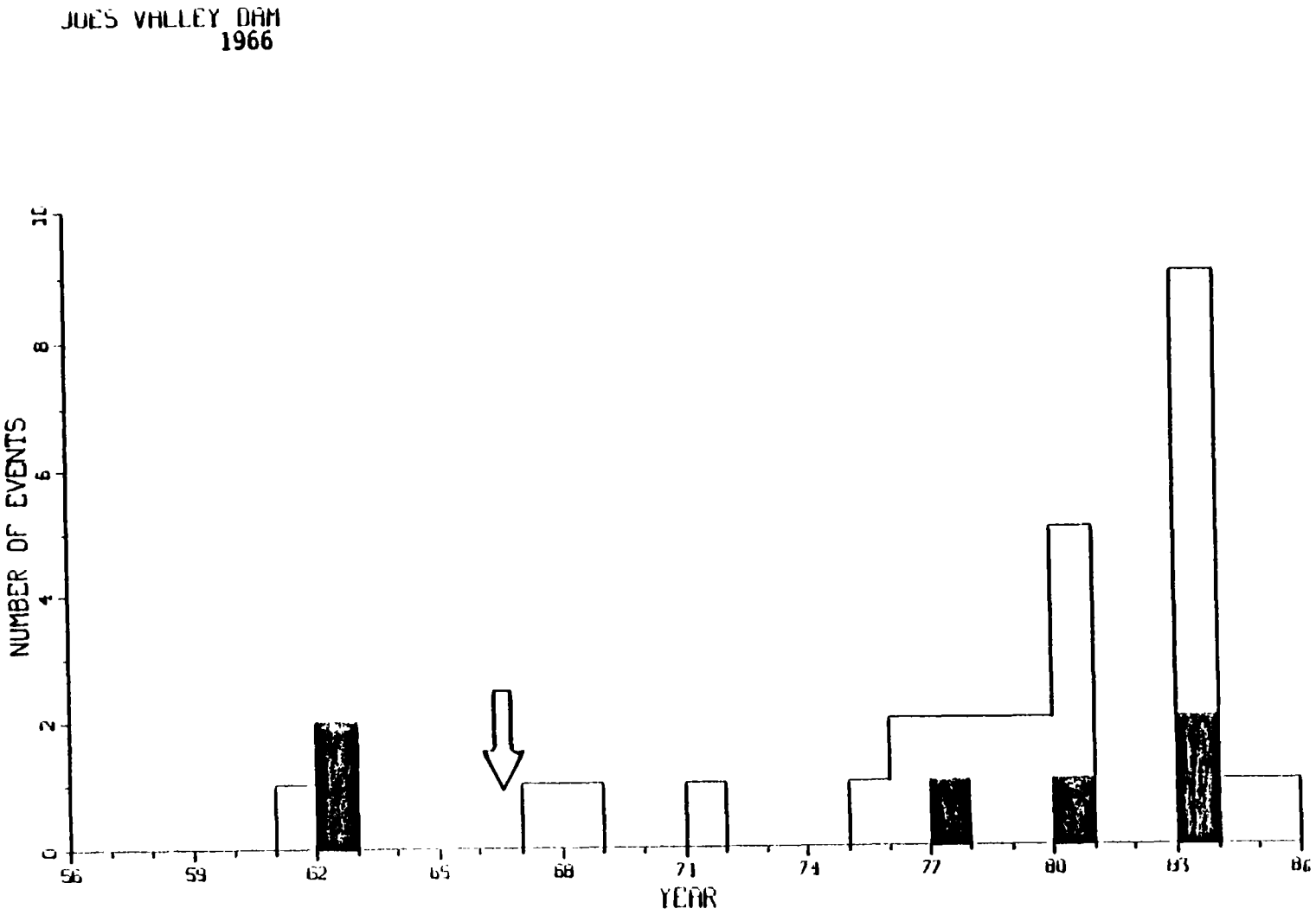


Figure B-2f. Yearly event count for Joes Valley Dam. Arrow signifies year of initial reservoir filling. Solid portions indicate events >

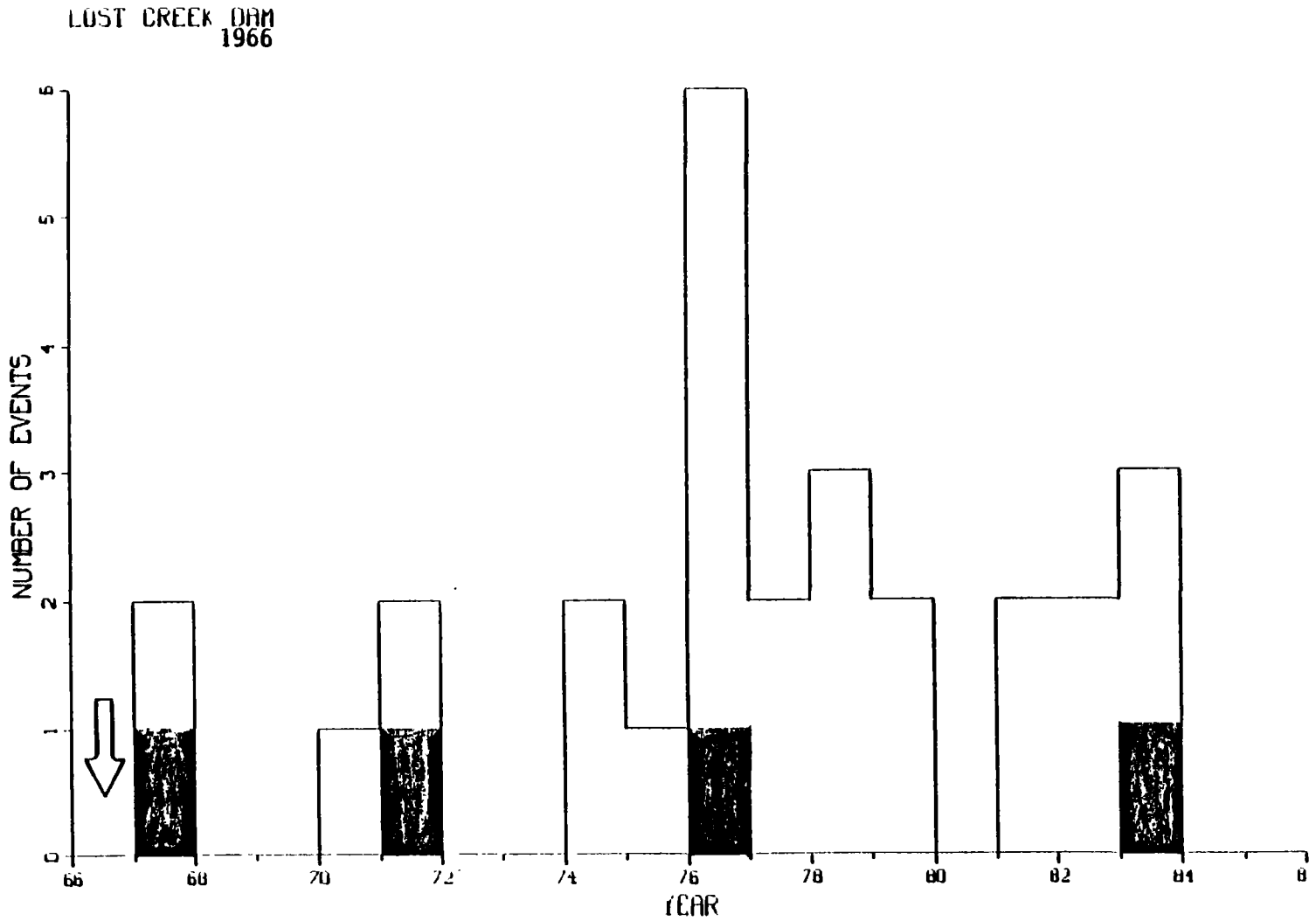


Figure B-2g. Yearly event count for Lost Creek Dam. Arrow signifies year of

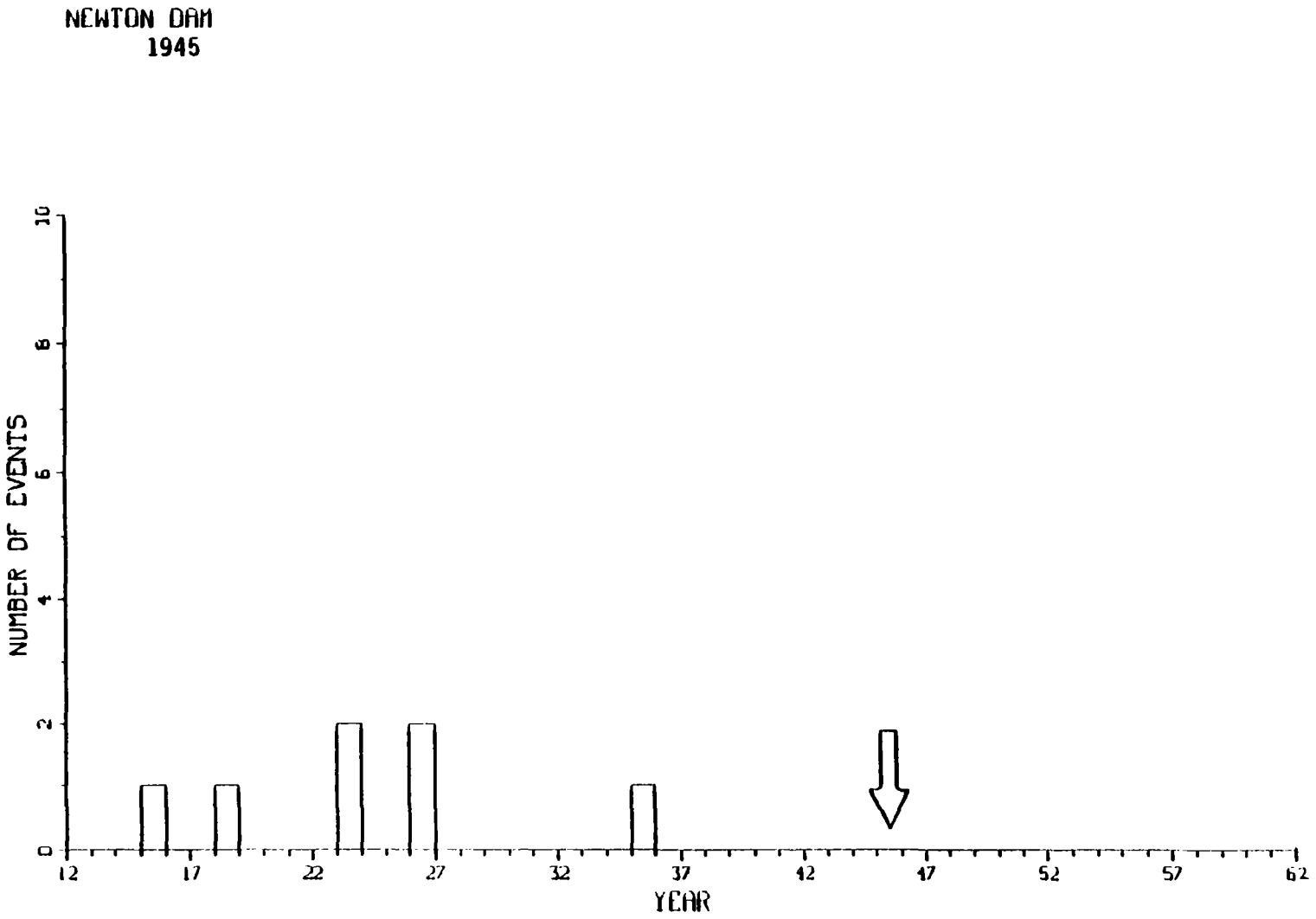


Figure B-2h. Yearly event count for Newton Dam. Arrow signifies year of initial reservoir filling

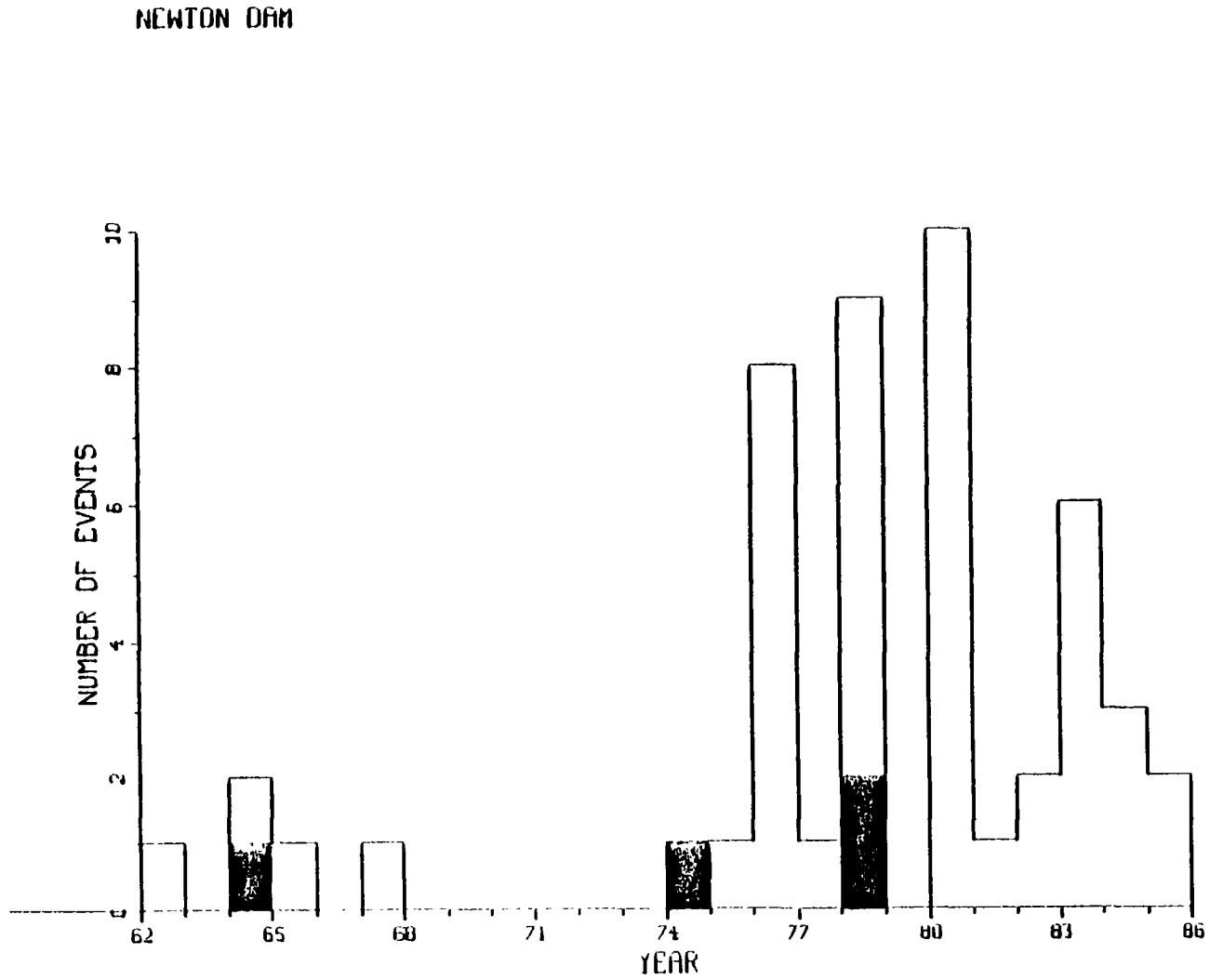


Figure B-2h (Cont'd). Solid portions indicate events ≥ magnitude 2.3.

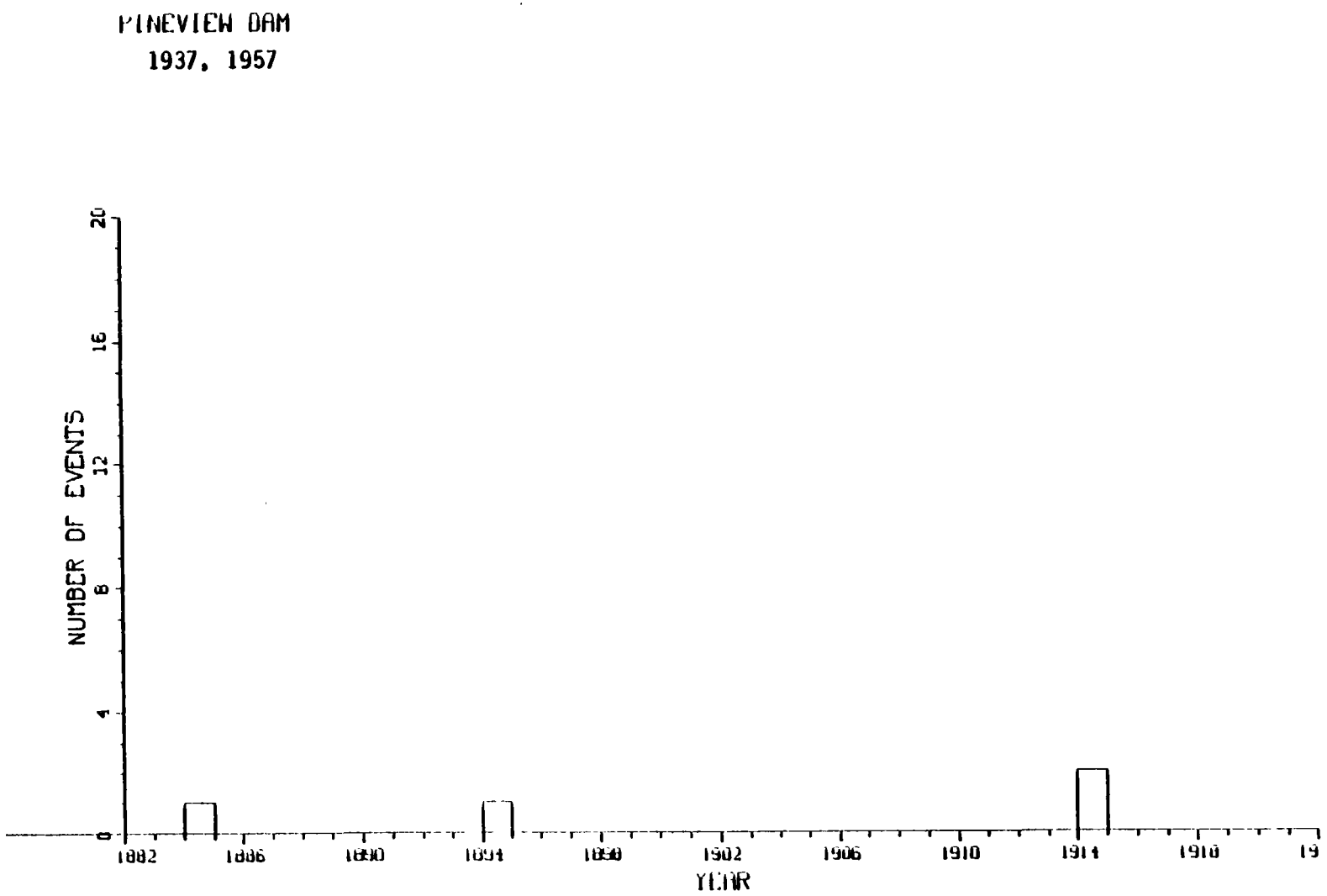


Figure B-2i. Yearly event count for Pineview Dam. Arrow signifies year of initial reservoir filling.

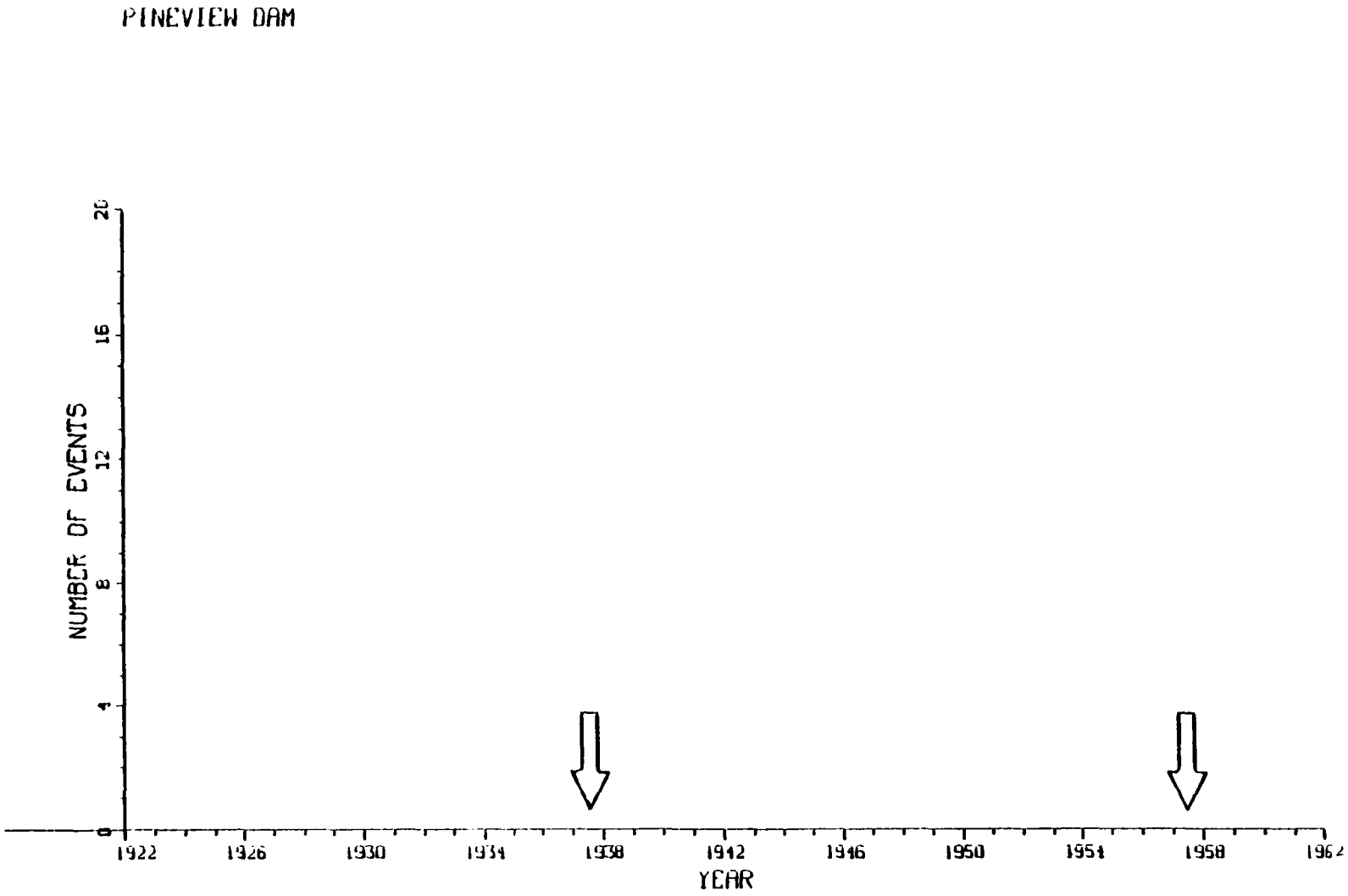


Figure B-2i (Cont'd)

PINEVIEW DAM

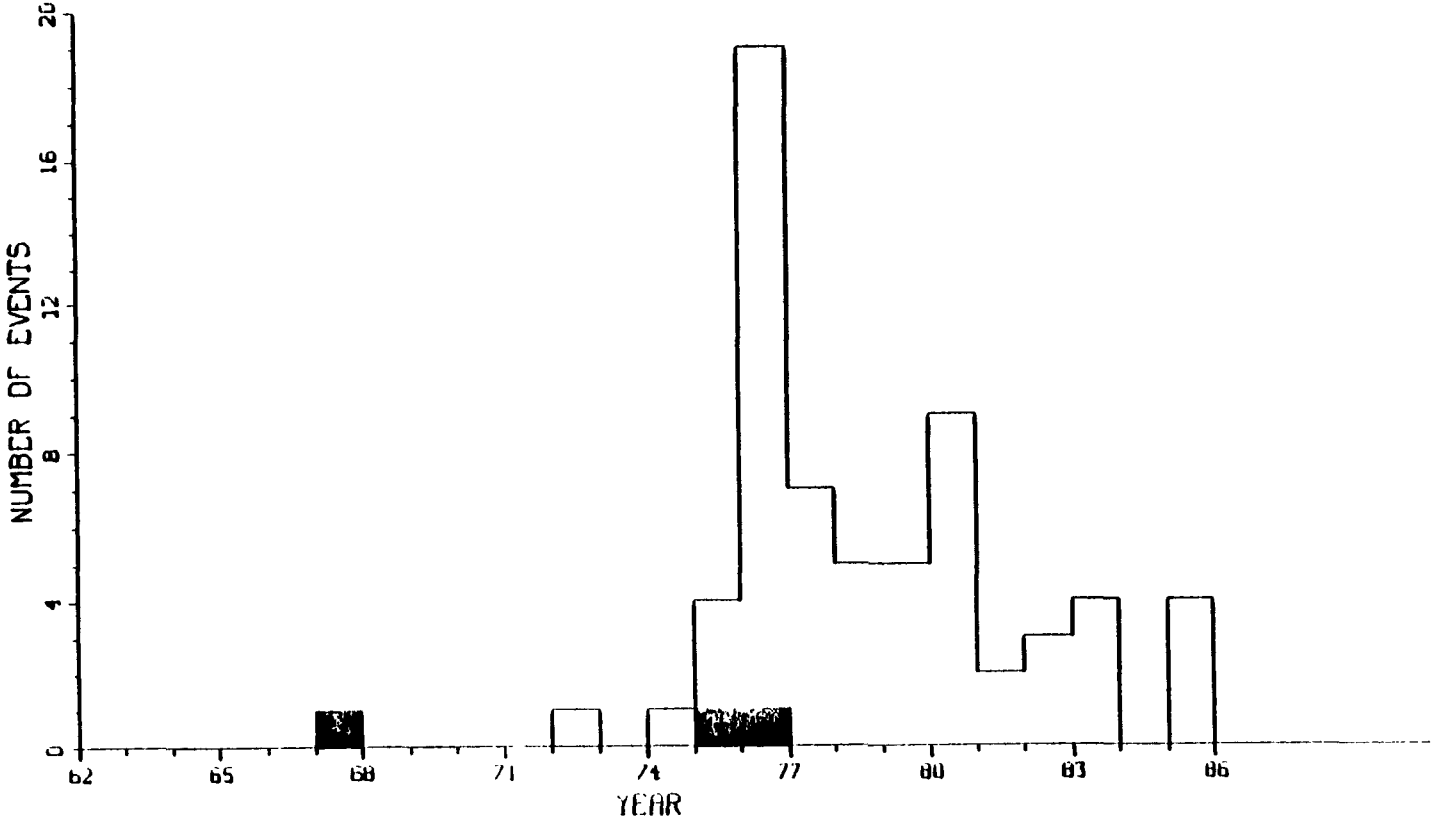


Figure B-2i (Cont'd)

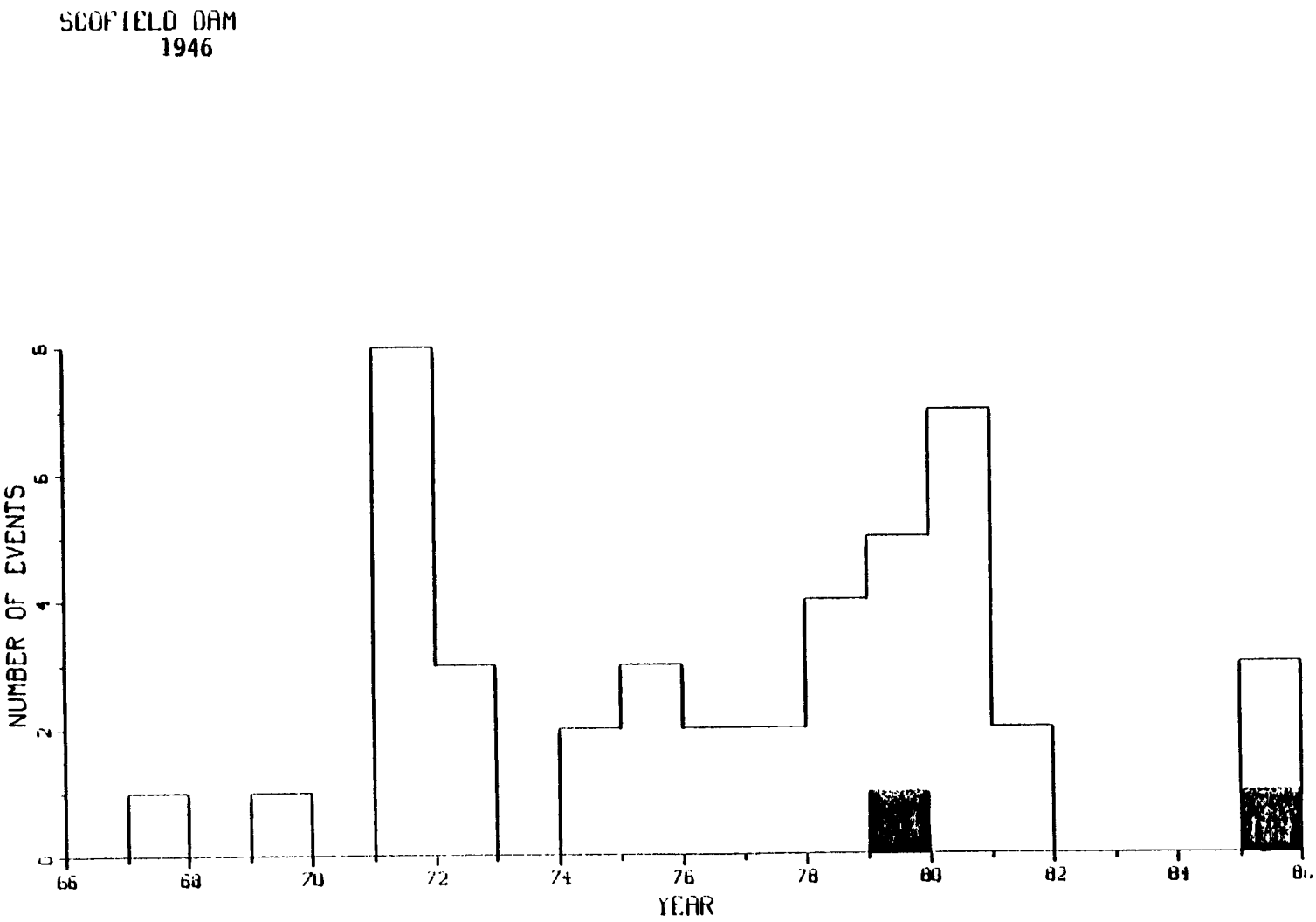


Figure B-2j. Yearly event count for Scofield Dam. Arrow signifies year of initial reservoir filling. Solid portions indicate events

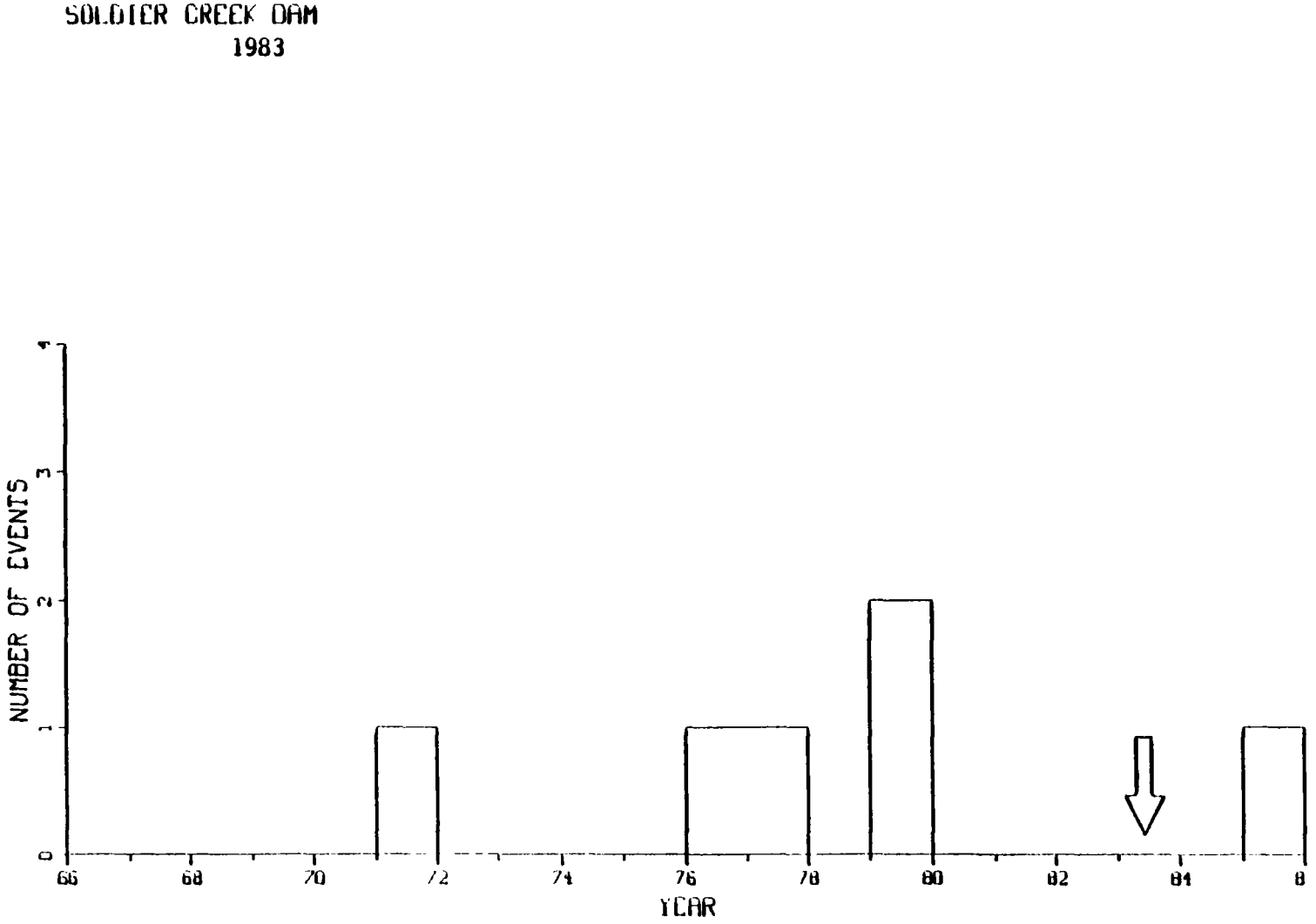


Figure B-24. Yearly event count for Soldier Creek Dam. Arrow signifies year of

STRAWBERRY DAM
1913

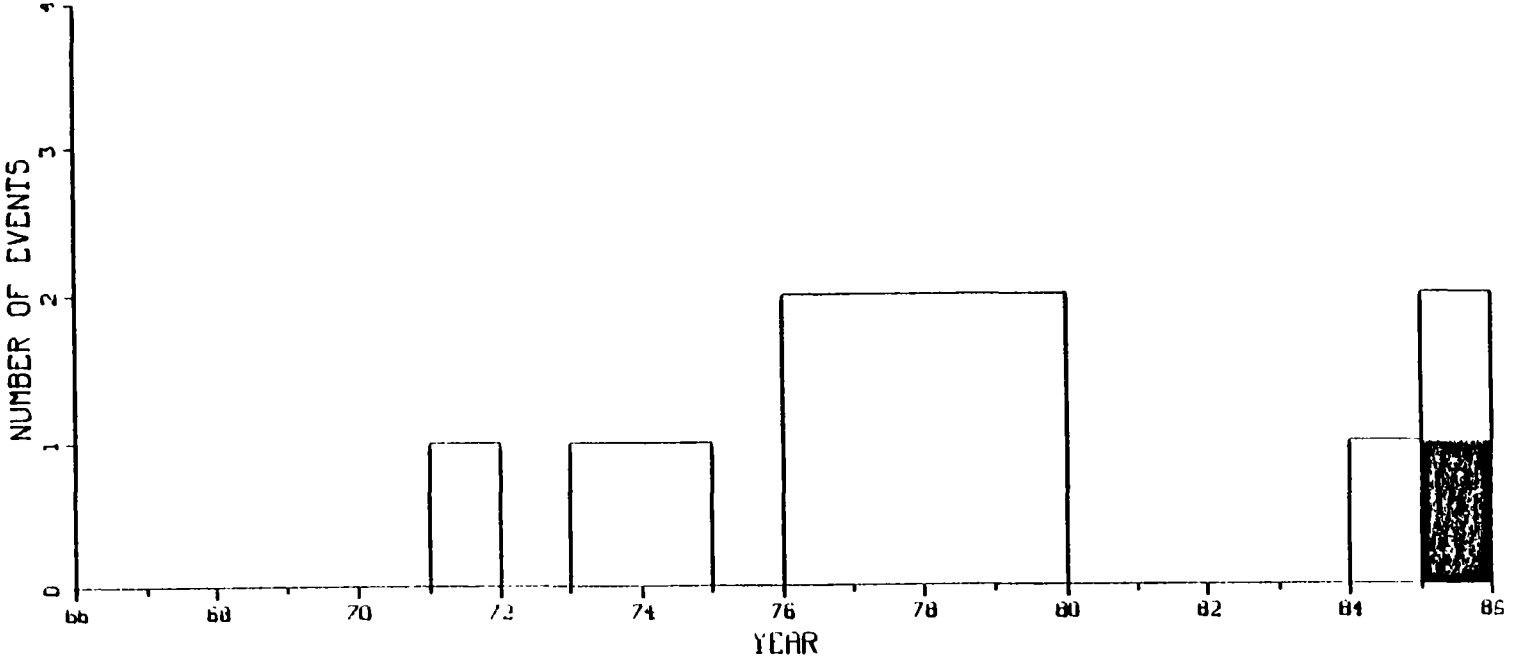


Figure B-21. Yearly event count for Strawberry Dam. Arrow signifies year of

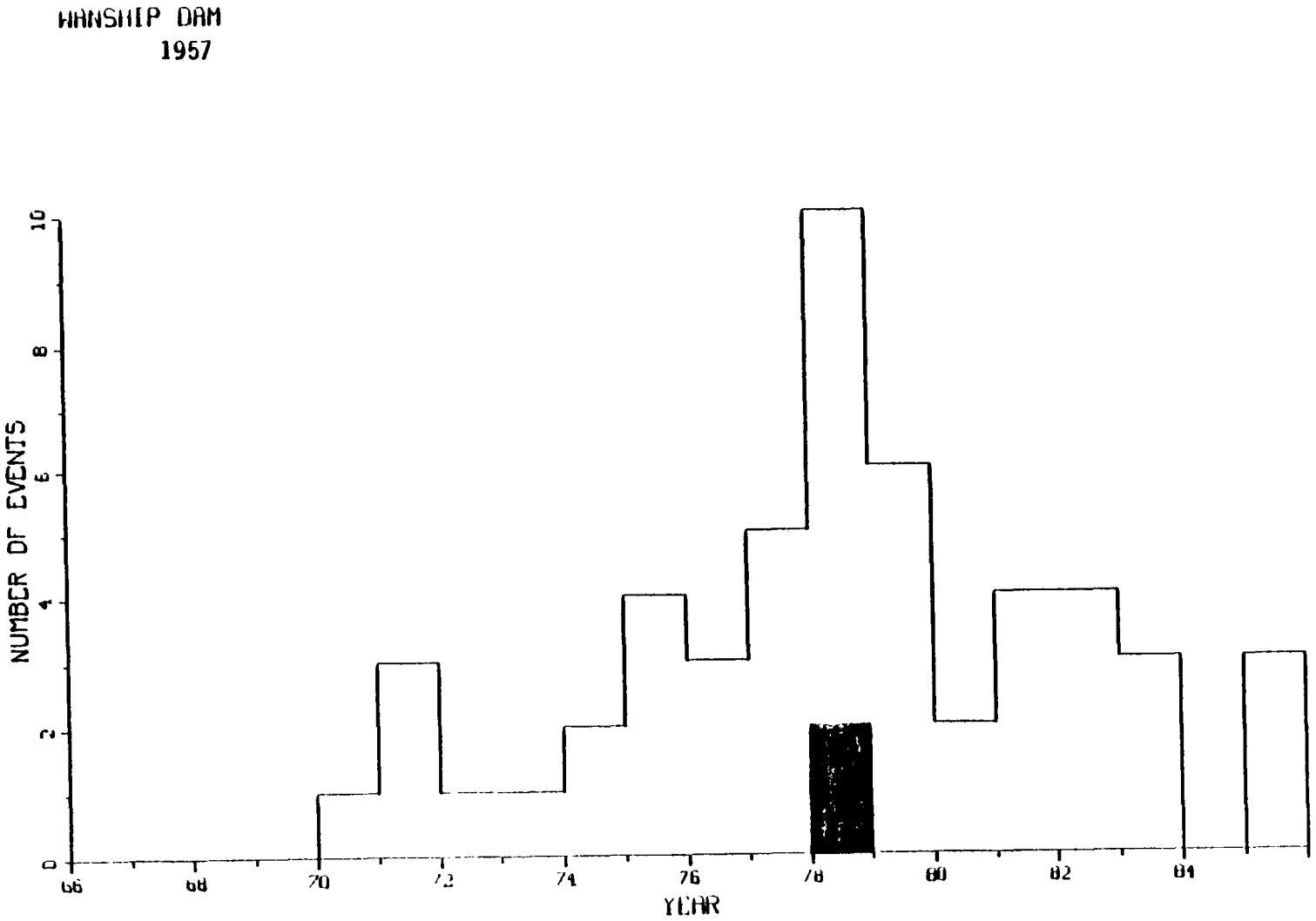


Figure B-2m. Yearly event count for Wanship Dam. Arrow signifies year of

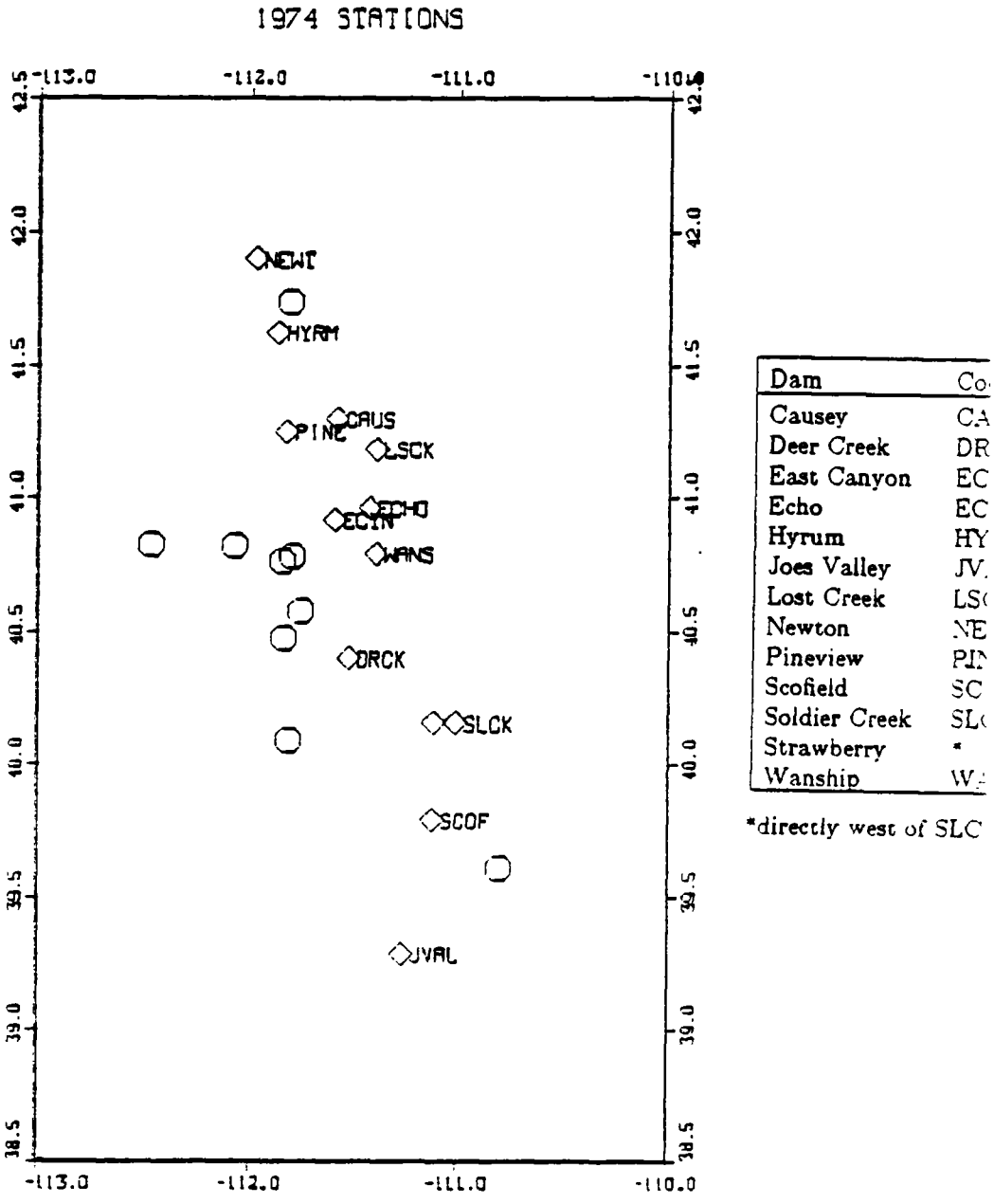


Figure B-3a. Stations (octagons) operated for 7 or more months of 1974. Dams shown as diamonds.

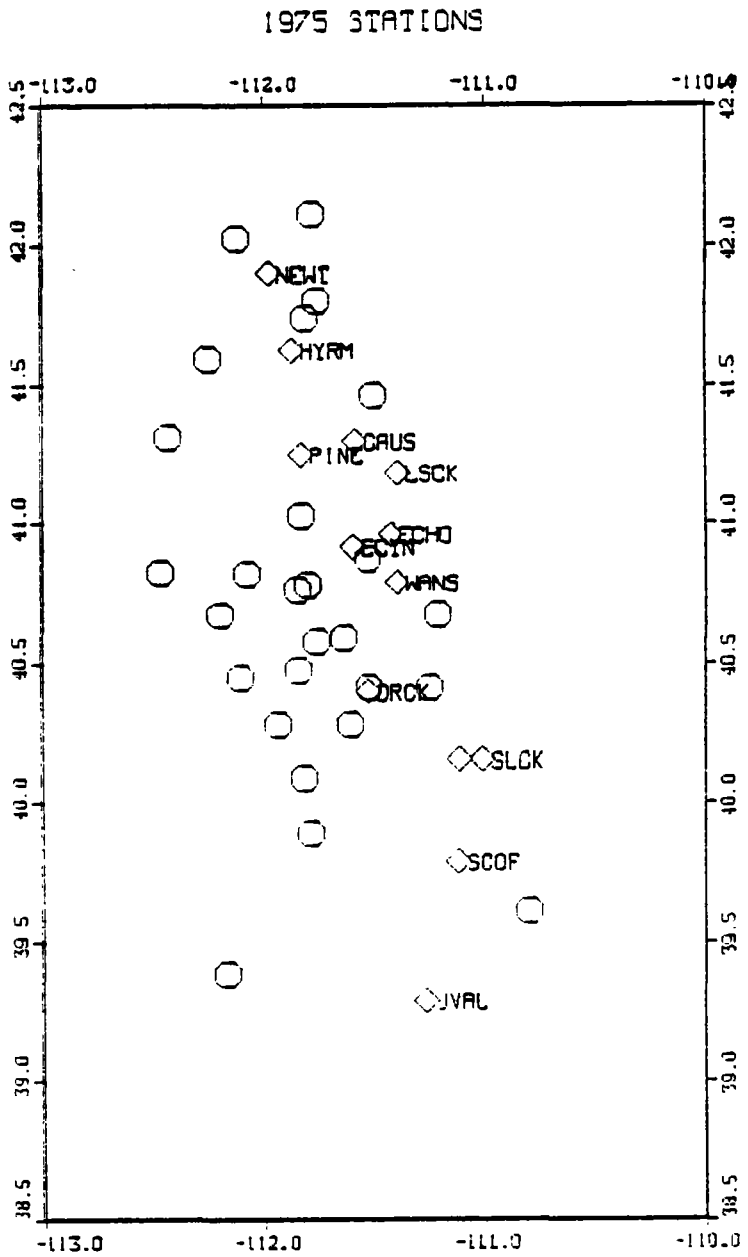


Figure B-3b. Stations (octagons) operated for 7 or more months of 1975. Dams shown as diamonds.

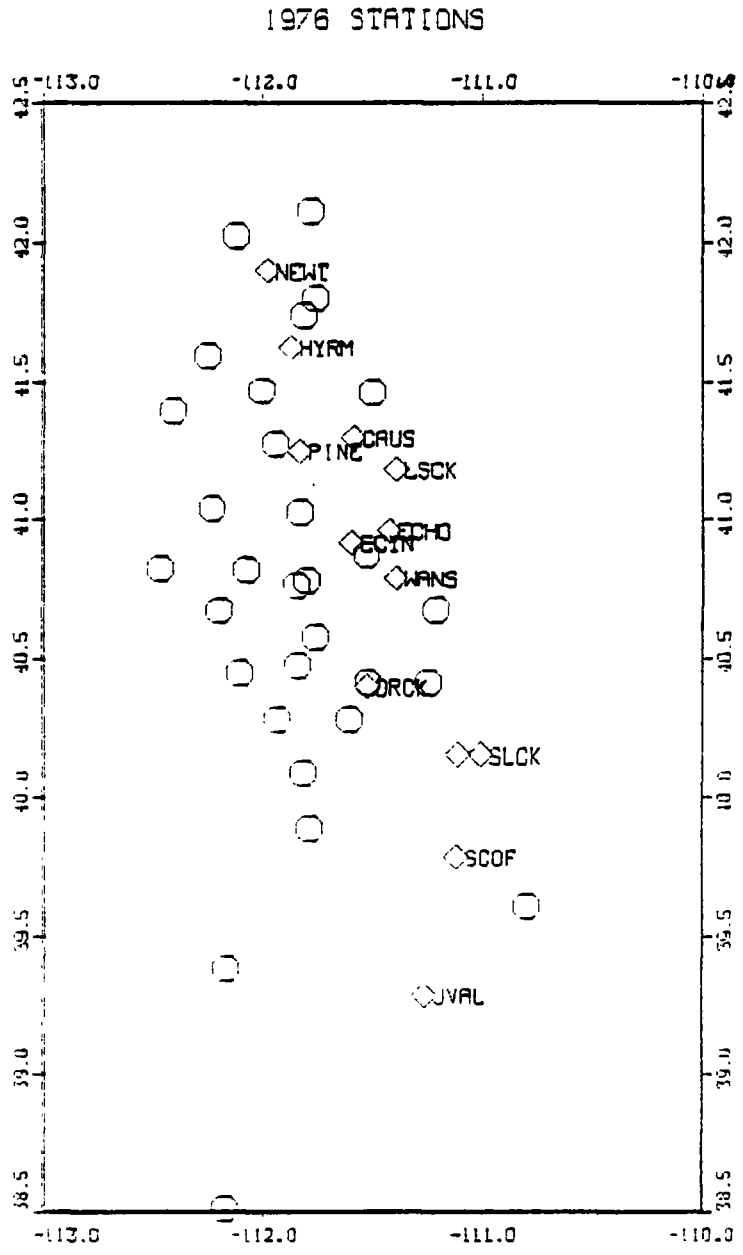


Figure B-3c. Stations (octagons) operated for 7 or more months of 1976. Dams shown as diamonds.

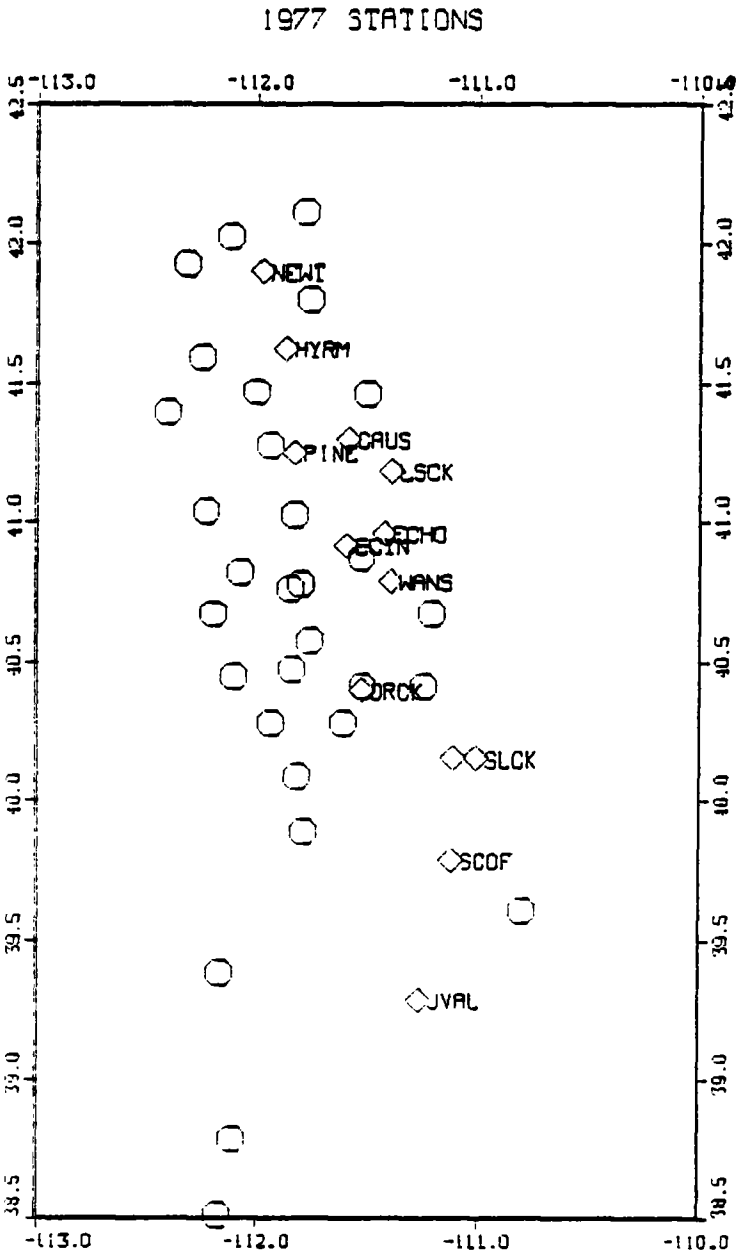


Figure B-3d. Stations (octagons) operated for 7 or more months of 1977. Dams shown as diamonds.

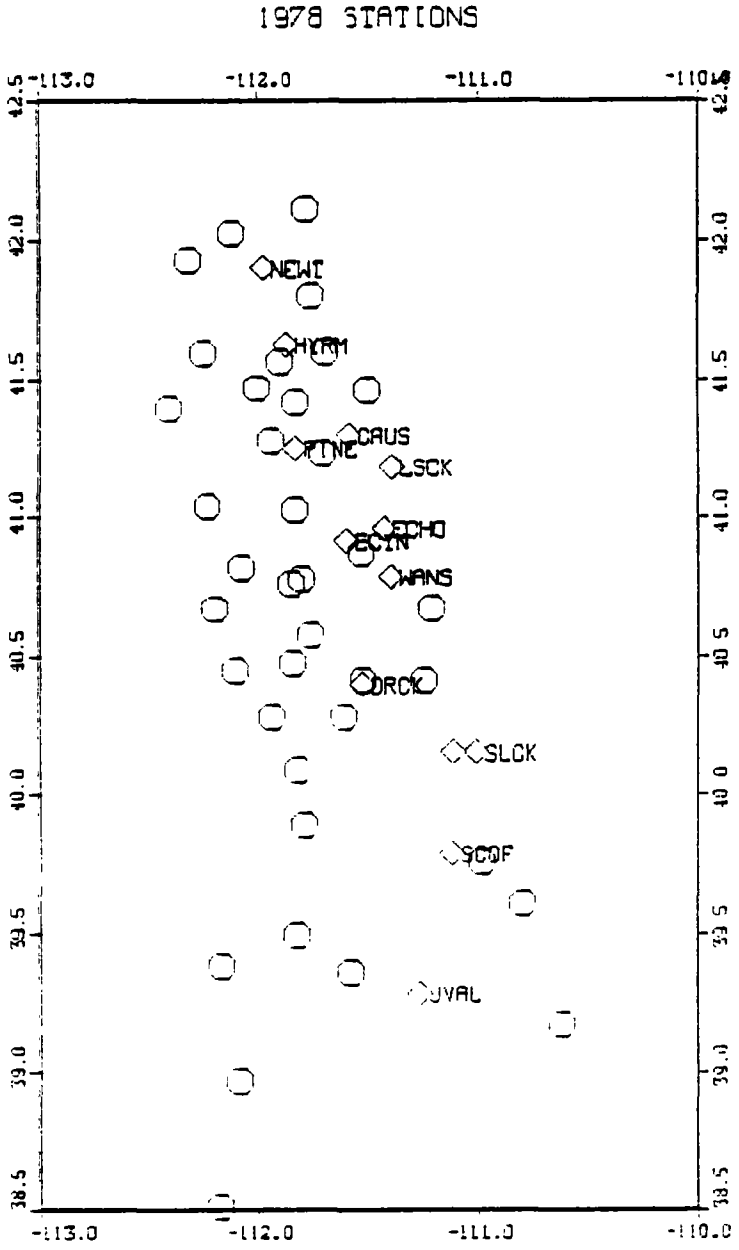


Figure B-3e. Stations (octagons) operated for 7 or more months of 1978. Dams shown as diamonds.

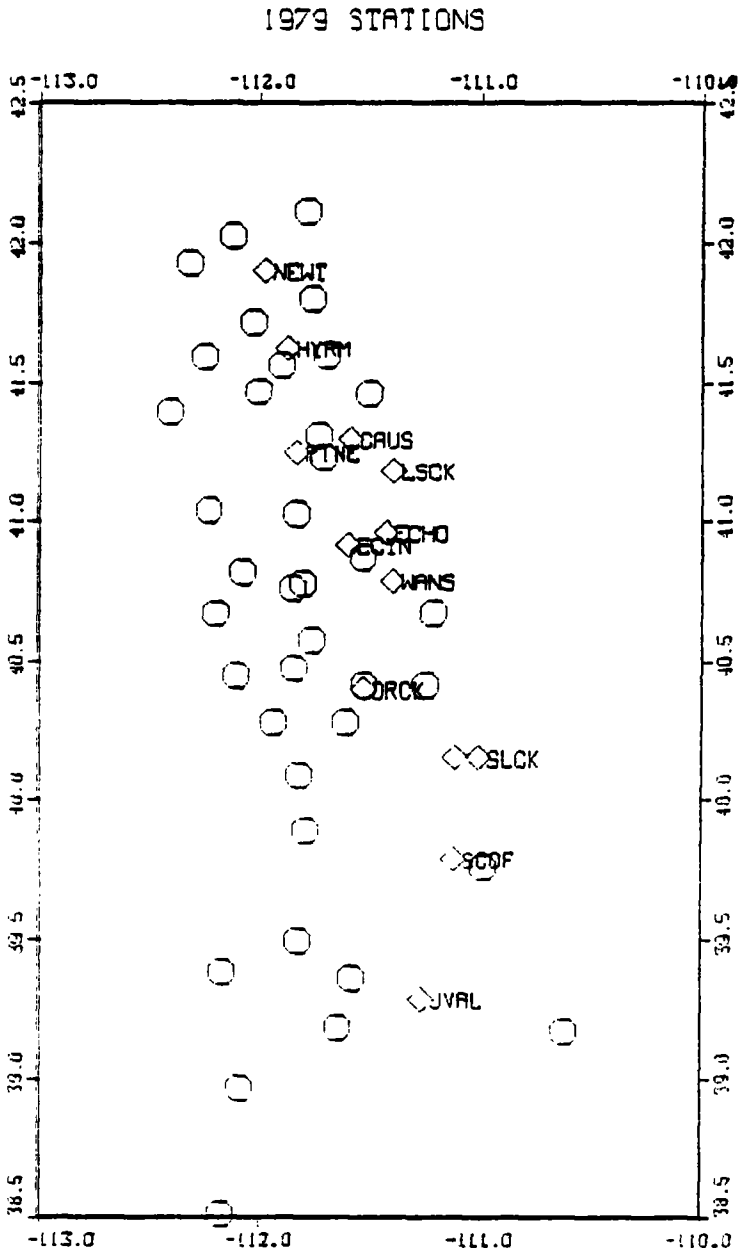


Figure B-3f. Stations (octagons) operated for 7 or more months of 1979. Dams shown as diamonds.

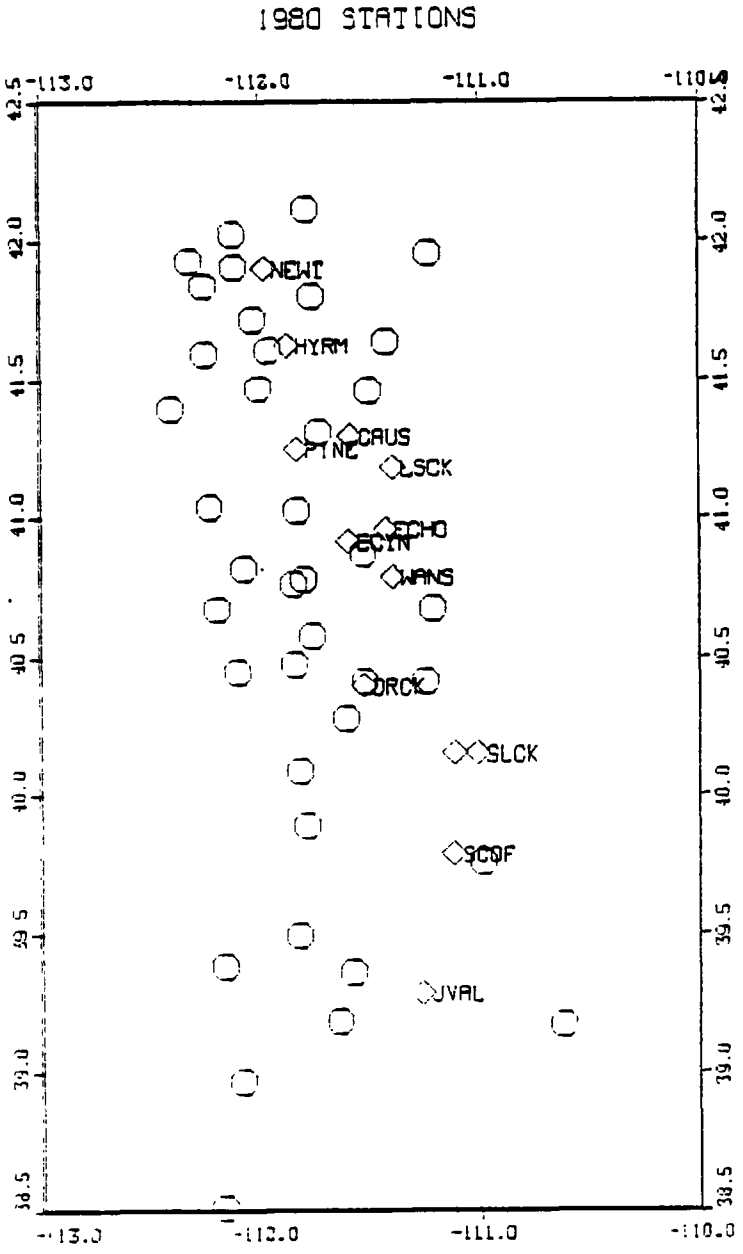


Figure B-3g. Stations (octagons) operated for 7 or more months of 1980. Dams shown as diamonds.

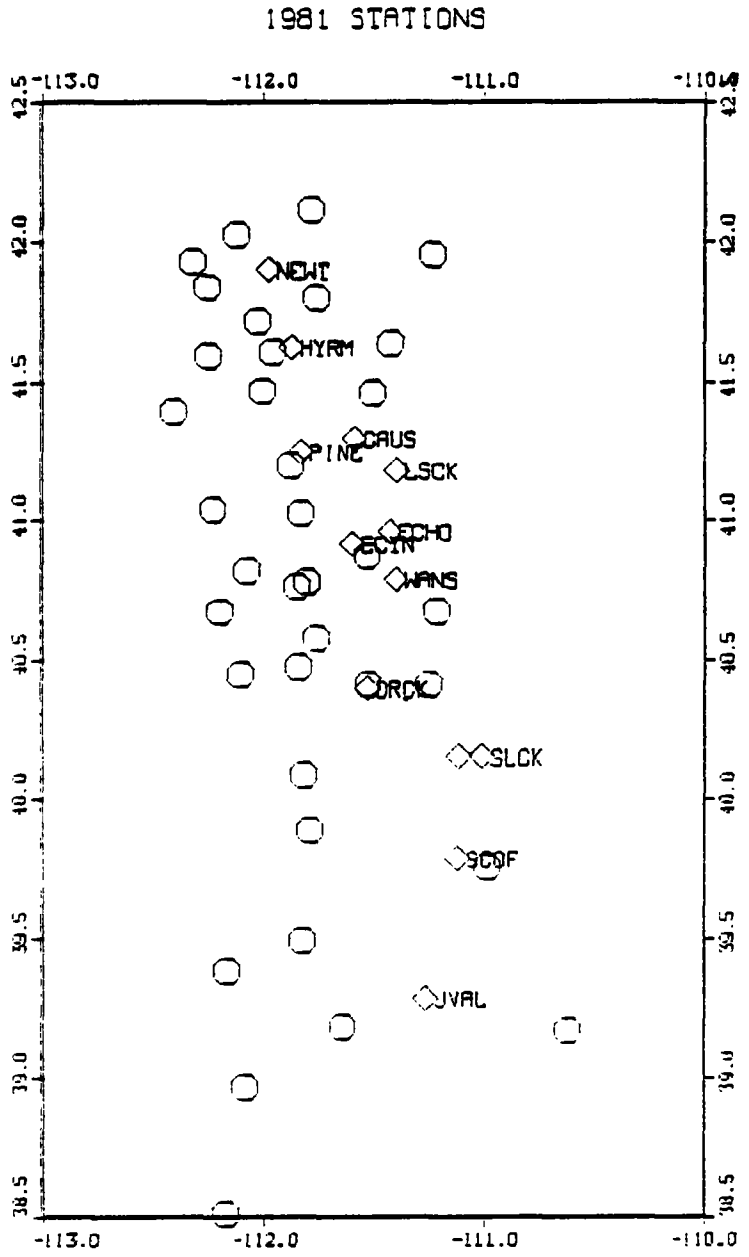


Figure B-3h. Stations (octagons) operated for 7 or more months of 1981. Dams shown as diamonds.

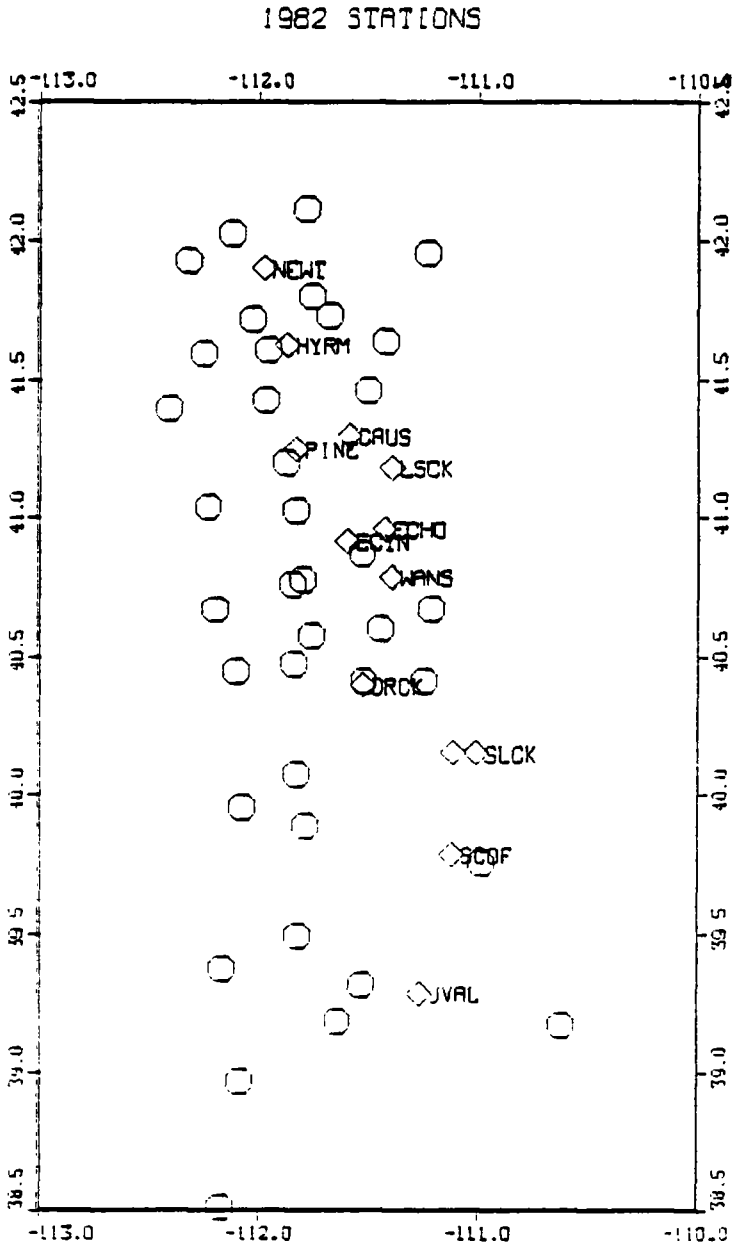


Figure B-3i. Stations (octagons) operated for 7 or more months of 1982. Dams shown as diamonds.

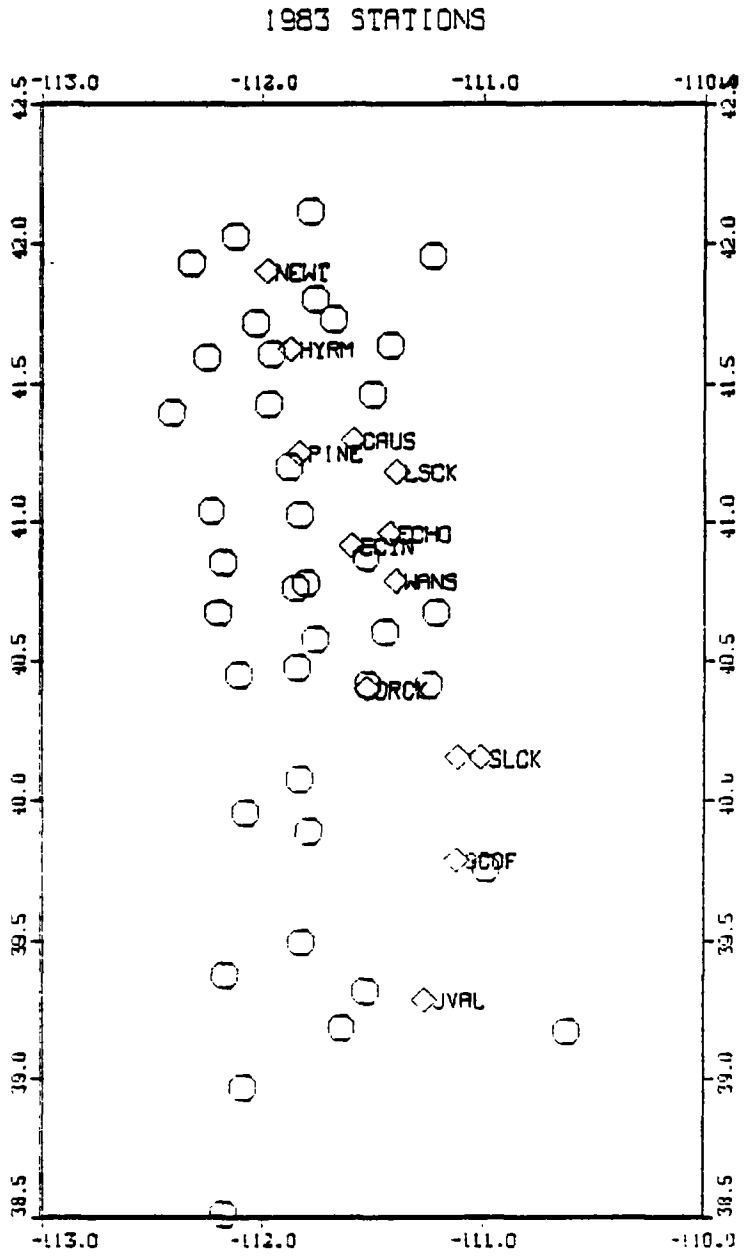


Figure B-3j. Stations (octagons) operated for 7 or more months of 1983. Dams shown as diamonds.

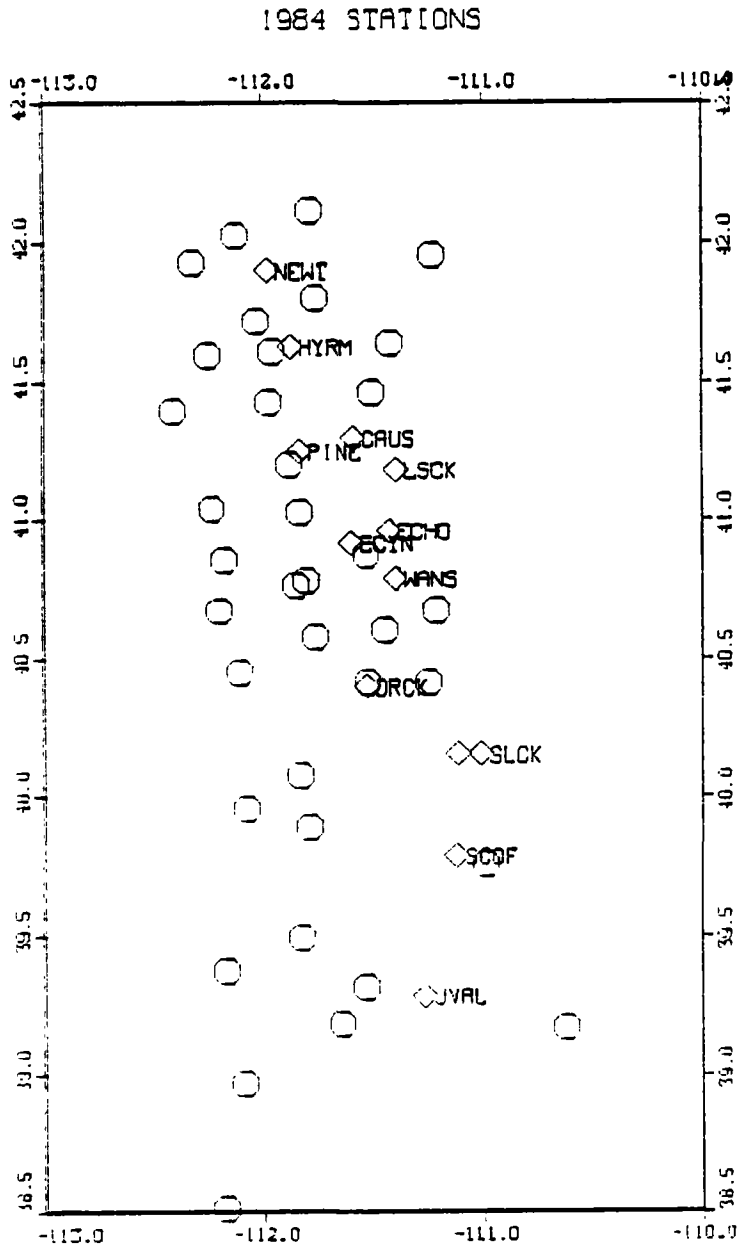


Figure B-3k. Stations (octagons) operated for 7 or more months of 1984. Dams shown as diamonds.

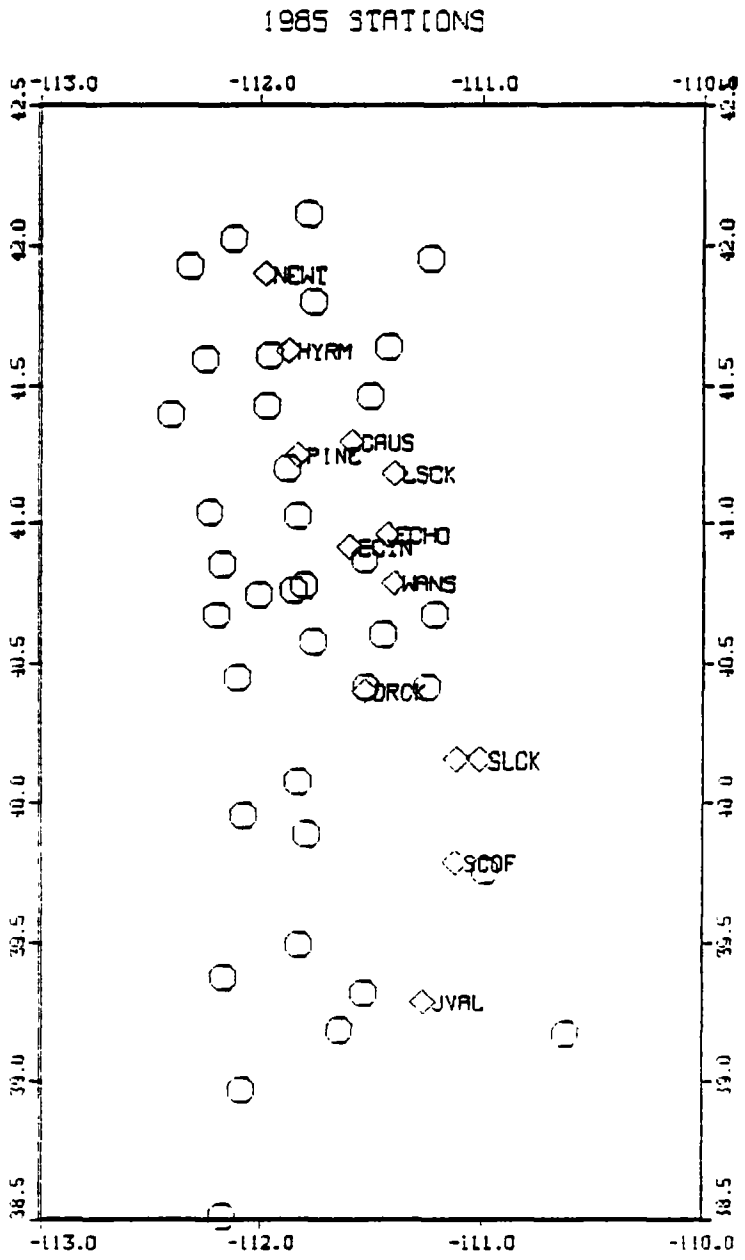


Figure 8-31. Stations (octagons) operated for 7 or more months of 1985. Dams shown as diamonds.

References

Arabasz, W.J., R.B. Smith, and W.D. Richins, 1979, Earthquake studies along the Wasatch Front, Utah: Network monitoring, seismicity, and seismic hazards, in Arabasz, W.J.. R.B. Smith, and W.D. Richins, eds., Earthquake studies in Utah, 1850-1978, University of Utah Seismograph Stations, Department of Geology and Geophysics, University of Utah, Salt Lake City, Utah, pp. 253-285.

_____, 1980, Earthquake studies along the Wasatch front, Utah: Network monitoring, seismicity, and seismic hazards, Bulletin of the Seismological Society of America, vol. 70, pp. 1479-1499.

Baecher, G.B., and R.L. Keeney, 1982, Statistical examination of reservoir induced seismicity, Bulletin of the Seismological Society of America, vol. 72, pp. 553-571.

Bones, D.G., 1978, Seismicity of the intermountain seismic belt in southeastern Idaho and western Wyoming, and tectonic implications, M.S. Thesis, Department of Geology and Geophysics, University of Utah, Salt Lake City, Utah, 131 pp.

Bufe, C.G., 1976, The Anderson Reservoir seismic gap - induced aseismicity?, Engineering Geology, vol. 10, pp.,255-263.

Carder, D.S., 1945, Seismic investigations in the Boulder Dam area, 1940-1944, and the influence of reservoir loading activity, Bulletin of the Seismological Society of America, vol. 35, pp. 175-192.

Foley, L.L., R.A. Martin, and J.T. Sullivan, 1986, Seismotectonic study for Joes Valley, Scofield, and Huntington north dams, Emery County and Scofield projects, Utah, Seismotectonic Report 86-7, U.S. Bureau of Reclamation, Denver, Colorado.

Gough, D.I., and Gough, W.I., 1970, Load-induced earthquakes at Lake Kariba, Geophysical Journal of the Royal Astronomical Society, vol. 21, pp. 79-101.

Guha, S.K., 1977, Premonitory crustal deformations, strains, and seismotectonic features (b-values) preceding Koyna earthquakes, Abstracts of the 1977 International Symposium on recent crustal movements, Stanford University, Palo Alto, CA.

Gupta, H.K., H. Narain, B.K. Rastogi, and I. Mohan, 1969, A study of the Koyna earthquake of December 10, 1967, Bulletin of the Seismological Society of America, vol. 59, pp. 1149-1162.

_____, B.K. Rastogi, and H. Narain, 1972, Common features of reservoir- induced seismic activities, Bulletin of the Seismological Society of America, vol. 62, pp. 481-492.

_____ and J. Combs, 1976, Continued seismic activity at the Koyna reservoir site, India, Engineering Geology, vol. 10, pp. 367-313.

_____ and B.K. Rastogi, 1976, Dams and Earthquakes, Elsevier Publishing, Amsterdam. 299 pp.

_____, C.V. Rama Krishna Rao, B.K. Rastogi, and S.C. Bhatia, 1980, Bulletin of the Seismological Society of America, vol. 70, pp. 1833-1847.

Jacob, K.H., W.D. Pennington, J. Armbruster, L. Seeber, and S. Farhatulla, 1979. Tarbela Reservoir, Pakistan: A region of compressional tectonics with reduced seismicity upon initial reservoir filling, Bulletin of the Seismological Society of America, vol. 69, pp. 1175-1193.

Kisslinger, C.K., 1976, A review of theories of mechanisms of induced seismicity, Engineering Geology, vol. 10, pp. 85-89.

Leith, W., D.W. Simpson, and C.H. Scholz, 1984, Two types of reservoir induced seismicity. presented at IASPEI Regional Assembly, Hyderabad, India.

Meade, R.B., 1982, The evidence for reservoir-induced macroearthquakes, State-of-the-art for assessing earthquake hazards in the United States, Report 19, U.S. Army Corps of Engineers, 194 pp.

Nuttli, O.W., 1979, The relation of sustained maximum ground acceleration and velocity to earthquake intensity and magnitude, State-of-the-Art for assessing earthquake hazards in the United States, Report no. 16, U.S. Army Engineer Waterway Experimental Station. Vicksburg, Miss., 74 pp.

Packer, D.R., J.R. Lovegreen, and J.L. Born, 1977, Reservoir-induced seismicity, vol. 6 (327 p.) in: Earthquake evaluation studies for Auburn dam, Woodward-Clyde Consultants, 8 v. NTIS report, PB-283 531/2GA, PC A15/MF A01.

_____, L.S. Cluff, P.L. Knuepfer, and R.J. Withers, 1980, Study of reservoir induced seismicity, U.S. Geological Survey Open-file Report 80-1092.

Piety, L.A., C.K. Wood, J.D. Gilbert, J.T. Sullivan, and M.H. Anders, 1986, Seismotectonic study for Palisades dam and reservoir, Palisades project, U.S. Bureau of Reclamation. Seismotectonic Report 86-3, 198 pp.

Rothé, J.P., 1970, Man-made earthquakes. Tectonophysics, vol. 9, pp. 215-238.

_____, 1973, Summary: Geophysics Report, in: Man-made lakes: their problems and environmental effects, Geophysical monograph 17, American Geophysical Union. Washington. D.C., pp. 441-454.

Schleicher. D., 1975, A model for earthquakes near Palisades reservoir, southeast Idaho, U.S. Geological Survey Journal of Research, vol. 3, pp. 393-400.

Simpson, D.W., 1976, Seismicity changes associated with reservoir loading, Engineering Geology, vol. 10, pp. 123-151.

_____, 1986. Triggered earthquakes, Annual Reviews of Earth and Planetary Science. vol. 14, pp. 21-42.

_____, and S.K. Negmatullaev, 1981, Induced seismicity at Nurek reservoir, Tadjikistan, USSR, Bulletin of the Seismological Society of America, vol. 71, pp. 1561-1586.

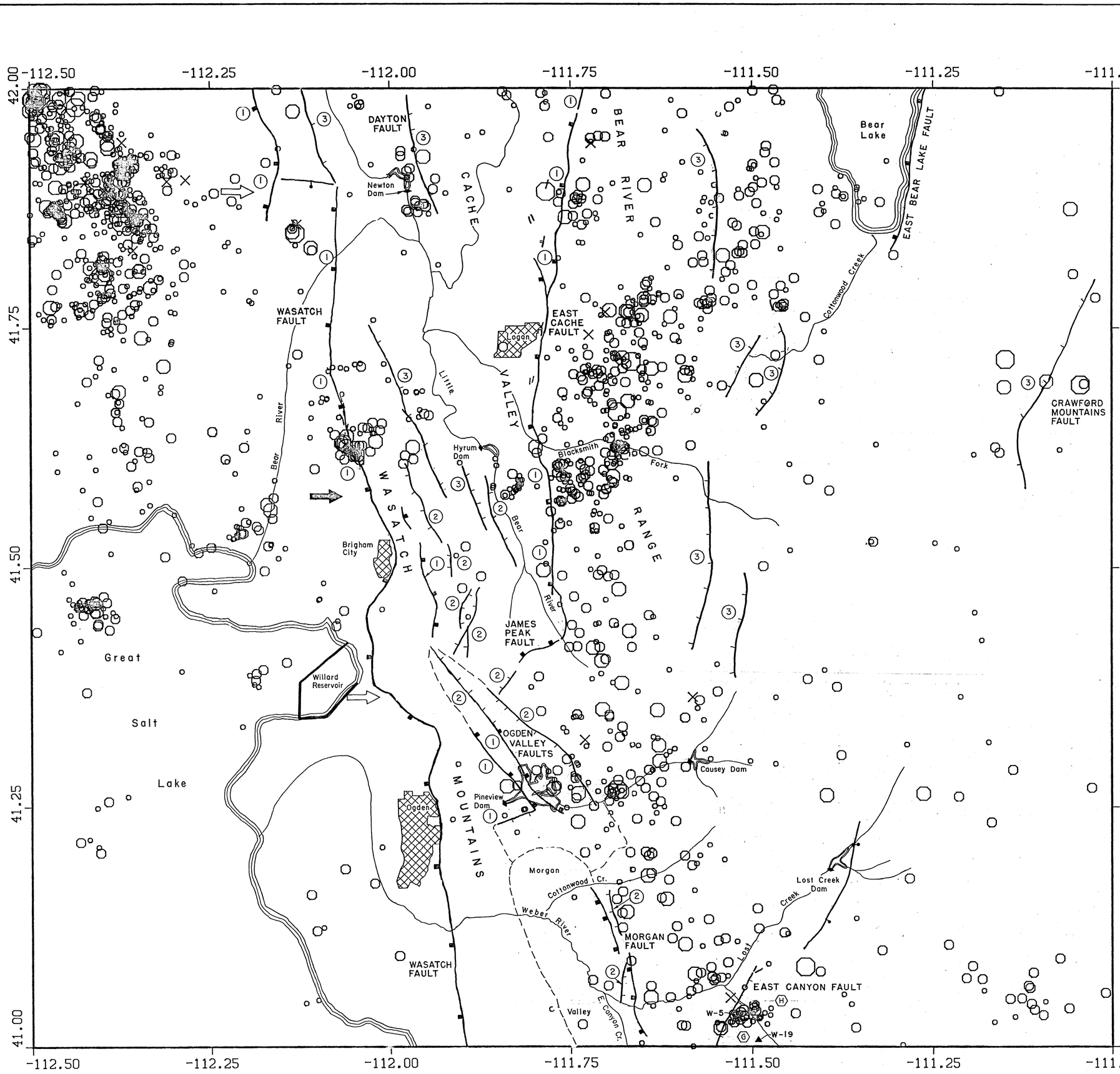
Smith, R.B., P.L. Winkler, J.G. Anderson, and C.H. Scholz, 1974, Source mechanisms of microearthquakes associated with underground mines in eastern Utah, Bulletin of the Seismological Society of America, vol. 64, pp. 1295-1317.

_____, and M.L. Sbar, 1974, Comtemporary tectonics and seismicity of the western United States with emphasis on the Intermountain seismic belt, Geological Society of America Bulletin, vol. 85, pp. 1205-1218.

Stuart-Alexander, D.E., and R.K. Mark, 1976, Impounding-induced seismicity associated with large reservoirs, U.S. Geological Survey Open-file Report 76-770.

Waldpole, R.E., and R.H. Meyers, 1985, Probability and Statistics for Engineers, MacMillan Publishing, New York, 639 pp.

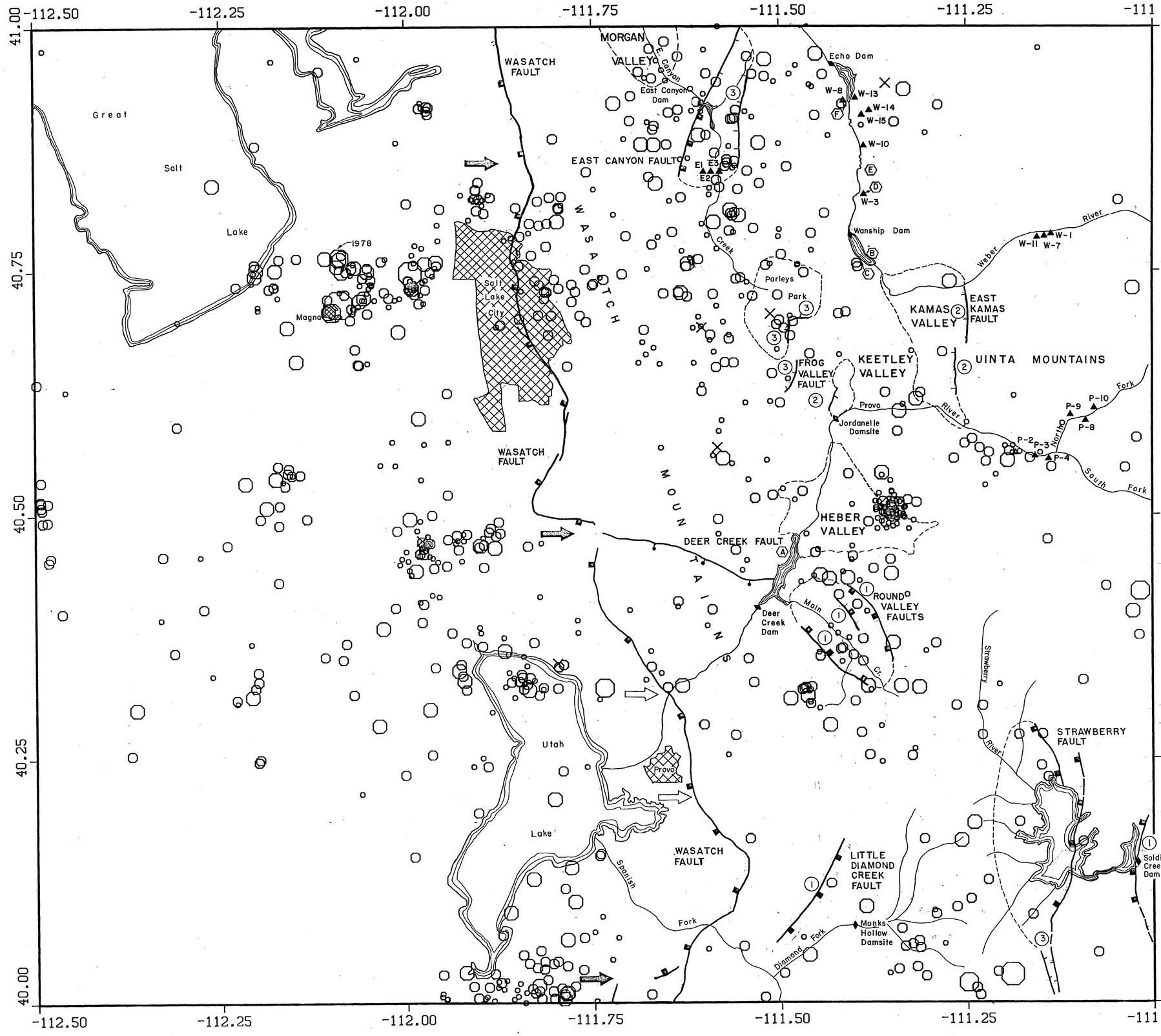
Williams, D.J., and W.J. Arabasz, 1988, Mining related seismicity in the Wasatch Plateau, Utah, PAGEOPH, in press.



CENTRAL UTAH REGIONAL SEISMOTECTONIC STUDY

SEISMICITY (OCTOBER, 1974 - JUNE, 1986) AND AGES OF NORMAL FAULTS IN THE NORTHERN PORTION OF THE BACK VALLEYS OF THE WASATCH MOUNTAINS

PLATE 1A



EXPLANATION

NORMAL FAULTS and ages of most recent displacement

Late Quaternary

Unlabelled – Indicates mapped scarps in late Quaternary deposits and/or age of displacement established by trenching, Wasatch fault from Swan and others (1980, 1981) and Machette and others (1987), Strawberry fault from Nelson and Van Arsdale (1986), other faults this study

(1) Inferred late Quaternary displacement, Stinking Springs fault from Nelson and Martin (1982), other faults this study

Quaternary ?

(2) Suspected Quaternary displacement, but mapping for this study shows or suggests no late Quaternary displacement

(3) Suspected Quaternary displacement based only on air photo mapping this study

Cenozoic

Post-Eocene but pre-Quaternary displacement

EARTHQUAKES

MAGNITUDE (M_L)

- 4.0 – 4.9
- 3.0 – 3.9
- 2.0 – 2.9
- 1.0 – 1.9
- < 1.0
- NO MAGNITUDE GIVEN

Epicenters from University of Utah catalog

SYMBOLS

Proposed segment boundaries of the Wasatch fault, solid arrows from Schwartz and Coppersmith (1984), open arrows from Machette and others (1987). Segments in table 7.1 are: Ogden (41.55°N – 40.8°N) Salt Lake City (40.8°N–40.5°N), Provo (40.5 N–40.0 N)

Outlines of the back valleys

▲ W-8 Soil profile locality not shown on other figures (tables 3.2 and 3.3)

(A) Amino acid sample locality (table 3.1)

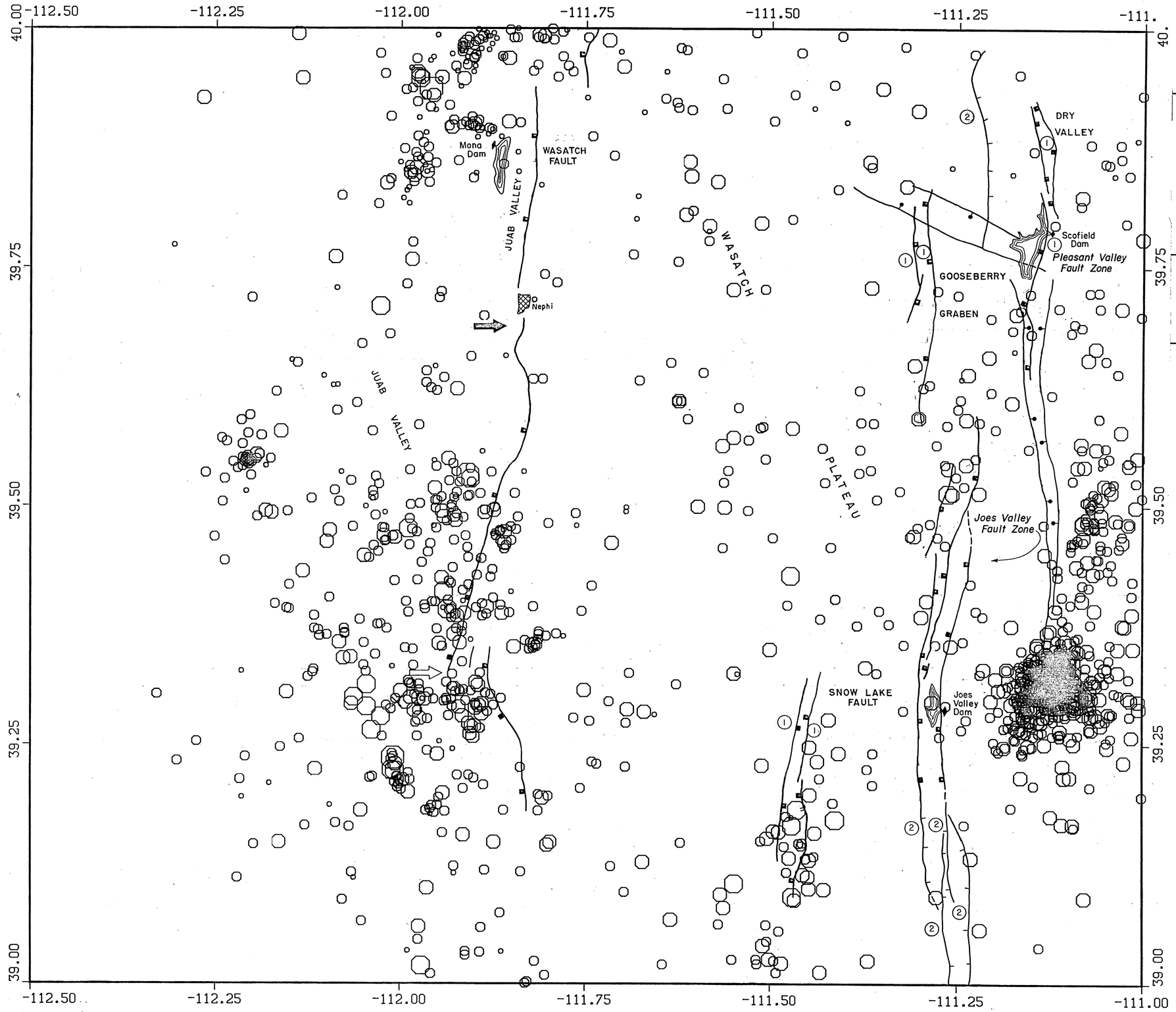
5 0 5 10 15

SCALE OF KILOMETERS

CENTRAL UTAH REGIONAL SEISMOTECTONIC STUDY

SEISMICITY (OCTOBER, 1974 – JUNE, 1986) AND AGES OF NORMAL FAULTS IN THE CENTRAL AND SOUTHERN PORTIONS OF THE BACK VALLEYS OF THE WASATCH MOUNTAINS

PLATE 1B



EXPLANATION

NORMAL FAULTS and ages of most recent displacement

Late Quaternary

Unlabelled - Indicates mapped scarps in late Quaternary deposits and/or age of displacement established by trenching, Wasatch fault from Schwartz and Coppersmith (1984), Joes Valley faults from Foley (1987) and Foley and others (1986)

(1)- Inferred late Quaternary displacement, from Foley (1987) and Foley and others (1986)

Quaternary ?

(2)- Suspected Quaternary displacement, but mapping of Foley and others (1986) shows or suggests no late Quaternary displacement

Cenozoic

Post-Eocene but pre-Quaternary displacement

EARTHQUAKES

MAGNITUDE (M_L)

- 4.0 - 4.9
- 3.0 - 3.9
- 2.0 - 2.9
- 1.0 - 1.9
- < 1.0
- NO MAGNITUDE GIVEN

Epicenters from University of Utah catalog

SYMBOLS

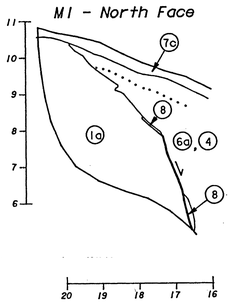
Proposed segment boundaries of the Wasatch fault, solid arrows from Schwartz and Coppersmith (1984), open arrows from Machette and others (1987) Segments in table 7.1 are Nephi (40.0°N-39.7°N) and Levan (39.7 N-39.3 N)

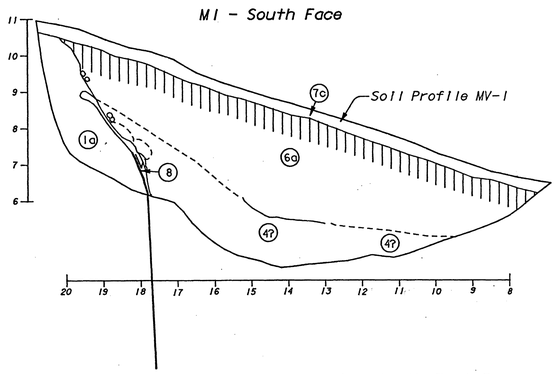
5 0 5 10 15
SCALE OF KILOMETERS

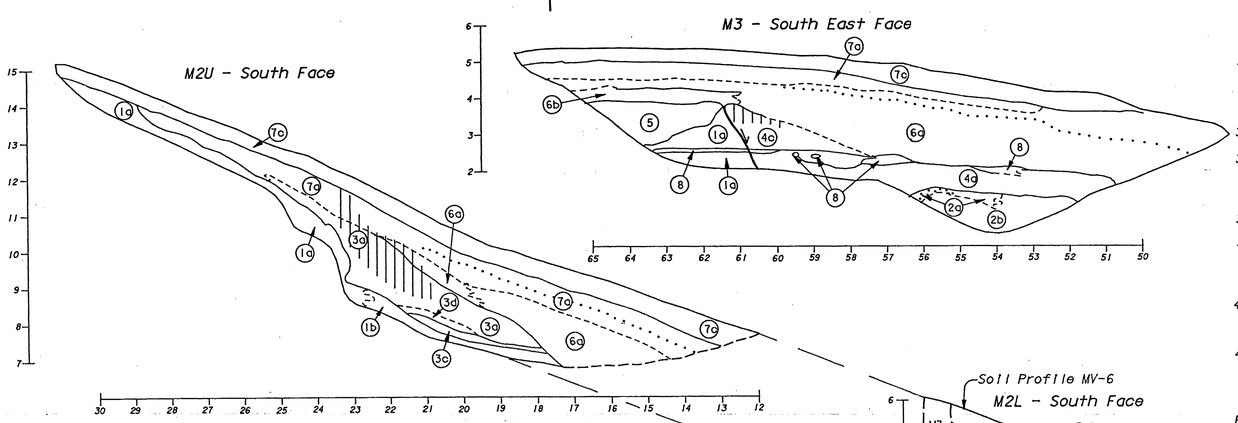
CENTRAL UTAH REGIONAL SEISMOTECTONIC STUDY

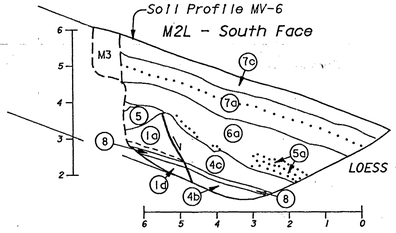
SEISMICITY (OCTOBER, 1974 - JUNE, 1986) AND AGES OF NORMAL FAULTS OF THE NORTHERN WASATCH PLATEAU

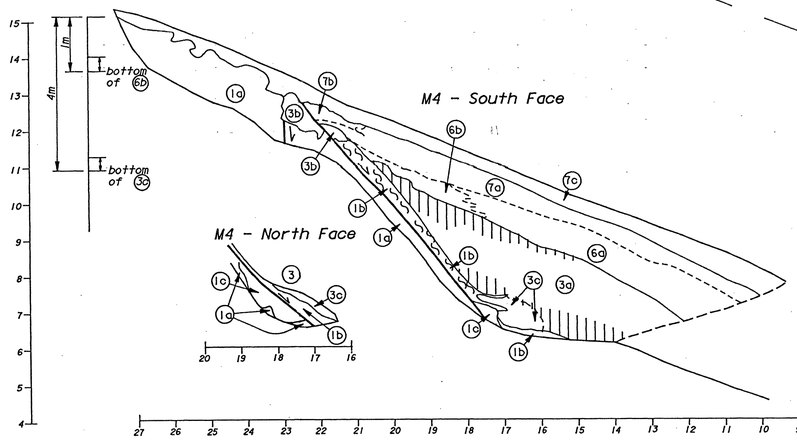
PLATE 1C











EXPLANATION

— Contacts, dashed where indistinct

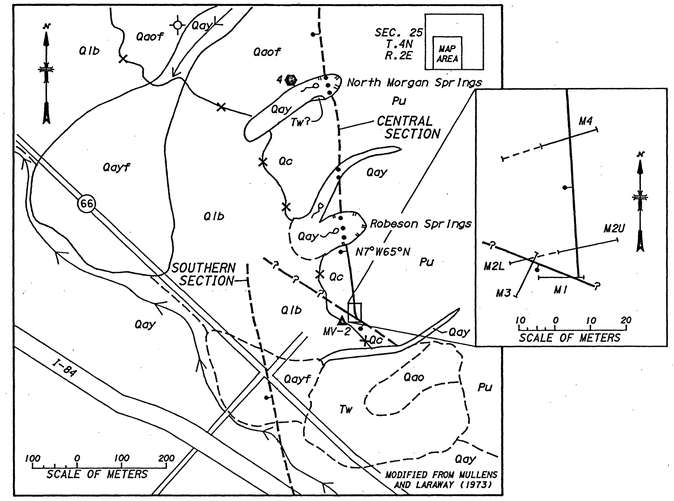
··· Soil horizon boundary

||| Zones of carbonate accumulation

Fault

§§ Fault zone

Unit Number	Trench In Which Unit Occurs	Unit Description
BEDROCK		
1a	M1, M2U M4	Dark grey (2.5Y 4/2) dolomite consisting of variably weathered rock which breaks readily to small chips, containing carbonate filled fractures near the ground surface with local zones of yellow (2.5Y 7/6) alteration; rock fabric is intact. DCd of Mullens and Laraway (1973)
1b	M2U, M4	Dark grey (2.5Y 4/2) fault breccia consisting entirely of soft, uncemented, non-plastic, silt-sized fragments interpreted to be part of the Morgan fault zone.
1c	M4	Yellow (2.5Y 7/8) plastic clay along Morgan fault zone interpreted to be fault gouge.
1d	M2L	Dark grey (2.5Y 4/2) limestone? with blobs of yellow (2.5Y 8/4) limey siltstone. Cl or Cll of Mullens and Laraway (1973)
COLLUVIUM		
2a	M3	Tan (7.5YR 7/4) clayey silt consisting of 10% angular, dolomite, limestone and clastic pebbles in a firm silty clay matrix containing pockets of carbonate.
2b	M3	Brown (7.5YR 5/6) unstratified, clayey silt consisting of 20% angular dolomite, limestone and clastic pebbles in a loose clayey silt matrix.
3a	M2U, M4	Light brown (10YR 6/4) mostly unstratified clayey silt consisting of 20% subangular dolomite (90%) and sandstone (10%) pebbles in a firm, clayey silt matrix containing crude 20° west dipping bedding near the base.
3b	M4	Yellow (10YR 7/4) unstratified, very hard, sandy silt with (1% pebbles).
3c	M4	Yellow (10YR 6/6) unstratified, gravelly clay consisting of 30% subangular dolomite (82%), limestone (11%) and sandstone (6%) pebbles in a hard, silty clay matrix.
3d	M2U	Same as 3 with 30% subangular dolomite and sandstone pebbles.
4a	M3, M1?	Dark brown (2.5YR 3/4) unstratified, silty clay consisting of 20% angular dolomite (20%), limestone (22%), pebbles and occassional cobbles in a firm silty clay matrix.
4b	M2L	Brown (10YR 6/8) unstratified, silty clay consisting of 20% angular siltstone (81%) and sandstone (19%) pebbles in a firm, silty clay matrix.
4c	M2L, M3, M1?	Yellow (10YR 7/6) unstratified silty clay consisting of 5% angular sandstone (72%) and siltstone (28%) in a silty clay matrix.
PEAT		
5	M2L, M3	Black (10YR 3/2) fiberous peat with local horizontal interbeds of brown silty clay.
5a	M2L	Dark brown silt with 10%? organic material, these are interpreted as buried A-horizons that formed concurrently with the unit 5.
LOESS - COLLUVIUM		
6a	M2U, M2L	Brown (7.5 YR 8/4-6/6) massive silt consisting of (1% pebbles in a clayey silt matrix grading upslope to 5% to 10% subangular and subrounded dolomite (7%) pebbles in a loose silt matrix.
6b	M4, M2U	Same as 6 with 10%-15% subangular predominately dolomite pebbles in a firm clayey silt matrix.
RECENT SLOPEWASH - COLLUVIUM		
7a	ALL	Light brown (7.5YR 7/4) gravelly silt consisting of 20%-30% angular and subangular dolomite pebbles and cobbles in a firm silt matrix. A cambic B-horizon and a BCa horizon are developed in this unit.
7b	M4	Dark brown (10YR 3/3 to 7.5YR 3/4) gravelly silt consisting of 20%-30% angular and subangular dolomite pebbles and cobbles in a loose matney of silt, scarp-derived colluvial wedge.
7c	ALL	Dark brown (10YR 3/3 to 7.5YR 3/4) gravelly silt consisting of 20% - 30% angular and subangular dolomite pebbles and cobbles in a loose matrix of silt and organic material, A-horizon.
SPRING DEPOSIT?		
8	M1, M2L, M3	Red (2.5YR 4/6) silty clay occurring as a thin continuous seam in M2L and M3, and a vertical decemminated zone in M1 with gradational boundaries.


SEC. 25 T.4N R.2E
MAP AREA
North Morgan Springs
CENTRAL SECTION
Robeson Springs
N7°W65°N
SOUTHERN SECTION
MV-2
I-84
66
Qay
Qaof
Qaof
Qay
Qay
Qc
Qay
Qay
Qay
Qay
Qay
Qay
Qay
Qay
Qay
Qay
Qc
Qc
Qaoc
Qaoc
Qao